UNIVERSITAT POLITÈCNICA DE VALÈNCIA

ESCUELA DE DOCTORADO

DEVELOPMENT AND CALIBRATION OF A GLOBAL GEOMETRIC DESIGN CONSISTENCY MODEL FOR TWO-LANE RURAL HIGHWAYS, BASED ON THE USE OF CONTINUOUS OPERATING SPEED PROFILES

DESARROLLO Y CALIBRACIÓN DE UN MODELO GLOBAL DE CONSISTENCIA DEL DISEÑO GEOMÉTRICO DE CARRETERAS CONVENCIONALES BASADO EN EL EMPLEO DE PERFILES CONTINUOS DE VELOCIDAD DE OPERACIÓN

DOCTORAL THESIS

Presented by:

FRANCISCO JAVIER CAMACHO TORREGROSA

Supervised by:

Dr. ALFREDO GARCÍA GARCÍA

NOVEMBER 2014

A todos los que me han hecho y me harán posible

Resumen

La seguridad vial es uno de los problemas más importantes de sociedad actual, causando centenares de miles de víctimas mortales cada año en todo el mundo.

En la generación de un accidente intervienen diversos factores, siendo los más relevantes el factor humano y la infraestructura, así como su interacción. Sobre dicha interacción se ha investigado mucho en los últimos años, ampliando la comprensión sobre el proceso de conducción y dando lugar a mejoras que, en muchos casos, todavía no han sido transcritas a las guías de diseño.

Algunos de estos avances se centran sobre la comprensión de los procesos cognitivos involucrados en la tarea de conducción; en la respuesta de los conductores y en la mejor estimación de la siniestralidad. Ligado a todo ello está el concepto de consistencia. Se entiende como tal al grado de adecuación entre las expectativas de los conductores y el comportamiento de la carretera. Así pues, una carretera inconsistente produce sorpresas en los conductores, potencialmente derivando en una mayor siniestralidad.

En esta tesis se desarrolla un modelo de consistencia global basado en el análisis de la velocidad de operación. Se han tratado más de 150 tramos homogéneos de carreteras convencionales de la Comunidad Valenciana, extrayendo diversos parámetros operacionales y determinando cuáles presentan una mayor relación con la siniestralidad.

Para posibilitar el estudio, se han creado diversas herramientas auxiliares, algunas de las cuales constituyen igualmente una importante innovación. Dos ejemplos son un nuevo método analítico-heurístico de restitución geométrica en planta basado en el azimut, así como una nueva metodología de tramificación de carreteras convencionales o unas expresiones para determinar de forma más precisa la velocidad de proyecto idónea para un tramo homogéneo.

El modelo de consistencia obtenido puede servir de base para la estimación de la siniestralidad, a través de safety performance functions. Con el objetivo de integrar todos estos avances, se propone una nueva metodología de diseño de carreteras que, complementando las actuales guías, permite considerar el carácter continuo de la seguridad vial en el proceso de diseño.

Resum

La seguretat viària és un dels problemes més importants de la societat actual, causant centenars de milers de víctimes mortals cada any a tot el món.

A la generació d'un accident de trànsit hi intervenen diversos factors, dels quals els més importants són el factor humà i la infraestructura, així com la seua interacció. Als últims anys s'ha investigat molt al voltant d'eixa interacció, ampliant el coneixement sobre el procés de conducció, donant lloc a millores que, en molts cassos, encara no hi han sigut transcrites a les guies de disseny.

Alguns d'aquests avanços es centren sobre la comprensió dels processos cognitius involucrats en la tasca de conducció; en la resposta dels conductors i en una millor estimació de la sinistralitat. Connectat amb tot això està el concepte de consistència. S'entén com a consistència del disseny geomètric al grau d'adequació entre les expectatives dels conductors i el comportament viari. Així doncs, una carretera inconsistent produeix sorpreses als conductors, derivant potencialment en una major sinistralitat.

En aquesta tesi es desenvolupa un model de consistència global basat en l'anàlisi de la velocitat d'operació. S'han tractat més de 150 seccions homogènies de carreteres convencional de la Comunitat Valenciana, extraient diversos paràmetres operacionals i determinant quals presenten una major relació amb la sinistralitat.

Per a possibilitar l'estudi, s'han creat diverses ferramentes auxiliars, algunes de les quals constitueixen igualment una important innovació. Dos exemples són un nou mètode analític-heurístic de restitució geomètrica en planta basat en l'azimut, així com una nova metodologia de tramificació de carreteres convencionals o unes expressions per a determinar de forma més precisa la velocitat de projecte idònia per a un segment homogeni.

El model de consistència obtingut pot emprar-se com a base per a una millor estimació de la sinistralitat, mitjançant safety performance functions. Amb l'objectiu d'integrar tots aquests avanços, es proposa una nova metodologia de disseny de carreters que, complementant les actuals guies de disseny, permet considerar el caràcter continu de la seguretat viària en el procés de disseny.

Abstract

Road safety is one of the most important problems in our society. It causes hundreds of fatalities every year worldwide.

A road accident may be caused by several concurrent factors. The most common are human and infrastructure. Their interaction is important too, which has been studied in-depth for years. Therefore, there is a better knowledge about the driving task. In several cases, these advances are still not included in road guidelines.

Some of these advances are centered on explaining the underlying cognitive processes of the driving task. Some others are related to the analysis of drivers' response or a better estimation of road crashes. The concept of design consistency is related to all of them. Road design consistency is the way how road alignment fits drivers' expectancies. Hence, drivers are surprised at inconsistent roads, presenting a higher crash risk potential.

This PhD presents a new, operating speed-based global consistency model. It is based on the analysis of more than 150 two-lane rural homogeneous road segments of the Valencian Region (Spain). The final consistency parameter was selected as the combination of operational parameters that best estimated the number of crashes.

Several innovative auxiliary tools were developed for this process. One example is a new tool for recreating the horizontal alignment of two-lane rural roads by means of an analytic-heuristic process. A new procedure for determining road homogeneous segments was also developed, as well as some expressions to accurately determine the most adequate design speed.

The consistency model can be integrated into safety performance functions in order to estimate the amount of road crashes. Finally, all innovations are combined into a new road design methodology. This methodology aims to complement the existing guidelines, providing to road safety a continuum approach and giving the engineers tools to estimate how safe are their road designs.

Table of Contents

List of Figures

List of Tables

1. Background

The proposed research is presented as the Thesis Dissertation of Mr. Francisco Javier Camacho Torregrosa, to get the rank of Philosophy Doctor. The author is Civil Engineer, by the Civil Engineering School of Universitat Politècnica de València (Spain). This research has been supervised by Professor Alfredo García García.

The title of the document is 'Development and Calibration of a Global Geometric Design Consistency Model for Two-Lane Rural Highways, based on the Use of Continuous Operating Speed Profiles'. This covers the main objective of the research and provides a major contribution compared to existing literature about several topics, including alignment recreation, road segmentation, accident estimation and road geometric consistency.

The author belongs to the Highway Engineering Research Group (HERG), of the aforementioned university. This group is directed by Professor Alfredo García García.

2. Introduction

Road safety is one of the most serious problems in our society, causing thousands of victims every year. Approximately 1.2 million people die and between 20 and 50 million are injured worldwide every year. Road fatalities will become the third cause of death by the year 2020, if the current trends remain unchanged.

Road safety is a difficult topic for research. The existence of several concurrent factors is very well known, but their contribution to road crashes is hard to analyze. Road safety research implies examining all the concurrent factors.

The human factor is present in nearly 90% of road accidents. However, these accidents tend to concentrate on certain locations, i.e., they are not randomly distributed. Research has shown that nearly 30% of crashes are due to infrastructure.

Guidelines tend to establish some thresholds for several design parameters. However, the effect of these parameters on drivers remains unknown in most cases. Human and infrastructure factors have normally been studied separately, while it is known that they present a strong interaction.

Recently, there has been an interest on the analysis of that interaction, due to the greater knowledge of the human behavior. The cognitive processes underlying the perception, processing and action of the drivers as a response of the infrastructure are therefore necessary.

The concept of geometric design consistency arises from that. We can define it as how the road layout and drivers' expectancies fit. Therefore, a consistent road is easily readable by drivers, not producing surprises. On the contrary, a non-consistent road tends to surprise drivers and hence hazardous situations are more frequent.

Expectancies can be classified as follows:

- A priori. Acquired by the drivers during all their driving life.
- Ad hoc. Acquired for a particular road segment while driving through it.

The analysis of road design consistency is a good way to reduce road crashes. There are several methods to evaluate it. The most common ones are those based on operating speed. Sudden operating speed changes, or disperse operating speed profiles are normally related to a higher crash risk.

Operating speed can be understood as the speed developed by drivers while they are only experiencing geometric constraints. It is normally established as the 85^{th} percentile of the observed speed under free-flow conditions. Operating speed profiles can also be depicted by means of operating speed models. Those models recreate the observed operating speed profile by means of geometric parameters, such as the length on tangents, radii on curves, etc. Operating speed is easily calculated. This is why the consistency methods based on it are very well known.

Geometric design consistency also has a strong relationship to road crashes. Therefore, most consistency criteria are established according to their safety effect. Crash modeling is a difficult task, since crashes are random, discrete and rare. This makes it impossible to use traditional statistical techniques. On the contrary, we need to use count models, combined with additional techniques in order to address specific problems, such as the large amount of zeros (just in case). Normally, the Negative Binomial distribution is applied.

This thesis dissertation presents a new global design consistency model, based on continuous operating speed profiles. The concept "global" means that this parameter does not focus on a particular curve, but in a global homogeneous segment. The application of this parameter to a global segment will allow us to estimate the number of accidents to compare different alternatives in the planning process.

The proposed consistency model is based on the operating speed evaluation. Therefore, we need some operating speed models and a computer application that applies them to a set of road segments. The operating speed models were previously developed by the Highway Engineering Research Group (HERG). Data consisted of more than 16,000 vehicles-kilometer, collected by using small GPS devices. They were placed on vehicles of actual drivers from the Valencian region of Spain. Therefore, continuous operating speed profiles were obtained. A computer application was also developed for filtering and processing all data.

Those operating speed models were based on geometric parameters. Therefore, a methodology for determining the horizontal alignment from a set of road sections was needed. This document proposes a new methodology for recreating the horizontal alignment from a set of points that represent a road centerline. Most current methodologies perform this task by examining curvature profiles. The proposed methodology uses the heading direction instead. This addresses several limitations to most of the existing methodologies. As a result, accurate radii, spiral

parameters and lengths can be obtained. Moreover, no fake geometric elements are introduced, as well as existing elements are not excluded.

The consistency model will be related to some operating speed indicators. This process will be carried out by comparing different sets of operating parameters to the number of road accidents. A safety performance function will be developed, considering exposure (AADT and length), as well as the consistency parameter. A negative binomial distribution will be assumed.

Finally, a new geometric design process is proposed. This process aims to combine all previous contributions, thus helping engineers to design safer two-lane rural roads. It is particularized for existing roads, new roads and for the planning stage.

3. State of the Art

3.1. Road Safety

Road safety has become a very important problem in our society. Over 1.2 million people die every year due to traffic in the entire world, as well as between 20 and 50 million people are injured. Considering the constant evolution of medical practices, as well as the higher live expectancy, by the year 2020 road fatalities will become the third cause of decease worldwide (it was the tenth cause by the year 2010).

Considering data from 2009, in the European Union every year 1,200,000 accidents with victims take place. Those accidents cause over 35,000 fatalities and 1,500,000 injuries. Besides the human live cost, economic consequences are also very important. Considering both direct and indirect costs, around 130 billion euros are lost in a year, representing about 2% of the Gross National Product of the EU.

The development level of the countries is also important. Developed countries apply modern countermeasures that keep low accident rates. On the other hand, underdeveloped countries present very low mobility levels, so the number of road accidents is also very low. Conversely, road accident rates are higher in developing countries.

Kopits and Cropper (2005) observed an inverse U-shaped relationship between the capita GDP and road fatality. Thus, road fatality firstly increases as the economy of a country does, and therefore decreases when the country becomes developed. The initial growth may be due to the rapid mobility increase of the country, not in accordance to the road safety knowledge development. This is typical for developing countries. Developed countries have better vehicles, infrastructure, knowledge and higher mobility, so the road safety rate decreases again. This problem reveals as very important if we consider that the number of developing countries is about to increase during the incoming years.

An accident is defined as an unforeseeable event that alters normal behavior of things and causes some damage. Thus, a road accident can be defined as an accident in which a moving vehicle is implied and takes place in the public road network.

Accidents are not completely random. Thus, it is necessary to know and understand their causes, circumstances and consequences in order to be able to prevent them or, at least, reduce their severity.

First of all, we are going to introduce some basic concepts related to road safety. Accidents can be classified considering several factors, but the most common are severity and typology.

According to the damage caused to the people implied in a road accident, victims can be classified as:

- Fatality. Person who dies instantly or within 30 days after the road accident takes place.
- Injury victim. Person who has been injured as a result of the road accident, but not resulting in a fatality. We distinguish two types:
    - Severe injury. Injury victim who needs to be hospitalized more than 24 h due to the road accident.
    - Slight injury. Victim who needs to be hospitalized less than 24 h.

The severity of a road accident is determined as the highest severity level of the people implied. Therefore, road accidents can be classified as:

- Accident with victims. Accident with at least one victim.
- Fatal accident. Accident with at least one fatality.
- Property Damage Only Accident. Accident with no victims.

The severity of an accident is influenced by several factors, such as the type or road users, the collision angle and the speed of the vehicles (Laureshyn et al., 2010).

Road accidents can also be classified according to their typology:

- Run off the road accident. The vehicle abandons the platform. The severity of the accident is highly dependent on the roadside configuration. This is normally a single-vehicle accident.
- Rear end accident. At least two vehicles are involved, depending this number on the traffic conditions. The vehicles drive in the same direction and collide because of the speed dispersion. This accident is very frequent in low-light conditions, traffic congestion or sudden speed reduction of the preceding vehicle.

- Head-on accident. Two vehicles driving in opposite directions collide. The cause of the accident might be diverse. The severity of this accident is normally maximum, due to the relative speed difference.
- Lateral accident. This accident normally takes place at intersections or curves. Two vehicles who drive in different (not opposite) directions collide. Its severity will be determined by the energy dissipated in the collision, as well as the vehicles type and location of the impact.

A collision implies a sudden kinetic energy release, causing a deformation of the vehicle(s). Kinetic energy (E_k) is determined, depending on the mass (m) of the object and its speed (v), according to Equation 1.

$$E_k = \frac{1}{2} \cdot m \cdot v^2 \quad (1)$$

Rear-end collisions usually present low severity, since the relative speed differential is low. On the other hand, head on accidents present the highest relative speed difference, and therefore the highest severity.

3.1.1. Concurrent factors

After introducing the road safety problem, as well as some generalities, this section focuses on why accidents take place. A very important effort has been done in this topic during the last years towards two directions: determining which factors are related to the likelihood of an accident to happen, and the underlying processes that take place when an accident happens. The first ones are known as concurrent factors. The second part is explained with road safety theories.

Concurrent factors are all aspects involved in the generation of road accidents. Most researchers distinguish three main concurrent factors and other two of less importance:

- Infrastructure factor. This factor is related to road design. Road infrastructure must be designed according to drivers' expectations. The zones that not meet the aforementioned condition might present higher crash rates. Some researchers estimate that this factor is behind over 30% of road accidents, on its own or combined with human factor. Hence the importance of its consideration and correct treatment (Treat et al., 1979).

- Human factor. This is the most important concurrent factor, since it is estimated to be behind over 90% of all road accidents. This factor focuses on the human being, analyzing both its physical and psychical aspects while performing the driving task. Its interaction with the infrastructure factor reveals as very important too.
- Vehicle factor. It focuses on how the vehicle can be involved in the generation of an accident. It gathers all possible issues with vehicle malfunctions, low maintenance issues, etc. As the technology develops, this factor reveals as less important.
- Traffic factor. This is a less important factor than the previous three. Traffic conditions do also have an effect on road crashes. One example is how the accident type changes depending on the different traffic states (congested or free-flow conditions).
- Environmental factor. This is not an important concurrent factor too. It includes all external factors that may affect the likelihood of having an accident. One example is weather conditions.

Figure 1 shows the three most important concurrent factors, as well as their relative importance to road accident likelihood. Depending on the factors involved in a road accident, very different solutions may arise. For instance, some problems related to human factor like drunk driving can be treated with psychological actions. On the other hand, consistency-related issues should be addressed through a road redesign. Industrial engineering deals with the vehicle factor. In addition, in most cases a road accident can be explained through the combination of several concurrent factors. Hence the importance of multidisciplinary teams to understand road safety.

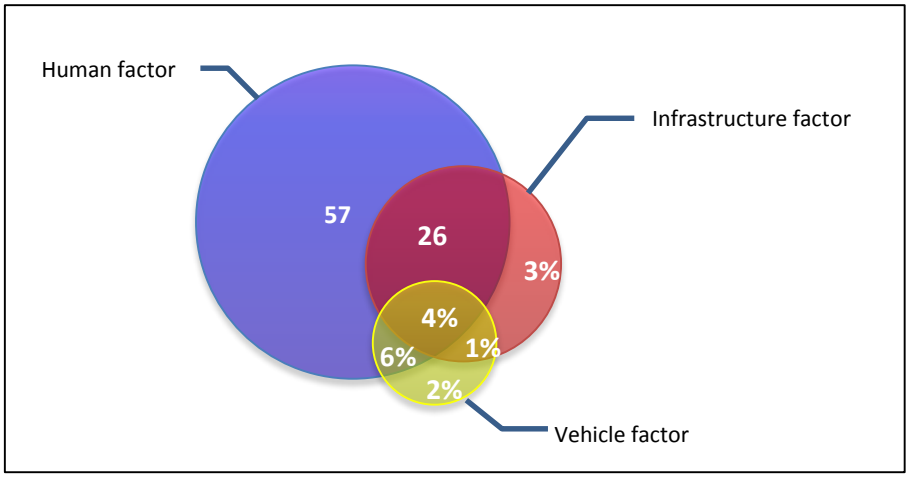

Figure 1. Road safety main concurrent factors.

These factors are also related to the accident severity. All of them can also act before, during or after the accident. The Haddon's Matrix (Table 1) classifies them according to the temporal irruption.

<table>
<tr><th></th><th>Before</th><th>During</th><th>After</th></tr>
<tr><td rowspan="7">Human</td><td>Physical conditions (fatigue, disorders, medication, alcohol…)</td><td rowspan="2">Physical conditions (reflexes)</td><td>Physical conditions (resistance to the impact).</td></tr>
<tr><td>Physiological conditions (stress, distractions, attitude…)</td><td rowspan="3">Own errors (bad perception of the road, bad assessment of the road performance, inappropriate negotiation of the curve…)</td><td rowspan="2">Physiological conditions (emotional shock)</td></tr>
<tr><td>Demographic profile (age, gender, profession, education…)</td><td rowspan="2">Experience and expertise (safety, conditions of the zone of the accident, emergency response, etc.)</td></tr>
<tr><td>Driving expertise and abilities (driving experience, knowledge of the vehicle and the road…)</td><td rowspan="4">Actions (post-accident maneuvers)</td></tr>
<tr><td>Previous maneuvers to the collision</td><td rowspan="3">Action (speed, braking, lateral position…)</td></tr>
<tr><td>Self-protection (seatbelt, helmet…)</td></tr>
<tr><td rowspan="3">Vehicle</td><td>Physical factors (type of vehicle, color, power…)</td><td rowspan="4">Passive safety activation (deformation resistance, airbag…)</td></tr>
<tr><td>Mechanical conditions (brake system, shock absorbers, lights…)</td><td rowspan="3">Path of the vehicle after the collision</td></tr>
<tr><td>General state of the vehicle</td></tr>
<tr><td>State previous to the collision (load, number of passengers, etc.)</td></tr>
<tr><td rowspan="4">Infrastructure and environment</td><td>Road geometry (horizontal and vertical alignment, cross-section).</td><td>Recovering area (shoulders, emergency lane, free-zones…)</td><td rowspan="2">Accident call</td></tr>
<tr><td>Pavement characteristics (skid resistance, roughness, etc.)</td><td rowspan="2">Environment conditions</td></tr>
<tr><td>Environment (urban or rural, signals, traffic flow, main users…)</td><td rowspan="2">Critical zones (transition zones, workzones, unusual environment, obstacles, etc.).</td><td rowspan="2">Pavement conditions</td></tr>
<tr><td>Road facilities (road signs, etc.).</td></tr>
</table>

Table 1. Haddon's Matrix. All concurrent factors are present, including when they act.

It's important to highlight that the number of road safety related concurrent factors is pretty big, hence the necessity to group them all into the abovementioned types. There exist other grouping possibilities, such as the one proposed by Wang, Quddus and Ison (2012).

3.1.1.1. Infrastructure factor

Infrastructure plays a major role in accident causation. In fact, this is why accidents tend to concentrate in certain locations, instead of dispersing randomly through the road network.

Most research focus on the horizontal alignment. Complex alignments are normally related to higher accident rates. Shankar, Mannering and Barfield (1996) found that the increased number of horizontal curves per kilometer increased the severity of the accidents. Milton and Mannering (1998) found that short road sections were less likely to experience accidents than longer sections.

Some other researchers found that a higher curvature is linked to a lower accident rate, which is counter-intuitive (Wang, Quddus and Ison, 2012). However, this might be because of the way the curvature was analyzed in that research. The difficulty at analyzing the paper of the road infrastructure on crashes is that it is normally linked to the human factor. This is why sometimes road users drive more carefully at more complex alignments.

Some of the most important aspects related to the infrastructure factor are:

- Road type and design-related parameters (design speed, etc.).
- Horizontal alignment.
- Vertical alignment.
- Combined horizontal and vertical alignment, paying special attention to sight distance and road perception.
- Cross-sectional parameters. Particularly important are the lane and shoulder widths, since they are highly connected to operating speed.
- Road margins.
- Road marking and signs.
- Pavement conditions.

3.1.1.2. Human factor

Human factor considers the issues related to driver reactions and behavior. This factor is highly related to human psychology, perception, reaction and learning processes. This is a complex area, so there exist several theories that try to explain them. These theories allow researchers to detect which level is more likely to be the cause of a road accident, and hence actuate on it.

Each driver presents different characteristics, abilities and limitations. They are also influenced by their particular circumstances, which may be related to the environment or not. Environment conditions affect all drivers at the same level, whereas personal circumstances obviously not. Some examples of environment-related circumstances are weather conditions, urban planning, orography, light conditions and more. Some driver-related circumstances are stress level, fatigue or alcohol consumption.

Hence, all those circumstances result in a high variability of the responses for the same road layout. This is the reason why the human-road interaction has to be deeply analyzed. This would allow engineers to design safer roads for everybody, foreseeing drivers' reactions.

3.1.1.3. Vehicle factor

This factor becomes less and less important in developed countries, due to the technological development of vehicles. In fact, vehicle related accidents are mostly due to a poor maintenance, punctures, blowouts, etc.

Nevertheless, it remains as a very important contributing factor in developing countries, since passive and active safety measures are not embedded in their vehicles.

3.1.1.4. Traffic factor

Accidents occur when traffic moves. These traffic characteristics affect road safety through both engineering and behavioral effects. We can distinguish four traffic-related parameters: speed, traffic flow, density and congestion (Wang, Quddus and Ison, 2012).

It seems clear that the speed has an influence on road safety. A higher speed implies more kinetic energy, more distance travelled during the perception and reaction time, and a narrower vision field. The higher kinetic energy implies a higher severity

once the accident has occurred. However, it is not clear how the speed affects the probability of having an accident.

Elvik, Christensen and Amundsen (2004) analyzed the effect of speed on road crashes. They found that speed and the number of road crashes are connected. However, more data and better statistical models should be applied in order to give more evidence to the conclusions. Taylor, Baruya and Kennedy (2002) employed 174 road segments in a cross-sectional analysis, confirming the results found by Elvik, Christensen and Amundsen. However, their model presented some flaws.

On the contrary, Baruya (1998) found an inverse relation between the average speed and accident frequency. The same conclusion was reached by Taylor, Lynam and Baruya (2000), who used data from the Netherlands, Sweden and England. Both of them attributed this phenomenon to inadequate design standards on the roads with a higher frequency.

Finally, Kockelman and Ma (2007) examined the freeway speed and speed variation preceding accidents in California, finding no evidence between the speed conditions and crash frequency.

The extreme variability between operating speed and crash rates can be explained through the driver-road interaction. From a physical point of view, a higher speed is linked to a higher accident risk: there is less time to react, the vision field is reduced, and maneuvers take more distance to be completed. However, the human factor compensates this, increasing the attention level and the workload demand. They also are more aware of the surrounding traffic and leave more distance from the preceding vehicle. The infrastructure effect is not negligible: the roads with higher design standards are normally those which present higher speeds.

Although it is not clear whether the average operating speed plays an important role on the generation of road accidents, it seems clearer that the operating speed dispersion does. A higher operating speed dispersion implies more interactions between vehicles, increasing the probability of having a crash.

In the 60s, Solomon (1964), Cirillo (1968) and Munden (1967) analyzed the relationship between the operating speed dispersion and crash rates in two and four lane roads. The former two concluded that crash rates were lower when the operating speeds were 15-20 kph higher than the average operating speed. Munden found that the lowest crash rates took place when the operating speeds were closer to the average speed.

Garber and Gadiraju (1989) analyzed the effect of the speed dispersion on road safety. They considered 36 road segments. They concluded that:

- A higher speed dispersion is related to a higher crash rate in all road segments.
- The speed dispersion is minimum when the difference between the operating and design speeds ranges from 8 to 16 kph.
- For average speeds from 40 to 112.5 kph, the speed dispersion decreases as the speed increases.
- The difference between the design speed and the speed limit has an important effect on the speed dispersion.
- The crash rate does not necessarily increase when the average speed increases.

Traffic volume is also related to accidents, especially to accident type. As it will be later indicated, exposure plays a major role in accident estimation. Ceder and Livneh (1982) analyzed crash rates for different traffic conditions and found that single and multiple crash rates behaved in different ways according to the traffic conditions.

Lord, Manar and Vizioli (2005) calculated three different functional forms of the traffic-crash rates relationship. They found that the use of traffic volume as the only explanatory variable might not be adequate. Instead, using density and V/C ratio offered a richer description. Zhou and Sisiopiku (1997) noticed that hourly crash rates presented a 'U' shape, decreasing while the V/C ratio increased.

Himes, Donnell and Porter (2011) examined the influence of the hourly traffic volume on the mean speed and its dispersion. They examined 79 sites of 8 roads in Pennsylvania and Virginia, finding that the hourly traffic volume was strongly correlated to the speed dispersion. An increase of 100 vph is associated with a decrease in speed deviation by 1.2 mph. Therefore, a higher traffic volume was found to produce a more uniform flow.

The effect of traffic density on road safety still remains almost unknown. The reason can be the difficulty of accurately estimating traffic density. Ivan, Wang and Bernardo (2000) noticed that single-vehicle accident rate increased as the ratio volume/capacity did, following a negative binomial distribution. The accident rate was the highest at a low volume/capacity ratio.

The proportion of heavy traffic also affects crash rates. One of the underlying reasons is the higher speed dispersion, as well as the more amount of passing maneuvers, being a higher conflict exposure to head-on crashes.

3.1.1.5. Environment factor

The environment factor covers some other aspects not considered previously, such as weather conditions, urban planning development, orography, etc. The affection is mostly due to an impairment by drivers (for instance, sun glares or low visibility).

Shankar, Mannering and Barfield (1996) found that rain may increase the possibility of injury rear-end crashes, if compared with PDO crashes. M. Abdel-Aty (2003) found that darker periods often lead to a higher accident severity.

3.1.2. Road Safety theories

Road safety theories try to determine why an accident has occurred. The better knowledge about the underlying phenomena would let researchers and practitioners to develop more suitable methods and policies for improving safety.

Figure 2 represents the most basic approach to understand how a road safety measure influences the final outcome of road accidents. A certain road safety measure affects several risk factors, producing a change in the final outcome, in terms of number of accidents or their severity.

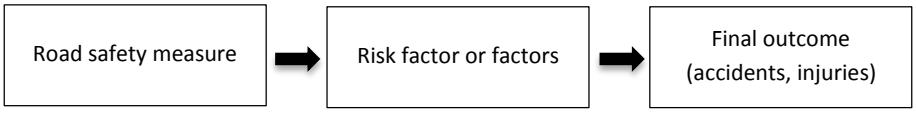

Figure 2. Influence of a road safety measure (Adapted from Elvik (2004)).

This simple model presents three important problems:

- The number of risk factors that should be considered is very large. Some of them remain even unknown or unmeasurable.
- Many of the road safety evaluation studies do not clearly identify and/or measure the risk factors influenced by the countermeasure.
- Some road safety measures present user behavioral adaptation, i.e., users get adapted to the countermeasure by changing their attitudes and behavior. Thus, the safety measure could indeed be counter-productive.

Evans (1991) suggested a two casual chain model that includes this phenomenon (Figure 3).

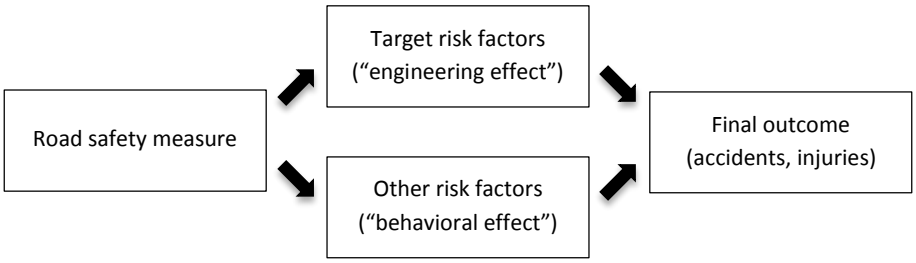

Figure 3. Evans' casual chain model.

This duality is the reason why road safety lacks of a solid theoretical ground, on the contrary to several other mature disciplines (Wang, Quddus and Ison, 2012). Instead, there exist some groups of theories that try to explain the user-road-crashes interaction. We can distinguish two ways of approaching to road safety:

- By means of the infrastructure factor. Several objective relationships can be established between some geometric or environmental parameters and road crashes. They will be discussed in section 3.1.3.
- Analysis of the human factor. This approach cannot estimate the number of road accidents. Instead, a better knowledge of the process is achieved.

There are some other theories that try to combine the best part of both approaches. Some of them try to explain driver's attitudes and behavioral change after a certain countermeasure is applied. Some others establish a general framework for driver behavioral adaptation due to infrastructure changes.

Elvik (2004) proposed a conceptual framework based on Evans' model (Figure 3). He proposed the following risk factors to be considered, as well as the behavioral adaptation:

- Kinetic energy. This is not a risk factor *per se*, since it does not cause harm as long as it is controlled. If a collision takes place, this energy is released, affecting the severity.
- Friction. This factor is related to the control and stability of the vehicle.
- Visibility. The more sight distance, the more time drivers have to process the information, hence reducing the likelihood of surprises.

- Compatibility. It refers to the difference that exists between different types of vehicles in terms of speed, mass, performance, etc.
- Complexity. It refers to the amount of information that a user has to process per unit of time.
- Predictability. It denotes the reliability at which the occurrence of a risk factor can be predicted in a given situation.
- Individual rationality. Individual users normally try to behave looking for their maximum benefit, i.e., satisfying their preferences.
- Individual vulnerability. When an accident occurs, some individuals are more exposed than others.
- System forgiveness. Some elements of the road should be designed in order to prevent accidents or reduce their severity. Some examples are clear margins, rumble strips, road lighting, and others.

In order to prevent counterproductive responses, Amundsen and Bjørnskau (2003) suggested to analyze the following factors, which already include the behavioral adaptation effect:

- How easily a certain countermeasure is noticed. Drivers are continuously scanning the road. When they notice a safety countermeasure, behavioral adaptation might occur. Thus, the best solution is to act without leaving them to know (obviously, this is not always possible).
- Historical antecedent of behavioral adaptation to basic risk factors. There is a higher probability of behavioral adaptation if it already took place before.
- Size of the engineering effect on generic risk factors. Large changes are more likely to be noticed by users.
- Whether or not a measure primarily reduces injury severity. Measures that reduce injury severity are less likely to lead to behavioral adaptation than measures that mostly act on reducing the likelihood of an accident.
- The likely size of the material damage incurred in an accident. Road users prefer the material damage in an accident to be as small as possible.
- Whether or not additional utility can be gained. Users try to maximize utility of the trip. For some road safety measures, it is difficult to see how road users could gain any benefit by changing their behavior.

Considering all these parameters, Elvik proposed a revised causal chain model that incorporated the relationships between road safety measures and driver behavior,

through behavioral adaptation (Figure 4). The result is termed as behavioral safety margin, indicating how road users assess their safety margin when travelling.

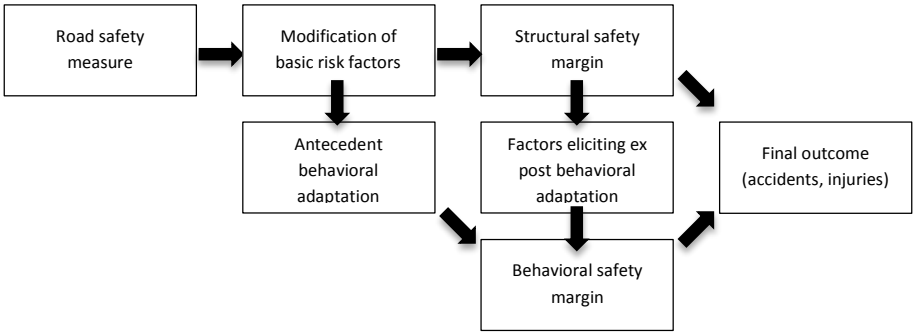

Figure 4. Elvik's revised casual chain model.

According to Elvik (2006), accidents may be explained according to a few general statistical regularities that determine the relationship between risk factors and accident occurrence. These regularities are called 'laws of accident causation'. He proposed the following laws:

- Universal law of learning. The ability to foresee undesirable traffic situations increases uniformly as the amount of travel (or conflicts) increases. This law also implies that the accident rate per unit of exposure decreases as the exposure increases.
- The law of rare events. The rarer a certain risk factor is encountered, the larger its effect results on accident rate. Moreover, its rareness makes this event more difficult to be learnt.
- The law of complexity. The more information rate the road user must attend to, the higher the probability of committing an error.
- The law of cognitive capacity. As the cognitive capacity of a road user approaches to their limits, the higher the probability of having an accident.

3.1.3. Road Safety measurement and estimation

3.1.3.1. Crash rates

When one deals with road safety, it reveals as necessary to compare the safety level of different roadway features. It is well known that a poorly road design induces

more accidents. However, a reliable tool to compare between the different road elements should be introduced.

The comparison of the number of crashes should not be used as a comparison tool between roadway features. The reason is that the number of accidents is also influenced by the exposure (i.e., traffic volume and length). The higher the exposure, the higher risk.

We can generically define crash rate as the ratio between the number of crashes and the exposure. There are different types of crash rates, depending on which accidents are considered. For instance, we can focus only on rear-end or fatal crashes.

For spot road elements, such as intersections, exposure is usually considered as the traffic volume that interacts with that element. For linear roadway elements, their length must also be considered. Equations 2 and 3 indicate how the exposure (*TT*) is measured in both cases. *L* (km) represents the length, while *AADT* (vpd) is the Annual Average Daily Traffic. In both cases the exposure is calculated for an entire year, but it can be easily adapted to a different period of time.

$$TT = 365 \cdot AADT \quad (2)$$

$$TT = 365 \cdot AADT \cdot L \quad (3)$$

The likelihood of having a road accident is very low. Therefore, crash rates are normally expressed in terms of 10^6 veh-km or similar.

Some researchers, such as Elvik (2010) have introduced the concept of 'conflict exposure', more linked to the learning process rather than on crash estimation. Thus, we will not cover that kind of exposure.

The most well-known crash rates are:

- Accident rate. Number of accidents per 10^6 vh-km.
- Crash rate. Number of accidents with victims per 10^6 vh-km.
- Fatality rate. Number of fatalities per 10^6 vh-km.
- Severity rate. Number of fatalities per accident with victims.
- Risk Index (EuroRAP). Number of severe injury or fatal accidents per 10^9 vh-km.
- Equivalent Property Damage Only Index (EPDO Index). Equivalent number of PDO crashes, applying the following conversion coefficients:

- PDO crash: 1.
- Slight injury accident: 3.5.
- Serious injury or fatal accident: 9.5.

The consideration of PDO crashes in the crash rates is controversial, because of underreporting. The number of accidents that actually take place on a certain roadway entity is higher than those reported. Underreporting may be due to several reasons, including low-severity accidents, lack of police enforcement, etc. The problem arises since underreporting is not randomly distributed. It depends on police enforcement, type of accident, location, type of vehicles, etc. This makes the analysis considering PDO crashes susceptible of being biased. It is also dependent on the severity of the road accident. According to Elvik and Borger Mysen (1999), the underreporting rate increases as the severity of the accident decreases. A 100% of fatal road accidents are assumed to be reported at developed countries. Hauer (2006) demonstrated that accidents involving trucks always present low underreporting rates, regardless of the severity of the accident.

Thus, PDO crashes should only be considered whether the total number of accidents is not enough to perform a valid statistical analysis. Such the case, conclusions should be handled carefully.

Road traffic safety analysis has been normally based on crash statistics because of data availability. However, it presents some problems because of their rareness. Hydén (1987) suggested that a pyramid relationship between frequency and severity of accidents existed. The higher the severity (vertical position of the pyramid), the lower the frequency (volume of the pyramid) (Figure 5).

Svensson (1998) introduced the concept of severity hierarchy, in which the traffic events pyramid concept is revised by adding the severity level to the conflicts. If the severity hierarchy of a particular site is represented, the most accurate shape will be a diamond (Figure 6). The least severe events in traffic are when only one vehicle, with no traffic and no other concurrent factors are present. Most traffic encounters are of medium severity: the road users have to operate their vehicles, but they see no problem.

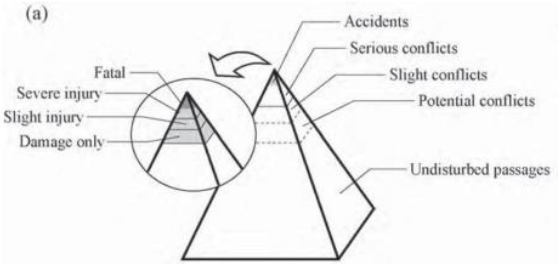

Figure 5. Traffic events pyramid (adapted from Hydén (1987)).

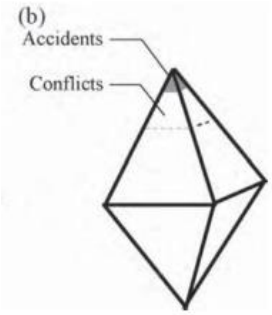

Figure 6. Dyamond representation of traffic events (adapted from Svensson (1998)).

Crash rates can be used for comparing the safety level of different roadway entities, or the evolution of a certain entity along time. However, they also present some drawbacks. They are calculated in terms of the number of accident and the exposure. This is perfectly valid as long as the exposure does not affect the generation of accidents. However, as it was previously stated, the traffic – at least – affects the accident-generation process. Hence, crash rates are biased by their exposure and should be handle with care.

Figure 7 shows one example. A possible relationship between the number of accidents and the exposure (in terms of AADT) is shown. Road 1 is safer than road 2, since it presents less accidents than Road 2 for every exposure value (its line is always beneath the Road 2's line). However, if we determine the crash rate for both roads, we find that Road 2 appears to be safer than Road 1, since it presents a lower crash rate. This is a typical situation for linear elements such as road segments (see Section

3.1.3.3.1). The more traffic flow is good from a safety perspective, since crash rates decrease.

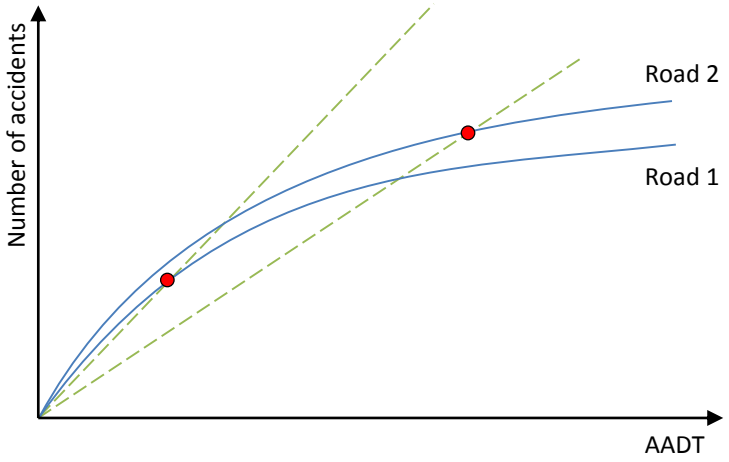

Figure 7. Crash rates are not valid here for comparing two road elements. Adapted from PIARC (2003).

As a recommendation, crash rates should only be used when the exposure level is similar for all the elements under analysis. If this is not the case, they could be used in combination with the corresponding safety performance function.

3.1.3.2. Statistical treatment of road safety

Foreseeing the future number of accidents in a certain road element is an important tool, since it allows engineers to compare different solutions in order to select the best one from the safety perspective.

This kind of analysis is valid not only for comparing different roadway entities, but also for estimating the number of accidents, as well as the factors involved. However, road crashes are not easy to model, since they are:

- Rare. They present a very low frequency, eventually including a high amount of zeros. This property, as well as their discrete character makes it necessary to use asymmetric, count distributions.
- Random. They do not present a clear behavior (i.e., we may have 0 accidents in one intersection one year and 7 accidents the following one).

This is an important issue, since it prevents us from using data collected during short periods of time.

- Discrete. They can only be integer, positive or null values. Hence, count distributions will be used.

Observed accidents is barely the count of the number of accidents at a certain location within a period of time. This is an unprocessed measurement. The observed number of accidents will approach the actual safety performance only if a high exposure has been observed (long-term measurement). This phenomenon is known as regression to the mean (RTM) (Figure 8).

Elvik and Vaa (2004) defined Regression to the Mean (RTM) as the tendency for an abnormally high number of accidents to return to values closer to the long-term mean; conversely abnormally low numbers of accidents tend to be succeeded by higher numbers. RTM occurs as a result of random fluctuation in the recorded number of accidents around the long-term expected number of accidents.

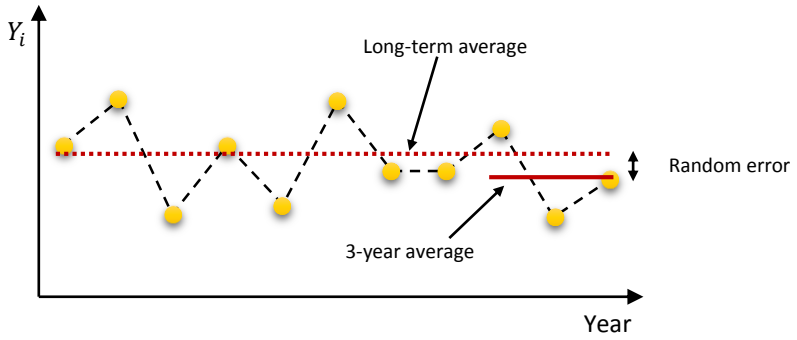

Figure 8. Regression to the Mean.

De Pauw et al. (2013) analyzed the impact of the Regression to the Mean effect, finding that its effect is higher for severe crashes than for slight injury crashes (37% vs. 9%). This was expected, since the frequency of crashes decreases as the severity increases. The Empirical Bayes Method was found to be a good tool for addressing this issue. They also highlighted the importance of correcting the RTM effect for evaluation studies when locations were selected based on their crash history.

3.1.3.2.1. Data and methodological issues

As discussed above, crash-frequency data are non-negative integers, which suggest the application of count-data regression methods. Accidents seem to behave

according to a Poisson process. However, there exist some issues that might invalidate this approach. According to Lord and Mannering (2010), the most common are:

- Overdispersion. A Poisson distribution is heteroskedastic, being the variance equal to the mean. In overdispersed data, the variance exceeds the mean. This is very frequent in crash counts.
- Underdispersion. This is not typical in crash counts, but might be the case for small databases with mall sample means.
- Time-varying explanatory variables. As explained above, the randomness of the accidents makes it necessary to consider large periods of time in the analysis. This way of proceeding alleviates the problems related to the crash randomness, but it does not take into consideration the possible variation of the explanatory variables. One example is the variation of traffic volume. We have previously explained that the traffic volume affects the road safety performance. However, we will normally consider the average traffic volume per day in the analysis, which is a single value. It is well known that traffic volume varies depending on the moment of the day and year, among other factors. The accidents that took place within a peak hour in the morning might present more than twice the AADT. The effect is the opposite for low-traffic situations. As a result, some information is lost in the final model, being added to the unexplained variability.
- Temporal and spatial correlation. When considering different elements coming from a larger one (e.g., taking different road segments from the same roadway entity), some unobserved effects are shared. These effects cannot be measured, but they exist. Therefore, in the final model some elements share some information, resulting in a model that lacks of precision. The same problem may arise when dividing a single road entity into several periods of time in order to avoid time-varying explanatory variables.
- Low sample-mean and small sample size. One of the most important problems in road safety is the small number of observations. In addition, there is normally a preponderance of zeros. Those problems combined may cause estimation problems in traditional count-frequency techniques. The result is normally a skewed distribution towards zero, producing incorrect estimations.
- Injury severity and crash type correlation. Crashes can be classified according to their severity level or their type. The most common approach

is to consider all crash types in the analysis. However, some researchers have tried to calibrate models for a single type of crash or a single severity group. This should not be done, since there appear specific statistical problems because the correlation among the different groups.

- Underreporting. This problem was previously introduced. This is why normally only accidents with victims are considered in the analyses.
- Omitted-variables bias. Crash estimation models are based on a set of independent parameters. Those models should consider all important parameters. On the contrary, their estimations might not be accurate.
- Endogenous variables. The explanatory variables should always be exogenous, i.e., they do not depend on the crash history of the roadway element. However, sometimes we are interested on adding endogenous parameters, in which their value is a consequence of the number of crashes. One example is the warning-signs frequency, which depends on the crash history of the road. In such the case, the model will indicate that warning signs negatively affect the safety level, since they are placed at the top hazardous locations. Not considering the endogeneity would lead to conclusions completely far from reality.
- Functional form. The functional form of the model establishes how explanatory variables affect the number of crashes. Most count-data models assume that explanatory variables influence the dependent variables in some linear manner. Some other researchers support that crash frequency models should be better fitted with complex non-linear relationships.
- Fixed parameters. Traditional models do not allow parameter estimates to vary across observations. Thus, the effect of the explanatory variable on the frequency of crashes is the same for all observations. However, due to the unobserved heterogeneity, one might expect the estimated parameters of some explanatory variables to differ across roadway segments. Some estimation models let those parameters to vary across observations, but their functional form is quite complex.

3.1.3.2.2. Modeling methods for analyzing crash-frequency data

A wide variety of methods have been developed to model the number of crashes depending on some parameters. Crash-frequency data are non-negative integers, so a normal distribution is not adequate. Poisson regression is considered as a good way to estimate road crashes. The Poisson process establishes that the probability of a

road entity i (i.e. intersection or road section) of having y_i accidents in a period of time is given by Equation 4.

$$P(y_i) = \frac{e^{-\lambda_i} \cdot \lambda_i^{y_i}}{y_i!} \quad (4)$$

In this expression, λ_i is the expected number of crashes in the same period of time for the roadway entity i. This is an asymmetric, heteroskedastic distribution, in which the mean is equal to the variance.

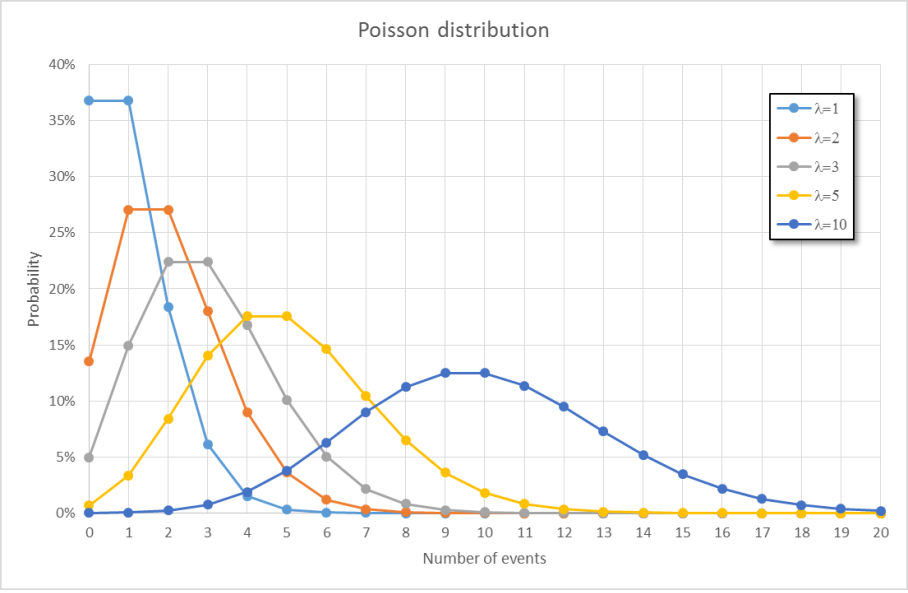

Figure 9. Poisson distribution for different λ values.

Poisson regression models estimate the Poisson parameter λ_i as a function of several explanatory variables, by means of the functional form shown in Equation 5. $\boldsymbol{X_i}$ is the vector that represents the explanatory variables, while $\boldsymbol{\beta}$ is the vector of the estimates.

$$\lambda_i = e^{\boldsymbol{\beta} \cdot \boldsymbol{X_i}} \quad (5)$$

This approach is valid when mean and variance are the same. However, accidents do not always behave that way. Overdispersion is one of the most important limitations of this model. The easiest way to overcome this limitation is the Negative Binomial (or Poisson-Gamma) regression.

The Negative Binomial distribution is shown in Equation 6. It is based on a Poisson functional form, but incorporating a gamma-distributed error term (e^{ε_i}) of mean 1 and variance α. This is known as the overdispersion parameter. The Poisson distribution is the particular case where $\alpha = 0$.

$$\lambda_i = e^{\boldsymbol{\beta} \cdot \boldsymbol{X_i} + \varepsilon_i} \tag{6}$$

The variance of the negative binomial distribution is calculated as shown in Equation 7. Therefore, the variance is higher than the mean value.

$$VAR[y_i] = E[y_i] \cdot \left[1 + \alpha \cdot E[y_i]\right] = E[y_i] + \alpha \cdot E[y_i]^2 \tag{7}$$

This is probably the most frequently used model for estimating road crashes because of its validity and simplicity. However, it also presents some limitations. The most important is that it cannot handle underdispersed data. It also has problems when considering low sample-mean values and small sample sizes.

Poisson-Lognormal distribution is an alternative to Poisson-Gamma. This approach has been recently proposed by several researchers. The difference is that the error term e^{ε_i} is lognormal- instead of gamma-distributed.

This approach offers more flexibility than the negative binomial distribution, but still suffers from some limitations. Model estimations are more complex and small sample sizes and low sample mean values are still a problem.

A more complex Poisson generalization is the Conway-Maxwell-Poisson distribution. The main advantage is that it can handle both underdispersed and overdispersed data. In addition, several common probability density functions are special cases of the Conway-Maxwell-Poisson (e.g. the geometric distribution, Bernoulli distribution and Poisson distribution). This approach lets the researchers to widely expand the types of crash-frequency data modeling problems.

This distribution produces more complex models. Hence, the negative binomial distribution is preferred when dealing with overdispersed data. Conversely, this is a very interesting approach for underdispersed data.

Despite of these advantages, this model can be negative influenced by low sample-mean and small sample bias. This is a recent approach to crash frequency modeling, so there are not many multivariate applications of the approach.

As mentioned above, one of the most important problems while modeling crash rates is the large amount of zeros. A possible solution are the zero-inflated-Poisson models. These models are based on the hypothesis that a "zero value" may be produced by two different processes (they are called "states"):

- Non-zero state. Locations where the estimated crashes are very low (zero), but they present the same characteristics as other locations (i.e., Poisson, Negative Binomial or Poisson-lognormal modelled).
- Zero state. Free-crash locations. Those locations are considered as very safe and hence they do not produce crashes.

The probability of a roadway entity of being in zero or non-zero state is determined by a binary logit or probit model (Equation 8).

$$\begin{cases} \Pr(y_i = 0) = p_i + (1 - p_i) \cdot e^{-\lambda_i} \\ \Pr(y_i = y) = \dfrac{(1 - p_i) \cdot e^{-\lambda_i} \cdot \lambda_i^y}{y!} \end{cases} \quad (8)$$

This kind of models have been very popular since its inception, due to their precision at characterizing data sets with large amount of zeros. On the other hand, this model has also received several criticisms due to its formulation. Roadway entities cannot present a zero probability of having crashes, due to the crash generation process itself.

The Poisson regression can also consider random effects, in order to account for temporal or spatial correlation. In this case, a vector that groups the different elements that might share unobserved effects is provided. As a result, the error term is distributed accounting for this variability.

There are some other models which are not based on the Poisson process. The first one is the Gamma model. This model can handle over- and under-dispersion. This is also a dual-state model, like ZIP models. Due to this limitation as well as its difficulty to be modeled, it has not been very popular.

The generalized estimating equation model has been applied to highway safety analysis to model crash data with repeated measurements. It allows researchers to overcome spatial and temporal correlation issues. Actually, this is not a regression model, but a method to estimate models with data characterized by serial

correlation. The selection of the correlation type can be critical when the database has omitted variables.

The generalized additive model has more flexibility than the traditional count-data models. They provide a more flexible functional form, involving smoothing functions for the explanatory variables of the model. This function represents a more flexible relationship in how explanatory variables are taken into account, not being limited to linear or logarithm relationships.

There are still limitations for this model, highlighting the complex modelling when including several parameters. They also use spline functions to smooth the relationships, which are more difficult to interpret than traditional count models. This approach is only recommended when dealing with endogeneity.

3.1.3.3. Tools to estimate and assess road safety

Some statistical issues with crash count data have been reported, as well as some modeling methodologies. Considering all of them, a better understanding of the crash generation process can be achieved.

There exist some specific tools for estimating or analyzing crashes. Some of them allow the designers to estimate the number of accidents depending on some factors. Some others are useful for determining whether a road countermeasure has been effective or not. All of them are mostly based on the previous concepts, but they have been adapted to the use mostly by road practitioners.

3.1.3.3.1. Safety Performance Functions

A Safety Performance Function is an expression that allows us to estimate the number of crashes in a certain roadway entity depending on some factors. The factors include some design and/or environmental features, as well as the exposure. The exposure may have an influence on the output or not. Those functions are normally calibrated considering a Negative Binomial distribution.

Their common functional form is shown in Equation 9 (intersections) and Equation 10 (road segments). *AADT* and length are normally given in vpd and km, respectively.

$$\lambda_i = E(y_i) = \beta_0 \cdot AADT_i^{\beta_1} \cdot e^{\sum_{j=2}^{k} \beta_j \cdot X_{ij}} \quad (9)$$

$$\lambda_i = E(y_i) = \beta_0 \cdot AADT_i^{\beta_1} \cdot L_i^{\beta_2} \cdot e^{\sum_{j=3}^{k} \beta_j \cdot X_{ij}} \quad (10)$$

X_{ij} represents the different parameters that are considered by the SPF, while β_{ij} are the corresponding estimates. The exposure is normally introduced in terms of elasticity. This is the functional form that produces the best adjustments, according to Oh et al. (2003).

The exposure is very important in those models. In fact, it explains most of the accident variability. However, the way to consider it has been very controversial. Some researchers support that the exposure does not affect the crash generation process, and so assuming $\beta_1 = \beta_2 = 1$. In recent years, most researchers assume that the *AADT* has a true effect on how accidents are generating, thus not enforcing $\beta_1 = 1$.

According to the *AADT* estimate, there are four possibilities:

- $\beta_1 = 0$. The number of crashes is not influenced by the traffic volume. Obviously, this is not true.
- $\beta_1 = 1$. The crash rate is the same regardless of the traffic volume. The number of crashes is proportional to *AADT*.
- $\beta_1 > 1$. The crash rate becomes higher as the traffic increases.
- $\beta_1 < 1$. The crash rate becomes lower as the traffic volume increases. This is the most common outcome for the *AADT* estimate, according to most safety performance functions.

The consideration of the segment length has remained more controversial. Some researchers include it in the analysis, obtaining a calibrated estimate. Some others do not, fixing it to 1 but performing a negative binomial regression, which may also be correct. In the last case, researchers assume that the road segment length does not have an influence on the crash rate. Some researchers indicate that it behaves in the opposite direction than *AADT*: a longer road segment leads to a higher crash rate. Some others, like Miauo, Song and Mallick (2003) and Lord, Manar and Vizioli (2005) affirm that road length does not affect crash rates.

Obviously, the length of the road segment might only be relevant if homogeneous road segments are considered. Thus, road segmentation becomes a very important issue. Resende and Benekohal (1997) indicated that only homogeneous road segments should be considered, based on traffic flow and geometric characteristics.

3.1.3.3.2. Before/After studies

Before/After studies are widely considered to be the most appropriate method to execute the evaluation of the effectiveness of traffic safety measures (de Pauw et al., 2013). It consists on comparing the number of accidents before and after the application of the countermeasure.

Although this may seem a simple approach, there are some problems due to the nature of road accidents. De Pauw et al. (2013) distinguished the following issues:

- Regression to the mean.
- Long-term trends affecting the number of crashes or injured road users.
- General changes in the number of crashes.
- Changes in traffic volumes.
- Any other specific events introduced at the same time as the road safety measure.

Due to the high variability of road crashes, the actual number of accidents at a certain location can never be known. However, the more years of data we have, the more precision about the outcome. When comparing the number of accidents before and after a countermeasure has been applied, at least 3-5 years before and after are suggested to use. Figure 10 shows how the accident randomness affects the results.

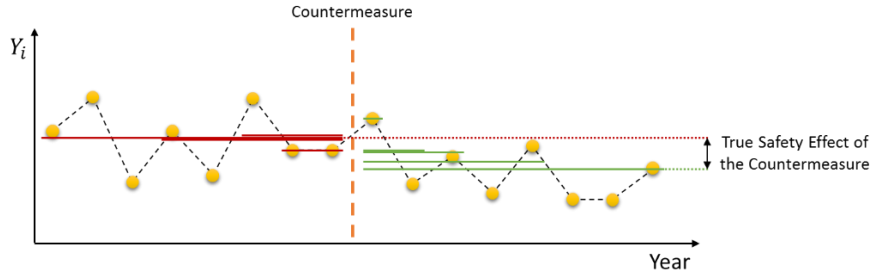

Figure 10. Variation of the estimated before/after effect depending on the number of years considered.

Several researchers have stated that the distribution of the expected mean of a Poisson-distributed count parameter follows a Gamma distribution. Considering this assumption, we cannot perfectly estimate the expected number of accidents, but we can determine a range that includes it with a certain probability.

According to it, we can use the properties of the Gamma distribution to estimate the range within the actual expected number of accidents is located. Figure 11

represents the variation of the lower and upper bound of the range for an estimation of three crashes/year. One can notice how the uncertainty is extreme for 1-2 years, but it is quite stable for more than 5 years. This is why at least 3 to 5 years are recommended to be used for before/after analyses. This is due to the Regression to the Mean (RTM) bias (de Pauw et al., 2013). If short periods of time are considered, the Empirical Bayes Method is suggested as a good tool to reduce this bias. If long periods of time are considered, there is no need to use an additional technique.

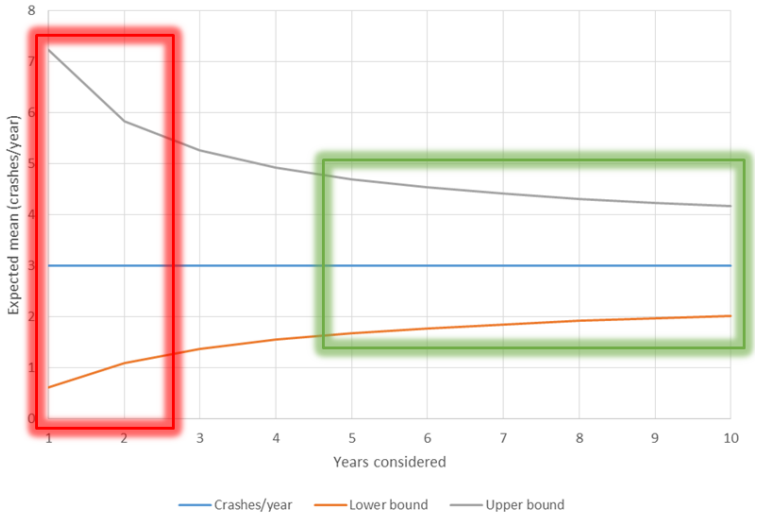

Figure 11. Confidence intervals for a gamma distribution depending on the number of years considered.

The accident outcome after the application of the countermeasure can also be affected by some other factors. Some examples are social awareness, traffic volume variations, etc. Those factors cannot be directly measured but they do exist. Thus, the effect of those other factors should be deducted in order to estimate the actual effect of the safety measure. We can do this by examining the crash variation in a control group. A control group is a set of similar roadway entities in which the countermeasure has not been applied. Thus, the variation of the number of crashes is only due to these general factors. Their comparison will let us to determine the true effect of the countermeasure.

3.1.3.3.3. Crash Modification Factors

A Crash Modification Factor (*CMF*) is a coefficient that lets us rapidly estimate the variation of the crash outcome due to a certain countermeasure. Considering y_0 the

initial number of accidents of the roadway entity i, the number of accidents after the countermeasure is applied (y_f) can be calculated as shown in Equation 11.

$$y_f = y_i \cdot CMF_{0\to f} \tag{11}$$

$CMF_{0\to f}$ is the crash modification factor that let us go from the initial to the final condition. Is worth pointing out that *CMFs* are normally not considered in terms of before-after situations, but referred to a base condition. The *CMF* is 1.0 for the base condition. Some *CMFs* refer to all accidents, while others refer to a certain subgroup (type of accident or severity).

Crash modification factors are a very simple and powerful tool, but they have to be handled with care. They were calibrated based on several Before/After analysis, considering certain conditions, such as traffic volume, cross-section, visibility, etc. A variation of those parameters might affect the outcome of crashes. Therefore, *CMFs* should only be applied when these additional conditions are satisfied.

There are many situations in which more than one *CMF* needs to be used. This is not a problem, as long as all conditions are satisfied. The uncertainty about the outcome also increases, as further discussed. A general formulation is given in Equation 12 (Wu et al., 2013). y_{rs} is the predicted number of crashes per year on a roadway element. y_{br} is the predicted number of crashes for the base conditions. CMF_j are all the crash modification factors to apply. Finally, C_r is a calibration factor for the highway element for local conditions.

$$y_{rs} = y_{br} \cdot C_r \cdot \prod_{j=1}^{n} CMF_j \tag{12}$$

The calibration factor for local conditions covers social, climatic and other aspects that vary across regions and have a certain effect on the number of accidents.

Sometimes, the *CMF* is not a single value but a function (Crash Modification Function). They are basically managed in the same way as crash modification factors.

CMFs are normally calibrated considering several Before/After analyses. Thus, there exist a certain degree of uncertainty, which is reflected in the variance of the *CMF*. This allows us to get an idea about their performance and the validity of the

outcome. Of course, the more *CMFs* we use in our analysis, the more uncertain the result becomes.

CMFs can be used together with safety performance functions for a better estimation of the number of crashes, according to the following steps:

1. Estimation of the number of accidents on a road geometric element for the base conditions. This can be done by means of a safety performance function (y_{br}).
2. Adjustment of the previous quantity for the local conditions, applying the *CMFs* and the geographical parameter (C_r). The estimated number of crashes is y_{rs}.
3. If some information about actual crashes is available, the Empirical Bayes method can be applied (further explained).

There are tons of crash modification factors available for designers. The AASTHO's Highway Safety Manual contains several of them, including their variance, accuracy and feasibility. All those *CMFs* covered by the part C of the HSM present a standard error less than 0.1, whereas *CMFs* that appear on part D present a standard error lower than 0.3. The webpage www.cmfclearinghouse.org also gathers several crash modification factors, classified depending on the road entity they refer to, accuracy, feasibility and so on.

CMFs should be handle with care. No risk exposure is considered, as well as interaction among the different parameters is not covered.

3.1.3.3.4. Empirical Bayes Method

The Empirical Bayes Method is based on the assumption that accident counts are not the only clue to the safety of a roadway entity. The other clue is how similar roadway entities behave. For instance, if we know that a certain roundabout presents 0 accidents in a year, but on average roundabouts present 0.56 accidents in a year, it would not be correct to assume that our roundabout is completely safe. In the same way, we already know that our roundabout behaves slightly better than the average roundabout. Hence, the actual crash probability of our roundabout should be within those values.

According to Hauer et al. (2002), the Empirical Bayes Method addresses two safety estimation issues:

- It increases the precision of estimates beyond what is possible when the available data is limited.
- It corrects the regression to the mean bias.

The Empirical Bayes Method considers both observed and estimated data. The expected number of accidents is calculated as shown in Equation 13.

$$E(\lambda/r) = \alpha \cdot \lambda + (1 - \alpha) \cdot r \tag{13}$$

$E(\lambda/r)$ represents the estimated number of accidents. λ is the expected number of accidents, according to the SPF estimation. r is the observed number of accidents. α is a weight parameter, that gives more importance to the estimated or the observed accidents, according to the reliability of the SPF. This parameter is calculated as Equation 14 shows, being μ the overdispersion parameter of the SPF.

$$\alpha = \frac{1}{1 + \lambda \cdot \mu} \tag{14}$$

Depending on the overdispersion parameter of the safety performance function, the estimated number of accidents will be closer to the SPF estimation or the observed accidents. Figure 12 shows one example.

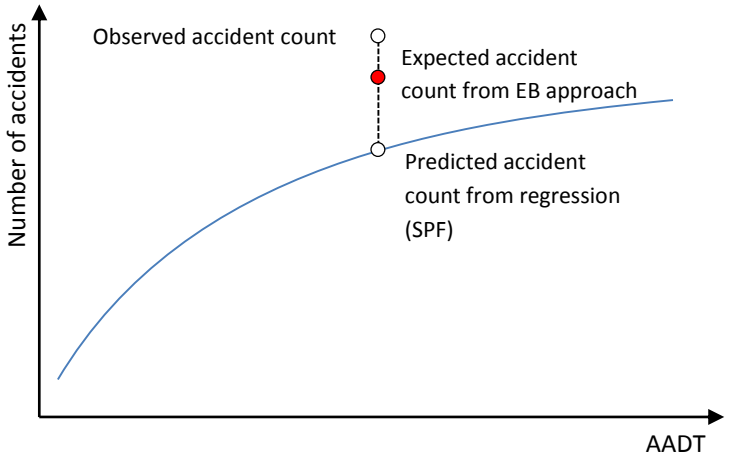

Figure 12. Graphical estimation of the expected accidents through the EBM.

Harwood et al. (2000) recommend to apply the Empirical Bayes procedure in the following cases:

- For estimating the number of accidents for the "do-nothing" alternative.
- Projects where the roadway cross-section is changed but the basic number of lanes remains the same. This includes, for instance, shoulder or lane widening projects.
- Projects with minor changes in the alignment.
- Projects in which a passing lane or a short four-lane section is added to increase passing opportunities.
- Any combination of the above.

On the contrary, the Empirical Bayes procedure is not applicable in the following cases:

- Projects where there is an important change in the alignment layout.
- Intersections where the number of legs is changed.

3.1.4. Road Safety Programs

Road safety is a very important social and economic problem. This is why tons of research have globally focused on it. This chapter analyzes how the different parts of the world address this problem.

3.1.4.1. Spain

Road safety in Spain began to be considered as a big issue in the final 1980s, due to the sudden increase of the fleet of vehicles, according to an increase of the mobility demand. In 1989, 110,000 crashes with victims took place in Spain, with 7,188 fatalities. The Spanish Administration got concerned about the problem, promoting some Road Safety Strategic Plans and a higher investment on road construction and maintenance. As a result, the number of fatalities has dramatically decreased, even more if it is compared also considering the mobility rate or the global number of vehicles.

Some policies have been transferred to the European Union as the integration level has increased. Thus, the global direction of the road safety policies are shared by all member states, presenting similar results, but with slight differences. For instance, Spain has been able to halve the number of fatalities from 2001 to 2010.

Figure 13 shows the evolution of the number of road accidents and fatalities from 2001 to 2010. The annual decrement of fatalities is about 6.9%, which is a very important factor. This reduction takes place both in rural and urban roads. However, the evolution of the number of road crashes is more stable, with a reduction rate of 0.9%. Thus leads us to think that the severity of road accidents is lower.

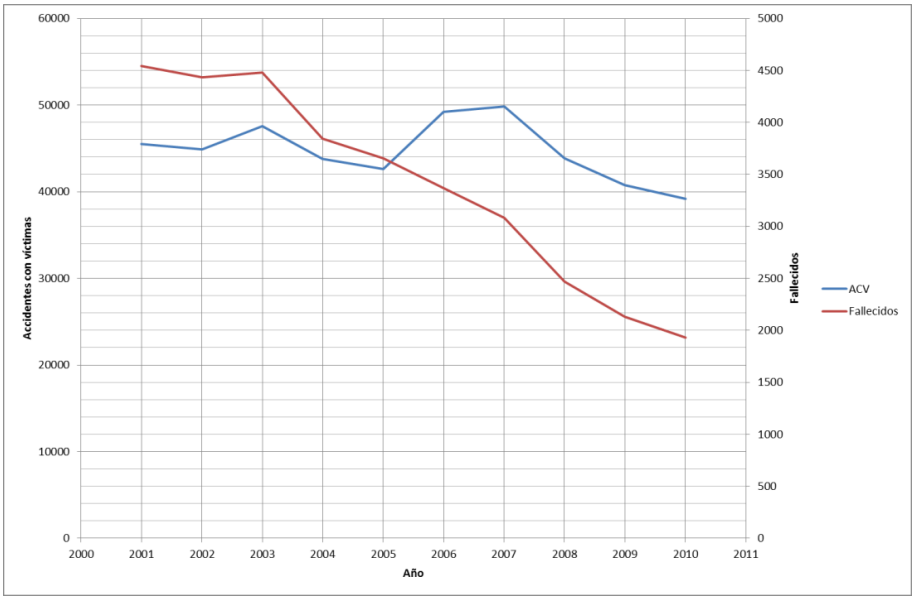

Figure 13. Evolution of the number of accidents with victims (blue) and fatalities (red) in Spain from 2001 to 2010.

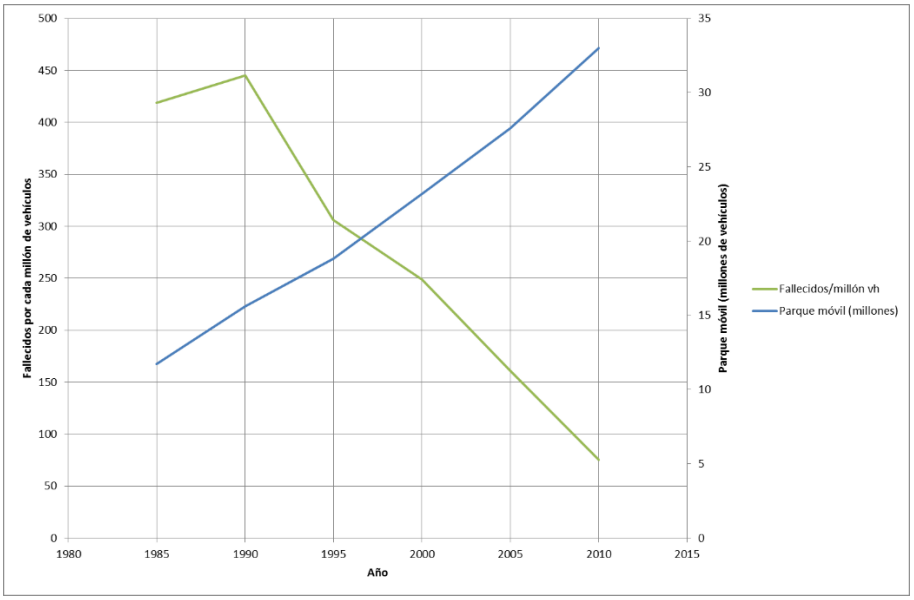

Figure 14. Evolution of the fatalities vs. million vehicles rate (green) and the total amount of vehicles (millions, blue)

The evolution of the fatalities is even more impressive if we compare it to the evolution of the fleet of vehicles (Figure 14).

Spain developed the Road Safety Strategic Plan between 2005 and 2008. The main objective was to reduce the number of fatalities by 40% compared to 2003. Some rapid measures were performed in 2004 and 2005, with good results. Some actions, like showing the consequences of fatal accidents were carried out in order to increase the social rejection to road crashes. As a result, the number of fatalities dropped by 42.6 %. However, the accidents in which a motorcycle was involved rose.

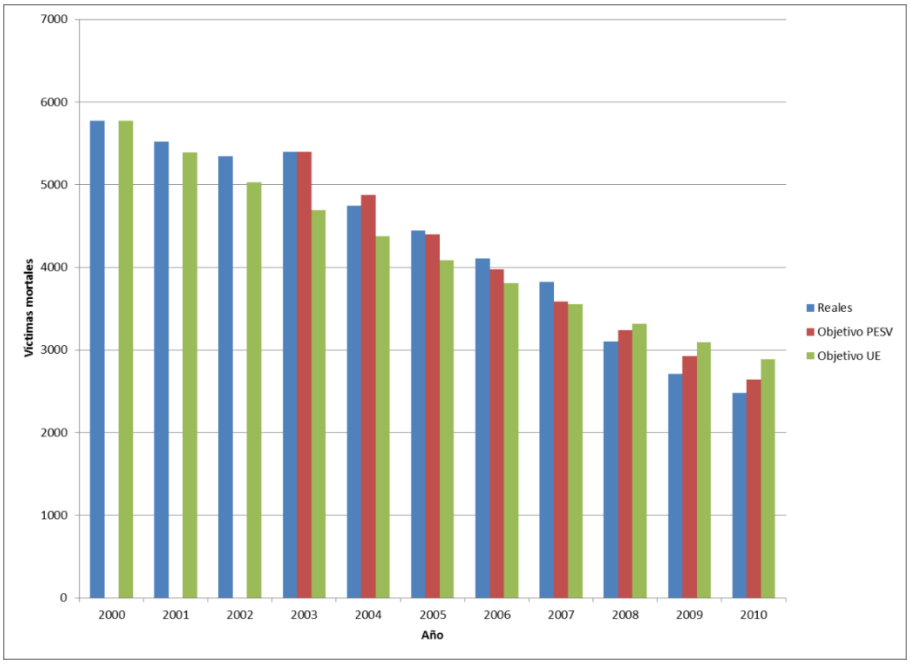

Figure 15. Fatalities in Spain due to road crashes. Last decade. They are compared to actual data and Spanish and European road safety programs.

The Road Safety Strategy 2010-2020 has been designed on the basis of the Road Safety Strategic Plan.

3.1.4.2. European Union

The current EU policy to halve accidents by 2010 is focused on the action on three pillars: infrastructure, driver and vehicle. Regarding the infrastructure factor, the European policies are most based on:

- Self-explaining roads. They should influence and guide a driver's behavior.
- Forgiving roadside. They should protect road users by providing them with a variety of safety measures and modern design implementations that will save their lives in the case of an accident.

In 2001, the European Union published the White Book of Transportation. The objective was to halve the number of fatalities from 2001 to 2010, going from 50,000 to 25,000 fatalities a year. In order to reach this objective, several measures were performed. This objective was revised in 2005, since the tendency was too low to

reach the global objective (5% of annual fatality reduction vs. 2% before). This revision proposed 32,500 fatalities in 2010 as the main goal.

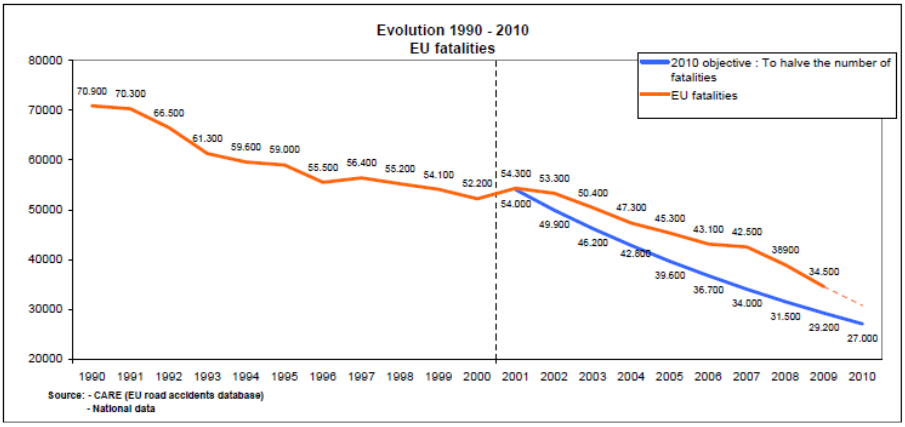

Figure 16. Number of fatalities due to road crashes 1990-2010. Comparison to the objective of the European Union.

The New Action Program on Road Safety of the European Union has been developed for the years 2011-2020. It aims for all countries to collaborate in reaching the highest standards in road safety. Thus, road safety is a shared responsibility. As a general objective, it intends to halve the number of fatalities due to road crashes from 2010 to 2020.

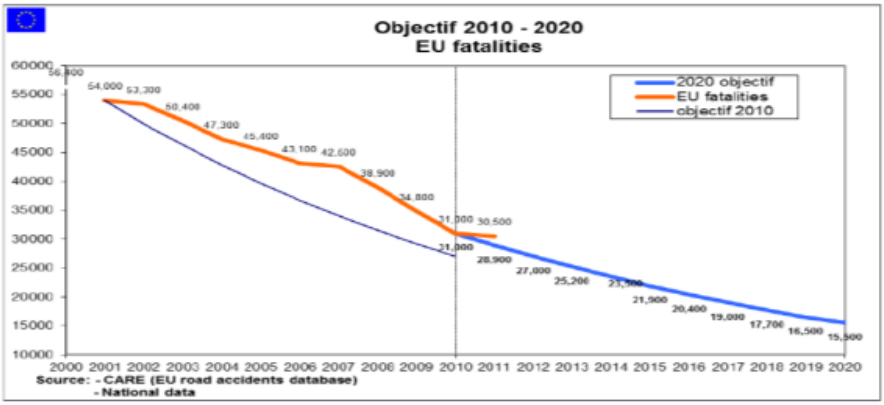

Figure 17. Evolution of fatalities due to road crashes 2000-2020. Comparison to the European Union's objective.

This goal is intended to be reached by means of strategic objectives oriented towards several concurrent factors, like human, infrastructure and vehicles.

3.1.4.3. Worldwide

The period 2011-2020 has been named as "Decade of Action" in road safety. It has been promoted by Russia, supported by more than 100 countries and declared by the United Nations General Assembly. This plan was launched in May, 11th 2011.

Its objective was to stabilize and reduce the estimated fatalities in road crashes worldwide by 2020. It is founded on the following pillars:

- Road safety management.
- Better infrastructures and a safer mobility.
- Safer vehicles.
- Safer road users.
- Better response to road accidents.

More information about the project can be found in www.decadeofaction.org.

3.2. Human factor. Traffic psychology

Traffic psychology is defined as the study of the behavior of road users and the psychological processes underlying that behavior. It attempts to identify the determinants of road user behavior with the aim of developing effective accident countermeasures (Rothengatter, 1997).

Human factor is crucial for understanding road safety. As explained in Section 3.1.1, this is the most important factor by itself and also in consideration with the infrastructure factor. Ogden (1996) defined the conditions of a safe road:

- Warns the driver of any substandard or unusual features.
- Informs the driver of conditions to be encountered.
- Guides the driver through unusual sections.
- Controls the drivers' passage through conflict points and road links.
- Forgives a driver's errant or inappropriate behavior.

Due to the interaction of infrastructure and human factors, problems have different ways to be addressed. Infrastructure solutions have to take into consideration drivers' internal processes; as well as social countermeasures. As explained below, the human response to engineering solutions is sometimes more important than the countermeasure itself. Evans (1990) distinguished two categories: human infrastructure (behavior, social norms, legislation…) and the engineering infrastructure (roads, vehicles, traffic control systems).

3.2.1. The driving task

Janssen (1979) proposed a driving behavior model in which all decisions are organized hierarchically in three steps: navigation, guidance and control. Alexander and Lunenfeld (1990) later completed this model (Figure 18).

- Navigation. This is a strategic/planning level. It includes the decision to drive, the route to choose, time to leave, etc. Several aspects do have influence at this level, such as driver's feelings, sleepiness, need of the trip, etc. All these decisions are taken before entering the vehicle.
- Guidance. This level appears once the previous one has been overcome. Decisions at this level are taken while driving, and are related to how to manage the vehicle within the traffic flow, how to deal with obstacles, curve negotiation, speed adaptation, and similar. These are conscious decisions, taken on purpose by drivers.

- Control. Almost all decisions at this level are automatic, taken unconsciously by drivers in response to several different stimuli. Some examples are speed variation, steering maneuvers, gear changing, etc.

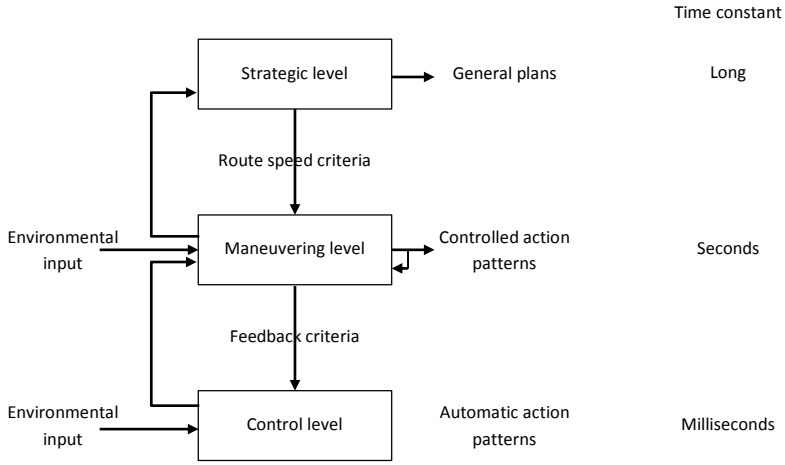

Figure 18. Hierarchical structure of the mobility/driving task (adapted from Shinar (2007)).

All the decisions made at every level of the driving task are performed accordingly to some criteria the driver would like to achieve. For instance, if the driver wants to reach the destination quickly:

- Navigation. The driver chooses the most direct, low traffic route.
- Guidance. The user drives faster, overtaking vehicles if possible and cutting some curves (if possible).
- Control. The driver adapts its driving behavior, limiting their braking behavior, as well as reducing the number of gear changes.

The scheme is not always going from navigation to control. Sometimes, user's experience from one level can make them to reconsider navigation decisions. One example is when a lot of traffic is found in one route and the driver reconsiders again the route to take. Hence, decisions at all levels may actually be taken at all times. This makes this model not so easy to be used. Moreover, some parameters actually do have influence on various levels of the hierarchical model, such as GPS systems. Thus, some more detailed hierarchical models have been proposed, including the most recent technologies and some other decision-taking loops. Despite of this fact,

this kind of navigation-guidance-control hierarchical models are not enough for explaining some behaviors.

These supplementary models focus on the variables that affect decisions, and consider drivers' limitations as well as the driving situation. Several kind of models are presented, focusing on different aspects of the human factor: attention and perception, motivation, decision-taking models and integrative models. They explain similar aspects from different points of view. At some points they clearly differ, but it is pretty useful to know all of them, since a global vision of the driving behavior can be reached thus.

3.2.1. Visual perception

The information perceived by drivers is mainly visual (Evans, 2004). Compared to the acoustic or haptic perception, the optical one has a portion about 90% (Dietze et al., 2008). Drivers try to perceive as much information as possible. Less information is required on familiar roads rather than on unfamiliar ones.

Often drivers must perform several tasks within short time intervals, thus requiring high attention levels. When the workload is high, the driver might fail to acquire all the needed information. The vision of the driver varies according to the workload level, thus being narrower when the workload gets higher (Andersen et al., 2011).

According to the visual system, various fields of perception can be identified:

- Field of view. Horizontal: 180º to 220º. Vertical: 130º (Biedermann, 1984).
- Visual field. It is the part of the field of view that can be well focused with moving eyes and unmoved head. Horizontal: 60º. Vertical: 40º (Berger, 1996).
- Useful field of view. Part of the visual field where the most information is received (Berger, 1996).

Stereoscopic vision is also very important, since it helps users to estimate distances. The human stereoscopic vision lets us to see a small range of 3D vision –less than 6 m – , so longer distances have to be estimated in comparison to know objects, object occlusion and distribution of light and shadow. Moving objects are perceived by the human eye up to 800 m.

The visual field depends on several parameters, but speed is a very important one. As the speed gets higher, the visual field becomes smaller (Babkov, 1975). The field

of view is also smaller if the alignment is discontinuous. Although the road user primarily focus on the road, they can also focus on other objects, if they are relevant.

Leutner (1974) developed a model in which the road is classified according to its distance to the driver and their possibilities:

- Zone 1: 600 m – 250 m. Orientation and information zone.
- Zone 2. 250 m – 75 m. Attendance and decision zone.
- Zone 3. Lower than 75 m. Acting zone.

3.2.2. Experience and learning. Hazard perception

'Exposure' can be defined as the occurrence of specific events that may generate conflicts between road users. A conflict is any event in which road users arrive at the same place at the same time or within a very short time interval. Some examples are crossing, braking or overtaking. In those cases, users must be aware of the situation in order to prevent road accidents. This definition of exposure is different than the one based on AADT. If the AADT increases 10 times, the conflict exposure increases far more (Elvik, 2010).

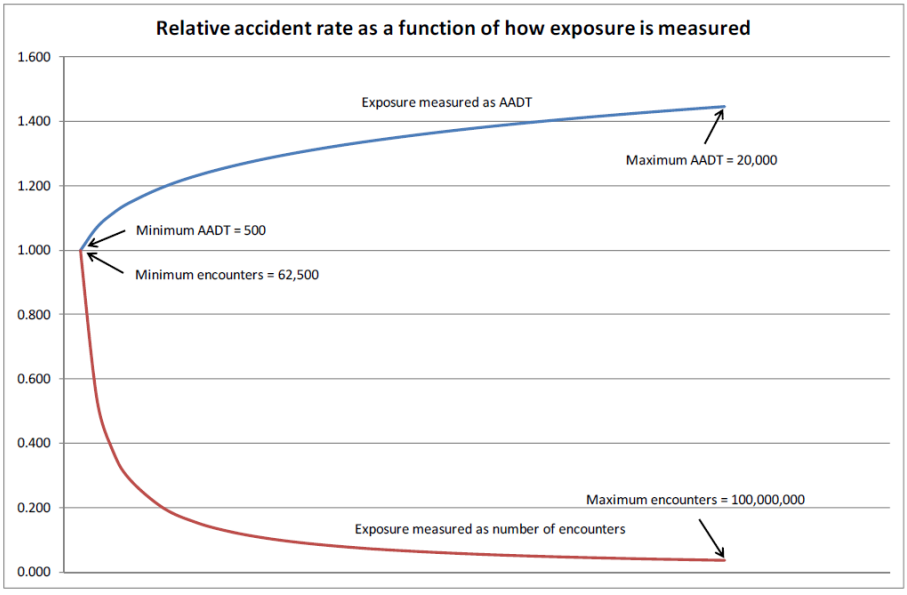

Figure 19. Crash rate as a function of how exposure is measured (Source: Elvik, 2010).

This definition of conflict exposure can be used as a surrogate measure to learning abilities. In most cases, the rate of accidents decreases as the number of events increases. This can be interpreted as a 'learning curve' (Elvik et al., 2009).

Some other studies, such as those developed by Sagberg (1998) and Hakamies-Blomqvist et al. (2002) do also achieve the same conclusions. Crash rates experience a big drop as the conflict exposure gets higher. Steeper learning curves indicate a faster learning by the users.

Driving learning efficiency is controlled by some other factors:

- Frequent events are associated with a lower probability of accident occurrence. The process of learning is very quick, because of their frequency.
- Control. Quick events are more risky and less easy to learn than slower events.
- Complexity. Complex events are more risky and less easy to learn than slower events.

The ability of identifying hazardous situations while driving is an important skill, since it prevents high workload demands in the driving task. This ability is mostly related to experience. Hence, novice drivers have problems at detecting potential conflicts, while experienced drivers might not. The familiarity to the road is also important, since the hazard locations are well located in familiar roads. The hazard perception skill can be improved from the experience.

Chapman and Underwood (1998) found that experienced drivers adapted the scanning patterns according to the road and traffic situation, while novice drivers used the same scanning patterns for all situations. Borowsky, Shinar and Oron-Gilad (2010) analyzed the effects of age and driving experience on the ability to detect hazards while driving. Their study showed that young, unexperienced drivers were more likely to commit hazard perception errors. They also found that the different groups paid attention to different zones when approaching to a 'T' intersection. Experienced drivers focused on the other roads, searching for incoming traffic that might be a problem. On the contrary, novice drivers kept their behavior, focusing on their own road and thus not foreseeing potential incoming traffic.

3.2.3. Information processing models

It is a well-known fact that our capacity to process information is limited. Considering the driving task, the problem arises because of the need to process a certain quantity of information within a limited time.

When driving, lots of information –most of them through the visual channel – are shown to us, but only a small portion can be attended and processed. In an ideal situation, the information rate to process is lower than our capacity. In case that critical information flows at a rate higher than our capacity, a failure is experienced. This failure can be missing some information, misperceiving information we attend to, or not considering all the information we should. If the missed information is critical, then the likelihood of a crash will increase.

The fact that we deal with information rates and not with information *per se* is very important. The amount of information between two points of a certain road might be constant, but the rate at which it flows depends on the speed we choose.

One generally accepted model is the one proposed by Wickens (1992) (Figure 20). In this model, our connection to the environment is carried out by the sensory receptors. All this information is briefly stored (during seconds), decaying rapidly. During those seconds, it is stored in a short-term sensory storage (STSS), and the user has to select what to keep and what to lose (i.e., all information not attended will be permanently lost to us). Our attendance to the external stimuli will determine the processing degree of the information.

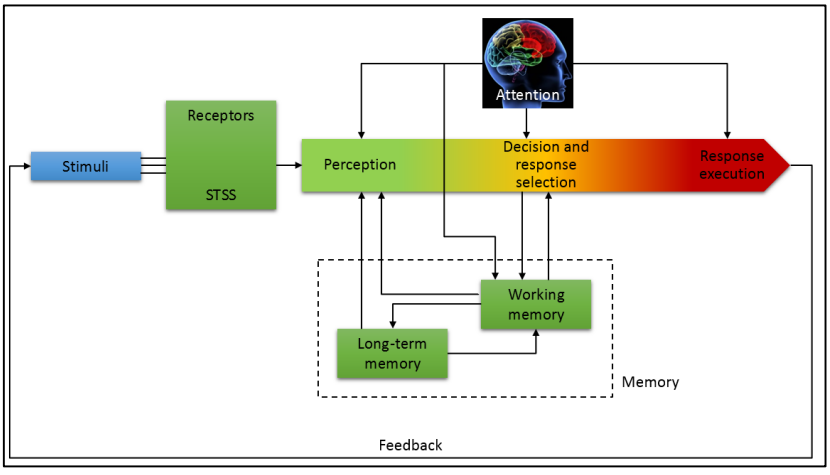

Figure 20. Wickens' Attention and Perception model (adapted from Shinar (2007)).

Considering the driving task, much of this information is barely acquired, processed at a minimal level. Thus, we are aware of the curves, signs and traffic, and we respond adequately to all of them, but the information is afterwards forgot.

Perception is not only limited to what information reaches our receptors, but also to the way we interpret it. This interpretation is based on our previous experiences, so our memory has a major role to play. The memory is divided into two storage mechanisms: short-term or working memory, and long-term memory. Both storage mechanisms are quite different:

- Storage capacity. The short-term memory (STM) is extremely limited. It cannot acquire more information without forgetting something. The long-term memory (LTM) works like being unlimited.
- Storage mechanism. Perceived information enters STM and may or may not be transferred to LTM.
- Nature of information. STM information is essentially visual or acoustic. LTM information is basically conceptual or semantic.
- Decay of information. STM information can be stored unless a new information enters our system. LTM information is always available, but sometimes difficult to remember.
- Retrieval of information. Retrieval from STM is immediate. Retrieval from LTM is sometimes difficult.

When driving, the STM and LTM are connected in order to identify which information is relevant, according to traffic laws. When a match is done, our perception focuses on it (for instance, a STOP sign, or another vehicle). Depending on our previous driving experience, we will focus on different aspects, thus making our perception more or less efficient.

The next stage is the decision process. Decisions are hugely based on our previous experience, so memory also plays a major role here. One example is when and how to brake our vehicle, how to negotiate certain curves, or how to interact with other vehicles.

After taking the most important decisions, it is time to respond. Considering this model, this is the first part where a motor action appears. The response may be faulty even if the decision was correct, depending on conditions and driver skills. A more experience driver usually responds better than a novice one does.

We can distinguish here two kind of processes: controlled and automated processes. Several studies (Schneider and Shifrin, 1977) indicate that complex tasks involve the automation of several sequences of behavior. Learning this sequences is hard, avoiding the user to perform more tasks at the same time. The advantage is that, once learned, they can perform them unconsciously. One example is changing gears.

The response creates an action, which induces new stimuli. Those are again captured by our sensors and the process continues. This is the so-called 'feedback loop'.

Attention is also crucial for the model. It can be defined as the resource of psychic energy that we devote to the task at any time. When driving, we normally block irrelevant sensor information in order to pay more attention to our visual perception. This phenomenon is more evident as the traffic situation is more complex. For instance, at hazardous sites we practically do not listen to the rest of passengers, and pay almost all our attention to the road layout.

3.2.4. Attention. Driving workload

'Attention' or 'workload' can be defined as the information rate that a person has to process per unit of time. As explained above, it is highly related to the human cognitive skills. There are two aspects related to attention that should be considered: the total amount of attentional capacity, and the portion of it that is dedicated to the driving task.

The capacity of attention is not constant. It depends on our particular circumstances, the moment of the day, and other factors. The proportion of attention on the driving task varies in time, depending on the driver's criterion. Experienced drivers are very efficient at managing their attention.

A driver may divide or focus their attention. When driving, normally drivers split their attention between driving and non-driving tasks. It is an automated behavior, normally well performed because of the high-control level acquired while learning to drive. On the other hand, drivers also focus their attention while they perceive lots of information but they only select the stimuli needed for a safe and efficient driving.

The driving workload should be neither too low nor too high. If it is too low, the will take more capacity for non-driving tasks. On the other hand, if it is too high, it may surpass driver's capabilities. In fact, one of the most common causes behind road accidents is the lack of attention, due to its poor management by drivers. The road,

traffic and environment situation requires more or less attention, being this attention level variable in time. This variation mostly depends on the information rate that has to be processed by drivers. Thus, driving at low speeds leads to lower attention requirements.

Figure 21 represents how the performance varies depending on the workload. For a low workload demand, the performance is also low. According to road design, this is represented by a very simple geometric layout combined with a simple environment. Drivers tend to get distracted, so the number of accidents is not minimum. These accidents are difficult to predict, since they spread almost randomly within these simple sections.

The workload demand increases as the complexity of the road segment does. Drivers respond accordingly, increasing their performance level. This can be done until an optimum performance level is achieved. At this point, all the capacity of the driver is used for the driving task. If the workload increases beyond this point, the performance dramatically collapses.

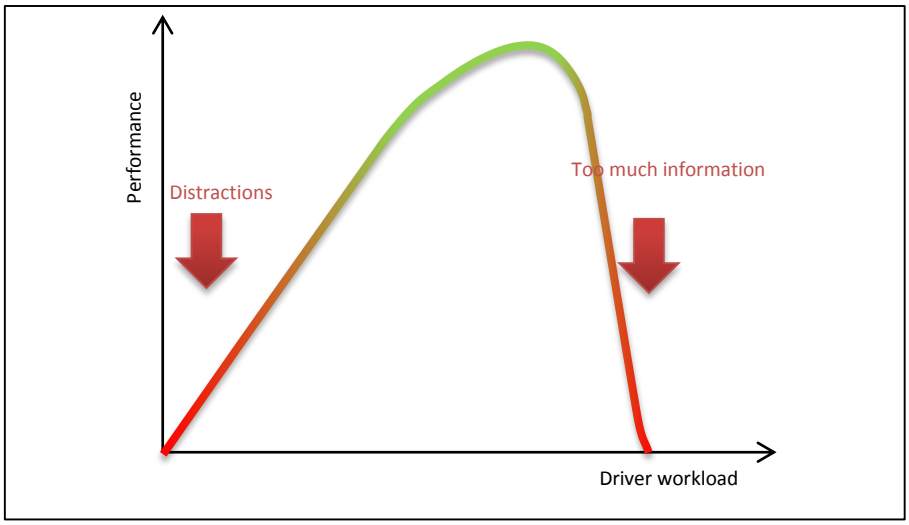

Figure 21. Relationship between performance and driver workload.

The driving situation is normally safe as long as our attention level is higher than the environmental demands. Experienced drivers know very well how to manage attention requirements. Thus, when the traffic situation becomes harder, they reduce their speed in order to reduce the information rate perceived and then decreasing the attention requirements (Elvik, 2006). Besides, they also expect in a

better way than novice drivers when the attention requirements are to increase, thus readapting their attention allocation. One example is observing the rest of the traffic in order to guess if a conflict is to appear, in order to foresee it.

Sometimes (but fortunately quite rarely), the attention requirements increase unexpectedly, surpassing the driver's performance level. This is the dangerous point where the likelihood of having a crash dramatically increases. The attention requirements may not be too high, but they appear when the driver is not prepared. Hence, it may end in a road accident (Figure 22).

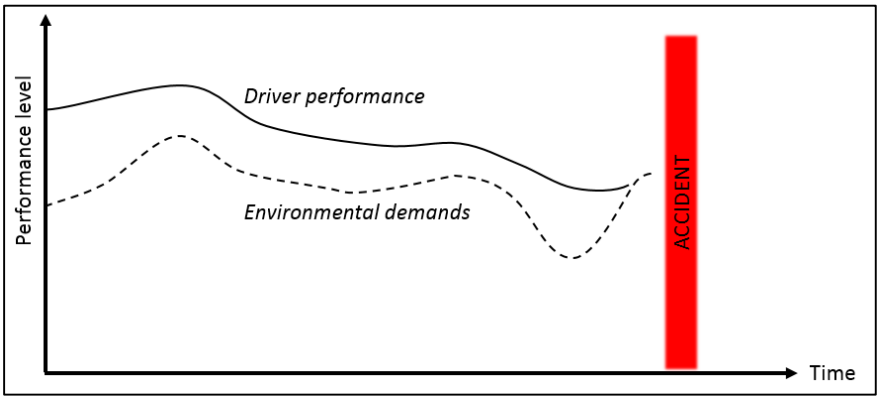

Figure 22. Driver mental workload overpassed by a sudden increase of the environmental demands.

Driving is more a matter of mental capacity rather than physical capacity. Impair drivers do know their limitations and hence put more mental attention on the driving task, thus leading to similar safety levels than physically fit drivers (Elvik, 2006). This is not true if the brain is affected by the impairment. One example is epilepsy, Alzheimer's disease and sleep apnea, which do affect accident rates.

3.2.5. Theories and models of driver behavior

Models of driver behavior try to describe, explain and predict driver behavior. They are used for understanding some underlying processes of accident causation, as well as drivers' attitudes. We can also use these models to predict drivers' reactions to certain circumstances, and to develop better road safety countermeasures, self-explaining roads, etc.

Those models are valid to explain why the introduction of certain road safety elements not only affect the infrastructure but they also have a real effect on driver

behavior. Sometimes the behavioral effect may negate the safety benefits of the countermeasure itself. Human behavior models are thus necessary in order to identify the reason and avoid this reaction.

3.2.5.1. Rational decision making models

Those models try to explain driving behavior on the basis that we are humans and take decisions following certain logic. By the way, the same condition of being humans is inherent to the fact that sometimes we take biased decisions, or we do not consider all the information available. Those models have to also consider these biasing effects in their schemes.

Sivak (2002) adapts the economic bounded and unbounded rationality concepts to driving behavior. Decisions based on unbounded rationality consider all possible information, with no biasing, taking all the time needed. Let's take as an example a pedestrian who wants to cross a street. If based on unbounded rationality, the pedestrian would exactly calculate the needed gap, besides determining the speed of the approaching vehicles. They would also have all possible time to perform this operation. Obviously, this is not the case. Instead, the pedestrian selects an approximate gap, based on their perception of the length of the street and the speed of approaching vehicles. Depending on the time not being able to cross, the need of gap decreases because of the pedestrian adds more parameters to the problem, such as taking more risk, stress level, etc. The pedestrian therefore does not consider all the information available, as well as they perform a biased, non-objective decision. This is called 'bounded rationality'. By simply observing road users we cannot determine their biasing level, so it is not possible to accurate estimate their behavior.

The previous model indicates why do we behave differently according to the external situation, but it assumes a complete control of our behavior. According to Ajzen (1991), this is not true. Ajzen's theory of planned behavior indicates that before any behavior it exists one intention. This intention is based on three different aspects: attitude towards the behavior (for instance, speeding), the subjective norm we embrace (the way we are influenced by society, friends, etc.), and the perceived control on this behavior (for instance, warning signs, existence of traffic or not, etc.). This is a model which is highly related to particular perceptions, so it is particularly useful for explaining aggressive driving, drunk driving and risky driving involving conscious violations (Shinar, 2007).

Fuller (2005) proposed one of the most important rational decision models, complementing the Wickens' model. That model did not focus on the attention allocation needs for each one of the processes, although being a major issue. Attention allocation is quite flexible, being able to rapidly change according to multiple factors, both endogenous and exogenous to the driver.

Fuller's model is depicted in Figure 23. The main diagonal line represents the threshold between a non-collision situation (left side) and a collision situation (right one). Collision situation does not need collision, since a lucky escape is also possible.

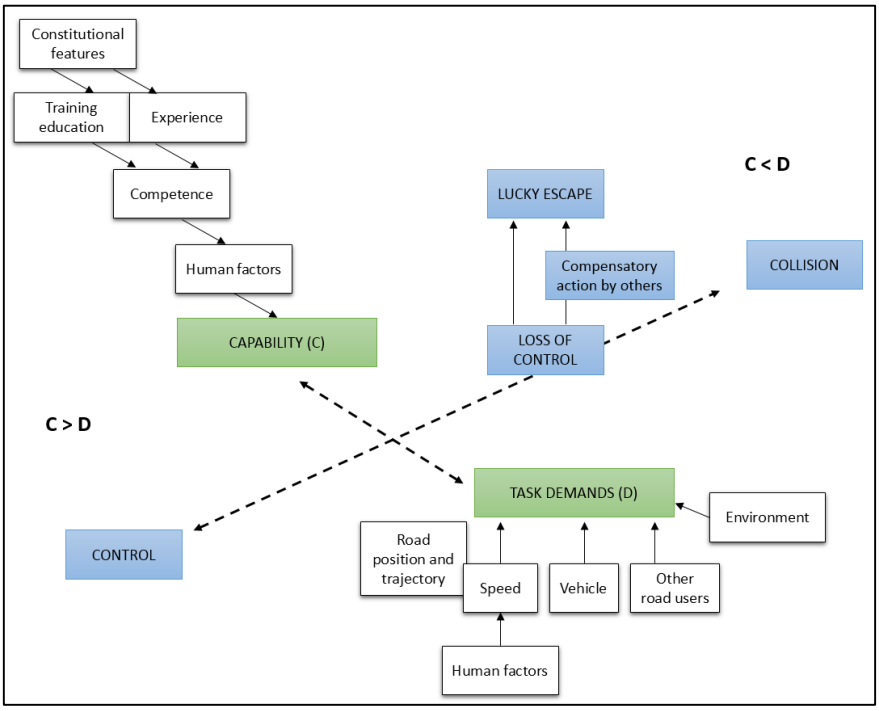

Figure 23. Fuller's model of driver behavior (adapted from Shinar (2007)).

Driver's capabilities are mostly based in their training education, experience and competence, as well as human factors. On the other hand, factors such as environment, vehicle and speed determine the task demands. Although speed is selected by drivers, the information rate to be processed depends on it, thus becoming a task demand parameter. This is why old users drive slower, trying to adapt the information rate to their capabilities. Fuller indicated that drivers are

motivated to keep a preferred level of task difficulty, being the speed variation the easiest way to manage it.

This can explain how drivers manage their abilities between driving and non-driving tasks. When driving through a reduced speed area, drivers tend to reduce their driving capabilities, thus performing a non-driving task, in order to keep the initial task difficulty level. In case the road needs too much attention to be paid, drivers tend to reduce their speed and hence the information rate and thus readapting their demand-capabilities equilibrium.

The previous statement is also the reason why engineers are continuing improving the safety of vehicles and infrastructures, but the overall safety level does not evolve in the same way. The reason is because drivers are dedicating less effort to the driving task.

Road inconsistencies can also be explained with this model. Drivers adapt their behavior to low-effort demanding roads but, in the case an inconsistency appears, the task amount suddenly increases, often surpassing driver's current capabilities and thus increasing the probability of an accident.

3.2.5.2. Motivational models

Motivational models of driver behavior focus on driver motivations, instead on driver capacity. Fuller's model incorporates motivations through the 'constitutional features', but they are not emphasized. Motivations include safety, performance, and economy, among other factors.

Several surveys have pointed out that safety is not one of the primary motivations that drivers consider (Mason-Dixon, 2005). Thus, how can it be included by driving behavior models? The answer is through a different parameter: risk. Risk is considered the multiplication of the probability of an unwanted event times the consequences of that event.

3.2.5.2.1. Risk minimization and risk compensation theories

Risk minimization models assume that people do not try to maximize safety, but to minimize risk. Summala (1988) argues that drivers tend to adapt their behavior searching a zero-risk level. The driver only changes their behavior when the risk level reaches certain subjective threshold. The risk perception is relative, and highly variable among different people.

This theory compares different risk levels in order to identify hazardous situations. Every road has an objective risk level. This risk is defined as a function of its geometric features, environment, etc. This risk is not measurable or perceptible by the road users. Conversely, each road user has its own risk level, calculated in a subjective way, depending on the characteristics that the driver is able to perceive. This is called perceived risk. Drivers assess the risk level and adopt different behaviors also considering their particular conditions (stress level, time restrictions, purpose of the trip, etc.), thus assuming more or less risk. This is a decision performed by each driver, only comparing the assumed risk to the risk perception. However, the perception of the risk is not the objective risk of the road. Hence the importance of allowing a good risk perception of the roads.

Road crashes tend to be higher at those locations where the perceived risk is quite lower than the objective one. In these cases, drivers underestimate the objective risk of the road, thus leading to hazardous situations more frequently.

Two different design decisions can be made, according to this theory: reducing the objective risk (the best one), or increasing the risk perception, in order to accommodate to the objective one.

3.2.5.2.2. Risk homeostasis model

This model, proposed by Wilde (1998), is maybe the best-know motivational model. According to it, we strive not to minimize risk, but to reduce it to a non-zero level which is comfortable to us. Hence, perceived risk is continuously analyzed in order to reach the personal threshold we desire. This perceived risk level is affected by the objective risk and by the driver's skills. Thus, the same situation may be risky for novice and old drivers, while not risky for young, aggressive drivers. The risk target also varies among people.

The most important effect of this model is that most infrastructure and vehicle improvements would have low or no long-term effect according to it. Thus, Wilde proposes that effective countermeasures should focus on changing the risk target, which can only be achieved through behavior modification.

This theory also accounts with several criticisms, summarized by Robertson (2002):

- Only a small percent of drivers have experienced a crash, so they cannot actually determine the risk of having one.

- The risk level is not only controlled by the driver. Some other drivers do exist, and their actions are relevant to the risk level.
- Most of the research that supports the risk homeostasis theory is flawed in its design or analysis.
- Data contradicts the model statements. Crashes have dramatically decreased during last years.
- The risk of a crash varies in several countries, also varying after some measures are taken. If this model is correct, then the risk of a crash should remain the same.

3.2.5.3. Integrative models

Basically two kinds of road behavior models have been presented: those ones based on information processing and motivational factors. Road behavior is in the end a mixture of both. Both kind of models cannot explain certain part of drivers' behavior, so they have to be considered together.

Reason et al. (1990) offered a different approach to road behavior, mixing motivations and task limitations. Their approach was done by means of analyzing aberrant behaviors, such as violations and errors.

Nearly all violations are deliberate actions that are considered to be unsafe behaviors. They can be observed, measured and documented. On the other hand, errors are not deliberate, and can be divided into slips, lapses and mistakes.

Errors are mainly caused by information processing flaws of the individual drivers. In contrast, violations are primarily motivationally caused, and have to be described relative to the specific context in which they occur.

The two types of behaviors are different: people who commit errors are not necessary likely to commit violations and vice versa. Reason et al. (1990) also investigated about the social factors that are behind violations. Young drivers are more likely to commit violations, whereas old drivers are to commit errors.

There can be identified four kinds of errors:

- Errors due to driver's capabilities saturation.
- Errors due to a flaw in the basic, unconscious driving tasks.
- Reasoning errors.
- Errors due to a misperception of the environment.

3.3. Road design

Geometric design is the main part of road design. It consists on determining the detailed layout of a road depending on some prior constraints. Some goals such as functionality, safety, comfort, environmental integration, harmony or aesthetics, economy and flexibility must be satisfied.

Although the result is tridimensional, its design is not conceived as such. Several attempts of horizontal, vertical and cross-section designs are performed, in an iterative process. The whole result is analyzed at each iteration, looking for the best balancing between goals and constraints.

The most important parameter in the design process is the design speed. The designer selects this speed according to factors such as the functional classification of the road, drivers' expected behavior, orography and land use. It influences some "road segment features", such as the minimum radius, sight distances, transition parameters and cross-section. Later on, a more detailed design is performed, keeping in mind this prior restriction and guidelines.

3.3.1. Speed concepts

3.3.1.1. Design speed

Design speed (v_d) is a selected speed used to determine the various geometric design features of the roadway (AASHTO, 2011). This speed is selected by road designers, and should also consider the anticipated operating speed, topography, the adjacent land use, and the functional classification of the highway. Safety, mobility and efficiency are a direct outcome of the design speed selection. On the contrary, there are some constraints such as environmental quality, economics, aesthetics, and social or political impacts.

Although the design speed is not the speed at which users will operate, it does influence on certain design parameters such as curve radii, sight distance, superelevation rate, etc. This is why this parameter is so important. A large difference between design and operating speed may therefore cause safety problems. AASHTO's Green Book (2011) reports that design speed should be consistent with the speeds that drivers are likely to expect on a given highway facility. Drivers do not adjust their speeds to the importance of the highway, but to their perception of the physical limitations of the highway and its traffic. The design

speed is used for determining minimum values for highway design such as horizontal curve radius and sight distance.

The AASHTO states the following about the selection of a design speed:

- The assumed design speed should be a logical one with respect to the topography, the adjacent land use, and the functional classification of the highway.
- Every effort should be made to use as high a design speed as practicable to attain a desired degree of safety, mobility and efficiency while under the constraints of environmental quality, economics, aesthetics, and social or political impacts.
- The design speed chosen should be consistent with the speed a driver is likely to expect.
- A highway of higher functional classification may justify a higher design speed than a less important facility in similar topography. A low design speed should not be assumed for a secondary road where the topography is such that drivers are likely to travel at high speeds.
- The design speed selected should fit the travel desires and habits of nearly all drivers.
- A pertinent consideration in selecting design speeds is the average trip length. The longer the trip, the greater the desire for a higher speed.

Functional classification	Terrain		
	Level	Rolling	Mountainous
Arterial	100-110	80-100	60-80
Collector	60-100	50-80	30-60
Local	50-80	30-60	30-50

Table 2. AASHTO Guidelines on Minimum Design Speed (kph) for rural highways.

The AASHTO does not include a feedback loop in the design process. Thus, the speed behavior resulting from the design alignment is not compared to the design features. There is a need for an iteration in the design process to check for and resolve disparities between the design speed and estimated operating speeds (Krammes, 2000). Thus, superelevation rates should be based on operating speed instead of on design speed.

The geometric features obtained with the design speed are considered minimum values, and drivers are encouraged to adopt higher values. With no maximum values

established, this design approach may lead to alignments with abrupt changes or considerable differences between successive elements (Hassan, Sayed and Tabernero, 2001).

The Spanish guidelines define design speed as the one that establishes the minimum geometric features of the different road geometric elements, in a safety and comfortable way. Therefore, the design speed of a road segment is the minimum of the design speeds of the individual geometric elements. The design speed of a single element is defined as the maximum speed that can be maintained along it in safe and comfort conditions, when the pavement is wet, tires are in good shape and weather, traffic and legal conditions are not a constraint. The Spanish guidelines also indicate that the design speed should be selected accordingly to the design speed of the adjacent road segments, as well as topographic and environment, climate, mobility, functional classification, homogeneity, economic conditions and the distance between adjacent accesses.

The Spanish guidelines indicate that the design speed should be selected considering the following aspects:

- Orography and roadside conditions.
- Environmental conditions.
- Functionality of the new road within the road network.
- Homogeneity of the road or the itinerary.
- Socio-economic conditions.
- Driveway density and minimum separation.

However, no quantitative guidance is given, so the designer has the final decision.

The process of selecting the design speed presents some issues. Krammes (2000) demonstrated that operating speeds for horizontal curves were often higher than the design speeds, which is clearly a problem. In fact, the design speed concept has been adapted in some countries to better ensure that design speeds are in agreement with estimated operating speeds.

Figure 24 shows the difference between the operating speed and the inferred design speed (kph). Data collected was of 138 horizontal curves in five states. As we can see, the operating speed is quite more stable than the design speed. For low-design speed curves, the operating speeds are quite higher than the design one. The opposite effect takes place for the high-design speed ones.

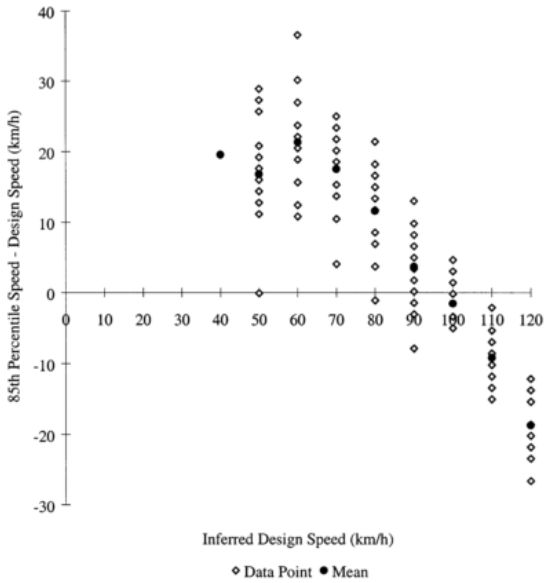

Figure 24. Difference between the operating speed and the inferred design speed (Source: Krammes (2000))

Krammes presented the following recommendations:

- The AASHTO should review recent data on the distribution of today's desired speeds on rural highways. The recommended minimum design speeds should represent a high percentile value of the desired speed distribution.
- Current AASHTO policy on the application of the selected design speed cannot guarantee that alignments with design speeds lower than 60 mph will promote uniform operating speed profiles.

Earlier, Leisch and Leisch (1977) proposed a new design speed concept for the United States that was based on the operating speed. They suggested that the difference between design and operating speeds should not exceed 15 kph. The difference between the operating speed for passenger cars and heavy vehicles should be limited to the same threshold.

Harwood, Neuman and Leisch (2000) suggested the following loop for determining design speeds:

1. The designer selects a design speed.

2. The designer develops a preliminary design for the facility.
3. The designer determines the operating speed profile and compares it to the design speed.
4. If the operating speed is less than or equal to the design speed, the design is acceptable and the preliminary design can be further developed.
5. On the contrary, the designer can:
    a. Select a higher design speed and go to step 2.
    b. Change the geometric design or other characteristics, maintaining the initial design speed.

Lamm (2002) suggested that the operating speed should be used for determining the design speed. Instead of being the most restrictive speed of the road segment, the average operating speed value was proposed as design speed. Thus, the design speed better reflects the general behavior of the road segment.

For doing so, they proposed an average Curvature Change Rate ($\emptyset CCR_s$), which is calculated using the CCR_s for all curves of a road segment (Equation (15). Tangents are not considered in this process.

$$\emptyset CCR_s = \frac{\sum_{i=1}^{i=n} CCR_{s_i} \cdot L_i}{\sum_{i=1}^{i=n} L_i} \quad (15)$$

Where:
$\emptyset CCR_s$: Average curvature change rate of the single curve for the observed roadway section without regarding tangents (gon/km).
CCR_{s_i}: curvature change rate of the single curve or unidirectional curved site i (gon/km).
L_i: length of curve or unidirectional curved site i (m).

The average CCR can be used for determining an average operating speed, according to the specific operating speed model applicable for the country. This is called average operating speed ($\emptyset v_{85}$). Lamm et al. (2007) suggest the use of this term as the basis for establishing the design speed for new designs and RRR-strategies.

Some other countries have guidelines in which the design speed is selected considering an iterative process or by means of some instructions based on quantitative criteria. The operating speed is also sometimes considered in the design process. Some examples are Australia and other European countries, where the

design speed concept has been reexamined in order to address disparities with operating speeds.

The UK's guidelines establish an iterative methodology to determine the design speed. A seed design speed is proposed for the road segment. Departing from this value, the road segment is completely designed and the operating speed profile is determined. This profile is compared to the design speed. The zones where the difference between both speeds is too high have to be redesigned.

The German guidelines indicate that the design speed should be used at first for determining the minimum radii of the horizontal curves, vertical curves and maximum grades. The operating speed profiles are then determined, considering the CCR and road width. These operating speed profiles are used for determining some other aspects, such as the superelevation rates of the horizontal curves. It is also suggested that the operating speed should not exceed the design speed more than 20 km/h.

The French design method is similar, but it determines the sight distance based on the operating speed profile. There are other consistency requirements that must be satisfied.

In all cases, the design speed is selected by the designer and it is applied to the whole road segment. This is why it is also known as "designated design speed". There is another definition of design speed: "inferred design speed". This definition applies to single geometric features which have a design speed definition. The inferred design speed is the design speed which would correspond to the design feature, according to its geometry. Inferred and designated design speeds are the same only for the limiting geometric design feature of the road segment.

3.3.1.2. Operating speed

AASTHO's Green Book (2011) defines operating speed as the speed at which drivers are observed operating their vehicles during free-flow conditions. Free-flow speeds are those observed from vehicles whose operation are unimpeded by traffic control devices or by other vehicles in the traffic stream. Typically, a 5 seconds headway is considered as free-flow conditions. The 85^{th} percentile of the distribution of observed speeds is the most frequently used measure of the operating speed associated with a particular location or geometric feature.

The operating speed is a way of representing the behavior of drivers. Drivers select their speed as a function of road geometric features, environment, urban planning, functional classification of the road, regulations, and other factors.

Drivers do not know the design speed of a road. However, this speed determines some geometric features of the road. Hence, there might appear safety problems if there is a big difference between design and operating speeds. This is why the operating speed estimation should somehow be considered while defining a design speed.

Determining the operating speed for already built up roads is very easy, since only observation is needed. The problem arises when one needs to estimate the operating speed for roads at the design stage. This estimation can be done through operating speed models.

Operating speed models are some expressions that allow us to estimate the operating speed at certain road geometric features mostly depending on their geometric design. Several research has been carried out in this way, as can be seen in the corresponding section. Several factors influence operating speeds:

- Geometric factors. Some road features impose operating speed restriction, such as horizontal curves or low sight-distance locations. Those points are known as operating speed controls. Exceeding the speed control would lead to less comfort and safety. Some examples are the radius of the horizontal curves, longitudinal grades at long tangents, etc. Other geometric factors still influence the operating speed, not being a speed control. Some examples are the lane and shoulder widths at tangents.
- Non-geometric factors. At geometric features where the geometry does not impose a control on the operating speed, drivers are free to select it. They perform their selection considering some geometric factors as well, but they might include some other variables in their decision. Some examples are the environment, functional classification of the road, etc. They mostly affect drivers' speeds in a psychological way. Hence, their inclusion in the models is more difficult.
- Social factors. Drivers are different. They present different stress level, hurry, purpose of the trip, experience, skills, etc. Vehicles are also different. All those parameters do also have an influence of the outcome. The problem is that operating speed models are calibrated for all drivers,

regardless of their social conditions. Thus, all these variables will lead to more or less operating speed dispersion.

3.3.2. Road safety consideration in the design process

Drivers mostly behave according to the geometric restrictions they find. Thus, they adapt to the local design of the geometric features, not attending to the design speed unless it imposes clear restrictions. Safety problems might exist if there is a large difference between the road design and drivers' behavior.

3.3.2.1. Road safety in the guidelines

One important issue with most current road design guidelines is that the drivers' final behavior is not checked. Most current guidelines give some design minimum/maximum criteria for the design of the different geometric features. Thus, it is assumed that a safe road is achieved when it meets the standards, being unsafe otherwise. Most current guidelines propose detailed methodologies to estimate the functionality or economic level of the design. However, road safety is several times not adequately considered. Many authors have expressed concern over the lack of quantitative safety considerations in the highway geometric design guidelines (Lamm, Psarianos and Cafiso, 2002).

Most current guidelines present the following two groups of inconsistencies:

- An inappropriate use of the design speed.
- A bad choice of the consecutive road geometric elements.

Several road design guidelines present old definitions of the design speed. The worst part is that they do not check if the drivers operate at a speed similar to the design speed. Recently, several research has been carried out in order to better define the design speed. However, these new concepts are still to be included in the different guidelines.

The minimum sight distance is normally defined in terms of the design speed. The designer must provide a visibility higher than the sight distance in the entire road segment. However, the sight distance is normally calculated with the design speed, so the SSD is underestimated along most of the road segment. In addition, users drive at the operating speed, which is normally higher than the design speed. Most of the current guidelines do not exclusively consider the design speed, but also do not have tools to estimate the operating speed profiles.

The maximum and minimum lengths of the tangents between two different curves is also controlled by the design speed. Some studies indicate that drivers' negotiation at these points depend on the operating speed, so these criteria should be redefined.

Guidelines normally only give some thresholds or maximum/minimum values for the design of the different geometric features. Thus, the designer is free to select a certain value within a large range. However, a few tools exist for establishing a good connection between the different types of elements.

The Spanish guidelines do not include a consistency evaluation into the road design. On the contrary, there are some recommendations to produce a balanced road design. They are based on the Safety Criteria I and II, applied on the inferred design speed and the design speed of the road.

- The design speed difference between two consecutive road segments should not exceed 30 kph.
- For two-lane rural highways, the difference between the inferred design speed and the design speed of the entire road segment should not exceed 20 kph.
- For consecutive curves with an intermediate tangent, the difference of the inferred design speed between both curves should not exceed 30 kph.
- The relationship between the radii of consecutive curves is controlled. Depending on the class of the road (Class 1 or 2), two relationships are given when the intermediate tangent is shorter than 400 m (Figure 25).
- The Spanish guidelines do not propose tools for determining homogeneous road segments.
- Lippold (1997) found that it was such a high difference in terms of probability of accidents depending on the balance degree of the consecutive geometric elements. Their results were integrated in the German Guidelines (Figure 26).

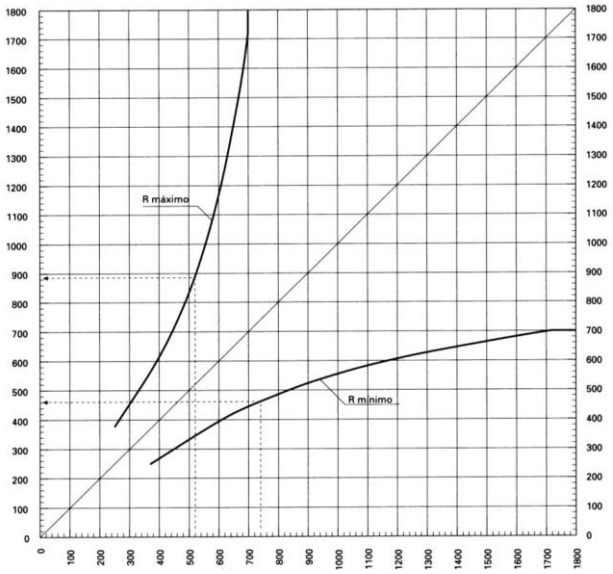

Figure 25. Radii relationship for consecutive curves with an intermediate tangent lower than 400 m, according to the Spanish guidelines. Roads belonging to Class 1.

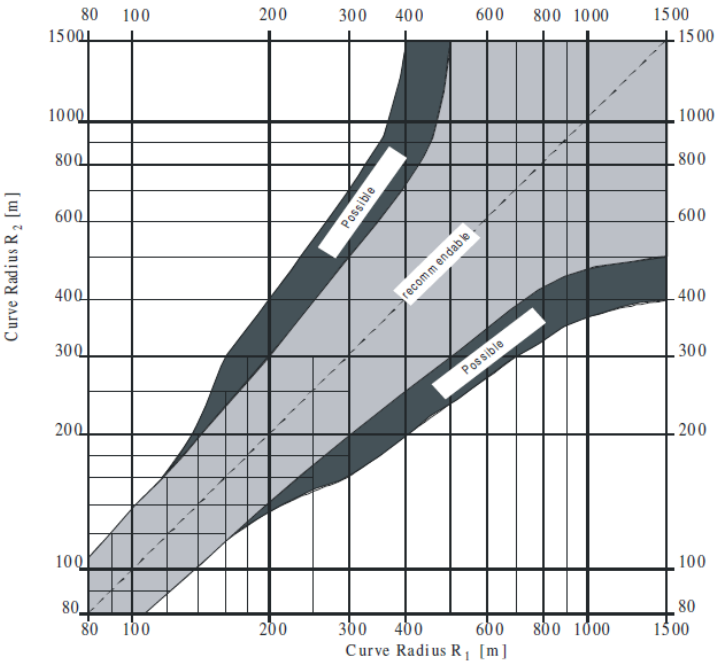

Figure 26. Balanced curve consecution. German guideline RAS-L (1997).

The AASHTO (2011) establishes a maximum relationship of 3:2 for designing consecutive horizontal curves.

Guidelines are gradually moving from a nominal to a substantive concept of safety. Nominal safety refers to the compliance of the design features of a road (lane width, curve radii, etc.) to prevailing design criteria. It is a yes/no concept. On the other hand, substantive safety refers to a quantitative way to estimate safety. It considers the frequency and nature of road accidents, thus allowing engineers to develop better designs and a most accurate comparison between different alternatives. Some recent guidelines do include consistency evaluation processes, as well as tools that allow engineers to estimate the number of crashes. This is very useful while selecting among different alternatives.

3.3.2.2. Highway Safety Manual (HSM)

The AASHTO Highway Safety Manual (HSM) provides analytical tools and techniques to estimate the expected number of crashes on road segments and intersections (AASTHO 2010). Most of them are based on the combination of three basic tools (safety performance functions, crash modification factors and the Empirical Bayes method). The purpose of the Highway Safety Manual is to assess the safety impacts of transportation project and program decisions at all stages of the development process:

- System Planning.
- Project Planning and Preliminary Engineering.
- Design and Construction.
- Operations and Maintenance.

The Highway Safety Manual is organized in four parts:

- Part A. Introduction, Human Factors and Fundamentals of Safety.
- Part B. Roadway Safety Management Process.
- Part C. Predictive Methods.
- Part D. Crash Modification Factors.

Part A describes the purpose and scope of the Highway Safety Manual. It also includes some fundamentals to be used in the next sections of the HSM. The chapters are:

- Chapter 1. Introduction and Overview.

- Chapter 2. Human Factors.
- Chapter 3. Fundamentals.

Part B presents some steps to monitor and reduce crash frequency and severity on existing road networks. Several network screening tools that account for the Regression to the Mean are presented. Some methods to evaluate the effectiveness of an individual treatment are also included. The chapters are:

- Chapter 4. Network screening.
- Chapter 5. Diagnosis.
- Chapter 6. Select Countermeasures.
- Chapter 7. Economic Appraisal.
- Chapter 8. Prioritize Projects.
- Chapter 9. Safety Effectiveness Evaluation.

Part C provides a predictive method for estimating expected average crash frequency at an individual site. This method is basically based on the use of safety performance functions. The chapters are:

- Chapter 10. Rural Two-Lane, Two-Way Roads.
- Chapter 11. Rural Multilane Highways.
- Chapter 12. Urban and Suburban Arterials.

Part D presents a collection of some *CMFs*:

- Chapter 13. Roadway Segments.
- Chapter 14. Intersections.
- Chapter 15. Interchanges.
- Chapter 16. Special Facilities.
- Chapter 17. Road Networks.

3.3.2.3. Interactive Highway Safety Design Model (IHSDM)

The Interactive Highway Safety Design Model (IHSDM) is a software decision-support tool that can be used to evaluate the safety and operational performance of existing or planned two-lane rural highways (Krammes and Hayden, 2003). This is an interactive, computer program composed by several modules that assess the engineers in the process of designing safer roads. It was developed by the US Federal Highway Administration (FHWA).

It consists of the following six modules:

- Crash prediction.
- Design consistency.
- Intersection review.
- Policy review.
- Traffic analysis.
- Driver/Vehicle.

The Crash Prediction Module (CPM) is an implementation of the crash prediction methods documented in Part C of the Highway Safety Manual. It includes capabilities to evaluate rural two-lane highways, rural multilane highways, urban/suburban arterials, freeway segments and freeway ramps/interchanges. The estimated number of crashes is based on the geometric design and traffic characteristics. It is based on the use of safety performance functions and crash modification factors.

The design consistency module helps diagnose safety concerns at horizontal curves. This module depicts operating speed profiles based on the operating speed profile developed by Fitzpatrick et al. (2000). This operating speed profile uses the radius as an input for the calculation of the operating speed for horizontal curves. This model also considers the vertical curvature. Along with those models, the Design Consistency Module also applies the TWOPAS equations for limiting the operating speed when steep grades are present. The current model checks design consistency considering Safety Criteria I and II.

The design consistency and crash prediction modules were developed based on field data from a sample of sites with specific geometric design features and traffic operational characteristics. Not all two-lane highways will contain geometric design parameters within the ranges used to develop the IHSDM. Donnell et al. (2009) used an arterial and a collector roads to compare the outputs of the IHSDM to the actual observations. The arterial road presented similar characteristics that those used for calibrating the IHSDM. The outputs were quite similar to the observed values. However, the collector road was designed differently. The results showed that it was difficult to predict design consistency to roads like that. Further research was suggested for supplementing the design consistency module.

The Intersection Review Module is an expert system that performs a diagnostic review to systematically evaluate an intersection design for typical safety concerns.

This module considers the intersection configuration, the horizontal and vertical alignment, and the intersection sight distance.

The Policy Review Module checks roadway-segment design elements for compliance with relevant highway geometric design policies. It is updated including the AASHTO's 2011 Green Book. This module also includes a tool for inputting policy tables from other agencies' design policies. The module is organized into four categories: cross-section, horizontal alignment, vertical alignment and sight distance.

The Traffic Analysis Module uses the TWOPAS traffic simulation model to estimate traffic quality of service measures for an existing or proposed design under current or projected future traffic flows.

The Driver/Vehicle module allows the user to evaluate how a drier would operate a vehicle within the context of a roadway design and to identify whether conditions exist in a given design that could result in loss of vehicle control. It consists on a driver performance model linked to a vehicle dynamics model.

3.3.3. Road segmentation

Roads are hardly ever designed as a whole. Instead, they are usually divided into different segments. Each one of the road segments presents a design speed and should be designed accordingly to the design features of the others.

Already built up roads are not an exception. When estimating the safety level of an existing road, some inputs such as road length, design speed, etc. are often required. In addition, global consistency methodologies and safety performance functions for road segments provide different results depending on how the road was divided. Thus, there is a need to define a criterion to divide roads into homogeneous road sections.

Zhang and Ivan (2005) noticed this problem for the first time when estimating crash rates for 1 km long road segments. They concluded that road crashes depended on the speed limit, CCR and the curvature of the geometric elements within the road segment.

The road segments resulting from a constant-length segmentation process are not homogeneous. This is why other researchers have provided other segmentation methods. Garber and Ehrhart (2000) divided the road considering major junctions.

They identified the operating speed dispersion and traffic volume as the most important parameters influencing road crashes.

Pardillo and Llamas (2003) performed two different kind of road divisions: a 1 km long road segments and segments between main road junctions. The latter ranged from 3 to 25 km long. They pointed out that access density, average sight distance, average speed limit and the proportion of overtaking impeding zones were correlated to crash rates. They also suggested 400 m as the minimum length for homogeneous road segments.

There are other segmentation methods which are based on the geometric characteristics of the road. The most well-known method is the "German procedure". This method distinguishes road segments according to their curvature change rate (CCR). Figure 27 shows how this process is carried out: a profile of the cumulative deflection angle versus the road station must be plotted. Hence, homogeneous road segments can be distinguished according to similar CCR behavior. CCR is defined as the sum of the absolute deflection angles over the length (km).

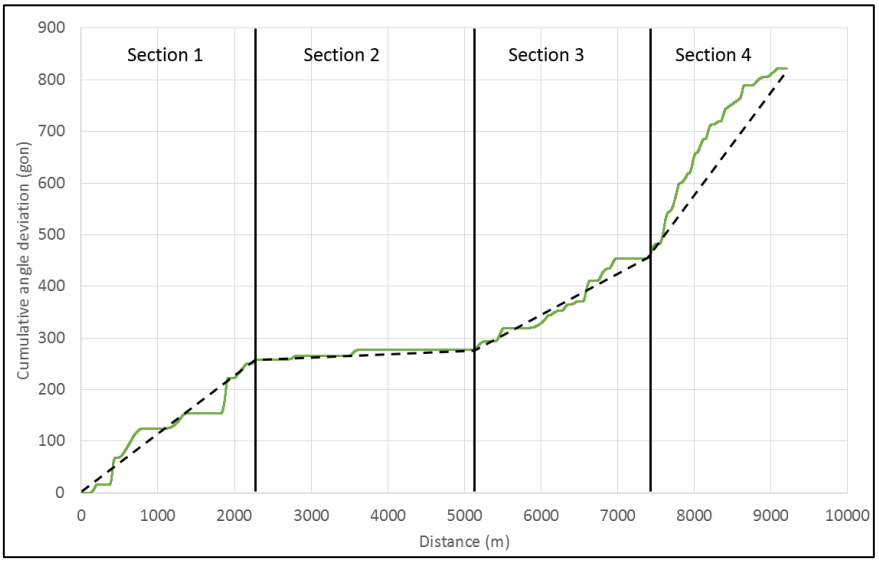

Figure 27. Determination of homogeneous road segments. German methodology.

Some other methodologies include additional geometric parameters. Abdel-Aty and Radwan (2000) divided a road of 227 km long into 566 road geometric segments. Geometric features such as lane and shoulder width, horizontal curvature, etc. were

considered in the analysis. They also determined a strong relationship to road crashes. They suggested 800 m to be the minimum road segment length.

Cafiso et al. (2010) presented a methodology for segmenting two-lane rural highways. This methodology was based on the following parameters:

- Average Annual Daily Traffic (AADT).
- Curvature Change Rate (CCR) and average paved width (W).
- Road Side Hazard Rating (RSH), according to their definition of this parameter.

The Roadside Hazard was evaluated using checklists filled in by inspectors for segments of 200 m.

The homogeneous road segments present a constant RSH value. They can be distinguished by minimizing the sum of squared deviations of the individual RSH values with respect to the mean and conducting a t-test in this process. A minimum length of 1000 m and a t-test significance level of 15% are suggested.

Cafiso, D'Agostino and Persaud (2013) investigated the importance of a correct segmentation on the estimation of road crashes given by safety performance functions. They tested five segmentation alternatives:

- Segmentation 1. Homogeneous segments with respect to AADT and curvature, as suggested by HSM.
- Segmentation 2. Data organized to have within each segment two curves and two tangents.
- Segmentation 3. Segments with constant AADT.
- Segmentation 4. Segments with a constant length (650 m).
- Segmentation 5. All the variables used in the stepwise procedure are constant within each segment with their original value.

They concluded that the poorest segmentation was Segmentation 5, since it yielded to very short segments. On the contrary, Segmentations 2 and 4 were the most promising ones. Segmentation 4 (constant length) was determined to be the better for practical application.

3.3.4. Recreation of the road geometry

Sometimes engineers need to work on already built-up roads. There may be several reasons, going from redesign to research purposes. In all those cases the geometry of the road needs to be extracted. The easiest way to do it is taking the design project, but in several cases this is not possible.

Instead, several researchers have developed methodologies to recreate the geometric alignment of roadway sections. This procedure consist on determining the horizontal and/or vertical road alignment from a set of *x*, *y*, *z* points that represent the road centerline.

This methodology can be divided in two steps: the determination of the set of points and the transformation of them into a horizontal and/or vertical alignment.

Finally, these methodology is not only useful for determining the actual alignment of a road, but for studying the actual behavior of drivers. This will let researchers to determine how the operating behavior fits the road alignment.

3.3.4.1. Centerline data extraction

This initial set of points can be obtained by means of different procedures. The most evident method – besides of expensive and slow – is the surveying and demarcation of the existing road.

GPS devices are a good way to determine the actual path of vehicles along a road. They provide latitude, longitude and altitude data along all the covered path. Depending on the frequency at which they record and store information, speed and acceleration data may be also obtained. Some factors such as the precision of the position are influenced by the GPS technology and the environment. If there are elements such as big buildings or tunnels, the precision will be lower. There are some modern systems that overcome these limitations, such as differential GPS. The reception frequency of these systems is also increasing.

Due to the general availability of GPS systems, as well as their affordability, there are several researchers that have focused on their use for road geometry restitution. Baffour (1997) used instrumented vehicles with GPS in order to obtain road geometry, longitudinal grade and superelevation rate. In 2002 they also determined the lateral slope of roads by using additional GPS receivers (Baffour, 2002).

Roh, Seo and Lee (2003) used different systems, such as RTK DGPS and GLONASS for determining some road alignments. They also compared the accuracy of both

systems. Veneziano, Hallmark and Souleyrette (2004) compared altitude data coming from GPS-photogrammetric restitution and LIDAR (Light Detection and Ranging). Young and Miller (2005) processed about 11 million GPS data coming from the Kansas Transportation Department. They showed how the error among several GPS receivers is highly correlated. This error is composed of two parts: a common one (bias error) and a random part (random error). The bias error is pretty higher than the random error. Thus, although the addition of both error terms might be relevant, the random term is several times negligible. This makes this methodology suitable for restoring road alignments.

Imran, Hassan and Patterson (2006) used GPS and GIS systems for studying the path of several vehicles and hence use these paths for restoring road horizontal alignment. Cai and Rasdorf (2008) proposed a GIS-LIDAR methodology for extracting road centerline instead of using DMI or GPS systems.

The advantages of GPS-based technology are the fast data extraction and their accuracy. The disadvantage is how those data are collected. GPS data reflect the vehicle's operation, not the road alignment. The vehicle cannot go through the centerline of the road, since it is incompatible with road operation. Thus, at least one trip in each direction is needed. Later on, both trips must be merged into a single one that corresponds to the road centerline. Unfortunately, this also reflects driver's operation and not road design. Drivers normally operate adding spiral transitions at locations where they are not. On right curves drivers operate very similar to road geometry, but they depict a smoother radius on left curves. Thus, the combined geometry is not the actual one. This is necessarily not a problem. In several situations, researchers do investigate on drivers' operation and hence this is a very good way to do it. The only problem is the possible bias due to the knowledge of drivers about the scope of the project.

There are other methods to obtain the road centerline without GPS data. This solves the bias due to drivers' operation, but it is a slower method. Easa et al. (2007) and Dong et al. (2007) used IKONOS imagery for determining the horizontal set of points of the road centerline. They transformed the image into grayscale and later applied the Canny edge detection procedure, thus allowing the automatic detection of road axes.

The road centerline can also be manually depicted. Two characteristics of the satellite image are needed: high resolution and good orthorectification. The first condition allows the user to zoom in the road up to an altitude where the road

centerline is clearly distinguished. The distance between points should not be necessarily the same. A higher point density is required at curved locations than at tangents. The second condition is also very important. At mountainous locations, the horizontal alignment might appear different depending on the position of the satellite which took the image, which may bias the results. There are several orthorectifying methodologies that combine the image with the topography, producing a valid image regardless of the position of the satellite.

3.3.4.2. Road alignment extraction

This is the second step of the road geometric restitution process. It consists on determining a road alignment from a series of x, y – and eventually z – coordinates. There are different procedures. Some of them are automatic, some of them not. Three main groups can be distinguished.

3.3.4.2.1. Spline application

Splines are 3-degree polynomic curves that fit a set of points. This is not a single function, but a series of functions that are connected in several ways at their boundary points. They can include some smoothing factors, as well as tangency conditions. This allows to store several geometric factors into a few parameters, thus reducing the data storage and processing needs. They also let engineers to restructure the distance between the points of the road centerline to a certain cadence.

In 1977, the Kansas Department of Transportation acquired data from their road network, thus producing a very large database, difficult to be managed. Data were obtained through a GPS device with a frequency of 1 second. Ben-Arieh et al. (2004) proposed the use of B-splines to condense and manage all these information. They only considered the horizontal alignment. The vertical alignment was not obtained because of the accuracy of the data. Nehate and Rys (2006) added the vertical component, developing a methodology for determining the available sight distance.

All these methodologies represent the road layout by means of a sequence of B-Splines, but the horizontal and vertical layout were not determined. Castro et al. (2006) developed a procedure for obtaining the geometric layout of two-lane rural roads. They used a GPS device placed in an instrumented vehicle, travelling at 80 km/h. The GPS frequency was 1 Hz. The vehicle operated in both directions, so the first step was to determine the set of points of the corresponding road centerline. The next step consists on determining the corresponding cubic spline geometry. This

geometry was compared to the design one, thus determining that 71% of the restored points were closer than 0.50 m to the actual road geometry. The maximum distance was of 1.00 m, and the average distance, 0.40 m.

Lipar et al. (2011) developed a different procedure for estimating the curvature of a set of points departing from GPS data. They first adapted the set of points to a B-spline curve, in order to later apply a stereographic projection. However, spiral transitions cannot be determined through this method.

Cafiso and di Graziano (2008) and later Garach et al. (2014) developed a spline-based methodology for recreating horizontal alignments. Their main contribution is that their approach allows them to fit altogether combinations of circular curves and spiral transitions. The methodology is therefore valid for curves with and without spiral transitions.

A band of tolerance was introduced, in order to set as a tangent all curvatures under this threshold. The curves were adjusted by placing trapezoids in the curvature diagram. The condition is that the area of the trapezoid should be the same than the area of the region determined by the graph of the truncated curvature function and the abscissa axis within the curve region.

3.3.4.2.2. Threshold-based detection of road geometric features

This kind of procedures use some thresholds to determine the boundaries between different road geometric elements.

Maybe the most important contribution was performed by Imran et al. (2006). They used high-accuracy-GPS devices at 10 Hz mounted on several vehicles travelling through two-lane rural roads at different speeds, ranging from 80 to 100 km/h.

Their adjustment was mainly based on the detection of the boundary points between tangents and curves. They developed the heading profile for all the road. Their basic assumption was that if the heading variation between two consecutive points was lower than a certain threshold, it could be considered as a tangent. Otherwise, it was considered a curve.

The next step was to determine the geometry of the curves. A circular curve follows the expression of the Equation 16, where (x_0, y_0) is the circular curve center and (x_i, y_i) are the points corresponding to the circumference of radius r.

$$\sqrt{(x_i - x_0)^2 + (y_i - y_0)^2} - r = 0 \quad (16)$$

The point where the spiral transitions begins and finishes is not known. They supposed that at least 50% of the central points of the curve belonged to the circular part of the curve. They therefore estimated the mean square error. After that, they varied the boundary points and recalculated the mean square error. This process continues until the optimal solution is achieved.

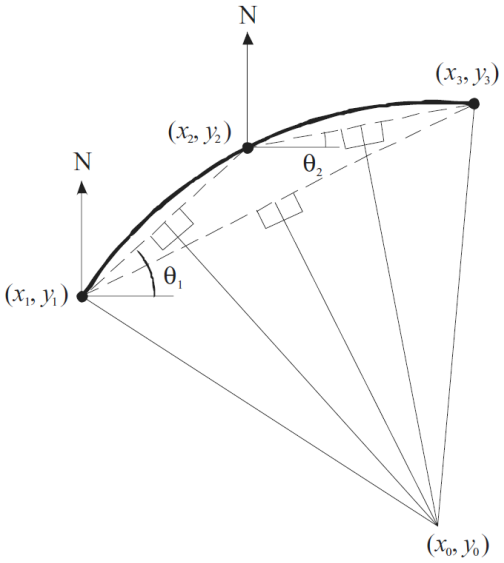

Figure 28. Adjustment of a curve as a function of two central points.

Additionally, they analyzed how GPS data frequency influenced the results. They used data collected at 0.1, 0.5 and 1 second interval. They determined that the difference of using 0.1 and 0.5 s data was negligible (1.55% vs. 1.40% error compared to the actual geometry). On the contrary, the difference was quite higher when using 1-second collected data (error of 2.34%).

3.3.4.2.3. Analytic solutions

The road elements present some geometric constraints, such as continuity or tangency. These conditions can be used for determining the horizontal alignment of the road. Due to the complexity of those relationships, there are a few methods of this group. The complexity of the road they can treat is also limited. Some assumptions are indeed needed.

Easa et al. (2007) used satellite imagery for detecting the horizontal layout of circular curves, as well as broken-back curves without intermediate tangent. The basic assumption was that no spiral transitions existed. It was a semi-automatic process. The user selects the zone where the curve exists and a computer program fits the optimal geometry. Figure 29 shows some geometric relationships between the different road elements.

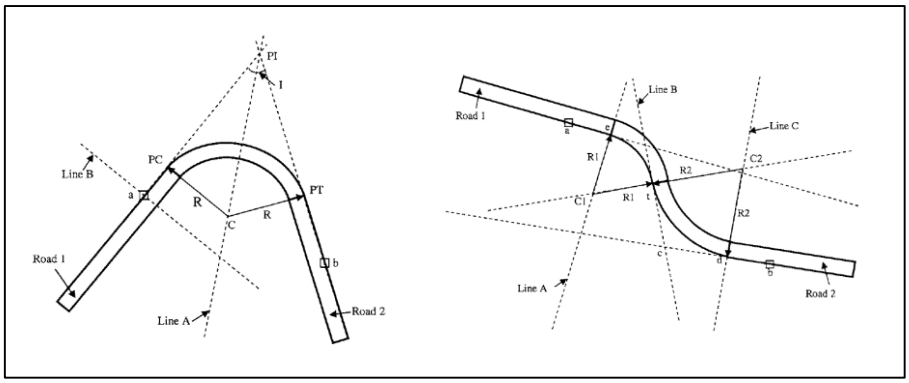

Figure 29. Some geometric relationships for simple horizontal layouts.

Dong et al. (2007) improved this methodology, also considering the transition curves. They adapted the transition curves to 3-degree functions, thus allowing in an easier way to perform the tangency condition both in the tangency and the curve points. The process is quite complex, so this methodology was limited to easy road layouts, as well as symmetric curve configurations. Figure 30 shows one example.

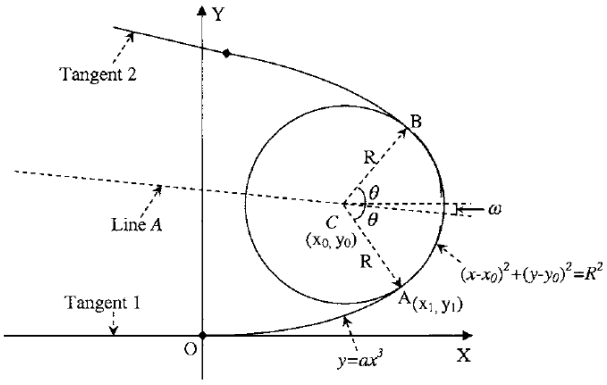

Figure 30. Geometric relationship for a sequence of spiral – circular curve – spiral.

Gikas and Strakatos (2012) presented a methodology based on fractal theory to recreate horizontal alignments. They pointed out that curvature and heading profiles include a lot of noise in the measurements. They used fractal theory to filter both. As a result, they created a much more readable curvature profile from which they could accurate estimate the initial/end points of each horizontal element. Once this has been detected, it is very easy to determine their characteristics analytically.

3.4. Infrastructure factor and its relation to human factor

3.4.1. Driver behavior according to road geometry

Road geometry affects drivers in several ways. The road design imposes some constraints to drivers, forcing them to vary direction and speed. There is a high variability of the drivers' response, so they do not always respond as expected. Some of these behaviors may lead to accidents or conflicts. This is why the relationship between geometry and driver behavior is so important.

Road geometry can be analyzed through several indicators. The most evident – but difficult to measure – is the evolution of their position, i.e., curve negotiation or lateral position. Hence, there are other, simpler indicators to study, such as the speed and the speed variation (longitudinal acceleration).

Speed is important since it is related to two factors: safety and performance. A higher speed implies a better performance, since drivers spend less time travelling. On the contrary, a higher speed is linked to a higher workload demand, altering the probability of an accident to appear. In addition, the kinetic energy increases, so the severity of a hypothetic accident also does. It is worth to mention that the speed dispersion has a higher influence than the speed magnitude on accident occurrence, but it is commented in the corresponding section.

The acceleration – speed variation – is also very important. In this topic, acceleration is normally divided into two components: longitudinal and lateral acceleration.

Longitudinal acceleration indicates how the operating speed varies. It is more related to safety rather than on comfort. Two indicators are worth to mention: speed reduction and deceleration. Both of them are highly related to road safety, since high speed reductions or decelerations are linked to a sudden variation of driver performance. An abrupt change is normally explained because of a driver surprise. The consequences might be a rear-end crash or a run-off the way accident. There are several safety performance functions that estimate crash rates based on speed reductions. There are also several speed reduction models, based on geometric features.

Lateral acceleration is linked to driver comfort and safety. Lateral acceleration is caused because of a variation of the direction of the speed. It is calculated as Equation 17, where v is the longitudinal operating speed and R is the local radius.

$$a_t = \frac{v^2}{R} \tag{17}$$

A lateral acceleration implies a centripetal force on drivers. This force is annoying for them, so they will try to reduce this acceleration. There are two ways of doing it: by reducing the operating speed or smoothing the radius. The analysis of how drivers try to compensate the centripetal force by changing their lateral evolution is called curve negotiation.

The centripetal force is also linked to vehicle stability (see Consistency Criterion III). The higher the centripetal force is, the higher the friction demand is. If the demanded friction is too high, the pavement will not be able to keep the vehicle onto it. This is why this parameter is also linked to road safety.

3.4.1.1. Curve negotiation

As we indicated in the corresponding section of the Human Factor chapter, there are two kinds of aberrant behaviors: violations and errors. This is highly related to curve negotiation, since both kinds of aberrant behaviors lead to different aberrant road behaviors. Depending on them, there are different types of accidents more likely to appear, as well as different solutions.

Aberrant behaviors can be due to:

- The driver negotiates the curve far away from its design on purpose (violation). One example is when the driver cuts a left-handed curve.
- The driver misperceives the curve and negotiates it in a non-convenient way for its actual design. This is an error. When drivers notice the actual road design, they might correct their behavior, possibly originating high lateral accelerations which might be dangerous.

A high accident concentration at a certain curve may be due to one of the aforementioned reasons. Both of them can be controlled through its design. The countermeasure for the first one will be something to prevent drivers to cut off the

curve. The countermeasure for the second one would be a redesign in order to let drivers to adequately perceive it.

Friedinger (1980) pointed out that the optical structure of the road space changes when going from a tangent to a curve. For some curves it is really difficult to follow a parallel path, probably increasing the likelihood of uncertainties and steering corrections.

It is not easy how to measure and quantify curve negotiation. Spacek (2005) distinguished two groups of track behavior:

- Normal behavior. The vehicle tracks basically follow the ideal line in the center of the driving lane.
- Extreme behavior. The vehicle tracks strongly differs from the ideal line. This is the group where both types of aberrant behaviors are located at.

Spacek (2005) analyzed drivers' curve negotiation at eight horizontal curves of two-lane rural highways (four in each direction). He used 12 autonomous measuring units (distanciometers), built in delineator poles. Thus, he could determine the vehicle's path with highly accurately, as well as determining the operating speeds. He also considered different vehicle's width for determining the center of each vehicle type: passenger cars 1.80 m, heavy vehicles 2.50 m, and motorcycles 0.80 m. All horizontal curves were isolated, presenting an inferred design speed lower than the speed limit. Radii ranged from 65 to 220 m. Deflection angle did from 48 to 146 gon. Longitudinal grade was limited to 3%. He measured over 200 vehicles for each curve.

A computer program was developed in order to determine speed, lateral acceleration and the radial friction, also considering the superelevation rate.

According to AGVS (1980), Spacek identified six track types (Figure 31):

- Ideal behavior (I). This is a symmetrical track path within a narrow area along the center of the lane. This is the idealized path of the design standards.
- Normal behavior (N). Symmetrical path track along the center of the lane, but within a somewhat broader area than with the ideal behavior and with slight cutting to the inside of the curve, without the vehicle edges touching the centerline.
- Correcting (K). S-shaped track path with increased drifting toward the outside of the curve and subsequent correction of the steering angle in the

second half of the curve. It is assumed that this track type corresponds to a misperception error by the driver.

- Cutting (C). A track path with strong cutting to the inside of the curve within the area of the circular arc. This is a conscious driving trying to compensate the centrifugal force.
- Swinging (S). Asymmetrical track path between the beginning and end of the curve with a pronounced tendency to drive on the right side at the beginning and an increasing drift to the left toward the end of the curve.
- Drifting (D). Asymmetrical track path between the beginning and end of the curve with a pronounced tendency to drive on the left side at the beginning of the curve and an increasing drift to the right toward the end.

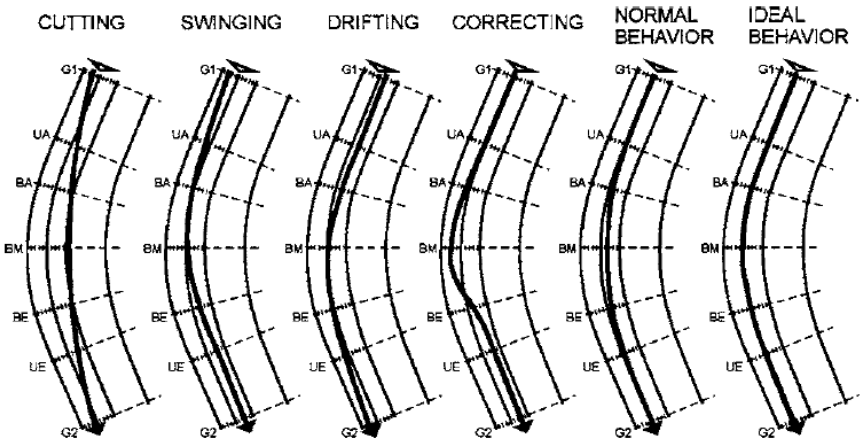

Figure 31. Different types of driver trajectories (Source: Spacek (2005)).

Those are the ideal track types. Not all observed paths followed by actual drivers fit one of these groups. A range zone was defined in order to classify the vehicles. 20% of all recorded trajectories did not fit any of the ideal track behavior shapes.

No evident relationships between track type and curve geometry were identified. The desired track types I and N were more frequent when the ratio A/R was between 0.33 and 0.50. The proportion of unwanted track types increased for ratios about 0.80 or when there was no spiral transition.

Said et al. (2007) used an instrumented vehicle for determining the conditions under the driver performance better fitted the road design. A 110-km long route was

chosen for the experiment, consisting of several highway classifications, design speeds, and both rural and urban highways. 30 volunteers, male and female, ranging from 20 to 50 years old drove the instrumented vehicle. The extracted data included vehicle path, vehicle's speed, centripetal force and heading to the preceding vehicle.

Considering the vehicle path, they found several curves where the drivers did not perceive the actual curvature before they should. This case was found for curves with and without spiral transitions. As a result, drivers had to rapidly correct their path with a sharper curve, thus producing a higher centripetal force.

On the contrary, curves with no perception problems presented a pretty different behavior. In those cases, if possible, drivers started their curve negotiation earlier the beginning of the curve, thus producing an operating curve smoother than the existing one. It is worth to highlight that previous research identified that road crashes at curves are more linked to the operating alignment than to the design one.

They also observed that in several cases spiral transitions designed according to guidelines were not enough for drivers to completely acquire the corresponding curvature. Thus, the drivers needed to compensate that by increasing their operational curvature and thus producing a safety hazard.

Othman et al. (2013) determined that the highest record of lateral acceleration and yaw rate took place on the curve entrance, regardless of the radius and the curve direction. The speed was found to be practically constant along all the curve, as reflected by previous literature. Thus, the lateral acceleration variations were mostly due to changes in the local operating curvature. They examined data from 5922 trips of seven passenger cars driven by 22 different drivers.

3.4.1.2. Longitudinal behavior. Operating speed

Operating speed is one of the most well-known factors of driver performance. There exist lots of research efforts carried out in this way. This better knowledge allows the correct estimation of a lot of performance factors as well as some relationships to road crashes, such as those developed considering the speed reduction or deceleration rates.

We can distinguish two kinds of speed:

- The speed developed under free-flow conditions, only being conditioned by the road geometry. This is known as operating speed. In order to use a

single parameter instead of a range of speed distributions, the 85th percentile of the free-flow speed is considered as operating speed. Normally a headway of 5 seconds is accepted for free-flow conditions.

- Speed influenced by other factors, such as traffic.

Some geometric design features impose a speed control on drivers. This means that there is a physical restriction to the operating speed. A higher speed means a lower stability. Thus, depending on the conditions, drivers will be enforced to select a speed lower than a certain value. On the other hand, there are several geometric features that are not a speed control. One example are tangents. In this case, speed is more controlled by social and risk perception, as well as the vehicle performance.

Therefore, the speed dispersion is different depending on the speed control imposed by the geometry. Operating speeds have been found to be normally distributed (Donnell et al., 2009). The same condition was found in Spain (Pérez-Zuriaga, 2012). However, as explained above, the mean and variance parameters of both speed distributions differ (Figure 32).

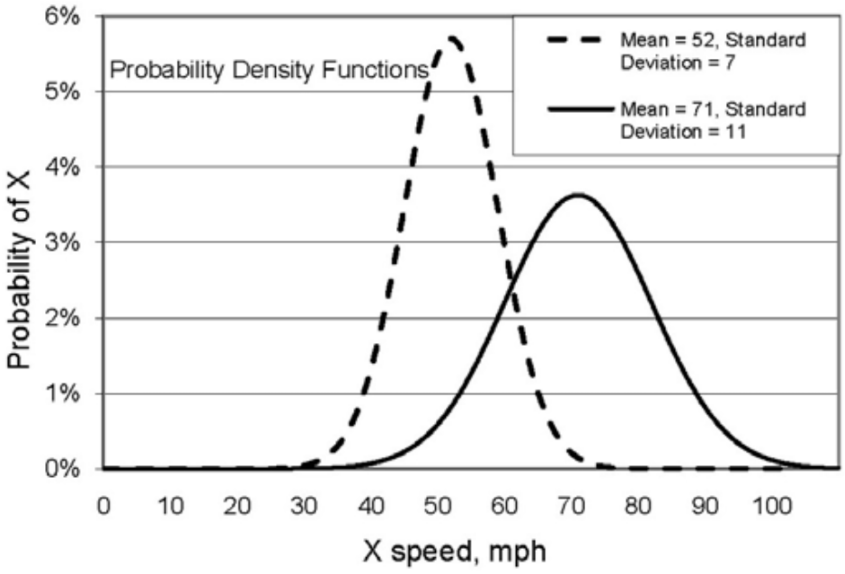

Figure 32. Example of probability density functions for tangent and curve sections. Adapted from Donnell et al. (2009).

The operating speed distribution for curves presents a lower mean as well as a lower dispersion. This is because of the geometric control imposed by the curve. This geometric control is normally the curve radius. The operating speed increases as the radius does. As the geometric control limitations disappear, the social factors take more place in the establishment of the operating speed, thus growing the speed dispersion.

The operating speed distribution for tangents normally presents a higher mean, as well as a higher dispersion. This is because there is no geometric control, so users select their speed (desired speed) accordingly.

As explained in the corresponding section, operating speed is the speed selected by drivers with no traffic or environmental restrictions, i.e., free-flow conditions. Hence, when we mention operating speed, we are referring to the whole distribution of speeds. This definition is not easy to deal with, since it is not a single value. Parameters such as the mean, variance and percentile should always be mentioned while talking about it. In order to avoid this, we normally consider the operating speed as the 85^{th} percentile of the free-flow speed.

The analysis of the operating speed is a good way to figure out drivers' behavior. For already built up roads the operating speed can be easily observed. On the contrary, the operating speed cannot be directly measured on non-built up roads. This makes it necessary to develop ways to estimate it. The most well-known procedure to estimate operating speeds is by means of operating speed models. These are some expressions that estimate the operating speed as a function of some – usually geometric – features. They were previously calibrated by means of observation, so we are introducing this at first.

There are several methodologies to observe operating speed. Spot data location methods are the simplest way to collect operating speed data. Radar guns are a different way. The user only has to stay in an area close to the road and point the gun towards the vehicle. The distance and speed of the vehicle is therefore obtained. This is a rapid and economic way to take operating speeds, but it presents three important issues:

- Cosine error. The person responsible of data collection has to stay completely perpendicular to the road. If this is not the case, the operating speed will be biased. This is especially problematic on horizontal curves, since the trajectory of the vehicles are continuously changing.

- Manual data collection. This is not an automatic data collection, so the user might commit some errors while collecting and writing down data.
- Driver biasing. Drivers perform naturally as long as they don't notice the data collection process. Hence, the data collector should be hided from the traffic stream, which is not always easy.

Some of these issues can be addressed by means of different road collection methods. Some examples are piezoelectric sensors embedded in the pavement and connected to traffic counters. Pneumatic tubes are a different possibility, although the drivers notice the system and they get biased.

The most important issue with spot-speed data collection is its own nature. They collect the operating speed at a single point. Therefore, the only output is the speed at that point, not having any information about the longitudinal speed variation. This is a major issue, since the location of the collecting device affects the results.

Spot-speed data collection systems on curves has normally been placed in their midpoint. The underlying hypothesis is that this is the point where the minimum operating speed is achieved. This hypothesis was later checked by Pérez-Zuriaga (2012). The selection of the operating speed location for data collection at tangents is normally more controversial. Some researchers select the midpoint of the tangent. Some others select 200 m or 100 m before the point of curvature. In all those cases, there is no evidence whether this is the location where the maximum operating speed (desired speed) is achieved. Moreover, there is no evidence whether the maximum operating speed has been reached. The more important issue appears when trying to estimate the speed reduction or deceleration rate on a tangent-to-curve transition. In the first case we need to know the maximum and minimum speeds reached, as well as if the desired speed was reached. In addition, for the second case we also need to know the exact location where they are achieved. This makes this data collection method impractical.

Some researchers, such as Misaghi and Hassan (2005), developed operating speed models for curves and a speed reduction model overcoming the existing limitations by means of collecting speed data at five spots along each curve.

Those errors can be addressed with continuous operating speed collection methods. All of them collect data on a longitudinal road section. Depending on the method, some other issues might appear.

Continuous operating speed can be obtained from video recordings. This requires a video camera installed on an elevated location. The video camera must have a good resolution, as well as a controlled lenses distortion. This is a very good way to record vehicles, since there are several possibilities to place the camera without disturbing the traffic. On the other hand, these recordings are also valid for restoring the vehicle's path, as well as for determining some other parameters.

On the other hand, this methodology is not valid for recording all places. A suitable, free of obstacles terrain should be available. Only a small section can be recorded, because of the amplitude of the lenses. The major issue is the post-processing requirements. Advanced software is required for analyzing all data.

Instrumented vehicles are a different way to obtain continuous operating speeds. This methodology consists on a vehicle equipped with different measuring devices, such as GPS, accelerometer, cameras, etc. The impressions of drivers can also be recorded. Thus, the accuracy and number of parameters are maximum. In addition, the post-processing is very fast. The disadvantage of this method is driver biasing. Drivers must be volunteers, often knowing the scope and aims of the research project, which might influence their response. Even in the case they are not aware of them, they are driving an instrumented vehicle which is not their own vehicle. Those devices and the different vehicle per se make it difficult for drivers to perform naturally, thus affecting the results.

An innovative continuous data collection methodology was presented by Pérez-Zuriaga et al. (2013). This consists on giving small GPS tracking devices to actual users of a certain road. Those GPS devices were placed outside the vehicle, thus affecting drivers as less as possible. In addition, they were encouraged to drive naturally. The scope of the research project was given by researchers at the second checkpoint. Drivers are aware of the GPS recording unit, although they do not know what it is. In addition, they performed a test to compare operating speeds with and without GPS devices, determining that drivers were not biased.

3.4.1.2.1. Operating speed estimation on horizontal curves

There are a lot of operating speed models for horizontal curves. Most of them only use one or two geometric parameters, since they impose a speed control for drivers. The parameter most widely used is the radius. Normally, the operating speed prediction models for horizontal curves do not consider the vertical alignment.

The R^2 parameter is given as a measure to estimate the goodness-of-fit of the adjustment. But this does not mean that a higher correlation parameter corresponds to a better model. Several more aspects do have influence, such as the number of elements, or whether the speed data is aggregated or not.

The variability of operating speed is due to some factors not considered in the model. Several of them are social factors, which highly depend on the region where the model is developed. This entails that one should be very confident on the validity of an operating speed model before applying it to a certain road. It is normally preferred a worse operating speed model for the same region than a better operating speed model calibrated for a different one.

Lamm, Hayward and Cargin (1986) developed some operating speed models for horizontal curves based on the curvature change rate (CCR) for a single curve. The curvature change rate measures how twisty an alignment is, dividing the sum of the absolute deflection angles (gon) over the length (km). It can be applied to a whole road segment (*CCR*) or to a horizontal curve, including spiral transitions (CCR_S) (Equation 18).

$$CCR_S = \frac{63700 \cdot \left(\frac{L_{cl1}}{2 \cdot R} + \frac{L_c}{R} + \frac{L_{cl2}}{2 \cdot R}\right)}{L_{cl1} + L_c + L_{cl2}} \tag{18}$$

They suggested the use of this parameter since it was more correlated to the operating speed than other geometric parameters, such as the curve radius, deflection angle, etc. They used horizontal curves from United States, Germany, Greece and Italy for the analysis.

Lamm and Choueiri (1987) analyzed 84 horizontal curves with a lane width of 3.65 m, obtaining the expressions in Equations 19 and 20.

$$v_{85} = 95.780 - 0.076 \cdot CCR \qquad R^2 = 0.84 \tag{19}$$

$$v_{85} = 96.152 - \frac{2803.769}{R} \qquad R^2 = 0.82 \tag{20}$$

Three years later, they analyzed 322 horizontal curves of two-lane rural highways. They found the radius as the most influencing factor. They developed the model shown in Equation 21.

$$v_{85} = 94.378 - \frac{3188.9}{R} \qquad R^2 = 0.79 \tag{21}$$

Kanellaidis et al. (1990) developed an operating speed model for curves considering 58 horizontal curves in Greece. The model is shown in Equation 22.

$$v_{85} = 129.88 - \frac{623.1}{\sqrt{R}} \qquad R^2 = 0.78 \qquad (22)$$

Morrall and Talarico (1994) related the operating speed of horizontal curves to the degree of curvature. In this case, the longitudinal grade for those curves ranged from -5% to +5%. Equation 23 resumes the model.

$$v_{85} = e^{4.561 - 0.0058 \cdot DC} \qquad R^2 = 0.63 \qquad (23)$$

The degree of curvature (DC) is defined as the angle which defines a 100 m long circular arc. It is related to the radius as expressed in Equation 24.

$$DC = \frac{5729.58}{R} \qquad (24)$$

This equation was later expressed in terms of curvature change rate by Lamm, Psarianos and Mailaender (1999) (Equation 25). This model also considers the transition curves.

$$v_{85} = e^{4.561 - 0.000527 \cdot CCR_S} \qquad R^2 = 0.63 \qquad (25)$$

Some operating speed models for horizontal curves include more than one parameter in their definition. Hence, they achieve a better correlation at the expense of needing more data. However, the difference in terms of correlation compared to the rest of models is not noticeable.

Krammes et al. (1995) developed a model based on the curve radius, its length and its deflection angle (Δ, in sexagesimal degrees) (Equation 26). They used 138 horizontal curves. This model was later validated by Collins and Krammes (1996). This is a very well-known model. It is valid for horizontal curves with and without spiral transitions.

$$v_{85} = 102.4 - \frac{2742}{R} + 0.012 \cdot L - 0.10 \cdot \Delta \qquad R^2 = 0.82 \qquad (26)$$

McFadden and Elefteriadou (2000) analyzed 78 horizontal curves, developing two operating speed models (Equations 27 and 28). Those models depend on the operating speed of the preceding tangent, which has been proved to be a reliable parameter for operating speed estimation.

$$v_{85} = 103.66 - 1.95 \cdot DC \qquad R^2 = 0.80 \qquad (27)$$

$$v_{85} = 41.62 - 1.29 \cdot DC + 0.0049 \cdot L - 0.12 \cdot \Delta + 0.95 \cdot v_T \qquad R^2 = 0.90 \qquad (28)$$

Fitzpatrick and Collins (2000) developed one of the most comprehensive models for operating speed estimation on horizontal curves. They kept the radius as the most important parameter, but they developed different equations depending on the horizontal-vertical alignment coordination. As a result, six operating speed models for passenger cars were developed. Table 3 (Equations 29 to 34) resumes the model.

Case	Model	N	R^2	MSE	Eq #
Horizontal curve with longitudinal grade ranging from 0% to 4% Horizontal curve with sag vertical curve	$v_{85} = 106.30 - \frac{3595.29}{R}$	28	0.92	2.84	(29)
Horizontal curve with longitudinal grade between 4% and 9%	$v_{85} = 96.46 - \frac{2744.49}{R}$	14	0.56	6.86	(30)
Horizontal curve with longitudinal grade ranging from -9% to 0%	$v_{85} = 100.87 - \frac{2720.78}{R}$	22	0.59	6.38	(31)
Horizontal curve combined with crest vertical, limited sight distance vertical curve (K<43)	$v_{85} = 101.90 - \frac{3283.01}{R}$	16	0.78	3.95	(32)
Horizontal tangent combined with crest vertical, limited sight distance vertical curve (K<43)	$v_{85} = 111.07 - \frac{175.95}{K}$	6	0.54	6.30	(33)
Horizontal tangent combined with sag vertical curve	$v_{85} = 100.19 - \frac{126.07}{K}$	5	0.68	3.51	(34)

Table 3. Fitzpatrick and Collins (2000) operating speed model.

N is the number of geometric features considered for each calibration. MSE is the Minimum Square Error. Due to the small amount of geometric curves considered in the analysis, this model should be carefully used.

Lamm, Psarianos and Cafiso (2002) developed a model for estimating operating speed on horizontal curves based on data extracted from Australia, Canada, France, Germany, Greece, Italy, Lebanon and United States. This model is composed by two expressions (Equations 35 and 36). In this case, *G* is the longitudinal grade of the road. Both expressions are valid only for CCR_S values lower than 1600 gon/km. The first expression should be used for longitudinal grades of 6% or lower, using the second expression otherwise.

$$v_{85} = 105.31 + 2 \cdot 10^{-5} \cdot CCR_S^2 - 0.071 \cdot CCR_S \qquad R^2 = 0.98 \qquad (35)$$

$$v_{85} = 86 - 3.24 \cdot 10^{9} \cdot CCR_S^3 + 1.61 \cdot 10^{-5} \cdot CCR_S^2 - 4.26 \cdot 10^{-2} \cdot CCR_S \qquad R^2 = 0.88 \qquad (36)$$

Castro et al. (2008) developed another equation for estimating the operating speed on horizontal curves of Spain (Equation (37). This equation is also dependent on the radius and it was calibrated with 18 horizontal curves.

$$v_{85} = 120.16 - \frac{5{,}596.72}{R} \qquad R^2 = 0.75 \qquad (37)$$

They later developed an operating speed model for Colombian curves (Castro et al., 2011) which depends on the length of the curve (L_c) and the deflection angle (Ω, gon) (Equation (38). The model was calibrated using 22 curves.

$$v_{85} = 91.1323 + 0.0328341 \cdot L_c - 0.481729 \cdot \Omega \qquad R^2 = 0.76 \qquad (38)$$

Some other researchers tried to overcome the barriers of this methodology by considering the operating speed values of different spots. The first example was carried out by Seneviratne and Islam (1994). They developed models for the initial point (point of curvature, PC), the midpoint (MC) and the final point of the curve (point of tangency, PT) (Table 4, Equations 39 to 41). Their models were based on data extracted from eight horizontal curves, which is considered a low sample. This is also the reason of their high regression coefficients.

These models show how the operating speed increases as the curve is covered by the user. The minimum degree of curvature was 6º.

Case	Model	R^2	Eq #
Point of Curvature	$v_{85} = 95.41 - 1.48 \cdot DC - 0.012 \cdot DC^2$	0.99	(39)
Midpoint	$v_{85} = 103.03 - 2.41 \cdot DC - 0.029 \cdot DC^2$	0.98	(40)
Point of Tangency	$v_{85} = 96.11 - 1.07 \cdot DC$	0.90	(41)

Table 4. Seneviratne and Islam (1994) operating speed model.

Gibreel et al. (2001) performed a similar approach, by considering five spot locations where the operating speed was measured. They also considered the tridimensional nature of the road. Hence, they selected 9 sections of a sag vertical curve combined with a horizontal curve, and 10 sections of a crest vertical curve combined with a horizontal curve.

They selected 5 points according to the following criteria (Figure 33 and Table 5):

- Point 1 was set at about 60-80 m on the preceding tangent, before the beginning of the spiral curve. This point was selected because it was where the driver may anticipate the effect of the 3D combination before travelling on it.
- Point 2 was the end of the spiral curve.
- Point 3 was the midpoint of the horizontal curve.
- Point 4 was the end of the horizontal curve and the beginning of the spiral transition.
- Point 5 was set out at 60-80 m on the departure tangent after the end of the spiral curve. The driver might still be affected by the 3D combination after travelling through it.

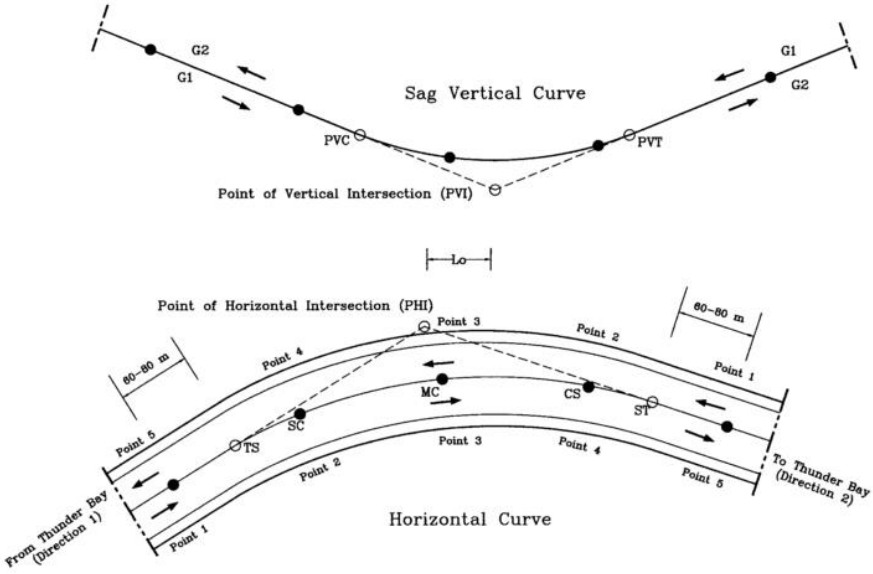

Figure 33. Spots where the operating speed was measured.

Model	R^2	Eq #
$v_{s1} = 91.81 + 0.010 \cdot r + 0.468 \cdot \sqrt{L_v} - 0.006 \cdot G_1^3 - 0.878 \cdot \ln A - 0.826 \cdot \ln L_0$	**0.98**	(42)
$v_{s2} = 47.96 + 7.217 \cdot \ln r + 1.534 \cdot \ln L_v - 0.258 \cdot G_1 - 0.653 \cdot A - 0.008 \cdot L_0 + 0.020 \cdot e^E$	**0.98**	(43)
$v_{s3} = 76.42 + 0.023 \cdot r + 2.30 \cdot 10^{-4} \cdot K^2 - 0.008 \cdot e^A - 1.23 \cdot 10^{-4} \cdot L_0^2 + 0.062 \cdot e^E$	**0.94**	(44)
$v_{s4} = 82.78 + 0.011 \cdot r + 2.067 \cdot \ln K - 0.361 \cdot G_2 - 0.036 \cdot e^E - 1.091 \cdot 10^{-4} \cdot L_0^2$	**0.95**	(45)
$v_{s5} = 109.45 - 1.257 \cdot G_2 - 1.586 \cdot \ln L_0$	**0.79**	(46)

Table 5. Gibreel et al. operating speed model for curves.

Where:

r: radius of the horizontal curve (m).
L_v: length of vertical curve (m).
E: superelevation rate (%).
A: algebraic difference in grades (%).
K: rate of vertical curvature (m).
G_1 and G_2: first and second grades in the direction of travel (%).
L_0: horizontal distance between point of vertical intersection and point of horizontal intersection (m).

Himes et al. (2011) developed a comprehensive research about the operating speed variability. The most important contribution was that they considered many exogenous and endogenous parameters into a 3-equation systems, performing a

3OLS regression. They collected data at 79 sites on eight roads in Pennsylvania and Virginia. Five of the roadways were two-lane rural and three were suburban two-lane. The operating speeds were collected using traffic counters.

$$\begin{cases} PSL = \alpha_{PSL} + X_{PSL} \cdot \beta_{PSL} + u_{PSL} \\ s = \alpha_s + X_s \cdot \beta_s + PSL \cdot \gamma_s + u_s \\ d = \alpha_d + X_d \cdot \beta_d + PSL \cdot \gamma_d + s \cdot \theta_d + u_d \end{cases} \quad (47)$$

Where:

PSL: Posted speed limit (kph).
s: mean speed (kph).
d: speed deviation (kph).
α: constant for posted speed limit, mean speed and speed deviation, respectively.
X: vector of exogenous variables (geometric traffic flow, etc.) for posted speed, mean speed and speed deviation, respectively.
β: vector of estimable regression parameters for exogenous variables.
u: random disturbance term for posted speed limit, mean speed, and speed deviation, respectively.
γ: estimable regression parameters for the posted speed limit endogenous variable in the mean speed deviation equation, respectively.
θ: estimable regression parameters for the mean speed and speed deviation endogenous variables.

They took an econometric approach to the problem, using three-stage least squares (3SLS). The 3SLS estimator addresses endogeneity and it is a full-information estimator, allowing error covariance. The error covariance may result from shared unobservables between posted speed, mean speed and speed deviation that are not included in the model.

They observed some parameters such as the horizontal curve direction, vertical curve type, adjacent land use, curb and gutter (present or not), rural/urban, median or turning lane, at-grade rail crossing an on-street parking.

They found that the speed deviation does not appear in the mean speed equation. Therefore the mean speed is not affected by speed deviation. However, the speed deviation is affected by the mean speed, as found by previous researchers.

They assumed that the operating speed was normally distributed, so the 85th percentile operating speed could be obtained by the mean speed plus a standard deviation.

3.4.1.2.2. Operating speed estimation on tangents

Tangents do not impose a speed control on drivers. Thus, the operating speeds on tangents are normally higher than on curves, as well as their speed dispersion. Instead of radius (this parameter makes no sense on tangents), some other parameters are normally considered. Some examples are the tangent length, the radius of the preceding and/or following curve, lane and shoulder width, etc.

Depending on how drivers perform on tangents according to the operating speed, tangents can be divided into two groups (Lamm et al., 1988):

- Independent tangents. They are pretty long tangents. Drivers can fully develop their desired speed. Thus, the maximum speed reached (and maintained) is not affected by any geometric control, such as the preceding or following curve. Operating speed dispersion is maximum in this case, thus only existing a few models. The correlation parameters are quite lower than for horizontal curves.
- Non-independent tangents. This is when the independence condition is not met. In this case, the tangent is shorter, so drivers cannot achieve their desired speed. They select a different, lower operating speed, based on their perception of the alignment constraints. Some parameters of the adjacent geometric controls might influence drivers' behavior. The operating speed dispersion is lower in this case (but higher than for horizontal curves).

Several researchers provided different desired speed values for independent tangents:

- Morrall and Talarico (1994): 95.7 km/h.
- Lamm and Choueiri (1987): 94.4 km/h.
- Ottesen and Krammes (2000): 97.9 km/h.
- Fitzpatrick and Collins (2000): 100 km/h.
- Easa (2003a): 100 km/h for two-lane rural highways with a 90 km/h speed limitation.

Polus, Fitzpatrick and Fambro (2000) developed a comprehensive study about drivers on tangents of different types. They developed classification criteria, as well as operating speed models for each one of those groups. Instead of the tangent length (T_L), they introduced a secondary variable, the Geometric Measure (*GM*), which also considers the constraining elements as well. There are two definitions of this measure, depending on a threshold (t) for the tangent length. This threshold was established to 150 m. Equations 48 and 49 show how this parameter is calculated.

$$GM_S = \frac{R_1 + R_2}{2}; L_T < t \quad (48)$$

$$GM_L = \frac{\left[L_T \cdot (R_1 \cdot R_2)^{\frac{1}{2}}\right]}{100}; L_T \geq t \quad (49)$$

Where:

R_1: radius of the preceding curve (m).

R_2: radius of the following curve (m).

L_T: tangent length (m).

Four groups of tangents were identified:

- Group 1. Radii of the preceding and following curves lower than 250 m. Tangent length lower than 150 m. Equation 50.
- Group 2. Radii of the preceding and following curves lower than 250 m. Tangent length between 150 and 1000 m. Equation 51.
- Group 3. Radius of both curves higher than 250 m. Tangent length between 150 and 1000 m. Equation 52.
- Group 4. Tangent length higher than 1000 m. Equation 53.

$$v_{85} = 101.11 - \frac{3420}{GM_S} \qquad R^2 = 0.553 \quad (50)$$

$$v_{85} = 98.405 - \frac{3184}{GM_L} \qquad R^2 = 0.684 \quad (51)$$

$$v_{85} = 97.73 - 0.00067 \cdot GM \qquad R^2 = 0.2 \quad (52)$$

$$v_{85} = 105.00 - \frac{22.953}{e^{0.00012 \cdot GM_L}} \qquad R^2 = 0.838 \quad (53)$$

Jessen et al. (2001) developed an operating speed model for tangents not based on geometric features. They considered other factors, such as speed limit (v_l) and *AADT* (Equation 54).

$$v_{85} = 70.2 + 0.434 \cdot v_l - 0.001307 \cdot AADT \quad (54)$$

Himes et al. (2011) found that the geometric design features on two-lane roads were not correlated with the posted speed limit. Hence, the speed limit should not be ignored as a predictor of operating speed. They examined the speed and speed limit of 79 locations, finding that there was a positive correlation between the posted speed limit and the mean speed. A one mph increase of the speed limit induces a 0.6 mph increase of the mean speed.

3.4.1.2.3. Operating speed variation and acceleration/deceleration rates

It is not possible to depict an operating speed profile if there is no speed transition between the different geometric features. The previous two sections have introduced some models to estimate operating speed at certain geometric elements, but speed transition rates are necessary to create a continuous operating speed profile.

Operating speed variation between the different geometric features is of a major importance. Two different approaches can be found:

- Analysis of the operating speed reduction. The scope is to relate operating speed reduction to road safety.
- Determination of acceleration and deceleration rates. The objective is to create operating speed profiles.

The operating speed reduction between two geometric features (normally between a tangent and a horizontal curve) has been several times related to crash frequency. The higher the speed reduction, the higher the crash rate.

Literature has commonly referred to this parameter as 85th percentile of the operating speed reduction. As a first sight, it might seem that it can be calculated as the difference between the operating speeds of a tangent and the following curve. However, this is not true, as shown by Hirshe (1987). Drivers do not behave uniformly, i.e., they might behave differently at tangents and curves, changing their percentile behavior. Thus, the drivers corresponding to the 85th percentile operating speed on the tangent and the one corresponding to the 85th percentile on the curve are not the same. Speed distributions are also quite different. Both conditions make

the 85th percentile of the operating speed reduction to be higher than the simple difference of the operating speeds.

Al-Masaeid et al. (1995) developed some expressions to estimate the 85th percentile of the operating speed reduction considering geometric parameters. Their expressions consider both the horizontal and vertical alignment, as well as the pavement conditions (Table 6).

Case	Model	Eq #
Level terrain	$\Delta v_{85} = 3.30 + 1.58 \cdot DC$	(55)
Constant longitudinal grade	$\Delta v_{85} = 1.84 + 1.39 \cdot DC + 4.09 \cdot P + 0.07 \cdot G^2$	(56)
Presence of vertical curvature	$\Delta v_{85} = 1.45 + 1.55 \cdot DC + 4 \cdot P + 0.00004 \cdot L_v^2$	(57)

Table 6. Al-Masaeid et al.'s operating speed models for tangent-to-curve transition.

Where:
DC: Degree of curvature (sexagesimal degrees).
P: Pavement condition (good shape: $P = 0$, $P = 1$ otherwise).
G: Longitudinal grade (%).
L_v^2: Length of the vertical curve within the horizontal curve (m).

They also studied the operating speed reduction between two consecutive curves, without intermediate tangent (Equation 58). R_1 and R_2 are the radii for both curves.

$$\Delta v_{85} = 5.081 \cdot \left(\frac{1}{R_2} - \frac{1}{R_1}\right) \qquad R^2 = 0.62 \qquad (58)$$

McFadden and Elefteriadou (2000) proposed two models to estimate the 85th percentile of the maximum operating speed reduction before a curve (Equations 59 and 60).

$$85\text{MSR} = -14.90 + 0.144 \cdot v_{85_{PC200}} + 0.01533 \cdot L_{APT} + \frac{954.55}{R} \qquad R^2 = 0.71 \qquad (59)$$

$$85\text{MSR} = -0.812 + \frac{998.19}{\text{R}} + 0.017 \cdot L_{APT} \qquad R^2 = 0.60 \qquad (60)$$

Where:
$85MSR$: 85th percentile of the maximum speed reduction into curve (km/h).
$v_{85_{PC200}}$: 85th percentile speed at 200 m prior to point of curvature (km/h).
R: horizontal curve radius (m).
L_{APT}: length of approach tangent (m).

They validated Hirshe's hypothesis, which states that the 85MSR is higher than the simple subtraction of the operating speeds.

Misaghi and Hassan (2005) developed a comprehensive study of the operating speed reduction, as well as its relationship to the operating speed difference.

- $\Delta_{85}v$. Operating speed reduction not exceeded by 85% or all users, driving at free-flow conditions, i.e. operating speed reduction. Its determination should be performed considering all individual operating speed reductions.
- Δv_{85}. Operating speed differential. It is the direct subtraction of the operating speed on the tangent and the following curve.

Some researchers have found relationships between both parameters, such as Misaghi and Hassan (2005) (Equation 61) and Castro et al. (2011) (Equation 62).

$$\Delta_{85}v = 0.97 \cdot \Delta v_{85} + 7.55 \qquad R^2 = 0.72 \qquad (61)$$
$$\Delta_{85}v = 0.704 \cdot \Delta v_{85} + 4.497 \qquad R^2 = 0.73 \qquad (62)$$

The other point of view for the study of speed variations between different geometric features is the conformation of the operating speed profile. Operating speeds for tangents and curves are normally calculated with the aim of depicting the operating speed profile of a road. Thus, speed transition models are required.

Traditionally, those models have been very difficult to calculate, since data was not available for the initial and final spots where the speed variation took place. Thus, these models are developing when continuous operating speed collection methods have been available. These models need to estimate not only the magnitude of the speed variation (acceleration/deceleration rate), but also where the speed change takes place.

First researchers proposed fixed values of acceleration and deceleration rates:

- Lamm et al. (1988) proposed 0.85 m/s^2 for acceleration and deceleration. These rates have been one of the most widely used in the entire world.

- Kockelke and Steinbrecher (1987) observed that acceleration and deceleration rates were mostly lower than 1.00 m/s^2, although higher values – up to 2.50 m/s^2 – were also recorded.
- Collins and Krammes (1996) observed acceleration rates ranging from 0.12 to 0.52 m/s^2 and deceleration rates ranging from 0.35 to 1.19 m/s^2.

Fitzpatrick et al. (2000) developed several models for estimating acceleration and deceleration rates (Table 7). Their most significant contribution was that the rates were not fixed, but varying depending on several parameters such as the curve radius.

Alignment condition	Deceleration rate	Acceleration rate
Horizontal curve with no vertical curve or with non-limiting sight distance vertical curve	0.00 $R \geq 436$ m $0.6794 - \frac{295.14}{R}$ (63) 175 m $\leq R < 436$ m 1.00 $R < 175$ m	0.00 $R > 875$ m 0.21 436 m $< R \leq 875$ m 0.43 250 m $< R \leq 436$ m 0.54 175 m $< R \leq 250$ m
Horizontal curve combined with sag vertical curve	1.00	0.54
Horizontal curve combined with limiting sight distance crest vertical curve		
Tangent combined with limiting sight distance crest vertical curve		

Table 7. Fitzpatrick et al.'s deceleration and acceleration models.

Crisman et al. (2004) developed similar speed variation rates, also depending on the curve radius (Table 8).

Radius (m)	Deceleration rate (m/s^2)	Acceleration rate (m/s^2)
R < 178	1.00	0.54
178 ≤ R < 437	0.50	0.43
437 ≤ R < 2187	0.20	0.20

Table 8. Crisman et al.'s deceleration and acceleration models.

Crisman et al. (2007) carried out a research focusing on the deceleration rates. They determined maximum, minimum and average rates for the percentiles 50th and 85th

of the operating speed. They found that in most cases deceleration took place in two phases:

- The driver detects the curve and stops accelerating.
- In a second phase, the driver brakes.

Figueroa and Tarko (2007) determined that the average deceleration rate was about 0.42 m/s^2. This value was clearly lower than the obtained by previous research, maybe because negligible and significant decelerations were mixed. As a result, they removed the negligible ones, thus leading to a deceleration rate of 0.69 m/s^2.

3.4.1.2.4. Operating speed profiles

An operating speed profile represents how the operating speed varies depending on the station for a certain road. It may present two possible natures:

- Observed operating speed profile. Only possible for existing road segments. It can only be obtained by applying continuous operating speed data collection methods.
- Estimated operating speed profile. Valid for non-existing and existing roads. This is depicted considering different operating speed models, as well as some construction rules.

This section contains some of the most important operating speed profile models, developed by different researchers along the last years. In most cases, they use their own operating speed models, which have already been introduced.

According to the operating speed profile model presented by Lamm, Psarianos and Cafiso (2002), the first step is to calculate the operating speed at horizontal curves according to Equations 35 and 36. The next step is the calculation of the operating speed on tangents. There are different cases depending on the length of the tangent (T_L). Acceleration and deceleration rates of 0.85 m/s^2 are used. Two additional parameters are defined (Figure 34):

- $T_{L_{\min}}$. Minimum length required for changing the speed from a curve to the next one. As the acceleration and deceleration rates are the same, its calculation is always the same. It is calculated as expressed in Equation 64.
- $T_{L_{\max}}$. Minimum length between two consecutive curves required for accelerating, reaching the desired speed on the tangent, and decelerating,

always using the corresponding acceleration and deceleration rates. It is calculated as expressed in Equation 65.

$$TL_{min} = \frac{\left|{v_{85}}_1^2 - {v_{85}}_2^2\right|}{2 \cdot a} = \frac{\left|{v_{85}}_1^2 - {v_{85}}_2^2\right|}{22.03} \quad (64)$$

$$TL_{max} = \frac{{v_{85}}_{Tmax}^2 - {v_{85}}_1^2}{2 \cdot a} + \frac{{v_{85}}_{Tmax}^2 - {v_{85}}_2^2}{2 \cdot a} = \frac{2 \cdot {v_{85}}_{Tmax}^2 - {v_{85}}_1^2 - {v_{85}}_2^2}{22.03} \quad (65)$$

Where:

v_{85_i}: operating speed of the corresponding curve ($i = 1,2$) (kph).

a: acceleration/deceleration rate (m/s^2).

${v_{85}}_{Tmax}^2$: desired speed, calculated with the operating speed model for curves but using $CCR_s = 0$ gon/km.

If the tangent is shorter than $T_{L_{\min}}$, the required acceleration/deceleration rate will be higher, thus being a risk factor. If the tangent is longer than $T_{L_{\max}}$, the driver reaches the desired speed and keeps it for some distance. If the tangent length remains between $T_{L_{\min}}$ and $T_{L_{\max}}$, the driver accelerates up to a maximum speed (lower than the desired speed), and decelerates before facing the second curve. This speed is calculated as expressed in Equation 66.

$$\frac{T_L - T_{Lmin}}{2} = \frac{{v_{85}}_T^2 - {v_{85}}_1^2}{22.03} \rightarrow v_{85_T} = \sqrt{11.016 \cdot (T_L - T_{Lmin}) + {v_{85}}_1^2} \quad (66)$$

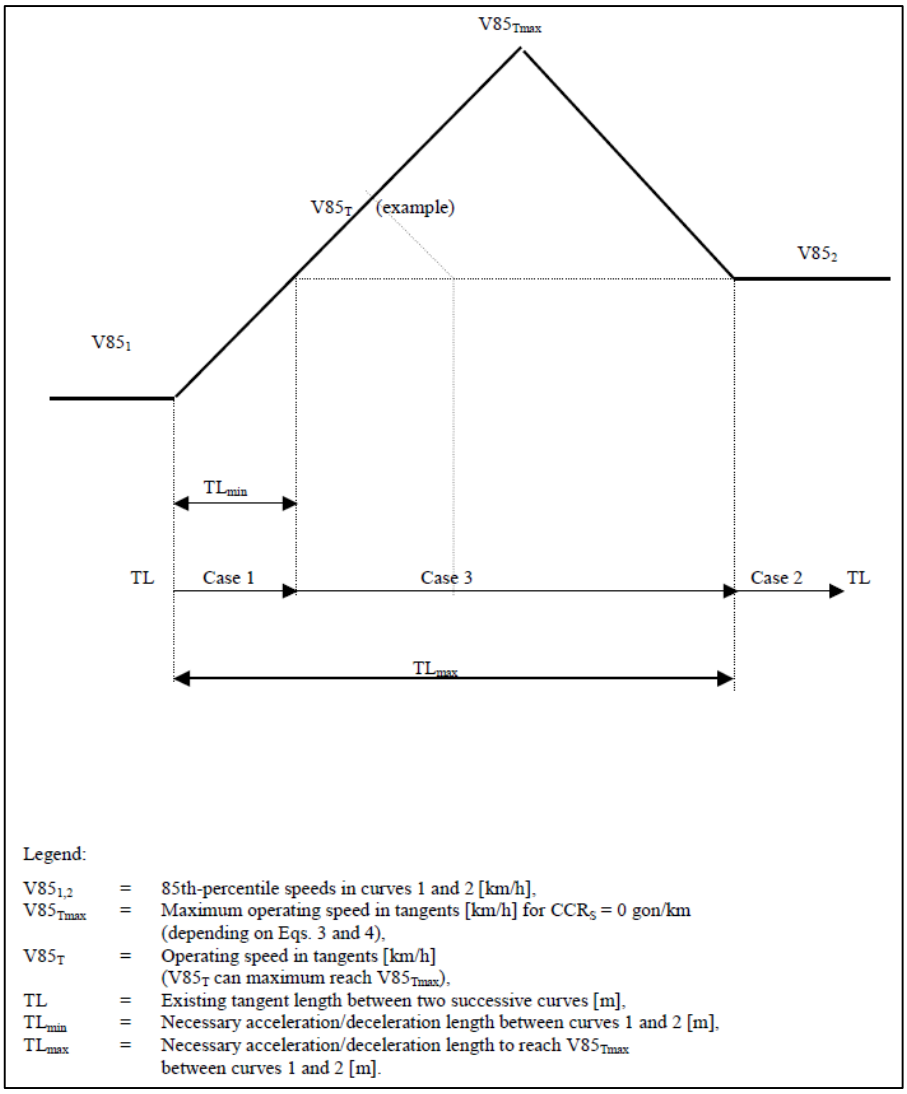

Figure 34. Lamm, Psarianos and Cafiso's operating speed model.

Ottesen and Krammes (2000) developed an operating profile speed model which considered operating speed models with more parameters. The procedure of conforming the final operating speed profile is similar. The operating speed for the horizontal curves remains constant along their length, only changing on tangent sections. This model also uses the acceleration and deceleration rates proposed by Lamm et al. (1988).

The first step is the calculation of the operating speed on curves according to their model for horizontal curves.

The operating speed at tangents depends on the tangent length. Three possibilities may exist (Figure 35):

- The tangent length between both curves is short. Drivers directly change their speed v_1 (first curve) to v_2 (second curve) at a constant acceleration/deceleration rate.
- The tangent is longer, so drivers can reach a speed higher than on both curves. However, this speed is lower than the desired speed.
- The tangent is long enough to allow drivers to reach the desired speed at least at one point.

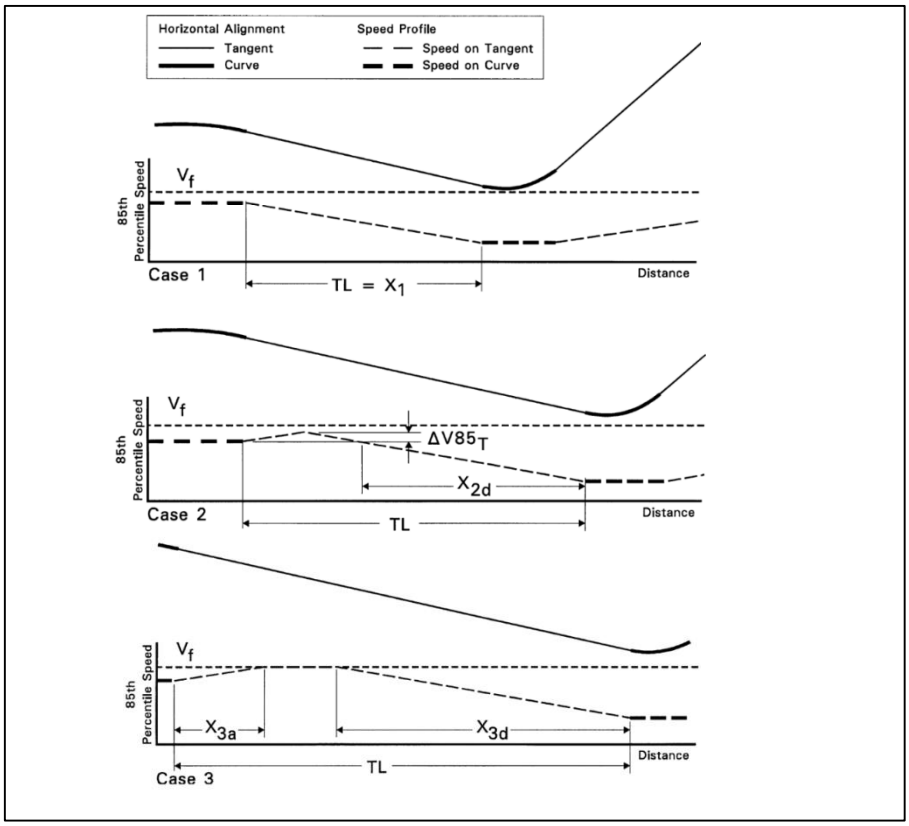

Figure 35. Ottesen and Krammes' (2000) operating speed profile model.

In order to better distinguish between those three cases, a new parameter, the critical length of the tangent, is defined (Equation 67). This is the tangent length required for allowing drivers to reach the desired speed at a single point.

$$L_{crit} = \frac{2 \cdot v_T^2 - v_1^2 - v_2^2}{25.92 \cdot a} \quad (67)$$

Where:

L_{crit} : Critical tangent length (m).
v_T: operating speed on the tangent (km/h).
v_{1-2} : operating speeds of the preceding (1) and following (2) curves (km/h).
a : acceleration/deceleration rate (0.85 m/s²).

Depending on the length of the tangent, three cases can be distinguished (Table 9).

Case	Condition	Equation	Vd reached?	Eq #
1	$L_T = X_1$	$X_1 = \frac{{v_{85_1}}^2 - {v_{85_2}}^2}{25.92 \cdot a}$	No	(68)
2.1	$L_T < L_{T_{crit}}$	$X_{2d} = \frac{{v_{85_1}}^2 - {v_{85_2}}^2}{25.92 \cdot a}$	No	(69)
		$v_{85_{T_{max}}} = v_{85_1} + \Delta v_{85_T}$		(70)
		$\Delta v_{85_T} = -2v_{85_1} + \frac{\sqrt{4{v_{85_1}}^2 + 44.06 \cdot (L_T - X_{2d})}}{2}$		(71)
2.2	$L_T = L_{T_{crit}}$	$X_{2a} = X_{3a} = \frac{v_f^2 - {v_{85_1}}^2}{25.92 \cdot a}$	Yes, but not sustained	(72)
3	$L_T > T_{L_{crit}}$	$X_{3a} = \frac{v_f^2 - {v_{85_1}}^2}{25.92 \cdot a}$	Yes, reached and sustained	(73)
		$X_{3d} = \frac{v_f^2 - {v_{85_2}}^2}{25.92 \cdot a}$		(74)

Where:
$X_{n,[a,d]}$: Distance traveled for case n during acceleration (a) or deceleration (d) (kph)
v_{85_n}: Operating speed on curve n
Δv_{85}: Difference between the operagint speeds (kph)
a: acceleration (or deceleration) rate = 0.85 m/s²
L_T: tangent length (m)
$L_{T_{crit}}$: Critical tangent length (m)
v_f: desired operating speed on long tangents (kph)

Table 9. Ottesen and Krammes' operating speed model.

This is a good model, although it presents an important drawback: several times the deceleration starts in a point where the following curve is not visible. Thus, deceleration rates are not always those defined by Lamm et al. (1988), being higher in these cases. Thus, their advanced operating speed profile model also considers the visibility profile, for determining the points where decelerations start.

The authors finally compare their operating speed model to the reality. They concluded the following:

- For curves with a degree of curvature lower than 5º, the model shows a speed reduction lower than the actual one.
- For curves with a degree of curvature higher than 5º, the model fits quite well the reality.
- The advanced model presents a higher dispersion than the original one.

Fitzpatrick and Collins (2000) presented a more advanced operating speed model. Their model takes into account not only the horizontal alignment but also the vertical one. This can be achieved because of their operating speed models for curves, which depend on the vertical alignment. They also consider TWOPAS equations and different acceleration and deceleration rates.

Their operating speed profile model is based on considering three different operating speed profiles and therefore selecting the lower speed for every station (Figure 36). The three operating speed profiles are:

- Desired speed (constant for the entire road segment). It was set to 100 km/h, according to Ottesen and Krammes (2000), who established the desired speed to 97.9 km/h.
- Operating speed on curves (operating speed models and acceleration/deceleration rates provided by Fitzpatrick et al. (2000)).
- Maximum operating speed considering TWOPAS equations.

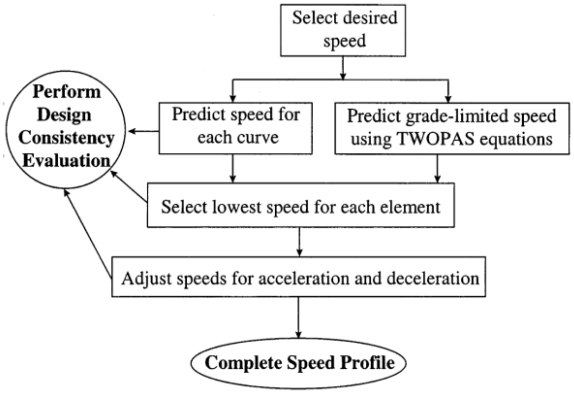

Figure 36. Operating speed models for consistency evaluation proposed by Fitzpatrick and Collins (2000).

The following assumptions are needed to conform the operating speed profile:

- The operating speed on curves is assumed to be uniform. Thus, speed transitions take place within the tangents. This is valid both for horizontal and vertical curves.
- Fitzpatrick et al. (2000) did not obtain acceleration/deceleration rates depending on horizontal and vertical alignment combinations. Thus, the most restrictive rate was selected for each situation.
- For crest vertical curves with limited sight distance, the acceleration behavior starts where both tangents intersect. This is because the speed control condition (low sight distance) is over, and drivers are thus free to reach their desired speed.
- Operating speed on curves cannot be higher than on tangents. Thus, estimated operating speeds for curves which violate this assumption will be moved to the highest operating speed of the adjacent tangents.
- The operating speed profile for complex geometries cannot be depicted with this model. This is the result of not considering horizontal and vertical alignment from a first moment, which might invalidate complex horizontal-vertical combinations.
- The operating speed model for curves is not valid for radii lower than 100 m. Thus, the minimum operating speed was set to 60 km/h.

The operating speed profile is composed by the three individual operating speed procedures. After the minimum speed value is selected for every station, acceleration and deceleration rates are applied. There are different speed transition cases, depending on some constraints. Some factors need to be defined first:

- Length available for speed change (LSC_a). This is the total length of the tangent.
- Critical length for complete acceleration and deceleration (LSC_c). This is the minimum theoretical length that a tangent needs to allow a complete acceleration (X_{fa}), reach the desired speed in a single point and decelerate before entering the second curve (X_{fd}). Acceleration and deceleration rates are those proposed by Fitzpatrick et al. (2000).
- Minimal length required for accelerating (or decelerating) from one curve to the next one (X_{ca} or X_{cd}, respectively).

Six behavior types can be found:

- Type A. The length is higher than the required distance for accelerating and decelerating. Thus, the desired speed is reached and maintained for some length (X_{fs}).

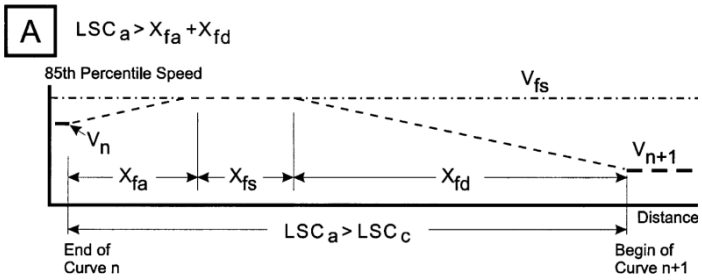

Figure 37. Fitzpatrick and Collins' operating speed model. Behavior type A.

- Type B. The tangent length does not leave drivers to reach the desired speed, but it is still higher than the one required to directly decelerate (or accelerate) to the next curve. A higher speed (lower than the desired one) is reached and kept for an instant.

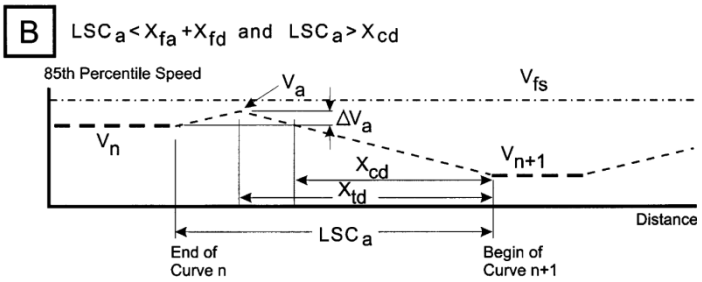

Figure 38. Fitzpatrick and Collins' operating speed model. Behavior type B.

- Case C. This is the theoretical case where the tangent length is exactly the same to reach the operating speed of the second curve using the required deceleration rate. This is only for deceleration cases.

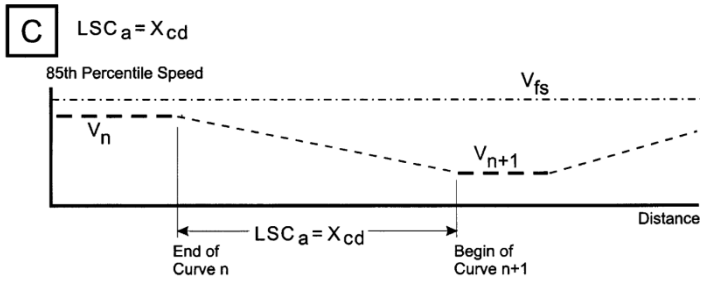

Figure 39. Fitzpatrick and Collins' operating speed model. Behavior type C.

- Case D. The tangent length is lower than the critical one. Thus, deceleration rates have to be higher than the standard ones. This is only for deceleration cases. Potential safety hazards may appear.

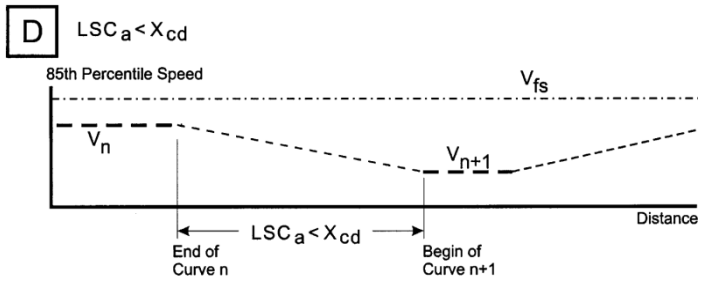

Figure 40. Fitzpatrick and Collins' operating speed model. Behavior type D.

- Case E. Theoretical case, where the length of the tangent is the critical one for accelerating and reach the operating speed of the second curve.

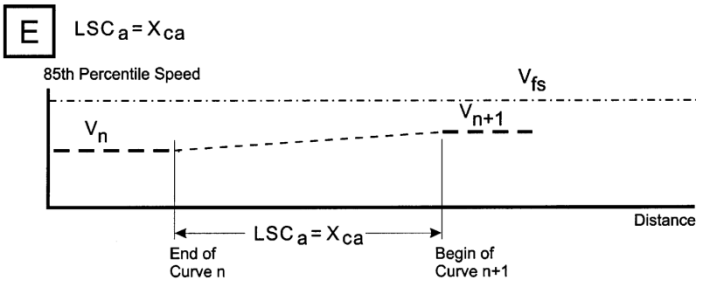

Figure 41. Fitzpatrick and Collins' operating speed model. Behavior type E.

- Case F. In this case, the tangent length is lower than the one of the case E. In contrast to case D, higher acceleration rates than the standard ones are not reached. Standard acceleration rates are applied, so the operating speed reached at the curve 2 is lower than before (v_{n+1}^{a}).

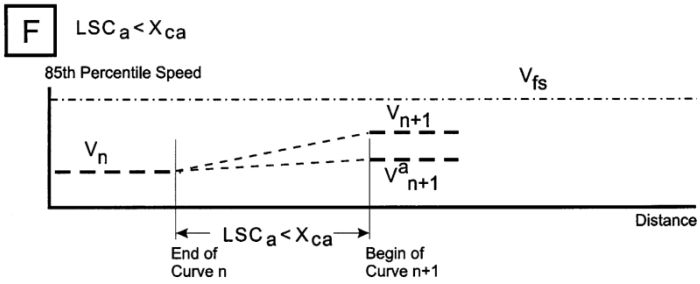

Figure 42. Fitzpatrick and Collins' operating speed model. Behavior type F.

$LSC_c = X_{fa} + X_{fd}$	(75)
$X_{fd} = \frac{v_{fs}^2 - v_{n+1}^2}{25.92 \cdot d}$	(76)
$X_{cd} = \frac{v_n^2 - v_{n+1}^2}{25.92 \cdot d}$	(77)
$X_{ca} = \frac{v_{n+1}^2 - v_n^2}{25.92 \cdot a}$	(78)
$X_{fa} = \frac{v_{fs}^2 - v_n^2}{25.92 \cdot a}$	(79)
$X_{fs} = LSC_a - X_{fd} - X_{fa}$	(80)
$X_{td} = \frac{v_a^2 - v_{n+1}^2}{25.92 \cdot d}$	(81)
$V_a = V_n + \Delta V_a$ *(The curve with the largest radius has to be used)*	(82)
$\Delta v_a = \frac{-2V_n + \sqrt{4V_n^2 + 44.06 \cdot (LSC_a - X_{cd})}}{2}$	(83)
$V_{n+1}^a = V_n + a \cdot LSC_a$	(84)

Where:
V_{fs}: desired operating speed on long tangents (kph)
V_n: operating speed on curve n (kph)
V_{n+1}: operating speed on curve $n+1$ (kph)
V_{n+1}^a: operating speed on curve $n+1$ determined as a function of the assumed acceleration rate (kph)
V_a: maximum achieved speed on roadway between curves for behavior type B (kph).

ΔV_a: difference between speed on curve n and the maximum achieved speed on roadway between curves for behavior type B (kph). a, d: acceleration and deceleration rates (m/s^2). LSC_c : critical length of roadway to accommodate full acceleration and deceleration (m). LSC_a: length of roadway available for speed changes (m). X_{fd}: length of roadway for deceleration from desired speed to curve $n+1$ (m). X_{cd}: length of roadway for deceleration from curve n to curve $n+1$ (m). X_{td}: length of roadway for deceleration from V_a to curve $n+1$ (m). X_{ca}: length of roadway for acceleration from curve n to curve $n+1$ (m). X_{fa}: length of roadway for acceleration from curve n to desired speed (m). X_{fs}: length of roadway between two speed limited curves at desired speed (m).

Table 10. Calculation of parameters for Fitzpatrick and Collins' model (2000).

This model was later improved by Easa (2003a), including the consideration of the sight distance for determining where acceleration and deceleration rates could start. The same operating speed models are considered for curves, tangents and acceleration and deceleration rates. The same hypotheses are assumed. The author suggest the use of the operating speed models for curves calibrated by Gibreel et al. (2001) if one does not want to assume a constant speed at curves.

The available distance for speed variations is different depending on the alignment. If there is no vertical variation, this value is the tangent length. If there is vertical variation, both horizontal and vertical alignments, as well as sight distance limitations have to be considered. There are five cases, organized in a similar way as Fitzpatrick and Collins (2000).

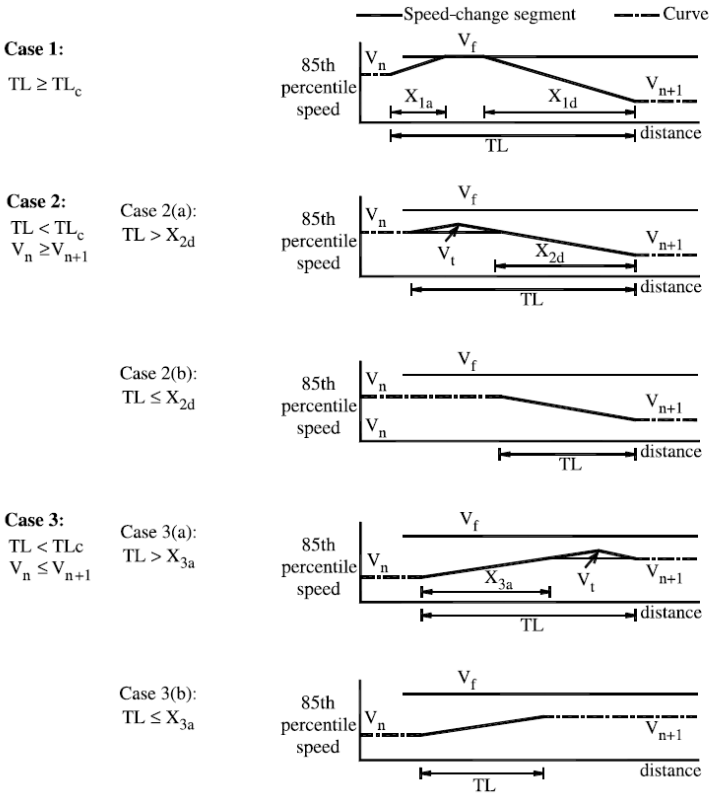

Figure 43. Cases for Easa's operating speed model (2003).

Case	Condition	Subcondition	Equation	Eq. #
1	$L_T \geq L_{T_{crit}}$		$X_{1a} = \frac{V_f^2 - V_n^2}{25.92 \cdot a}$	(85)
			$X_{1d} = \frac{V_f^2 - V_{n+1}^2}{25.92 \cdot d}$	(86)
			$L_{T_{crit}} = X_{1a} + X_{1d}$	(87)
2	$L_T < L_{T_{crit}}$ $V_n \geq V_{n+1}$	$L_T > X_{2d}$	$X_{2d} = \frac{V_n^2 - V_{n+1}^2}{25.92 \cdot d}$	(88)
			$V_t = \sqrt{V_n^2 + 25.92 \cdot \left(\frac{ad}{a+d}\right) \cdot (L_T - X_{2d})}$	(89)
		$L_T \leq X_{2d}$	$d' = \frac{V_n^2 - V_{n+1}^2}{25.92 \cdot L_T}$	(90)
3	$L_T < L_{T_{crit}}$ $V_n \leq V_{n+1}$	$L_T > X_{3a}$	$X_{3a} = \frac{V_{n+1}^2 - V_n^2}{25.92 \cdot a}$	(91)
			$V_t = \sqrt{V_{n+1}^2 + 25.92 \cdot \left(\frac{ad}{a+d}\right) \cdot (L_T - X_{3a})}$	(92)
		$L_T \leq X_{3a}$	$V_{n+1}^a = \sqrt{V_n^2 + 25.92 \cdot a \cdot L_T}$	(93)

Where:
L_T: length of the intermediate tangent (m)
$L_{T_{crit}}$: critical tangent length (m)
$X_{n,[a,d]}$: distance for element n under acceleration or deceleration conditions (m)
V_f: desired speed on the intermediate tangent (kph)
V_t: maximum speed reached on the tangent (if not the desired speed) (kph)
V_n, V_{n+1}: operating speed on the curve n or $n+1$ (kph)
a, d: acceleration and deceleration rates (m/s^2)

Table 11. Parameters of Easa's operating speed model.

They also provided an improved model, which also considers the possibility of having a sight obstruction. The stopping sight distance is calculated as the sum of two distances: the one required for perception and reaction (D_{pr}) and another one for stopping the vehicle (D_r):

$$D_{pr} = 0.278 \cdot v \cdot t \quad (94)$$

$$D_r = \frac{v_0^2 - v_{n+1}^2}{25.92 \cdot d} \quad (95)$$

Where v is the operating speed of the vehicle at the point where the controlling horizontal curve is visible, and t is the perception and reaction time (assumed to be 2.5 s). v_0 is the initial operating speed, while v_{n+1} is the operating speed of the horizontal curve that establishes the speed control. d is the available distance for the speed variation.

However, the available distance is:

$$D_a = S_a - 0.278 \cdot v \cdot t \tag{96}$$

There are three possible cases.

Case 1. The available distance is higher than the required one. The base model is applied. Otherwise, the operating speed profile must be corrected based on the available sight distance. The new deceleration rate is:

$$d' = \frac{v_f^2 - v_{n+1}^2}{25.92 \cdot D_a} \tag{97}$$

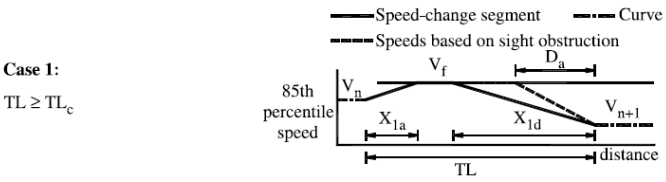

Figure 44. Easa's operating speed profile model. Case 1.

Case 2. The driver tends to accelerate until they see the obstruction or reach the desired speed. The higher speed is calculated as:

$$v_t' = [v_n^2 + 25.92 \cdot a \cdot (TL - S_a)]^{\frac{1}{2}} \tag{98}$$

Hence, the deceleration rate results in:

$$d' = \frac{v_t'^2 - v_{n+1}^2}{25.92 \cdot D_a} \tag{99}$$

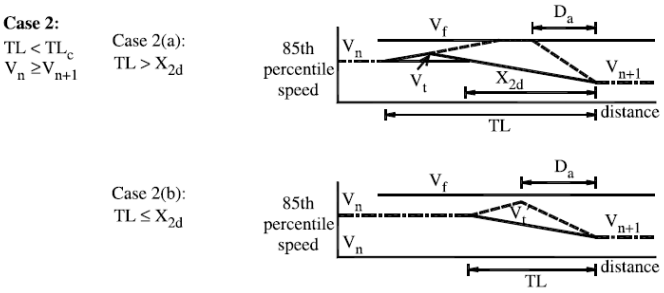

Figure 45. Easa's operating speed profile model. Case 2.

Case 3. This case is similar to case 2, but the desired speed is not reached.

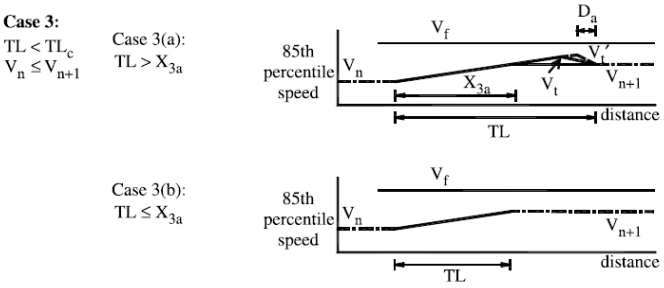

Figure 46. Easa's operating speed profile model. Case 3.

Crisman et al. (2004) introduces a new operating speed profile model. Their methodology includes the consideration of two operating speed profiles (one per direction). They considered their operating speed models for curves and tangents. The validity of this model is for longitudinal grades up to 3%. The procedure is the following:

- Definition of homogeneous road segments, according to the German procedure.
- Calculation of the *CCR* for each homogeneous segment. Determination of the lane and shoulder width. Calculation of the desired speed of the road segment.
- Calculation of the operating speed on the horizontal curves.
- Calculation of the operating speed on tangents. Transition curves and circular curves with radius higher than 2200 m are included in this group.
- Incorporation of the acceleration and deceleration rates.

Polus and Mattar-Habib (2004) developed an operating speed model for the analysis of design consistency. Operating speeds on horizontal curves are calculated with Krammes et al. (1995) operating speed model. Operating speed on tangents are calculated according to Polus, Fitzpatrick and Fambro (2000) model. Acceleration and deceleration rates were not defined, but they used 3 seconds for decelerations and 4 seconds for acceleration. In both cases, 1 second of those was located within the curved section, being the rest on the tangent.

This model was later improved by Polus et al. (2005), where the vertical alignment was included by means of the TWOPAS equations. The minimum value of both operating speed profiles was selected for every station, as previous models did.

3.4.2. Road safety estimation depending on road design

There is a huge research effort that tries to estimate the safety performance of two-lane rural highways. Some of them have produced safety performance functions for estimating the number of accidents in a road segment depending on some conditions. Some others examine the impact of a change of a geometric feature on the safety conditions. Both of them are covered here. Only geometric and environmental conditions are considered here. However, the most accurate safety performance functions consider operational measures, such as design consistency. They will be examined in Section 3.5.

It is well known that a large number of accidents is explained by the risk exposure (length and traffic volume). Harwood et al. (2000) developed the following expression to estimate the number of accidents in a year (crashes / year) in terms of traffic volume (vpd) and length (miles):

$$y_i = AADT \cdot L \cdot 365 \cdot 10^{-6} \cdot e^{0.4865} \qquad \boldsymbol{R^2 = 0.65} \qquad (100)$$

They considered a negative binomial distribution. As it can be seen, crash rates are not affected by length and AADT. This will change in later literature.

Cafiso et al. (2010) also developed a safety performance function to estimate the number of accidents as a function of the exposure. In this case, the AADT was assumed to influence crash rates, but the length was still considered not a factor.

$$y_i = e^{-7.123} \cdot L \cdot AADT^{0.731} \qquad \boldsymbol{AIC = 417.6} \qquad (101)$$

Although exposure was the most important factor for estimating road accidents, some other parameters were also considered. The authors calibrated a more detailed model, in which additional parameters were included:

$$\begin{aligned} & y_i \\ & = AADT \cdot L \cdot 365 \cdot 10^{-6} \\ & \cdot e^{0.6409+0.1388 \cdot State+0.0846 \cdot LW+0.0591 \cdot SW+0.0668RHR+0.0084DD} \\ & \cdot \sum WH_i e^{0.045 \cdot DEG_i} \cdot \sum WV_i e^{0.4652 \cdot V_i} \cdot \sum WG_i e^{0.1048 \cdot GR_i} \end{aligned} \qquad \boldsymbol{R^2 = 0.65} \qquad (102)$$

Where:

$State$: Location of roadway segment (0 for Minnesota, 1 for Washington).
LW: lane width (ft).
SW: Shoulder width (ft).
RHR: roadside hazard rating. This is an integer, ranging from 1 to 7.
DD: driveway density (driveways per mi).
WH_i: weigth factor for the i^{th} horizontal curve in the roadway segment, the proportion of the total roadway segment length represented by the portion of the i^{th} horizontal curve that lies within the segment. The total weights must sum 1.0.
DEG_i: degree of curvature for the i^{th} horizontal curve (degrees per 100 ft).
WV_j: weight factor for the j^{th} crest vertical curve in the roadway segment; the proportion of the total roadway segment length represented by the portion of the j^{th} crest vertical curve that lies within the segment. The total weights must sum 1.0.
V_j: Crest vertical curve grade rate for the j^{th} vertical curve within the roadway segment in percent change in grade per 100 ft.
WG_k: weight factor for the k^{th} straight grade segment, the proportion of the total roadway segment length represented by the portion of the k^{th} straight grade segment that lies within the segment. The total weights must sum 1.0.
GR_k: absolute value of grade for the k^{th} straight grade on the segment (%).

The authors suggest the use of the first model to have a good approach while using network screening tools; and the second one while an accurate estimation of the number of accidents is intended.

Some other researchers have focused on examining the effect of certain geometric features, such as the curvature of the road segment. Considering the sharpness of the horizontal curves, the general finding is that sharper curves produce more accidents (Othman et al., 2013). This can be due to different phenomena, such a high workload demand, a sudden change of the workload, or erroneous maneuvers.

Zegeer et al. (1991) analyzed over 13,000 curves in Washington State, evaluating the relationship between curve features and crashes. They also concluded that sharper curves, narrower curve width, lack of spiral transitions and increased superelevation deficiency were linked to a higher accident rate. The length of the curve and AADT were also considered to affect crash rates:

$$AR = AADT \cdot L_C \cdot (1.94 + 0.24 \cdot DC - 0.026 \cdot W - 0.25 \cdot Spirals \qquad \boldsymbol{R^2 = 0.35} \qquad (103)$$

Where AR is the estimated accident rate (total accidents / million vehicle miles), $AADT$ the traffic volume (vpd), L_C the length of the curve (miles), W the section width (feet), and $Spirals$ is 0 if no spiral transitions are present, 1 otherwise.

This was one of the first approaches to accident modeling in horizontal curves. This is also why it also presented some statistical problems. For instance, they modeled the accident rate instead of the number of accidents, the use of the normal distribution, and the consideration of all accidents without removing PDO crashes.

They later developed a *CMF* to estimate the variation in the number of accidents depending on some geometric conditions (Zegeer et al., 1992):

$$CMF = \frac{1.55 \cdot L_C + \frac{80.2}{R} - 0.012 \cdot S}{1.55 \cdot L_C} \qquad (104)$$

Where:

L_C: length of the horizontal curve (mi).
R: radius of the horizontal curve (ft).
S: 1 if there is spiral transition, 0 otherwise.

Othman et al. (2013) compared the driver's operation along a set of thousands of horizontal curves to their crash rates. They found that the entrance of the horizontal curve was the most hazardous part, since the highest lateral accelerations were

presented here. This was valid for smooth curves ($R > 400\ m$). Drivers performed in the same way for the entrance and middle part of sharper curves. Thus, extreme lateral accelerations were not present.

The convenience of the horizontal curves to include spiral transitions is not clear. Most design standards recommend the use of spiral transition curves. They provide a gradual increase in the centrifugal force, a convenient arrangement for superelevation, and a good roadway appearance. However, many studies have claimed that spiral transitions should not be considered in the horizontal alignment, since they allow drivers to maintain high speeds (Tom, 1995). This study indicated that curves with no spiral transitions present lower crash rates. Perco (2006) found that the spiral transition should imitate the drivers' natural steering path. Thus, no too long spiral transitions were recommended. The average time for the steering path was set in 2.25 seconds. Said et al. (2007) also concluded that spiral curves would help to produce alignments conforming to the natural vehicle path but the current design of spiral curves should be revised. In fact, the current guidelines for designing spiral transitions are based on research during 1930s and 1940s.

Said et al. (2009) developed some cubic relationships between the spiral length and the drivers' comfort level. They provided some recommendations for adapting the spiral design to drivers' operation.

Horizontal curvature misperception can also be attributed to how the superelevation rate is set. Krammes (2000) stated that drivers have difficulty judging curvature and appropriate speeds from the approaching tangent to a horizontal curve. He indicated that the superelevation rate might be one of the reasons, since different states apply different superelevation design. Maximum superelevation rates should be established in order to provide more uniformity.

The effect of superelevation is felt only when the vehicle has entered the curve. This is the reason why superelevation should be based on the operating speed rather than on the design speed (Krammes, 2000).

It was indicated that a large sight distance is recommended in order to give the road users enough time to form correct expectations. Thus, inadequate sight distance is a common accident contributing factor. Sight distance is the result of the general alignment of the road and its roadside.

Silyanov (1973) observed a negative relationship between stopping sight distance and accident rate in the former Soviet Union. Babkov (1975) reported that the lack

of proper sight distance was the main reason for about 8-10% of the accidents in the former Soviet Union.

The AASHTO Green Book Edition of 1965 indicated that the number of accidents on the curves with limited sight distance was significantly higher than that on the other curves (Gibreel et al., 1999).

The calculation of the Stopping Sight Distance (SSD) using 3D models is recommended (Hassan et al., 2000), since their results are highly different to those achieved with 2D models.

3.4.2.1. Cross-section and roadside conditions

Cross section affects the likelihood of several kinds of road accidents. For a normal cross-section configuration, the greater the lane and shoulder widths, the fewer the accidents. This effect is not linear: for very wide lanes and/or shoulders, drivers tend to speed up their vehicles, thus the road safety decreases. Himes et al. (2011) found that a one-foot increase in the total shoulder width is associated with a 0.33 mph increase of the operating speed. This produces a lower vision field, increasing the driver workload.

Pignataro (1973) found that the total accident rate per million vehicle-miles on two-lane rural highways decreased from 5.5 to 2.4 as the pavement width increased from 5.0 to 7.5 m. He also found that the accident rate decreased by 22% for two-lane rural highways with low traffic volume and by 47% for two-lane rural highways with high traffic volume when the pavement width was widened from 5.5 to 6.7 m.

Silyanov (1973) collected data from Russia, Germany and other European countries and established the following relationship between accident rate and pavement width:

$$AR = \frac{1}{0.173 \cdot W - 0.21} \quad (105)$$

Where AR is the accident rate (accidents per million vehicle-kilometer), and W is the pavement width (m).

Babkov (1975) got similar conclusions. He observed that the accident rate decreased by 50% when pavement width increased from 4.5 to 6.5 m. He also concluded that an insufficient shoulder width would cause an increase in the accident rate. Thus, the shoulder width should not be lower than 3.0 m.

The effect for both lane and shoulder with is greater for high traffic volumes, as can be seen in Figures Figure 47 and Figure 48 (Harwood et al., 2000).

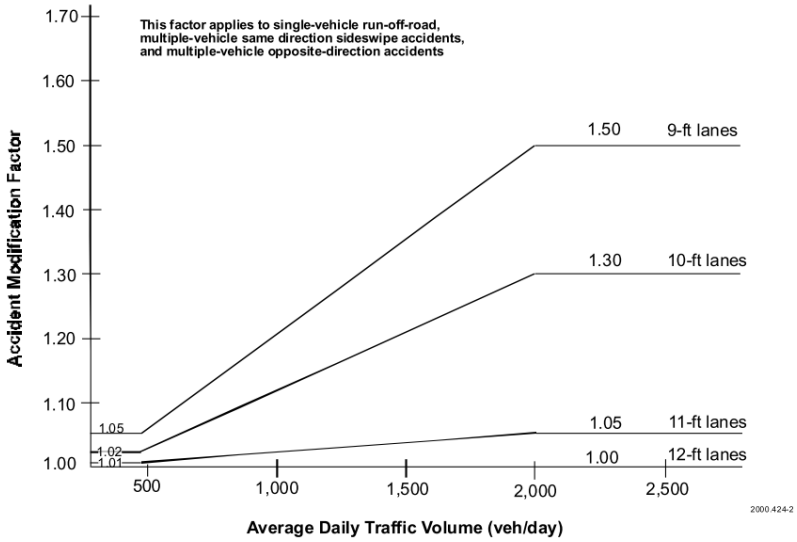

Figure 47. Recommended AMF for lane width (Harwood et al., 2000).

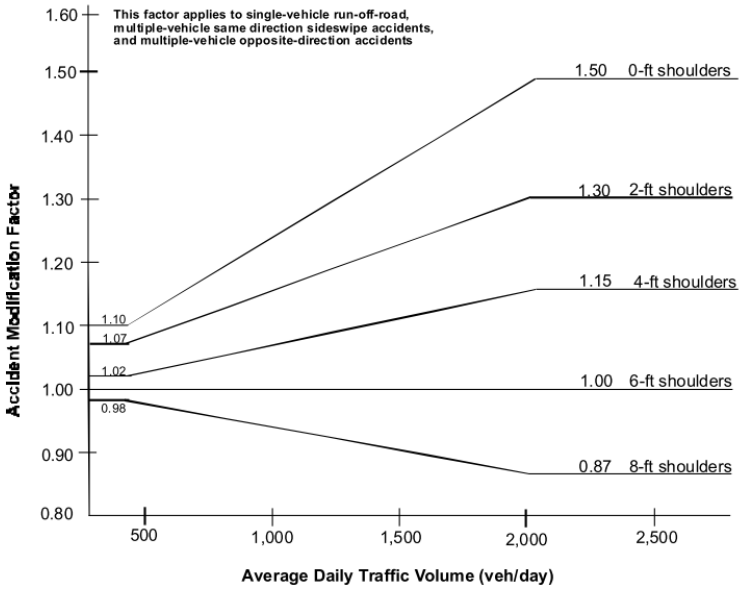

Figure 48. Recommended AMF for shoulder width (Harwood et al., 2000).

Road centerline and edgelines have also a true effect on road safety. Several studies point out that the relative increase in accident risk can be assumed equal to 20% for missing or ineffective edge lines and centerlines (Cafiso, la Cava and Montella, 2007b).

Daytime delineation is effectively accomplished with pavement markings. The problem arises at nighttime or rainfall conditions, where chevron alignment signs have demonstrated to be an effective countermeasure. Missing or ineffective chevrons and damage or missing guideposts or barrier deflectors can lead to accident risk increase equal to 30% (Cafiso, la Cava and Montella, 2007b).

Roadside conditions are also important. The main safety effect of roadside deals with accident severity and not with accident probability. In fact, some authors point out that the severity of an accident is more related to the roadside conditions rather than to the curve sharpness (Hummer et al, 2010).

Zegeer et al. (1988) developed a roadside hazard rating system to characterize the accident potential for roadside designs on two-lane highways. This scale rates the roadside hazard from 1 (no problem) to 7 (very hazardous). Ratings 1 and 2 are for recoverable situations, while ratings above 5 are for non-recoverable situations. The severity of a virtual accident also increases according to this rating. This roadside hazard rating can be used as a parameter in a safety performance function in order to estimate the number of crashes.

Cafiso et al. (2010) developed a Roadside Hazard Index (RSH), considering some indicators related to the roadside conditions, aggregated in segments of 200 m.

They established that a Road Safety Inspection has to be carried out for both directions, assigning a score (0= not present, 1=low risk, 2=high risk) to five different roadside items. The relative weights for specific roadside safety hazard items were:

- Embankments: 3.
- Bridges: 5.
- Dangerous terminals and transitions: 2.
- Trees, utility poles and rigid obstacles: 2.
- Ditches: 1.

The overall value of RSH_i is a weighted mean of the five roadside items:

$$RSH_i = \frac{\sum_{k=1}^{2} \max\left(Score_{ijk} \cdot Weight_j\right)}{2} \quad (106)$$

Where k is the direction of the survey.

There roadside hazard ratings include some subjective perception by the experts, but this is part of the methodology (Cafiso et al, 2006).

3.4.2.2. Number of intersections and driveways

Direct accesses to roads can significantly increase the number of accidents. The problem is not only the number and type of accesses but also where they a connected to the main road (e.g. accesses on horizontal curves).

Harwood et al. (2000) identified that a high frequency of dangerous accesses (40 accesses/km) increased crash rates to about 135%. They presented the following *CMF*:

$$CMF = \frac{0.2 + (0.05 - 0.005 \cdot \ln AADT) \cdot DD}{0.2 + (0.05 - 0.005 \cdot \ln AADT) \cdot 5} \quad (107)$$

Where DD is the driveway density (driveways per mile).

The driveway density has also an effect on the traffic operation. Himes et al. (2011) found that a one-unit increase in the number of access points within 1000 ft of the road is associated with a 0.29 mph reduction in the mean speed.

3.4.2.3. Speed limit

The speed limit, in combination with the operating speed, has also an important role to play in road safety. This speed is fixed to a value that is considered safe, depending on some geometric and environmental features of the road. These features are sometimes evident, such a sharp curve. The operating speed is in this case similar to the speed limit, since the drivers notice the speed control and adapt their behavior.

In other cases, the underlying cause of the speed limitation is not evident for drivers. Thus, two groups are formed: those who respect the speed limit and those who prefer to keep an operating speed according to the road layout and conditions. This situation produces the following problems:

- The speed dispersion before the geometric control increases, thus increasing the likelihood of crashes.

- There might appear sudden speed reductions when the cause of the speed limitation gets evident for all drivers. This might occur or not, depending on the limitation itself. A sharp curve is a clear speed control, but an intersection might not.

As a result, it is recommended the posted speed to reflect the operating speed of the road. Otherwise, the probability of having an accident increases. Krammes (2000) indicated that the current warning and advisory speed signing system in the United States was not accurate. Many horizontal curves are signed with unrealistically low advisory speeds, affecting their credibility. As a result, at some locations it would be a good countermeasure to slightly rise the speed limit, in order to reduce the speed dispersion.

This way of placing posted speed limits is linked to the concept of self-explaining roads. Where a difficult condition is obvious, drivers are more apt to accept lower speed operation than where there is no apparent reason for it. Drivers do not adjust their speeds to the importance of the highway, but to their perception of the physical limitations and traffic thereon. Self-explaining roads are those designed to be easily interpreted by drivers and hence induce an adequate driving behavior (Camacho-Torregrosa et al., 2013). Non-consistent roads can infer sudden operating changes to road users, including changes on the workload demand. These changes may end in errors in the selection of the speed or the trajectory (Cafiso and la Cava, 2009).

Reduced design speeds are sometimes necessary for some facilities, but designers should not expect that drivers would adapt to them only because of the speed limit. Posted or advisory speed limits alone cannot constrain driver speeds to an arbitrary design speed in areas where the geometrics permit higher travel speeds (Harwood et al., 2000).

3.4.2.4. Pavement conditions

Al-Masaeid (1997) analyzed the influence of the pavement conditions on crash rates on two-lane rural highways, for single and multiple crash rates. They found that an increase in the IRI level would reduce the single-vehicle accident rate. The effect was the contrary for multiple-vehicle crashes.

The skid resistance of the pavement plays a major role in vehicle stability. Several studies indicate that crash rates increase when the skid resistance drops below certain value (about 10%) (Cafiso, la Cava and Montella, 2007b).

Buddhavarapu et al. (2012) analyzed the relationship between the pavement condition and the accident severity. They found that it existed a low correlation between the different pavement parameters and the probability of a crash becoming fatal.

The drivers also adapt their behavior to their perception of the pavement conditions. Road users drive at lower speeds when the pavement is in bad shape. This is good for non-consistent roads, where the geometric conditions might increase the number of crashes but the low speeds operate in the opposite way. In such the case, a change in the pavement conditions may let the road users think that the road presents a better performance that it actually does, increasing the crash rate.

3.5. Road design consistency

Interaction between infrastructure and human factors is very important. This is why several sections have been dedicated to its analysis. Users see how the road behaves and use this information in order to reduce their mental workload on the driving task. This is what we call driver's expectancies.

However, this is not always an advantage. Sometimes, the road suddenly changes its behavior, against drivers' expectations. In this case, the mismatch between expectancies and road behavior makes the crash likelihood to increase.

Road design consistency is related to this phenomenon. It refers to how the road behavior meets users' expectancies. Driver expectancy is defined as "an inclination, based upon previous experience, to respond in a set manner to a roadway or traffic situation" (Rowan et al., 1980). A consistent road means no surprises, a lower probability of having an accident. On the contrary, a poor consistent road will produce several surprises, increasing the risk.

Alexander and Lunenfeld (1990) defined two kinds of expectancies:

- *A priori.* Based on all the driver's experience, since they got their driving license. They are based on experience accumulated over a long period.
- *Ad hoc.* Expectancies based on the behavior of the road the driver is driving through. Based on experience gained very recently.

Näätänen and Summala (1976) suggested that expectancies were "recently weighted", i.e. the expectancies have a stronger effect on drivers' behavior as they are more recent.

Although the concept may be clear, the way of measuring it might not. How do we measure the fitting degree between the road behavior and drivers' expectations? This cannot be directly performed. Thus, several researchers have proposed different indicators. The most important can be classified in the following groups:

- Drivers' operation. Those methodologies are based on examining how drivers operate along a certain road or element. Some indicators are the operating speed, curve negotiation, speed reduction, lateral acceleration, lateral friction, etc. Two main methodologies can be identified:
    - Operating speed. This is the most extended group of methodologies to measure design consistency. The reason is

because operating speed is a very well-known, easy to measure indicator.

    - Vehicular stability. It evaluates the risk level attained by drivers while performing along a certain curve.
- Alignment indices. Quantitative indicators that resume the general character of a road. Extreme values of those indicators are thought to be related to a more inconsistent road.
- Driver workload. Consistent roads suppose a lower workload for drivers. There are some methods that indirectly evaluate this parameter.

Several researchers have pointed out the high relationship between consistency and road safety. Thus, several safety performance functions have been calibrated, which appear in the following sections.

3.5.1. Operating speed methods

Operating speed is a good indicator to represent how drivers behave depending on the road features. In addition, this parameter is easy to obtain and interpret. This is why this was the first measure available in the literature to evaluate design consistency (Hassan, 2004). Thus, several relationships between the operating speed and the number of crashes have been developed. Some of them do not explicitly include the concept of "consistency", but they refer to the speed reduction due to a surprise. Hence, this concept is implicitly included.

Leisch and Leisch (1977) developed a speed-based consistency evaluation process for the United States. However, this procedure was not widely used. This method is characterized by the following aspects:

- It considers both passenger car and truck speeds.
- It considers the combined effects of horizontal and vertical alignment.
- It varies deceleration rates approaching and acceleration rates departing curves as a function of the approaching tangent and curves.

The main weakness of this method is that it is based on information collected from 1965 to 1973, which should be updated.

Lindeman and Ranft (1978) analyzed the operating speed dispersion on horizontal curves depending on their geometry. Their found that sharp and smooth curves behaved in different ways. The speed dispersion for sharp curves increased as their radius did. On the contrary, the speed dispersion was constant at a maximum value for smooth curves.

Zegeer (1990) studied more than 100 fatal crashes and other more than 100 crashes with victims at horizontal curves. They concluded that the speed was an important factor involved in the probability and severity of accidents.

There are other speed definitions that may be linked to road crashes, such as the design speed and the speed limit. They are part of the infrastructure factor, but they may interact with the operating speed and lead to higher crash rates.

The operating speed based consistency models examine the operating speed profile, guessing how drivers' expectancies might be violated. These methods are widely used, since there is a lot known about operating speed. Moreover, a change in the operating speed is a clear indicator of an inconsistency, while a change in the mental workload is not.

The operating speed profile is the drivers' speed response to the road alignment. Thus, inconsistencies can be detected by examining its performance. For instance, a very smooth operating speed profile indicates that drivers read the road very well, with small changes in their workload. On the other hand, abrupt changes of the operating speed profile indicate surprises and a poor design.

There are two ways of evaluating the consistency on two-lane rural roads: local and global methodologies.

- Local methodologies are more extended than global ones. They examine local problems with the operating speed, such as sudden speed reductions or high differences between the design and operating speeds. They are appropriate for locating where the inconsistency problems appear.
- Global methodologies. They examine the global operating speed variation on a road segment. As a difference to local methodologies, they do not focus where the problem is, but they can be introduced into safety performance functions in order to estimate the number of crashes.

Geometric design consistency evaluation methodologies are a good tool to assist engineers at designing better roads. They can be useful for assessing the safety level

of an existing road, selecting among different alternatives, performing a better road design, etc.

3.5.1.1. Local evaluation methods

Local evaluation methods are valid for examining where the operating speed profile produces problems, focusing them and providing different solutions. Most methods of this group focus on examining where high speed variations take place. It was found very soon that speed consistency was highly related to road safety, so researchers focused on its measurement and the development of smoother operating speed profiles.

Leisch and Leisch (1977) proposed three consistency criteria for road design:

- The difference between design speeds of two consecutive road segments should not exceed 10 mi/h.
- The difference between the operating speeds for two consecutive road geometric elements should not exceed 10 mi/h. Only passenger cars were considered in this definition.
- The difference between operating speeds for passenger vehicles and trucks should not exceed 10 mi/h.

The 10 mph threshold was based on the perception that under most circumstances drivers can reasonably manage this speed variation. In addition, they found that a high difference between the operating speeds of cars and trucks was linked to a higher crash rate.

McLean (1979) examined the relationship between horizontal curve design and operating speeds at 120 curves in Australia. He noted three criticisms to the design speed and consistency relationship:

- Roadway designs that conform to design speed standards do not ensure a consistent alignment.
- Designs that conform to a specified design speed do not ensure compatibility between combinations of design elements.
- Free-flow design speeds and design speed are not necessarily equal.

He suggested that the inferred design speed for consecutive elements should not differ more than 10 kph, and never 15 kph.

Lamm and Choueiri (1995) proposed three criteria for road design consistency. Those criteria were developed comparing speed variation to crash rates. The three criteria are:

- Criterion I. It evaluates the difference between design and operating speeds. It corresponds to a reasonable agreement between the design speed and the actual driving behavior.
- Criterion II. It evaluates the operating speed difference between two consecutive road geometric features. This speed variation should be limited to certain threshold.
- Criterion III. It compares the side friction demand to the maximum skid resistance (vehicular stability).

McFadden and Elefteriadou (2000), based on a research carried out by Krammes et al. (1995), proposed that the 85th percentile of the maximum speed reduction before a curve (85MSR) was a better estimator of the local consistency than the operating speed difference. They provided two models to calculate it.

The Interactive Highway Safety Design Model (IHSDM), developed in United States by the Federal Highway Administration (FHWA) has an entire module for estimating design consistency, based on Lamm's Safety Criteria I and II.

3.5.1.1.1. Comparison of design and operating speeds

As previously mentioned, the design speed is selected by the road designer in order to calculate some geometric features of an entire road segment. This speed is not known by drivers, but they are influenced by those features, such as the minimum radius, minimum sight distance, etc. Some other parameters are not directly influenced by this speed, such as the radii of the rest of the curves. Drivers operate mostly considering this last parameter. Hence, design and operating speeds should be similar, in order to prevent hazardous situations.

The selection of the design speed for much road designs has been based on two principles (Krammes et al., 1995):

- All curves within a section of road should be designed for the same speed.
- The design speed should reflect the uniform speed at which a high percentage of drivers desire to operate.

The aim of this way to proceed was to achieve consistency in order that most drivers could safety operate at their desired speed along the whole section of the road. Thus, an inconsistency appeared when they had to decelerate from their desired speed in order to safely negotiate certain alignment features.

This criterion was first introduced by Lamm et al. (1988), as Safety Criterion I. There were defined three consistency thresholds depending on the difference between the operating speed and the design speed:

- $v_{85} - v_d \leq 10\ \mathrm{km/h}$. Good consistency. The road does not need any change.
- $10\ \mathrm{km/h} < v_{85} - v_d \leq 20\ \mathrm{km/h}$. Fair consistency. Some parameters, such as the sight distance, should be changed in order to accommodate them to the operating speed requirements.
- $v_{85} - v_d > 20\ \mathrm{km/h}$. Poor consistency. The difference between design and operating speeds is too high. The road should be redesigned in order to reduce this difference.

They established these thresholds based on the crash frequency variations among them. They proposed the design speed to be calculated with the average operating speed ($\emptyset v_{85}$). Therefore, if using their proposed operating speed models, the consistency thresholds can be given in terms of curvature change ratio:

- Good consistency: $\left|CCR_{s_i} - \emptyset CCR_s\right| \leq 180\ \mathrm{gon/km}$.
- Fair consistency: $180\ \mathrm{gon/km} < \left|CCR_{s_i} - \emptyset CCR_s\right| \leq 360\ \mathrm{gon/km}$.
- Poor consistency: $\left|CCR_{s_i} - \emptyset CCR_s\right| > 360\ \mathrm{gon/km}$.

Once an inconsistency has been detected, the engineer should examine the operating speed profile for determining the best solution. For instance, if the inception of the design speed is a single curve, normally it would be preferred to redesign this curve in order to raise the design speed. On the other hand, sometimes a combination of very smooth road geometric features lead to a local increase of the operating speed. In this case, the accommodation of certain parameters to the operating speed might be preferred.

Lamm also suggested to change the definition of design speed. The definition based on the most restrictive road geometric feature would not be the most appropriate for establishing some design parameters for the rest of the road segment. He

proposed to consider the average operating speed instead, better meeting the general character of the road segment.

An additional drawback of this methodology is that the design speed is only known if the road project is available. Otherwise, the design speed should be inferred for each geometric feature. This is not easy, since several design parameters have to be evaluated, such as sight distance, parameter for vertical curves, superelevation rate, curve radii, etc.

Ng and Sayed (2004) developed a safety performance function considering the difference of the operating and design speeds (108):

$$Y_{i,5} = e^{-3.380} \cdot L^{0.8920} \cdot AADT^{0.5913} \cdot e^{0.009091 \cdot (v_{85} - v_d)} \quad (108)$$

This safety performance function estimates the number of road crashes in 5 years ($Y_{i,5}$) in terms on this difference, $AADT$ (vpd) and the length of the curve (km).

Wu et al. (2013) analyzed the relationship between consistency and road crashes. They calculated the consistency level for two two-lane rural roads of Pennsylvania, with more than 40 geometric elements each. The consistency was determined with the IHSDM Consistency Review Module. They reflected an evident relationship between the difference of the operating and inferred design speeds and road crashes. The higher this difference, the higher the crash rate. They recommended this difference to be further investigated.

3.5.1.1.2. Comparison of the operating speed of consecutive geometric features

The previous criterion presented some issues in its definition, as well as in its application. Some of them were the design speed definition and inference. Moreover, it is also not clear how drivers' surprises or expectancies violations are considered in this definition.

A different way to estimate design consistency is by means of the examination of the operating speed variation. This procedure is much extended, because its relationship to safety as well as it is very easy to calculate. This is known as Safety Criterion II.

Since the early 1930s it is well known that a high operating speed variability exists between tangents and curves. This relationship may be linked to the likelihood of road crashes (Fitzpatrick et al., 2000).

Babkov (1968) suggested that the operating speed difference between two consecutive horizontal curves should not exceed by 15% the operating speed of the first one.

Lamm et al. (1988) defined the Safety Criterion II considering the safety performance according to this variation. They also developed an operating speed model for horizontal curves, based on the degree of curvature (DC). Thus, they could correlate the operating restrictions to the road design. They defined the following thresholds:

- $\left|v_{85_{i+1}} - v_{85_i}\right| \leq 10$ km/h . Good consistency. No action is required. $\Delta DC \leq 5º$, $|\Delta CCR_s| \leq 180$ gon/km.
- 10 km/h $< \left|v_{85_{i+1}} - v_{85_i}\right| \leq 20$ km/h. Fair consistency. This is not a major issue for drivers, but they should be warned at least. ΔDC is between 5º and 10º, 180 gon $< |\Delta CCR_s| \leq 360$ gon/km.
- $\left|v_{85_{i+1}} - v_{85_i}\right| > 20$ km/h . Poor consistency. The operating speed difference is pretty high. This zone of the alignment should be redesigned. $\Delta DC > 5º$, $|\Delta CCR_s| > 360$ gon/km.

The geometric relationships were established according to the operating speed model shown in Equation 18.

This difference should not be confused with the 85th percentile of the operating speed reduction. Hirshe's hypothesis (Hirshe, 1987) establishes that both concepts are different. This is why several other researchers have focused on estimating the operating speed reduction as well as relating it to crash rates. One example is Al-Masaeid et al. (1995), who developed three equations that related the 85th percentile of the operating speed reduction to the crash rate. Considering Safety Criterion II, horizontal curves with a radius higher than 412 m are always consistent.

Kanellaidis et al. (1990) developed operating speed models for horizontal curves and tangents. They suggested that a consistent road design could be achieved if the difference between two consecutive road geometric features was limited to 10 km/h.

Anderson et al. (1999) examined consistency and crash rates on more than 5000 horizontal curves, considering Safety Criterion II. Table 12 shows the results. Crash rates increase dramatically as the consistency gets worse.

Consistency – Lamm's Criterion II	Number of curves	Crash rate (accidents with victims/10^6veh-km)
Good	4518	0.46
Fair	622	1.44
Poor	147	2.76

Table 12. Crash rates for good, fair and poor consistency. Safety Criterion II.

The establishment of three consistency ranges is good from a design point of view, since it gives direct instructions to designers. However, it presents some problems.

The first one is related to where the thresholds should be located. These thresholds were defined considering data from some specific locations. However, different thresholds could be established for different geographic zones, like Korea (Lee et al., 2000) or Italy (Cafiso, 2000).

The second issue is related to how the calculations were performed. It was limited to OLS, linear regression. This is not a good approach, as it was previously indicated (see Section 3.1.3.2).

In addition, the speed ranges are very wide. A literal interpretation of Safety Criterion II indicates that no difference exists between $\Delta v_{85} = 10.1$ kph and $\Delta v_{85} = 20$ kph, which is not true. A continuous function would be a better tool.

All the previous assumptions are also extensible to the Safety Criterion I.

In addition, the use of the simple subtraction of the operating speeds is not a good approach to the actual phenomenon, as stated by Hirshe (1987). Different parameters should be used instead, like $\Delta_{85}v$ or *85MSR*. However, some researchers have calibrated relationships linking these parameters to Δv_{85}, such as Misaghi and Hassan (2005) and Castro et al. (2011) (Equations 61 and 62).

The operating speed reduction in a tangent-to-curve transition is not a consistency parameter by itself. However, this is highly related to road accidents, so several researchers have estimated its influence on crash rates.

Anderson et al. (1999) also developed some safety performance functions in terms of exposure and speed reduction, considering more than 5,000 horizontal curves:

$$Y_{i,3} = e^{-7.1977} \cdot AADT^{0.9224} \cdot L_C^{0.8419} \cdot e^{0.0662 \cdot \Delta v_{85}} \qquad \boldsymbol{R_{FT} = 0.179} \qquad (109)$$

$$Y_{i,3} = e^{-0.8571} \cdot MVKT \cdot e^{0.0780 \cdot \Delta v_{85}} \qquad \boldsymbol{R_{FT} = 0.168} \qquad (110)$$

Where:
$Y_{i,3}$ Estimated number of accidents at a certain curve, in three years.
$AADT$: Average Annual Daily Traffic (vpd).
$MVKT$: exposure (millions of vehicles-km in three years).
L_C: length of the horizontal curve (km).
Δv_{85}: speed reduction (kph).

Both models were found to be statistically related to road crashes, but with a weak relationship.

Anderson and Krammes (2000) further developed Fitzpatrick et al.'s research. They estimated the crash rate as a function of the operating speed reduction in tangent-to-curve transitions. This speed reduction was calculated with Ottesen and Krammes' (2000) model:

$$AR = 0.54 + 0.27 \cdot \Delta v_{85} \qquad \boldsymbol{R^2 = 0.93} \qquad (111)$$

$$AR = 0.18 + 0.23 \cdot DC \qquad \boldsymbol{R^2 = 0.91} \qquad (112)$$

Where:
AR: *Accident Rate*, in 10^6 vh-km).
Δv_{85}: Operating speed reduction (kph).
DC: Degree of curvature (degrees).

Ottesen and Krammes determine the speed reduction in terms of the degree of curvature. This is why the second expression was also provided exclusively in terms of geometry. As previously indicated, the operating speed of curves of a degree of curvature lower than 4º remains very similar to tangents. Hence, the crash rate is minimum. The high R^2 is because they grouped all their data into eleven groups, thus only fitting eleven points for determining crash rates (ecological fallacy).

Ng and Sayed (2004) developed a safety performance function depending on the speed reduction:

$$Y_{i,5} = e^{-3.796} \cdot L^{0.8874} \cdot AADT^{0.5847} \cdot e^{0.04828 \cdot \Delta v_{85}} \qquad (113)$$

Where $Y_{i,5}$ is the estimated number of accidents in five years.

Naturalistic driving data collected by instrumented vehicles is a technique that can provide information directly related to the driving task and performance.

Cafiso, di Graziano and la Cava (2005) used an instrumented vehicle in order to correlate some operating parameters to crash rates. The Driving Instrumented Vehicle Acquisition System (DIVAS) of the University of Catania was used. This is a standard medium-class car equipped with high accuracy instruments (GPS, optical odometer, gyroscope, accelerometer, etc.). It can acquire and collect in-field data under actual traffic conditions. It also measures some psychophysiological parameters, such as the electrocardiogram.

They collected data from 15 test drivers on actual roads. They confirmed that a coordinate sequence of curves does not produce an unexpected driving event even if short bending radii are adopted. However, a long tangent followed by a sharp curve does. High speed gradients of about 2 m/s^2 were found, which are quite higher than 0.85 m/s^2, usually considered. High transversal accelerations and local maximum curvatures higher than the design ones were also observed. The lack of transition curves was also found to be an inconsistency factor.

They finally recommended Lamm's Criterion II to be used for consistency evaluation, partially complemented by Lamm's Criterion I. Additionally, at some points Lamm's criterion III could also help to determine road design consistency.

Later, Cafiso and la Cava (2009) compared the driving tests to the number of accidents in 5 years, using the Empirical Bayes method. They found that the maximum driving speed differential between two successive elements and between the average section speed and the minimum single element speed were good safety performance indicators. In fact, both indicators were not correlated, and the authors suggested to use both in a complementary way. In fact, speed variations exclusively based on the operating speed may underestimate the effective change in the driving task.

3.5.1.2. Inertial evaluation methods

3.5.1.2.1. Consistency density index

Wu et al. (2013) compared the output of the consistency module of the IHSDM to the crash rates at two case study highways in central Pennsylvania. They defined δ as the difference between the operating speed and the inferred design speed for each point of the road, only when the operating speed was higher than the design speed.

They compared the δ distribution to the crash rates for three years, observing that the highest crash rates were achieved for a higher δ. The Empirical Bayes Method was used for considering more accurate data. A more detailed study showed that most of the problems were due to limited sight distance on crest vertical curves. Crash rates were developed with the IHSDM Crash Prediction Module, using the Empirical Bayes Method.

Model A uses the continuous δ parameter. Model B uses a segmented δ, not varying within the same consistency region according to Safety Criterion I. The dependent parameter for all cases is the number of crashes per year.

	Model A	Model B
Presence of a horizontal curve	0.272	0.295
Log of AADT	0.816	0.916
Log of element length	0.829	0.847
δ fair (base=good)		0.316
δ poor (base=good)		0.245
δ	0.009	
Constant	-3.314	-3.693
AIC	754.7	757
Observations	560	560

Table 13. Statistical adjustments for models A and B.

They also defined the consistency density to account for the effect of elements upstream and downstream of the study element. Hence, for a certain element, the consistency measure (δ) is:

$$\delta = \delta_{i-1} + \delta_i + \delta_{i+1} \tag{114}$$

Where δ_j is the consistency parameter for each one of the corresponding elements. Thus, they developed models C and D, in the same way as A and B (Table 14).

	Model C	Model D
Presence of a horizontal curve	0.264	0.265
Log of AADT	0.701	1.034
Log of element length	0.933	0.940
Sum of δ around the element	0.004	
Design inconsistency density (fair)		0.065
Design inconsistency density (poor)		0.015
Constant	-2.846	-3.954

AIC	686.2	689.4
Observations	532	532

Table 14. Statistical adjustments for models C and D.

They found that consistency is highly related to the number of accidents. The greater the continuous δ, the higher the crash risk (model A). Poor and fair design consistency levels are related to a higher expected total crash frequency (model B). Similar conclusions were found with the density expressions of δ. The low value of the coefficient for the element length (see models A and B) was attributed to the short length of the elements that were considered.

3.5.1.2.2. Inertial Consistency Index

García et al. (2013) presented a new consistency index that was based on the difference between the inertial operating speed and the operating speed itself. The inertial operating speed was introduced as the moving average of the operating speed, considering a length of 1000 m. They considered that this parameter reflects drivers' expectations, since it is based on the road behavior during the last 1000 m. On the contrary, the operating speed profile reflects actual road layout. Hence, a big difference between both estimators reflects a lack of consistency.

They considered 1,686 tangent-to-curve transitions, extracted from 88 two-lane rural road segments in Spain. They estimated the operating speed profiles with local models, and classified all transitions in different groups, according to this model. They proposed the following consistency thresholds, which are very similar to those proposed by Lamm for the Safety Criterion I:

- $\left|v_{85_{inertial}} - v_{85}\right| \leq 10$ km/h. Good consistency.
- $10 \text{ km/h} < \left|v_{85_{inertial}} - v_{85}\right| \leq 20$ km/h. Fair consistency.
- $\left|v_{85_{inertial}} - v_{85}\right| > 20$ km/h. Poor consistency.

3.5.1.3. Global consistency evaluation

Local consistency models mostly focus on the speed dispersion in a local area of the road. However, some road segments may not present local inconsistencies but induce a high workload demand because of speed variation. Global consistency models examine the variability of the operating speed along a road segment. These kind of methodologies were first introduced by Polus and Mattar-Habib (2004). These models do not define road design consistency according to thresholds, but in a continuous way. They have an additional advantage: the consistency value can be

included in a safety performance function to estimate the number of accidents. This is more accurate than estimating the number of accidents for a single curve. In addition, this can be used in the alternative selection stage of the project. However, these models cannot detect where local inconsistencies are, so they have to be used

The consistency model introduced by Polus and Mattar-Habib (2004) is based on the following hypothesis: a road alignment with so many speed variations forces a high variation of the driver workload. Hence this road alignment is not consistent, even if no local inconsistencies are found.

The segmentation process is of a high importance here. Polus proposed the German methodology. They used nine two-lane rural road segments in Israel, ranging from 1.5 to 8.4 km long. They developed their own operating speed profile model, based on Ottesen and Krammes' model for horizontal curves and Polus, Fitzpatrick and Fambro's model for tangents.

The Polus' consistency model is composed by two auxiliary parameters: R_a and σ. The second one is operating speed dispersion. The first one is calculated as the area between the operating speed and the average operating speed, divided by the length of the road segment (Equation 115).

$$R_a = \frac{\sum|a_i|}{L} \tag{115}$$

Where:

$|a_i|$: sum of the regions between the operating speed profile and the average operating speed (m/s).

L: length of the road segment (m).

Equation 116 shows the final consistency model, based on both previous parameters.

$$C = 2.808 \cdot e^{-0.278 \cdot R_a \cdot \frac{\sigma}{3.6}} \tag{116}$$

This expression was obtained exclusively according to road geometry. The operating speed models were only valid for horizontal curves.

According to the consistency model and the observed number of crashes, they also determined three consistency ranges:

- Good consistency: $C > 2$ m/s.
- Fair consistency: $1 < C \leq 2$ m/s.

- Poor consistency: $C \leq 1$ m/s.

They also calibrated a relationship to road crashes, using 34 two-lane rural road segments in Israel. They considered the crash rate instead of the number of accidents (Equation 117).

$$ECR = 0.5215 \cdot e^{-0.3583 \cdot C} \qquad R^2 = 0.304 \qquad (117)$$

Where ECR is the estimated crash rate (accidents with victims), per 10^6 veh-km.

García and Camacho-Torregrosa (2009) adapted the same global consistency model to estimate the crash rate in Spanish roads. They used 43 two-lane rural road segments (Equation 118).

$$ECR = 0.36108 \cdot e^{-0.3363 \cdot C} \qquad R^2 = 0.279 \qquad (118)$$

Garach (2013) developed an enhanced version of the Polus consistency model. They indicated that the original consistency model equation was not the ideal for consistency analysis. Thus, they developed Equation (119, also dependent on R_a and σ).

$$C = \frac{195.073}{\left(\frac{\sigma}{3.6} - 5.7933\right) \cdot (4.1712 - R_a) - 26.6047} + 6.7826 \qquad (119)$$

This model was developed in this way in order to fit the same thresholds as proposed by Polus et al. In addition, they proposed a Safety Performance Function able to estimate the number of accidents with victims as a function of the consistency (C), AADT and length (L) of the road segment (Equation (120).

$$Y = e^{-8.7282} \cdot AADT^{1.0674} \cdot L^{0.8179} \cdot e^{-0.1931 \cdot C} \qquad \text{AIC} = 958.82 \qquad (120)$$

Echaveguren (2012) adapted Polus' consistency model to Chilean roads. They used five road segments of 2 to 13 km long. The operating speed was collected in two ways: they used a 10 Hz GPS tracker, and they also developed an operating speed profile considering Fitzpatrick and Collins model. They concluded that the Polus' consistency model is good for determining the consistency value of a road segment, but the road segmentation should be accurately performed.

Polus et al. (2005) improved their previous consistency model by adding the speed dispersion due to the vertical alignment, through the TWOPAS equations.

Their integrated consistency model is based on adding the effect of the operating speed dispersion due to the interaction of passenger cars and heavy vehicles. A new parameter, A_{CT}, was introduced. It is the area between the operating speed profile obtained from their operating speed profiles as well as the TWOPAS equations. The integrated consistency model is calculated as shown in Equation 121.

$$IC = (2.808 \cdot e^{-0.278 \cdot R_a \cdot \sigma}) \cdot e^{-0.01 \cdot A_{CT}} \quad (121)$$

Where:

IC: Integrated consistency.

R_a: Area beneath the operating speed profile and the average operating speed profile, divided by the segment length (m/s).

σ: Operating speed dispersion (m/s).

A_{CT}: Normalized area between the operating speed profile for trucks and passenger cars (m/s).

The threshold for good, fair and poor consistency were not changed from their previous model.

They later calibrated a relationship between the integrated consistency model and the crash rates for two sets of roads (Mattar-Habib, Polus and Farah, 2008). 26 road segments from northern Israel and 83 road segments from Germany were selected. All road segments connected two major junctions, with minor intersections in between them. However, no road segments with cross-sectional changes or big AADT variations were considered. Crash data were available for three years, from 2003 to 2005. PDO crashes were not considered.

They developed two safety performance functions for roads in Israel and Germany. They performed a better adjustment than in previous cases, since they considered the number of accidents instead of the crash rate. They used a Poisson regression, developing Equations 122 (Israel) and 123 (Germany):

$$\ln(\lambda_i) = \ln(1.256 \cdot 10^{-5}) + 1.677 \cdot \ln(AADT) + 0.061 \cdot L - 0.228 \cdot IC \quad \text{Log-lik.=186.86} \quad (122)$$

$$\ln(\lambda_i) = \ln(6.902 \cdot 10^{-3}) + 0.635 \cdot \ln(AADT) + 0.226 \cdot L - 0.144 \cdot IC \quad \text{Log-lik.=-140.58} \quad (123)$$

Where λ_i is the number of accidents with victims in a year, L is the length of the road segment (km), $AADT$ the average annual daily traffic (vpd) and IC is their integrated consistency model. This is a better way to estimate accidents, although the exposure parameters were not adequately considered. $AADT$ is considered in an elasticity term, which is ok. However, the length of the road segment was considered as a geometric parameter, which might not be adequate since it is an exposure term. In addition, we can see how the $AADT$ affects the number of crashes in a very different way.

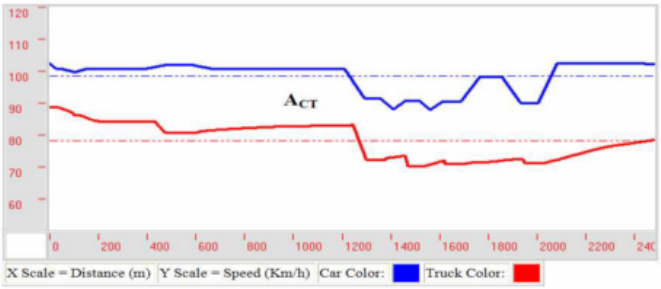

GENERAL ROAD DATA
NUMBER OF LANES: 2
ROAD COEFFICIENT: 1.00
LENGHT: 2486 m
TERRAIN: Level
SPEED PROFILE PARAMETERS - CARS
AVERAGE SPEED: 98.23 km/hr
RELATIVE AREA (Ra): 0.97 m/sec
STANDARD DEVIATION (STD): ±5.96 km/hr
CONSISTENCY: 1.79
CONSISTENCY EVALUATION: Acceptable Consistency
SPEED PROFILE PARAMETERS AND CONSISTENCY - TRUCKS
AVERAGE SPEED: 78.05 km/hr
RELATIVE AREA (Ra): 1.40 m/sec
STANDARD DEVIATION (STD): 5.49 km/hr
CONSISTENCY: 1.55
CONSISTENCY EVALUATION: Acceptable Consistency
INTEGRATED CONSISTENCY MODEL
BOUNDED AREA BETWEEN PROFILES (ACT): 5.89 m/sec
OVERALL CONSISTENCY: 1.69
OVERALL CONSISTENCY EVALUATION: Acceptable Consistency

Figure 49. HSPC (Highway Speed Profile and Consistency) Program Output (Mattar-Habib, Polus and Farah, 2008).

Most global consistency models use different forms of the speed dispersion. Their use has been more common since a better knowledge has been achieved in the recent years. Himes et al. (2011) developed a comprehensive model for estimating speeds based on several exogenous and endogenous parameters. This allow

engineers to develop better consistency, speed dispersion based models to analyze the operating speed and the operating speed dispersion.

3.5.2. Vehicular stability

When a vehicle enters a curve, there are several forces acting over it, which cause the change of its direction. Due to the change of its direction, a centripetal force appears. This force tends to throw the vehicle away from the road. Some other friction-related forces, as well as part of the mass of the vehicle compensate the first one and keeps the vehicle on the pavement.

Figure 50 shows the simplified model with all forces. f_t is the side friction demanded in order to keep the vehicle on the pavement. v is the speed at which the vehicle enters the curve.

Some factors, such as the radius and the superelevation rate, are decided in the design stage. Some of them, such as the superelevation rate, may depend on the design speed (depending on the guidelines). On the other hand, different drivers select different speeds. The side friction demand is therefore a result of the combination of previous factors. The higher the speed, the higher the side friction demand.

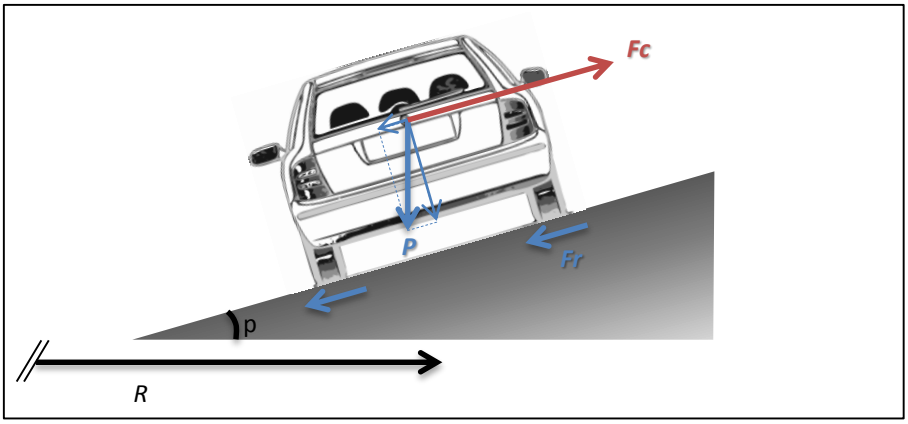

Figure 50. Forces acting on the vehicle when negotiating a curve.

$$F_c = m \cdot \frac{v^2}{R} \quad (124)$$

$$P = m \cdot g \quad (125)$$

$$F_r = f_t \cdot F_N = f_t \cdot P \cdot \cos p \quad (126)$$

A global equilibrium of forces can be established in the x axis:

$$f_t \cdot P \cdot \cos p + P \cdot \sin p = F_c$$

$$m \cdot g \cdot (f_t \cdot \cos p + \sin p) = m \cdot \frac{v^2}{R}$$

$$g \cdot (f_t \cdot \cos p + \sin p) = \frac{v^2}{R}$$

The superelevation rate is almost negligible. Hence:

$$\sin p \approx \tan p \approx p$$
$$\cos p \approx 1$$

$$g \cdot (f_t + p) = \frac{v^2}{R}$$

$$v^2 = g \cdot R \cdot (f_t + p)$$

Adopting $g = 9.8\ \mathrm{m/s^2}$ and changing the speed to km/h, it yields to:

$$v^2 = 127 \cdot R \cdot (p + f_t) \quad (127)$$

The side friction can be expressed in terms of the rest of parameters:

$$f_t = \frac{v^2}{127 \cdot R} - p \quad (128)$$

As it can be seen, the sharper the curve, higher the speed or lower the superelevation rate, a higher skid resistance is required. However, there is a maximum side friction that the pavement is able to offer. If the demanded side friction tends to exceed the pavement skid resistance, the equilibrium of all forces is not satisfied and hence the vehicle escapes from the pavement. This happens for a friction demand in the area of $0.50g$ for passenger cars, and from $0.24g$ to $0.35g$ for trucks, depending on their loading and configuration (Pratt and Bonneson, 2008).

The lateral acceleration is not introduced in this equation, but it also has something to say. Its value is highly related to drivers comfort. The higher the speed, the higher the centripetal force and hence the lateral acceleration.

Drivers begin to feel uncomfortable for side friction demands quite lower than the friction limits of tires. They react to this discomfort by reducing their speed. The Green Book recommends design-side friction factors conservatively below the point where most drivers feel discomfort.

Design speed (mph)	Design-side friction factor (g)
10	0.38
15	0.32
20	0.27
25	0.23
30	0.20
35	0.18
40	0.16
45	0.15
50	0.14
55	0.13
60	0.12
65	0.11
70	0.10
75	0.09
80	0.08

Table 15. Design-side friction factors based on upper limit of driver comfort (AASHTO, 2011)

The design-side friction factors decrease as the curve speed increases because the drivers desire less side friction demand as the speed increases. As the speed increases, the heading change becomes more noticeable for drivers. Thus, more steering effort is required to stay properly within the travel lane. These conditions require a high concentration and thus the cone of vision is reduced. As the curve speed increases, these undesirable conditions occur at lower side friction demand levels (Pratt and Bonneson, 2008).

This kind of consistency evaluation examines the vehicular stability of a vehicle when driving through a curve. Therefore, it evaluates the inferred design conditions of the curve but considering the operational parameters. There are different approaches to the same phenomenon.

3.5.2.1. Comparison between demanded and assumed side friction

This consistency criterion compares the demanded side friction (due to the operating speed) to the required side friction to keep the vehicle on the pavement (assumed side friction). This method is recommended for evaluating design consistency by ensuring that enough side friction (f_R) supply is available to meet the side friction demand (f_{RD}) as vehicles negotiate a horizontal curve.

Side friction (f_R) is calculated considering the inferred design speed for each individual curve. Side friction demand (f_{RD}) is determined as a function of the operating speed. This criterion was introduced by Lamm, Psarianos and Mailaender (1999) as the Safety Criterion III.

This model presents some drawbacks, but it is very simple to use. This is why this model is the most extended among all which deal with vehicle stability.

The assumed side friction was calculated using the 1984 edition of the AASHTO Green Book. Relationships relating f_R to v_d were first developed by regression of the maximum permissible tangential friction recommended in the United States, Germany, France, Sweden and Switzerland as a quadratic function of the design speed. This is later multiplied by a factor of 0.925 in order to reduce the maximum side friction compared to the tangential friction, due to tires-pavement interaction. An additional factor (n) is applied, depending on the terrain (Hassan, 2004). Thus, the side friction can be calculated from the inferred design speed with Equations 129 and 130.

$$f_R = n \cdot 0.925 \cdot f_T \quad (129)$$

$$f_T = 0.58 - 4.92 \cdot 10^{-3} \cdot v_d + 1.81 \cdot 10^{-5} \cdot v_d^2 \quad (130)$$

Where:
f_T skid resistance for ideal conditions.
v_d inferred design speed (km/h).
n ratio to apply on the transversal skid resistance. It is 0.40 for mountainous roads, 0.45 for level terrains and new designs, and 0.60 for already existing roads.

The demanded side friction is calculated by means of the vehicular stability equation (Equation 131).

$$f_{RD} = \frac{v_{85}^2}{127 \cdot R} - e \quad (131)$$

Where f_{RD} is the demanded skid resistance, v_{85} is the operating speed (km/h), and e is the superelevation rate (%).

The consistency parameter is the difference between both values, calculated according to Equation 132.

$$\Delta f_R = f_R - f_{RD} \tag{132}$$

Lamm also gave three different consistency classifications according to the thresholds shown in Table 16.

Consistency	Lamm's Criterion III
Good	$\Delta f_R \geq 0.01$
Fair	$0.01 > \Delta f_R \geq -0.04$
Poor	$\Delta f_R < -0.04$

Table 16. Consistency thresholds for Safety Criterion III.

This method is widely known because of its simplicity. Although the end user is benefited from a simpler model, this one may be too simplistic. The interaction between the tires and the pavement is extremely complex, being this expression too simple. It depends on more factors, and its relationship with the pavement type is not so strong. The tangential and side friction values are almost the same in all AASHTO editions. All friction values have been based on the same research that was carried out in the 1930s and 1940s, with slight differences (Hassan, 2004). This expression considers the radius of the curve, but this is not the one performed by drivers, who tend to smooth it.

Additionally, there are some issues relating the statistical modelling that was used for determining these thresholds. All the drawbacks exposed for Safety Criteria I and II are also valid here, such as the geographical variability, the OLS regression and the wide consistency zones.

Ng and Sayed (2004) developed the following safety performance function to estimate the number of accidents with victims in five years ($Y_{i,5}$) as a function of the exposure (km and vpd) and Lamm's Safety Criterion III.

$$Y_{i,5} = e^{-3.303} \cdot L^{0.8733} \cdot AADT^{0.5680} \cdot e^{-2.194 \cdot \Delta f_R} \tag{133}$$

3.5.2.2. Models based on the kinetic energy

The side friction demand is determined in terms of the operating speed on the curves. However, this speed is highly dependent on the operating speed at the approaching tangent. Bonneson (2000) developed the following relationship between the side friction demand and curve and tangent speed:

$$f_t = 0.259 - 0.00359 \cdot v_{85T} - 0.0214 \cdot (v_{85T} - v_{85C}) \quad (134)$$

In this expression, f_t is the side friction demand at 85th percentile curve speed (g), and v_{85T} and v_{85C} are operating speeds for tangent and curve, respectively (mph).

This equation gives the side friction demand for any combination of operating speeds of tangents and curves. If they are set the same, the resulting side friction is the one at which the 85th percentile passenger car driver does not reduce the speed. This friction level is about 0.05 to 0.10g lower than the values provided by the AASHTO.

Pratt and Bonneson (2008) identified the side friction differential as a curve severity measure, since drivers are more likely to lose the control of their vehicles when they experience side friction demand that they find excessive. This may happen for low speed reduction levels when the operating speed on the tangent is high. Hence, curves should be assessed based on the energy reduction calculated from the estimated curve and approach tangent speeds.

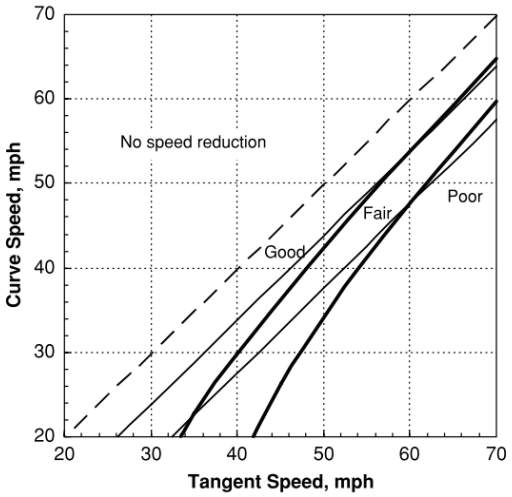

Figure 51. Comparison of speed reduction and energy reduction thresholds for the model developed by Pratt and Bonneson (2008).

3.5.2.3. Safety margin methods

The safety margin concept is used in several fields of civil engineering. It is based on examining the difference between the critical and actual lateral acceleration, friction or speed.

According to the AASHTO (2011), the minimum curve radius is calculated as:

$$R_{min} = \frac{v^2}{127 \cdot (e_{max} + f_{max})} \tag{135}$$

Where e_{max} and f_{max} are the máximum permissible design superelevation and side friction coefficient. The maximum value of the sideways friction coefficient for design depends upon the design speed for a curve.

For radii greater than the minimum radius, the design superelevation and side friction are less than their maximum values. The AASHTO proposes five methods to distribute superelevation and side friction according to the curve radius.

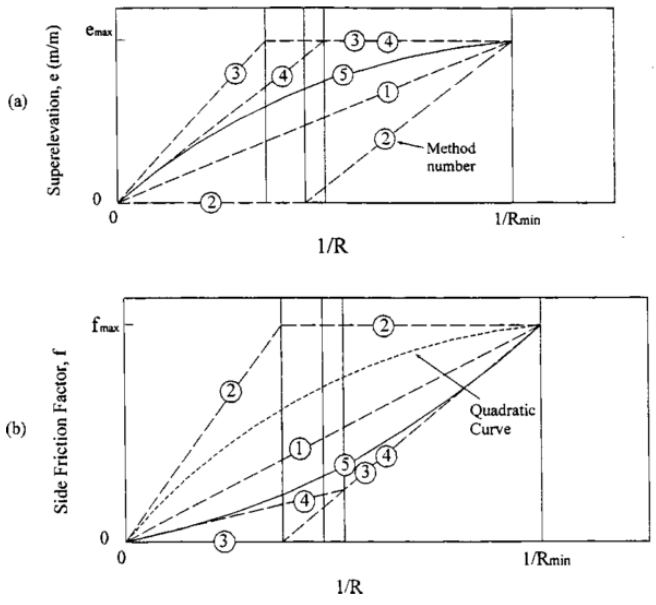

Figure 52. AASHTO methods of distributing superelevation and side-friction.

Nicholson (1998) defined margin of safety as the difference between the limiting speed and the design speed. The limiting speed (v_L) is the one that requires the maximum friction coefficient (f_{max}), which is used for design. It is calculated as:

$$v_L = \sqrt{127 \cdot R \cdot (e + f_{max})} \tag{136}$$

The difference between the limiting speed and the design speed can be considered a design margin of safety. A good design will try to maximize this safety margin. Drivers tend to operate considering ad hoc expectations, so their operation at one curve affects how they face the following one. Thus, the safety margin of a curve also is influenced by the operating speed of the previous one.

The variation of the safety margin along a highway section arises mainly from the variation of the superelevation rate. Therefore, it is desirable to distribute the superelevation rate in order to produce small variations of the safety margins (better design consistency) and a large average safety margin for each curve (greater safety).

Nicholson (1998) compared the safety margins of the AASHTO methods of distributing e and f. He found that Method 2 provided the smallest mean and variance, while Method 3 resulted in the largest mean and variance. Nicholson concluded that Method 1 (linear distribution) appeared to be the best. Easa (1999) completed the previous analysis, by adding an unsymmetrical parabolic curve, as described by AASHTO, showing that Method 5 was the best.

Easa (2003b) presented a new method to distribute superelevation rates along a road segment, in order to maximize the safety margin mean and to minimize its dispersion.

3.5.3. Alignment Indices

Alignment Indices are parameters which resume the general character of a road segment in a single value. They are very easy to calculate and interpret, so some researchers have suggested their use for design consistency evaluation. Some relationships to safety have been proposed as well. Because of their simplicity, some guidelines do also include them in the road design process, such as the Italian standards.

Some of the alignment indices are applied to the whole road segment, such as the ratio between the largest and the sharpest radii of a road segment. Some others are

different for each geometric element, such as the Curvature Change Ratio. Thus, depending on the definition of the alignment index, an inconsistency can be found if either of the following situations takes place:

- An abrupt change of an alignment index for two successive geometric elements.
- A high variability of an alignment index.
- A high difference between a certain geometric feature of one geometric element and the average value of the alignment index.

Polus (1980) noticed that the crash rate was lower if the alignment indices presented less dispersion.

Some examples of alignment indices are (Fitzpatrick et al., 2000):

- Horizontal alignment indices:
  - Curvature change rate (CCR).
  - Curvature degree.
  - Ratio between the curved length and the whole road segment (CL:RL).
  - **Average radius (AR).**
  - **Average tangent (AT).**
  - **Ratio between a certain radius and the average radius (CRR).**
  - Ratio between the largest and the sharpest radii (RR).
  - Ratio between the length of a tangent and the average length of all tangents (TL:AT).
- Vertical alignment indices:
  - Vertical CCR (V CCR).
  - **Average vertical curvature (AVC).**
  - Average vertical grade (V AG).
- Combined alignment indices:
  - Combined CCR.

However, the same authors indicated that the best alignment indices were those marked in bold.

CRR is a good estimator of the number of crashes. It is not a single value for all the road segment, but varies for each curve. This alignment index does not perform well

for the sharpest and smoothest curves of a certain alignment. This might be since this parameter does not take into account the length of the curve.

Anderson et al. (1999) developed an expression that estimates the number of accidents with victims considering the CRR. 5,287 horizontal curves were tested, with a total of 1,747 accidents from 1993 to 1995. However, 93.2 % of those curves experienced zero or one accident in the the 3-year period.

$$Y_{i,3} = e^{-5.932} \cdot AADT^{0.8265} \cdot L_C^{0.7727} \cdot e^{-0.3873 \cdot CRR} \quad (137)$$

This expression estimates the number of accidents in three years ($Y_{i,3}$) as a function of the exposure ($AADT$ and L_C in vpd and km) and the CRR index.

Ng and Sayed (2004) developed a similar equation to estimate the number of accidents in five years ($Y_{i,5}$).

$$Y_{i,5} = e^{-3.159} \cdot L_C^{0.8898} \cdot AADT^{0.5906} \cdot e^{-0.3606 \cdot CRR} \quad (138)$$

The length of the curve is also in km.

The ratio between the maximum and minimum radii is also a well-known alignment index. It is calculated as follows:

$$RR = \frac{R_{max}}{R_{min}} \quad (139)$$

This alignment index provides a single value for the entire road segment. As the RR index gets closer to 1, the general character of the road segment is more homogeneous, indicating a higher consistency.

Previous research have indicated that this parameter does not perform well. For instance, a road segment might perform quite homogeneous, only with a sharper curve. In this case, the RR parameter might indicate that the road segment is not adequate, which might not be true.

In addition, a similar RR for two road segments may be interpreted in very different ways. For instance, it is not the same having 1000 and 500 m as the maximum and

minimum radii than 200 and 100 m. This issue can be addressed by combining this parameter with the average radius.

The average vertical curvature parameter is determined as follows:

$$AVC = \frac{\sum \frac{L_i}{|A|_i}}{n} \tag{140}$$

Where:
AVC: Average vertical curvature (m/%).
L_i: length of the vertical curve i (m).
$|A|_i$: Absolute algebraic difference of the longitudinal grade (m).
n: Number of vertical curves of the road segment.

This parameter is strongly correlated to the available sight distance.

Anderson et al. (1999) developed a safety performance function for the previous three road safety indices. They estimated the number of accidents with victims within 3 years. The correlation parameter was quite higher than for their model with CRR. The reason is because these three parameters are for an entire road segment, which always produces better correlations than when a single curve is fitted. 282 road segments were used for the former two, and 249 for the last one. $AADT$ is expressed in vpd, while the length of the road segment is in km. The length for the road segments ranged from 6.4 to 32 km.

$$Y_{i,3} = e^{-7.845} \cdot AADT^{0.995} \cdot L^{1.108} \cdot e^{-0.000137 \cdot AR} \qquad R^2 = 0.6726 \tag{141}$$

$$Y_{i,3} = e^{-7.859} \cdot AADT^{0.988} \cdot L^{1.058} \cdot e^{0.0043 \cdot RR} \qquad R^2 = 0.6651 \tag{142}$$

$$Y_{i,3} = e^{-8.297} \cdot AADT^{1.052} \cdot L^{1.167} \cdot e^{-0.0028 \cdot AVC} \qquad R^2 = 0.6880 \tag{143}$$

The authors indicated that high part of the correlation is explained by the exposure parameters ($AADT$ and L). In fact, the alignment index explains from 0.66 to 3.29% of the variability. However, the authors remark that the crash rates behave accordingly to what they expected.

Fitzpatrick et al. (2000) performed a sensitivity analysis for several alignment indices. They determined that the most adequate alignment indices for estimating the number of accidents were the average radius and the average longitudinal grade of the road. The CRR was not selected. However, they highlighted that the best way to

estimate the number of accidents was with operational consistency measurements, rather than on alignment indices.

3.5.4. Driver workload

Driver workload can be defined as a measurement of the mental effort that a person assigns for a certain activity. It is not linked to the task difficulty, but to the human factor. Hence, it reflects in a better way the actual definition of design consistency. On the contrary, it is still too difficult to measure how the driver workload is affected by the road design.

According to section 3.2.4, drivers adapt their performance according to the workload requirements of the road segment. According to driver workload demand, a road accident may happen in the following two cases:

- Some point of the road is very complex, overpassing driver's capacity. The performance dramatically decreases and some information is missing.
- The driving workload is not a problem. Drivers adapt their performance to the workload demand. If a sudden workload demand appears, drivers might not be able to adapt their performance, thus increasing the probability of an accident.

The difference between both situations is that in the second one, the driver would be able to respond to it in a good way if the road alignment would not have "trained them" to perform in that way. This is completely connected to design consistency. However, we previously stated that the workload can be managed by the driver by means of adjusting their operating speed. Thus, both situations are somehow the same. This meets the conclusions provided by Wooldridge (1994), who identified two hazardous situations according to workload demand:

- Those sites with a high workload demand.
- Locations with a sudden increase of the workload demand.

Heger (1995) compared the distribution of the mental workload capacity and the mental workload demand in order to determine a nominal safety distance (Figure 53). The mental workload demand is narrower, since it is adapted to the certain situation, which is almost the same for all drivers. The mental workload capacity is quite more disperse, since it depends on particular conditions of drivers. The nominal safety distance is defined as the distance, in terms of mental workload, from the 85th

percentile of the mental workload demand and the 15th percentile of the mental workload capacity.

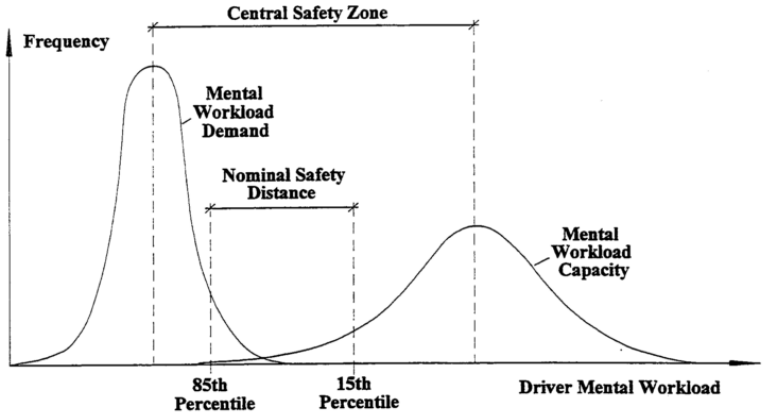

Figure 53. Relationship between Mental Workload Demand and Mental Workload Capacity (Heger, 1995).

The difficulty of dealing with this kind of parameters is how to measure them. This research field is in continuous evolution, due to the new technology possibilities. Smiley proposed four basic approaches:

- Primary task measures: as the task becomes more difficult, performance deteriorates.
- Secondary task measures: while performing a primary task, the driver also performs a secondary task. The more difficult the primary task, the poorer performance of the secondary task.
- Physiological measures: as the primary task increases in difficulty, physiological arousal increases.
- Subjective measures: as the primary task increases in difficulty, so does the driver's estimate of their own workload.

Therefore, we can distinguish four approaches to measure consistency:

- Visual Demand (VD).
- Subjective perception scales.
- Measurement of psychophysiological parameters.
- Other methods.

3.5.4.1. Visual Demand methods

Examining the visual requirements to perform the driving task is an indicator of the driver workload. Drivers are supported on visual perceptions by far more than in other stimuli.

Visual Demand can be understood as the amount of visual information that the driver needs for maintaining an adequate control of the vehicle. These methods try to determine the minimum information required for performing the driving task. It consists on impeding the driver's vision at a certain rate along the road (Wooldridge et al, 2000).

Krammes et al. (1995) proposed a visual demand technique to determine the design consistency of horizontal curves. They used visual occlusion techniques. The driver is assumed to need to attend to the roadway only for part of the total driving time. As the roadway becomes more complex, the driver spends more time acquiring visual information. In their experiments, the road users were forced to drive with their eyes closed, only opening them when they needed some information to keep the vehicle on the pavement. The total amount of time they need to be with the eyes open is related to the workload demand. The higher the time, the higher the workload.

They developed the following relationship between the workload level of a horizontal curve (WL, in %) and the degree of curvature:

$$WL = 0.193 + 0.016 \cdot DC \qquad R^2 = 0.90 \qquad (144)$$

Fitzpatrick et al. (2000) performed an experiment with 24 volunteers driving an instrumented vehicle, using the visual occlusion technique. They employed a LCD visor that was either under the control of the driver or the experimenter. They established two objectives:

- Assess driver workload imposed by roadway geometric features.
- Assess driver tolerance for increases in workload imposed by roadway geometric features.

They tested three different courses with some geometric features. They finally calibrated the following expression, based on a sample size of 670 curves:

$$VD_L = 0.285 + \frac{23.133}{R} \qquad R^2 = 0.526 \qquad (145)$$

The attention level also varies between familiar and unfamiliar drivers. Obviously, unfamiliar drivers need to pay more attention and thus the visual demand is higher. Wooldridge et al. (2000) proposed two models to estimate the visual demand for horizontal curves, depending on the familiarity with the road. The model for familiarized users is Equation 146, while the Equation 147 represents the model for unfamiliar ones.

$$VD_{LF} = 0.198 + \frac{29.2}{R} \quad (146)$$

$$VD_{LU} = 0.173 + \frac{43.0}{R} \quad (147)$$

They also examined pairs of curves, but no significant results were achieved.

This model only depends on the curve radius. Thus, the visual demand increases as the radius decreases. However, the sharpest curves are designed for a lower operating speed environment, so the drivers have more time to process the perceived information (Hassan, Sayed and Tabernero, 2001).

The visual demand for unfamiliar drivers is higher for all radii lower than 552 m. Thus, this value was established as the logical limit to the model. A relationship between the visual demand and safety performance has yet to be documented (Hassan, 2004).

Ng and Sayed (2004) developed a safety performance function for each kind of driver, considering the models proposed by Wooldridge et al. (2000):

$$Y_{i,5} = e^{-4.679} \cdot L^{0.8873} \cdot AADT^{0.5841} \cdot e^{4.566 \cdot VD_{LF}} \quad (148)$$

$$Y_{i,5} = e^{-4.297} \cdot L^{0.8866} \cdot AADT^{0.5831} \cdot e^{3.076 \cdot VD_{LU}} \quad (149)$$

Easa and He (2006) evaluated the visual demand on three-dimensional highway alignments, using a driving simulator. 15 people participated in the experiment, where nine two-dimensional and 3D hypothetical alignments for two-lane rural roads were tested. They found that the visual demand on 3D curves varies significantly with the inverse of the horizontal curve radius and the inverse of the vertical curvature. In addition, the age of the subject has a significant effect. A driver older than 65 needs 35-40% more workload on 3D alignments than younger drivers.

Visual demands for full, half and first 30 m of 3D curves were calculated as follows:

$$VDF = 0.1668 + 28.6502 \cdot RINV + 1.2826 \cdot KINV \cdot C_{type}(C) + 0.9592 \cdot KINV \cdot C_{type}(S) + 0.0032 \cdot Age \quad \mathbf{R^2 = 0.80} \quad (150)$$

$$VDH = 0.1685 + 37.2199 \cdot RINV + 1.0282 \cdot KINV \cdot C_{type}(C) + 0.6457 \cdot KINV \cdot C_{type}(S) + 0.0029 \cdot Age \quad \mathbf{R^2 = 0.57} \quad (151)$$

$$\log VD30 = -1.5148 + 85.3096 \cdot RINV + 0.0084 \cdot Age \quad \mathbf{\frac{Pchisq}{DF} = 0.01} \quad (152)$$

Where:
$RINV$: Inverse of horizontal curve radius (m^{-1}).
$KINV$: Inverse of K (absolute value for crest or sag vertical curves).
$C_{type}(C)$ and $C_{type}(S)$: Nominal variables for C and S curves.
Age: Age of the subject.

The visual demand for full, half and first 30 m on the tangent was calculated as:

$$VDF = 0.2022 + 11.2527 \cdot RINVP + 0.0028 \cdot Age \quad \mathbf{R^2 = 0.35} \quad (153)$$
$$VDH = 0.1940 + 19.9492 \cdot RINVP + 0.0029 \cdot Age \quad \mathbf{R^2 = 0.35} \quad (154)$$
$$VD30 = 0.1837 + 19.8707 \cdot RINVP + 0.0036 \cdot Age \quad \mathbf{R^2 = 0.35} \quad (155)$$

Where $RINVP$ is the inverse of radius of the preceding curve (m^{-1}).

3.5.4.2. Qualitative scale methods

A different way to determine the driver demand that the road imposes to the drivers is by using qualitative, subjective scales. In this case, drivers are asked about the performance along a certain road, just after driving through it. The results are used for determining the workload demand and hence the design consistency level.

Messer (1980) established a methodology to estimate the workload demand based on measuring certain geometric features of the road. The underlying hypothesis is that the workload demand should be higher for curves with a high deflection angle. He developed the following expression:

$$WL_n = \left(U \cdot E \cdot S \cdot R_f\right) + (C \cdot WL_l) \quad (156)$$

Where:
WL_n: Estimated workload demand for the geometric element n.

U: Unfamiliarity factor. It depends on the road classification and its situation).
E: Expectancy factor of the geometric element. It is $C - 1$ if the geometric element is similar to the previous one. 1 otherwise.
S: Sight distance factor.
R_f: Potential workload demand for the general road geometric element.
C: Overlapping factor. This factor depends on the distance between the geometric elements.
WL_l: Workload demand of the previous geometric element.

This research also provides several figures and tables to determine all these coefficients. However, the sources are not given. All geometric elements with $WL_n \leq 1$ are considered as good consistent. On the contrary, $WL_n > 6$ indicates a poor consistency.

Considering this consistency definition, a poor consistency can be addressed in several ways: change of a certain geometric feature, separate the geometric elements, or increase the sight distance before the consistency issue. He also recommended not to propose horizontal curves with excessive length, since they tend to accumulate accidents. He also gave some recommendations to coordinate horizontal and vertical curves, as well as for intersection design.

Another option is the Modified Cooper-Harper scale, which is widely used in aircraft testing (Fitzpatrick et al., 2000) (Table 17).

The procedure for workload rating is quite more complex than using the visual demand method. However, there is no research about the relationship visual demand – crash rates. Wooldridge (1994) observed that the highest collision rate was for $WL = 6$ in the Messer Scale. A clearer trend was found when grouping the road sections using a workload yaw defined as the difference between the workload of a feature and the moving average of the workload.

Difficulty level	Demand	Anchors	Rating
Very easy	No mental effort needed to drive	As easy as driving a straight, flat road	1
Easy	Little mental effort needed to drive		2
Little difficulty	Some mental effort needed to drive		3
Minor difficulty	Moderate mental effort needed to drive		4
Difficult	Considerable mental effort needed to drive	By concentrating you can steer a smooth path	5
Very difficult	High mental effort needed to drive		6
Major difficulty	Maximum mental effort needed to drive		7
Very major difficulty	Maximum mental effort needed to stay in lane		8
Almost impossible	Maximum mental effort needed to stay on road		9
Impossible	Cannot stay on the road	Curves are too sharp to stay on road	10

Table 17. Modified Cooper-Harper scale.

3.5.4.3. Psychophysiological measurement

A poor consistency is linked to a sudden variation of the workload demand. Although this is a drivers' internal process, they reflect the difficulty through some physical responses, such as the blink rate or heartbeat. Thus, a slow blink rate may indicate a low workload, while a high heartbeat rate indicates a high workload.

In this case, it is also necessary to compare these values to their normal state. These factors vary a lot among different people, as well as depending on the specific moment (Heger, 1995).

3.5.5. Other methods

There are some other consistency measurement methods.

3.5.5.1. Checklists

The AASHTO (1972) published a checklist that consisted in a set of points that a road segment should gather in order to offer a good consistency level. This methodology is not used, since it is more than 40 years old. In addition, it is not a quantitative measurement method, and it does not present any quantitative relationship to road safety:

Factors to Consider in the General Review		
Cross-Section Markings	Lighting	Road Surface
Guide Signs & Route Markers	Missing Information	Sight Distance
Geometry	Terrain	Signals
Land Use	Traffic	Warning & Regulatory Signs
	Road Type	Weather
Detailed Analyses		
Navigation Expectancies	Guidance Expectancies	Special Features

Table 18. Some aspects covered by the checklist (AASHTO, 1972).

3.5.5.2. Combined models

Cafiso et al. (2010) developed a comprehensive model to estimate the number of accidents based on a combination of exposure, geometry, consistency and context variables.

They used 107 homogeneous segments on a total of 168.20 km of roads. The length of these road segments ranged from 0.50 to 4.29 km. Road segments were determined according to exposure, roadside hazard (RSH) and CCR.

As consistency terms, they used the following ones:

- Polus' global consistency model.
- Local consistency criteria (see Equations (157 to (159).

$$\Delta V_n = \frac{\sum_{s=1}^{n_{\Delta V}} \Delta V_s}{n_{\Delta V}} \quad (157)$$

$$\Delta V_{10} = \frac{N(\Delta V > 10)}{L_{SH}} \quad (158)$$

$$\Delta V_{20} = \frac{N(\Delta V > 20)}{L_{SH}} \quad (159)$$

Where:

ΔV_s: speed differential (km/h).
ΔV_n: Average speed differential (km/h).
ΔV_{10}: ΔV_{10} density (1/km).
ΔV_{20}: ΔV_{20} density (1/km).
$n_{\Delta V}$: number of speed differentials in the homogeneous section (HS).
$N(\Delta V > 10)$: Number of speed differentials higher than 10 km/h in the homogeneous section.
$N(\Delta V > 20)$: Number of speed differentials higher than 20 km/h in the homogeneous section.

The context-related variable was the driveway-density (DD), obtained from RSI checklists.

The curve ratio was defined as:

$$CR = \frac{\sum_{j=1}^{k} L_{Cj}}{L_{HS}} \tag{160}$$

Where L_{HS} is the total length of the homogeneous section (km) and L_{Cj} is the length of the j^{th} curve in the homogeneous section composed by k curves.

A negative binomial distribution was used. They obtained 19 models, highlighting the following ones:

$$y_i = e^{-6.682} \cdot L \cdot AADT^{0.619} \cdot e^{0.0646 \cdot DD - 1.89 \cdot CR + 0.0691 \cdot s} \qquad \boldsymbol{AIC = 407.4} \tag{161}$$

$$y_i = e^{-7.812} \cdot L \cdot AADT^{0.753} \cdot e^{0.067 \cdot DD - 1.948 \cdot CR + 0.0872 \cdot \Delta v_{10} + 0.185 \cdot RSH} \qquad \boldsymbol{AIC = 407.4} \tag{162}$$

Where:

y_i: number of crashes in a year.
L: road segment length (km).
$AADT$: traffic volume (vpd).
DD: driveway density (number of driveways/km).
CR: curve ratio.
s: standard deviation of speed (kph).
Δv_{10}: speed differentials density (higher than 10 kph).
RSH: roadside hazard rating.

Those models should be compared to the one in which only the exposure is presented (Section 3.4.2).

3.5.5.3. Global Criteria

The different consistency criteria would give different consistency rates for the same road feature. Thus, Lamm et al. (1995) proposed a global consistency indicator. It combined the results of his previous three criteria. This is not a well-known consistency factor. Table 19 shows its determination.

Criteria I, II and III (the order does not matter)			Result
Good	Good	Good	Good
Good	Good	Fair	Good
Good	Good	Poor	Good
Good	Fair	Fair	Fair
Good	Fair	Poor	Fair
Good	Poor	Poor	Poor
Fair	Fair	Fair	Fair
Fair	Fair	Poor	Fair
Fair	Poor	Poor	Poor
Poor	Poor	Poor	Poor

Table 19. Global consistency criteria (Lamm et al., 1995).

However, some inconsistencies should never be permitted. Some of them are also correlated, so a more quantitative criterion was recommended (Hassan, Sayed and Tabernero, 2001).

Ng and Sayed (2003) tried to develop a global quantitative criterion considering $|v_{85} - v_d|$, Δv_{85}, Δf_R, CRR, VD_{LU} and VD_{LF}. They demonstrated that each one of those criteria alone had a significant relationship with collision frequency. They also tried to combine two of them in order to obtain a better accuracy, but no results were found. As Hassan (2004) demonstrated, all those criteria depend mainly on the curvature, so they are strongly correlated, even though it may not be linear.

They later developed several safety performance functions for indicators of each one of the general consistency criteria. Equation 163 is only valid for horizontal curves, while the Equation 164 is valid for horizontal curves and tangents.

$$Y_{i,5} = e^{-3.369} \cdot L^{0.8858} \cdot AADT^{0.5841} \cdot e^{0.0049 \cdot (v_{85} - v_d) + 0.0253 \cdot \Delta v_{85} - 1.177 \cdot \Delta f_R} \quad (163)$$

$$Y_{i,5} = e^{-2.338} \cdot L^{1.092} \cdot AADT^{0.4629} \cdot e^{IC \cdot (0.022 \cdot \Delta v_{85} - 1.189 \cdot \Delta f_R)} \quad (164)$$

IC is a dummy variable, 0 for tangents and 1 for horizontal curves.

They also evaluated some other expressions considering each one of the consistency criteria on their own. As it can be seen, slight more variability is achieved when combining some of them.

3.5.6. Implementation of the consistency into the road design process

Horizontal alignment design mainly involves the design of horizontal curves and tangents. Several researchers have developed methods to design horizontal and vertical alignments using different objectives. These methods can be classified into three categories:

- Optimization methods. They address construction costs for horizontal or horizontal/vertical (combined) alignments.
- Speed-profile methods. Their goal is the maximization of the design consistency, based on trial and error. They consider horizontal or combined alignments.
- Special methods. Mostly based on expert systems or addressing some other measures such as collision cost.

Construction cost is the main criterion of alignment design in existing methods. However, no systematic method is available to maximize design consistency in highway alignment design (Easa and Mehmood, 2007).

The process for optimizing and evaluating design consistency for new alignments would involve trial and error. This does not guaranty that the best solution is achieved; as well as this is a time-consuming process.

Easa and Mehmood (2007) developed an optimization model looking for maximizing the design consistency. Their model was based on the operating speed profile developed by Fitzpatrick and Collins (2000). Given a tentative alignment, they developed a procedure that calculated the best alignment considering some physical and functional constraints. The objective function was to minimize the mean speed difference of successive geometric features along the highway section. Another useful objective was to minimize the maximum speed difference. However, this model presented some limitations, such as only the horizontal alignment was considered. In addition, some other factors such as the cost were not considered.

3.6. Limitations of the current knowledge

We have reviewed the state of the art of several fields: road safety, human factor and traffic psychology, road design, infrastructure factor and road design consistency. As a result, we have identified some gaps of the current knowledge, which are summarized as follows.

There are three important concurrent factors in road safety: infrastructure, human and vehicle factors. The interaction between the infrastructure and human factors are of a major importance. Human behavior is very difficult to estimate, since it does not respond to a cause-consequence structure. Road safety theories try to explain this behavior. Several theories were presented, showing their advantages and disadvantages. The important fact is that there is not a driving behavior theory able to explain everything, but all theories can be used in a complementary way.

Driver behavior is caused by road design. Drivers respond to the road layout, and this response can be measured. Thus, it is necessary to establish good tools to design and analyze road design. Design speed is a fundamental parameter for this task. However, there is some controversy about how it should be measured and considered in the design stage. This is, in part, due to the ambiguity at establishing homogeneous road segments. Some methodologies have been explained. The recreation of the road geometry plays also a major role in road research. Most existing methodologies are based on the analysis of the curvature, so they also lack of accuracy while recreating complex geometries.

There is a lot investigated about how drivers response to road design. We have shown some of the most well-known operating speed models. Operating speed models for curves generally present a good accuracy. This is not true for tangents, where there is a high operating speed dispersion. In addition, those models present high geographical variations.

Road design consistency is a good tool to estimate the number of road accidents. There are four main ways to calculate it, although the operating speed is the best-known. There are two kinds of consistency models: local and global ones. Global models are useful for being introduced as a part of a Safety Performance Function, in order to estimate the number of accidents. However, there is little literature about them, especially about how the affection of the exposure parameters.

4. Objectives

The main objective of this research is the development of a global consistency model for two-lane rural roads. This model should be related to road crashes, therefore enabling the possibility to estimate them and thus design safer roads. This parameter could also be used in the planning stage, for prioritizing alternatives.

Some additional objectives are:

- Development of a methodology for recreating the horizontal alignment of road segments. Starting from a polyline that represents the centerline of a road section, this methodology is able to identify the horizontal alignment. A computer application will also be programmed for performing this task.
- Development of a computer application able to depict the operating speed profiles departing from operating speed models and a horizontal alignment.
- Development of a segmentation methodology that allows us to split a road section into homogeneous road segments. The global consistency model will be applied to those homogeneous segments.
- Extraction and analysis of different operating speed indicators, extracted from a set of road segments. Some of them will also be related to road geometry, in order to provide an optimum road design.
- Development of a new procedure for designing, redesigning and planning of roads, considering the previous contributions.

5. Hypotheses

This research is based on several hypotheses. The most important being:

- Accidents are not randomly distributed: there are some contributing factors involved in their generation and severity. Some of them, such as the human and infrastructure factor, are very frequent. In addition, their interaction is of a major importance.
- The infrastructure and human factors present a very strong interaction. Therefore, a change on the infrastructure does not always produce the desired effect on drivers' behavior. Thus, the human factor should be studied.
- Road accidents are random, discrete and rare. This makes it necessary to use count models for their analysis. In addition, depending on other factors, different statistical techniques or even different approaches might be needed.
- The reporting of Property Damage Only (PDO) crashes is not homogeneous. It depends on factors such as policy enforcement, type of crash, environment, time of the day, etc. Therefore, their number is normally biased. This is why only accidents with victims are usually considered in the analysis.
- Design consistency can be defined as how the road behavior and drivers' expectancies fit. It is a good way to estimate the influence of the infrastructure on road safety.
- Road design consistency is linked to road safety, so we can develop safety performance functions in which we can estimate the number of accidents as a function of the consistency model and some exposure parameters.
- Road design consistency can be studied through analyzing operating speed variation through a homogeneous road segment. Some of these criteria are centered on local variations and other on global variations.
- The operating speed is an optimum way to estimate the drivers' response to road geometry.
- The operating speed can be assumed to be the 85^{th} percentile of the measured speed under free-flow conditions. It cannot be measured for non-existing roads, so several models have been developed based on measurements from actual roads.
- We can assume that a vehicle is travelling under free-flow conditions if the headway is at least 5 seconds, according to most research.

- Operating speed models are normally calculated on the basis of the horizontal and, if existing, the vertical alignment. Those alignments can be obtained from a series of depicted points that represent their horizontal position (and altitude, if needed). A parameter is normally needed for doing such task: curvature or heading direction.
- Road safety is not an absolute value. We cannot ensure a zero-crash state on roads. This means that following guidelines does not ensure absolute safety. On the contrary, road safety is a continuum: the variation of certain parameters will gradually change the results.

6. Methodology

This Doctoral Thesis develops a new global geometric design consistency model, based on the relationship between the operating speed behavior and road accidents. Continuous operating speed profiles are used in the analysis. Those models were specifically developed for the Valencian region, in a previous research (Pérez-Zuriaga, 2012).

A large set of two-lane rural road highway sections will be selected within all the Valencian region. The operating speed profiles will be developed for all of them, according to the aforementioned operating speed models. Some performance indicators will be extracted from them and later related to the number of crashes. The consistency parameter will be defined as the performance indicator that better estimates road crashes. Figure 54 shows the general layout of the project.

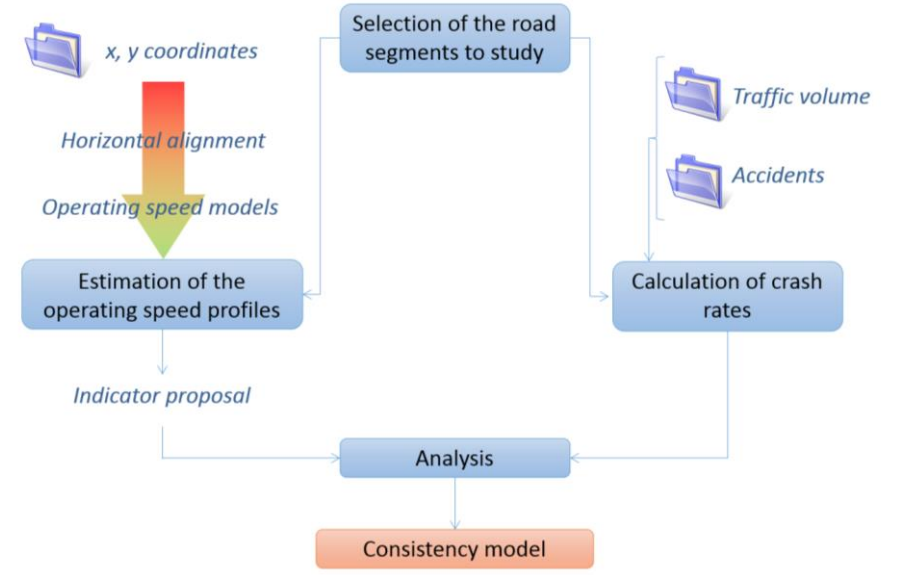

Figure 54. General layout of the study.

6.1. Data acquisition

Traffic volume, crashes and geometry are required from a large number of two-lane rural road segments. Moreover, road segments cannot be directly defined, since the segmentation procedure is based on geometrical variations, which are not a priori known.

The first step is the selection of a large number of two lane rural road sections in the Valencian region. Traffic and accident data must also be available for those road segments.

The operating speed profiles will be developed for all of them. Hence, the selected road sections must meet the conditions for operating speed models to be applied. Those conditions are:

- Two-lane rural road sections. No special requirements about their cross-section have to be met.
- Rural environment.
- Level terrain. Operating speed models were calibrated for level terrain and therefore only horizontal alignment parameters were considered. Therefore, the maximum longitudinal grade is limited to 3%.
- Major junctions are allowed within the road sections. This is because road segments have to be later extracted, and this will be a road segmentation criterion. Traffic volume changes and intersection-related accidents are clearly considered in their corresponding databases, so it is not a problem from this point of view.
- Traffic volume will affect exposure. This phenomenon will be covered by the corresponding safety performance function. However, interaction between the consistency criterion and traffic volume will not be studied. In order to reduce the variability, medium AADT road sections are considered.
- The road sections must be in good shape. This includes pavement condition, marking and guiding posts. Minor roads are not considered due to these conditions.
- The road must be covered by a good, high-resolution satellite imagery. This is in order to depict the centerline.

For all those road sections, the following data have to be collected:

- Geometry.

- Traffic volume during last years.
- Road crashes (number, location, typology, severity, etc.).

Geometric data was extracted from satellite imagery. The road centerline was depicted as a polygonal line. The distance between points is not a problem, so it presented a higher density at curved locations, as shown in Figure 55.

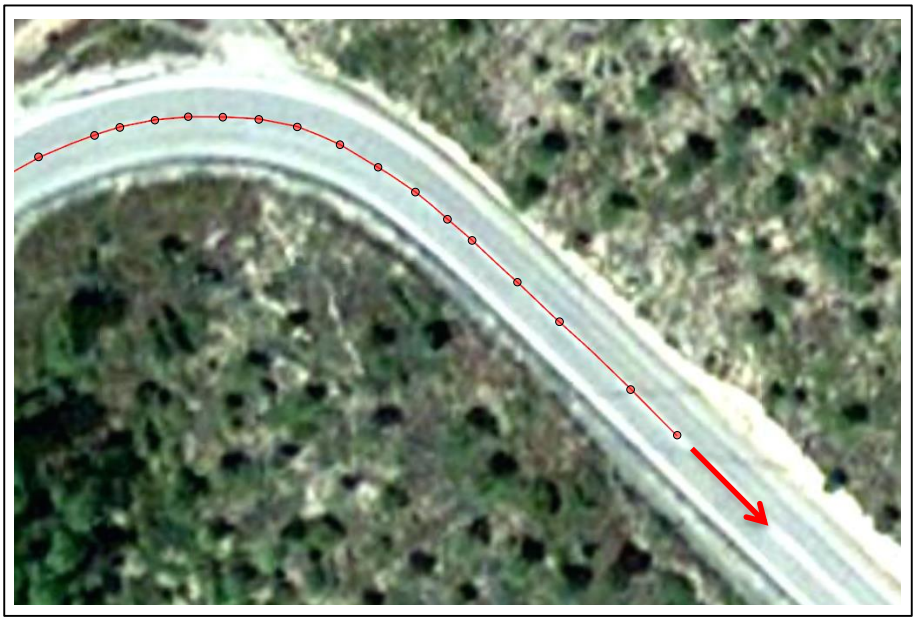

Figure 55. Extraction of the road centerline.

Each road segment was an individual polygonal. A computer program was developed in order to process all individual polylines and extracting the corresponding geometry.

Crash data was available since 1999, provided by the different road administrations. All reported accidents include severity, date and time, consequences and observations, as well as their milepost location.

Figure 56. Accident data acquisition form.

Traffic volume data is downloadable from the corresponding administrations. Data for the last 13 years exists for almost all road segments. The traffic volume values are divided by major intersections.

CV	Tramo	Pk Ini	Inicio	Pk Fin	Fin	Pk Est.	IMD 2006	%P	IMD 2007	%P	IMD 2008	%P	IMD 2009	%P	IMD 2010	%P
CV-36	036050	10+500	Accés Mas del Jutge	12+800	A-7(Accés Calicanto)	11+300	18.872	16	21.376	16	21.529	13	19.045	12	19.233	10
CV-37	037030	0+000	CV-374	0+000	CV-50	0+000	-	-	-	-	-	-	-	-	-	-
CV-40	040010	0+000	A-7(Cerdà)	3+400	CV-645(Annauir)	2+800	23.028	12	24.000	10	20.544	11	21.147	12	20.145	11
CV-40	040020	3+400	CV-645(Annauir)	11+000	CV-60(Accés L'Olleria)	8+100	22.981	-	23.900	-	-	-	22.222	-	22.670	-
CV-40	040030	11+000	CV-60(Accés L'Olleria)	16+300	CV-650(Poligon L'Altet)	12+000	21.403	10	22.757	9	22.336	9	17.285	8	20.131	8
CV-40	040040	16+300	CV-650(Poligon L'Altet)	19+900	CV-81(Accés Ontinyent)	17+900	22.600	-	23.500	-	-	-	-	-	17.499	-
CV-40	040050	19+900	CV-818Accés Ontinyent)	24+600	N-340(Albaida)	23+300	18.451	9	19.200	9	-	-	15.159	9	14.297	8
CV-41	041010	0+000	CV-50(Alzira)	4+240	CV-543(Cogullada)	0.900	14.949	-	15.453	-	16.071	9	13.838	6	12.732	4
CV-41	041020	4+240	CV-543(Cogullada)	8+350	CV-560(Accés La Pobla	6+500	9.723	4	11.091	4	10.358	4	10.102	3	10.395	3
CV-41	041030	8+350	CV-560(Accés La Pobla Llarga)	11+990	CV-575(Maunel)	8+900	5.773	6	6.776	6	6.711	5	6.646	4	7.348	5

Figure 57. AADT data for different road segments.

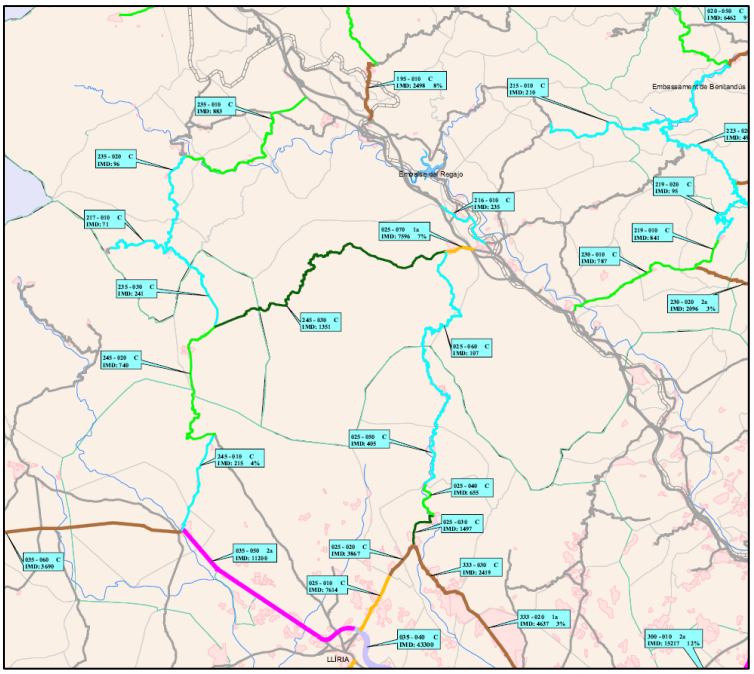

Figure 58. AADT map.

Due to the randomness of traffic accidents, a long period was considered for road crashes. Conversely, those data have to be handle with care. This is a very long time period, so there is a certain probability that some countermeasures had been applied. Thus, the history of those road segments should be reviewed. Road traffic volume variations was also reviewed, in order to detect some related issues.

6.2. Development of the operating speed models

The operating speed models considered in this doctoral thesis were explicitly developed in previous research (Pérez-Zuriaga et al., 2010). These operating speed models were calibrated with data extracted from GPS receivers placed on actual drivers.

The operating speed model for curves is divided into two expressions, depending whether the radius is higher than 400 m or not. Several researchers found that the behavior of operating speed changed at 400 m, which was also found in this research. Equation 165 shows the operating speed model for horizontal curves.

$$\begin{cases} v_{85} = 97.4254 - \dfrac{3310.94}{R}; 400\text{ m} < R \leq 950\text{ m} \\ v_{85} = 102.048 - \dfrac{3990.26}{R}; 70\text{ m} < R \leq 400\text{ m} \end{cases} \qquad R^2 = 0.76 \quad (165)$$

The operating speed for tangents is calculated depending on the speed developed on the previous horizontal curve (v_{85C}, km/h) and its radius (R, m). L (m) is the tangent length (Equation 166).

$$v_{85} = v_{85C} + \left(1 - e^{-\lambda \cdot L}\right) \cdot (110 - v_{85C}) \qquad R^2 = 0.52 \quad (166)$$

λ is an additional parameter that is determined with Equation 167.

$$\lambda = 0.00135 + (R - 100) \cdot 7.00625 \cdot 10^{-6} \quad (167)$$

Acceleration and deceleration rates were also developed, depending on the radius of the geometric feature that supposed a geometric control. Both speed transition rates are in m/s^2. Equation 168 shows the deceleration rate and Equation 169 shows the acceleration rate.

$$d = 0.313 + \frac{114.436}{R} \qquad R^2 = 0.70 \quad (168)$$

$$a = 0.41706 + \frac{65.93588}{R} \qquad R^2 = 0.71 \quad (169)$$

The following construction rules were proposed for depicting the operating speed profile:

- The operating speed remains constant along all the circular section of the horizontal curve. Therefore, speed transitions can only take place on tangents and spiral curves. This rule can only be violated if there are two consecutive circular curves, or a sudden speed jump is observed. In this case, this rule is only valid for the geometric feature that produces the lowest operating speed profile.
- If there exists a tangent with an estimated operating speed lower than the both adjacent horizontal curves, this speed will be substituted by the lowest operating speed of those curves.

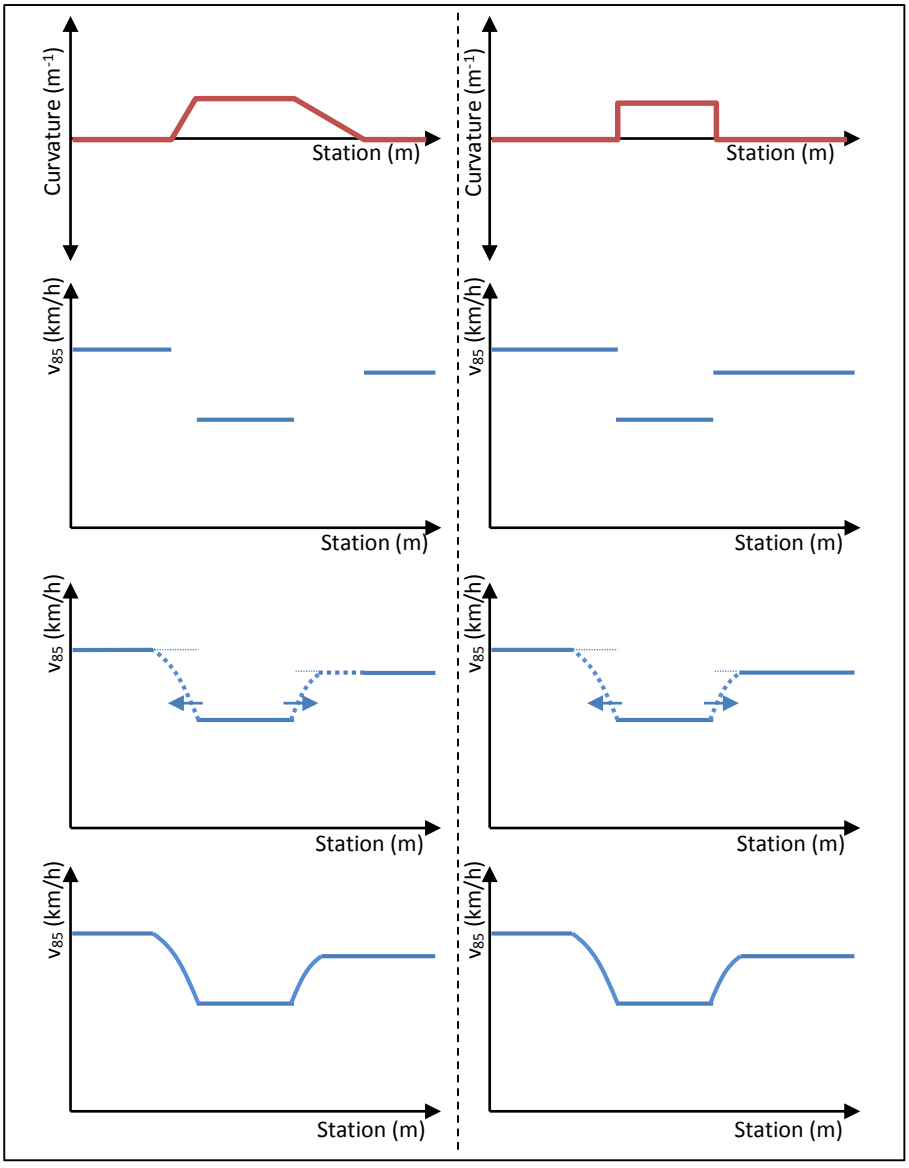

Figure 59. Operating speed profile construction.

6.3. Determination of the centerline coordinates

All road sections were depicted from satellite imagery. Thus, a set of *(latitude, longitude)* points that represented the road centerline was available for obtaining the horizontal alignment. However, two additional processes were needed:

- Creation of a set of *(x, y)* coordinates, separated at a constant distance (1 m), which is more suitable for the following process. This section covers this process.
- Determination of the horizontal alignment. This process will be fully developed in the following section.

In this case, all centerlines were composed by a single path. However, in some other cases the centerline may not be depicted from satellite imagery, but collected by GPS devices placed on some vehicles. Such the case, it is necessary to join several trajectories into a single one. This section describes how this process is performed, being our situation the particular case when the number of trajectories to join is 1.

6.3.1. Input data

Data are normally provided in a *(latitude, longitude)* format. In order to manage all these coordinates, a transformation to an *(x, y)* format must be applied. In addition, some filtering tools were developed in order to establish the initial and final points of the road section, etc.

The computer program is able to manage the following information for each point. Of course, some of them are only valid when using GPS devices.

- Date.
- Time.
- Latitude.
- Longitude.
- Instant speed.
- Heading direction.
- Altitude.

The program is able to deal with several input coordinate systems. Regardless of this format, the program always works with a virtual origin closer to the input points, in order to reduce the computer memory requirements.

If they are in a latitude, longitude format, the Earth is assumed to be an ellipsoid of local radius R_T (Figure 60). The (*x*, *y*) coordinates are calculated as follows:

$$x_i = \left(\frac{\pi}{180} \cdot Long_i - Long_0\right) \cdot R_T \cdot \cos\left(Lat_i \cdot \frac{\pi}{180}\right) \quad (170)$$

$$y_i = \left(\frac{\pi}{180} \cdot Lat_i - Lat_0\right) \cdot R_T \quad (171)$$

Where:

x_i, y_i: coordinates of each point in the *(x, y)* system.
$Lat_i, Long_i$: coordinates of each point in the *(latitude, longitude)* system.
$Lat_0, Long_0$: coordinates of the virtual origin *(latitude, longitude)* system.
R_T: Local radius of the Earth (m).

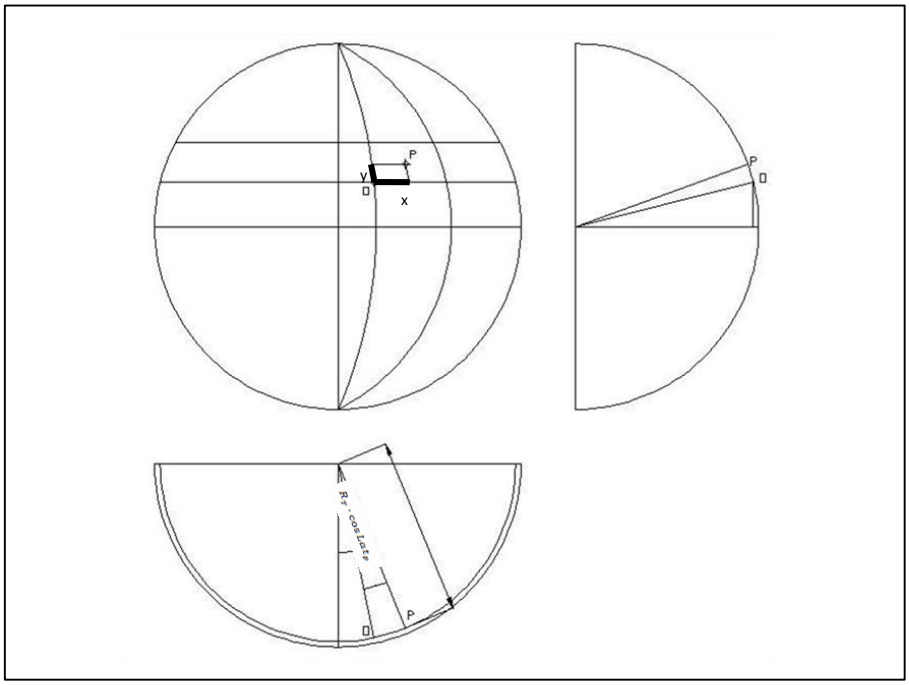

Figure 60. Determination of the local coordinates.

If the input coordinates are in the UTM system, there is no need of additional transformation. The program only moves all points to a closer virtual origin in order to use less memory while performing calculations.

The user now needs to indicate to the program which is the beginning and the final point of the trajectory to be processed. As it was previously indicated, there may be more than one trajectory in the calculation (in both directions), so the user has to manually indicate where is the initial and final point, assisted by a map. The user also has to indicate the approximate heading of the trajectory at the initial and final points. Those directions don not need to be accurately determined, allowing an error of even 80 gon. Figure 61 shows the initial and final points, their directions and several trajectories in both directions to be merged into a single one.

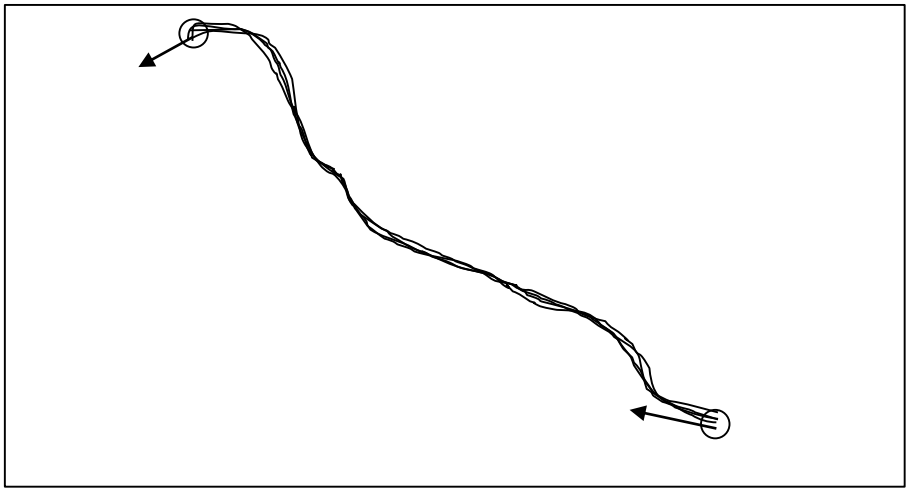

Figure 61. Initial information for determining the merged path.

6.3.2. Calculation of the merged path

This section describes how the merged path is produced from several polylines. The resulting path presents a constant separation between points, which is normally set to 1 m.

The program works under a Microsoft Office Excel environment. In order to better understand the process, several screenshots of the different steps are shown.

The first step consists on determining where the initial and final points are located in each individual path. The program takes the initial and final points introduced by the user and calculates the geometric distance between every point and the initial and final points. All the points which are closer to either the initial or final point than a certain threshold are marked (Figure 62). This threshold is user-defined, varying depending on the data origin. For instance, if the track has been recorded with a 1

Hz GPS receiver, travelling at 100 km/h, the threshold should be something like 40 m. On the contrary, maybe the initial or final points might not be detected.

Date	Time	Latitude	Longitude	Speed	Course	Altitude	x	y	Extremo	Tramo	Tipo	Flotante
01/01/2006	1	1	1	1	1	-20,977	1000	1000				
02/01/2006	1	1	1	1	1	-21,133	1004,519	991,489				
03/01/2006	1	1	1	1	1	-21,249	1007,243	982,071				
04/01/2006	1	1	1	1	1	-21,328	1008,631	972,236				
05/01/2006	1	1	1	1	1	-21,35	1009,171	962,266				
06/01/2006	1	1	1	1	1	-21,451	1009,157	952,225				
07/01/2006	1	1	1	1	1	-21,529	1008,615	941,92				
08/01/2006	1	1	1	1	1	-21,573	1007,643	931,444				
09/01/2006	1	1	1	1	1	-21,616	1006,329	921,109				
10/01/2006	1	1	1	1	1	-21,666	1004,813	910,97	1			
11/01/2006	1	1	1	1	1	-21,673	1003,069	900,79	1			
12/01/2006	1	1	1	1	1	-21,675	1001,564	890,921	1			
13/01/2006	1	1	1	1	1	-21,678	999,877	880,794	1			
14/01/2006	1	1	1	1	1	-21,649	998,343	870,872	1			
15/01/2006	1	1	1	1	1	-21,669	996,848	860,933	1			
16/01/2006	1	1	1	1	1	-21,687	995,123	850,79				
17/01/2006	1	1	1	1	1	-21,689	993,658	840,891				
18/01/2006	1	1	1	1	1	-21,683	992,104	830,976				
19/01/2006	1	1	1	1	1	-21,687	990,474	820,939				
20/01/2006	1	1	1	1	1	-21,659	989,055	811,168				
21/01/2006	1	1	1	1	1	-21,68	987,341	801,021				
22/01/2006	1	1	1	1	1	-21,63	985,941	791,309				
23/01/2006	1	1	1	1	1	-21,596	985,915	780,909				
24/01/2006	1	1	1	1	1	-21,586	985,052	770,569				
25/01/2006	1	1	1	1	1	-21,546	984,559	760,557				
26/01/2006	1	1	1	1	1	-21,55	983,031	750,389				

Figure 62. "1" indicates that those points are close to the initial point set by the user.

This algorithm is convenient since it focuses where the next step should work on. On the contrary, the next process would be too slow.

The next step consist on adding the initial and final exact points, according to the introduced points by the user. Obviously, each trajectory presents close but not exact points to those boundary points. Thus, these new points have to be created.

It is assumed that the initial point for each trajectory is the closest point of it to the user-defined initial point (Figure 63). Thus, for all points of the individual trajectories marked with a "1", the following process is repeated:

1. A straight section is created between the first and the second points (points A and B).
2. A perpendicular straight line is created departing from the user-defined initial point.
3. The intersection of previous lines is calculated. There are two possibilities:
    a. The intersection point is between points A and B. In this case, the exact initial point has been found, so it is inserted in the data series.
    b. The intersection point is not between A and B. Thus, points B and C should be chosen and the process restarted until the previous condition is satisfied.

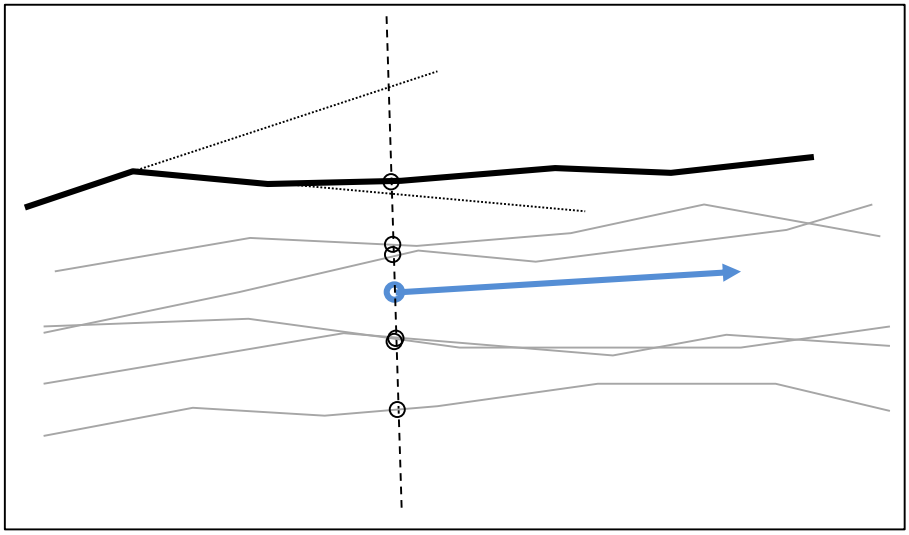

Figure 63. Development of the merged path from the individual paths. Grey: individual trajectories. Blue: vector of the merged path. Black: individual trajectory that is being evaluated at this iteration.

The individual trajectories are then marked once the initial and final exact points have been determined for all of them (Figure 64). The value “1” is established for forward direction, being “-1” otherwise.

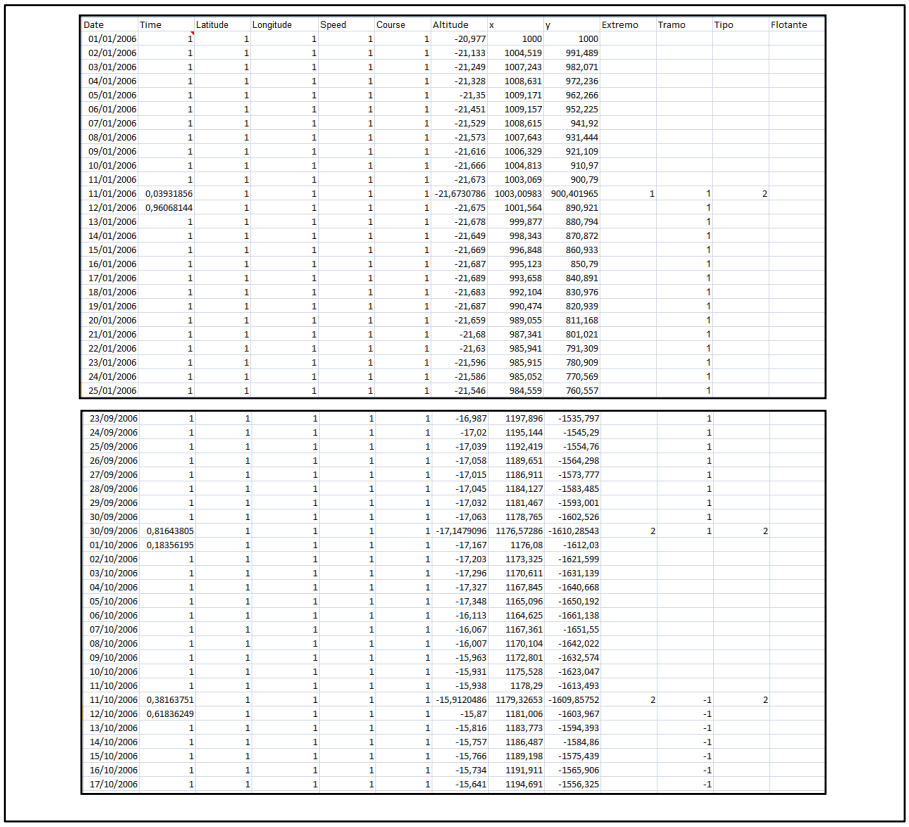

Date	Time	Latitude	Longitude	Speed	Course	Altitude	x	y	Extremo	Tramo	Tipo	Flotante
01/01/2006	1	1	1	1	1	-20,977	1000	1000				
02/01/2006	1	1	1	1	1	-21,133	1004,519	991,489				
03/01/2006	1	1	1	1	1	-21,249	1007,243	982,071				
04/01/2006	1	1	1	1	1	-21,328	1008,631	972,236				
05/01/2006	1	1	1	1	1	-21,35	1009,171	962,266				
06/01/2006	1	1	1	1	1	-21,451	1009,157	952,225				
07/01/2006	1	1	1	1	1	-21,529	1008,615	941,92				
08/01/2006	1	1	1	1	1	-21,573	1007,643	931,444				
09/01/2006	1	1	1	1	1	-21,616	1006,329	921,109				
10/01/2006	1	1	1	1	1	-21,666	1004,813	910,97				
11/01/2006	1	1	1	1	1	-21,673	1003,069	900,79				
11/01/2006	0,03931856	1	1	1	1	-21,6730786	1003,00983	900,401965	1	1	2	
12/01/2006	0,96068144	1	1	1	1	-21,675	1001,564	890,921		1		
13/01/2006	1	1	1	1	1	-21,678	999,877	880,794		1		
14/01/2006	1	1	1	1	1	-21,649	998,343	870,872		1		
15/01/2006	1	1	1	1	1	-21,669	996,848	860,933		1		
16/01/2006	1	1	1	1	1	-21,687	995,123	850,79		1		
17/01/2006	1	1	1	1	1	-21,689	993,658	840,891		1		
18/01/2006	1	1	1	1	1	-21,683	992,104	830,976		1		
19/01/2006	1	1	1	1	1	-21,687	990,474	820,939		1		
20/01/2006	1	1	1	1	1	-21,659	989,055	811,168		1		
21/01/2006	1	1	1	1	1	-21,68	987,341	801,021		1		
22/01/2006	1	1	1	1	1	-21,63	985,941	791,309		1		
23/01/2006	1	1	1	1	1	-21,596	985,915	780,909		1		
24/01/2006	1	1	1	1	1	-21,586	985,052	770,569		1		
25/01/2006	1	1	1	1	1	-21,546	984,559	760,557		1		
23/09/2006	1	1	1	1	1	-16,987	1197,896	-1535,797		1		
24/09/2006	1	1	1	1	1	-17,02	1195,144	-1545,29		1		
25/09/2006	1	1	1	1	1	-17,039	1192,419	-1554,76		1		
26/09/2006	1	1	1	1	1	-17,058	1189,651	-1564,298		1		
27/09/2006	1	1	1	1	1	-17,015	1186,911	-1573,777		1		
28/09/2006	1	1	1	1	1	-17,045	1184,127	-1583,485		1		
29/09/2006	1	1	1	1	1	-17,032	1181,467	-1593,001		1		
30/09/2006	1	1	1	1	1	-17,063	1178,765	-1602,526		1		
30/09/2006	0,81643805	1	1	1	1	-17,1479096	1176,57286	-1610,28543	2	1	2	
01/10/2006	0,18356195	1	1	1	1	-17,167	1176,08	-1612,03				
02/10/2006	1	1	1	1	1	-17,203	1173,325	-1621,599				
03/10/2006	1	1	1	1	1	-17,296	1170,611	-1631,139				
04/10/2006	1	1	1	1	1	-17,327	1167,845	-1640,668				
05/10/2006	1	1	1	1	1	-17,348	1165,096	-1650,192				
06/10/2006	1	1	1	1	1	-16,113	1164,625	-1661,138				
07/10/2006	1	1	1	1	1	-16,067	1167,361	-1651,55				
08/10/2006	1	1	1	1	1	-16,007	1170,104	-1642,022				
09/10/2006	1	1	1	1	1	-15,963	1172,801	-1632,574				
10/10/2006	1	1	1	1	1	-15,931	1175,528	-1623,047				
11/10/2006	1	1	1	1	1	-15,938	1178,29	-1613,493				
11/10/2006	0,38163751	1	1	1	1	-15,9120486	1179,32653	-1609,85752	2	-1	2	
12/10/2006	0,61836249	1	1	1	1	-15,87	1181,006	-1603,967		-1		
13/10/2006	1	1	1	1	1	-15,816	1183,773	-1594,393		-1		
14/10/2006	1	1	1	1	1	-15,757	1186,487	-1584,86		-1		
15/10/2006	1	1	1	1	1	-15,766	1189,198	-1575,439		-1		
16/10/2006	1	1	1	1	1	-15,734	1191,911	-1565,906		-1		
17/10/2006	1	1	1	1	1	-15,641	1194,691	-1556,325		-1		

Figure 64. Detection of road segments.

Figure 65 and Figure 66 show some screenshots of the computer program. They show some tools for assisting the user in determining which trajectories should be considered and which not.

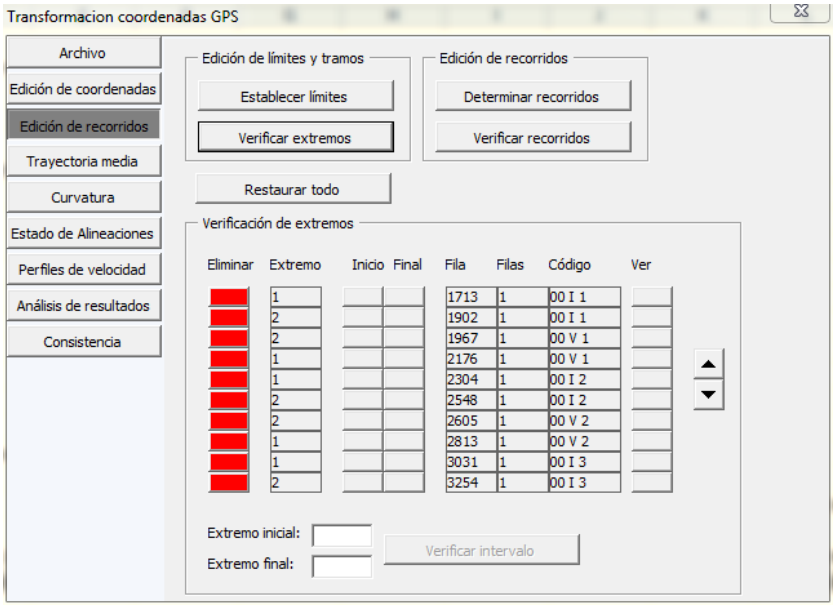

Figure 65. Selection of valid individual trajectories.

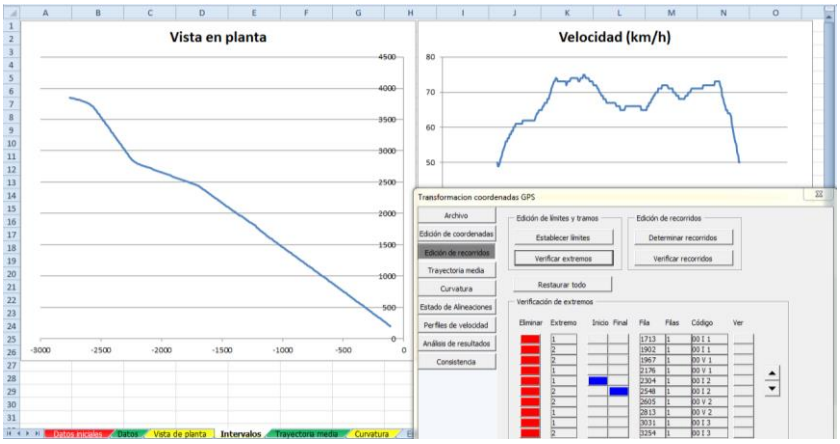

Figure 66. Selection of individual trajectories. Path and speed profiles.

The computer program builds the merged path considering all individual trajectories at the same time. The process is the following one:

1. The program saves for each individual path the initial point of the next iteration. This is for performing faster calculations. Initially, all those points belong to the same straight line (the perpendicular one to the initial vector).
2. The average points for the forward and backward directions are calculated. The average point of those determine the first point of the centerline.
3. The program initiates the calculation of the next point. A straight segment of 1 m length is determined. The direction of this segment is the one introduced by the user (initial vector).
4. A perpendicular line is plotted from previous point (point 2 in Figure 67). All the intersection points between this line and the individual trajectories are determined.
5. With all previous individual points, the average forward direction and backwards direction points are determined. The merged path point is the average value of those (point 2').
6. The procedure is repeated from step 3 until no more points belonging to the average path are found. In this case, the vector to consider is the one which connects the previous two points: 1' and 2'.

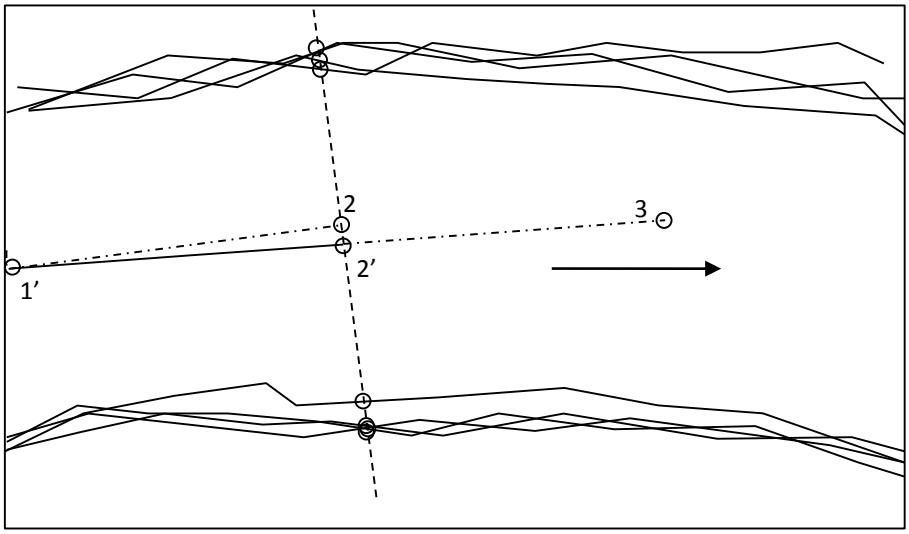

Figure 67. Creation of a new point of the average path. The previous segment is extended 1 m, generating point 2. A perpendicular line is created, cutting all road segments in both directions. An average point is generated for each direction. The midpoint is then determined (2'). The process is started again, creating point 3.

The final result is shown on Figure 68. For each individual trajectory, its intersection between the perpendicular vector belonging to the average path is calculated as mentioned for the starting point (see Figure 69).

Sometimes, GPS devices record values far away from the trajectory, due to reception errors. The algorithm also includes a function that takes away those points, by considering a confidence interval (Figure 71).

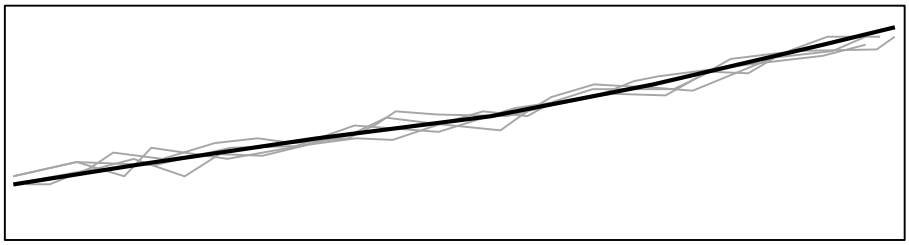

Figure 68. Merged path (black line) and individual paths (gray lines)

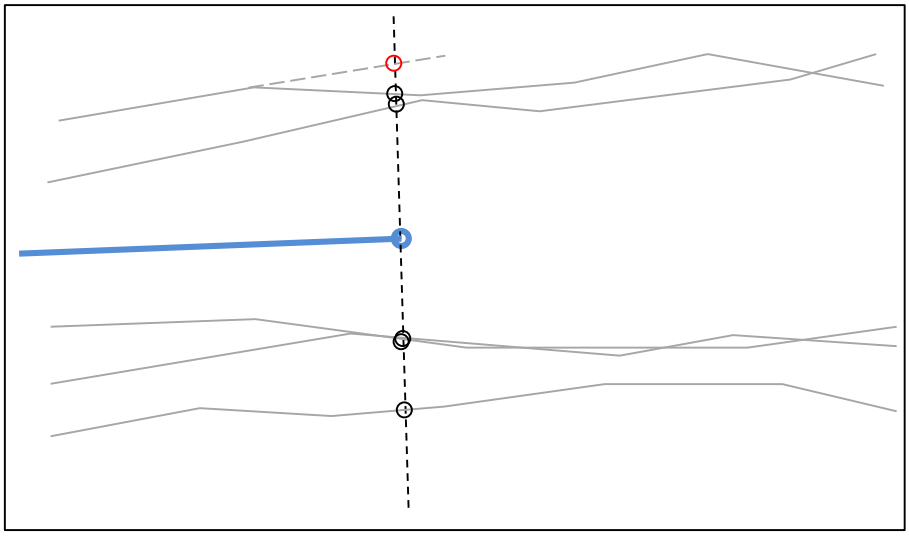

Figure 69. Creation of the midpoint of the average path. The red point is neglected since it does not belong to an individual trajectory (its intersection belongs to a previous segment).

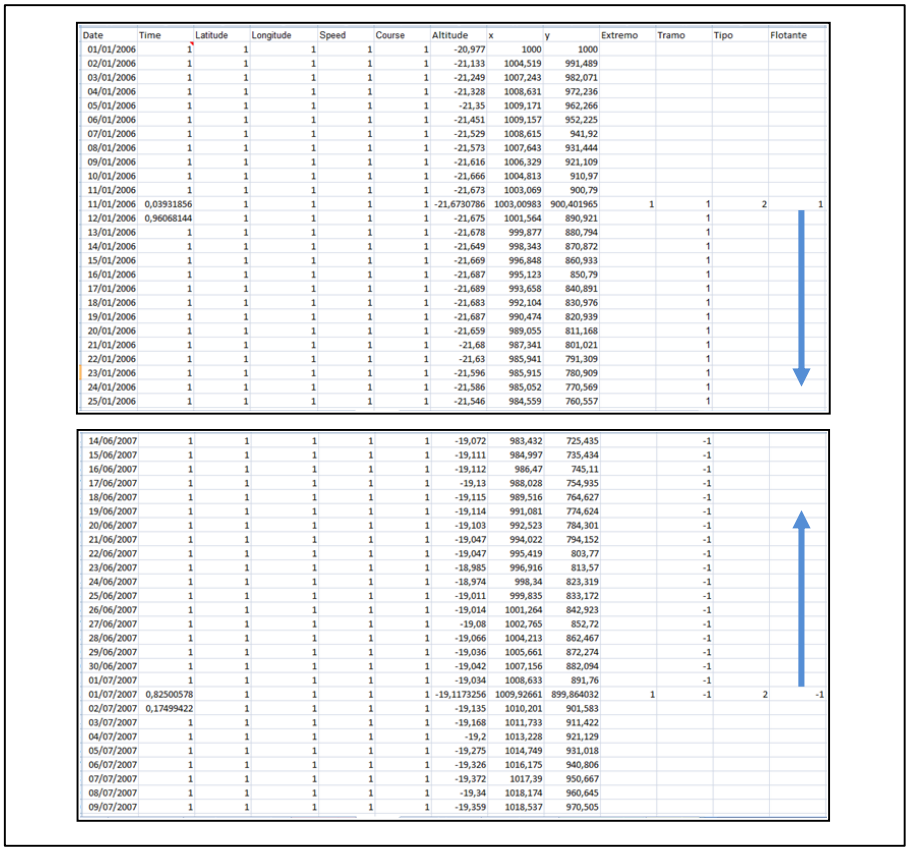

Date	Time	Latitude	Longitude	Speed	Course	Altitude	x	y	Extremo	Tramo	Tipo	Flotante
01/01/2006	1	1	1	1	1	-20,977	1000	1000				
02/01/2006	1	1	1	1	1	-21,133	1004,519	991,489				
03/01/2006	1	1	1	1	1	-21,249	1007,243	982,071				
04/01/2006	1	1	1	1	1	-21,328	1008,631	972,236				
05/01/2006	1	1	1	1	1	-21,35	1009,171	962,266				
06/01/2006	1	1	1	1	1	-21,451	1009,157	952,225				
07/01/2006	1	1	1	1	1	-21,529	1008,615	941,92				
08/01/2006	1	1	1	1	1	-21,573	1007,643	931,444				
09/01/2006	1	1	1	1	1	-21,616	1006,329	921,109				
10/01/2006	1	1	1	1	1	-21,666	1004,813	910,97				
11/01/2006	1	1	1	1	1	-21,673	1003,069	900,79				
11/01/2006	0,03931856	1	1	1	1	-21,6730786	1003,00983	900,401965	1	1	2	1
12/01/2006	0,96068144	1	1	1	1	-21,675	1001,564	890,921		1		
13/01/2006	1	1	1	1	1	-21,678	999,877	880,794		1		
14/01/2006	1	1	1	1	1	-21,649	998,343	870,872		1		
15/01/2006	1	1	1	1	1	-21,669	996,848	860,933		1		
16/01/2006	1	1	1	1	1	-21,687	995,123	850,79		1		
17/01/2006	1	1	1	1	1	-21,689	993,658	840,891		1		
18/01/2006	1	1	1	1	1	-21,683	992,104	830,976		1		
19/01/2006	1	1	1	1	1	-21,687	990,474	820,939		1		
20/01/2006	1	1	1	1	1	-21,659	989,055	811,168		1		
21/01/2006	1	1	1	1	1	-21,68	987,341	801,021		1		
22/01/2006	1	1	1	1	1	-21,63	985,941	791,309		1		
23/01/2006	1	1	1	1	1	-21,596	985,915	780,909		1		
24/01/2006	1	1	1	1	1	-21,586	985,052	770,569		1		
25/01/2006	1	1	1	1	1	-21,546	984,559	760,557		1		

14/06/2007	1	1	1	1	1	-19,072	983,432	725,435		-1		
15/06/2007	1	1	1	1	1	-19,111	984,997	735,434		-1		
16/06/2007	1	1	1	1	1	-19,112	986,47	745,11		-1		
17/06/2007	1	1	1	1	1	-19,13	988,028	754,935		-1		
18/06/2007	1	1	1	1	1	-19,115	989,516	764,627		-1		
19/06/2007	1	1	1	1	1	-19,114	991,081	774,624		-1		
20/06/2007	1	1	1	1	1	-19,103	992,523	784,301		-1		
21/06/2007	1	1	1	1	1	-19,047	994,022	794,152		-1		
22/06/2007	1	1	1	1	1	-19,047	995,419	803,77		-1		
23/06/2007	1	1	1	1	1	-18,985	996,916	813,57		-1		
24/06/2007	1	1	1	1	1	-18,974	998,34	823,319		-1		
25/06/2007	1	1	1	1	1	-19,011	999,835	833,172		-1		
26/06/2007	1	1	1	1	1	-19,014	1001,264	842,923		-1		
27/06/2007	1	1	1	1	1	-19,08	1002,765	852,72		-1		
28/06/2007	1	1	1	1	1	-19,066	1004,213	862,467		-1		
29/06/2007	1	1	1	1	1	-19,036	1005,661	872,274		-1		
30/06/2007	1	1	1	1	1	-19,042	1007,156	882,094		-1		
01/07/2007	1	1	1	1	1	-19,034	1008,633	891,76		-1		
01/07/2007	0,82500578	1	1	1	1	-19,1173256	1009,92661	899,864032	1	-1	2	-1
02/07/2007	0,17499422	1	1	1	1	-19,135	1010,201	901,583				
03/07/2007	1	1	1	1	1	-19,168	1011,733	911,422				
04/07/2007	1	1	1	1	1	-19,2	1013,228	921,129				
05/07/2007	1	1	1	1	1	-19,275	1014,749	931,018				
06/07/2007	1	1	1	1	1	-19,326	1016,175	940,806				
07/07/2007	1	1	1	1	1	-19,372	1017,39	950,667				
08/07/2007	1	1	1	1	1	-19,34	1018,174	960,645				
09/07/2007	1	1	1	1	1	-19,359	1018,537	970,505				

Figure 70. Here is how the floating points evolve for forward and backward trajectories.

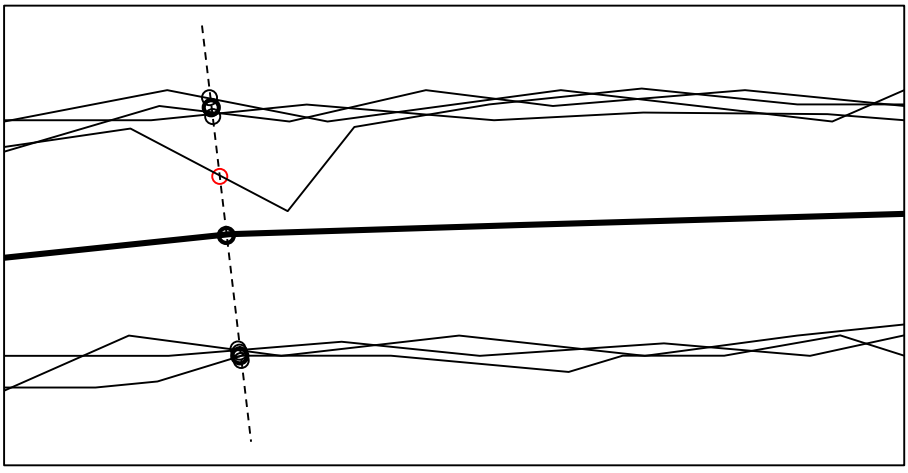

Figure 71. The red point is deleted since it seems to be an outlier.

This is a long process, highly dependent on the number of trajectories to consider, the number of points, the distance between the centerline points, etc. However, it is not dependent on the geometry of the road segment. When determining the centerline of a single road segment (just the case to consider here), the performance is about 1 km per 3 seconds (Intel Core i5 processor, 4 GB RAM).

Initially, the user selected which distance between points they want to consider. A 5 m distance was recommended. However, computers are quite faster today, so now only 1 m is allowed, which is very fast and accurate.

The program finally allows the user to export the trajectory into a kml file, which can be opened with Google Earth (Figure 72).

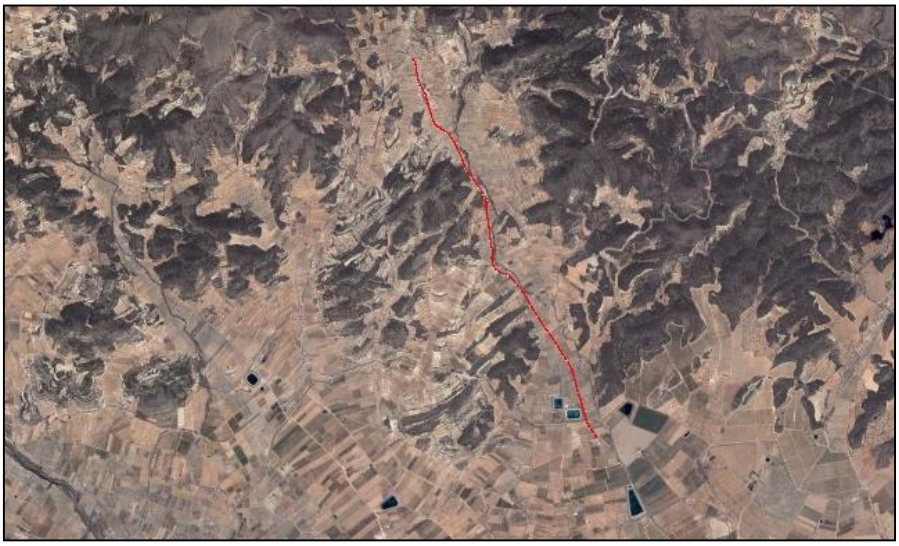

Figure 72. Merged path exported to Google Earth.

6.4. Determination of the horizontal alignment

This section explains how the horizontal alignment can be obtained departing from a series of points belonging to a polyline that represents the road centerline. The horizontal alignment is a series of three kinds of geometric elements that compose the road. Those geometric elements are:

- Tangents. Null curvature.

- Circular curves. Constant curvature.
- Spiral transitions. Linear variation curvature.

A horizontal alignment provides the sequence of those geometric elements, as well as their properties, such as length, radius or parameter.

The horizontal alignment can be depicted by means of the curvature profile. This is why most previous research have been focused on extracting the horizontal alignment departing from the curvature parameter. However, this way of proceeding presents several drawbacks, since curvature is an unstable parameter. Thus, a different methodology was developed in order to better compose the final horizontal alignment. This methodology is based on the use of the heading direction instead of curvatures.

A variation of the first methodology was also developed first. This methodology allows researchers to estimate the local curvature performed by individual drivers, which may be useful for analyzing curve negotiation.

6.4.1. Analysis of the local curvature

The local curvature can be easily obtained by determining the radius of the curve that goes through a set of three different, 2D points (Figure 73). However, this procedure produces curvature diagrams that present a high level of noise, thus being impractical to interpret them. This problem increases as the points become closer. The reason is because the error in the curvature measurement is due to slight transversal errors. As the longitudinal distance gets lower, the higher the curvature error is.

Thus, a filtering algorithm was created in order to develop more accurate, with less error, curvature diagrams. The entire process is divided into four, ordered steps:

- Determination of an initial curvature profile, based on 3, 5, 7, etc. points.
- Adjustment of the previous diagram by means of the gradient method.
- Adjustment of very large curvatures.
- Longitudinal analysis of the curvature profile. Filtering of the anomalous data.

It is worth to indicate that this process is not needed for determining the horizontal alignment from the polyline that represents the road centerline. This procedure is only suggested for analyzing the local curvature performed by drivers.

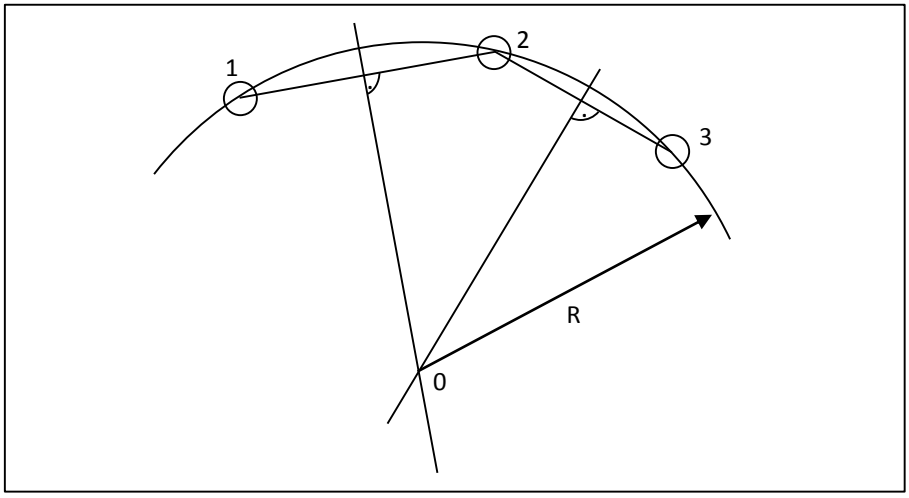

Figure 73. Determination of a circle that go through three points.

6.4.1.1. Creation of the seed curvature profile

The original, 3-points based curvature profile presents excessive noise. This is because the depicted curvature is based on a completely local curvature, which may not be representative of drivers' behavior. If the points were at a higher distance, the curvature would better reflect the reality.

One solution is to determine the curvature based on more than three points. This adds a global behavior to the curvature calculation at each point. Hence, the error is reduced and a smoother curvature profile is achieved. Of course, the more points are included, the smoother the curvature profile results. On the contrary, adding too many points to the curvature calculation will produce too smooth curvature diagrams, which are neither useful for researchers.

A new parameter is defined: "cadence". It indicates the number of points to consider at each side of the central point. Thus, if cadence is 1, the total number of points is 3. For a cadence of 2, the number of points is 5, and so on. The number of points (n) is determined from the cadence parameter (k) as shown in Equation 172.

Figure 74 shows some examples.

$$n = 2 \cdot k + 1 \tag{172}$$

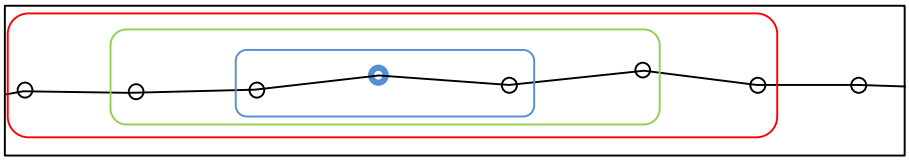

Figure 74. Selected points for different cadences.

The local curvature is always calculated by using only three points. Indeed, when the cadence is higher than 1, all the possible combinations of three points are selected of all of them, thus producing several circumferences. The one which best fits to all the points is the selected for determining the final curvature value. The number of circumferences to determine at each location is calculated with Equation 173, being n the number of points and k the cadence.

$$\binom{n}{3} = \binom{2k+1}{3} \tag{173}$$

The circumference which best fits all points is determined as the one which presents the lower MSE (mean square error) between all the considered points and the particular solution of the circumference. The MSE is determined for each partial solution according to Equation 174. Figure 75 shows some combinations considered for a cadence of 2.

$$MSE = \sum_{P_1}^{P_{2k+1}} (R_m - \overline{P_0 P_i})^2 \tag{174}$$

Where:

P_i: Each point considered of the centerline.

k: Cadence.

R_m: Radius of the circumference.

P_0: Center of the circumference.

$\overline{P_0 P_i}$: Distance between the center of the circumference and each point considered of the centerline.

The cadence value is introduced by the user. It influences on two main aspects: the smoothness of the curvature profile and the speed of the calculation. A cadence value from 3 to 6 is recommended. Higher values make this process too slow (it is based on a combinatory formulation), and result in a too smooth profile, which might

hide sharp local curvatures. The effect of the cadence can be seen on Figure 76 and Figure 77.

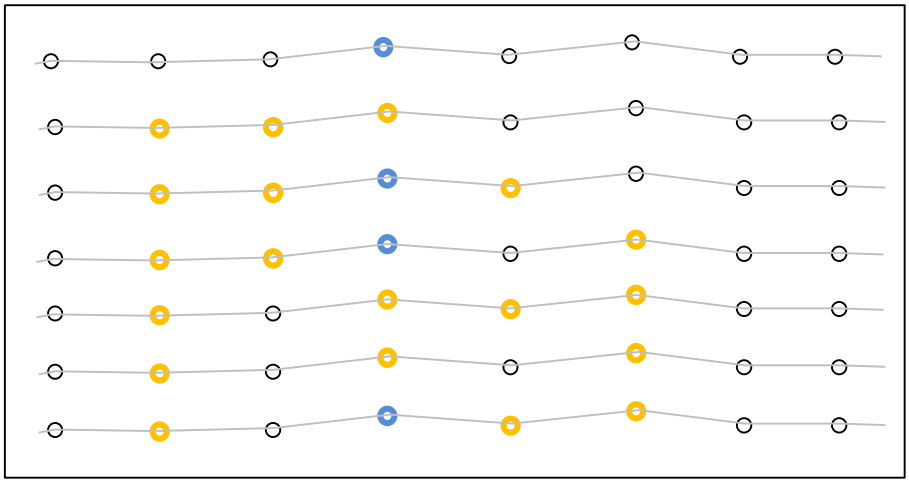

Figure 75. Several combinations of points for cadence=2.

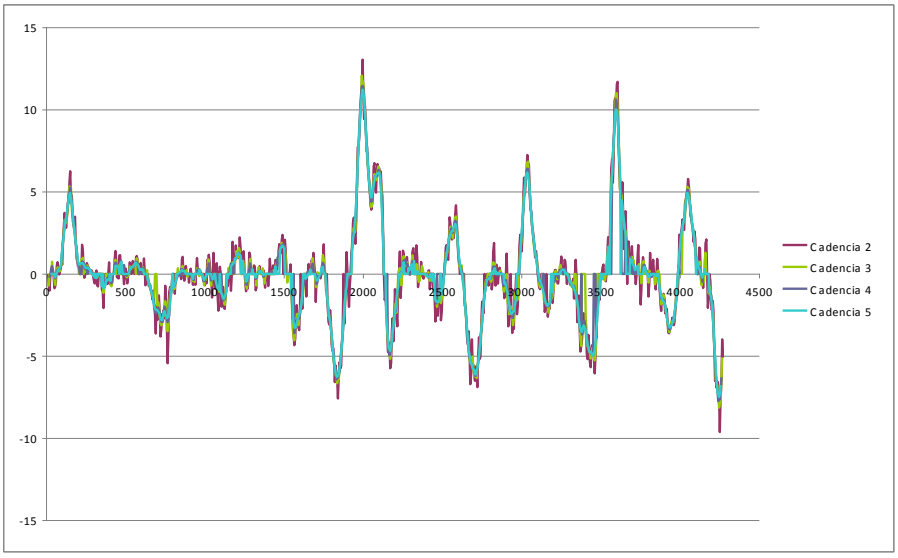

Figure 76. Curvature profile for different cadence values.

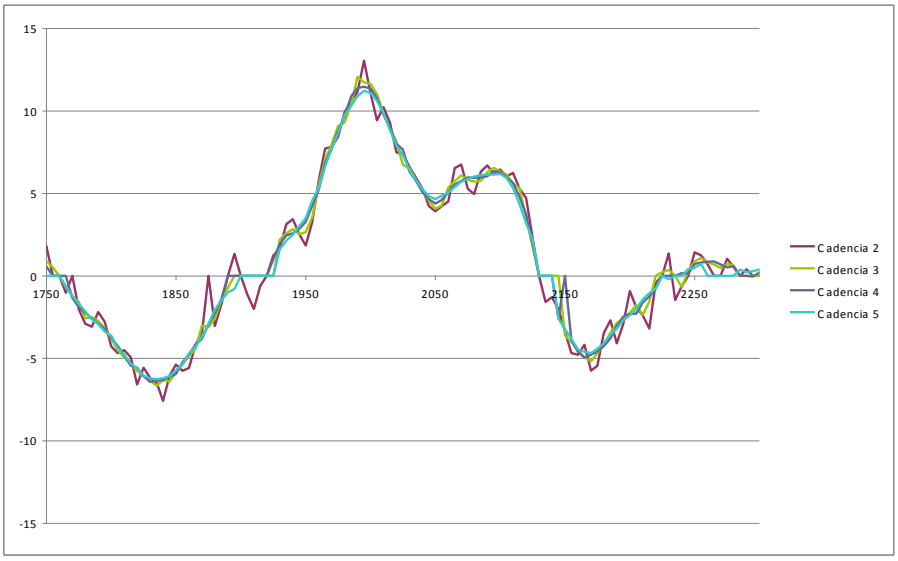

Figure 77. Curvature profile for different cadence values. Zoom in.

6.4.1.2. Application of the gradient method

The best circumference obtained by means of the previous procedure might not be the best, since a discrete number of solutions have been tried. The gradient methods allows to overcome this issue. It is based on the hypothesis that if we consider the 2D space as a continuum of MSE solutions, a local minimum can be encountered.

This space of solutions cannot be transformed to a functional form, so the minimum error cannot be determined by means of an analytical solution. Instead, the space of solutions is discretized, and several of them are tried in order to reach the best value. Since the objective is to find a solution with the minimum error, the algorithm is called “gradient method”.

The algorithm developed was implemented in the program. From the previous solution for each point, it tries four different new centers for the circumference, by varying it at a distance δ. It calculates the MSE for each partial solution, and moves the center of the circumference to the one which presents the lowest MSE. The previous solution is also included. Figure 78 shows one example. This process is repeated until all the new solutions present a higher MSE than the previous one.

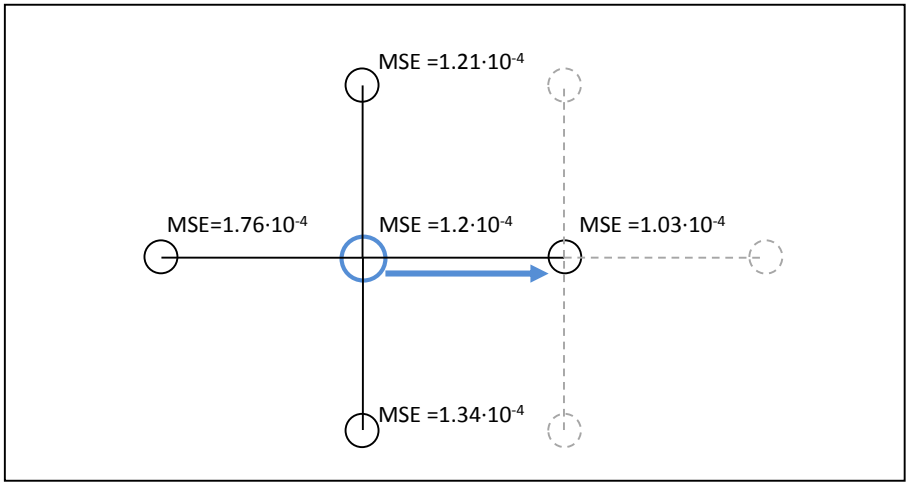

Figure 78. Center optimization based on the calculation of the lowest MSE.

When this point is reached, the program recalculates halves the distance to $\delta/2$ and starts again (Figure 79). The user controls the initial value of δ and the number of divisions. An accuracy of 1 m is recommended, which is pretty accurate and also fast to reach. Figure 80 shows how the best-fitting center is found by this algorithm.

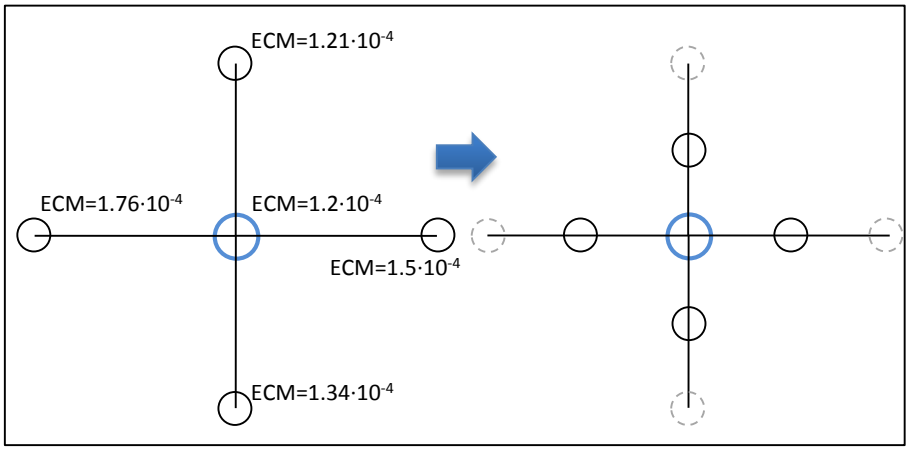

Figure 79. Distance reduction when no better point is reached.

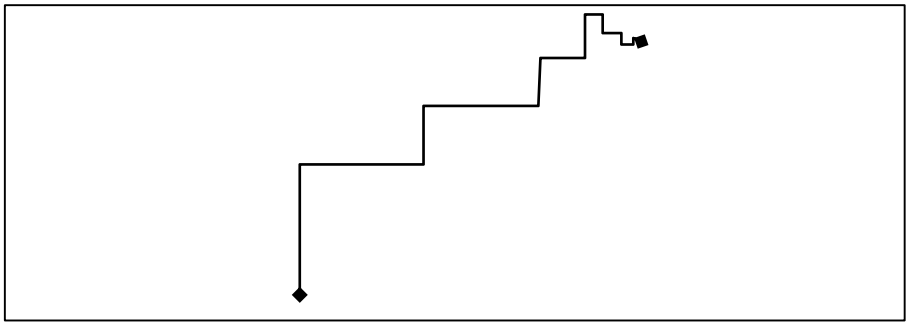

Figure 80. Example of the movement created by the center while being optimized.

6.4.1.3. Filtering of the low curvature values

The curvature data obtained from the previous method is quite good. Nevertheless, it can be enhanced by means of two additional algorithms. A disadvantage of previous methods is that tangent sections are never reached, since a curvature (even a negligible one) always exists. This algorithm determines when a section performs more like a tangent and a null curvature should be considered.

A good procedure to determine if a road section should be considered as a tangent is considering the circumferences performed in the first step. If the curve presents a large radius, almost all centers will fall in a certain region of the plane. The average center will be close to the actual center determined by the previous step. Thus, the previous solution must not be changed.

If the section belongs to a tangent one, the center of the circumferences fall almost randomly at both sides of the road. Thus, the average value of all centers is very close to the road, while the best circumference, achieved in the previous step, is so far away from it (see Figure 81). Therefore, in this case the curvature should be changed to 0.

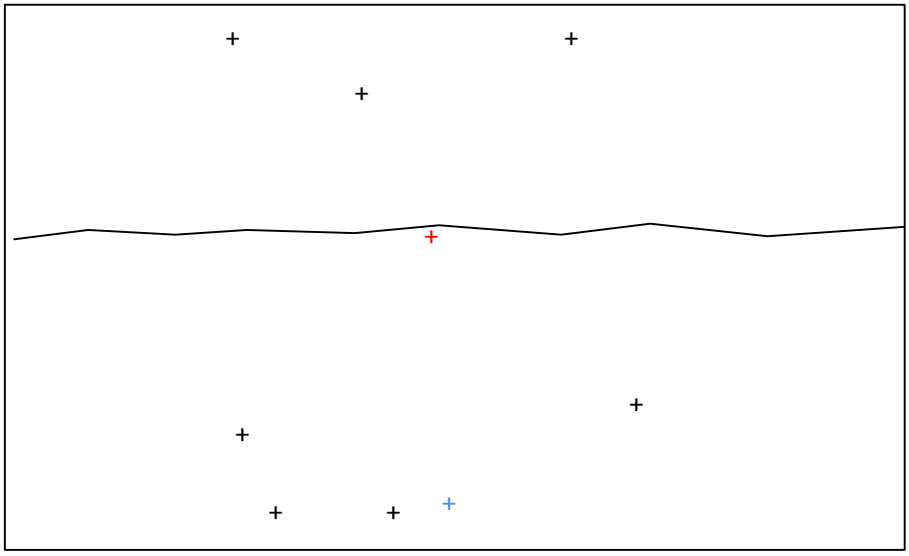

Figure 81. Correction of tangent-like sections.

6.4.1.4. Longitudinal analysis

All previous steps only consider each point individually, as well as the closest ones. However, a longitudinal analysis may add more information to determine the curvature profile.

Some procedures can be performed in order to produce smoother curvature profiles. However, the traditional algorithms are not adequate, since they might hide sharp curvatures. The proposed algorithm only focuses at certain points where the curvature value is clearly different. The following cases are treated (Figure 82):

- Null curvature point surrounded by to non-curvature points (to the same direction). The null curvature point will be changed by the average value of those points.
- Non-null curvature point surrounded by two non-curvature points before and after. In this case, the curvature of the point is changed to zero.

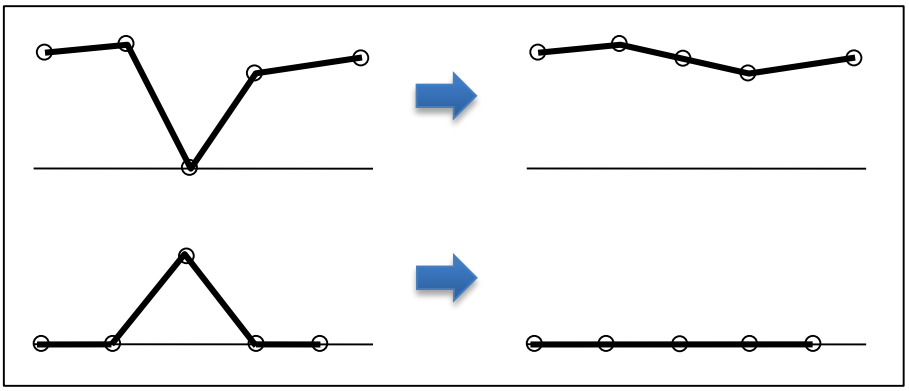

Figure 82. Longitudinal error correction.

6.4.2. Restitution of the horizontal alignment

The next step is to determine the horizontal alignment based on the polyline that represents the road centerline. A lot of previous effort has been carried out in order to obtain this solution, most of them considering the properties of the curvature profile.

Determining the geometric elements that compose the horizontal alignment of a road from a set of data points is not easy. Previous research used an initial curvature profile estimated from the points. Unlike the road alignment, the curvature profile is not smooth and even may not be continuous. It is composed of horizontal lines with $\kappa = 0$ that represent tangents, horizontal lines with $\kappa \neq 0$ that represent circular curves, and sloped straight lines that represent spiral transitions. Such a profile was meant to help identify the presence of spirals and compound circular curves.

Dealing with the heading direction can overcome several of these difficulties. This procedure was specifically developed for this doctoral thesis.

6.4.2.1. Use of the heading for geometric restitution

The horizontal curvature of a road strongly affects the safety and comfort of travel, and that is why curvature profiles are widely used in road design and road alignment analysis. Three kinds of geometric elements are used in designing the horizontal alignment of roads: tangents, circular curves, and spiral transitions. These are the components that closely follow the natural vehicle paths, and the existing design standards apply to the parameters of these curves. Each type of curve has a distinct curvature profile shape.

Analyzing the horizontal alignment based on the heading profile instead of the curvature profile presents two important advantages:

- As demonstrated in the corresponding section, the heading profile is considerably less sensitive to measurement error, which allows the alignment components to be easily identifiable, even including visual inspection by the user. This benefit is clear when comparing the heading profile to the curvature profile.
- The road heading must always be continuous. This means that the heading value presented by a geometric element at its final point must always be the same as the initial heading value of the following geometric element. Consequently, fitting the alignment in this way allows sharing some information longitudinally, thereby addressing some issues produced by the randomness of the data. Moreover, in most cases the heading's first derivative is also continuous (except when a large radius of the circular curve eliminates the necessity of using spiral transitions), meaning that a continuity in the heading's slope profile must also be satisfied, thus adding more information. The curvature profile does not present this property, and the different geometric elements must be independently fitted, producing less accurate solutions.

For the reasons previously explained, the heading profile will be used to represent the horizontal alignment. Curvature is related to heading direction as shown in Equation 175.

$$\kappa = \frac{1}{R} = \frac{d\theta}{ds} \tag{175}$$

Where:

$\kappa = \frac{1}{R}$: Curvature($[L]^{-1}$), where R is the horizontal radius.
θ: Heading direction (rad).
s: Distance.

Therefore, the different geometric elements can also be described according to their heading properties, as shown in Table 20.

Like the curvature profile, the heading profile can be defined as the representation of the heading direction of the alignment, depending on the station. Figure 83 shows one example of a right-handed horizontal curve. In the heading profile, tangents are horizontal lines, circular curves are sloped lines, where spiral transitions are parabolic curves.

Geometric element	Curvature		Heading	
Tangent	$\kappa = 0$	(176)	$\theta = \int 0 \cdot ds = \theta_k$	(177)
Circular curve	$\kappa = c_k$	(178)	$\theta = \int c_k \cdot ds = c_k \cdot s + \theta_k$	(179)
Spiral transition	$\kappa = \frac{s + d_o}{A^2}$	(180)	$\theta = \int \frac{s + d_o}{A^2} \cdot ds = \frac{1}{A^2} \cdot \left[\frac{s^2}{2} + d_0 \cdot s + \theta_k\right]$	(181)

κ: Curvature (m^{-1}).

θ: Heading (gon).

s: Distance measured from the beginning of the geometric element (m).

A: Parameter of the spiral transition (m).

d_0, c_k, θ_k: Constants.

Table 20. Curvature and heading properties for the geometric elements.

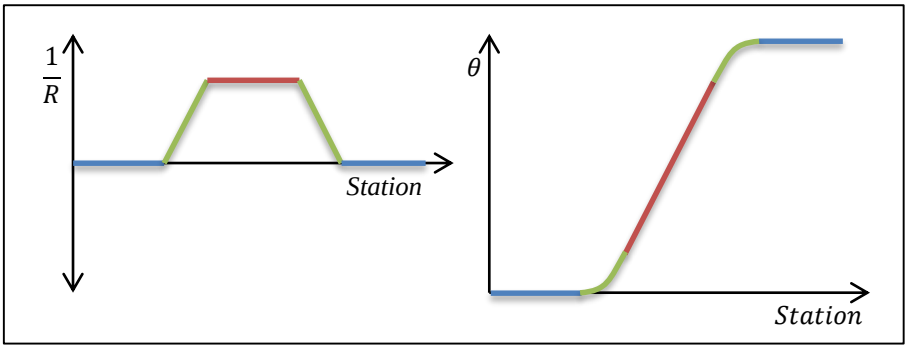

Figure 83. Curvature and heading profile for a tangent-to-curve-to-tangent sequence with transition curves.

6.4.2.2. Assessment of the error of curvature and heading parameters

One of the advantages of using the heading direction is the lower error. Thus, the obtained diagrams are quite more readable, even with no smoothing or filtering processes that may affect the results. We are going to demonstrate it by comparing the error level of both parameters.

An extraction of point location data from the alignment yields a sequence of (x, y) coordinates. These coordinates can be converted to the corresponding initial heading profile *(s, θ)* by calculating Δs and θ with the Equations 182 and 183:

$$\Delta s_i = \sqrt{\Delta x_i^2 + \Delta y_i^2} \qquad (182)$$

$$\theta_i = \arctan\left(\frac{\Delta y_i}{\Delta x_i}\right) \tag{183}$$

Where the coordinates (x_i, y_i) represent the point i located at distance s_i from the beginning of the alignment. Thus:

$$\Delta x_i = x_{i+1} - x_i \tag{184}$$
$$\Delta y_i = y_{i+1} - y_i \tag{185}$$

According to the relationship between curvature and heading direction, the curvature can be determined as:

$$\kappa_i = \frac{\theta_{i+1} - \theta_i}{\Delta s_i} \tag{186}$$

Let us assume that there is a constant longitudinal separation between the points of the alignment of μ_s. The standard deviation of this error is σ_s. The lateral error ε_l is the distance between the point and the actual alignment. Its mean value is $\mu_l = 0$ and the standard deviation is σ_l.

The identification of the different highway alignment elements is possible if the error of the corresponding parameter is lower than the change itself. In order to test this, we are going to assume that $\sigma_{\Delta\theta}$ is the standard estimation error in θ and $\sigma_{\Delta\kappa}$ is for κ. Of course, the standard estimation of separation is quite smaller than μ_s. Thus, it can be assumed:

$$\varepsilon_\theta \cong \frac{\varepsilon_l}{m_s} \tag{187}$$

Another assumption is that ε_l is independent and normally distributed. Thus, the estimation errors of changes in heading and curvature can be approximated using the linear term of the Taylor series. The approximate standard errors of both are shown in Equations 188 and 189.

$$\sigma_{\Delta\theta} = \frac{\sqrt{2}}{m_s} \cdot \sigma_l \tag{188}$$

$$\sigma_{\Delta\kappa} = \frac{2}{m_s^2} \cdot \sigma_l \tag{189}$$

Transversal errors of 5, 10 and 20 cm are normal when manually depicting a road centerline from satellite imagery. The distance between points might be of 5, 10 or 20 m. Table 21 presents the standard errors in the estimates of headings changes and curvature changes calculated for any two consecutive points of the horizontal alignment. The corresponding detectable changes in the headings and curvature profiles are also provided. They are assumed to be twice the estimation standard error. The table indicates that, in the majority of cases, the curvature profiles are too noisy to allow convenient identification and estimation of curves. On the contrary, the heading profile is less noisy, and even small changes in the headings can be conveniently detected.

Lateral standard error (m)	Alignment points interval Δs (m)	Heading profile		Curvature profile	
		Std. error of θ change estimate (rad)	Minimum detectable change in heading (^{o})	Std. error of κ change estimate (1/m)	Largest radius of detectable isolated curve (m)
0.02	2	0.0141	1.6	0.01000	50 x
0.02	5	0.0057	0.64	0.00160	312 x
0.02	10	0.0028	0.3	0.00040	1250
0.05	2	0.0354	4.1 x	0.02500	20 x
0.05	5	0.0141	1.6	0.00400	124 x
0.05	10	0.0071	0.83	0.00100	500 ?

Table 21. Comparison of the noise effect on curvature- and heading- based procedures.

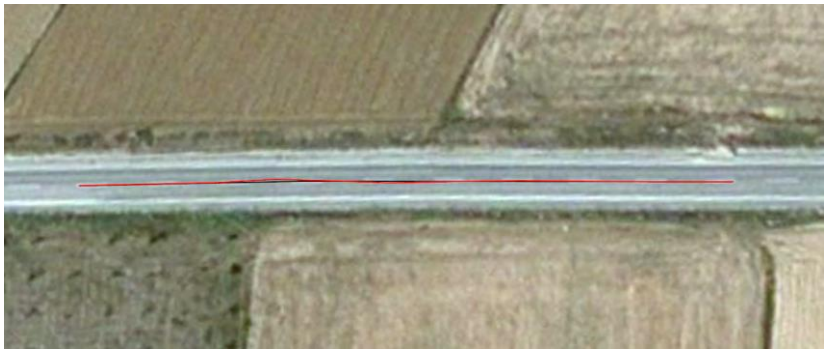

Figure 84. The black line represents the actual road centerline. Small variations of the clicked centerline (red) produce such a high noise in the curvature profile, making it unreadable. Those errors are quite lower in the heading profile.

Figure 85 shows a different approach to the error sensitivity of the method. A tangent-to-curve transition is shown, where no spiral transition exists. The radius of the curve is 200 m, which can be assumed to be medium. A random, standard error of 5 cm was introduced. The separation of points is 5 cm. The heading and curvature profiles are depicted. In both cases, the noise produced by the error term can be clearly seen. However, only in the case of the heading profile the change of geometric element can be clearly seen, since the variation of the heading is quite higher than its error. Hence, no smoothing processes are required.

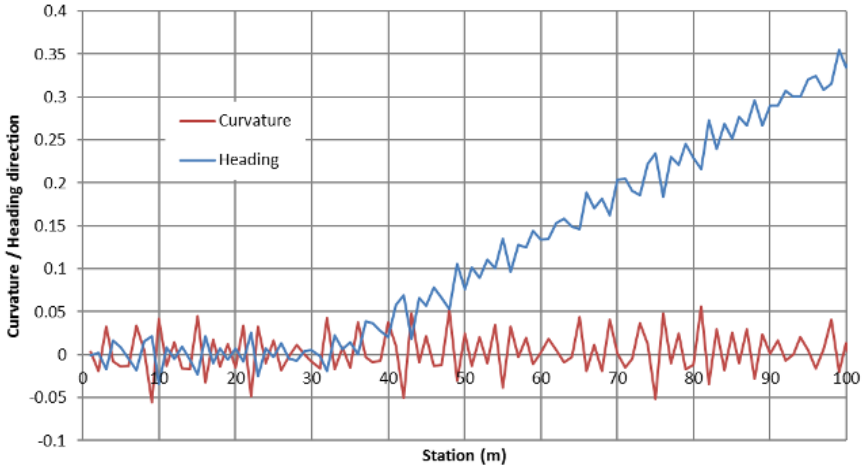

Figure 85. Comparison of a tangent-to-circular curve transition with artificial randomness. The heading methodology clearly indicates where the geometric element change is located.

Another consideration of the location error is its impact on the accuracy of s in the estimated curvature and heading profile. Since the Δs calculated with Equation 2 is not measured exactly along the alignment but rather along a line that tends to be at a slight skew to the alignment due to the lateral errors e_l, the distance s is overestimated and this overestimation is growing with distance. Fortunately, the longitudinal error e_s is negligible when evaluating the driving convenience and safety. For example, a statistical simulation that followed the stated earlier assumptions has shown that a point one kilometer away from the beginning is expected to be shifted by approximately 0.35 m if the data points on the alignment are separated by two meters and the lateral location accuracy is 0.02 m (standard deviation). This overestimation may require adjustments if the reconstructed location of the alignment is important.

It can be concluded that, to produce good results, the alignment points separated by two meters (Δs=2 m) should not have the standard measurement error exceeding 0.02 meter. This paper shows how to utilize heading profiles to fit horizontal alignments to data points obtained from manual image-based data collection. Another data collection method previously discussed uses drivers' paths. Camacho et al. (2010) developed a method that combines different paths followed by drivers into a single one called the "average path" with the alignment points separated at 1 m.

Thus, this overestimation requires adjustments if the reconstructed location of the alignment is important. In the case of extracting the geometric features of the road alignment, this inaccuracy can be neglected.

Figure 86 shows one example of heading profile. Although some noise is detected, all the different average geometric features are detected with no problem. It is worth to indicate that no previous refinement process has been applied, so no biasing is added.

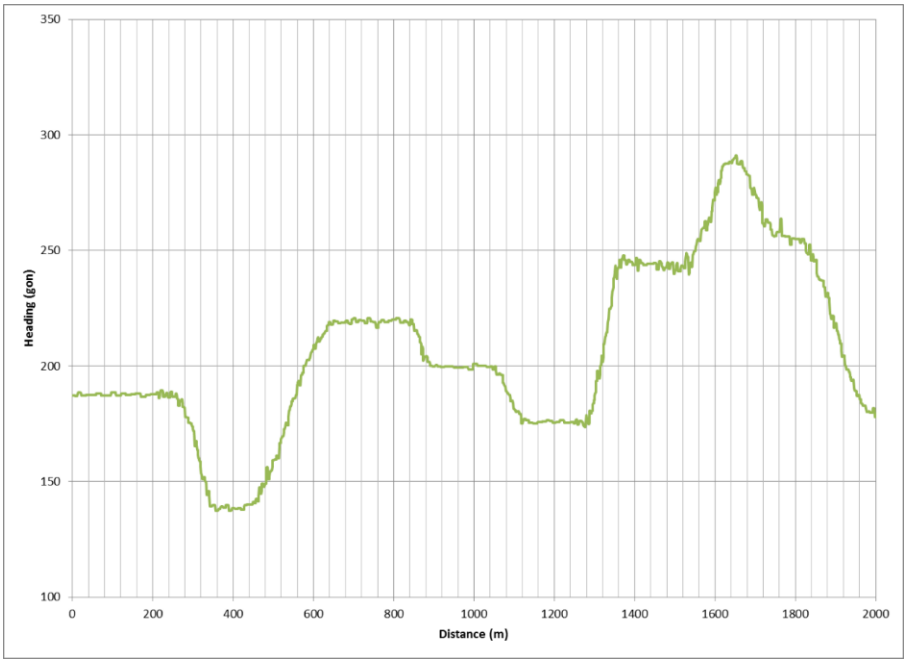

Figure 86. Example of heading profile.

6.4.2.3. General formulation and solution of the problem

The horizontal alignment restoration problem can be described in general terms as fitting the three types of alignment components by minimizing the square-mean error of heading estimates while preserving the continuity of the heading at the stitching points between the geometric elements. The continuity of the heading's first derivative (curvature) must also be preserved where transition curves are used. The decision variables include the parameters of the alignment curves and the stitching points. The continuity conditions are the constraints of the problem. Table 20 shows that a tangent heading curve has one parameter, a circular curve – two, and a transition curve – three.

The heading profile is quite readable, so the number of geometric elements is known and only the stitching points and the parameters of the geometric elements have to be solved. Thus, the problem is a mixed integer optimization problem. There are a limited number of discrete positions for the stitching points. On the other hand, knowing the stitching points allows fitting individual heading curves that are continuous functions. The general strategy is to separate the integer and continuous problems by solving them interchangeably until the solution converges. Fortunately,

when the stitching points are known (or solved), the number of constraints and decision variables can be made equal in all cases. Thus, only one set of curves exists that meets the continuity and smoothness conditions. These curves can be easily calculated from the system of linear equations that represents the continuity and smoothness conditions at the stitching points. Figure 87 shows the process.

The overall solving strategy includes:

1. Balancing the number of curve parameters with the number of continuity/smoothness conditions.
2. Solving the system of linear equations to obtain feasible curves for the current stitching points.
3. Finding the best stitching points for the current set of curves.
4. Repeating steps 2 and 3 until the solution converges.

Decomposition of the entire problem by dividing the alignment into shorter pieces is another strategy used to simplify and speed up the search for the solution. The midpoints of known geometric elements are the natural choice. After solving all the sub-problems, the entire alignment can be obtained by combining the solutions of sub-problems.

The following section discusses selected cases in a more specific and analytical manner. A heuristic procedure of finding the best stitching points is also presented and demonstrated with examples.

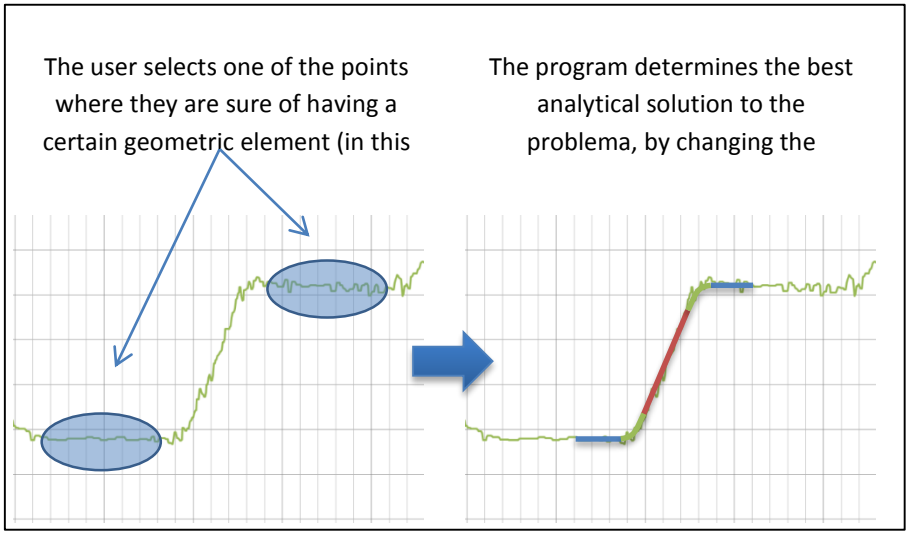

Figure 87. Selection of the points belonging to tangent sections.

The solutions for each problems are presented here. They are later discussed, including the constraints, parameters, and conditions. Table 22 shows those solutions.

The final stitching of all sub-problems is also indicated.

Geometric sequence	Geometric elements								
Isolated curve between two tangents	R	Cl	C	Cl	R				
Isolated curve between two tangents with no spiral transitions	R	C	R						
Two isolated curves with intermediate tangent (reverse or broken-back curves)	R	Cl	C	Cl	R	Cl	C	Cl	R
Two non-isolated curves with intermediate tangent	C	Cl	R	Cl	C				
Compound curve	C	Cl	C						
Tangent-to-curve transition	R	Cl	C						
Curve-to-tangent transition	C	Cl	R						
Stitching of a tangent section	R								
Stitching of a circular curve section	C								

Table 22. Sequences of elements with analytic solution.

Figure 88 shows the main form of the computer program. It allows the user to introduce the points between which the solution is going to be determined, and the

type of geometric composition. It also allows the user to stitch tangents, curves, and to modify the plotted profile, in order to be more accurate.

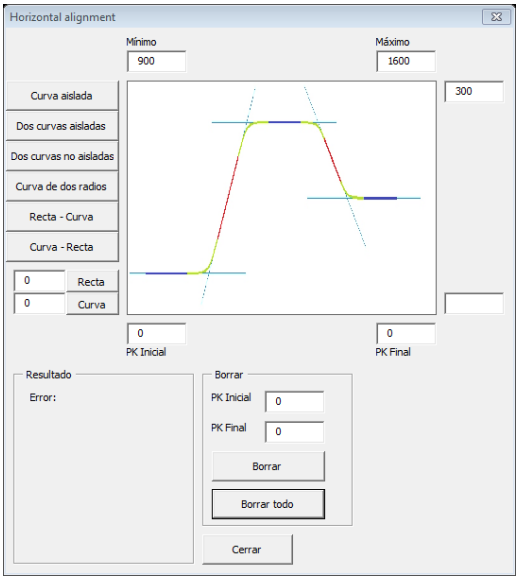

Figure 88. Form for calibrating the horizontal alignment based on the heading direction.

6.4.2.3.1. Isolated curve

This adjustment problem is valid for all horizontal curves with or without spiral transitions. It is first explained the case with spiral transitions, and later the particularization for the second problem.

As shown in Figure 89, the curve is clearly between two tangents. The user can clearly select one point within each tangent and the program will determine which stitching points produce the solution that better fits to the existing geometry.

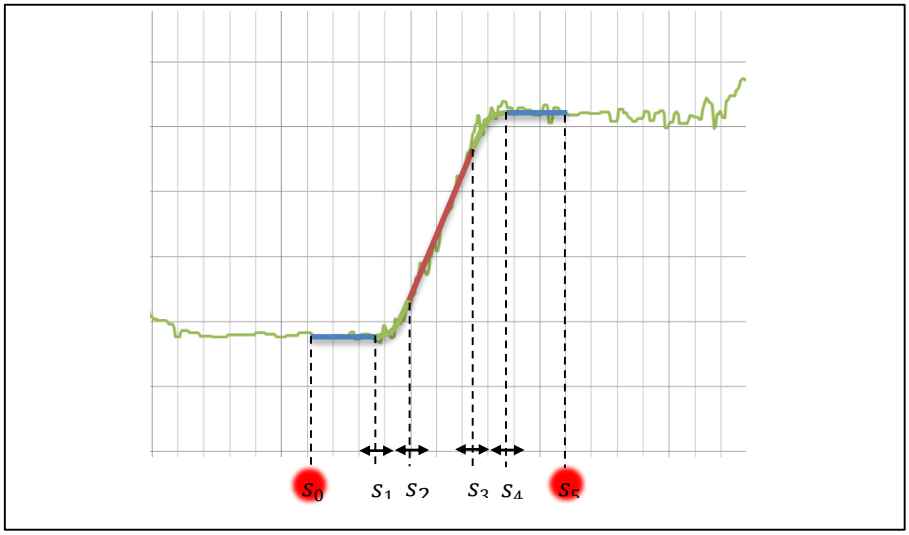

Figure 89. Layout of horizontal isolated curve.

The geometric elements are:

- Tangent T_1: $\theta_{T_1} = c_1$
- Clothoid Cl_1: $\theta_{Cl_1} = a_2 \cdot s^2 + b_2 \cdot s + c_2$
- Circular curve C: $\theta_C = b_3 \cdot s + c_3$
- Clothoid Cl_2: $\theta_{Cl_2} = a_4 \cdot s^2 + b_4 \cdot s + c_4$
- Tangent T_2: $\theta_{T_2} = c_5$

The stitching points are those connecting the different geometric elements, as well as those two points indicated by the user:

- Beginning point (user-defined): s_0
- Stitching point between T_1 y Cl_1: s_1
- Stitching point between Cl_1 y C: s_2
- Stitching point between C y Cl_2: s_3
- Stitching point between Cl_2 y T_2: s_4
- Ending point (user-defined): s_5

Figure 89 shows that the stitching points (s_i, $i = 1, 2, 3, 4$) must present continuity on heading and its slope (first derivative: curvature). Thus, the following conditions must be achieved:

Point s1:

Heading continuity: $\theta_{T_1} = \theta_{Cl_1}$

$$c_1 = a_2 \cdot s_1^2 + b_2 \cdot s_1 + c_2 \tag{190}$$

Curvature continuity: $\theta'_{T_1} = \theta'_{Cl_1}$

$$0 = 2 \cdot a_2 \cdot s_1 + b_2 \tag{191}$$

Point s2:

Heading continuity: $\theta_{Cl_1} = \theta_C$

$$a_2 \cdot s_2^2 + b_2 \cdot s_2 + c_2 = b_3 \cdot s_2 + c_3 \tag{192}$$

Curvature continuity: $\theta'_{Cl_1} = \theta'_C$

$$2 \cdot a_2 \cdot s_2 + b_2 = b_3 \tag{193}$$

Point s3:

Heading continuity: $\theta_C = \theta_{Cl_2}$

$$b_3 \cdot s_3 + c_3 = a_4 \cdot s_3^2 + b_4 \cdot s_3 + c_4 \tag{194}$$

Curvature continuity: $\theta'_C = \theta'_{Cl_2}$

$$b_3 = 2 \cdot a_4 \cdot s_3 + b_4 \tag{195}$$

Point s4:

Heading continuity: $\theta_{Cl_2} = \theta_{T_2}$

$$a_4 \cdot s_4^2 + b_4 \cdot s_4 + c_4 = c_5 \tag{196}$$

Curvature continuity: $\theta'_{Cl_2} = \theta'_{T_2}$

$$2 \cdot a_4 \cdot s_4 + b_4 = 0 \tag{197}$$

Therefore, eight constraints must be satisfied:

$$\begin{cases} c_1 = a_2 \cdot s_1^2 + b_2 \cdot s_1 + c_2 \\ 0 = 2 \cdot a_2 \cdot s_1 + b_2 \\ a_2 \cdot s_2^2 + b_2 \cdot s_2 + c_2 = b_3 \cdot s_2 + c_3 \\ 2 \cdot a_2 \cdot s_2 + b_2 = c_3 \\ b_3 \cdot s_3 + c_3 = a_4 \cdot s_3^2 + b_4 \cdot s_3 + c_4 \\ b_3 = 2 \cdot a_4 \cdot s_3 + b_4 \\ a_4 \cdot s_4^2 + b_4 \cdot s_4 + c_4 = c_5 \\ 2 \cdot a_4 \cdot s_4 + b_4 = 0 \end{cases} \tag{198}$$

And there are ten unknown parameters:

$$c_1, a_2, b_2, c_2, b_3, c_3, a_4, b_4, c_4, c_5$$

It is worth to highlight that the stitching points are not unknown parameters, since their optimal values will be calculated based on a heuristic approach.

The number of constraints is lower than the unknown parameters, so there are infinite solutions to the problem. Nevertheless, c_1 and c_5 are in fact known, since they are the heading directions of the preceding and the following tangent of the curve (Equations 199 and 200):

$$c_1 = \theta_{T_1} \tag{199}$$
$$c_5 = \theta_{T_2} \tag{200}$$

Thus, the number of unknowns is the same as constraints, so there is a unique solution to the problem. Now we are going to solve it.

$$\begin{cases} \theta_{T_1} = a_2 s_1^2 + b_2 s_1 + c_2 \\ 0 = 2a_2 s_1 + b_2 \\ a_2 s_2^2 + b_2 s_2 + c_2 = b_3 s_2 + c_3 \\ 2a_2 s_2 + b_2 = b_3 \\ b_3 s_3 + c_3 = a_4 s_3^2 + b_4 s_3 + c_4 \\ b_3 = 2a_4 s_3 + b_4 \\ a_4 s_4^2 + b_4 s_4 + c_4 = \theta_{T_2} \\ 2a_4 s_4 + b_4 = 0 \end{cases} \quad (201)$$

Taking Equation 202:

$$0 = 2a_2 s_1 + b_2 \rightarrow b_2 = -2a_2 s_1 \quad (202)$$

Substituting b_2 in Equations 190 and 191:

$$\theta_{T_1} = a_2 s_1^2 - 2a_2 s_1^2 + c_2 \rightarrow \theta_{T_1} = -a_2 s_1^2 + c_2 \rightarrow c_2 = \theta_{T_1} + a_2 s_1^2 \quad (203)$$

$$2a_2 s_2 - 2a_2 s_1 = b_3 \rightarrow a_2 = \frac{b_3}{2(s_2 - s_1)} \quad (204)$$

Now b_2 and c_2 can be replaced in Equation 192:

$$a_2 s_2^2 - 2a_2 s_1 s_2 + \theta_{T_1} + a_2 s_1^2 = b_3 s_2 + c_3 \quad (205)$$

Thus leading to:

$$a_2 (s_1 - s_2)^2 + \theta_{T_1} = b_3 s_2 + c_3 \quad (206)$$

Equations 204 and 206 can now be merged, by substituting a_2 in the last one:

$$\frac{b_3}{2(s_2 - s_1)} (s_1 - s_2)^2 + \theta_{T_1} = b_3 s_2 + c_3 \quad (207)$$

Obtaining:

$$\frac{b_3}{2}(s_2 - s_1) + \theta_{T_1} = b_3 s_2 + c_3$$

$$b_3(s_2 - s_1) + 2\theta_{T_1} = 2b_3 s_2 + 2c_3$$

$$b_3(s_2 - s_1) - 2b_3 s_2 = 2c_3 - 2\theta_{T_1}$$

$$b_3(s_2 - s_1 - 2s_2) = 2\left(c_3 - \theta_{T_1}\right)$$

$$b_3(s_1 + s_2) = 2\left(\theta_{T_1} - c_3\right)$$

$$b_3 = \frac{2\left(\theta_{T_1} - c_3\right)}{s_1 + s_2} \quad (208)$$

Similarly, departing from Equation 197:

$$2a_4 s_4 + b_4 = 0 \rightarrow b_4 = -2a_4 s_4 \quad (209)$$

Substituting b_4 in Equations 196 and 195:

$$a_4 s_4^2 - 2a_4 s_4^2 + c_4 = \theta_{T_2} \rightarrow -a_4 s_4^2 + c_4 = \theta_{T_2} \rightarrow c_4 = \theta_{T_2} + a_4 s_4^2 \quad (210)$$

$$b_3 = 2a_4 s_3 - 2a_4 s_4 \rightarrow a_4 = \frac{b_3}{2(s_3 - s_4)} \quad (211)$$

Now b_4 and c_4 can be substituted in Equation 194:

$$b_3 s_3 + c_3 = a_4 s_3^2 - 2a_4 s_3 s_4 + \theta_{T_2} + a_4 s_4^2 \quad (212)$$

Thus leading to:

$$b_3 s_3 + c_3 = a_4(s_3^2 - 2s_4 s_3 + s_4^2) + \theta_{T_2}$$

$$b_3 s_3 + c_3 = a_4(s_3 - s_4)^2 + \theta_{T_2} \quad (213)$$

Now a_4 can be substituted in Equation 213, obtaining:

$$b_3 s_3 + c_3 = \frac{b_3}{2(s_3 - s_4)}(s_3 - s_4)^2 + \theta_{T_2}$$

$$b_3 s_3 + c_3 = \frac{b_3}{2}(s_3 - s_4) + \theta_{T_2}$$

$$2b_3 s_3 + 2c_3 = b_3(s_3 - s_4) + 2\theta_{T_2}$$

$$2b_3 s_3 - b_3(s_3 - s_4) = 2\theta_{T_2} - 2c_3$$

$$b_3(2s_3 - s_3 + s_4) = 2\theta_{T_2} - 2c_3$$

$$b_3 = \frac{2\left(\theta_{T_2} - c_3\right)}{s_3 + s_4} \tag{214}$$

One can observe that we have to expressions that relate b_3 and c_3 to already known parameters. Thus, the following equation system can be solved:

$$\begin{cases} b_3 = \dfrac{2\left(\theta_{T_1} - c_3\right)}{s_1 + s_2} \\ b_3 = \dfrac{2\left(\theta_{T_2} - c_3\right)}{s_3 + s_4} \end{cases} \tag{215}$$

$$\frac{2\left(\theta_{T_1} - c_3\right)}{s_1 + s_2} = \frac{2\left(\theta_{T_2} - c_3\right)}{s_3 + s_4}$$

$$(s_3 + s_4)\left(\theta_{T_1} - c_3\right) = (s_1 + s_2)\left(\theta_{T_2} - c_3\right)$$

$$s_3\theta_{T_1} + s_4\theta_{T_1} - c_3 s_3 - c_3 s_4 = s_1\theta_{T_2} + s_2\theta_{T_2} - s_1 c_3 - s_2 c_3$$

$$s_1 c_3 - c_3 s_3 - c_3 s_4 + s_2 c_3 = s_1\theta_{T_2} + s_2\theta_{T_2} - s_3\theta_{T_1} - s_4\theta_{T_1}$$

$$c_3(s_1 - s_3 - s_4 + s_2) = \theta_{T_2}(s_1 + s_2) - \theta_{T_1}(s_3 + s_4)$$

$$c_3 = \frac{\theta_{T_2}(s_1 + s_2) - \theta_{T_1}(s_3 + s_4)}{(s_1 + s_2) - (s_3 + s_4)} \tag{216}$$

b_3 can also be obtained:

$$\begin{cases} b_3 = \dfrac{2\left(\theta_{T_1} - c_3\right)}{s_1 + s_2} \\ b_3 = \dfrac{2\left(\theta_{T_2} - c_3\right)}{s_3 + s_4} \end{cases} \rightarrow \begin{cases} c_3 = \theta_{T_1} - \dfrac{b_3(s_1 + s_2)}{2} \\ c_3 = \theta_{T_2} - \dfrac{b_3(s_3 + s_4)}{2} \end{cases}$$

$$\theta_{T_1} - \frac{b_3(s_1 + s_2)}{2} = \theta_{T_2} - \frac{b_3(s_3 + s_4)}{2}$$

$$b_3(s_3 + s_4) - b_3(s_1 + s_2) = 2\theta_{T_2} - 2\theta_{T_1}$$

$$b_3 = \frac{2\left(\theta_{T_1} - \theta_{T_2}\right)}{(s_1 + s_2) - (s_3 + s_4)} \tag{217}$$

Those parameters allow us to determine the rest of the unknown parameters. They are shown in Table 23.

c_1	θ_{T_1}	(218)
a_2	$\dfrac{\theta_{T_1} - \theta_{T_2}}{\left((s_1 + s_2) - (s_3 + s_4)\right)(s_2 - s_1)}$	(219)
b_2	$\dfrac{2\left(\theta_{T_2} - \theta_{T_1}\right)s_1}{\left((s_1 + s_2) - (s_3 + s_4)\right)(s_2 - s_1)}$	(220)
c_2	$\theta_{T_1} + \dfrac{\left(\theta_{T_1} - \theta_{T_2}\right)s_1^2}{\left((s_1 + s_2) - (s_3 + s_4)\right)(s_2 - s_1)}$	(221)
b_3	$\dfrac{2\left(\theta_{T_1} - \theta_{T_2}\right)}{(s_1 + s_2) - (s_3 + s_4)}$	(222)
c_3	$\dfrac{\theta_{T_2}(s_1 + s_2) - \theta_{T_1}(s_3 + s_4)}{(s_1 + s_2) - (s_3 + s_4)}$	(223)
a_4	$\dfrac{\theta_{T_1} - \theta_{T_2}}{\left((s_1 + s_2) - (s_3 + s_4)\right)(s_3 - s_4)}$	(224)
b_4	$\dfrac{2\left(\theta_{T_2} - \theta_{T_1}\right)s_4}{\left((s_1 + s_2) - (s_3 + s_4)\right)(s_3 - s_4)}$	(225)
c_4	$\theta_{T_2} + \dfrac{\left(\theta_{T_1} - \theta_{T_2}\right)s_4^2}{\left((s_1 + s_2) - (s_3 + s_4)\right)(s_3 - s_4)}$	(226)
c_5	θ_{T_2}	(227)

Table 23. Parameters for an isolated curve.

This demonstrates that for a given values of the points s_0 and s_5 (frontier, user-defined points), every set of (s_1, s_2, s_3, s_4) produces a unique solution to the problem. Thus, it is now only necessary to determine how the set of (s_1, s_2, s_3, s_4) points are found. A heuristic approach is presented, minimizing the minimum square error between the original headings and the fitted alignment.

The heuristic adjustment must consider some other obvious constraints of the problem. The geometric sequence has an order and cannot be changed. In addition, at least one point is required for tangents, two points for circular points and three points for spiral transitions, depending on the degree of the corresponding equations.

Both conditions can be expressed as:

$$\left.\begin{aligned} s_0 &< s_1 \\ s_1 &< s_2 - 2 \\ s_2 &< s_3 - 1 \\ s_3 &< s_4 - 2 \\ s_4 &< s_5 \end{aligned}\right\} \tag{228}$$

The heuristic approach tries all the different possibilities for all parameters. It is described as follows:

1. A seed (s_1, s_2, s_3, s_4) solution is proposed by the program. A first fitting solution is determined and the MSE is determined.
2. Variation of the stitching point s_1 between s_0 and s_2 , meeting the corresponding constraints. A solution is determined for all cases, calculating the MSE. The point s_1 will be moved to the location that produces the minimum MSE.
3. All the stitching points s_i, $i = 1, 2, 3, 4$ are moved between the stitching points s_{i-1} and s_{i+1}, according to the corresponding conditions. For each case, the stitching point is moved to the point where the solution produces the lowest MSE. This algorithm is applied to the following sequence of points: $s_1, s_2, s_3, s_4, s_3, s_2$. Finally, a provisional solution is determined and the MSE calculated.
4. The process is repeated until the MSE is not improved any more. This provisional solution is defined as the best and the process has concluded.

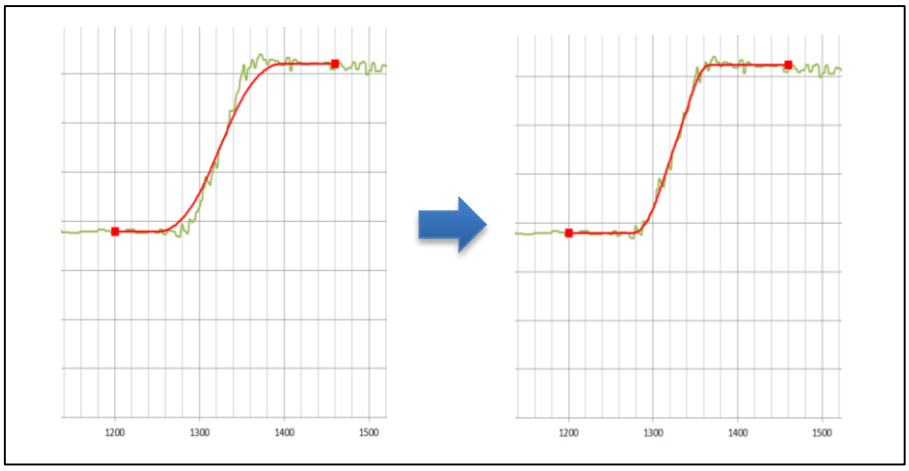

Figure 90. First (l) and final (r) optimizations of an isolated curve.

Once the best solution has been achieved, the parameters of the geometric features can be determined, considering the heading variation as well as the length of the elements.

6.4.2.3.2. Isolated curve without spiral transitions

The previous solution is valid for fitting isolated curves with spiral transitions. However, spiral transitions are not always used for road design. If the previous algorithm is applied to an isolated curve with no spiral transitions, the program will converge to a solution with minimum spirals (i.e., 2 m long). This is quite similar to the reality, but a more exact approach can be done by means of removing those spiral transitions.

A sequence of tangent – circular curve – tangent presents continuity of heading but not of curvature. Thus, only one equation can be applied for each one of the stitching points. Thus, only two equations are available.

The sequence of geometric elements is described as:

- Tangent T_1: $\theta_{T_1} = c_1$
- Circular curve C: $\theta_C = b_2 \cdot s + c_2$
- Tangent T_2: $\theta_{T_2} = c_2$

There are only two stitching points:

- Beginning point (user-defined): s_0
- Stitching point between T_1 and C: s_1
- Stitching point between C and T_2: s_2
- Ending point (user-defined): s_3

Two conditions must be satisfied:

Point s1:

Heading continuity: $\theta_{T_1} = \theta_C$

$$c_1 = b_2 \cdot s_1 + c_2 \tag{229}$$

Point s2:

Heading continuity: $\theta_C = \theta_{T_2}$

$$b_2 \cdot s_2 + c_2 = c_3 \tag{230}$$

Unknowns c_1 and c_3 are already known, since they are the heading value of the first and second tangents. Therefore, the resulting equation system is:

$$\begin{cases} \theta_{T_1} = b_2 \cdot s_1 + c_2 \\ b_2 \cdot s_2 + c_2 = \theta_{T_2} \end{cases} \tag{231}$$

The solution to the system is:

$$b_2 = \frac{c_3 - \theta_{T_1}}{s_2 - s_1} \tag{232}$$

$$c_2 = \theta_{T_1} - \frac{\theta_{T_2} - \theta_{T_1}}{s_2 - s_1} \cdot s_1 \tag{233}$$

There is no a heuristic approach to solve this problem. In fact, the user actually does not known whether the curve they are trying to determine has spiral transitions or not. Therefore, they fit the curve to the general isolated curve problem. If that algorithm produces a solution with minimum spiral transitions, a switching function

changes the algorithm and the solution without spiral transitions is calculated. The MSE is also determined. If this solution will be considered as the best if it presents a lower MSE.

6.4.2.3.3. Reverse and broken-back curves with tangents

A common road geometric sequence is two curves with an intermediate tangent. This sequence can be fitted by applying twice the previous algorithm. This way of proceeding is recommended when the intermediate tangent can be clearly distinguished, so the user can select the corresponding points in it.

The problem arises if the intermediate tangent is very short, or even negligible. In this case, the user is not sure about which point to select, so the result is probably biased by its decision.

This is why a particular solution to the two-curve sequence is determined and developed. The user can select the initial and final points of this sequence, and the program will determine which solution fits better. This procedure is also valid when no intermediate tangent exists, thus producing a 1 m long tangent.

The sequence of geometric elements is the following ones:

- Tangent T_1: $\theta_{T_1} = c_1$
- Clothoid Cl_1: $\theta_{Cl_1} = a_2 \cdot s^2 + b_2 \cdot s + c_2$
- Circular curveC_1: $\theta_{C_1} = b_3 \cdot s + c_3$
- Clothoid Cl_2: $\theta_{Cl_2} = a_4 \cdot s^2 + b_4 \cdot s + c_4$
- Tangent T_2: $\theta_{T_2} = c_5$
- Clothoid Cl_3: $\theta_{Cl_3} = a_6 \cdot s^2 + b_6 \cdot s + c_6$
- Circular curve C_2: $\theta_{C_2} = b_7 \cdot s + c_7$
- Clothoid Cl_4: $\theta_{Cl_4} = a_8 \cdot s^2 + b_8 \cdot s + c_8$
- Tangent T_3: $\theta_{T_3} = c_9$

Those stitching points are defined (Figure 91):

- User-defined initial point: s_0
- Transition point between T_1 and Cl_1: s_1
- Transition point between Cl_1 and C_1: s_2
- Transition point between C and Cl_2: s_3
- Transition point between Cl_2 and T_2: s_4

- Transition point between T_2 and Cl_3: s_5
- Transition point between Cl_3 and C_2: s_6
- Transition point between C_2 and Cl_4: s_7
- Transition point between Cl_4 and T_2: s_8
- User-defined final point: s_9

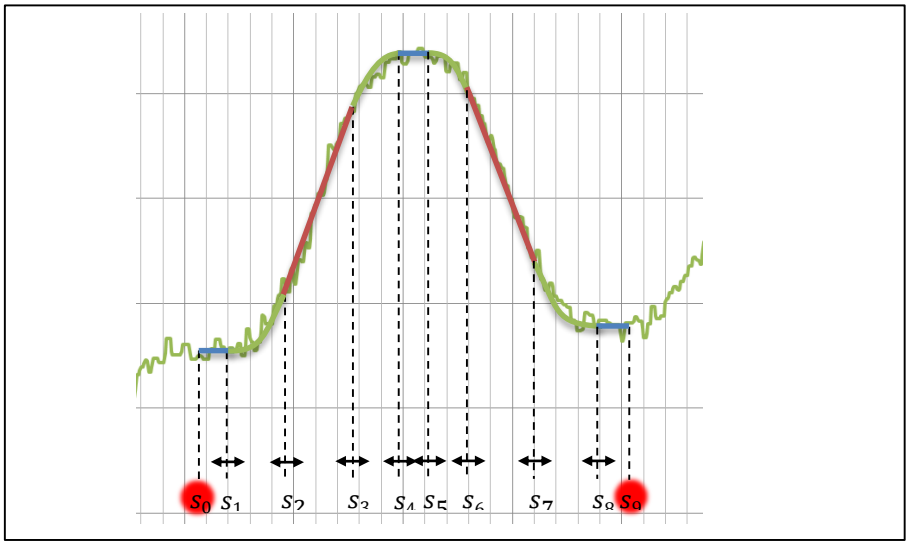

Figure 91. Layout of a combination of two isolated curves.

Continuity of heading and curvature must be maintained in all the stitching points. The values of the different parameters are obtained in the same way (Table 24).

c_1	θ_{T_1}	(234)
a_2	$\frac{\theta_{T_1} - \theta_{T_2}}{\big((s_1 + s_2) - (s_3 + s_4)\big)(s_2 - s_1)}$	(235)
b_2	$\frac{2\big(\theta_{T_2} - \theta_{T_1}\big)s_1}{\big((s_1 + s_2) - (s_3 + s_4)\big)(s_2 - s_1)}$	(236)
c_2	$\theta_{T_1} + \frac{\big(\theta_{T_1} - \theta_{T_2}\big)s_1^2}{\big((s_1 + s_2) - (s_3 + s_4)\big)(s_2 - s_1)}$	(237)
b_3	$\frac{2\big(\theta_{T_1} - \theta_{T_2}\big)}{(s_1 + s_2) - (s_3 + s_4)}$	(238)
c_3	$\frac{\theta_{T_2}(s_1 + s_2) - \theta_{T_1}(s_3 + s_4)}{(s_1 + s_2) - (s_3 + s_4)}$	(239)
a_4	$\frac{\theta_{T_1} - \theta_{T_2}}{\big((s_1 + s_2) - (s_3 + s_4)\big)(s_3 - s_4)}$	(240)
b_4	$\frac{2\big(\theta_{T_2} - \theta_{T_1}\big)s_4}{\big((s_1 + s_2) - (s_3 + s_4)\big)(s_3 - s_4)}$	(241)
c_4	$\theta_{T_2} + \frac{\big(\theta_{T_1} - \theta_{T_2}\big)s_4^2}{\big((s_1 + s_2) - (s_3 + s_4)\big)(s_3 - s_4)}$	(242)
c_5	θ_{T_2}	(243)
a_6	$\frac{\theta_{T_2} - \theta_{T_3}}{\big((s_5 + s_6) - (s_7 + s_8)\big)(s_6 - s_5)}$	(244)
b_6	$\frac{2\big(\theta_{T_3} - \theta_{T_2}\big)s_5}{\big((s_5 + s_6) - (s_7 + s_8)\big)(s_6 - s_5)}$	(245)
c_6	$\theta_{T_2} + \frac{\big(\theta_{T_2} - \theta_{T_3}\big)s_5^2}{\big((s_5 + s_6) - (s_7 + s_8)\big)(s_6 - s_5)}$	(246)
b_7	$\frac{2\big(\theta_{T_2} - \theta_{T_3}\big)}{(s_5 + s_6) - (s_7 + s_8)}$	(247)
c_7	$\frac{\theta_{T_3}(s_5 + s_6) - \theta_{T_2}(s_7 + s_8)}{(s_5 + s_6) - (s_7 + s_8)}$	(248)
a_8	$\frac{\theta_{T_2} - \theta_{T_3}}{\big((s_5 + s_6) - (s_7 + s_8)\big)(s_7 - s_8)}$	(249)
b_8	$\frac{2\big(\theta_{T_3} - \theta_{T_2}\big)s_8}{\big((s_5 + s_6) - (s_7 + s_8)\big)(s_7 - s_8)}$	(250)
c_8	$\theta_{T_3} + \frac{\big(\theta_{T_2} - \theta_{T_3}\big)s_8^2}{\big((s_5 + s_6) - (s_7 + s_8)\big)(s_7 - s_8)}$	(251)
c_9	θ_{T_3}	(252)

Table 24. Parameters for a set of two consecutive curves.

For a given user-defined points s_0 and s_9 all the different sets of $(s_1, s_2, s_3, s_4, s_5, s_6, s_7, s_8)$ produce a single solution to the problem. As before, the only question is how to determine the best sequence.

The sequence of road geometric elements is known, so the following constraints can be established:

$$\left.\begin{aligned} s_0 &< s_1 \\ s_1 &< s_2 - 2 \\ s_2 &< s_3 - 1 \\ s_3 &< s_4 - 2 \\ s_4 &< s_5 \\ s_5 &< s_6 - 2 \\ s_6 &< s_7 - 1 \\ s_7 &< s_8 - 2 \\ s_8 &< s_9 \end{aligned}\right\} \tag{253}$$

The heuristic approach is the following:

1. Considering the initial and final points defined by the user, the program establishes a seed set of $(s_1, s_2, s_3, s_4, s_5, s_6, s_7, s_8)$ points. The first solution is determined and the MSE calculated. This is the first provisional solution.
2. Variation of the stitching point s_1 between s_0 and s_2, meeting the corresponding constraints. A solution is determined for all cases, calculating the MSE. The point s_1 will be moved to the location that produces the minimum MSE.
3. All the stitching points s_i, $i = 1, 2, 3, 4, 5, 6, 7, 8$ are moved between the stitching points s_{i-1} and s_{i+1}, according to the corresponding conditions. For each case, the stitching point is moved to the point where the solution produces the lowest MSE. This algorithm is applied to the following sequence of points: $s_1, s_2, s_3, s_4, s_5, s_6, s_7, s_8, s_7, s_6, s_5, s_4, s_3, s_2$. Finally, a provisional solution is determined and the MSE calculated.
4. The process is repeated until the MSE is not improved any more. This provisional solution is defined as the best and the process has concluded.

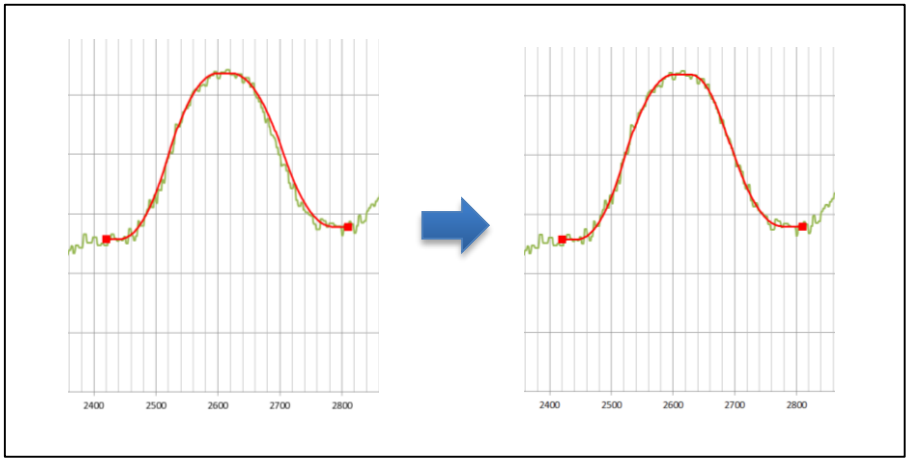

Figure 92. First (l) and final (r) solutions of the broken-back curve.

6.4.2.3.4. Series of n curves

The previous problem can be expanded to the case of n consecutive sequences of tangents and isolated curves with spiral transitions. The main advantage of this procedure is that the algorithm converges to a unique solution, even if all tangents present a negligible length.

The heuristic process has to consider $4n$ boundary points, n being the number of circular curves. The number of resulting equations from the stitching points is $8n$ (two for each point). With $i = 1 \dots n$ being each one of the circular curves, the stitching points are the following:

- Tangent T_i: from s_{4i-4} to s_{4i-3}
- Clothoid Cl_{2i-1}: from s_{4i-3} to s_{4i-2}
- Circular curve C_i: from s_{4i-2} to s_{4i-1}
- Clothoid Cl_{2i}: from s_{4i-1} to s_{4i}

Each curve adds nine unknown parameters, and the last tangent adds an additional one. Thus, there are $9n + 1$ unknowns. However, the tangent-related parameters are known since they can be directly obtained once the position of their stitching point is defined. There are $n + 1$ tangents, hence the same number of parameters. Thus, the final number of unknowns is $8n$, i.e., the same of constraints. Therefore, the problem has a unique solution. The solution to the system is presented in Table 25:

c_{4i-3}	θ_{T_i}	(254)
a_{4i-2}	$\frac{\theta_{T_i} - \theta_{T_{i+1}}}{\big((s_{4i-3} + s_{4i-2}) - (s_{4i-1} + s_{4i})\big)(s_{4i-2} - s_{4i-3})}$	(255)
b_{4i-2}	$\frac{2\big(\theta_{T_{i+1}} - \theta_{T_i}\big)s_{4i-3}}{\big((s_{4i-3} + s_{4i-2}) - (s_{4i-1} + s_{4i})\big)(s_{4i-2} - s_{4i-3})}$	(256)
c_{4i-2}	$\theta_{T_i} + \frac{\big(\theta_{T_i} - \theta_{T_{i+1}}\big)s_{4i-3}^2}{\big((s_{4i-3} + s_{4i-2}) - (s_{4i-1} + s_{4i})\big)(s_{4i-2} - s_{4i-3})}$	(257)
b_{4i-1}	$\frac{2\big(\theta_{T_i} - \theta_{T_{i+1}}\big)}{(s_{4i-3} + s_{4i-2}) - (s_{4i-1} + s_{4i})}$	(258)
c_{4i-1}	$\frac{\theta_{T_{i+1}}(s_{4i-3} + s_{4i-2}) - \theta_{T_i}(s_{4i-1} + s_{4i})}{(s_{4i-3} + s_{4i-2}) - (s_{4i-1} + s_{4i})}$	(259)
a_{4i}	$\frac{\theta_{T_i} - \theta_{T_{i+1}}}{\big((s_{4i-3} + s_{4i-2}) - (s_{4i-1} + s_{4i})\big)(s_{4i-1} - s_{4i})}$	(260)
b_{4i}	$\frac{2\big(\theta_{T_{i+1}} - \theta_{T_i}\big)s_{4i}}{\big((s_{4i-3} + s_{4i-2}) - (s_{4i-1} + s_{4i})\big)(s_{4i-1} - s_{4i})}$	(261)
c_{4i}	$\theta_{T_{i+1}} + \frac{\big(\theta_{T_i} - \theta_{T_{i+1}}\big)s_{4i}^2}{\big((s_{4i-3} + s_{4i-2}) - (s_{4i-1} + s_{4i})\big)(s_{4i-1} - s_{4i})}$	(262)
c_5	$\theta_{T_{i+1}}$	(263)

Table 25. Parameters for a set of *n* consecutive curves.

The heuristic process is the same than in the previous cases, but the number of stitching points to fit is clearly higher. In addition, the seed solution used for initiating the problem is very important, since it determines how fast the solution is reached. Thus, the user is encouraged to indicate to the program the zone where the tangents are more likely to be.

6.4.2.3.5. Reverse and broken-back curves without tangents

This is a particular solution to the previous problem, but in this case the preceding and following tangents are not available. The user should consider using this case when there appears a sequence of several curves with no intermediate tangents. Hence, the user must select initial and final points belonging to the circular part of the curves.

The sequence of geometric elements is the following:

- Circular curve C_1: $\theta_{C_1} = b_1 \cdot s + c_1$
- Clothoid Cl_1: $\theta_{Cl_1} = a_2 \cdot s^2 + b_2 \cdot s + c_2$
- Tangent T: $\theta_T = c_3$
- Clothoid Cl_2: $\theta_{Cl_2} = a_4 \cdot s^2 + b_4 \cdot s + c_4$
- Circular curve C_2: $\theta_{C_2} = b_5 \cdot s + c_5$

The stitching points are:

- User-defined initial point: s_0
- Transition point between C_1 y Cl_1: s_1
- Transition point between Cl_1 y T: s_2
- Transition point between T y Cl_2: s_3
- Transition point between Cl_2 y C_2: s_4
- User-defined final point: s_5

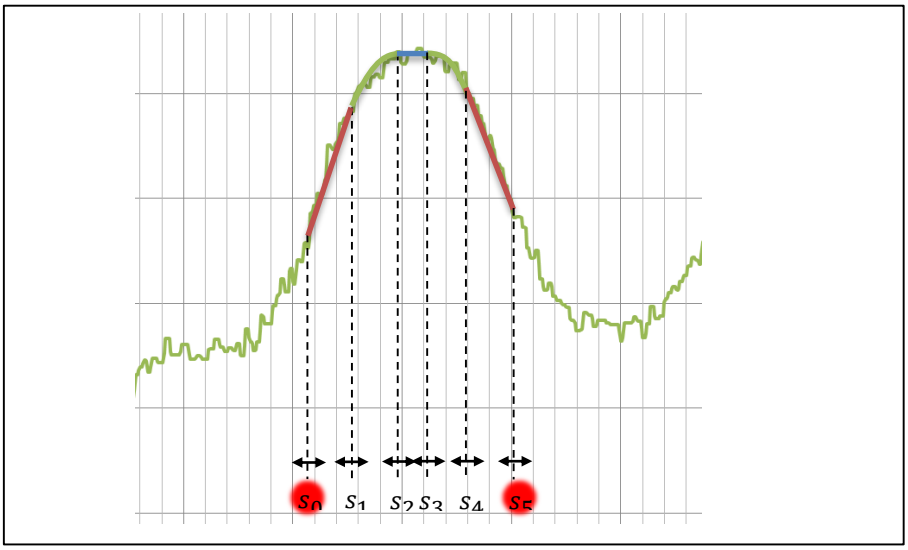

Figure 93. Layout of a broken-back (or reverse) curve.

Continuity of heading and curvature must be satisfied for all the stitching points:

Point s1:

Continuity of heading: $\theta_{C_1} = \theta_{Cl_1}$

$$b_1 \cdot s_1 + c_1 = a_2 \cdot s_1^2 + b_2 \cdot s_1 + c_2 \quad (264)$$

Continuity of curvature: $\theta'_{C_1} = \theta'_{Cl_1}$

$$b_1 = 2a_2 s_1 + b_2 \quad (265)$$

Point s2:

Continuity of heading: $\theta_{Cl_1} = \theta_T$

$$a_2 \cdot s_2^2 + b_2 \cdot s_2 + c_2 = c_3 \tag{266}$$

Continuity of curvature: $\theta'_{Cl_1} = \theta'_T$

$$2 \cdot a_2 \cdot s_2 + b_2 = 0 \tag{267}$$

Point s3:

Continuity of heading: $\theta_T = \theta_{Cl_2}$

$$c_3 = a_4 \cdot s_3^2 + b_4 \cdot s_3 + c_4 \tag{268}$$

Continuity of curvature: $\theta'_T = \theta'_{Cl_2}$

$$0 = 2 \cdot a_4 \cdot s_3 + b_4 \tag{269}$$

Point s4:

Continuity of heading: $\theta_{Cl_2} = \theta_{C_2}$

$$a_4 \cdot s_4^2 + b_4 \cdot s_4 + c_4 = b_5 \cdot s_4 + c_5 \tag{270}$$

Continuity of curvature: $\theta'_{Cl_2} = \theta'_{C_2}$

$$2 \cdot a_4 \cdot s_4 + b_4 = b_5 \tag{271}$$

Finally, the problem to solve is an eight-equation system (Equation 272).

$$\begin{cases} b_1 \cdot s_1 + c_1 = a_2 \cdot s_1^2 + b_2 \cdot s_1 + c_2 \\ b_1 = 2a_2 s_1 + b_2 \\ a_2 \cdot s_2^2 + b_2 \cdot s_2 + c_2 = c_3 \\ 2 \cdot a_2 \cdot s_2 + b_2 = 0 \\ c_3 = a_4 \cdot s_3^2 + b_4 \cdot s_3 + c_4 \\ 0 = 2 \cdot a_4 \cdot s_3 + b_4 \\ a_4 \cdot s_4^2 + b_4 \cdot s_4 + c_4 = b_5 \cdot s_4 + c_5 \\ 2 \cdot a_4 \cdot s_4 + b_4 = b_5 \end{cases} \quad (272)$$

Like in previous cases, the first and last geometric features are known, since they can be obtained from the heading profile. In previous cases those geometric elements were tangents, so the average heading value was very easy to obtain. In this case, those elements are circular curves, which are a bit more difficult, but they can be determined. This is de case for the parameters b_1, c_1, b_5 and c_5.

Thus, there are seven unknown parameters to be solved: a_2, b_2, c_2, c_3, a_4, b_4, c_4. However, $c_3 = \theta_T$, where θ_T is the heading value of the intermediate tangent. It can be easily determined from the heading profile and the stitching points s_2 and s_3. Hence, the unknown parameters to be determined are: a_2, b_2, c_2, a_4, b_4 and c_4.

As one can observe, this problem is clearly different than the previous ones. In this case, the number of unknowns is lower than the constraints, so this problem can only be solved under certain conditions. These conditions can be obtained by adjusting the parameters c_2 and c_4. Two different solutions will appear, depending on the equations used for the procedure. Therefore, the solution only exists when both solutions lead to the same result.

Departing from equations 265 and 267:

$$b_2 = b_1 - 2a_2 s_1 \quad (273)$$

$$b_2 = -2a_2 s_2 \quad (274)$$

Solving the system:

$$b_1 - 2a_2 s_1 = -2a_2 s_2$$

$$2a_2 s_1 - 2a_2 s_2 = b_1$$

$$2a_2(s_1 - s_2) = b_1$$

$$a_2 = \frac{b_1}{2(s_1 - s_2)} \tag{275}$$

$$b_2 = -2a_2 s_2 = \frac{b_1 s_2}{x_2 - s_1} \tag{276}$$

Equations 275 and 276 now only share one unknown parameter (c_2). It is going to be determined from both of them.

Considering Equation 264:

$$b_1 s_1 + c_1 = \frac{b_1 s_1^2}{2(s_1 - s_2)} - \frac{b_1 s_1 s_2}{s_1 - s_2} + c_2$$

$$c_2 = b_1 s_1 + c_1 - \frac{b_1 s_1^2}{2(s_1 - s_2)} + \frac{b_1 s_1 s_2}{s_1 - s_2}$$

$$c_2 = \frac{2b_1 s_1 (s_1 - s_2)}{2(s_1 - s_2)} + \frac{2c_1 (s_1 - s_2)}{2(s_1 - s_2)} - \frac{b_1 s_1^2}{2(s_1 - s_2)} + \frac{2b_1 s_1 s_2}{2(s_1 - s_2)}$$

$$c_2 = \frac{2b_1 s_1 (s_1 - s_2) + 2c_1 (s_1 - s_2) - b_1 s_1^2 + 2b_1 s_1 s_2}{2(s_1 - s_2)}$$

$$c_2 = \frac{2b_1 s_1^2 - 2b_1 s_1 s_2 + 2c_1 s_1 - 2c_1 s_2 - b_1 s_1^2 + 2b_1 s_1 s_2}{2(x_1 - x_2)}$$

$$c_2 = \frac{b_1 s_1^2 + 2c_1 s_1 - 2c_1 s_2}{2(s_1 - s_2)} \tag{277}$$

Considering Equation 268:

$$\frac{b_1 s_2^2}{2(s_1 - s_2)} - \frac{b_1 s_2^2}{s_1 - s_2} + c_2 = c_3$$

$$\frac{b_1 s_2^2}{2(s_1 - s_2)} - \frac{2b_1 s_2^2}{2(s_1 - s_2)} + c_2 = c_3$$

$$c_2 = c_3 + \frac{b_1 s_2^2}{2(s_1 - s_2)} \tag{278}$$

Those c_2 values must be the same. Thus, both expressions can be equaled:

$$\frac{b_1 s_1^2 + 2c_1 s_1 - 2c_1 s_2}{2(s_1 - s_2)} = c_3 + \frac{b_1 s_2^2}{2(s_1 - s_2)}$$

$$\frac{b_1 s_1^2 + 2c_1 s_1 - 2c_1 s_2 - b_1 s_2^2}{2(s_1 - s_2)} = c_3$$

$$\frac{b_1 (s_1^2 - s_2^2)}{2(s_1 - s_2)} + \frac{2c_1 (s_1 - s_2)}{2(s_1 - s_2)} = c_3$$

$$\frac{b_1 (s_1 + s_2)(s_1 - s_2)}{2(s_1 - s_2)} + \frac{2c_1 (s_1 - s_2)}{2(s_1 - s_2)} = c_3$$

$$b_1 \frac{(s_1 + s_2)}{2} + c_1 = c_3$$

$$\frac{(s_1 + s_2)}{2} = \frac{c_3 - c_1}{b_1} \quad (279)$$

Thus, the solution for c_2 only exists if the Equation 279 is satisfied. Let us see which condition is that. If we determine the intersection between the first circular curve and the tangent:

$$\left.\begin{matrix} \theta = b_1 s + c_1 \\ \theta = c_3 \end{matrix}\right\} \rightarrow b_1 s + c_1 = c_3 \rightarrow s = \frac{c_3 - c_1}{b_1} \quad (280)$$

So the second term is the point where the heading of the first circular curve and the intermediate tangent virtually intersect. On the other hand, the first term of Equation (279 indicates the center of the heading of the clothoid. Thus, the additional constraint is that the parabolic curve that represents the heading of the spiral transition must be centered in the virtual intersection of the tangent and the first curve heading expressions.

This procedure can be repeated for the second spiral transition, giving the same constraint. Departing from Equations 269 and 271:

$$b_4 = -2a_4 s_3 \quad (281)$$

$$b_4 = b_5 - 2a_4 s_4 \quad (282)$$

Combining both expressions:

$$-2a_4 s_3 = b_5 - 2a_4 s_4$$

$$a_4 = \frac{b_5}{2(s_4 - s_3)} \tag{283}$$

$$b_4 = -2a_4 s_3 = \frac{b_5 s_3}{s_3 - s_4} \tag{284}$$

Substituting a_4 and b_4 in Equations 268 and 270:

$$c_3 = \frac{b_5 s_3^2}{2(s_4 - s_3)} - \frac{b_5 s_3^2}{s_4 - s_3} + c_4$$

$$c_3 = \frac{b_5 s_3^2}{2(s_4 - s_3)} - \frac{2b_5 s_3^2}{2(s_4 - s_3)} + c_4$$

$$c_4 = c_3 + \frac{b_5 s_3^2}{2(s_4 - s_3)} \tag{285}$$

$$\frac{b_5 s_4^2}{2(s_4 - s_3)} - \frac{b_5 s_3 s_4}{s_4 - s_3} + c_4 = b_5 s_4 + c_5$$

$$c_4 = \frac{2b_5 s_4(s_4 - s_3) + 2c_5(s_4 - s_3) + 2b_5 s_3 s_4 - b_5 s_4^2}{2(s_4 - s_3)}$$

$$c_4 = \frac{2b_5 s_4^2 - 2b_5 s_3 s_4 + 2c_5 s_4 - 2c_5 s_3 + 2b_5 s_3 s_4 - b_5 s_4^2}{2(s_4 - s_3)}$$

$$c_4 = \frac{b_5 s_4^2 + 2c_5 s_4 - 2c_5 s_3}{2(s_4 - s_3)} \tag{286}$$

Both expressions can be combined:

$$c_3 = \frac{b_5 s_4^2 + 2c_5 s_4 - 2c_5 s_3 - b_5 s_3^2}{2(s_4 - s_3)}$$

$$c_3 = \frac{b_5(s_4^2 - s_3^2) + 2c_5(s_4 - s_3)}{2(s_4 - s_3)}$$

$$c_3 = \frac{b_5(s_4^2 - s_3^2)}{2(s_4 - s_3)} + \frac{c_5(s_4 - s_3)}{(s_4 - s_3)}$$

$$c_3 = \frac{b_5(s_4 + s_3)(s_4 - s_3)}{2(s_4 - s_3)} + \frac{c_5(s_4 - s_3)}{(s_4 - s_3)}$$

$$c_3 = b_5\frac{(s_4 + s_3)}{2} + c_5$$

$$\frac{(s_4 + s_3)}{2} = \frac{c_3 - c_5}{b_5} \quad (287)$$

Which is the same constraint that Equation 279, but for the second transition curve.

This is the moment when the number of constraints and unknown parameters are the same, so a unique solution exists for the problem. They are shown in Table 26.

b_1	b_1	(288)
c_1	c_1	(289)
a_2	$\frac{b_1}{2(s_1 - s_2)}$	(290)
b_2	$\frac{b_1 s_2}{s_2 - s_1}$	(291)
c_2	$c_3 + \frac{b_1 s_2^2}{2(s_1 - s_2)}$ or $\frac{b_1 s_1^2 + 2c_1 s_1 - 2c_1 s_2}{2(s_1 - s_2)}$	(292)
c_3	θ_T	(293)
a_4	$\frac{b_5}{2(s_4 - s_3)}$	(294)
b_4	$\frac{b_5 s_3}{s_3 - s_4}$	(295)
c_4	$c_3 + \frac{b_5 s_3^2}{2(s_4 - s_3)}$ or $\frac{b_5 s_4^2 + 2c_5 s_4 - 2c_5 s_3}{2(s_4 - s_3)}$	(296)
b_5	b_5	(297)
c_5	c_5	(298)
Midpoint of Cl_1	Centered in the virtual intersection between C_1 and T	
Midpoint of Cl_2	Centered in the virtual intersection between T and C_2	

Table 26. Parameters for a curve-to-tangent-to-curve transition.

Those new kind of restrictions make it necessary to change the adjustment process, since not all $s_i, i = 1 \dots 4$ values are valid. Therefore, instead of varying the position of the stitching points, it was decided to work with the virtual intersections between both curves and the intermediate tangent. Those points are defined as s_A and s_B, for the first and the second curves, respectively. They are calculated as follows:

$$s_A = \frac{s_1 + s_2}{2} \tag{299}$$

$$s_B = \frac{s_3 + s_4}{2} \tag{300}$$

Considering the length of the spiral transitions L_{Cl_1} and L_{Cl_2}, the following relationships exist between the stitching points and s_A and s_B:

$$s_1 = s_A - \frac{L_{Cl_1}}{2} \tag{301}$$

$$s_2 = s_A + \frac{L_{Cl_1}}{2} \tag{302}$$

$$s_3 = s_B - \frac{L_{Cl_2}}{2} \tag{303}$$

$$s_4 = s_B + \frac{L_{Cl_2}}{2} \tag{304}$$

The sequence of the geometric elements must not be forgot. Thus, the following restrictions still have to be considered:

$$\left.\begin{aligned} s_0 &< s_1 - 1 \\ s_1 &< s_2 - 2 \\ s_2 &< s_3 \\ s_3 &< s_4 - 2 \\ s_4 &< s_5 - 1 \end{aligned}\right\} \tag{305}$$

These restrictions cannot now be satisfied by varying the position of the stitching points, but varying the length of the spiral transitions for each position of s_A and s_B.

The heuristic process to determine the best solution is the following:

1. An initial, seed solution is created by the program. Two candidates of s_A and s_B are proposed. The length of the spiral transitions is set to the minimum (2 m). Calculation of the stitching points and determination of the MSE.

2. Increase of the length of each spiral transition. Determination of the solution and calculation of the MSE. This process is repeated until the spiral transition reaches the adjacent stitching points. The solution that produces the lowest MSE is considered.
3. Alternative variation of s_A and s_B and repetition of the process. This process is repeated until the adjacent stitching points are met.

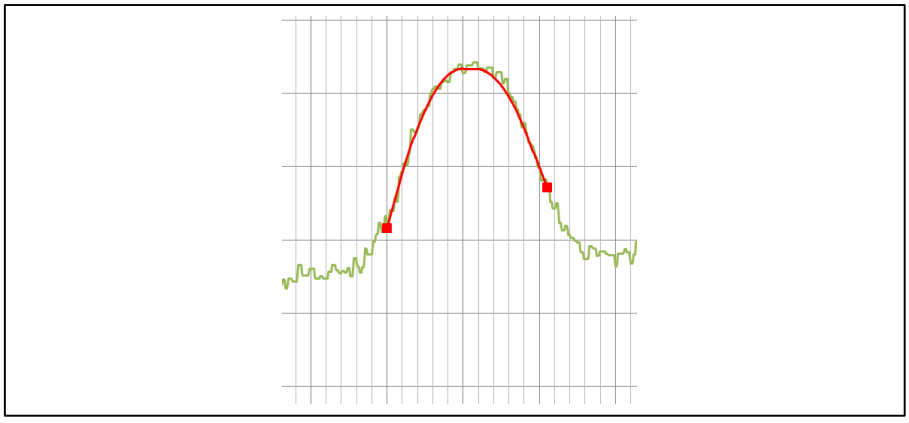

Figure 94. Broken-back final solution.

6.4.2.3.6. Compound curves

This is the case of having two consecutive circular curves, only separated by a spiral transition.

The sequence of geometric elements is so simple:

- Circular curve C_1: $\theta = b_1 s + c_1$
- Clothoid Cl: $\theta = a_2 s^2 + b_2 s + c_2$
- Circular curve C_2: $\theta = b_3 s + c_3$

There are four singular points:

- Initial, user-defined point: s_0
- Stitching point between C_1 y Cl: s_1
- Stitching point between Cl y C_2: s_2
- Final, user-defined point: s_3

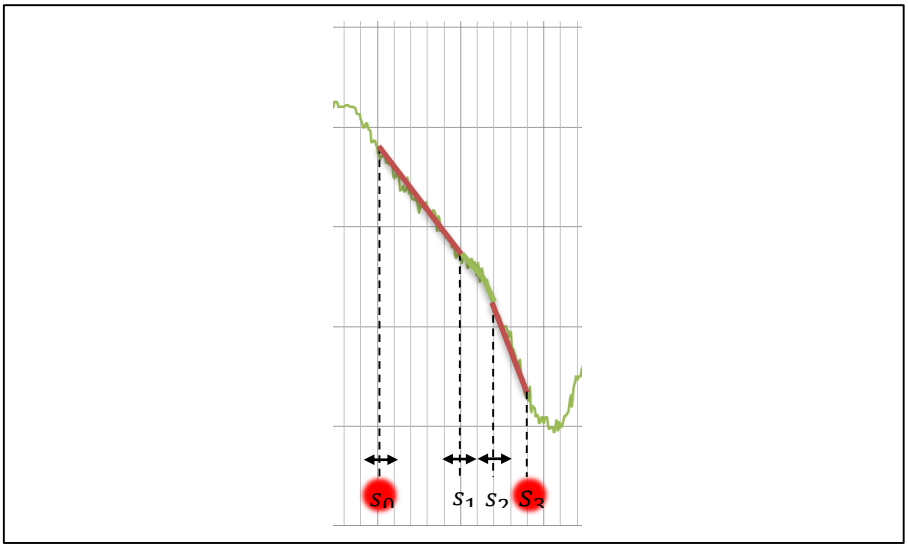

Figure 95. Layout of a compound curve.

The constraints for all the stitching points are continuity on heading and curvature, like in the previous cases. Like in the last case, the parameters of the first and last geometric elements are known: b_1, c_1, b_3 and c_3. Thus, there are only three unknowns (a_2, b_2, c_2) for four constraints:

Point s1:

Continuity of heading: $\theta_{C_1} = \theta_{Cl}$

$$b_1 s_1 + c_1 = a_2 s_1^2 + b_2 s_1 + c_2 \tag{306}$$

Continuity of curvature: $\theta'_{C_1} = \theta'_{Cl}$

$$b_1 = 2a_2 s_1 + b_2 \tag{307}$$

Point s2:

Continuity of heading: $\theta_{Cl} = \theta_{C_2}$

$$a_2 s_2^2 + b_2 s_2 + c_2 = b_3 s_2 + c_3 \tag{308}$$

Continuity of curvature: $\theta'_{Cl} = \theta'_{C_2}$

$$2a_2 s_2 + b_2 = b_3 \tag{309}$$

The equation system results as:

$$\begin{cases} b_1 s_1 + c_1 = a_2 s_1^2 + b_2 s_1 + c_2 \\ b_1 = 2a_2 s_1 + b_2 \\ a_2 s_2^2 + b_2 s_2 + c_2 = b_3 s_2 + c_3 \\ 2a_2 s_2 + b_2 = b_3 \end{cases} \tag{310}$$

From Equations 307 and 309:

$$b_2 = b_1 - 2a_2 s_1 \tag{311}$$
$$b_2 = b_3 - 2a_2 s_2 \tag{312}$$

Equaling both expressions:

$$b_1 - 2a_2 s_1 = b_3 - 2a_2 s_2$$

$$a_2 = \frac{b_3 - b_1}{2(s_2 - s_1)}$$

$$b_2 = b_3 - \frac{s_2(b_3 - b_1)}{(s_2 - s_1)}$$

$$b_2 = \frac{b_3(s_2 - s_1) - s_2(b_3 - b_1)}{(s_2 - s_1)}$$

$$b_2 = \frac{b_3 s_2 - b_3 s_1 - b_3 s_2 + b_1 s_2}{(s_2 - s_1)}$$

$$b_2 = \frac{b_1 s_2 - b_3 s_1}{(s_2 - s_1)} \tag{313}$$

There is only one unknown left and two additional constraints to fit. Hence, c_2 can be obtained from two Equations:

From Equation 306:

$$b_1 s_1 + c_1 = \frac{b_3 - b_1}{2(s_2 - s_1)} s_1^2 + \frac{b_1 s_2 - b_3 s_1}{(s_2 - s_1)} s_1 + c_2$$

$$\frac{2b_1 s_1 (s_2 - s_1) + 2c_1 (s_2 - s_1)}{2(s_2 - s_1)} = \frac{b_3 s_1^2 - b_1 s_1^2}{2(s_2 - s_1)} + \frac{b_1 s_1 s_2 - b_3 s_1^2}{(s_2 - s_1)} + c_2$$

$$c_2 = \frac{2b_1 s_1 s_2 - 2b_1 s_1^2 + 2c_1 s_2 - 2c_1 s_1 - b_3 s_1^2 + b_1 s_1^2 - 2b_1 s_1 s_2 + 2b_3 s_1^2}{2(s_2 - s_1)}$$

$$c_2 = \frac{-b_1 s_1^2 + 2c_1 s_2 - 2c_1 s_1 + b_3 s_1^2}{2(s_2 - s_1)} \quad (314)$$

Considering Equation 308:

$$\frac{b_3 s_2^2 - b_1 s_2^2}{2(s_2 - s_1)} + \frac{2b_1 s_2^2 - 2b_3 s_1 s_2}{2(s_2 - s_1)} + c_2 = b_3 s_2 + c_3$$

$$c_2 = \frac{2b_3 s_2^2 - 2b_3 s_1 s_2 + 2c_3 s_2 - 2c_3 s_1 - b_3 s_2^2 + b_1 s_2^2 - 2b_1 s_2^2 + 2b_3 s_1 s_2}{2(s_2 - s_1)}$$

$$c_2 = \frac{b_3 s_2^2 + 2c_3 s_2 - 2c_3 s_1 - b_1 s_2^2}{2(s_2 - s_1)} \quad (315)$$

The additional constraint comes from equaling both expressions:

$$\frac{b_3 s_2^2 + 2c_3 s_2 - 2c_3 s_1 - b_1 s_2^2}{2(s_2 - s_1)} = \frac{-b_1 s_1^2 + 2c_1 s_2 - 2c_1 s_1 + b_3 s_1^2}{2(s_2 - s_1)}$$

$$b_3 s_2^2 + 2c_3 s_2 - 2c_3 s_1 - b_1 s_2^2 = -b_1 s_1^2 + 2c_1 s_2 - 2c_1 s_1 + b_3 s_1^2$$

$$b_3 s_2^2 - b_1 s_2^2 + b_1 s_1^2 - b_3 s_1^2 = 2c_1 s_2 - 2c_1 s_1 - 2c_3 s_2 + 2c_3 s_1$$

$$(b_1 - b_3)(s_1^2 - s_2^2) = 2(s_1 - s_2)(c_3 - c_1)$$

$$(b_1 - b_3)(s_1 + s_2)(s_1 - s_2) = 2(s_1 - s_2)(c_3 - c_1)$$

$$\frac{(s_1 + s_2)}{2} = \frac{c_3 - c_1}{b_1 - b_3} \quad (316)$$

This condition is similar than for the case of reverse and broken back curves without tangents. The virtual intersection of the heading expressions for both curves must be in the mid transition curve. The first term of Equation 316 is the midpoint of the heading of the transition curve, while the second term is that virtual intersection, as shown in Equation 317:

$$\left.\begin{matrix}\theta = b_1 s + c_1 \\ \theta = b_3 s + c_3\end{matrix}\right\} \rightarrow b_1 s + c_1 = b_3 s + c_3 \rightarrow s = \frac{c_3 - c_1}{b_1 - b_3} \quad (317)$$

Finally, Table 27 shows how all the parameters are calculated as a function of the already known variables.

b_1	b_1	(318)
c_1	c_1	(319)
a_2	$\frac{c_3 - b_1}{2(s_2 - s_1)}$	(320)
b_2	$\frac{b_1 s_2 - c_3 s_1}{(s_2 - s_1)}$	(321)
c_2	$\frac{-b_1 s_1^2 + 2c_1 s_2 - 2c_1 s_1 + b_3 s_1^2}{2(s_2 - s_1)}$ or $\frac{b_3 s_2^2 + 2c_3 s_2 - 2c_3 s_1 - b_1 s_2^2}{2(s_2 - s_1)}$	(322)
b_3	b_3	(323)
c_3	c_3	(324)
Midpoint of clothoid Cl	Centered in the intersection of C_1 and C_2	(325)

Table 27. Parameters of a circle-spiral-circle transition.

The heuristic process to determine the best location of the stitching points is performed in a similar way than for previous adjustment problems. In this case, the station of the midpoint of the spiral transition is s_M (Equation 326). The length of the spiral transition is L_{Cl}.

$$s_M = \frac{s_1 + s_2}{2} \quad (326)$$

The stitching points are calculated considering s_M and the length of the spiral transition:

$$s_1 = s_M - \frac{L_{Cl}}{2} \tag{327}$$

$$s_2 = s_M + \frac{L_{Cl}}{2} \tag{328}$$

While calculating the solution, the following restrictions must be satisfied:

$$\left.\begin{matrix} s_0 < s_1 - 1 \\ s_1 < s_2 - 2 \\ s_2 < s_3 - 1 \end{matrix}\right\} \tag{329}$$

The following heuristic process was proposed:

1. The program proposes a seed solution based on establishing the midpoint between s_0 and s_3 as s_M. The length of the spiral transition is set to the minimum (2 m). The stitching points s_1 and s_2 are calculated and the geometric solution is determined. The MSE is calculated.
2. The program increases the length of the spiral transition and new solutions are determined. The MSE is calculated for each one.
3. This process is repeated until the spiral transition arrives to the end of the circular curves. Then s_M is changed towards the left and right sides, repeating the previous process.
4. The last process is repeated for all possibilities. The solution with the lowest MSE is left as the final one.

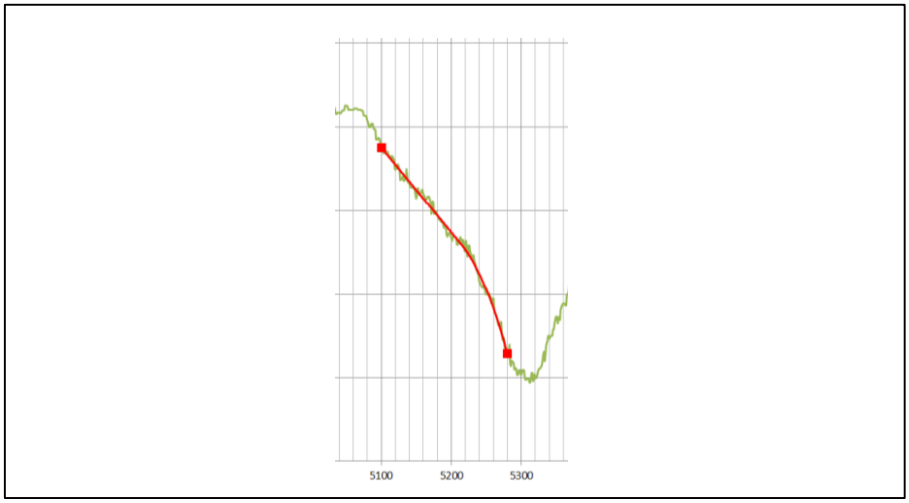

Figure 96. Final solution of the compound curve adjustment.

6.4.2.3.7. Tangent-to-curve transition

This is a particular case of the previous one. In this case, the first curve becomes a tangent, so $b_1 = 0$ and $c_1 = \theta_T$. Thus, we are not going to solve this case but the last expressions are particularized (Table 28).

c_1	θ_T	(330)
a_2	$\frac{c_3}{2(s_2 - s_1)}$	(331)
b_2	$\frac{-c_3 s_1}{(s_2 - s_1)}$	(332)
c_2	$\frac{2\theta_T s_2 - 2\theta_T s_1 + b_3 s_1^2}{2(s_2 - s_1)}$ or $\frac{b_3 s_2^2 + 2c_3 s_2 - 2c_3 s_1}{2(s_2 - s_1)}$	(333)
b_3	b_3	(334)
c_3	c_3	(335)
Midpoint of clothoid Cl	Centered in the intersection of T and C	(336)

Table 28. Parameters of a tangent-to-curve transition.

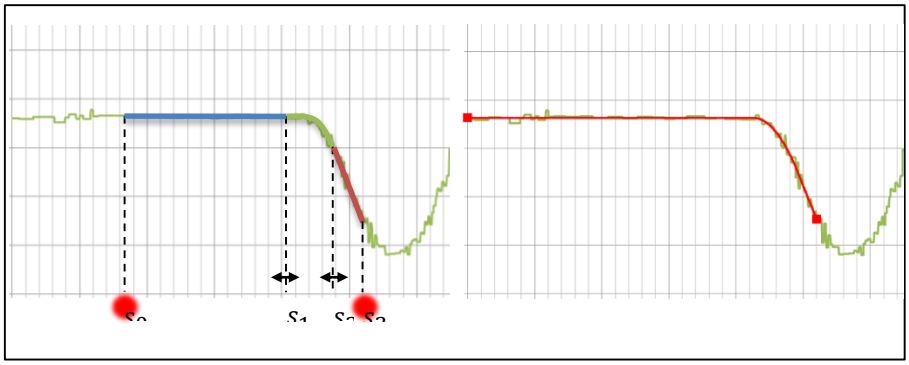

Figure 97. Tangent-to-curve layout and final solution.

6.4.2.3.8. Curve-to-tangent transition

Similar case than the previous one. In this case, $b_3 = 0$ and $c_3 = \theta_T$. Estimations of the parameters are shown in Table 29.

b_1	b_1	(337)
c_1	c_1	(338)
a_2	$\frac{\theta_T - b_1}{2(s_2 - s_1)}$	(339)
b_2	$\frac{b_1 s_2 - \theta_T s_1}{(s_2 - s_1)}$	(340)
c_2	$\frac{-b_1 s_1^2 + 2c_1 s_2 - 2c_1 s_1}{2(s_2 - s_1)}$ or $\frac{2\theta_T s_2 - 2\theta_T s_1 - b_1 s_2^2}{2(s_2 - s_1)}$	(341)
c_3	θ_T	(342)
Midpoint of clothoid Cl	Centered in the intersection of C_1 and C_2	(343)

Table 29. Parameters of a curve-to-tangent transition.

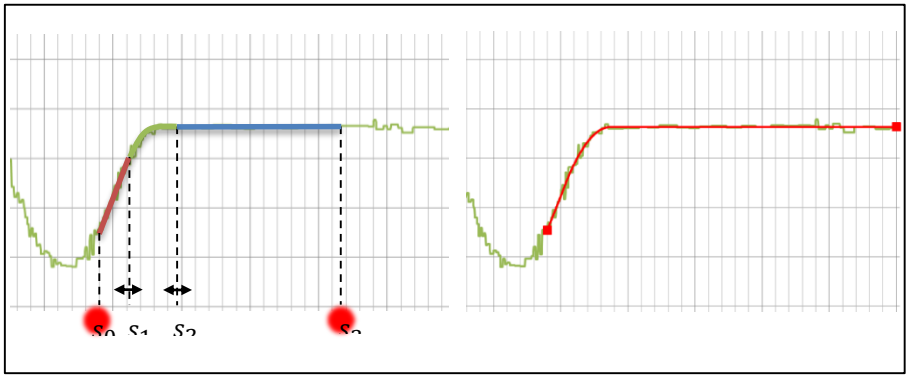

Figure 98. Curve-to-tangent layout and final solution.

6.4.2.3.9. Tangent adjustment

The problem of fitting an entire road to a horizontal alignment has been decomposed into single pieces. This makes it easier to achieve a solution, thus reducing the computational time. However, all these pieces need to be merged into a single solution to the entire road alignment.

When a sequence of two isolated curves are separately fitted, the intermediate is partially fitted twice (one for each partial solution). Both heading values must be very similar and close to the actual solution. However, a single value must be reached.

An algorithm was developed in order to achieve a single solution for all these kind of tangents. At this point, there is the advantage of knowing the exact points where the tangent starts and ends, since it was previously fitted. Hence, the solution is simply by calculating the average heading value considering all points between those.

The final solution presents a single value of heading for the whole tangent, a bit different than those previously calibrated. This is also why the individual problems must be fitted considering such a high portion of tangents: the final, merged solutions will be more accurate, too.

Figure 99 shows an example of how this process works.

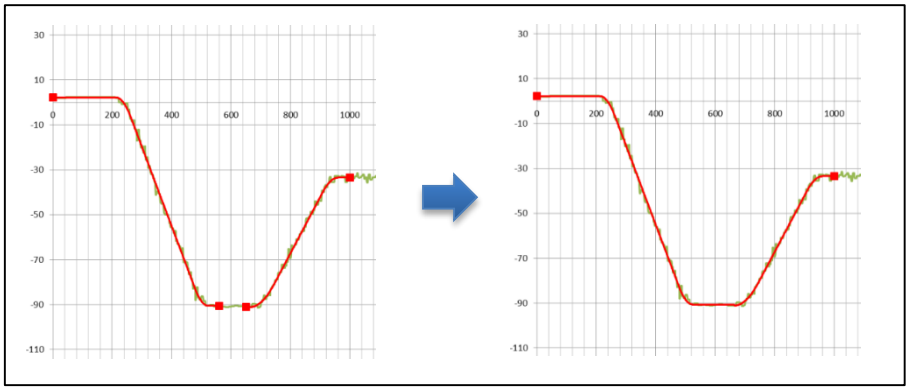

Figure 99. Merging of solutions through a tangent section.

6.4.2.3.10. Circular curve adjustment

This case is similar to the previous one. Instead of having a tangent, in this case the intermediate geometric element is a curve. Like in the previous case, the stitching, frontier points to the adjacent geometric features are known. Thus, it is so easy to determine the final solution for the circular curve, like in the previous case. Figure 100 shows one example.

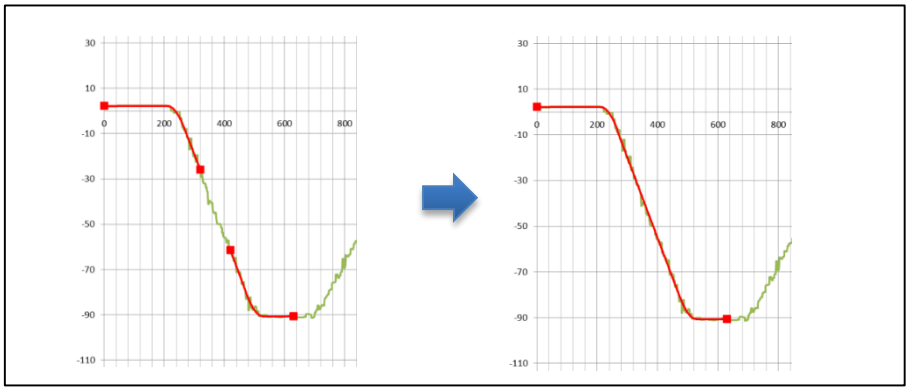

Figure 100. Merging of solutions through a curve section.

6.4.3. Determination of the horizontal alignment

Once the heading profile is completely fitted, the horizontal alignment can be determined, based on the properties of the different parameters and their relationship to the geometric characteristics. Figure 101 and Table 30 show the intermediate and final results of the adjustment of a road segment.

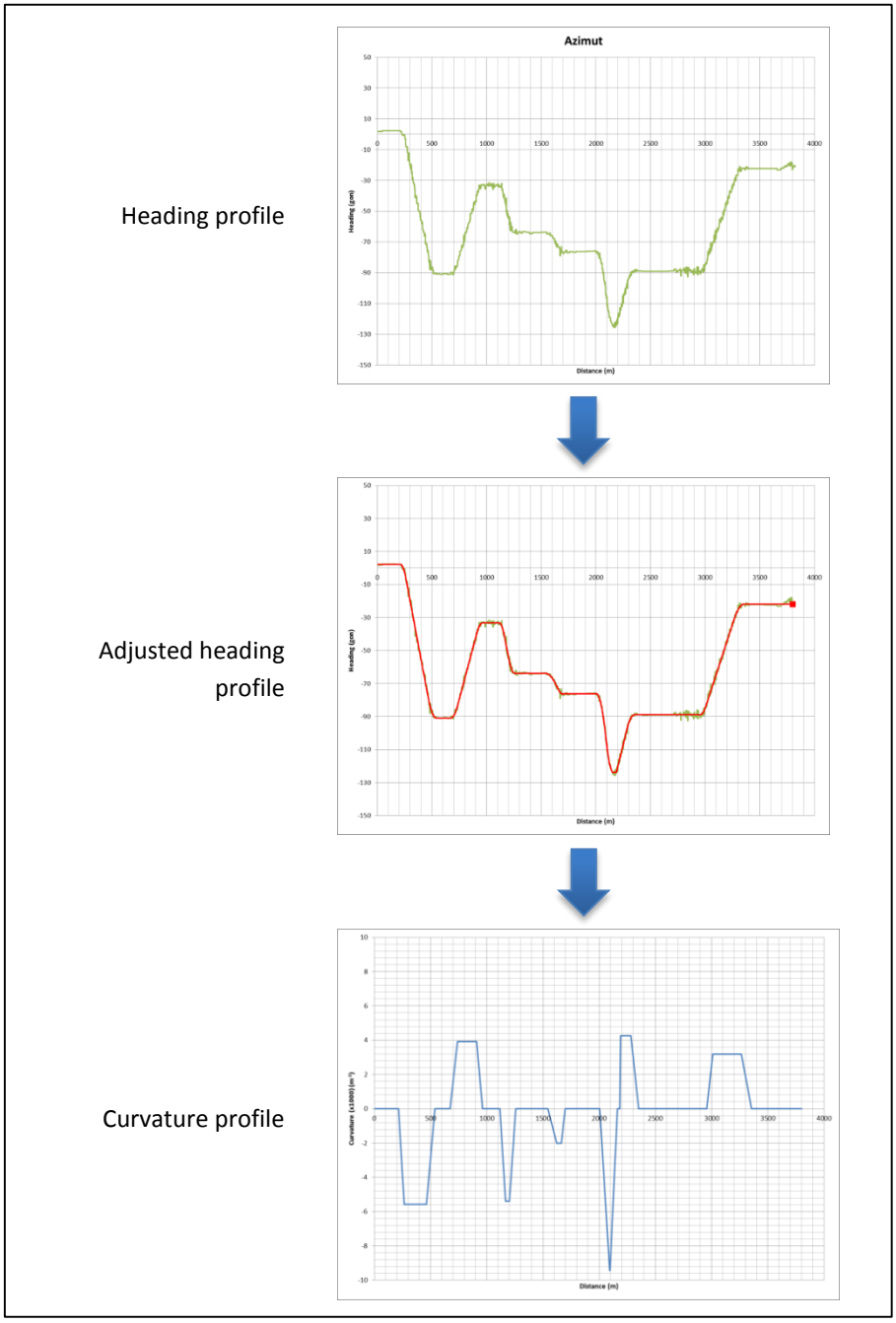

Figure 101. Curvature extraction from an initial heading profile.

Element	St_i (m)	St_f (m)	θ_i (gon)	θ_f (gon)	R | A (m)
Tangent	0	214	2.22	2.22	
Clothoid	214	265	2.21	-6.99	97
Circular curve	265	462	-7.35	-76.85	-180
Clothoid	462	540	-77.20	-90.85	119
Tangent	540	675	-90.77	-90.77	
Clothoid	675	738	-90.71	-82.74	128
Circular curve	738	910	-82.49	-39.87	255
Clothoid	910	962	-39.63	-33.27	116
Tangent	962	1116	-33.23	-33.23	
Clothoid	1116	1166	-33.16	-41.89	97
Circular curve	1166	1201	-42.24	-53.89	-186
Clothoid	1201	1257	-54.23	-63.66	103
Tangent	1257	1545	-63.79	-63.79	
Clothoid	1545	1622	-63.92	-68.93	197
Circular curve	1622	1662	-69.06	-74.07	-495
Clothoid	1662	1697	-74.20	-76.38	134
Tangent	1697	2006	-76.29	-76.29	
Clothoid	2006	2092	-76.12	-102.23	96
Circular curve	2092	2095	-102.83	-104.03	-106
Clothoid	2095	2161	-104.63	-123.85	84
Tangent	2161	2185	-123.85	-123.85	
Clothoid	2185	2192	-123.83	-122.90	41
Circular curve	2192	2282	-122.63	-98.49	235
Clothoid	2282	2350	-98.22	-88.88	129
Tangent	2350	2956	-88.87	-88.87	
Clothoid	2956	3009	-88.85	-83.37	130
Circular curve	3009	3265	-83.16	-31.26	313
Clothoid	3265	3357	-31.05	-21.89	170
Tangent	3357	3801	-21.89	-21.89	

Table 30. Example of horizontal alignment data.

6.4.4. Genetic Algorithms to improve the final solution

The previous methodology provides a very accurate solution for all lengths, parameters and radii of an existing alignment. Therefore, its results can be used for research purposes or to generate an operating speed profile.

However, nothing has been indicated about the validity of these results for road redesign. Although all previous parameters are very similar to the actual ones, all of them might present slight variations. All these errors are cumulative, so the first part of a certain road is probably very similar to the actual one, but some kilometers later it will differ several meters.

In order to address this issue, we must take a further step. We need to compare the recreated and the existing alignment in terms of (x, y) coordinates. The enhancement of the original solution can be performed through a Genetic Algorithm (GA) approach.

The hypothesis is that curves and radii are well fitted by the heading algorithm. Thus, we can state that the difference between the actual road and the recreated one is due to small differences in lengths of the different elements. Figure 102 shows the adjustment to a certain road. We can see how the algorithm has very well detected the slope of the heading that represent the horizontal curves. Thus, we can assume that the radii are well calculated.

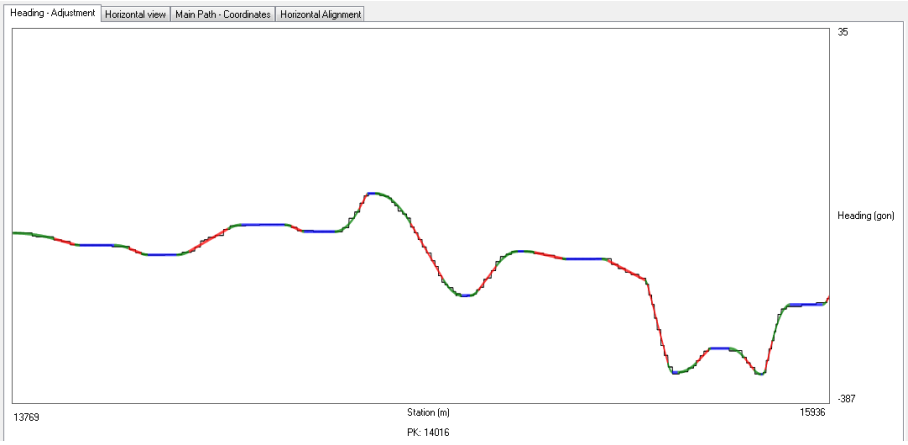

Figure 102. Heading adjustment to a certain road.

As a result, the genetic algorithm will be mainly focused on changing the lengths of the different elements. However, there is a slight chance to change the radius of the horizontal curves. The user can control all these parameters. The program always keeps continuity in curvature and heading between all elements, so after each mutation the adjacent elements are also recalculated.

The program works in a simple way, since it has demonstrated that provides a good solution to the problem. The steps are the following:

1. Selection of two consecutive tangents and their intermediate elements.
2. Mutation of the lengths of the intermediate elements and the tangents. The total length of the elements is maintained. The mutation probability is established as 70%, but it can be controlled by the user. The tangent function is used for the mutation.
3. Mutation of the radius of the intermediate circular curves. This probability is quite lower than the one for the lengths (10%), but it gives a chance to the radii to change. It is used a tangent function again.
4. Change of the parameters of the adjacent transition curves to readapt to the new situation and keep continuity in heading and curvature.
5. The new solution is depicted at a constant station distance of 1 m.
6. Comparison of the solution to the actual road. Calculation of the error.
7. If the mutated solution provides a lower error than the original one, this solution is established as the optimum and the process starts again.
8. When the original function mutes 200 times with no optimum solution, the process is repeated from Step 1 with the next sequence of tangents.
9. The algorithm continues until all the horizontal alignment has been adjusted.

The error function is calculated by means of Equation (344.

$$E = \sum_{s_0}^{s_f} \sqrt{\left(x_s - x_{a_s}\right)^2 + \left(y_s - y_{a_s}\right)^2} \tag{344}$$

Where:

E: Error of the solution.
s: station (1 m interval), ranging from the initial station (s_0) and the final station (s_f).
(x_s, y_s): Coordinates of the recreated solution at station s.
(x_{s_a}, y_{s_a}): Coordinates of the actual road at station s.

It is worth to indicate that the previous function considers all the magnitude of the error, i.e., including both longitudinal and transversal errors. It would be better to only consider the transversal error, regardless of the station. However, this

calculation takes too much time for current processors and is not recommended. Nevertheless, the error calculation algorithm provides a very good final solution.

6.5. Determination of the operating speed profiles

The consistency parameter is founded on the examination of the operating speed profiles of road segments. Thus, it is necessary to accurately obtain them. For this, it is necessary a horizontal alignment and some operating speed models. The horizontal alignment can be determined thanks to the procedure previously presented. The operating speed models were those developed for the Valencian region of Spain.

A computer program was developed in order to create the operating speed profiles for each road section. Two operating speed profiles are created: one for each direction of travel. This program only requires a horizontal alignment and a selection of the operating speed models to apply.

The computer program determines the operating speed profiles in three steps:

1. Calculation of the operating speed for tangents and circular curves. The operating speed is maintained constant along the whole geometric element.
2. Elimination of the anomalous operating speeds. One example is a tangent with an operating speed lower than those of the adjacent curves. In this case, the operating speed of the tangent is moved to the minimum value of the adjacent curves.
3. The operating speed profiles are determined by means of the acceleration and deceleration rates. As a hypothesis, the operating speed that imposes the speed control is kept without any variation.

Figure 103 shows one example of operating speed profile determined with the program. The blue lines represent the original operating speed for tangents, and the red ones for curves. The final operating speed is depicted in green.

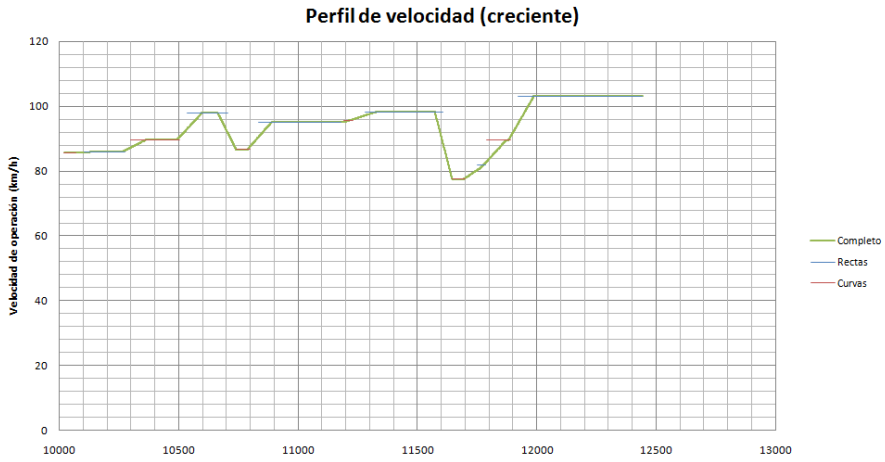

Figure 103. Example of operating speed profile (forward direction).

6.6. Road segmentation

All the selected road sections present different characteristics according to geometry, traffic, environment, and boundary conditions. Hence, they are heterogeneous road sections and they should divided into different homogeneous road segments.

The division was performed according to three different criteria:

- Major junctions.
- Geometry.
- Operation.

6.6.1. Major junctions

Homogeneous road segments must not contain major intersections or driveways. This is because major junctions:

- Normally imply an important change of traffic volume.
- Dramatically changes drivers' ad hoc expectations.
- The operating speed is affected.
- Accidents tend to concentrate at intersections, hence biasing crash rates.

Therefore, major junctions were defined as criteria for establishing road homogeneous segments.

6.6.2. Geometry

Additionally, a road segment without major junctions may present a heterogeneous geometry. These variations should be also detected as a road segment division criterion. The German methodology was suggested. The geometry of all road segments has to be determined, in order to depict their accumulated absolute deflection angle profile. Some geometric homogeneous segments can be therefore determined. A minimum road segment length of 2000 m will be established, according to the German methodology.

6.6.3. Operation

An additional road segmentation criteria was developed in this case. Homogeneous road segments must somehow present similar characteristics according to drivers' ad hoc expectations.

Drivers perform according to road geometry and road conditions, developing a certain operating speed. Thus, the operating speed is the response to a certain stimuli. Thus, if we examine the operating speeds achieved for a certain distance along a road segment, it will somehow reflect driver's ad hoc expectations.

A new parameter, called inertial operating speed, was introduced. It reflects this phenomenon. It is calculated as the average operating speed along the last 1000 m for every station. Obviously, there are two inertial operating speed profiles, one for each direction of travel. Figure 104 represents this.

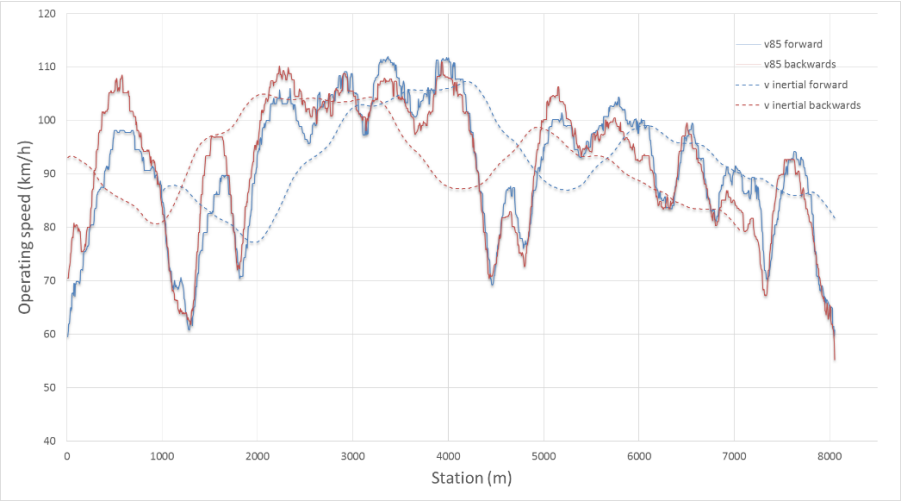

Figure 104. Operating and inertial operating speed profiles. Both directions.

The inertial operating speed indicates the expectations of drivers for each station, based on the operating speed recently developed. As it can be seen in Figure 104, the inertial operating speed is hardly influenced by local geometric features. It presents global ascending, descending or level trends, which can be associated to drivers' behavior. Thus, a change of this behavior can be interpreted as a change of the road homogeneous segment.

The local minimums and maximums of the inertial operating speed profile can be used for detecting where the drivers' expectations change. Thus, those points will be considered for dividing the original road section. Moreover, several of those points coincide with the division points created by the German methodology for determining homogeneous road segments. This is because the operating speed is a response to road geometry, so geometric changes normally imply operational changes.

The inertial operating speed profile is also influenced because of local inconsistencies. They may produce local minimums that are the result of the sudden deceleration of drivers, but not because of a change on their global behavior. Hence, it is needed to remove the local inconsistencies first.

Inconsistencies are identified here as a large difference between the drivers' expectations (inertial operating speed) and the road behavior (operating speed). Hence, the difference between the inertial operating speed and the operating speed

itself is a good indicator. It is known as inertial operating speed difference. The inertial operating speed difference profile will let us know where inconsistencies are located at. Figure 105 shows some local inconsistencies of the same road section.

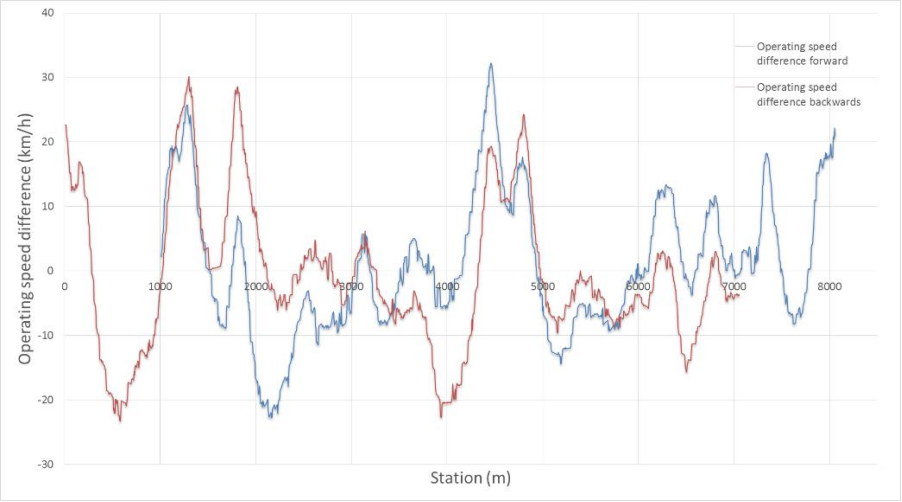

Figure 105. Inconsistencies in the inertial – operating speed profile.

It is also worth to point out that this criteria (as well as major junction criteria) can generate road segments shorter than 2000 m. This threshold was only established for the German procedure.

6.6.4. Determination of the homogeneous road segments

The road sections selected for this study will be divided into homogeneous segments, according to the three criteria presented. If some divisions coming from different criteria are in a close area, the following order prevails:

1. Major junctions.
2. Geometry.
3. Operational.

In addition, there are two types of road segments according to the constraining conditions at their initial and final points. A road segment can be defined as constrained when it starts and/or ends in an intersection, interchange, roundabout or urban zone. On the contrary, a road segment is free (or non-constrained) when both the initial and final points do not satisfy this condition.

The purpose of separating those kind of road segments is the difference of drivers at acquiring the expectations. Drivers clearly know when a constrained road segment starts, but this is not true for free road segments. Therefore, the process how drivers acquire *ad hoc* expectations clearly differs depending on the constraining conditions.

6.7. Calibration of the consistency parameter

The consistency parameter will be determined by examining its relationship to road crashes. It will be by means of a safety performance function. Only accidents with victims will be considered, as stated above. In order to reduce the variability of road crashes, the accidents of ten years will be considered. Equation 345 shows the safety performance function expression, according to Oh et al. (2003):

$$Y_{i,10} = e^{\beta_0} \cdot L^{\beta_1} \cdot AADT^{\beta_2} \cdot e^{\beta_3 \cdot C} \quad (345)$$

Where:

$Y_{i,10}$: Accidents with victims of the road segment in 10 years.
β_i: Regression coefficients.
L: Length of the road segment (km).
$AADT$: Average Annual Daily Traffic (vpd).
C: Global consistency index.

Road segment length and AADT are considered as exposure parameters. A Negative Binomial distribution is assumed, since it is a good solution to model over dispersed, count data.

Exposure parameters are introduced as elasticity terms. This is because of the better interpretation of the results. Hence, it will be possible to determine how the crash rates are affected depending on the traffic volume and the road segment length. In case the road length has no influence on crash rates, the β_1 coefficient will be automatically set to 1.

In addition, several trials will be performed depending on the type of road segment, i.e., constrained or not, or altogether. Therefore, a better knowledge of how these conditions affect drivers' behavior will be achieved.

The consistency parameter will be formed by means of different operating speed related indicators. Some of them are referred to entire operating speed profile, while some others are to local decelerations or speed reductions.

The first indicator considered was the average operating speed ($\bar{v}_{85}$, km/h). This is a good estimator of the road functional classification. This was also considered for determining some of the additional indicators:

- $\sigma_{v_{85}}$ (km/h). Operating speed dispersion of the road. It is calculated considering both speed profiles of the entire segment. It does not consider the isolated geometric elements, but discretizing the operating speed profile in segments of 1 m length.
- R_a (m/s). Area enclosed by the operating speed profile and the average operating speed. It is finally divided by the road segment length. This is a different way of calculating the operating speed dispersion.
- $E_{a,j}$ (m/s). Area enclosed by the operating speed profile and $\bar{v}_{85} \pm j$ km/h. It also measures the operating speed dispersion, but it is more sensitive to extreme behaviors. It was calculated considering $j = 10$ and $j = 20$ km/h.
- L_j (%). Quotient between the total length of the road segment where the operating speed is higher than j km/h more than the average operating speed and its total length. It is a measure that tries to determine how the dispersion behaves. It was also calculated considering $j = 10$ and $j = 20$ kph.

Figure 106 shows all those indicators.

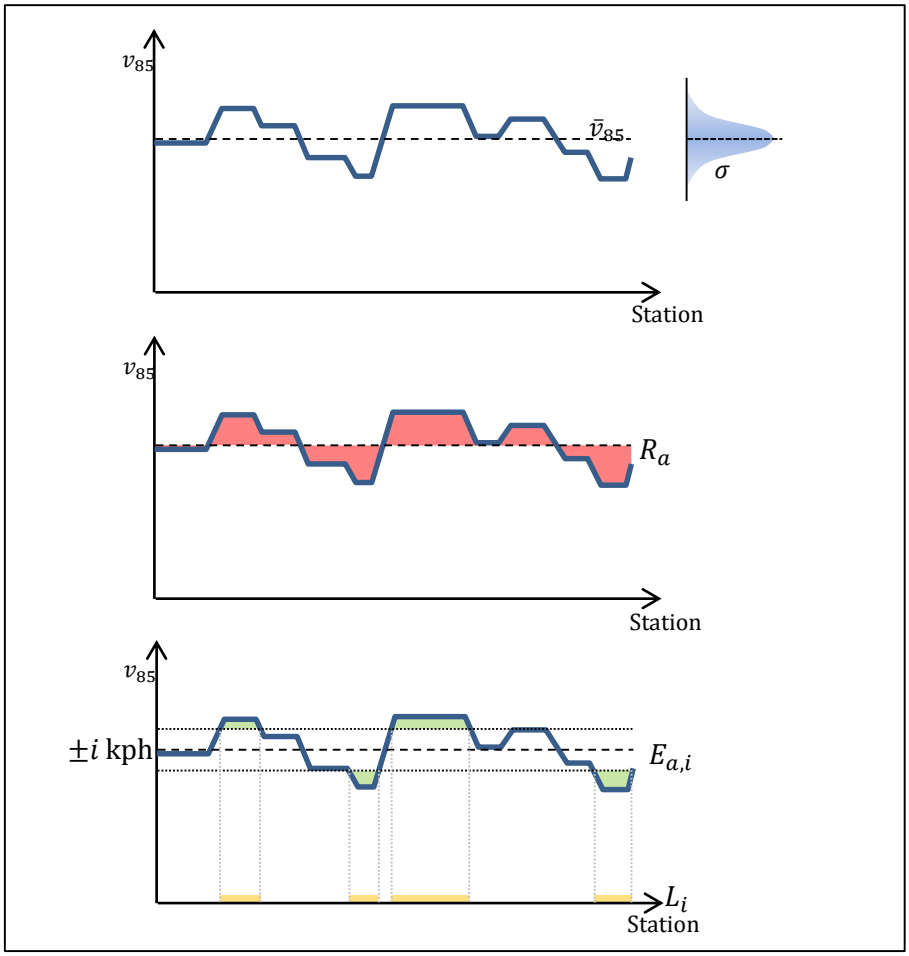

Figure 106. Global operating speed indicators. "i" is either 10 or 20 kph.

Besides examining the global speed behavior of the operating speed profiles, some other parameters describing local decelerations were obtained. Three different parameters can describe speed reduction: speed reduction *per se* (Δv_{85}, km/h), deceleration length (l, m) and deceleration rate (d_{85}, m/s^2). The last one can be derived from the former two as:

$$d_{85} = \frac{(v_{max}^2 - v_{min}^2)}{2 \cdot l} \cdot \frac{1}{3.6^2} \quad \textbf{(346)}$$

Where:

v_{max}: Operating speed before the deceleration (km/h).
v_{min}: Operating speed after the deceleration (km/h).
l: length of the speed transition (m).

Figure 107 shows all the basic parameters for the analysis of speed reductions.

All operating speed profiles were also examined looking for local decelerations. The following parameters were determined for each road segment:

- Average speed reduction ($\overline{\Delta v_{85}}$) (km/h).
- Average speed reduction dispersion ($\sigma_{\Delta v_{85}}$) (km/h).
- Average length used for speed reductions ($\bar{L}_{\Delta v_{85}}$) (m).
- Average deceleration rate ($\overline{d_{85}}$) (m/s^2).
- Deceleration rate dispersion ($\sigma_{d_{85}}$) (m/s^2).
- Number of speed reductions (N).
- Deceleration length ratio (L_d) (m). It is the ratio between the total segment length under deceleration conditions and the total length of the road segment.

Not all decelerations were considered. The operating speed profiles sometimes produce operating speed reductions of minimum values, which are negligible. In fact, they are lower than the accuracy of the operating speed models used for horizontal curves and tangents. Hence, different analysis will be performed in order to determine the minimum speed reduction threshold.

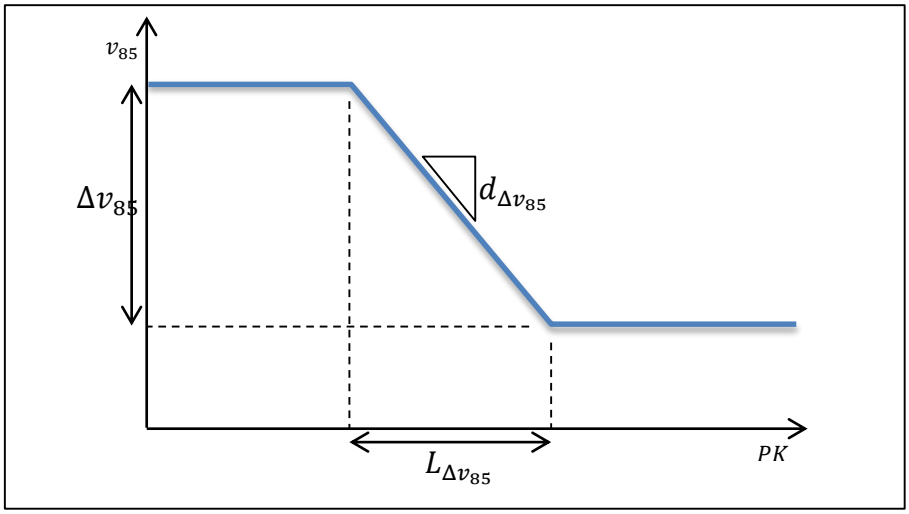

Figure 107. Local operating speed indicators.

6.8. Computer application

A computer application was developed, including all the possibilities reflected in this section. This was programmed in Visual Basic for Applications (VBA), embedded into Microsoft Office Excel 2007-2013. Several spreadsheets were used for storing and managing all data.

This application allows:

- GPS data extraction. Determination of the individual operating speed and individual heading.
- Merging of trajectories in order to determine the operating behavior. Management of all the individual trajectories, as well as their portions.
- Google Earth plotting of the merged trajectory.
- Analysis of the local curvature of the individual trajectories.
- Recreation of the geometry, according to the heading methodology previously presented.
- Determination of the horizontal alignment of a road segment.
- Construction of operating speed profiles from GPS data.
- Construction of operating speed profiles from several models.
- Determination of the altitude profile of road segments, based on GPS data collection.

The main form allows the user to access the different options. It consists on several tabs in the left side, showing different panes depending on the option selected:

- File. Main options like load, reload, save, export to Google Earth and close.
- Data import. It allows the user to import the main data, considering different types of coordinates.
- Trajectory analysis. Analysis and creation of individual trajectories. It allows the user to select which individual trajectories are going to be considered in the merged trajectory and/or the operating speed profile.
- Average trajectory. With this pane, the user will be able to create the merged trajectory, considering different options.
- Local curvature. Analysis of the local curvature. There are several options of cadence, gradient, etc.
- Horizontal layout. Tools for recreating the geometry and developing the horizontal alignment.
- Operating speed profiles. Tools for determining the operating speed profiles from actual drivers, and developing some others based on operating speed models.
- Analysis of results. Allows the user to extract some operational parameters to use in further research.
- Consistency. Allows to assess the consistency of the road segment, according to some models.

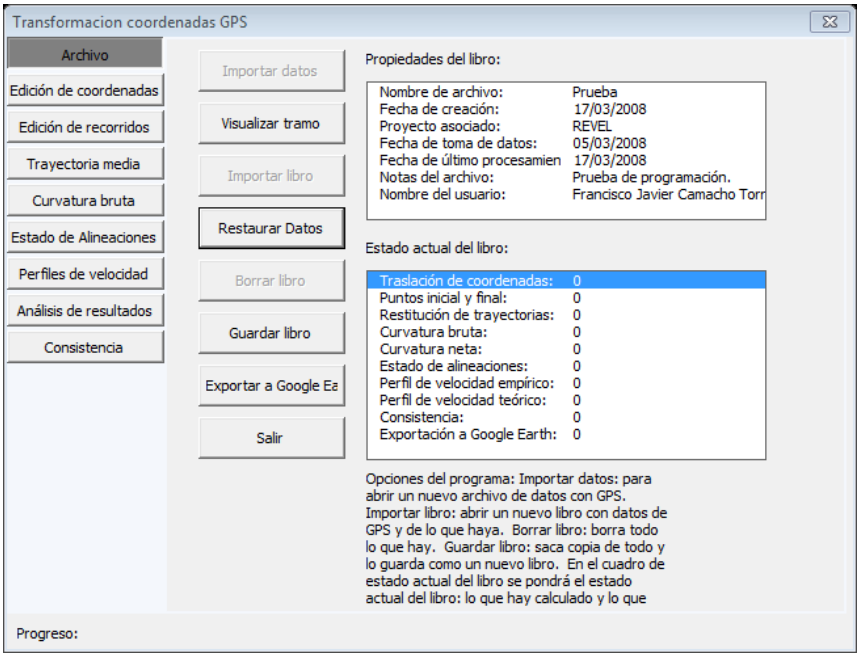

Figure 108. Main form of the computer application.

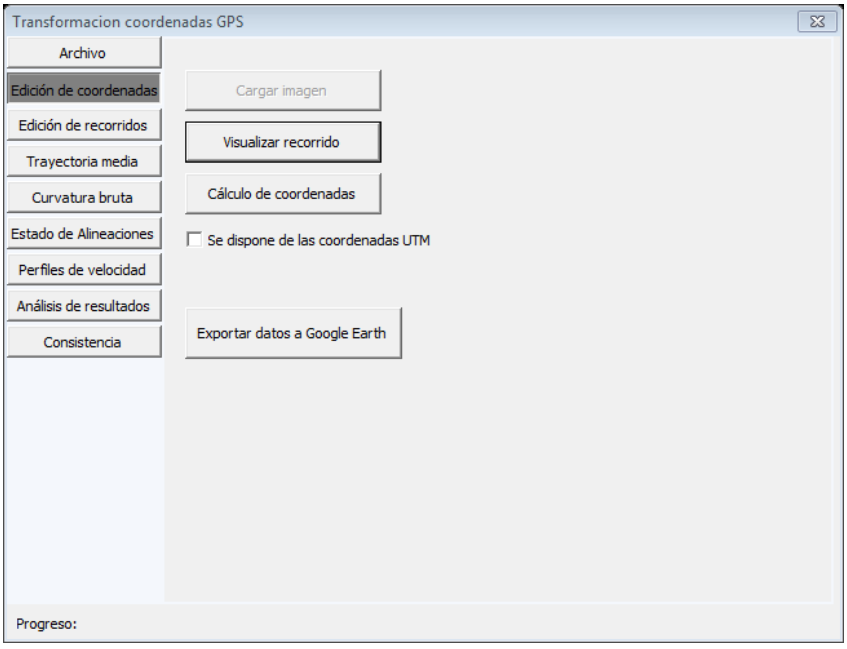

Figure 109. Form for coordinate edition.

Figure 110 shows the pane to edit individual trajectories. When considering several trajectories, the user might not want to use some of them. This allows the user to take them out from the analysis. There are several options:

- Establish boundary points. The user indicates to the program the approximate beginning and end of the road segment to be analyzed.
- Check boundary points. The program will show the user the tentative boundary points. The user might want to remove some of them, if some points are more times than needed. Otherwise, an error will occur.
- Determine individual trajectories. The program establishes the accurate initial and final points of all individual trajectories. This process is needed for merging all of them.
- Check individual trajectories. The user can analyze the path and speed profile for all trajectories. They might want to remove some of them, due to a bad performance of the road users. This tool is for this.

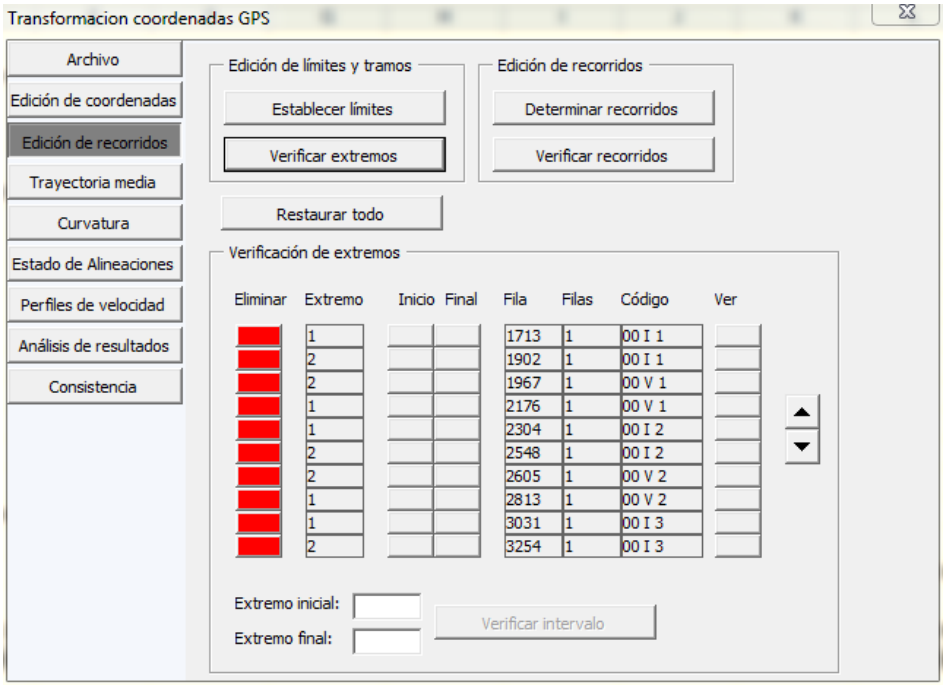

Figure 110. Window for filtering all individual trajectories.

Figure 111 pane allows the merging of all trajectories. Both directions can be merged together or separately. The last option is recommended when both of them substantially differ or when individual paths are only in one direction. The user can select the distance between the points. However, this option has been defined to 1 m.

There is another option to directly fit one road segment from the initial data. This option is only valid when all the points of the input data belong to the same, one direction, trajectory. In this case, the previous steps are not needed.

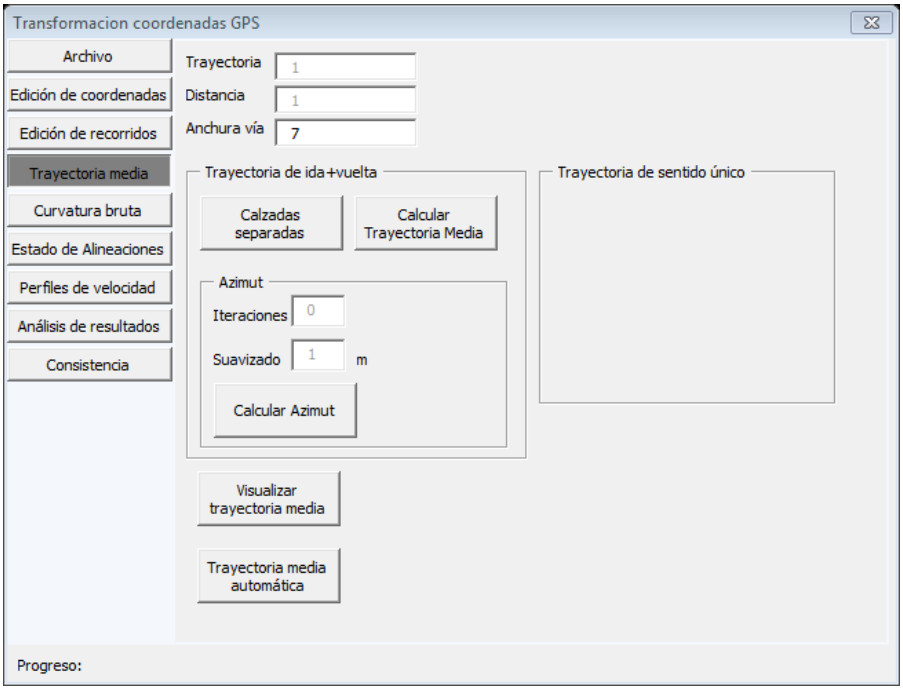

Figure 111. Form for developing the average path of all individual road segments.

The local curvature pane (Figure 112) allows the user to determine the local curvature departing from the merged trajectory. The user can select different cadences, gradients and some more options.

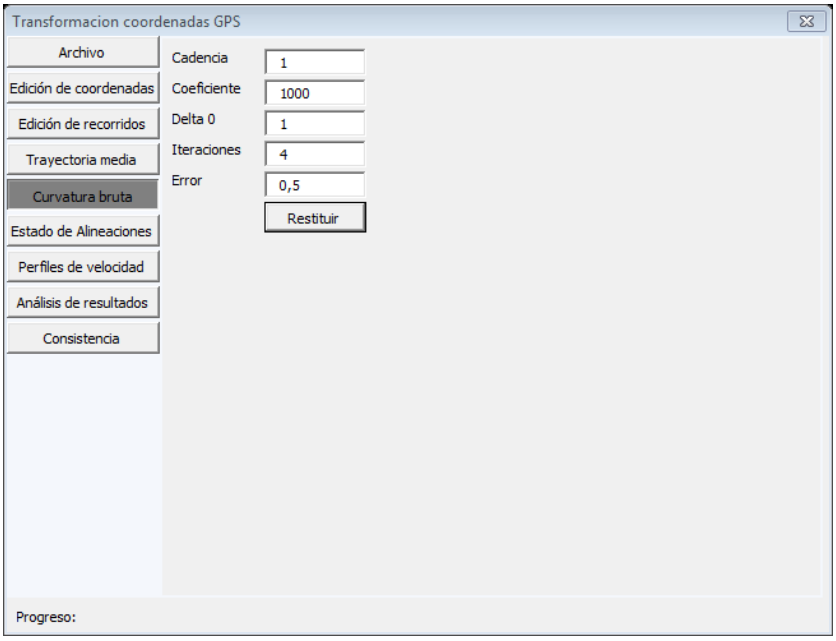

Figure 112. Local curvature extraction form.

The pane that allows the creation of the horizontal alignment is shown in Figure 113.

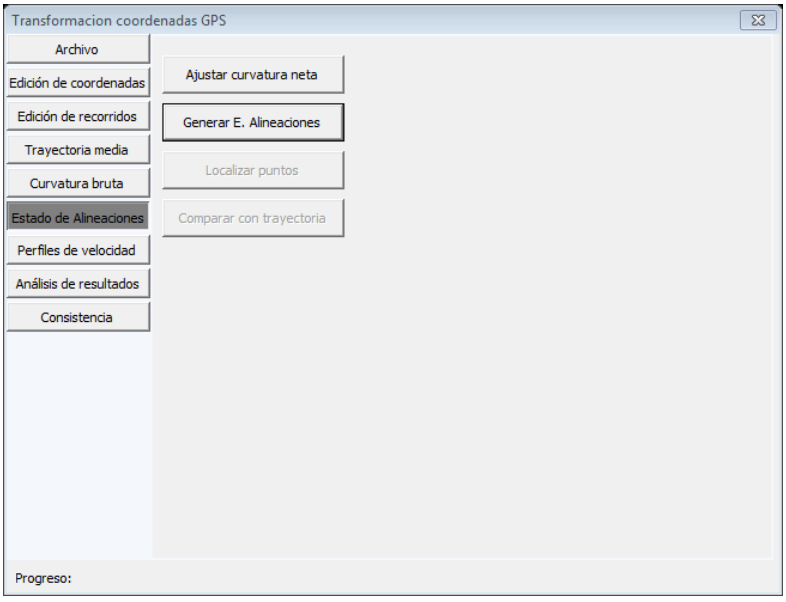

Figure 113. Adjustment of the horizontal alignment.

The operating speed pane is a bit more complex (Figure 114). It is divided into two sections:

- Determination of the operating speed profile based on operating speed profile models. The user can choose different models for curves, tangents and speed transition rates.
- Extraction and analysis of operating speed profiles from a set of drivers. Several percentiles can be extracted. Some smoothing tools are also available.

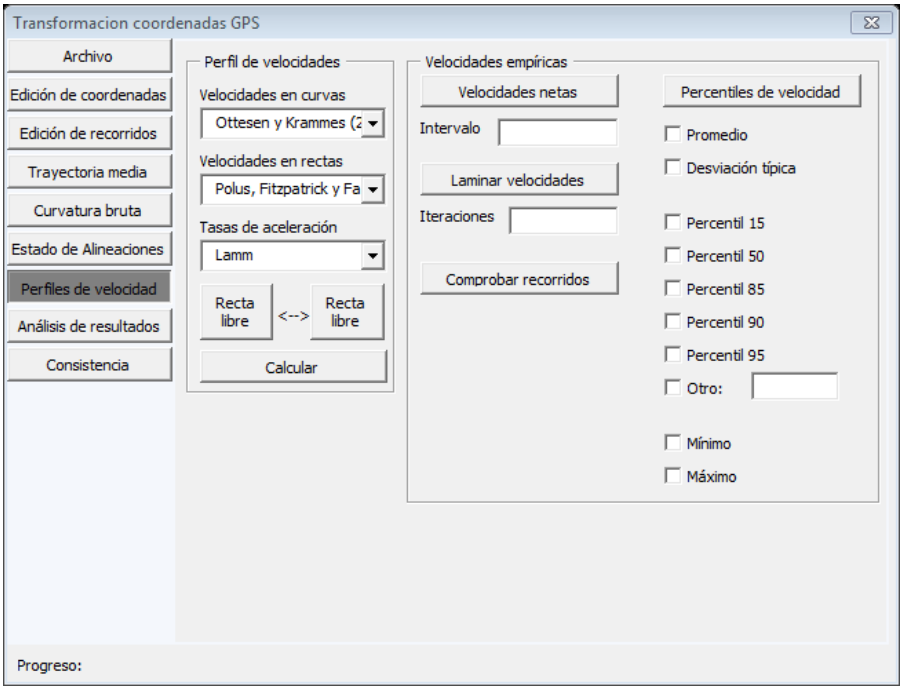

Figure 114. Development of the operating speed profiles. Several operating speed models (as well as construction rules) can be selected.

7. Development

7.1. Selection of road segments

An initial set of 65 two-lane rural road sections was selected in the Valencian region of Spain. All of them belong to the Infrastructure, Territory and Environment Department of Valencian Government or the Valencian Province Council. Table 31 and Figure 115 show them.

Figure 115. Initial road sections under study.

Code	Road	Begin	End	Initial station	Final station
1	CV-11	Urban	Intersection	0+710	10+550
2	CV-12	Intersection	Intersection	0+050	23+790
3	CV-14	Intersection	Urban	0+230	19+600
4	CV-15	Free	Urban	55+670	64+840
5	CV-15	Urban	Free	68+510	72+460
6	CV-25	Urban	Urban	15+850	19+770
7	CV-60	Roundabout	Free	0+090	22+680
8	CV-700	Roundabout	Urban	21+760	26+270
9	CV-700	Urban	Urban	27+520	38+610
10	CV-700	Urban	Urban	44+390	52+770
11	CV-715	Urban	Urban	10+390	16+290
12	CV-715	Urban	Urban	40+280	46+440
13	CV-83	Roundabout	Urban	14+270	23+530
14	CV-840	Urban	Urban	20+688	11+437
15	CV-860	Roundabout	Roundabout	0+090	4+640
16	CV-925	Intersection	Roundabout	14+190	24+930
17	CV-935	Roundabout	Intersection	6+000	9+910
18	CV-941	Roundabout	Roundabout	1+190	6+390
19	CV-949	Intersection	Free	0+020	6+980
20	CV-25	Urban	Urban	10+280	15+110
21	CV-35	Urban	Urban	87+120	95+910
22	CV-41	Roundabout	Roundabout	5+780	7+050
23	CV-41	Roundabout	Roundabout	9+750	11+910
24	CV-41	Roundabout	Roundabout	12+100	18+420
25	CV-42	Roundabout	Roundabout	1+870	3+060
26	CV-42	Roundabout	Roundabout	3+260	4+990
27	CV-42	Roundabout	Roundabout	5+150	7+370
28	CV-811	Roundabout	Roundabout	0+800	4+490
29	CV-900	Roundabout	Roundabout	10+270	11+070
30	CV-15	Roundabout	Roundabout	0+080	7+560
31	CV-820	Roundabout	Roundabout	12+320	12+320
32	CV-20	Urban	Urban	12+200	27+070

Code	Road	Begin	End	Initial station	Final station
33	CV-50	Urban	Roundabout	50+740	74+510
34	CV-805	Interchange with freeway	Interchange with freeway	2+070	13+090
35	CV-10	Roundabout	Roundabout	48+230	80+510
36	CV-15	Roundabout	Urban	9+630	15+550
37	CV-18	Roundabout	Roundabout	1+220	2+310
38	CV-50	Urban	Roundabout	33+890	39+660
39	CV-720	Urban	Urban	2+500	8+780
40	CV-806	Urban	Roundabout	0+790	6+680
41	CV-840	Roundabout	Interchange with freeway	14+550	20+590
42	CV-827	Roundabout	Urban	0+180	9+890
43	CV-35	Urban	Urban	68+340	86+640
44	CV-35	Urban	Roundabout	53+510	67+050
45	CV-333	Roundabout	Roundabout	3+850	8+390
46	CV-801	Urban	Intersection	0+420	9+070
47	CV-820	Urban	Roundabout	8+950	10+860
48	CV-755	Urban	Urban	0+000	0+650
49	CV-50	Urban	Urban	42+210	48+830
50	CV-15	Urban	Free	17+850	38+020
51	CV-50	Urban	Roundabout	76+240	83+740
52	CV-16	Roundabout	Roundabout	8+890	10+050
53	CV-18	Roundabout	Roundabout	3+350	8+000
54	CV-18	Roundabout	Roundabout	2+570	3+100
55	CV-439	Roundabout	Free	0+270	12+590
56	CV-222	Roundabout	Roundabout	0+530	6+450
57	CV-245	Urban	Urban	0+620	3+270
58	CV-245	Urban	Roundabout	3+770	6+690
59	CV-585	Roundabout	Roundabout	0+160	5+980
60	CV-790	Intersection	Roundabout	0+020	5+890
61	CV-11	Urban	Roundabout	10+660	19+320
62	CV-17	Roundabout	Roundabout	0+230	3+370
63	CV-403	Roundabout	Roundabout	2+050	3+320

Code	Road	Begin	End	Initial station	Final station
64	CV-407	Urban	Roundabout	0+500	2+160
65	CV-720	Urban	Urban	0+020	2+380

Table 31. Initial road sections under study.

7.2. Determination of the homogeneous segments

All the road sections had to be divided into homogeneous segments. In addition, the geometric and operational parameters had to be obtained. This process has been previously explained. Here are some examples of it.

7.2.1. Determination of the horizontal alignment

All road sections were depicted using Google Earth. The computer program was applied and the horizontal geometry was extracted. The horizontal alignments for all sections are in Appendix III.

Figure 116. Example of how the polyline is created. Notice the higher density on the horizontal curve.

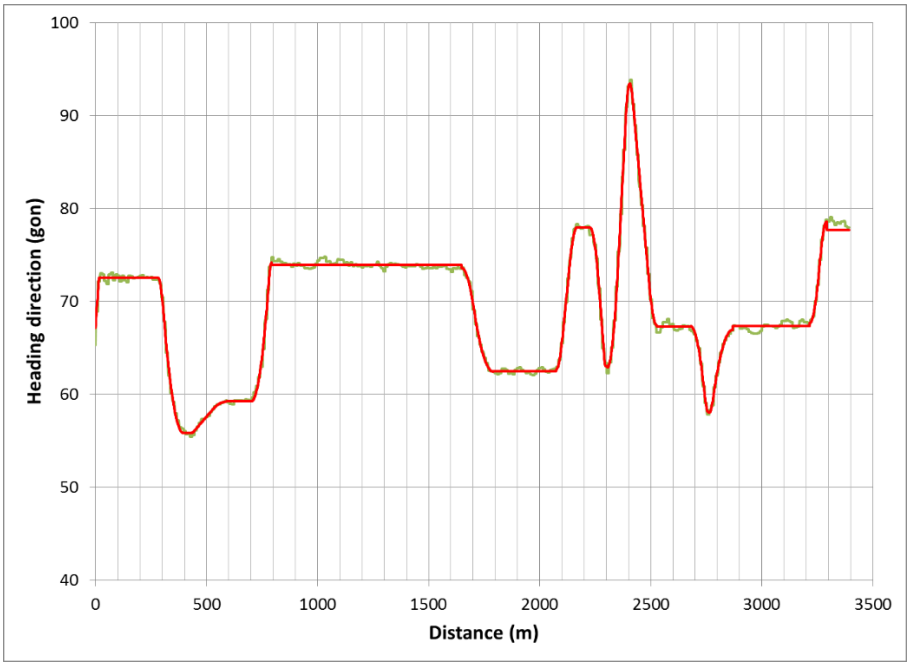

Figure 117. Recreation of the alignment based on the heading direction. The green line represents raw data, while the red one is the adjusted alignment. Road section 31.

7.2.2. Determination of the operating speed profiles

The operating speed profiles were determined for all road sections. In addition, the inertial operating speed profiles were also developed, for further determining the homogeneous road segments.

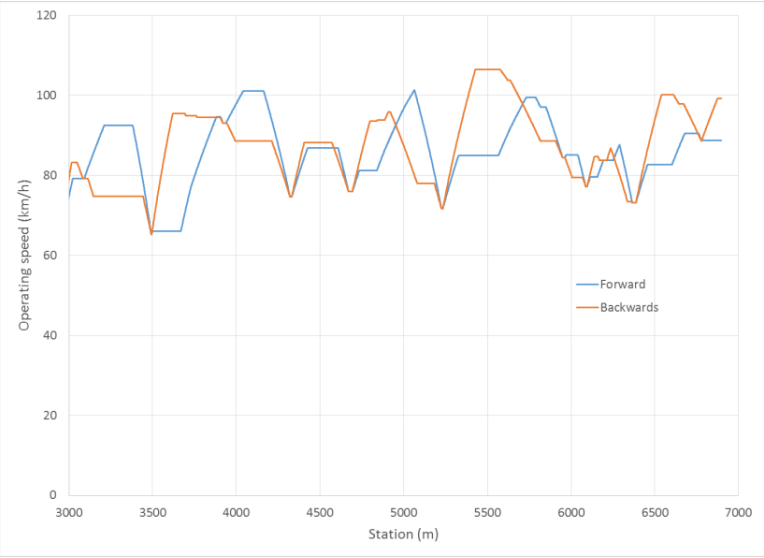

Figure 118. Example of the operating speed profiles (road segment 19.2).

7.2.3. Road segmentation

Considering the traffic volume variations, the CCR diagram, and the variation of the inertial operating speed, the road sections were divided into 158 homogeneous road segments.

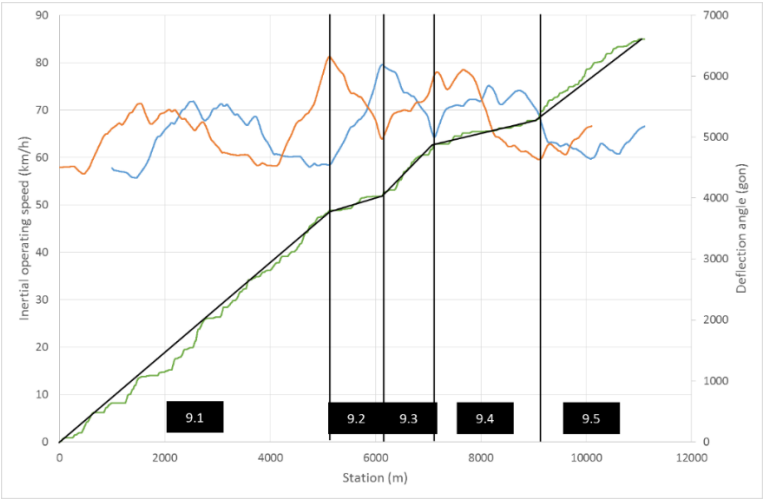

Figure 119. Determination of the homogeneous road segments from a road section (road section 9).

The 158 road segments were also classified according to their constraining conditions:

Road segment	Initial station	End station	Length (m)	Boundary conditions
1.1	0+710	10+550	9885	Constrained
2.1	0+050	2+570	2504	Constrained
2.2	2+570	9+760	7151	Free
2.3	9+760	10+960	1192	Free
2.4	10+960	11+510	553	Free
2.5	11+510	12+560	1042	Free
2.6	12+560	16+340	3765	Free
2.7	16+340	17+550	1205	Free
2.8	17+550	18+270	717	Free
2.9	18+270	19+320	1051	Free
2.10	19+320	23+790	1665	Constrained
3.1	0+230	5+380	5112	Constrained
3.2	5+380	10+150	4771	Free
3.3	10+150	13+480	3318	Free
3.4	13+480	15+100	1635	Free
3.5	15+100	16+080	987	Free
3.6	16+080	19+600	3512	Constrained
4.1	55+670	56+840	1159	Free
4.2	56+840	58+790	1946	Free
4.3	58+790	60+800	2011	Free
4.4	60+800	62+390	1584	Free
4.5	62+390	63+800	1402	Free
4.6	63+800	64+840	1043	Constrained
5.1	68+510	70+900	2369	Constrained
5.2	70+900	72+460	1556	Free
6.1	15+850	19+770	3893	Constrained
7.1	0+090	15+730	15645	Constrained
7.2	15+730	22+680	6971	Free
8.1	21+760	26+270	4533	Constrained
9.1	27+520	32+690	5141	Constrained

Road segment	Initial station	End station	Length (m)	Boundary conditions
9.2	32+690	33+630	963	Free
9.3	33+630	34+660	1017	Free
9.4	34+660	36+560	1911	Free
9.5	36+560	38+610	2070	Constrained
10.1	44+390	47+490	3089	Constrained
10.2	47+490	48+720	1220	Free
10.3	48+720	49+530	800	Free
10.4	49+530	52+770	3273	Constrained
11.1	10+390	12+880	2483	Constrained
11.2	12+880	15+230	2368	Free
11.3	15+230	16+290	1053	Constrained
12.1	40+280	42+360	2081	Constrained
12.2	42+360	44+360	1999	Free
12.3	44+360	46+440	2092	Constrained
13.1	14+270	16+320	1974	Constrained
13.2	16+320	17+690	1326	Free
13.3	17+690	19+530	1772	Free
13.4	19+530	20+570	997	Free
13.5	20+570	23+530	2999	Constrained
14.1	20+688	18+501	2165	Constrained
14.2	18+501	15+548	2948	Free
14.3	15+548	13+266	2277	Free
14.4	13+266	11+437	1821	Constrained
15.1	0+090	4+640	4536	Constrained
16.1	14+190	17+180	2972	Constrained
16.2	17+180	18+520	1322	Free
16.3	18+520	24+930	6394	Constrained
17.1	6+000	9+910	3906	Constrained
18.1	1+190	6+390	5202	Constrained
19.1	0+020	3+060	2997	Constrained
19.2	3+060	6+980	3901	Free
20.1	10+280	13+200	2868	Constrained

Road segment	Initial station	End station	Length (m)	Boundary conditions
20.2	13+200	15+110	1900	Constrained
21.1	87+120	89+200	2080	Constrained
21.2	89+200	92+240	2871	Free
21.3	92+240	93+490	1226	Free
21.4	93+490	95+910	2428	Constrained
22.1	5+780	7+050	1451	Constrained
23.1	9+750	11+910	2265	Constrained
24.1	12+100	13+720	1611	Constrained
24.2	13+720	14+710	1000	Free
24.3	14+710	18+420	3705	Constrained
25.1	1+870	3+060	1254	Constrained
26.1	3+260	4+990	1735	Constrained
27.1	5+150	7+370	2254	Constrained
28.1	0+800	1+780	1071	Constrained
28.2	1+780	3+760	1996	Free
28.3	3+760	4+490	721	Constrained
29.1	10+270	11+070	841	Constrained
30.1	0+080	2+230	2095	Constrained
30.2	2+230	6+010	3773	Free
30.3	6+010	7+560	1539	Constrained
31.1	12+320	14+400	2075	Constrained
31.2	11+000	12+320	1321	Constrained
32.1	12+200	15+340	3138	Constrained
32.2	15+340	27+070	11659	Constrained
33.1	50+740	53+400	2557	Constrained
33.2	53+400	55+200	1728	Free
33.3	55+200	57+300	2038	Free
33.4	57+300	61+400	3023	Free
33.5	61+400	62+000	567	Free
33.6	62+000	71+500	10478	Free
33.7	71+500	74+510	2465	Constrained
34.1	2+070	4+560	2489	Constrained
34.2	4+560	8+250	3692	Free

Road segment	Initial station	End station	Length (m)	Boundary conditions
34.3	8+250	13+090	4651	Constrained
35.1	48+230	65+320	17085	Constrained
35.2	65+320	69+570	4256	Free
35.3	69+570	80+510	10823	Constrained
36.1	9+630	12+520	2890	Constrained
36.2	12+520	15+550	3021	Constrained
37.1	1+220	2+310	1089	Constrained
38.1	33+890	39+660	5750	Constrained
39.1	2+500	8+780	6311	Constrained
40.1	0+790	6+680	5826	Constrained
41.1	14+550	20+590	6032	Constrained
42.1	0+180	2+280	2097	Constrained
42.2	2+280	3+270	993	Free
42.3	3+270	4+180	912	Free
42.4	4+180	6+390	2206	Free
42.5	6+390	9+890	3262	Constrained
43.1	68+340	70+950	2589	Constrained
43.2	70+950	76+290	5348	Free
43.3	76+290	79+780	3472	Free
43.4	79+780	80+730	943	Free
43.5	80+730	83+650	2893	Free
43.6	83+650	86+640	2995	Constrained
44.1	53+510	58+040	4651	Constrained
44.2	58+040	62+450	4421	Free
44.3	62+450	67+050	4499	Constrained
45.1	3+850	6+510	2658	Constrained
45.2	6+510	8+390	1925	Constrained
46.1	0+420	3+700	3280	Constrained
46.2	3+700	5+580	1979	Free
46.3	5+580	9+070	3218	Constrained
47.1	8+950	10+860	1791	Constrained
48.1	0+000	0+650	642	Constrained

Road segment	Initial station	End station	Length (m)	Boundary conditions
49.1	42+210	46+310	4101	Constrained
49.2	46+310	48+830	2498	Constrained
50.1	17+850	21+490	3635	Constrained
50.2	21+490	26+140	4647	Free
50.3	26+140	28+480	2333	Free
50.4	28+480	32+110	3617	Free
50.5	32+110	36+130	4000	Free
50.6	36+130	38+020	1885	Free
51.1	76+240	83+740	7509	Constrained
52.1	8+890	10+050	1252	Constrained
53.1	3+350	8+000	4522	Constrained
54.1	2+570	3+100	520	Constrained
55.1	0+270	9+350	9082	Constrained
55.2	9+350	12+590	2910	Free
56.1	0+530	5+470	4940	Constrained
56.2	5+470	6+450	1231	Constrained
57.1	0+620	3+270	2352	Constrained
58.1	3+770	6+000	2229	Constrained
58.2	6+000	6+690	853	Constrained
59.1	0+160	3+100	2944	Constrained
59.2	3+100	4+120	1018	Free
59.3	4+120	5+290	1169	Free
59.4	5+290	5+980	676	Constrained
60.1	0+020	1+990	1966	Constrained
60.2	1+990	5+890	3908	Constrained
61.1	10+660	17+920	7218	Constrained
61.2	17+920	19+320	1390	Constrained
62.1	0+230	3+370	3117	Constrained
63.1	2+050	3+320	1228	Constrained
64.1	0+500	2+160	1633	Constrained
65.1	0+020	2+380	2367	Constrained

Table 32. Homogeneous road segments to be considered.

Finally, there were 62 free road segments and 96 constrained ones, for a total of 158 road homogeneous segments.

7.3. Determination of the input data

After determining the homogeneous road segments, it was time to calculate AADT, accidents and operational parameters.

7.3.1. AADT

The average AADT of all years was considered. Table 33 shows the AADT value for all years, as well as the average value.

Section	2011	2010	2009	2008	2007	2006	2005	2004	2003	2002	2001	Avg.
1.1	1704	1705	1923	2330	1971	2086	2208	1835	969	1226	1758	1801
2.1	811	658	735	730	1252	1080	777	1046	603	921	792	859
2.2	811	658	735	730	1252	1080	777	1046	603	921	792	859
2.3	811	658	735	730	1252	1080	777	1046	603	921	792	859
2.4	811	658	735	730	1252	1080	777	1046	603	921	792	859
2.5	811	658	735	730	1252	1080	777	1046	603	921	792	859
2.6	811	658	735	730	1252	1080	777	1046	603	921	792	859
2.7	811	658	735	730	1252	1080	777	1046	603	921	792	859
2.8	811	658	735	730	1252	1080	777	1046	603	921	792	859
2.9	811	658	735	730	1252	1080	777	1046	603	921	792	859
2.10	811	658	735	730	1252	1080	777	1046	603	921	792	859
3.1	1198	1190	1039	1131	1424	1467	1844	1141	1224	1250	1148	1285
3.2	1108	1097	1147	1179	1254	1282	1334	1042	1026	1250	1163	1177
3.3	697	645	727	811	926	849	857	799	682	885	862	804
3.4	697	645	727	811	926	849	857	799	682	885	862	804
3.5	697	645	727	811	926	849	857	799	682	885	862	804
3.6	697	645	727	811	926	849	857	799	682	885	862	804
4.1	1119	780	1193	1266	1250	1280	979	825	801	967	1017	1035
4.2	1119	780	1193	1266	1250	1280	979	825	801	967	1017	1035
4.3	1119	780	1193	1266	1250	1280	979	825	801	967	1017	1035
4.4	1119	780	1193	1266	1250	1280	979	825	801	967	1017	1035
4.5	1119	780	1193	1266	1250	1280	979	825	801	967	1017	1035

Section	2011	2010	2009	2008	2007	2006	2005	2004	2003	2002	2001	Avg.
4.6	1178	1349	1498	1441	650	1647	1373	791	1045	859	929	1158
5.1	908	1076	1190	1083	1434	1466	1033	662	883	660	631	1011
5.2	908	1076	1190	1083	1434	1466	1033	662	883	660	631	1011
6.1	767	525	373	217	341	405	436	446	429	451	442	406
7.1	8775	8271	9015	10723	10827	9678	11713	7773	5550	5370	4229	9714
7.2	8694	8507	8004	9487	9121	7193	10672	9602	5550	5370	4229	7773
8.1	442	522	612	453	694	458	558	437	406	512	411	506
9.1	442	522	612	453	694	458	558	437	406	512	411	506
9.2	442	522	612	453	694	458	558	437	406	512	411	506
9.3	442	522	612	453	694	458	558	437	406	512	411	506
9.4	442	522	612	453	694	458	558	437	406	512	411	506
9.5	442	522	612	453	694	458	558	437	406	512	411	506
10.1	442	522	612	453	694	458	558	437	406	512	411	506
10.2	442	522	612	453	694	458	558	437	406	512	411	506
10.3	442	522	612	453	694	458	558	437	406	512	411	506
10.4	442	522	612	453	694	458	558	437	406	512	411	506
11.1	2524	2524	3161	2659	3457	2697	2870	3308	3218	3031	2323	2924
11.2	2524	2524	3161	2659	3457	2697	2870	3308	3218	3031	2323	2924
11.3	2524	2524	3161	2659	3457	2697	2870	3308	3218	3031	2323	2924
12.1	294	572	359	339	500	245	447	384	339	500	583	426
12.2	294	572	359	339	500	245	447	384	339	500	583	426
12.3	294	572	359	339	500	245	447	384	339	500	583	426
13.1	5060	5778	5635	5413	5881	6039	5180	6038	5686	5391	4765	5580
13.2	4951	5555	5152	5174	5881	6039	5180	6038	5686	5391	4765	5486
13.3	4951	5555	5152	5174	5881	6039	5180	6038	5686	5391	4765	5486
13.4	4951	5555	5152	5174	5881	6039	5180	6038	5686	5391	4765	5486
13.5	4951	5555	5152	5174	5881	6039	5180	6038	5686	5391	4765	5486
14.1	2170	2126	2262	2949	3345	2873	4182	4143	3357	3512	2536	3128
14.2	2170	2126	2262	2949	3345	2873	4182	4143	3357	3512	2536	3128
14.3	2170	2126	2262	2949	3345	2873	4182	4143	3357	3512	2536	3128
14.4	2170	2126	2262	2949	3345	2873	4182	4143	3357	3512	2536	3128
15.1	3868	4256	4256	4462	4990	4239	5945	6041	5392	5009	5212	4980
16.1	891	1978	1178	1177	1245	1256	1308	1444	1128	1128	1010	1285

Section	2011	2010	2009	2008	2007	2006	2005	2004	2003	2002	2001	Avg.
16.2	891	1978	1178	1177	1245	1256	1308	1444	1128	1128	1010	1285
16.3	891	1978	1178	1177	1245	1256	1308	1444	1128	1128	1010	1285
17.1	1859	1922	1902	2456	2479	2730	2651	3382	3111	2500	2751	2588
18.1	3395	3407	3828	4444	4094	4131	2515	3913	2953	2866	2570	3472
19.1	691	797	641	793	740	887	925	823	753	778	995	813
19.2	691	797	641	793	740	887	925	823	753	778	995	813
20.1	896	894	494	313	421	655	758	575	324	430	419	528
20.2	896	894	494	313	421	655	758	575	324	430	419	528
21.1	514	647	491	569	548	469	440	410	396	630	602	520
21.2	514	647	491	569	548	469	440	410	396	630	602	520
21.3	514	647	491	569	548	469	440	410	396	630	602	520
21.4	514	647	491	569	548	469	440	410	396	630	602	520
22.1	10213	10395	10102	10358	11091	9723	8418	5212	8500	7800	10420	9201
23.1	7200	7348	6646	6711	6776	5773	5512	8703	6650	6389	6389	6689
24.1	8056	8237	8589	8790	9333	8833	8853	7925	7620	9066	7473	8471
24.2	8056	8237	8589	8790	9333	8833	8853	7925	7620	9066	7473	8471
24.3	8056	8237	8589	8790	9333	8833	8853	7925	7620	9066	7473	8471
25.1	4433	4313	5531	6611	6384	4758	5350	9558	8922	9506	8500	6943
26.1	4433	4313	5531	6611	6384	4758	5350	9558	8922	9506	8500	6943
27.1	4929	4607	5216	6931	7258	5158	6812	5353	7092	8248	8769	6544
28.1	657	713	1296	659	832	718	729	1020	1015	1084	684	875
28.2	657	713	1296	659	832	718	729	1020	1015	1084	684	875
28.3	657	713	1296	659	832	718	729	1020	1015	1084	684	875
29.1	7109	6994	7643	5232	7276	7869	7129	6212	5197	4998	12880	7143
30.1	9228	9305	9569	10514	10340	9849	8499	8219	9684	7017	5914	8891
30.2	7512	6179	5696	6624	5858	5923	4797	4481	5236	4514	3974	5328
30.3	7512	6179	5696	6624	5858	5923	4797	4481	5236	4514	3974	5328
31.1	3157	3403	2873	3840	6336	4694	5238	4998	5230	4243	3904	4475
31.2	3157	3403	2873	3840	6336	4694	5238	4998	5230	4243	3904	4475
32.1	3461	3796	5209	5382	4564	4232	5842	4047	4335	5232	2770	4540
32.2	874	538	929	899	1053	935	940	614	599	459	522	748
33.1	1115	968	1016	1481	1756	2013	1999	775	1188	920	847	1296
33.2	1115	968	1016	1481	1756	2013	1999	775	1188	920	847	1296

Section	2011	2010	2009	2008	2007	2006	2005	2004	2003	2002	2001	Avg.
33.3	1115	968	1016	1481	1756	2013	1999	775	1188	920	847	1296
33.4	1115	968	1016	1481	1756	2013	1999	775	1188	920	847	1296
33.5	4361	4798	5043	5099	5011	4373	4054	1826	2480	1560	1487	3573
33.6	5033	5314	5411	5611	5650	4962	4348	1826	2480	1560	1487	3864
33.7	4370	4517	5309	4246	5512	4852	4538	4682	4688	4830	4042	4721
34.1	1632	2234	1504	1766	1990	2528	1960	1995	1884	6778	6395	2903
34.2	1632	2234	1504	1766	1990	2528	1960	1995	1884	6778	6395	2903
34.3	1632	2234	1504	1766	1990	2528	1960	1995	1884	6778	6395	2903
35.1	4675	3549	6888	4550	5054	4370	6060	5581	4867	4589	4619	5012
35.2	4675	3549	6888	4550	5054	3325	3547	3536	2855	3252	2996	3955
35.3	2682	2878	2998	3096	3159	3094	2497	2887	2402	2365	2723	2809
36.1	5596	4984	5471	5125	6237	5721	4743	3834	4210	3491	3728	4754
36.2	3403	3141	3452	3508	5223	3606	3185	2663	2942	2736	2870	3332
37.1	23160	23849	24712	26935	26265	25702	25107	25800	24807	26497	20476	25015
38.1	5379	5091	5105	4710	6044	4416	5271	5675	6200	5761	4159	5243
39.1	405	490	419	337	348	354	255	287	416	367	352	362
40.1	3901	3746	4747	4299	3755	5273	5567	5941	5141	9325	6109	5390
41.1	2170	2126	2262	2949	3345	2873	4182	4143	3357	3512	2536	3128
42.1	298	377	441	374	433	372	420	338	358	272	453	383
42.2	298	377	441	374	433	372	420	338	358	272	453	383
42.3	298	377	441	374	433	372	420	338	358	272	453	383
42.4	298	377	441	374	433	372	420	338	358	272	453	383
42.5	298	377	441	374	433	372	420	338	358	272	453	383
43.1	2159	2261	2279	2496	2012	1771	1958	1844	1921	1580	1457	1957
43.2	1792	1836	1881	1924	1421	1244	1420	1300	1245	1094	1031	1439
43.3	1524	1526	1592	1507	990	860	1029	904	753	740	720	1062
43.4	1524	1526	1592	1507	990	860	1029	904	753	740	720	1062
43.5	1524	1526	1592	1507	990	860	1029	904	753	740	720	1062
43.6	1524	1526	1592	1507	990	860	1029	904	753	740	720	1062
44.1	2502	2665	2660	2371	2211	2257	2088	1884	1750	2450	2245	2258
44.2	2502	2665	2660	2371	2211	2257	2088	1884	1750	2450	2245	2258
44.3	2350	2366	2548	2455	1909	2030	1883	1933	1639	2450	2245	2145
45.1	4053	4265	4369	4623	4932	4637	4471	4022	3086	3210	3147	4076

Section	2011	2010	2009	2008	2007	2006	2005	2004	2003	2002	2001	Avg.
45.2	2898	3173	3243	3587	4226	3528	3251	2943	2274	2570	2494	3128
46.1	517	778	592	508	452	405	478	497	518	647	593	546
46.2	517	778	592	508	452	405	478	497	518	647	593	546
46.3	640	758	811	719	639	602	725	773	814	1275	1102	821
47.1	3157	3403	2873	3840	6336	4694	5238	4998	5230	4243	3904	4475
48.1	766	913	1041	606	718	601	622	543	949	922	1795	871
49.1	2483	2544	2743	2913	2899	2819	2712	2748	2623	2281	2479	2676
49.2	2483	2544	2743	2913	2899	2819	2712	2748	2623	2281	2479	2676
50.1	2432	2325	2558	2792	4774	2670	2495	2144	2380	2402	2490	2703
50.2	2432	2325	2558	2792	4774	2670	2495	2144	2380	2402	2490	2703
50.3	2432	2325	2558	2792	4774	2670	2495	2144	2380	2402	2490	2703
50.4	2432	2325	2558	2792	4774	2670	2495	2144	2380	2402	2490	2703
50.5	1914	1882	2080	2111	2189	1594	1729	1627	1717	1674	1754	1835
50.6	2137	2455	2209	2343	2360	1305	2040	1830	1895	1822	1819	2007
51.1	4370	4517	5309	4246	5512	4852	4538	4682	4688	4830	4042	4721
52.1	4347	4304	5116	7336	7470	10954	11726	13741	14352	13591	14661	10325
53.1	12610	12762	12914	16390	16624	14655	13020	15852	16292	15365	12524	14639
54.1	12611	12762	12914	16390	16624	14655	13020	15852	16292	15365	12524	14639
55.1	401	373	233	347	352	490	393	467	350	350	350	370
55.2	211	244	127	196	204	387	378	365	350	350	350	295
56.1	5087	5369	4811	7191	7420	6245	5827	7798	7043	7285	6501	6549
56.2	5087	5369	4811	7191	7420	6245	5827	7798	7043	7285	6501	6549
57.1	188	209	191	413	170	214	216	197	165	158	155	208
58.1	188	209	191	413	170	214	216	197	165	158	155	208
58.2	188	209	191	413	170	214	216	197	165	158	155	208
59.1	3094	3286	3105	3530	4019	3393	3488	3248	4050	3850	3576	3554
59.2	3094	3286	3105	3530	4019	3393	3488	3248	4050	3850	3576	3554
59.3	3094	3286	3105	3530	4019	3393	3488	3248	4050	3850	3576	3554
59.4	3094	3286	3105	3530	4019	3393	3488	3248	4050	3850	3576	3554
60.1	2036	1774	2562	1803	1969	1676	2431	2020	2045	1778	1603	1966
60.2	2417	2404	3130	2463	2612	2168	3080	2448	2601	2379	2123	2540
61.1	3514	3181	3460	4865	4236	4218	4046	2156	2153	2020	2334	3266
61.2	3514	3181	3460	4865	4236	4218	4046	2156	2153	2020	2334	3266

Section	2011	2010	2009	2008	2007	2006	2005	2004	2003	2002	2001	Avg.
62.1	18379	19315	19986	23017	21232	18227	16925	11680	11802	11557	9650	16339
63.1	13610	13610	13375	15075	12380	20988	12726	16055	14779	14971	7802	14176
64.1	10623	10972	12140	12486	16676	16223	10299	13611	13227	14973	10878	13148
65.1	405	490	419	337	348	354	255	287	416	367	352	362

Table 33. AADT of all road segments.

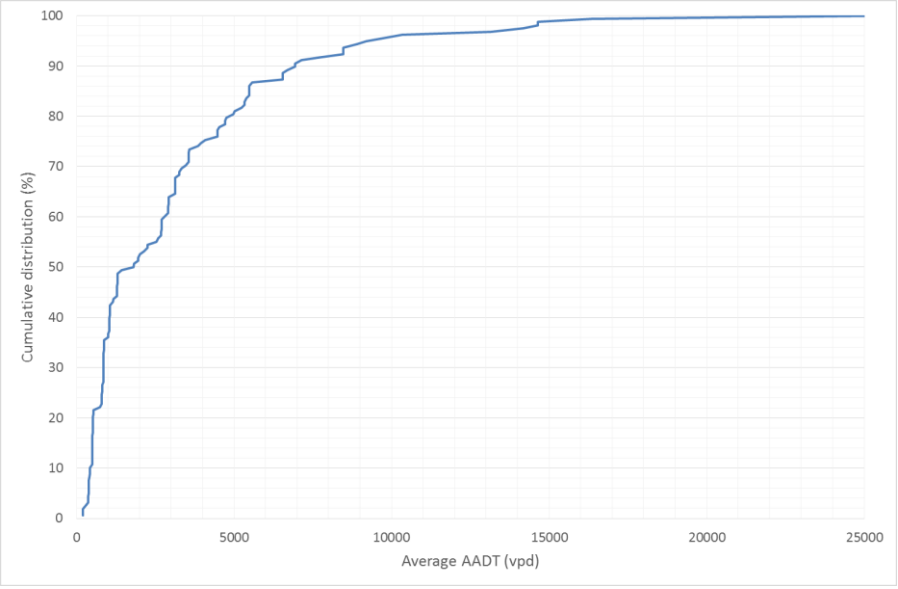

Figure 120. Distribution of the average AADT.

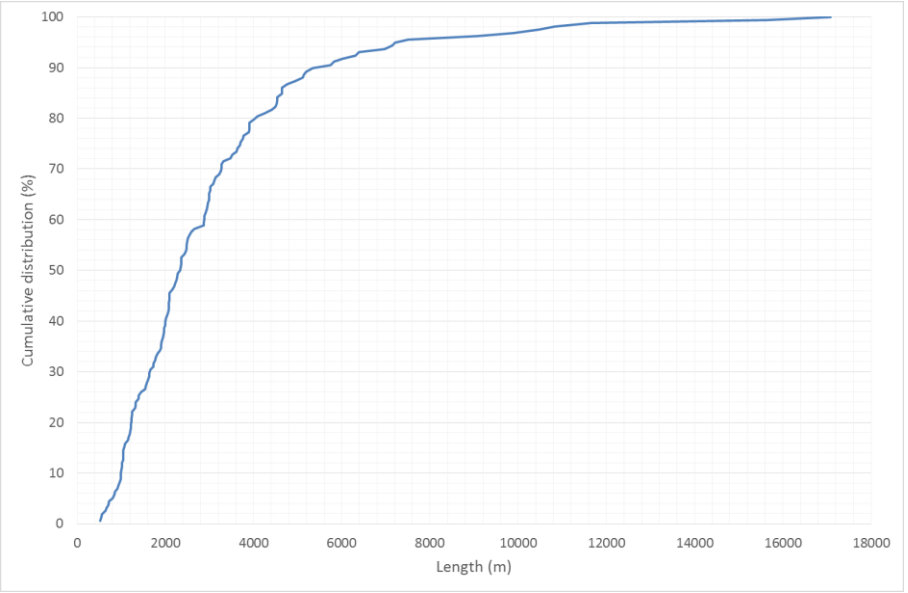

Figure 121. Distribution of the length of road segments.

7.3.2. Number of accidents

The number of accidents was calculated for each road segment. For this, all accidents with victims were examined, looking for their location and causes. The direction of travel was not considered since it was unknown. The AADT is calculated as the average AADT for all years. The number of accidents with victims is also rescaled to 10 years.

Road segment	Boundary conditions	Length (m)	AADT	Accidents with victims
1.1	Constrained	9885	1801	7
2.1	Constrained	2504	859	1
2.2	1	7151	859	4
2.3	1	1192	859	2
2.4	1	553	859	1
2.5	1	1042	859	0
2.6	1	3765	859	1
2.7	1	1205	859	0
2.8	1	717	859	0

Road segment	Boundary conditions	Length (m)	AADT	Accidents with victims
2.9	1	1051	859	0
2.10	Constrained	1665	859	2
3.1	Constrained	5112	1286	6
3.2	Free	4771	1177	4
3.3	Free	3318	804	3
3.4	Free	1635	804	1
3.5	Free	987	804	0
3.6	Constrained	3512	804	2
4.1	Free	1159	1036	0
4.2	Free	1946	1036	1
4.3	Free	2011	1036	3
4.4	Free	1584	1036	1
4.5	Free	1402	1036	1
4.6	Constrained	1043	1158	1
5.1	Constrained	2369	1012	3
5.2	Free	1556	1012	1
6.1	Constrained	3893	407	1
7.1	Constrained	15645	9714	47
7.2	Free	6971	7774	29
8.1	Constrained	4533	506	2
9.1	Constrained	5141	506	3
9.2	Free	963	506	1
9.3	Free	1017	506	0
9.4	Free	1911	506	1
9.5	Constrained	2070	506	0
10.1	Constrained	3089	506	4
10.2	Free	1220	506	0
10.3	Free	800	506	2
10.4	Constrained	3273	506	6
11.1	Constrained	2483	2925	2
11.2	Free	2368	2925	6
11.3	Constrained	1053	2925	1

Road segment	Boundary conditions	Length (m)	AADT	Accidents with victims
12.1	Constrained	2081	427	1
12.2	Free	1999	427	3
12.3	Constrained	2092	427	3
13.1	Constrained	1974	5581	5
13.2	Free	1326	5486	5
13.3	Free	1772	5486	1
13.4	Free	997	5486	2
13.5	Constrained	2999	5486	4
14.1	Constrained	2165	3129	14
14.2	Free	2948	3129	6
14.3	Free	2277	3129	5
14.4	Constrained	1821	3129	1
15.1	Constrained	4536	4980	10
16.1	Constrained	2972	1285	2
16.2	Free	1322	1285	1
16.3	Constrained	6394	1285	4
17.1	Constrained	3906	2588	9
18.1	Constrained	5202	3472	37
19.1	Constrained	2997	813	10
19.2	Free	3901	813	4
20.1	Constrained	2868	528	3
20.2	Constrained	1900	528	3
21.1	Constrained	2080	520	1
21.2	Free	2871	520	0
21.3	Free	1226	520	1
21.4	Constrained	2428	520	2
22.1	Constrained	1451	9202	8
23.1	Constrained	2265	6690	1
24.1	Constrained	1611	8472	11
24.2	Free	1000	8472	16
24.3	Constrained	3705	8472	30
25.1	Constrained	1254	6943	2

Road segment	Boundary conditions	Length (m)	AADT	Accidents with victims
26.1	Constrained	1735	6943	3
27.1	Constrained	2254	6544	8
28.1	Constrained	1071	875	0
28.2	Free	1996	875	2
28.3	Constrained	721	875	1
29.1	Constrained	841	7143	2
30.1	Constrained	2095	8891	4
30.2	Free	3773	5328	10
30.3	Constrained	1539	5328	4
31.1	Constrained	2075	4476	4
31.2	Constrained	1321	4476	4
32.1	Constrained	3138	4541	14
32.2	Constrained	11659	749	34
33.1	Constrained	2557	1296	5
33.2	Free	1728	1296	4
33.3	Free	2038	1296	0
33.4	Free	3023	1296	4
33.5	Free	567	3573	0
33.6	Free	10478	3865	14
33.7	Constrained	2465	4722	7
34.1	Constrained	2489	2903	2
34.2	Free	3692	2903	5
34.3	Constrained	4651	2903	5
35.1	Constrained	17085	5013	41
35.2	Free	4256	3955	9
35.3	Constrained	10823	2810	15
36.1	Constrained	2890	4754	4
36.2	Constrained	3021	3333	7
37.1	Constrained	1089	25015	8
38.1	Constrained	5750	5243	13
39.1	Constrained	6311	363	2
40.1	Constrained	5826	5390	9

Road segment	Boundary conditions	Length (m)	AADT	Accidents with victims
41.1	Constrained	6032	3129	18
42.1	Constrained	2097	384	0
42.2	Free	993	384	4
42.3	Free	912	384	1
42.4	Free	2206	384	3
42.5	Constrained	3262	384	4
43.1	Constrained	2589	1958	9
43.2	Free	5348	1440	1
43.3	Free	3472	1062	1
43.4	Free	943	1062	1
43.5	Free	2893	1062	2
43.6	Constrained	2995	1062	4
44.1	Constrained	4651	2258	16
44.2	Free	4421	2258	12
44.3	Constrained	4499	2146	5
45.1	Constrained	2658	4076	0
45.2	Constrained	1925	3129	2
46.1	Constrained	3280	547	3
46.2	Free	1979	547	1
46.3	Constrained	3218	822	0
47.1	Constrained	1791	4476	5
48.1	Constrained	642	871	1
49.1	Constrained	4101	2676	5
49.2	Constrained	2498	2676	11
50.1	Constrained	3635	2703	9
50.2	Free	4647	2703	7
50.3	Free	2333	2703	3
50.4	Free	3617	2703	2
50.5	Free	4000	1836	3
50.6	Free	1885	2008	8
51.1	Constrained	7509	4722	9
52.1	Constrained	1252	10325	3

Road segment	Boundary conditions	Length (m)	AADT	Accidents with victims
53.1	Constrained	4522	14640	49
54.1	Constrained	520	14640	2
55.1	Constrained	9082	371	2
55.2	Free	2910	295	1
56.1	Constrained	4940	6549	19
56.2	Constrained	1231	6549	3
57.1	Constrained	2352	209	0
58.1	Constrained	2229	209	1
58.2	Constrained	853	209	0
59.1	Constrained	2944	3555	12
59.2	Free	1018	3555	2
59.3	Free	1169	3555	1
59.4	Constrained	676	3555	6
60.1	Constrained	1966	1966	1
60.2	Constrained	3908	2541	3
61.1	Constrained	7218	3267	15
61.2	Constrained	1390	3267	5
62.1	Constrained	3117	16339	12
63.1	Constrained	1228	14176	4
64.1	Constrained	1633	13149	3
65.1	Constrained	2367	363	1

Table 34. Length, AADT and accidents with victims for all road segments.

7.3.3. Operational parameters

The operational parameters were extracted for all road segments. However, the operating speed for four road segments was completely stable. Hence, no decelerations were found and those road segments were not considered for the next step. The operational parameters for all road segments are in Table 35 and Table 36.

	$\bar{v}_{85}$	$\sigma_{v_{85}}$	R_a	$E_{a,10}$	$E_{a,20}$	L_{10}	L_{20}
1.1	108.68	2.829	0.503	0.104	0	0.0309	0
2.1	103.18	9.717	2.229	0.924	0.182	0.1938	0.0191
2.2	90.96	7.699	1.751	0.651	0	0.1759	0
2.3	79.01	7.921	1.899	0.596	0	0.1505	0
2.4	98.19	5.217	1.003	0.322	0.064	0.0741	0.0108
2.5	75.28	8.191	1.987	0.817	0	0.2164	0

	$\bar{v}_{85}$	$\sigma_{v_{85}}$	R_a	$E_{a,10}$	$E_{a,20}$	L_{10}	L_{20}
2.6	96.74	6.117	1.385	0.334	0	0.1049	0
2.7	83.47	7.505	1.819	0.699	0	0.2203	0
2.8	100.90	6.458	1.482	0.356	0	0.0906	0
2.9	82.99	4.836	1.198	0	0	0	0
2.10	91.24	11.41	2.651	2.009	0	0.4663	0
3.1	96.51	8.962	2.101	1.199	0.153	0.3279	0.0269
3.2	83.34	7.851	1.690	0.920	0	0.2536	0
3.3	92.36	12.88	3.253	2.540	0.236	0.5861	0.0414
3.4	95.34	6.193	1.332	0.592	0	0.1755	0
3.5	84.87	3.918	0.946	0	0	0	0
3.6	88.23	10.92	2.543	1.716	0.134	0.4034	0.0195
4.1	105.93	6.192	1.112	0.448	0.155	0.0962	0.0254
4.2	73.37	7.912	1.867	0.889	0	0.2456	0
4.3	84.40	11.00	2.703	1.679	0	0.4047	0
4.4	107.23	5.119	1.021	0.311	0.019	0.0773	0.0034
4.5	74.94	6.767	1.431	0.559	0.012	0.1426	0.0021
4.6	95.91	4.193	0.831	0.183	0	0.0460	0
5.1	98.34	12.00	2.867	1.976	0.630	0.4653	0.0956
5.2	76.81	8.652	1.994	1.068	0	0.2917	0
6.1	62.48	6.323	1.318	0.370	0.070	0.0872	0.0102
7.1	108.55	2.782	0.458	0.042	0.031	0.0060	0.0032
7.2	107.06	2.727	0.630	0	0	0	0
8.1	65.19	8.166	1.847	0.765	0.208	0.1979	0.0320
9.1	62.80	8.944	1.982	0.791	0.250	0.1725	0.0352
9.2	80.93	12.40	2.827	2.162	0.873	0.4553	0.1443
9.3	64.22	9.450	2.315	1.396	0.118	0.3829	0.0206
9.4	73.05	12.51	2.866	2.178	0.679	0.4735	0.0994
9.5	63.07	8.174	1.860	0.586	0.069	0.1432	0.0120
10.1	70.26	12.18	2.806	1.908	0.632	0.4171	0.0862
10.2	57.78	2.591	0.676	0	0	0	0
10.3	64.87	9.001	2.159	0.776	0.263	0.1737	0.0406
10.4	67.85	7.303	1.690	0.776	0	0.2360	0
11.1	74.13	12.11	2.959	2.206	0.254	0.5044	0.0449
11.2	63.76	7.393	1.678	0.457	0.137	0.1083	0.0234
11.3	78.69	7.851	1.728	0.727	0.113	0.1813	0.0175
12.1	69.67	11.44	2.795	2.138	0	0.5281	0
12.2	63.27	8.868	2.133	1.211	0	0.3451	0
12.3	56.99	6.008	1.242	0.264	0.123	0.0530	0.0195
13.1	107.36	2.509	0.689	0	0	0	0
13.2	100.72	2.468	0.475	0	0	0	0
13.3	109.84	0.758	0.079	0	0	0	0
13.4	101.06	2.697	0.510	0	0	0	0
13.5	106.55	8.905	1.520	0.717	0.651	0.0997	0.0838
14.1	89.03	11.00	2.315	1.529	0.646	0.3327	0.0898
14.2	106.00	4.975	1.088	0.284	0	0.0842	0
14.3	89.88	7.869	1.789	0.729	0.142	0.1941	0.0223
14.4	77.99	9.525	2.088	1.162	0.385	0.2696	0.0683
15.1	100.58	7.565	1.688	0.428	0.093	0.0974	0.0101
16.1	84.61	9.100	2.027	0.996	0.282	0.2357	0.0452
16.2	69.62	10.77	2.370	1.477	0.456	0.3309	0.0608
16.3	81.31	10.28	2.245	1.392	0.448	0.3185	0.0687
17.1	94.02	11.93	2.838	1.951	0.613	0.4402	0.0958

	$\bar{v}_{85}$	$\sigma_{v_{85}}$	R_a	$E_{a,10}$	$E_{a,20}$	L_{10}	L_{20}
18.1	77.84	10.83	2.592	1.798	0.079	0.4386	0.0130
19.1	68.55	9.451	2.192	1.204	0.225	0.3116	0.0352
19.2	86.51	8.853	1.989	1.076	0.144	0.2749	0.0253
20.1	72.32	12.08	2.721	1.863	0.675	0.3917	0.0988
20.2	63.81	6.782	1.502	0.457	0	0.1184	0
21.1	68.28	10.86	2.331	1.578	0.644	0.3408	0.0990
21.2	96.45	13.56	3.362	3.099	0.610	0.8018	0.0815
21.3	68.59	9.806	2.211	1.289	0.111	0.3046	0.0191
21.4	76.75	8.334	2.007	0.845	0.019	0.2365	0.0032
23.1	99.98	8.358	1.618	0.682	0.603	0.1150	0.0960
24.1	96.89	12.32	2.862	2.059	0.627	0.4692	0.0806
24.2	88.33	8.020	1.759	0.568	0	0.1215	0
24.3	103.48	7.604	1.584	0.500	0.445	0.0894	0.0761
25.1	94.33	11.18	2.577	1.259	0.691	0.2535	0.0956
27.1	98.69	8.212	1.671	0.635	0.555	0.1171	0.0978
28.1	92.52	9.457	2.223	1.352	0.262	0.3412	0.0462
28.2	79.84	8.131	1.827	0.849	0.092	0.2252	0.0155
28.3	76.27	5.921	1.377	0.266	0	0.0638	0
30.1	99.04	6.515	1.600	0	0	0	0
30.2	109.58	1.796	0.215	0.031	0	0.0094	0
30.3	99.98	7.929	2.082	0.985	0	0.3486	0
31.1	97.37	8.331	1.971	0.974	0	0.2813	0
31.2	88.53	9.956	2.125	1.493	0.349	0.3701	0.0492
32.1	88.66	9.060	2.005	1.185	0	0.3006	0
32.2	72.18	9.903	2.198	1.247	0.338	0.2922	0.0514
33.1	85.56	11.66	2.618	1.871	0.655	0.4002	0.1030
33.2	69.04	7.508	1.561	0.735	0.104	0.1844	0.0170
33.3	83.78	9.122	2.013	0.984	0.352	0.2319	0.0574
33.4	93.47	12.23	3.027	2.365	0.418	0.5900	0.0628
33.5	75.12	11.44	2.696	1.864	0.434	0.4346	0.0715
33.6	106.10	3.030	0.657	0	0	0	0
33.7	94.34	6.922	1.440	0.443	0	0.095	0
34.1	93.66	7.229	1.779	0.605	0	0.1893	0
34.2	103.41	5.846	1.369	0.388	0	0.1110	0
34.3	86.03	5.115	0.954	0.298	0.035	0.0754	0.0048
35.1	105.76	5.294	1.183	0.314	0	0.1010	0
35.2	96.62	6.342	1.430	0.461	0	0.1399	0
35.3	103.17	6.123	1.415	0.293	0	0.0815	0
36.1	89.79	10.37	2.382	1.737	0.206	0.4370	0.0306
36.2	106.41	5.699	1.098	0.464	0	0.1155	0
37.1	94.79	9.838	2.244	1.364	0.256	0.3406	0.0303
38.1	105.25	6.132	1.293	0.341	0	0.0694	0
39.1	63.16	6.516	1.316	0.455	0.082	0.1092	0.0134
40.1	96.29	8.815	2.133	1.134	0.059	0.3214	0.0096
41.1	91.26	10.16	2.412	1.690	0.123	0.4433	0.0202
42.1	91.51	9.019	2.230	1.114	0.048	0.2996	0.0081
42.3	56.52	3.864	0.929	0	0	0	0
42.4	65.63	8.705	1.888	1.025	0.084	0.2600	0.0138
42.5	69.81	8.359	1.938	0.741	0.151	0.1883	0.024
43.1	73.75	8.79	2.131	0.895	0.057	0.2379	0.0086
43.2	97.75	9.683	2.307	1.300	0.157	0.3361	0.0269
43.3	78.77	10.22	2.421	1.499	0.117	0.3716	0.0180
43.4	61.80	6.120	1.433	0.578	0	0.1882	0

	$\bar{v}_{85}$	$\sigma_{v_{85}}$	R_a	$E_{a,10}$	$E_{a,20}$	L_{10}	L_{20}
43.5	80.14	8.833	2.070	0.957	0.133	0.2407	0.0219
43.6	105.66	10.02	1.827	0.836	0.630	0.1239	0.0742
44.1	88.48	11.94	2.770	2.027	0.441	0.4537	0.0682
44.2	83.94	8.574	1.949	0.967	0	0.2491	0
44.3	99.59	6.688	1.288	0.299	0.128	0.0629	0.0136
45.1	106.87	6.626	1.051	0.311	0.233	0.0459	0.0265
45.2	96.90	9.562	2.051	1.090	0.281	0.2709	0.0311
46.1	65.28	11.45	2.403	1.699	0.650	0.3741	0.0847
46.2	76.45	8.743	1.862	0.974	0.209	0.2237	0.0358
46.3	63.85	8.446	1.964	0.737	0	0.1834	0
47.1	86.76	10.82	2.410	1.744	0.531	0.4154	0.0873
48.1	56.62	3.447	0.822	0	0	0	0
49.1	101.28	5.065	1.128	0.136	0	0.0380	0
49.2	76.26	12.30	3.112	2.497	0	0.6086	0
50.1	98.01	12.48	3.062	2.732	0.657	0.7052	0.1026
50.2	97.52	8.046	1.912	0.798	0	0.2214	0
50.3	84.65	9.011	2.030	1.453	0	0.3994	0
50.4	99.04	11.25	2.733	1.463	0.497	0.3572	0.0731
50.5	106.22	4.777	1.069	0.137	0.023	0.0332	0.0038
50.6	92.47	7.615	1.735	0.658	0	0.1633	0
51.1	98.80	7.342	1.721	0.464	0.046	0.1365	0.0051
52.1	90.50	8.601	1.627	0.879	0.454	0.2008	0.0623
53.1	102.19	6.232	1.382	0.386	0	0.1021	0
55.1	66.24	8.299	1.870	0.829	0.139	0.2127	0.0209
55.2	99.49	8.465	2.050	1.116	0.003	0.3256	0.0006
56.1	90.33	8.856	1.919	1.025	0.222	0.2522	0.0333
56.2	78.50	7.276	1.741	0.738	0	0.2307	0
57.1	84.17	10.06	2.202	1.312	0.473	0.3010	0.0741
58.1	84.22	7.481	1.712	0.657	0	0.1849	0
58.2	73.40	2.944	0.666	0	0	0	0
59.1	75.57	11.60	2.803	2.032	0.298	0.4853	0.0477
59.2	66.41	7.769	1.897	0.644	0	0.1917	0
59.3	83.13	8.774	2.135	0.900	0	0.2405	0
59.4	64.27	3.291	0.835	0.015	0	0.0051	0
60.1	72.22	8.857	1.981	0.791	0.085	0.1877	0.0091
60.2	64.41	7.275	1.583	0.602	0.033	0.1660	0.0055
61.1	104.54	6.333	1.077	0.266	0.216	0.0379	0.0241
61.2	95.30	10.64	2.345	1.216	0.379	0.2731	0.0434
62.1	102.04	6.745	1.328	0.554	0	0.1227	0
63.1	88.11	11.83	2.671	2.021	0.463	0.4613	0.0639
64.1	95.40	11.51	2.479	1.482	0.851	0.3123	0.1194
65.1	67.43	8.245	1.843	1.014	0	0.2737	0

Table 35. Operational global parameters for all road segments.

	$\overline{\Delta v_{85}}$	$\bar{d}_{85}$	$\sigma_{\Delta v_{85}}$	$\sigma_{d_{85}}$	$\bar{L}_{\Delta v_{85}}$	L_d	N
1.1	9.045	0.5523	6.017	0.1246	119	0.0421	7
2.1	11.267	0.7620	10.835	0.2315	105.5	0.0842	4
2.2	11.227	0.9003	9.548	0.1298	84.42	0.1947	33
2.3	8.473	1.0767	9.018	0.1314	52	0.1526	7

	$\overline{\Delta v_{85}}$	$\bar{d}_{85}$	$\sigma_{\Delta v_{85}}$	$\sigma_{d_{85}}$	$\bar{L}_{\Delta v_{85}}$	L_d	N
2.4	8.066	1.0181	11.162	0.8397	38.66	0.1048	3
2.5	9.179	1.2791	8.005	0.6082	38.71	0.1300	7
2.6	11.477	0.8116	6.188	0.1110	100.93	0.2010	15
2.7	8.753	1.0088	7.962	0.1729	53.5	0.1331	6
2.8	9.478	0.6772	6.056	0.2155	99	0.2761	4
2.9	6.940	1.0148	3.964	0.1022	43.14	0.1436	7
2.10	13.441	0.9310	7.888	0.1794	100.25	0.120	4
3.1	10.380	0.819	9.753	0.2058	86	0.1261	15
3.2	7.711	0.9839	6.921	0.1732	49.31	0.1498	29
3.3	7.813	0.9924	6.369	0.2048	54.05	0.1466	18
3.4	9.590	0.7910	8.860	0.2038	77.75	0.1902	8
3.5	5.332	0.9362	4.555	0.0302	38	0.0962	5
3.6	10.218	0.8658	7.957	0.2332	79.21	0.2142	19
4.1	27.300	1.019	0	0	199	0.085	1
4.2	13.689	1.4038	10.690	0.3412	52.28	0.1880	14
4.3	12.389	1.0544	12.279	0.2714	71.4	0.1775	10
4.4	18.395	0.7748	6.688	0.1083	180.5	0.1139	2
4.5	6.843	1.2136	6.161	0.2142	32.76	0.1519	13
4.6	15.355	1.3573	0	0	76	0.0364	1
5.1	10.845	0.7389	11.405	0.4419	93.5	0.1184	6
5.2	11.558	1.3486	8.963	0.1478	53.5	0.1719	10
6.1	8.145	1.9540	8.934	0.5651	19.41	0.132	53
7.1	3.657	0.4271	2.035	0.0608	68	0.0651	30
7.2	3.726	0.4639	2.647	0.0511	63.84	0.0595	13
8.1	7.745	1.8882	7.177	0.6590	19.54	0.1034	48
9.1	8.025	2.1315	8.852	0.6211	18.54	0.1099	61
9.2	15.472	1.7019	11.253	0.5430	57.8	0.3001	10
9.3	11.039	2.0796	9.278	0.9612	22.84	0.1460	13
9.4	13.160	1.6894	13.266	0.6926	44.21	0.1619	14
9.5	6.932	2.1329	7.022	0.5328	17.86	0.1294	30
10.1	10.900	1.9012	11.874	0.4574	26.48	0.1071	25
10.2	3.557	2.1425	2.816	0.4967	6.84	0.0364	13
10.3	10.953	2.0960	9.406	0.6262	32.85	0.143	7
10.4	10.283	1.7920	7.934	0.5044	31	0.1373	29
11.1	12.913	1.7611	10.895	0.7044	40.58	0.1389	17
11.2	7.723	1.9091	7.082	0.4023	21.05	0.1511	34
11.3	13.589	1.2363	12.017	0.3011	63.66	0.272	9
12.1	9.632	1.9130	10.009	0.6781	27.32	0.1641	25
12.2	8.819	2.2407	8.914	0.8171	17.46	0.1135	26
12.3	4.836	2.3083	5.833	0.4968	10.46	0.0700	28
13.1	3.139	0.5696	0	0	44	0.0111	1
13.2	2.781	0.5515	2.675	0.0408	42.2	0.0795	5
13.3	5.723	0.5700	0	0	83	0.023	1
13.4	4.893	0.5972	3.351	0.0341	66.75	0.1339	4
13.5	5.482	0.4404	0	0	103	0.0171	1
14.1	21.167	1.3850	17.663	0.6937	78.25	0.1445	8
14.2	10.096	0.6620	8.170	0.1276	109.28	0.1297	7
14.3	12.186	0.9643	9.116	0.2836	78.69	0.2246	13
14.4	12.441	1.2735	7.606	0.3323	55.53	0.228	15
15.1	5.7949	0.6381	4.887	0.0877	68.18	0.0826	11
16.1	19.971	1.192	8.811	0.2099	106.36	0.1968	11
16.2	12.563	1.7661	11.541	0.4046	43.4	0.1641	10
16.3	16.581	1.2821	12.504	0.3961	75.59	0.2187	37

	$\overline{\Delta v_{85}}$	$\bar{d}_{85}$	$\sigma_{\Delta v_{85}}$	$\sigma_{d_{85}}$	$\bar{L}_{\Delta v_{85}}$	L_d	N
17.1	18.724	0.9590	10.404	0.3423	131.3	0.1680	10
18.1	13.445	1.5255	8.426	0.5330	55.17	0.1485	28
19.1	12.092	1.7744	12.186	0.3203	35.88	0.149	25
19.2	13.667	1.0480	11.218	0.2763	78.04	0.2100	21
20.1	12.307	1.7893	9.859	0.4470	41.21	0.2299	32
20.2	8.602	2.0318	6.285	0.4405	21.1	0.1665	30
21.1	9.164	1.8667	9.219	0.7000	27.80	0.1403	21
21.2	14.267	1.1185	14.696	0.8662	65.3	0.1137	10
21.3	9.541	1.8648	8.308	0.6136	29.36	0.2634	22
21.4	10.423	1.3648	8.132	0.3398	43.22	0.160	18
23.1	4.730	0.5723	3.380	0.0768	62	0.1368	10
24.1	12.883	0.8438	4.294	0.2161	114	0.1061	3
24.2	14.448	0.9872	8.130	0.0248	101	0.202	4
24.3	4.842	0.5174	3.469	0.1200	73.83	0.0597	6
25.1	7.271	0.7058	8.979	0.1243	73.33	0.0877	3
27.1	7.529	0.6272	6.683	0.1024	85.5	0.0758	4
28.1	6.595	0.8685	5.898	0.3186	47	0.0877	4
28.2	11.568	1.1735	9.475	0.1940	60	0.2254	15
28.3	6.124	1.0346	6.639	0.3030	30.57	0.1484	7
30.1	6.036	0.6658	3.216	0.0153	68.75	0.0656	4
30.2	10.507	0.7453	2.735	0.1298	113	0.0299	2
30.3	10.021	0.7039	7.985	0.2334	93	0.0906	3
31.1	13.653	0.8506	7.871	0.1449	110.62	0.2133	8
31.2	7.674	0.8915	5.168	0.1515	57.77	0.1968	9
32.1	9.542	0.9348	10.513	0.3305	57.09	0.2001	22
32.2	10.980	1.5289	8.893	0.3919	41.42	0.1900	107
33.1	19.817	1.3286	13.770	0.2703	93	0.1819	10
33.2	7.040	1.5699	5.038	0.5502	23.66	0.1644	24
33.3	9.878	1.0735	9.412	0.1976	57.07	0.1961	14
33.4	16.557	0.9965	13.059	0.3981	102.9	0.1702	10
33.5	21.590	1.6861	11.577	0.3704	79.33	0.4204	6
33.6	4.044	0.4888	3.013	0.0787	63.5	0.0787	26
33.7	7.310	0.6793	4.619	0.2306	69.25	0.1124	8
34.1	6.975	0.7448	7.448	0.1638	64.28	0.1808	14
34.2	3.743	0.4883	5.261	0.2087	40.57	0.1044	19
34.3	4.675	0.8602	5.301	0.0952	35.6	0.1148	30
35.1	6.225	0.5292	5.600	0.1463	81.8	0.0837	35
35.2	8.192	0.7839	7.321	0.1038	72.26	0.1273	15
35.3	8.019	0.6271	5.428	0.1245	93.11	0.1118	26
36.1	13.213	0.9171	11.353	0.3093	85.33	0.1328	9
36.2	13.449	0.7546	4.474	0.0015	135	0.0446	2
37.1	3.013	0.7963	0	0	26	0.0119	1
38.1	6.925	0.5441	4.408	0.0967	97.9	0.0851	10
39.1	7.563	1.9588	7.231	0.5808	18.54	0.0940	64
40.1	13.725	0.9232	8.681	0.1414	101.62	0.1395	16
41.1	11.105	0.9216	7.444	0.2008	82.48	0.1709	25
42.1	16.439	1.1910	10.278	0.2551	89.16	0.1276	6
42.3	3.171	1.8120	2.952	0.9473	6.3	0.0345	10
42.4	8.315	1.8113	7.377	0.5949	24.07	0.1473	27
42.5	12.349	1.7265	9.369	0.3598	39.07	0.1617	27
43.1	7.114	2.5246	6.950	6.0840	32.84	0.1585	25
43.2	9.217	0.8041	9.260	0.2631	68.48	0.1600	25

	$\overline{\Delta v_{85}}$	$\bar{d}_{85}$	$\sigma_{\Delta v_{85}}$	$\sigma_{d_{85}}$	$\bar{L}_{\Delta v_{85}}$	L_d	N
43.3	13.113	1.2769	7.383	0.2694	65.26	0.1785	19
43.4	5.797	1.7142	6.092	0.3869	16.8	0.0890	10
43.5	10.810	1.2038	9.459	0.1978	55.53	0.1439	15
43.6	18.576	1.0907	16.180	0.0291	122.33	0.0614	3
44.1	9.627	1.2194	9.642	1.0543	64.22	0.1519	22
44.2	13.601	1.1108	9.505	0.2194	76.64	0.2166	25
44.3	5.429	0.6702	5.989	0.1526	54.84	0.0792	13
45.1	4.583	0.4761	5.843	0.1628	62.5	0.0705	6
45.2	13.629	0.7406	8.892	0.1705	125.33	0.1953	6
46.1	10.983	2.1538	11.893	0.6189	27.87	0.2082	49
46.2	14.600	1.7396	8.527	0.7049	57.33	0.2173	15
46.3	7.948	1.8470	8.084	0.6236	20.91	0.1104	34
47.1	9.132	0.8622	8.803	0.2622	62.6	0.1747	10
48.1	3.542	2.1809	2.841	0.3301	6.77	0.0475	9
49.1	5.477	0.6138	5.040	0.1338	64.83	0.1423	18
49.2	7.324	1.2231	4.815	0.4405	40.72	0.1467	18
50.1	7.519	0.9364	6.147	0.2203	55.69	0.0995	13
50.2	13.626	0.8906	8.140	0.1251	106.64	0.1606	14
50.3	6.402	0.9585	6.161	0.1800	44.92	0.1348	14
50.4	15.036	0.9757	10.644	0.2089	103.77	0.1291	9
50.5	10.493	0.7284	7.596	0.2887	104.83	0.0786	6
50.6	13.727	0.9334	9.750	0.0855	98.42	0.1827	7
51.1	6.675	0.6905	5.352	0.1299	70.25	0.1637	35
52.1	6.310	0.7734	6.188	0.1508	51.6	0.1030	5
53.1	7.972	0.6294	7.824	0.1889	85.07	0.1222	13
55.1	8.454	1.7125	7.421	0.5355	26.29	0.1505	104
55.2	13.356	0.8685	10.411	0.1697	105.62	0.1451	8
56.1	13.804	0.9710	11.647	0.3076	84.34	0.1963	23
56.2	9.2827	1.1853	6.182	0.1679	46.12	0.1498	8
57.1	10.983	1.0898	11.287	0.1900	60.18	0.1407	11
58.1	12.412	1.0477	7.256	0.1497	74.88	0.1512	9
58.2	7.734	1.3205	2.331	0.1619	33	0.1160	6
59.1	14.799	1.4769	12.808	0.5789	58.64	0.1693	17
59.2	7.024	1.6422	5.713	0.3188	24.90	0.1347	11
59.3	17.540	1.3330	10.762	0.2917	90	0.2311	6
59.4	4.836	1.6375	5.119	0.1872	13.87	0.0821	8
60.1	10.744	1.7678	8.540	0.5513	29.27	0.1340	18
60.2	7.201	1.7906	6.914	0.6584	19.25	0.1256	51
61.1	4.654	0.5003	4.978	0.1354	63.16	0.1093	25
61.2	5.339	0.6398	5.044	0.2048	53.83	0.2337	12
62.1	8.809	0.6155	10.665	0.1893	91	0.0583	4
63.1	21.740	1.2930	18.541	0.1463	114.33	0.1396	3
64.1	7.779	0.6783	6.773	0.1172	80.71	0.1729	7
65.1	9.271	1.7983	7.813	0.6052	25.52	0.1347	25

Table 36. Operational local parameters for all road segments.

Some operational parameters refer to the same phenomenon, such as R_a and the speed dispersion. Hence, they should not be considered together in the same analysis and a correlational analysis was performed for all operational parameters (Table 37).

	CCR	$\bar{v}_{85}$	$\sigma_{v_{85}}$	R_a	$E_{a,10}$	$E_{a,20}$	L_{10}	L_{20}	$\overline{\Delta v_{85}}$	$\bar{d}_{85}$	$\sigma_{\Delta v_{85}}$	$\sigma_{d_{85}}$	$\bar{L}_{\Delta v_{85}}$	L_d	N
C		-0.871	-0.023	0.002	-0.052	-0.098	-0.044	-0.090	-0.187	-0.869	0.029	0.236	-0.750	0.013	0.428
$\bar{v}_{85}$	-0.871		-0.200	-0.232	-0.150	0.027	-0.162	0.006	0.006	0.918	-0.218	-0.286	0.802	-0.259	-0.449
$\sigma_{v_{85}}$	-0.023	-0.200		0.980	0.929	0.659	0.898	0.658	0.501	-0.213	0.644	0.165	0.028	0.481	0.119
R_a	0.002	-0.232	0.980		0.939	0.567	0.928	0.574	0.479	-0.237	0.631	0.185	-0.016	0.484	0.108
$E_{a,10}$	-0.052	-0.150	0.929	0.939		0.608	0.985	0.616	0.486	-0.185	0.577	0.149	0.035	0.405	0.063
$E_{a,20}$	-0.098	0.027	0.659	0.567	0.608		0.502	0.991	0.301	-0.042	0.385	0.036	0.099	0.168	-0.016
L_{10}	-0.044	-0.162	0.898	0.928	0.985	0.502		0.513	0.478	-0.188	0.565	0.157	0.022	0.412	0.071
L_{20}	-0.090	0.006	0.658	0.574	0.616	0.991	0.513		0.307	-0.056	0.385	0.043	0.082	0.200	-0.009
$\overline{\Delta v_{85}}$	-0.187	0.006	0.501	0.479	0.486	0.301	0.478	0.307		-0.132	0.662	0.033	0.493	0.457	-0.081
$\bar{d}_{85}$	-0.869	0.918	-0.213	-0.237	-0.185	-0.042	-0.188	-0.056	-0.132		-0.274	-0.472	0.695	-0.172	-0.422
$\sigma_{\Delta v_{85}}$	0.029	-0.218	0.644	0.631	0.577	0.385	0.565	0.385	0.662	-0.274		0.160	0.080	0.501	0.125
$\sigma_{d_{85}}$	0.236	-0.286	0.165	0.185	0.149	0.036	0.157	0.043	0.033	-0.472	0.160		-0.243	0.115	0.172
$\bar{L}_{\Delta v_{85}}$	-0.750	0.802	0.028	-0.016	0.035	0.099	0.022	0.082	0.493	0.695	0.080	-0.243		0.008	-0.406
L_d	0.013	-0.259	0.481	0.484	0.405	0.168	0.411	0.200	0.456	-0.177	0.500	0.115	0.008		0.183
N	0.428	-0.449	0.119	0.108	0.063	-0.016	0.071	-0.009	-0.081	-0.422	0.125	0.172	-0.406	0.183	

Table 37. Correlation matrix among all operational parameters.

Table 37 shows the correlations between the different parameters. We can distinguish some groups of variables that are highly correlated (red), and some other with a mid-correlation (yellow). Figure 122 shows the resulting groups of correlated parameters.

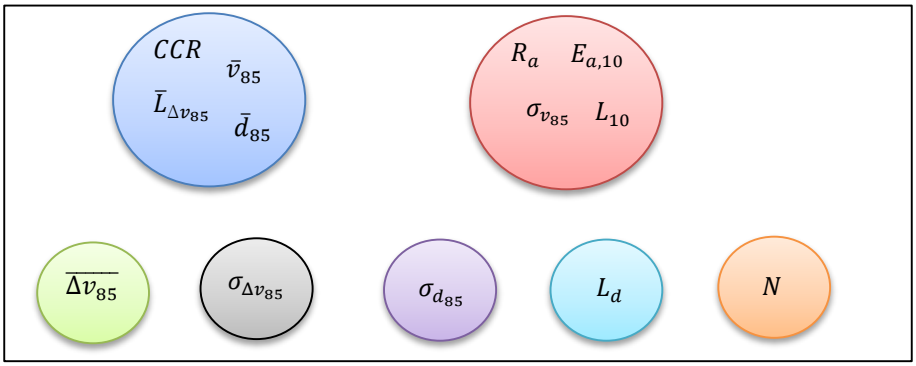

Figure 122. Groups of parameters.

At a first sight, the ideal situation would be to calibrate the consistency relationship to road accidents using only one parameter of each group. For the expressions that consider more than one parameter, these parameters should not belong to the same group. However, it was discovered that in some cases a good adjustment could be obtained by mixing two high correlated parameters. This can be explained because both parameters are different just where the difference is needed to provide a higher accuracy to the final model.

7.4. Calibration of the Consistency Parameter

A model is going to be calibrated considering one or two operational parameters. Three different subsets of data are considered: free, constrained and all road segments. This allows us to better determine the influence of the boundary conditions for the road segments.

7.4.1. Determination of the functional form

According to the statistic methods valid for count data, a negative binomial regression is performed. This is preferred rather than the Poisson distribution. In addition, it can perfectly handle overdispersion.

However, the Negative Binomial distribution is a generalized form of the Poisson distribution, with $\alpha = 0$, being α the overdispersion parameter.

The number of zeros should also be analyzed. If we had a large amount of zeros, the negative binomial distribution would not be appropriate. A Zero-Inflated Negative Binomial regression should be used instead. Figure 123 shows the frequency distribution for all accidents. As it can be seen, the amount of zeros is not too high, so a Negative Binomial regression is selected.

The program "R" is used for performing all statistical calibrations. The AIC (Akaike Information Criterion) is given in all regressions, as a measure of the goodness of fit. The overdispersion parameter is also given in the final models.

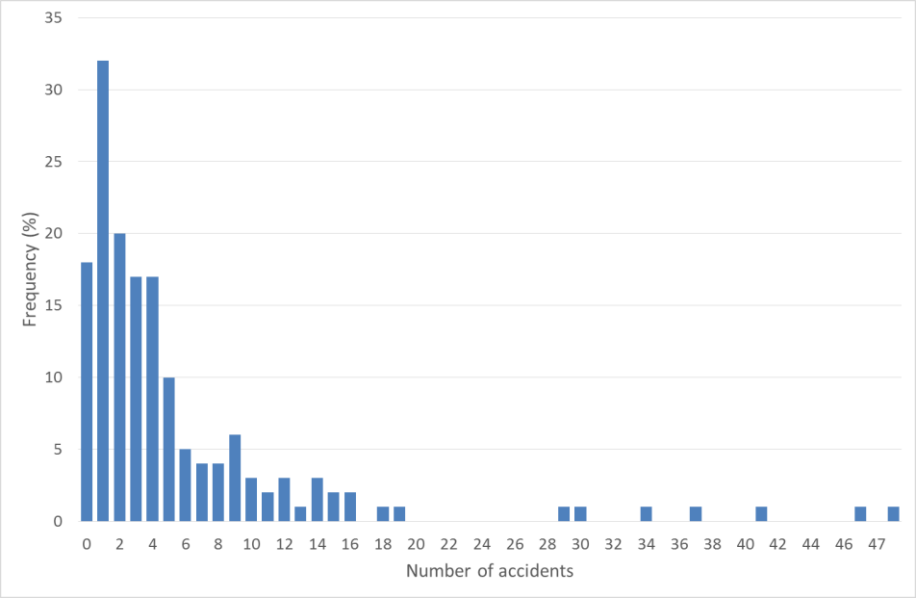

Figure 123. Distribution of the number of accidents.

7.4.2. Determination of the exposure influence

It is well known that accidents are highly affected by the exposure. Indeed, several previous researchers have developed safety performance functions that only depend on the exposure. A consistency parameter will be included in the safety performance function to be calibrated. In order to determine how the consistency parameter affects the result, a first calibration is performed only with the exposure. This will allow us to determine how the following consistency parameters affect the predictions, and if it is worth to consider them or not.

In all cases, the logarithm of the outcome is estimated with a linear combination of the predictors:

$$\ln(y_i) = \beta_0 + \beta_1 \cdot \ln L + \beta_2 \cdot \ln AADT \quad (347)$$

Thus, the final expression of the accidents in terms of exposure results as:

$$y_i = e^{\beta_0} \cdot L^{\beta_1} \cdot AADT^{\beta_2} \quad (348)$$

Where:

L: length of the road segment (km).
$AADT$: Average Annual Daily Traffic (vpd).

Table 38 shows the outcomes of the adjustment for free, constrained and all road segments.

Subset		β_0	β_1	β_2	AIC	α
		–	$\ln L$	$\ln AADT$		
All	Estimate	-4.16565	0.97389	0.61301	712.27	0.28555
	$\Pr(>\|z\|)$	$< 2 \cdot 10^{-16}$	$< 2 \cdot 10^{-16}$	$< 2 \cdot 10^{-16}$		
Free	Estimate	-5.5596	0.7370	0.8080	234.45	0.13316
	$\Pr(>\|z\|)$	$2.39 \cdot 10^{-10}$	$1.03 \cdot 10^{-7}$	$3.13 \cdot 10^{-12}$		
Constrained	Estimate	-3.65890	1.00638	0.55137	477.7	0.29789
	$\Pr(>\|z\|)$	$4.95 \cdot 10^{-10}$	$< 2 \cdot 10^{-16}$	$5.37 \cdot 10^{-15}$		

Table 38. Statistical adjustment – models only considering exposure.

We can see how all parameters are statistically significant, as expected. The length estimate is quite similar to 1 for all and constrained road segments. This indicates that the number of accidents is linearly affected by the length of the road segment under consideration. However, this is not true for free road segments, in which the higher the length, the lower the crash rate ($\beta_1 < 1$). This agrees with most of the previous research.

The AADT estimate is always ranging from 0 to 1. This indicates that a higher AADT results in lower crash rates. This agrees with most previous research.

The AIC results will be compared to those determined for the consistency models.

7.4.3. Calibration with one parameter

A first calibration with only one consistency parameter is performed. Each one of the operational parameters will serve us as the consistency term. Table 39 shows the estimates for the models calibrated with all operational parameters, one by one, considering all road segments. All parameters not statistically significant at a 95%

confidence level are highlighted in red. Table 40 and Table 41 show the same information for free and constrained road segments.

Parameter		β_0	β_1	β_2	β_3	AIC	α
		–	$\ln L$	$\ln AADT$	C		
CCR	Estimate	-5.2596612	1.0229543	0.7250004	0.0010109	707.16	0.2665
	$\Pr(>\|z\|)$	$< 2 \cdot 10^{-16}$	$< 2 \cdot 10^{-16}$	$< 2 \cdot 10^{-16}$	0.00507		
$\bar{v}_{85}$	Estimate	-3.77054	1.09419	0.80858	-0.02322	697.75	0.2328
	$\Pr(>\|z\|)$	$1.01 \cdot 10^{-15}$	$< 2 \cdot 10^{-16}$	$< 2 \cdot 10^{-16}$	$2.95 \cdot 10^{-5}$		
$\sigma_{v_{85}}$	Estimate	-4.87450	1.00084	0.64333	0.05347	709	0.2586
	$\Pr(>\|z\|)$	$< 2 \cdot 10^{-16}$	$< 2 \cdot 10^{-16}$	$< 2 \cdot 10^{-16}$	0.0208		
R_a	Estimate	-4.88365	1.00394	0.64700	0.22486	708.48	0.2562
	$\Pr(>\|z\|)$	$< 2 \cdot 10^{-16}$	$< 2 \cdot 10^{-16}$	$< 2 \cdot 10^{-16}$	0.0145		
$E_{a,10}$	Estimate	-4.60077	0.99307	0.63982	0.21017	708.96	0.2573
	$\Pr(>\|z\|)$	$< 2 \cdot 10^{-16}$	$< 2 \cdot 10^{-16}$	$< 2 \cdot 10^{-16}$	0.019		
$E_{a,20}$	Estimate	-4.20791	0.97814	0.61398	0.16215	713.9	0.2836
	$\Pr(>\|z\|)$	$< 2 \cdot 10^{-16}$	$< 2 \cdot 10^{-16}$	$< 2 \cdot 10^{-16}$	0.546		
L_{10}	Estimate	-4.58400	0.98974	0.63965	0.81590	709.68	0.2606
	$\Pr(>\|z\|)$	$< 2 \cdot 10^{-16}$	$< 2 \cdot 10^{-16}$	$< 2 \cdot 10^{-16}$	0.0287		
L_{20}	Estimate	-4.21671	0.97814	0.61454	1.25313	713.79	0.2828
	$\Pr(>\|z\|)$	$< 2 \cdot 10^{-16}$	$< 2 \cdot 10^{-16}$	$< 2 \cdot 10^{-16}$	0.49		
$\overline{\Delta v_{85}}$	Estimate	-4.54928	0.99114	0.63181	0.02175	712.08	0.2714
	$\Pr(>\|z\|)$	$< 2 \cdot 10^{-16}$	$< 2 \cdot 10^{-16}$	$< 2 \cdot 10^{-16}$	0.130		
$\bar{d}_{85}$	Estimate	-6.81776	1.08378	0.83601	-0.72692	694.57	0.2232
	$\Pr(>\|z\|)$	$< 2 \cdot 10^{-16}$	$< 2 \cdot 10^{-16}$	$< 2 \cdot 10^{-16}$	$3.29 \cdot 10^{-6}$		
$\sigma_{\Delta v_{85}}$	Estimate	-4.81451	0.98276	0.65601	0.03952	709.88	0.2682
	$\Pr(>\|z\|)$	$< 2 \cdot 10^{-16}$	$< 2 \cdot 10^{-16}$	$< 2 \cdot 10^{-16}$	0.0318		
$\sigma_{d_{85}}$	Estimate	-4.44833	0.97826	0.63874	0.22905	709.46	0.2681
	$\Pr(>\|z\|)$	$< 2 \cdot 10^{-16}$	$< 2 \cdot 10^{-16}$	$< 2 \cdot 10^{-16}$	0.0172		
$\bar{L}_{\Delta v_{85}}$	Estimate	-4.263719	0.991764	0.657077	-0.003949	710.92	0.2786
	$\Pr(>\|z\|)$	$< 2 \cdot 10^{-16}$	$< 2 \cdot 10^{-16}$	$< 2 \cdot 10^{-16}$	0.067		
L_d	Estimate	-4.64714	0.99224	0.64154	1.74170	711.97	0.2718
	$\Pr(>\|z\|)$	$7.57 \cdot 10^{-16}$	$< 2 \cdot 10^{-16}$	$< 2 \cdot 10^{-16}$	0.112		
N	Estimate	-4.905256	0.780094	0.706399	0.012243	707.04	0.2572
	$\Pr(>\|z\|)$	$< 2 \cdot 10^{-16}$	$8.74 \cdot 10^{-13}$	$< 2 \cdot 10^{-16}$	0.00777		

Table 39. Estimates for all road segments.

Adding a consistency parameter does not always improve the safety performance function. Table 39 shows in red those parameters which clearly are not statistically significant ($\Pr(>|z|)$ higher than 0.05). We can observe how in most of these cases, the model is even worse than the one predicted only considering exposure parameters (*AIC* higher than 712.27). There are two parameters that are clearly related to road accidents (their $\Pr(>|z|)$ is clearly lower than 0.05 and their corresponding model present the lowest *AIC* values). These parameters are the average operating speed and the average deceleration rate. We can also observe that their overdispersion parameters are lower than in other cases.

Parameter		β_0	β_1	β_2	β_3	AIC	α
		–	$\ln L$	$\ln AADT$	C		
CCR	Estimate	-6.631065	0.851248	0.909525	0.001157	232.04	0.1053
	Pr(> |z|)	$2.22 \cdot 10^{-11}$	$4.54 \cdot 10^{-9}$	$7.70 \cdot 10^{-14}$	0.0275		
$\bar{v}_{85}$	Estimate	-5.156144	0.913649	0.980499	-0.021021	230.8	0.0857
	Pr(> |z|)	$1.57 \cdot 10^{-9}$	$1.37 \cdot 10^{-9}$	$2.98 \cdot 10^{-14}$	0.013		
$\sigma_{v_{85}}$	Estimate	-6.48090	0.75908	0.88819	0.04066	235.28	0.1179
	Pr(> |z|)	$9.29 \cdot 10^{-8}$	$2.79 \cdot 10^{-8}$	$8.42 \cdot 10^{-11}$	0.26		
R_a	Estimate	-6.2434	0.7502	0.8691	0.1264	235.73	0.1225
	Pr(> |z|)	$1.31 \cdot 10^{-7}$	$4.35 \cdot 10^{-8}$	$1.66 \cdot 10^{-10}$	0.375		
$E_{a,10}$	Estimate	-5.68251	0.73825	0.82081	0.03218	236.41	0.1321
	Pr(> |z|)	$1.93 \cdot 10^{-7}$	$9.68 \cdot 10^{-8}$	$1.04 \cdot 10^{-9}$	0.846		
$E_{a,20}$	Estimate	-5.1568	0.7207	0.7660	-0.9263	234.63	0.1140
	Pr(> |z|)	$1.17 \cdot 10^{-8}$	$8.71 \cdot 10^{-8}$	$6.14 \cdot 10^{-11}$	0.177		
L_{10}	Estimate	-5.57375	0.73706	0.80945	0.01469	236.45	0.1332
	Pr(> |z|)	$4.22 \cdot 10^{-7}$	$1.03 \cdot 10^{-7}$	$2.37 \cdot 10^{-9}$	0.983		
L_{20}	Estimate	-5.1634	0.7208	0.7667	-5.7771	234.82	0.1149
	Pr(> |z|)	$1.34 \cdot 10^{-8}$	$9.25 \cdot 10^{-8}$	$7.03 \cdot 10^{-11}$	0.199		
$\overline{\Delta v_{85}}$	Estimate	-5.689924	0.745747	0.815948	0.006053	236.38	0.1289
	Pr(> |z|)	$1.34 \cdot 10^{-8}$	$1.24 \cdot 10^{-7}$	$8.72 \cdot 10^{-12}$	0.783		
$\bar{d}_{85}$	Estimate	-7.4849	0.8956	0.9586	-0.6084	232.3	0.1093
	Pr(> |z|)	$2.43 \cdot 10^{-9}$	$1.46 \cdot 10^{-8}$	$5.40 \cdot 10^{-13}$	0.0351		
$\sigma_{\Delta v_{85}}$	Estimate	-6.78255	0.76373	0.91413	0.05256	234.1	0.1055
	Pr(> |z|)	$6.41 \cdot 10^{-9}$	$1.23 \cdot 10^{-8}$	$4.80 \cdot 10^{-12}$	0.113		
$\sigma_{d_{85}}$	Estimate	-6.4790	0.7728	0.9034	0.6842	235.29	0.1328
	Pr(> |z|)	$1.62 \cdot 10^{-7}$	$6.95 \cdot 10^{-8}$	$7.82 \cdot 10^{-10}$	0.276		
$\bar{L}_{\Delta v_{85}}$	Estimate	-5.544843	0.747961	0.824520	-0.002145	235.97	0.1361
	Pr(> |z|)	$2.91 \cdot 10^{-10}$	$1.03 \cdot 10^{-7}$	$3.13 \cdot 10^{-12}$	0.494		
L_d	Estimate	-6.2227	0.7910	0.8526	1.8367	235.13	0.1071
	Pr(> |z|)	$7.57 \cdot 10^{-10}$	$2.00 \cdot 10^{-8}$	$4.75 \cdot 10^{-13}$	0.217		
N	Estimate	-6.49767	0.54443	0.90899	0.02520	233.06	0.1163
	Pr(> |z|)	$7.77 \cdot 10^{-11}$	0.0013	$4.57 \cdot 10^{-13}$	0.0603		

Table 40. Estimates for free road segments.

When examining free road segments, this effect is even more dramatic. All but three parameters are not eligible due to their low significance in their corresponding models. The other three parameters are *CCR* (a geometric one) and those two indicated for all road segments: average deceleration rate and average operating speed. These parameters hardly enhance the exposure-only model, since the *AIC* goes from 234.45 to 230.80 for the average operating speed model.

Parameter		β_0	β_1	β_2	β_3	AIC	α
		–	$\ln L$	$\ln AADT$	C		
CCR	Estimate	-4.4255976	1.0280685	0.6311256	0.0006884	477.89	0.2923
	Pr(> |z|)	$6.71 \cdot 10^{-8}$	$< 2 \cdot 10^{-16}$	$7.84 \cdot 10^{-12}$	0.156		
$\bar{v}_{85}$	Estimate	-3.416705	1.110393	0.742510	-0.021276	471.38	0.2578
	Pr(> |z|)	$2.62 \cdot 10^{-9}$	$< 2 \cdot 10^{-16}$	$8.74 \cdot 10^{-15}$	0.00311		
$\sigma_{v_{85}}$	Estimate	-4.57360	1.07050	0.58012	0.06990	474.83	0.2538
	Pr(> |z|)	$1.80 \cdot 10^{-10}$	$< 2 \cdot 10^{-16}$	$< 2 \cdot 10^{-16}$	0.028		
R_a	Estimate	-4.66454	1.08446	0.58732	0.32074	473.08	0.2439
	Pr(> |z|)	$2.05 \cdot 10^{-11}$	$< 2 \cdot 10^{-16}$	$< 2 \cdot 10^{-16}$	0.00893		
$E_{a,10}$	Estimate	-4.2861	1.0706	0.5799	0.3067	472.34	0.2433
	Pr(> |z|)	$3.66 \cdot 10^{-12}$	$< 2 \cdot 10^{-16}$	$< 2 \cdot 10^{-16}$	0.00555		
$E_{a,20}$	Estimate	-3.75117	1.02325	0.55315	0.25024	479.08	0.2931
	Pr(> |z|)	$3.22 \cdot 10^{-10}$	$< 2 \cdot 10^{-16}$	$3.74 \cdot 10^{-15}$	0.431		
L_{10}	Estimate	-4.27334	1.06566	0.57967	1.26371	472.44	0.2451
	Pr(> |z|)	$3.73 \cdot 10^{-12}$	$< 2 \cdot 10^{-16}$	$< 2 \cdot 10^{-16}$	0.00571		
L_{20}	Estimate	-3.76157	1.02320	0.55365	1.89543	478.92	0.2915
	Pr(> |z|)	$2.88 \cdot 10^{-10}$	$< 2 \cdot 10^{-16}$	$3.27 \cdot 10^{-15}$	0.377		
$\overline{\Delta v_{85}}$	Estimate	-4.16802	1.02456	0.57642	0.02934	477.06	0.2780
	Pr(> |z|)	$2.88 \cdot 10^{-10}$	$< 2 \cdot 10^{-16}$	$6.30 \cdot 10^{-16}$	0.0959		
$\bar{d}_{85}$	Estimate	-6.35827	1.11084	0.78187	-0.68247	468.24	0.2421
	Pr(> |z|)	$7.50 \cdot 10^{-11}$	$< 2 \cdot 10^{-16}$	$3.42 \cdot 10^{-16}$	0.000398		
$\sigma_{\Delta v_{85}}$	Estimate	-4.22264	1.01515	0.58622	0.03581	477.01	0.2800
	Pr(> |z|)	$3.72 \cdot 10^{-10}$	$< 2 \cdot 10^{-16}$	$5.71 \cdot 10^{-16}$	0.0981		
$\sigma_{d_{85}}$	Estimate	-3.92685	1.01502	0.57446	0.19665	476.34	0.2789
	Pr(> |z|)	$6.75 \cdot 10^{-11}$	$< 2 \cdot 10^{-16}$	$6.00 \cdot 10^{-16}$	0.0512		
$\bar{L}_{\Delta v_{85}}$	Estimate	-3.806904	1.030065	0.595613	-0.003847	477.83	0.2908
	Pr(> |z|)	$1.44 \cdot 10^{-10}$	$< 2 \cdot 10^{-16}$	$1.19 \cdot 10^{-14}$	0.164		
L_d	Estimate	-4.12959	1.00745	0.57920	1.91272	478.08	0.2856
	Pr(> |z|)	$1.69 \cdot 10^{-9}$	$< 2 \cdot 10^{-16}$	$1.89 \cdot 10^{-15}$	0.183		
N	Estimate	-4.195333	0.863701	0.620386	0.007890	477.37	0.2832
	Pr(> |z|)	$1.17 \cdot 10^{-9}$	$4.11 \cdot 10^{-10}$	$8.69 \cdot 10^{-14}$	0.131		

Table 41. Estimates for constrained road segments.

More parameters are eligible as consistency parameter for constrained road segments. The average operating speed and the average deceleration rate are also included. In this case, adding a consistency parameter clearly enhances the safety performance function, since AIC goes from 477.7 to 468.24 (average deceleration rate).

7.4.4. Calibration with two parameters

The consistency parameter should not be limited to only consider one operational parameter. Instead, several combinations of parameters should be tried for determining the best adjustment.

A first approach to the problem was performed by means of an Artificial Neural Network (ANN) approach. This method allows us to examine hidden relationships between elements, showing us which parameters should be further explored.

However, a direct approach with all data would indicate us that road accidents are most dependent on the exposure (AADT and length). This is not the objective of this step. We want to determine which operational parameters are more related to road crashes, excluding the influence of the exposure. Thus, only the operational parameters should be used for the ANN formulation, comparing them to the crash rate.

The computer application RapidMiner was used in this step. Only one hidden layer was proposed. The training cycles was set to 100,000, with a learning rate of 0.3 and a momentum of 0.15. The error threshold was $\varepsilon = 10^{-7}$. In order to check the validity of the ANN, the calibration was performed with a random 85% of data. The 15% left was used for validation purposes. Figure 124 indicates the structure of the model.

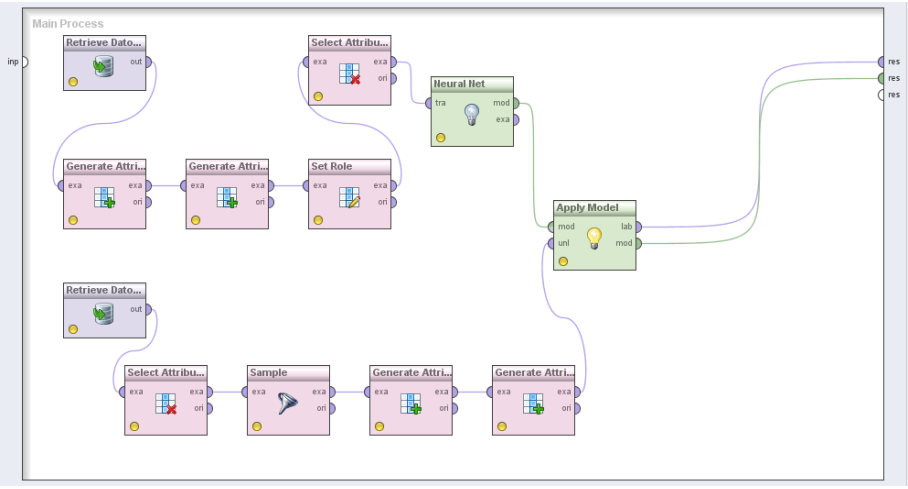

Figure 124. Screenshot of the RapidMiner structure for creating the Artificial Neural Network.

Figure 125 shows the ANN layout. As it can be seen, there are two variables that present strong connections: average deceleration and average speed.

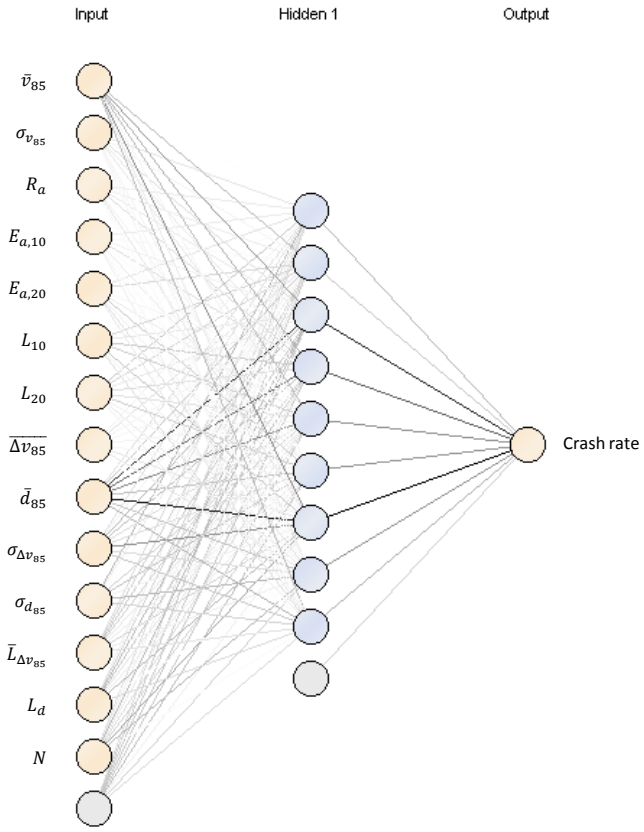

Figure 125. Structure of the ANN. Darker lines represent stronger relationships.

As Figure 125 shows, the most relevant parameters were the average operating speed and the average deceleration. However, some other combinations were tried for the final model.

N	L_d	$\bar{L}_{\Delta v_{85}}$	$\sigma_{d_{85}}$
710.412	707.089	700.422	710.115
708.251	714.032	708.694	709.696
701.717	709.826	714.263	708.357
700.781	709.729	714.218	708.629
695.849	709.427	713.319	706.643
706.505	713.836	714.260	708.479
696.133	710.013	713.651	707.433
706.124	713.885	714.242	708.344
700.751	712.207	714.118	706.623
705.112	702.700	713.222	710.429
702.615	710.525	714.180	707.723
708.241	709.427	709.315	712.2
708.635	714.226	711.394	709.315
705.166	713.626	714.226	709.427
709.708	705.166	708.635	708.241

	CCR	$\bar{v}_{85}$	$\sigma_{v_{85}}$	R_a	$E_{a,10}$	$E_{a,20}$	L_{10}	L_{20}	$\overline{\Delta v_{85}}$	$\bar{d}_{85}$	$\sigma_{\Delta v_{85}}$
CCR	711.524	705.860	705.502	705.146	705.727	711.244	706.217	711.020	703.245	708.074	705.499
$\bar{v}_{85}$	705.860	697.217	713.416	712.917	711.321	714.184	711.925	714.112	714.094	694.658	713.128
$\sigma_{v_{85}}$	705.502	713.416	709.063	708.982	709.436	713.678	709.879	713.590	709.808	696.467	709.465
R_a	705.146	712.917	708.982	709.173	709.636	713.560	710.145	713.483	709.812	696.777	709.598
$E_{a,10}$	705.727	711.321	709.436	709.636	710.428	713.360	710.811	713.328	709.964	702.361	710.399
$E_{a,20}$	711.244	714.184	713.678	713.560	713.360	714.042	713.383	714.005	712.995	711.505	712.785
L_{10}	706.217	711.925	709.879	710.145	710.811	713.383	711.271	713.356	710.606	702.691	711.001
L_{20}	711.020	714.112	713.590	713.483	713.328	714.005	713.356	713.978	712.998	711.401	712.671
$\overline{\Delta v_{85}}$	703.245	714.094	709.808	709.812	709.964	712.995	710.606	712.998	713.047	702.490	710.710
$\bar{d}_{85}$	708.074	694.658	696.467	696.777	702.361	711.505	702.691	711.401	702.490	698.801	699.490
$\sigma_{\Delta v_{85}}$	705.499	713.128	709.465	709.598	710.399	712.785	711.001	712.671	710.710	699.490	710.873
$\sigma_{d_{85}}$	710.115	709.696	708.357	708.629	706.643	708.479	707.433	708.344	706.623	710.429	707.723
$\bar{L}_{\Delta v_{85}}$	700.422	708.694	714.263	714.218	713.319	714.260	713.651	714.242	714.118	713.222	714.180
L_d	707.089	714.032	709.826	709.729	709.427	713.836	710.013	713.885	712.207	702.700	710.525
N	710.412	708.251	701.717	700.781	695.849	706.505	696.133	706.124	700.751	705.112	702.615

Table 42 shows all the potential combinations by multiplying two of each individual parameters. Only the AIC value is presented. The combinations with the lower AIC will be further explored.

$\sigma_{\Delta v_{85}}$	$\sigma_{d_{85}}$	$\bar{L}_{\Delta v_{85}}$	L_d	N
704.908	709.353	713.229	708.434	707.057
713.558	710.731	707.310	713.974	713.569
714.164	710.932	709.140	712.589	714.120
713.897	711.045	699.139	714.262	713.522
713.492	710.159	701.973	712.346	714.098
704.916	710.555		706.256	711.890
714.097	710.474	709.128		712.877
714.203	712.089	709.600	712.484	

	CCR	$\bar{v}_{85}$	$\sigma_{v_{85}}$	R_a	$E_{a,10}$	$E_{a,20}$	L_{10}	L_{20}	$\overline{\Delta v_{85}}$	$\bar{d}_{85}$	$\sigma_{\Delta v_{85}}$	$\sigma_{d_{85}}$	$\bar{L}_{\Delta v_{85}}$	L_d	N
CCR															
$\bar{v}_{85}$			702.677	702.473	706.168	713.378	706.843	713.244	707.553	697.624			710.274	714.191	712.987
$\sigma_{v_{85}}$		707.977		710.146	709.059	714.151	710.395	714.039	712.758	713.907			700.966	713.292	712.105
R_a		709.073	709.565		709.496	714.257	710.519	714.199	712.104	713.988			712.586	714.199	713.236
$E_{a,10}$													707.077	714.056	714.079
$E_{a,20}$													712.800	714.090	713.216
L_{10}													706.511	714.087	714.045
L_{20}													706.543	714.216	713.215
$\overline{\Delta v_{85}}$		709.147	714.264	714.035	712.142	714.207	712.342	714.263		711.343			707.390	714.060	712.789
$\bar{d}_{85}$		695.376	711.881	713.163	713.816	713.946	713.965	714.126	712.100				713.169	711.559	709.526
$\sigma_{\Delta v_{85}}$													712.276	712.227	709.720
$\sigma_{d_{85}}$															
$\bar{L}_{\Delta v_{85}}$															
L_d															
N															

Table 43 shows the potential combinations by dividing the parameters on the left by the parameters on the top of the table. Some of these combinations are not possible, since they provide infinite values. They are marked in black.

	CCR	$\bar{v}_{85}$	$\sigma_{v_{85}}$	R_a	$E_{a,10}$	$E_{a,20}$	L_{10}	L_{20}	$\overline{\Delta v_{85}}$	$\bar{d}_{85}$	$\sigma_{\Delta v_{85}}$	$\sigma_{d_{85}}$	$\bar{L}_{\Delta v_{85}}$	L_d	N
CCR	711.524	705.860	705.502	705.146	705.727	711.244	706.217	711.020	703.245	708.074	705.499	710.115	700.422	707.089	710.412
$\bar{v}_{85}$	705.860	697.217	713.416	712.917	711.321	714.184	711.925	714.112	714.094	694.658	713.128	709.696	708.694	714.032	708.251
$\sigma_{v_{85}}$	705.502	713.416	709.063	708.982	709.436	713.678	709.879	713.590	709.808	696.467	709.465	708.357	714.263	709.826	701.717
R_a	705.146	712.917	708.982	709.173	709.636	713.560	710.145	713.483	709.812	696.777	709.598	708.629	714.218	709.729	700.781
$E_{a,10}$	705.727	711.321	709.436	709.636	710.428	713.360	710.811	713.328	709.964	702.361	710.399	706.643	713.319	709.427	695.849
$E_{a,20}$	711.244	714.184	713.678	713.560	713.360	714.042	713.383	714.005	712.995	711.505	712.785	708.479	714.260	713.836	706.505
L_{10}	706.217	711.925	709.879	710.145	710.811	713.383	711.271	713.356	710.606	702.691	711.001	707.433	713.651	710.013	696.133
L_{20}	711.020	714.112	713.590	713.483	713.328	714.005	713.356	713.978	712.998	711.401	712.671	708.344	714.242	713.885	706.124
$\overline{\Delta v_{85}}$	703.245	714.094	709.808	709.812	709.964	712.995	710.606	712.998	713.047	702.490	710.710	706.623	714.118	712.207	700.751
$\bar{d}_{85}$	708.074	694.658	696.467	696.777	702.361	711.505	702.691	711.401	702.490	698.801	699.490	710.429	713.222	702.700	705.112
$\sigma_{\Delta v_{85}}$	705.499	713.128	709.465	709.598	710.399	712.785	711.001	712.671	710.710	699.490	710.873	707.723	714.180	710.525	702.615
$\sigma_{d_{85}}$	710.115	709.696	708.357	708.629	706.643	708.479	707.433	708.344	706.623	710.429	707.723	712.2	709.315	709.427	708.241
$\bar{L}_{\Delta v_{85}}$	700.422	708.694	714.263	714.218	713.319	714.260	713.651	714.242	714.118	713.222	714.180	709.315	711.394	714.226	708.635
L_d	707.089	714.032	709.826	709.729	709.427	713.836	710.013	713.885	712.207	702.700	710.525	709.427	714.226	713.626	705.166
N	710.412	708.251	701.717	700.781	695.849	706.505	696.133	706.124	700.751	705.112	702.615	708.241	708.635	705.166	709.708

Table 42. AIC values for the statistical analysis of all combinations of two operational parameters.

	CCR	$\bar{v}_{85}$	$\sigma_{v_{85}}$	R_a	$E_{a,10}$	$E_{a,20}$	L_{10}	L_{20}	$\overline{\Delta v_{85}}$	$\bar{d}_{85}$	$\sigma_{\Delta v_{85}}$	$\sigma_{d_{85}}$	$\bar{L}_{\Delta v_{85}}$	L_d	N
CCR															
$\bar{v}_{85}$	708.322		702.677	702.473	706.168	713.378	706.843	713.244	707.553	697.624	704.908	709.353	713.229	708.434	707.057
$\sigma_{v_{85}}$	711.017	707.977		710.146	709.059	714.151	710.395	714.039	712.758	713.907	713.558	710.731	707.310	713.974	713.569
R_a	711.072	709.073	709.565		709.496	714.257	710.519	714.199	712.104	713.988	714.164	710.932	709.140	712.589	714.120
$E_{a,10}$															
$E_{a,20}$															
L_{10}															
L_{20}															
$\overline{\Delta v_{85}}$	711.445	709.147	714.264	714.035	712.142	714.207	712.342	714.263		711.343	713.897	711.045	699.139	714.262	713.522
$\bar{d}_{85}$	708.356	695.376	711.881	713.163	713.816	713.946	713.965	714.126	712.100		713.492	710.159	701.973	712.346	714.098
$\sigma_{\Delta v_{85}}$															
$\sigma_{d_{85}}$															
$\bar{L}_{\Delta v_{85}}$	712.276	713.169	707.390	706.543	706.511	712.800	707.077	712.586	700.966	710.274	704.916	710.555		706.256	711.890
L_d	712.227	711.559	714.060	714.216	714.087	714.090	714.056	714.199	713.292	714.191	714.097	710.474	709.128		712.877
N	709.720	709.526	712.789	713.215	714.045	713.216	714.079	713.236	712.105	712.987	714.203	712.089	709.600	712.484	

Table 43. AIC values for the statistical division of all combinations of two operational parameters.

Hence, the following combinations of operational parameters were found to be interesting for further development:

- $\bar{v}_{85} \cdot \bar{d}_{85}$; *AIC*=694.6577

- $\frac{\bar{v}_{85}}{\bar{d}_{85}}$; *AIC*=695.3756
- $N \cdot E_{a,10}$; *AIC*=695.8485
- $N \cdot L_{10}$. *AIC*=696.1328
- $\sigma_{v_{85}} \cdot \bar{d}_{85}$; *AIC*=696.4666
- $R_a \cdot \bar{d}_{85}$; *AIC*=696.7768

It is worth to highlight that the best combinations are obtained by mixing continuous and local parameters. The deceleration rate is one of the most important, which remarks the importance of defining operating speed profile models based on accurate deceleration rates.

Those relationships were further explored, changing their indexes. Tables 13 to 18 reflect where the best AIC is achieved.

$\bar{v}_{85}$ \ $\bar{d}_{85}$	1/10	1/9	1/8	1/7	1/6	1/5	1/4	1/3	1/2	1	2	3	4	5
1/10	694.6	694.1	693.7	693.4	693.1	692.9	692.8	692.8	693.0	694.3	698.6	702.6	705.6	707.5
1/9	695.3	694.6	694.0	693.6	693.3	693.0	692.8	692.8	692.9	694.3	698.6	702.6	705.5	707.5
1/8	696.3	695.4	694.6	694.0	693.5	693.1	692.9	692.8	692.9	694.3	698.5	702.6	705.5	707.5
1/7	698.1	696.6	695.5	694.6	693.9	693.4	693.0	692.8	692.9	694.2	698.5	702.6	705.5	707.5
1/6	701.1	698.9	697.1	695.6	694.5	693.8	693.2	692.9	692.9	694.2	698.4	702.5	705.5	707.5
1/5	706.2	703.1	700.2	697.7	695.9	694.5	693.6	693.1	692.9	694.1	698.4	702.5	705.5	707.5
1/4	712.5	709.8	706.2	702.3	698.9	696.3	694.5	693.4	693.0	694.0	698.3	702.4	705.4	707.5
1/3	713.6	714.3	713.6	710.8	706.2	701.1	697.0	694.4	693.2	693.9	698.1	702.3	705.4	707.4
1/2	707.8	709.4	711.2	713.1	714.3	712.5	706.2	698.8	694.4	693.7	697.8	702.1	705.3	707.4
1	701.6	702.2	703.0	704.0	705.6	707.9	711.2	714.3	706.3	694.7	697.0	701.5	704.9	707.2
2	699.0	699.2	699.5	699.9	700.5	701.3	702.8	705.5	711.4	706.5	696.9	700.6	704.4	707.1
3	698.1	698.2	698.4	698.7	699.0	699.5	700.3	701.9	705.6	714.3	700.5	700.5	704.1	707.0
4	697.9	698.0	698.1	698.3	698.5	698.8	699.3	700.4	702.9	711.7	707.3	701.8	704.1	707.0
5	698.0	698.1	698.2	698.3	698.4	698.7	699.1	699.8	701.5	708.6	712.6	704.6	704.6	707.1

Table 44. AIC values for all multiplying combinations between the average operating speed and the average deceleration rate.

The parameter $\bar{v}_{85} \cdot \bar{d}_{85}$ is somewhat unstable. A slight difference of the exponents of both parameters may lead to accurate or inaccurate estimations of road crashes. The best adjustment is achieved for $\sqrt[9]{\bar{v}_{85}} \cdot \sqrt[3]{\bar{d}_{85}}$, which indicates that deceleration has a bigger effect than the average operating speed in this parameter. However, this is a complex functional form and is not recommended.

$\bar{v}_{85}$	5	4	3	2	1	1/2	1/3	1/4	1/5	1/6	1/7	1/8	1/9	1/10
5	697.2	696.7	696.3	696.0	695.6	694.8	694.3	693.9	693.6	693.4	693.3	693.2	693.1	693.1
4	697.2	696.6	696.2	695.9	695.4	694.6	694.1	693.7	693.5	693.3	693.2	693.1	693.1	693.0
3	697.2	696.6	696.1	695.8	695.3	694.4	693.9	693.6	693.4	693.2	693.1	693.0	693.0	692.9
2	697.1	696.5	696.0	695.6	695.0	694.2	693.7	693.4	693.2	693.1	693.0	693.0	692.9	692.9
1	697.1	696.4	695.9	695.5	694.8	694.0	693.5	693.3	693.1	693.0	693.0	692.9	692.9	692.9
1/2	697.0	696.4	695.8	695.2	694.5	693.7	693.3	693.1	693.0	693.0	692.9	692.9	692.9	692.9
1/3	697.0	696.2	695.6	695.0	694.2	693.5	693.2	693.0	693.0	692.9	692.9	692.9	692.9	692.9
1/4	696.9	696.1	695.4	694.7	693.8	693.3	693.1	693.1	693.0	693.0	693.0	693.0	693.0	693.0
1/5	697.0	696.2	695.4	694.5	693.8	693.4	693.4	693.4	693.4	693.4	693.4	693.4	693.4	693.4
1/6	698.4	697.6	696.8	696.0	695.4	695.2	695.2	695.2	695.2	695.2	695.2	695.2	695.2	695.2
1/7	702.5	702.0	701.5	700.9	700.4	700.2	700.1	700.1	700.1	700.1	700.1	700.1	700.1	700.0
1/8	705.8	705.5	705.2	704.9	704.5	704.4	704.3	704.3	704.3	704.2	704.2	704.2	704.2	704.2
1/9	708.0	707.9	707.7	707.5	707.3	707.2	707.1	707.1	707.1	707.1	707.1	707.1	707.1	707.1
1/10	709.5	709.4	709.2	709.1	709.0	708.9	708.9	708.9	708.9	708.9	708.9	708.9	708.9	708.9

$\bar{d}_{85}$: 1/10, 1/9, 1/8, 1/7, 1/6, 1/5, 1/4, 1/3, 1/2, 1, 2, 3, 4, 5

Table 45. AIC values for all dividing combinations between the average operating speed and the average deceleration rate.

The parameter $\bar{v}_{85}/\bar{d}_{85}$ is pretty more stable than the previous one. The best adjustment is achieved for $\sqrt[10]{\bar{v}_{85}}/\sqrt[5]{\bar{d}_{85}}$. However, there are simpler forms that also provide a good adjustment. The expression $\sqrt[3]{\bar{v}_{85}/\bar{d}_{85}}$ is recommended, since it combines an easy functional form and a good AIC value (693.11705).

$E_{a,10}$ \ N	1/10	1/9	1/8	1/7	1/6	1/5	1/4	1/3	1/2	1	2	3	4	5
1/10	708.1	707.8	707.5	707.0	706.4	705.7	704.6	703.4	702.3	704.9	709.1	709.7	709.6	709.4
1/9	708.0	707.7	707.3	706.9	706.3	705.5	704.5	703.1	702.0	704.7	709.1	709.7	709.6	709.4
1/8	707.8	707.5	707.1	706.7	706.1	705.3	704.2	702.9	701.7	704.5	709.0	709.7	709.6	709.4
1/7	707.6	707.3	706.9	706.5	705.9	705.1	704.0	702.6	701.4	704.3	708.9	709.6	709.5	709.4
1/6	707.4	707.1	706.7	706.2	705.6	704.8	703.7	702.3	701.0	703.9	708.8	709.6	709.5	709.3
1/5	707.1	706.8	706.4	705.9	705.3	704.5	703.4	701.9	700.4	703.4	708.6	709.5	709.4	709.3
1/4	706.8	706.5	706.1	705.6	705.0	704.1	703.0	701.4	699.7	702.7	708.4	709.4	709.4	709.2
1/3	706.5	706.2	705.8	705.3	704.7	703.8	702.6	700.9	698.9	701.6	708.0	709.2	709.2	709.1
1/2	706.3	706.1	705.7	705.2	704.6	703.8	702.6	700.7	698.0	699.6	707.3	708.8	708.9	708.8
1	707.2	706.9	706.7	706.3	705.8	705.2	704.1	702.3	698.9	695.8	705.2	707.8	708.2	708.2
2	709.5	709.3	709.2	709.0	708.7	708.4	707.8	706.7	704.2	696.4	701.4	706.0	707.0	707.2
3	711.4	711.3	711.3	711.2	711.0	710.8	710.5	709.9	708.5	702.3	698.2	704.5	706.2	706.6
4	712.8	712.8	712.8	712.7	712.6	712.5	712.4	712.1	711.4	707.8	697.4	702.9	705.5	706.1
5	713.7	713.7	713.7	713.6	713.6	713.6	713.5	713.3	713.0	711.1	701.0	701.0	704.8	705.8

Table 46. AIC values for all combinations between the number of decelerations and Ea,10.

The parameter $E_{a,10} \cdot N$ is quite stable. The best combination is achieved for the original form (exponent 1 for both parameters). However, a slight variation of the exponent that affects N provides quite inaccurate estimations. In addition, the parameter $E_{a,10}$ is zero for smooth road segments, so the estimation of road accidents would be less accurate in those cases.

L_{10} \ N	1/10	1/9	1/8	1/7	1/6	1/5	1/4	1/3	1/2	1	2	3	4	5
1/10	708.2	708.0	707.6	707.2	706.6	705.8	704.9	703.6	702.5	705.0	709.2	709.8	709.7	709.5
1/9	708.1	707.8	707.5	707.0	706.5	705.7	704.7	703.4	702.2	704.8	709.1	709.7	709.6	709.4
1/8	708.0	707.7	707.3	706.9	706.3	705.5	704.5	703.2	702.0	704.6	709.0	709.7	709.6	709.4
1/7	707.8	707.5	707.2	706.7	706.1	705.4	704.3	703.0	701.7	704.4	709.0	709.7	709.6	709.4
1/6	707.6	707.3	707.0	706.5	705.9	705.2	704.1	702.7	701.3	704.1	708.9	709.6	709.6	709.4
1/5	707.4	707.1	706.8	706.3	705.7	704.9	703.8	702.4	700.9	703.6	708.7	709.6	709.5	709.3
1/4	707.2	706.9	706.6	706.1	705.5	704.7	703.6	702.0	700.3	703.0	708.5	709.4	709.4	709.3
1/3	707.1	706.8	706.4	706.0	705.4	704.5	703.4	701.7	699.6	701.9	708.2	709.3	709.3	709.2
1/2	707.1	706.8	706.5	706.0	705.5	704.7	703.5	701.6	698.9	700.0	707.5	709.0	709.1	709.0
1	708.0	707.8	707.5	707.2	706.7	706.1	705.1	703.3	699.8	696.1	705.5	708.0	708.4	708.4
2	710.4	710.3	710.2	710.0	709.7	709.4	708.8	707.8	705.3	696.8	701.4	706.4	707.4	707.6
3	712.4	712.4	712.3	712.2	712.1	711.9	711.7	711.2	710.0	703.8	697.7	704.7	706.5	706.9
4	713.6	713.6	713.6	713.6	713.5	713.4	713.3	713.1	712.6	709.7	697.5	702.8	705.8	706.4
5	714.2	714.1	714.1	714.1	714.1	714.1	714.1	714.0	713.8	712.7	703.3	700.6	704.9	706.0

Table 47. AIC values for all combinations between the number of decelerations and L,10.

The parameter $L_{10} \cdot N$ behaves in a similar way than the previous one. The best adjustment is obtained for the original form. The parameter L_{10} is neither valid for smooth road segments, so this parameter is not recommended.

$\sigma_{d_{85}}$	5	4	3	2	1	1/2	1/3	1/4	1/5	1/6	1/7	1/8	1/9	1/10
1/10	710.2	709.5	708.8	708.1	707.2	706.0	704.7	703.6	702.5	701.5	700.5	699.7	699.0	698.3
1/9	710.1	709.5	708.7	708.0	707.0	705.6	704.2	703.0	701.8	700.8	699.8	699.0	698.2	697.6
1/8	710.1	709.4	708.6	707.8	706.8	705.2	703.7	702.3	701.0	700.0	699.0	698.2	697.4	696.8
1/7	710.0	709.3	708.5	707.7	706.4	704.6	702.9	701.4	700.1	699.0	698.1	697.2	696.5	696.0
1/6	709.9	709.2	708.4	707.4	706.0	703.9	702.0	700.4	699.0	697.9	697.0	696.2	695.6	695.1
1/5	709.8	709.1	708.2	707.1	705.4	702.9	700.8	699.1	697.7	696.7	695.8	695.1	694.6	694.2
1/4	709.7	708.8	707.8	706.6	704.5	701.5	699.2	697.5	696.2	695.3	694.6	694.0	693.6	693.3
1/3	709.4	708.5	707.3	705.8	703.1	699.5	697.1	695.6	694.5	693.8	693.4	693.0	692.8	692.7
1/2	708.9	707.7	706.3	704.2	700.6	696.6	694.6	693.6	693.1	692.7	692.6	692.5	692.4	692.4
1	707.6	706.0	703.8	700.8	696.5	694.0	693.5	693.5	693.5	693.6	693.6	693.7	693.8	693.8
2	706.7	704.9	702.5	700.0	697.9	697.6	697.8	697.9	698.1	698.2	698.2	698.3	698.3	698.4
3	707.5	705.9	704.2	702.7	701.9	702.0	702.1	702.3	702.3	702.4	702.4	702.5	702.5	702.5
4	708.6	707.4	706.2	705.4	705.1	705.2	705.3	705.3	705.4	705.4	705.4	705.5	705.5	705.5
5	709.5	708.6	707.9	707.4	707.2	707.3	707.3	707.4	707.4	707.4	707.5	707.5	707.5	707.5

$\bar{d}_{85}$

Table 48. AIC values for all combinations between the deceleration rate dispersion and the average deceleration rate.

The parameter $\sigma_{v_{85}} \cdot \bar{d}_{85}$ is quite stable, presenting a wide region of good adjustment. The best value is achieved for $\sqrt[10]{\sigma_{v_{85}}} \cdot \sqrt{\bar{d}_{85}}$, although it is a complex functional form. Other simpler expressions could be selected instead.

$\bar{d}_{85}$ \ R_a	5	4	3	2	1	1/2	1/3	1/4	1/5	1/6	1/7	1/8	1/9	1/10
1/10	711.3	710.5	709.5	708.4	706.9	705.4	704.2	703.1	702.1	701.2	700.3	699.5	698.8	698.2
1/9	711.3	710.5	709.5	708.3	706.7	705.1	703.8	702.6	701.5	700.5	699.6	698.8	698.1	697.5
1/8	711.3	710.4	709.4	708.2	706.5	704.7	703.2	701.9	700.8	699.8	698.8	698.0	697.3	696.7
1/7	711.2	710.4	709.3	708.0	706.2	704.2	702.6	701.2	699.9	698.9	697.9	697.1	696.5	695.9
1/6	711.2	710.3	709.2	707.8	705.8	703.5	701.7	700.2	698.9	697.8	696.9	696.1	695.5	695.0
1/5	711.1	710.2	709.0	707.5	705.2	702.6	700.6	698.9	697.6	696.6	695.7	695.0	694.5	694.0
1/4	711.0	710.0	708.8	707.1	704.4	701.3	699.1	697.4	696.1	695.2	694.4	693.9	693.4	693.1
1/3	710.8	709.7	708.3	706.4	703.1	699.4	697.0	695.5	694.4	693.7	693.2	692.8	692.6	692.4
1/2	710.4	709.2	707.5	705.0	700.8	696.6	694.5	693.4	692.8	692.5	692.3	692.2	692.1	692.1
1	709.3	707.6	705.2	701.8	696.8	693.9	693.3	693.2	693.3	693.3	693.4	693.5	693.6	693.6
2	708.0	705.9	703.3	700.5	698.0	697.5	697.7	697.8	698.0	698.1	698.2	698.2	698.3	698.3
3	707.9	706.2	704.4	702.9	701.9	701.9	702.1	702.2	702.3	702.4	702.4	702.4	702.5	702.5
4	708.5	707.3	706.3	705.5	705.1	705.2	705.3	705.3	705.4	705.4	705.4	705.5	705.5	705.5
5	709.2	708.5	707.9	707.5	707.3	707.3	707.4	707.4	707.4	707.4	707.5	707.5	707.5	707.5

Table 49. AIC values for all combinations between Ra and the average deceleration rate.

The parameter $R_a \cdot \bar{d}_{85}$ is also quite stable. The best adjustment is for $\sqrt[10]{R_a} \cdot \sqrt{\bar{d}_{85}}$. This is also a complex functional form, so other expressions should be tried instead.

We can see how the best adjustments are obtained for parameters that combine the average deceleration. Several functional forms were tried. Finally, the parameter $\sqrt[3]{\bar{v}_{85}/\bar{d}_{85}}$ is recommended due to its simplicity and low AIC value. In addition, the average operating speed and the average deceleration presented a strong relationship in the ANN calibration. However, the other relationships will also be further explored, in order to provide useful conclusions for road design.

7.5. Estimation of the number of accidents

According to the global consistency model presented, Table 50 shows the estimates to be used in the safety performance function. Three safety performance functions are provided, for all, free and constrained road segments. All parameters were significant at a 95% confidence level.

Subset		β_0	β_1	β_2	β_3	AIC	α
		–	$\ln L$	$\ln AADT$	$\sqrt[3]{\frac{\bar{v}_{85}}{\bar{d}_{85}}}$		
All	Estimate	-4.26225	1.13196	0.85298	-0.42896	693.12	0.2174
	Pr(> |z|)	$< 2 \cdot 10^{-16}$	$< 2 \cdot 10^{-16}$	$< 2 \cdot 10^{-16}$	$2.22 \cdot 10^{-6}$		
Free	Estimate	-5.5819	0.9265	0.9934	-0.3403	231.89	0.0980
	Pr(> |z|)	$6.76 \cdot 10^{-11}$	$8.95 \cdot 10^{-9}$	$8.11 \cdot 10^{-13}$	0.0285		
Constrained	Estimate	-3.91602	1.16103	0.80150	-0.41954	466.4	0.2331
	Pr(> |z|)	$6.43 \cdot 10^{-12}$	$< 2 \cdot 10^{-16}$	$< 2 \cdot 10^{-16}$	0.000161		

Table 50. Safety Performance Functions for estimating the number of accidents – final consistency model.

For all and constrained road segments, the AIC models are the best among all adjustments with one parameter. On the contrary, the model for free road segments is not the best. However, it was preferred to establish a unique functional form for all kinds of road segments.

Therefore, the consistency parameter is established as:

$$C = \sqrt[3]{\frac{\bar{v}_{85}}{\bar{d}_{85}}} \tag{349}$$

In order to use similar units, it is preferred to use the operating speed in m/s. This makes it necessary to change the term β_3 in all safety performance functions (see Table 51).

Subset		β_0	β_1	β_2	β_3	AIC	α
		–	$\ln L$	$\ln AADT$	$\sqrt[3]{\frac{\bar{v}_{85}}{\bar{d}_{85}}}$		
All	Estimate	-4.26225	1.13196	0.85298	-0.6574322	693.12	0.2174
	Pr(> |z|)	$< 2 \cdot 10^{-16}$	$< 2 \cdot 10^{-16}$	$< 2 \cdot 10^{-16}$	$2.22 \cdot 10^{-6}$		
Free	Estimate	-5.5819	0.9265	0.9934	-0.5215502	231.89	0.0980
	Pr(> |z|)	$6.76 \cdot 10^{-11}$	$8.95 \cdot 10^{-9}$	$8.11 \cdot 10^{-13}$	0.0285		
Constrained	Estimate	-3.91602	1.16103	0.80150	-0.6429949	466.4	0.2331
	Pr(> |z|)	$6.43 \cdot 10^{-12}$	$< 2 \cdot 10^{-16}$	$< 2 \cdot 10^{-16}$	0.000161		

Table 51. Final forms of the safety performance functions with the consistency parameter.

The units of this consistency parameter can be established based on a dimensional analysis (Equation (352).

$$C = \sqrt[3]{\frac{[L]/[T]}{[L]/[T]^2}} = \frac{[L]^{\frac{1}{3}} \cdot [T]^{-\frac{1}{3}}}{[L]^{\frac{1}{3}} \cdot [T]^{-\frac{2}{3}}} = [T]^{\frac{1}{3}} \quad (350)$$

7.6. Determination of the consistency thresholds

The consistency parameter is valid for estimating the number of crashes, and to determine the potential of improvement of a certain solution at the design stage. Due to its connection to road crashes, it is not necessary to establish certain thresholds for good, fair and poor design consistency. However, this division is sometimes useful for assisting road designers in taking some decisions.

Therefore, the output was clustered into three groups of consistency: poor, fair and good. Those clusters were determined using the software RapidMiner 6.0, with 50 max runs, and the method of Bregman Divergences for determining the measure types, and the divergence as Squared Euclidean Distance. The maximum optimization steps was set to 100. The consistency parameter was the only one to consider in the cluster analysis.

Figure 126 represents crash rates as a function of the consistency, separated into three groups for poor, fair and good consistency, as follows:

- Poor consistency: C is lower than 2.55 $s^{1/3}$.
- Fair consistency: C is between 2.55 and 3.25 $s^{1/3}$.
- Good consistency: C is higher than 3.35 $s^{1/3}$.

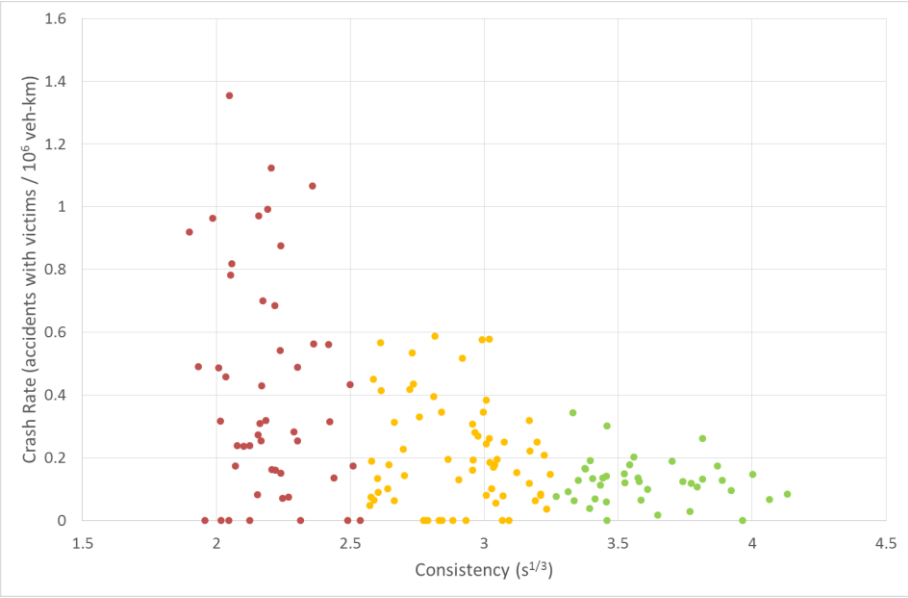

Figure 126. Relationship between the crash rate and the consistency parameter. Red, yellow and green dots represent poor, fair and good consistency road segments.

The three groups obtained present clear differences in both average crash rate and dispersion (uncertainty) about the outcome. It was decided to not distinguish between segment types (free vs. constrained).

8. Discussion

8.1. Recreation of the geometry

A new analytical-heuristic methodology has been presented for recreating the horizontal alignment of roads. This methodology is based on the use of the heading as a surrogate measure. A computer program was developed to assist the user through the entire process. This methodology provides important advantages compared to previous ones, such as:

- The heading profile presents quite less noise than the curvature profile. Thus, no previous smoothing and/or filtering processes are required. This prevents the inclusion or removal of spiral transitions, low-deflection curves, flat curves, etc.
- The heading of the road centerline must always be continuous. Thus, the final heading of a geometric element must be the same of the beginning of the following road geometric element. Therefore, fitting the alignment in this way allows sharing some information longitudinally thereby addressing some issues produced by the randomness of the data. In addition, in most cases the heading's first derivative is also continuous, adding more information to solve the problem.

Those two advantages provide some new possibilities to fit complex alignments and smooth curves. In addition, all the geometric elements are found, thus allowing a better knowledge of the geometry in order to accurately determine all their properties. Several previous methodologies were not able to find a solution, while other needed smoothing algorithms, which might hide or introduce short or flat geometric elements. The new method does not require smoothing; all geometric elements, even short or smooth ones, can be identified.

8.1.1. Data collection

An initial set of point locations must be in the Cartesian system (x, y coordinates), which may be obtained in several ways. GPS-equipped vehicles can be used for determining the typical vehicle paths, sometimes called "operating paths." Nowadays, the locations of designed and existing roads are typically available on electronic maps and orthorectified images with embedded geo-coordinates. Therefore, the geo-coded locations of the centerline road point sequence can be

obtained by the user manually from such maps and aerial imagery. In many cases of existing roads, design documentation does not exist or retrieving the paper-based design documentation is not practical when an alternative of high quality orthogonal and geo-coded images are available.

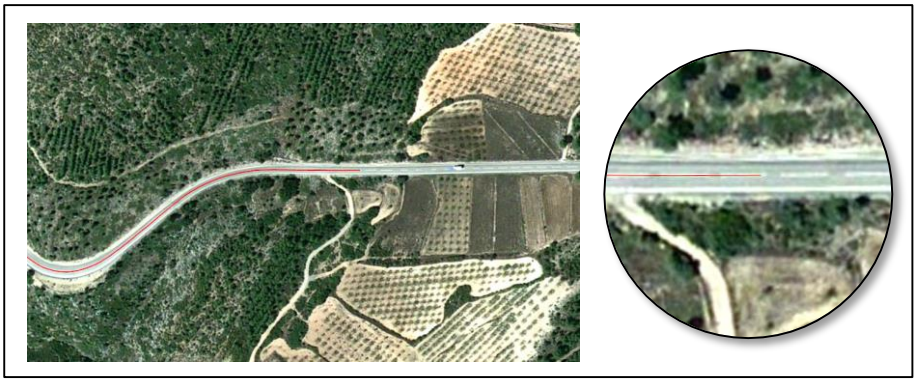

Figure 127. Depicting the road centerline from satellite imagery.

The results achieved with this methodology mostly depend on the accuracy at what the road centerline was depicted. Points should not be depicted too far from each other. This distance may be variable, depending on the curvature. Points should be located closer where a sharper curvature is observed.

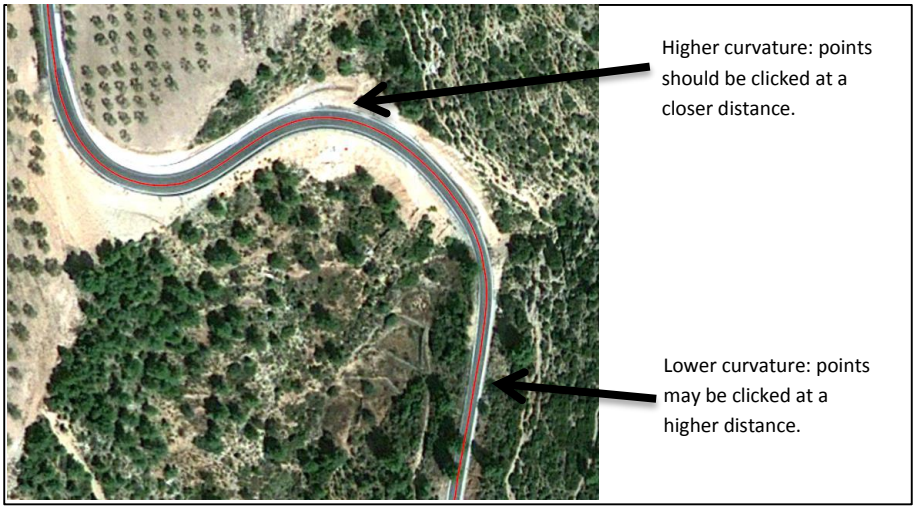

Figure 128. Complex sequence of geometric elements.

8.1.2. Advantages of the proposed methodology and comparison to other methods

One of the most important advantages of the proposed method is that it accurately detects all the geometric elements of the road. The obtained solution is much more accurate than solutions obtained by several other methods. Figure 129 shows the horizontal alignment obtained by two different methods: the curvature-based method presented by Camacho et al. (2010) and the proposed method. The primary cause of the poor performance of the other method is the wrong number of geometric elements. It generates an error that increases with the distance from the origin. In addition, the length of the different elements is not well determined with the curvature-based methodology, too.

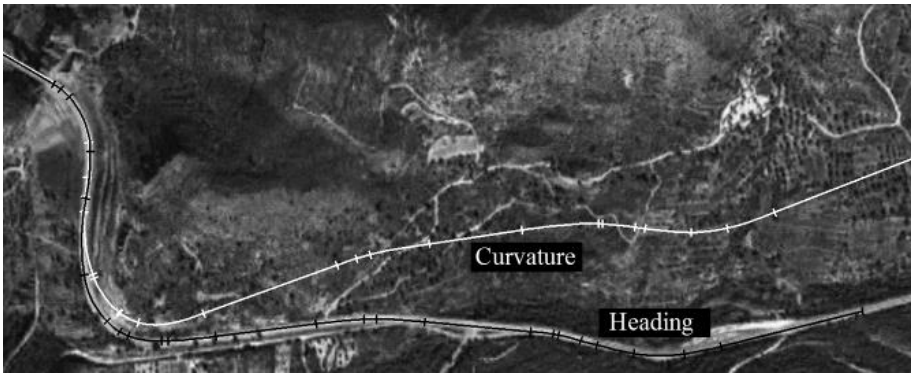

Figure 129. Comparison between the horizontal alignment recreation by means of the curvature and the heading methodologies.

Flat circular curves have small curvatures that can be easily overlooked in the presence of noisy data (particularly if the curve has a small deflection angle). The opposite may also happen when the noise of the curvature profile is confused with a small curvature. Therefore, a non-existing curve might be added or an actual curve removed.

Using the heading direction eliminates this difficulty. A horizontal curve always imposes a change of the heading, regardless of its radius. Hence, all curves are found with this methodology. Figure 130 shows one example of a low-deflection angle curve, hardly visible. However, the change in the heading direction is obvious.

Figure 130. Low-deflection angle curve. The heading methodology allows us to detect this kind of curves.

Several curvature-based methodologies employ user-defined thresholds for detecting the existence and position of different geometric elements. These thresholds depend on the user's criteria and affect the results. In addition, it is common than user-defined thresholds are valid for a certain range of geometric characteristics but not for others, leading to incorrect solutions.

A comparison of radii and lengths of circular curve obtained with the curvature-based method presented by Camacho et al. (2010) and the proposed method was performed. A set of 200 isolated, horizontal curves were randomly extracted from 10 two-lane rural highways in Spain. These roads were those used in the calibration of the operating speed models by Pérez-Zuriaga et al (2010). The curves were selected in order to have a wide range of radii and lengths. Figure 131 shows the comparison of the results from the two methods (estimated radii and lengths of the selected curves). As one can see, the radii obtained with both methodologies are almost identical, while their lengths are significantly different. Radii are similar because it is determined with the sharpest part of the curve. Hence, the curvature-based methodology focuses on zones where the sharpest part is observed, in which the noise has a lower effect. However, this comparison was performed only with all isolated curves detected with both methodologies. Nearly all smooth horizontal curves were detected by the heading methodology but not by the curvature-based one. In addition, the curvature method merged most of the compound curves into a single radius curve. The heading procedure could easily distinguish both curves and provide both radii. According to the length comparison, the estimations from both approaches clearly differ. The curvature-based method provides longer curves than the heading-based one. This can be explained because the initial and final points of the horizontal curves present low curvature, which may be confused with the noise

of the curvature profile. This problem does not exist in the case of the heading profile.

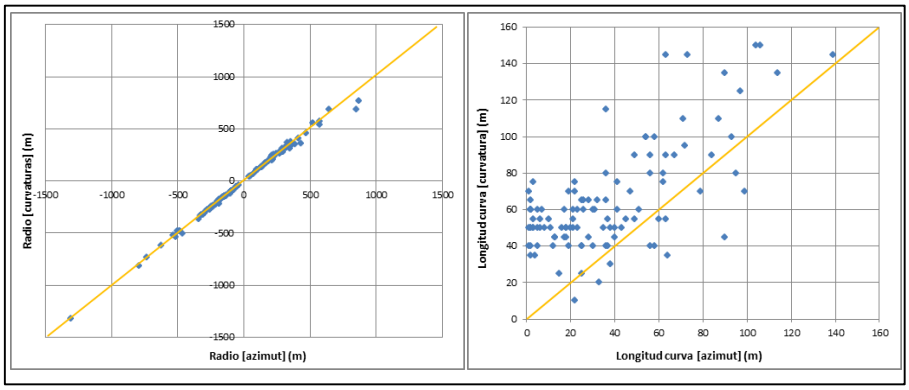

Figure 131. Comparison of length and radii for heading and curvature-based approaches.

The heuristic process used for determining the best location of s_i stitching points evaluates all possible solutions before fitting the final one. The average distance between data points - one meter - is sufficiently precise to obtain accurate estimates of the horizontal alignment. Figure 132 shows the comparison between the estimated and actual geometry of a certain road alignment (road CV-660, station 16+250 to station 19+250). The horizontal curves were correctly detected except one curve composed of two consecutive curves and a very short intermediate tangent. The estimated geometry is sufficiently close to the actual geometry for the purpose of evaluating local curvature from the safety point of view.

The accuracy of the results depends on selected Δs. In this case, $\Delta s = 1\ \mathrm{m}$, is acceptable for safety and mobility analysis that requires curve radius and length. A lower Δs should be used, such as 1 mm if the estimated alignment is need for the road redesign. In this case, further steps that deal directly to the *(x, y)* coordinates are recommended.

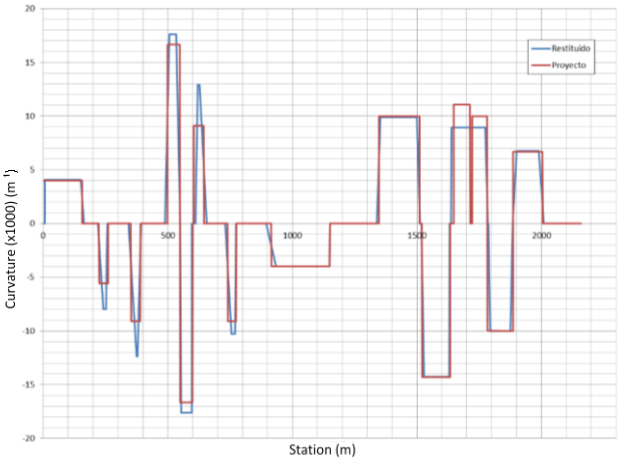

Figure 132. Projected road (red) vs. recreated alignment (blue).

The Genetic Algorithm approach provides a powerful tool to boost the heading solution to a (*x*, *y*)-fitted one. In this case, the accuracy of the solution can be directly observed by the user, since the horizontal distance deviation is one of the parameters controlled by the error function. Figure 133 shows an intermediate step of the adjustment of a very complex road (17 km of the northern part of the road CM-1006). We can see how the algorithm has very well fitted the northern part of the road, while the south part is still with the heading solution. We can also observe how the heading solution to the horizontal alignment recreation is similar in shape to the actual road, which indicates how accurate is the heading algorithm. Figure 134 shows the same road after being completely adjusted by the genetic algorithm approach. Figure 135 and Figure 136 are two details of the adjusted road, in order to show how tangents (blue), circular curves (red) and spiral transitions (green) are fitted. The actual road is depicted in black.

Figure 133. Coordinates view of the adjustment of a horizontal alignment (the road increases from up to down). We can see where the genetic algorithm is working at.

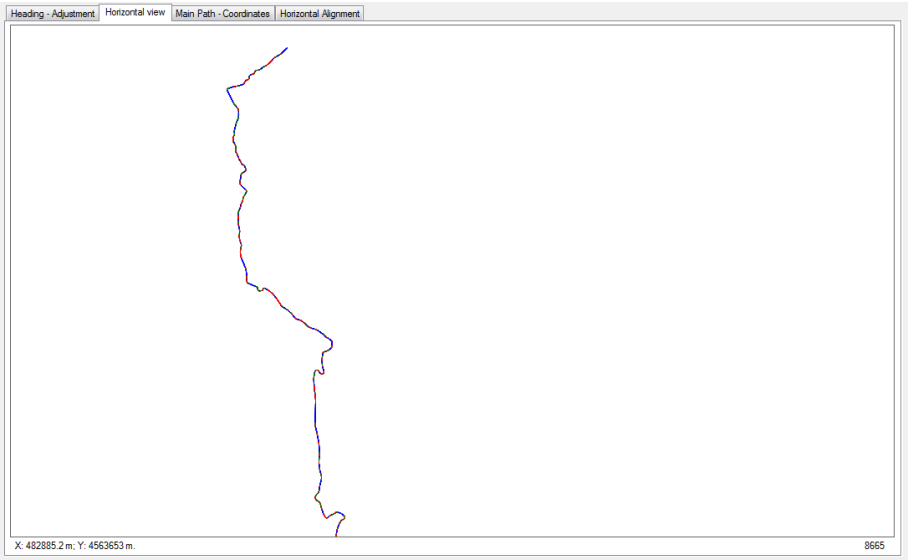

Figure 134. Coordinates view of the complete adjustment of a horizontal alignment.

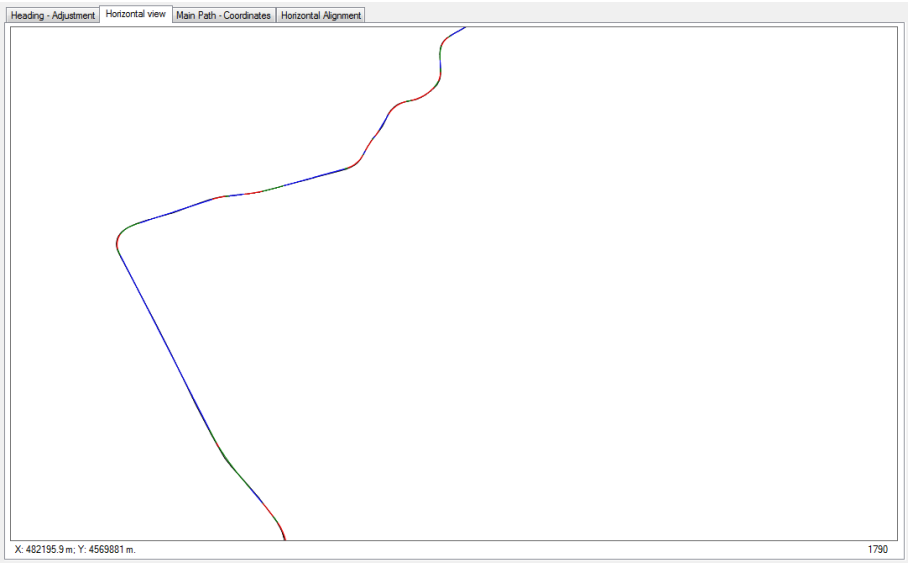

Figure 135. Zoom in of the previous alignment, northern section of the road.

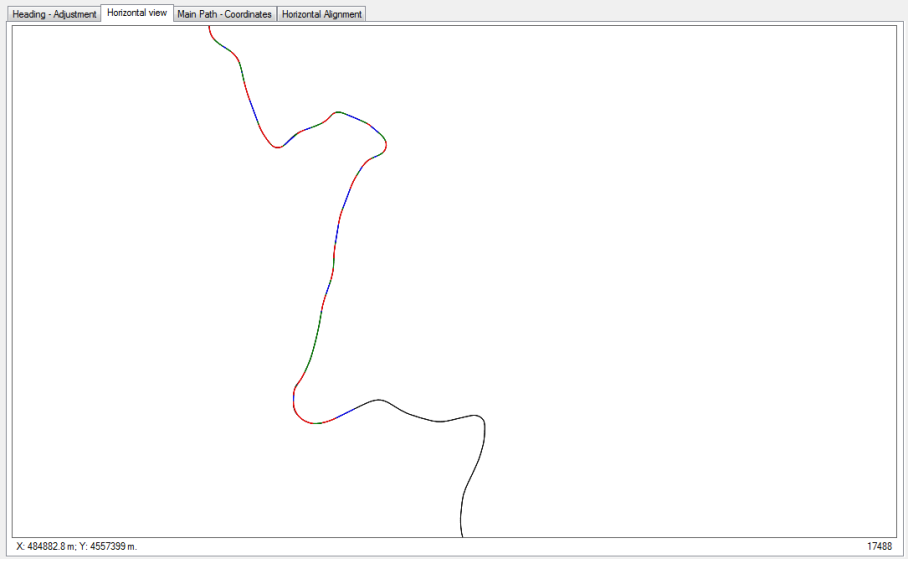

Figure 136. Zoom in of the previous alignment, southern section of the road. The road has not been completely recreated (we can see the original (*x*, *y*) poliline in black in the south part). It was left on purpose in order to give an idea about how accurate the final solution is.

8.2. Analysis of the consistency parameter and its relationship with road crashes

Three expressions for determining the number of accidents with victims in terms of the exposure and the consistency parameter have been determined. The importance of having those relationships is not only for estimating the number of accidents with victims, but also because of the better comprehension of how the input parameters affect the result. In this case, the type of road segment, the length, the traffic volume and the consistency parameter will be analyzed.

The exposure parameters were introduced in terms of elasticity. This allows us to easily determine the crash rate, in order to perform better comparisons.

Equations 351, 352 and 353 estimate the road crashes for all, free and constrained road segments depending on the exposure and consistency.

$$y_i = e^{-4.26225} \cdot L^{1.13196} \cdot AADT^{0.85298} \cdot e^{-0.6574 \cdot C} \quad (351)$$

$$y_i = e^{-5.5819} \cdot L^{0.9265} \cdot AADT^{0.9934} \cdot e^{-0.5216 \cdot C} \quad (352)$$

$$y_i = e^{-3.91602} \cdot L^{1.16103} \cdot AADT^{0.8015} \cdot e^{-0.6430 \cdot C} \quad (353)$$

Where:

$$C = \sqrt[3]{\frac{\bar{v}_{85}}{\bar{d}_{85}}} \quad (354)$$

Crash rates (accidents with victims per 10^6 veh-km) can be obtained by applying the following expression:

$$CR = \frac{y_i}{L \cdot AADT \cdot 0.00365} \quad (355)$$

Thus, the expressions for estimating crash rates in terms of million vehicle-km are:

$$CR_i = e^{1.350778} \cdot L^{0.13196} \cdot AADT^{-0.14702} \cdot e^{-0.6574 \cdot C} \quad (356)$$

$$CR_i = e^{0.031128} \cdot L^{-0.0735} \cdot AADT^{-0.0066} \cdot e^{-0.5216 \cdot C} \quad (357)$$

$$CR_i = e^{1.697008} \cdot L^{0.16103} \cdot AADT^{-0.1985} \cdot e^{-0.6430 \cdot C} \quad (358)$$

The type of road segment does not dramatically influence the number of crashes. Instead, the most important effect is how it changes the behavior of the rest of the exposure parameters. This is why the behavior of those parameters will be later examined.

Figure 137 and Figure 138 represent the estimation of road crashes depending on the exposure parameter (X and Y axis) and the type of road segment. Constrained road segments are in red, while free road segments are in green. The first figure is plotted for a poor consistency level ($C = 2$) and the second one for a good consistency level ($C = 4.25$). The number of crashes is clearly different when the consistency parameter changes. The influence of the type of road segment is quite lower than the consistency effect. Figure 139 and Figure 140 show the evolution of crash rates instead. They will be in-depth commented in the next chapter.

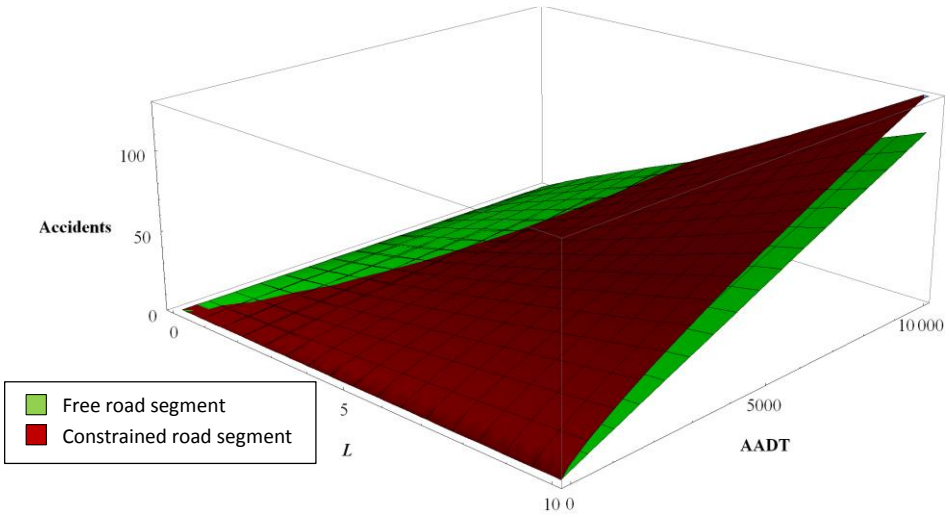

Figure 137. Estimation of road accidents as a function of the exposure. Poor consistency.

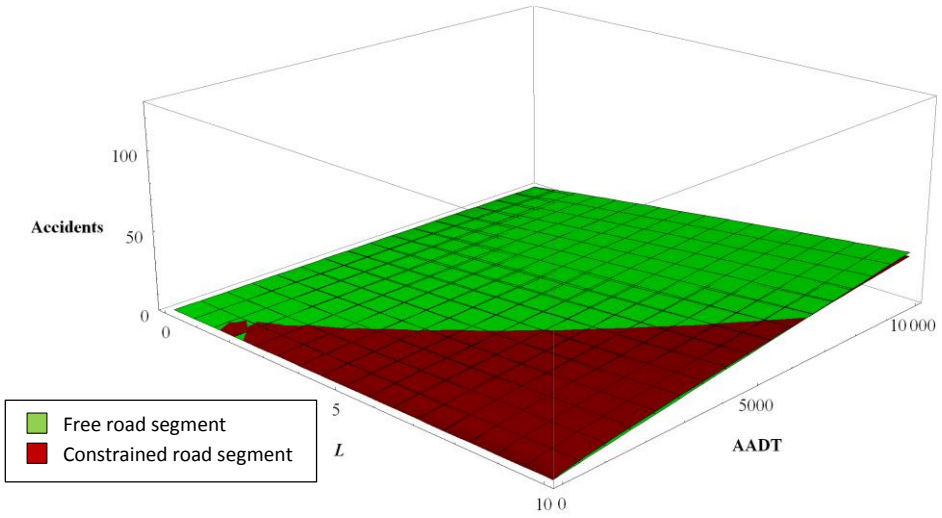

Figure 138. Estimation of road accidents as a function of the exposure. Good consistency.

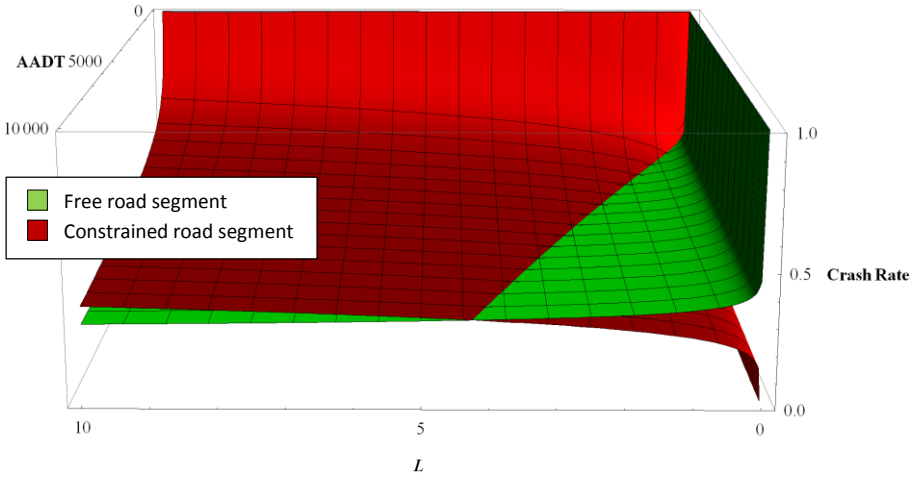

Figure 139. Estimation of crash rates as a function of the exposure. Poor consistency.

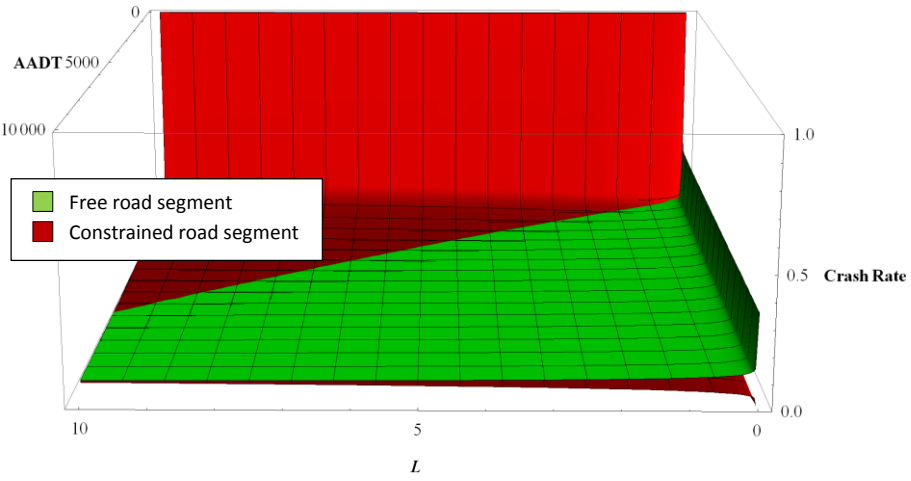

Figure 140. Estimation of crash rates as a function of the exposure. Good consistency.

8.2.1. Effect of the road length

The most important effect of the type of road segment is not the change of the number of crashes, but the change of the estimates. We can see how the exposure parameters change a lot depending on the type of road segment, especially the length.

From a theoretical point of view, the number of crashes should be proportional to the length. This is the reason why several previous research forced its estimate to be 1. This can be considered true as long as the road segment is not homogeneous.

The road behavior roughly remains unchanged through homogeneous road segments. Thus, a change of the homogeneous road segment is identified with a change of the road behavior. Hence, the length might also be a parameter to be considered in the consistency analysis.

In fact, results show that the factors affecting the exposure parameters differ from 1. Moreover, those factors behave in different ways depending on whether the road segment is free or constrained. For free road segments, the length estimate is 0.9265 (lower than 1), while for constrained ones is 1.16103 (higher than 1). This indicates that for free road segments, the crash rate increases as the road segment length does; while it behaves in the opposite direction for constrained road segments.

This different behavior may be explained in terms of *ad hoc* expectations. Each road homogeneous segment behaves differently in terms of design consistency. Some of them are consistent, thus demanding a low driver workload. Some others are non-consistent instead, requiring a higher mental effort or workload.

However, drivers adapt their driving skills to their perception of the mental effort required by the road segment. This means that a consistency change from one road segment to the following one might be a problem, if the second segment is less consistent. Drivers learn from road behavior, thus adapting their expectations, but this does not happen instantly. When the road segment changes, the road behavior does, hence forcing the driver to readapt their expectancies. Here is where the difference between constrained and free road segments appears. On constrained road segments, the drivers clearly notice that they are entering into a new road segment. Hence, they pay more attention along the first meters of the new road segment, in order to acquire their new expectancies.

On the contrary, drivers are not aware of entering into a new road segment when it is a free one. As a result, they still apply the expectations for the previous road segment, which might not be the adequate. After travelling a certain distance through the road segment, drivers unconsciously form their new expectancies.

This phenomenon can be explained by examining the length estimate. For constrained road segments, the drivers are adapting their expectancies to the road behavior as they are travelling along the road segment. As a result, they drive very carefully along the first meters, so the likelihood of having a crash is low. As they assimilate this behavior and transform it into their expectancies, they start to pay less attention and the crash rate stabilizes to a certain rate. This is why the longer the road segment, the higher the crash rate (Figure 141). This effect is the same for good and poor consistency, although crash rates are quite more stable for good consistency (Figure 142).

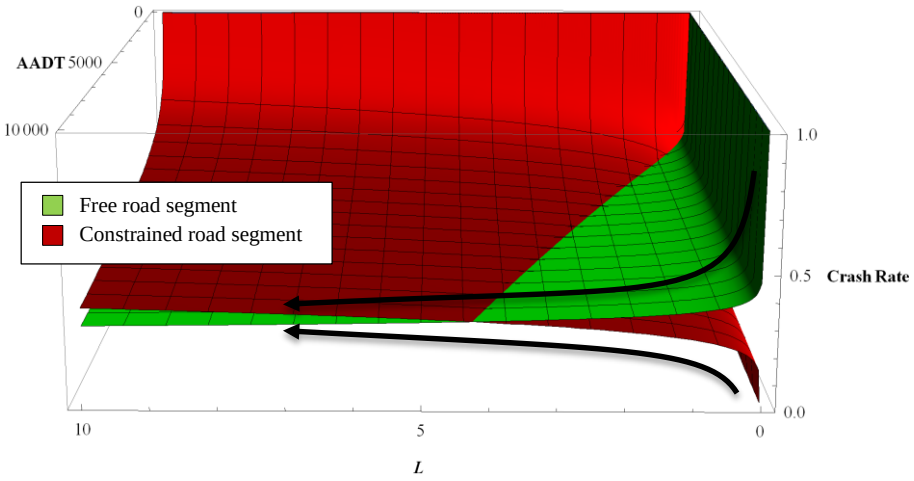

Figure 141. Evolution of the crash rate for free (green) and constrained (red) road segments according to the length. Poor consistency.

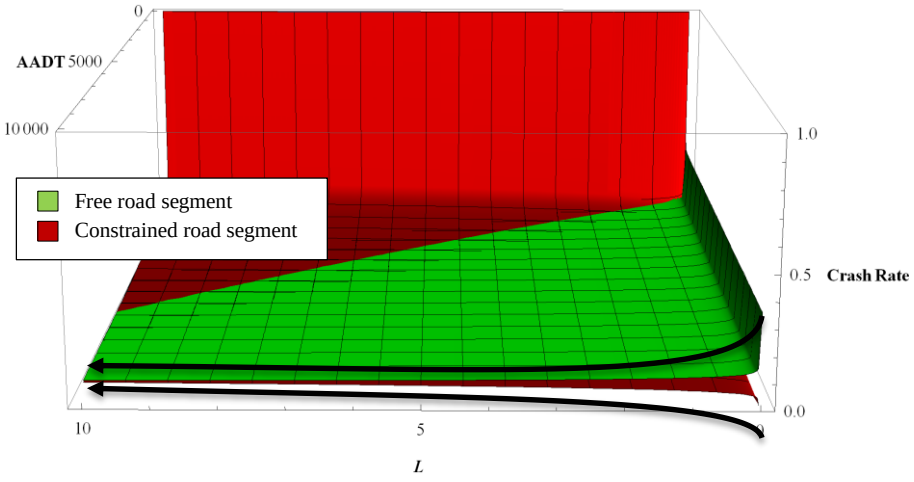

Figure 142. Evolution of the crash rate for free (green) and constrained (red) road segments according to the length. Good consistency.

On the contrary, drivers do not notice when they get into a new free road segment. Hence, they still apply the expectancies of the previous road segment to the current one. This is particularly bad for non-consistent road segments. For consistent road segments, there is almost no variation with the road length.

The convergence of the crash rate estimation for both types of road segments is also important. A change of road segment is not quite important when the consistency of the segment is good. This can be seen in Figure 142, where the type of road segment hardly affects the estimation of road crashes. In fact, the crash rate for both kind of road segments tends to be the same for long road segments.

8.2.2. Effect of the AADT

The AADT also affects the number of crashes differently depending on the road segment type. The AADT estimate for free road segments is quite close to 1, which indicates that crash rates are not affected by AADT. For constrained road segments, this estimate is lower than 1, so a higher AADT implies a lower crash rate, which agrees with most previous research.

When going along a road segment, drivers do not only focus on the road geometry, but also on traffic conditions (AADT). Depending on traffic conditions, drivers will react in different ways, performing a more or less aggressive driving. The lower the AADT, the more aggressive behavior is expected, since drivers do not expect other vehicles. This is why a low traffic road is about to present a higher crash rate.

This effect is even more dramatic for drivers who are familiarized with the road. The knowledge of the road allows them to perform maneuvers even with no visibility, which may be quite hazardous depending on the AADT. This condition is relaxed for high AADT values (Figure 143).

Constrained road segments are normally close to towns or zones where drivers incorporate to a new road, so familiarized drivers are more common. On the other hand, free road segments are part of longer road sections, thus decreasing the familiarity of drivers with the road.

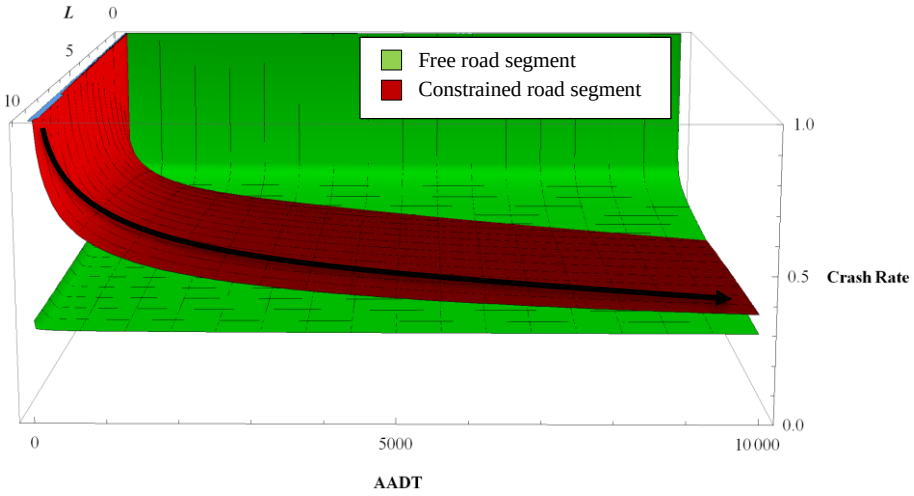

Figure 143. Evolution of the crash rate for free (green) and constrained (red) road segments according to the AADT. Poor consistency.

A good consistency partially relaxes this issue. A better road alignment provides less opportunities of having low sight distance situations, as well as drivers find no need to perform risky maneuvers, since their performance is already good. Figure 144 shows how crash rates are hardly affected by an AADT variation.

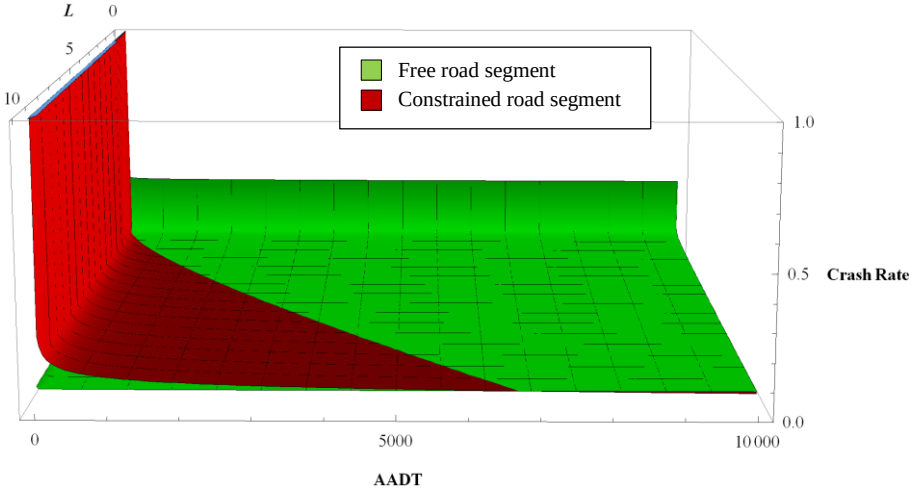

Figure 144. Evolution of the crash rate for free (green) and constrained (red) road segments according to the AADT. Good consistency.

8.2.3. Effect of the consistency parameter

We have seen how the crash rate behavior is quite different depending to the exposure, type of road segment and consistency. As one can expect, a good consistency makes the crash rate less dependent of the other factors, also producing a quite lower crash rate. Crash predictions substantively differ for both road segment types for a low consistency. On the contrary, a good consistency makes the estimations of both road segment types to converge. This is because a consistent road segment is not a problem for drivers, regardless of their concentration on the driving task.

Constrained road segments are more exposed to consistency variations. If we assume $y_{C=4}$ the number of accidents for a certain road segment with a good consistency level ($C = 4$), we can estimate the variation of the number of accidents as a function of the design consistency. The relative number of road accidents (Δy) can be obtained as:

$$\Delta y = \frac{y_C}{y_{C_0}} = \frac{e^{\beta_0} \cdot L^{\beta_1} \cdot AADT^{\beta_2} \cdot e^{\beta_3 \cdot C}}{e^{\beta_0} \cdot L^{\beta_1} \cdot AADT^{\beta_2} \cdot e^{\beta_3 \cdot 4}} = e^{\beta_3 \cdot (C-4)} \quad (359)$$

This expression can be calculated for all types of road segments (Equations 360, 361 and 362 for all, free and constrained road segments, respectively):

$$\Delta y = e^{-0.6574 \cdot (C-4)} \quad (360)$$

$$\Delta y = e^{-0.5216 \cdot (C-4)} \quad (361)$$

$$\Delta y = e^{-0.6430 \cdot (C-4)} \quad (362)$$

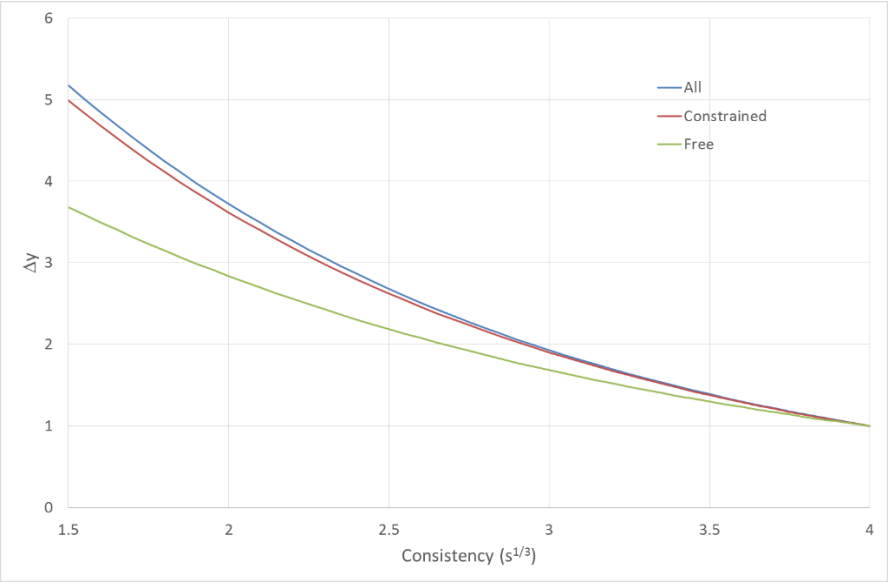

Figure 145. Evolution of road accidents depending on the road consistency.

Therefore, constrained road segments are more affected by consistency rather than free ones. This is the global behavior of road segments, regardless of their AADT and length. As one can see in Figure 137, long, low-consistent constrained road segments tend to produce quite more accidents than free road segments of the same condition. This might be explained due to the mixture of familiar and unfamiliar drivers, which creates two samples of drivers which behave differently. This separation can be clearly noticed for poor consistency, but has much less effect for consistent road segments. It is worth to highlight that those road segments are long enough, so all drivers have acquired their expectations. Hence, the effect may only be explained because of this mixture of drivers. In fact, it can be seen in Figure 137 and Figure 139 how the number of accidents is still higher on free road segments when shorter lengths are compared. Designers should consider this while designing constrained road segments.

Figure 146 shows four parameters of all the road segments: AADT, length, consistency, and crash rate (color of the points, going from 0 (dark blue) to 1.354 (red)). We can see how a lower consistency value leads to a higher crash rate.

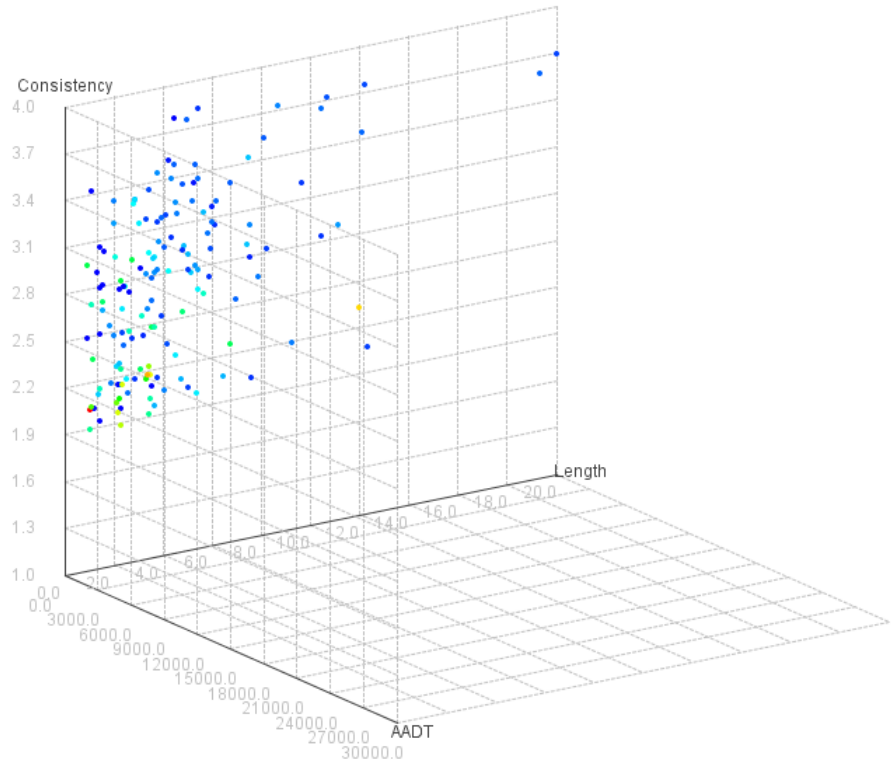

Figure 146. Crash rate (color of the points, from 0 (dark blue) to 1.354 (red)) as a function of the AADT, length and consistency.

8.2.3.1. Interaction between the average operating speed and the average deceleration rate

A lower consistency may result from a low average operating speed or a high average deceleration rate. Figure 147 shows the interaction of both parameters, compared to crash rates (size of the circles). As it was previously detected, both parameters are correlated. However, the average deceleration rate adds a bit more variability to the average operating speed. A higher average operating speed is linked to a better road. For a given average operating speed, the higher the deceleration rate, the higher the crash rate. The consistency result as a result of the primary indicators is depicted in Figure 148.

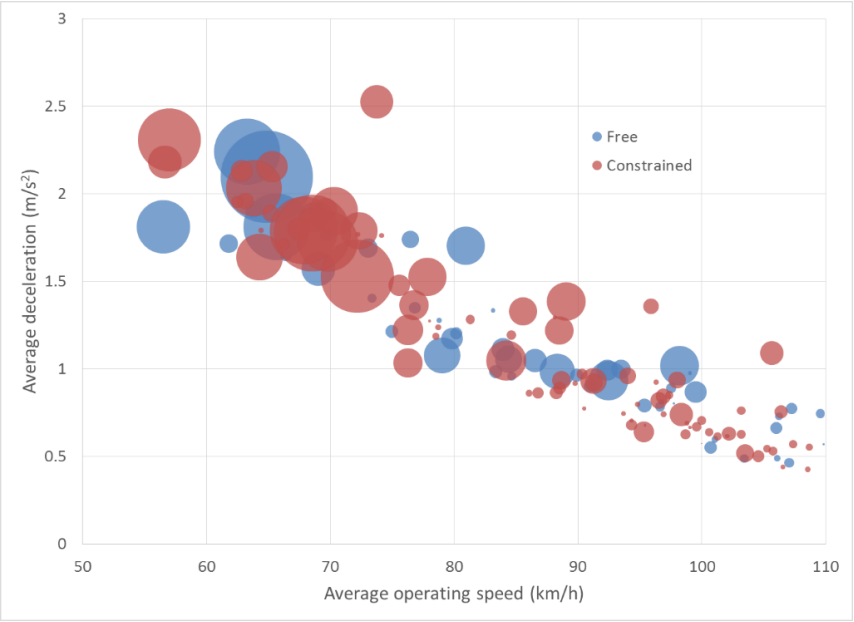

Figure 147. Comparison of average deceleration and average operating speed.

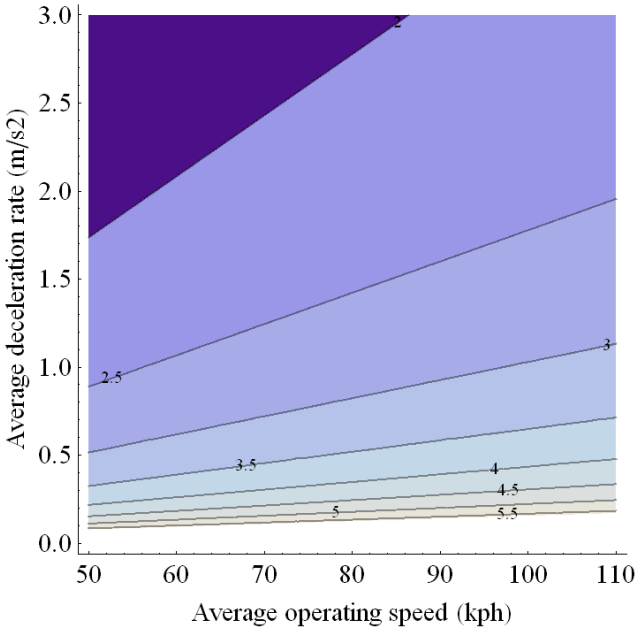

Figure 148. Consistency as a function of both input parameters.

The highest consistency values can only be obtained for road segments with high average operating speed and small deceleration rates. This can be obtained through a low CCR value and large radii. Figure 149 represents an example of operating speed profile from the less hazardous groups of road segments.

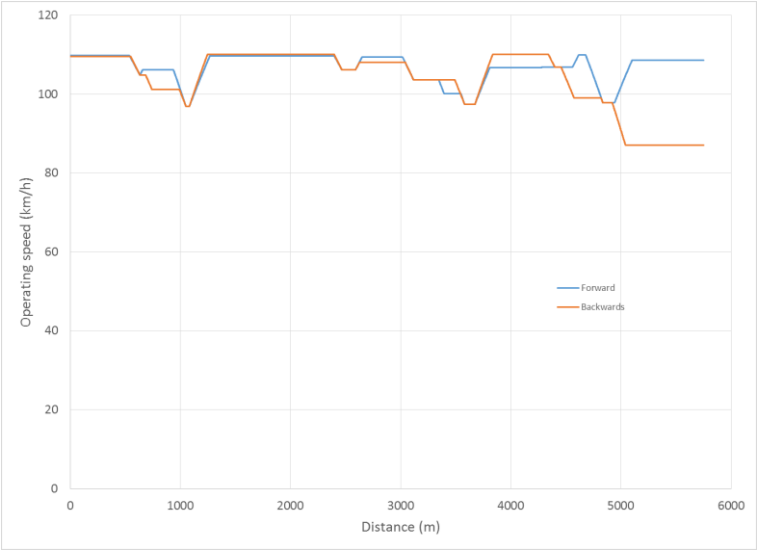

Figure 149. Operating speed profiles of a consistent road segment. Road segment 38.1.

If a road segment presents some medium-radii curves, the average deceleration increases, thus leading to a lower average operating speed. However, the desired speed is still often reached. This makes the consistency parameter to be lower. The speed dispersion increases (Figure 150).

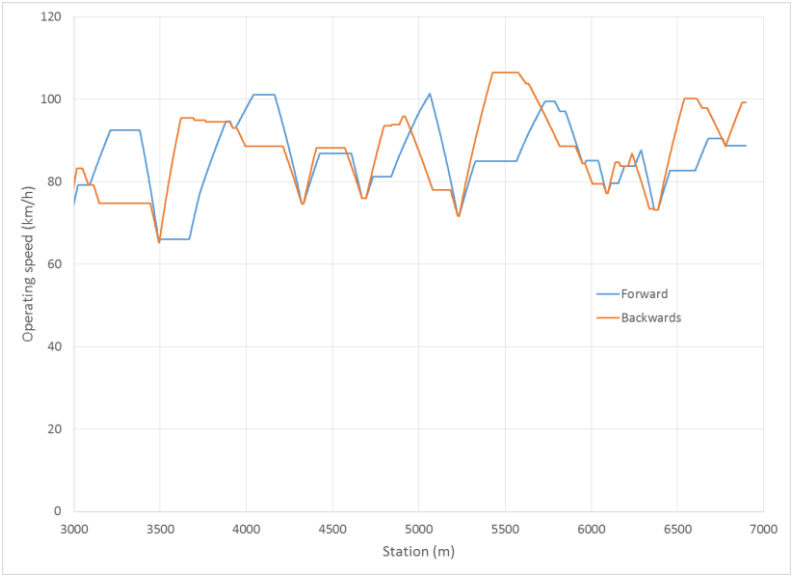

Figure 150. Operating speed profiles of a fair consistent road segment. Road segment 19.2.

There are other road segments that are mostly composed by medium radius curves. Hence, there are a lot of decelerations, which makes the operating speed even lower (Figure 151). In this case, the operating speed is reduced because a large amount of decelerations. The desired speed is hardly reached.

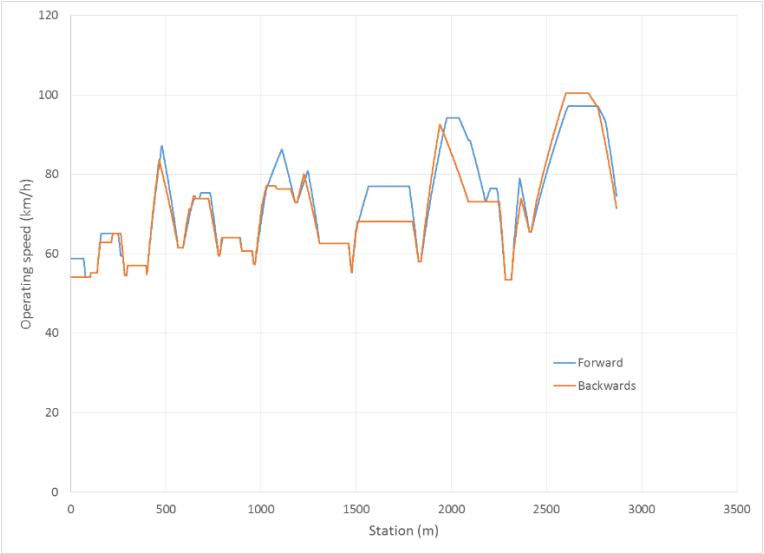

Figure 151. Operating speed profiles of a fair consistent road segment. Road segment 20.1.

Finally, there are some road segments that present a higher CCR, impeding drivers to develop a higher operating speed. This is the case with the lowest operating speeds (Figure 152). There are some medium tangents in which drivers develop a higher speed, but they are soon forced to decelerate again.

In road segments that present a high CCR, drivers cannot reach a high operating speed since they are always constrained by a geometric control. Decelerations are maximum and the speed variation behaves in this way. The low average speed and the high average deceleration rate indicate that the operating speed profile combines very different kinds of speed reductions. Thus, the drivers cannot accommodate expectancies and the situation is the most hazardous.

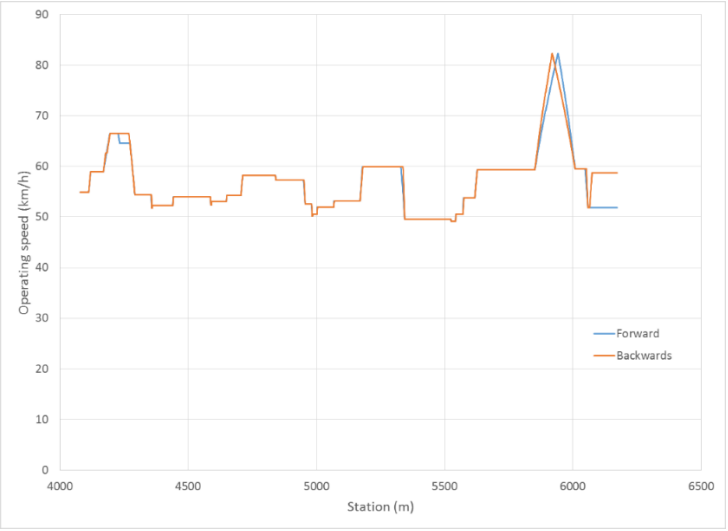

Figure 152. Operating speed profiles of a poor consistent road segment. Road segment 12.3.

A final analysis of the consistency parameter should be performed. This parameter is composed by two variables: the average operating speed and the average deceleration rate. Thus, it is necessary to have both of them when analyzing consistency. However, some operating speed models do not include a deceleration rate that varies with geometry. One example is the well-known 0.85 m/s^2 deceleration rate. In this case, the proposed consistency model would be in fact composed by only one parameter: the average operating speed.

This is not a problem. As we initially indicated when we analyzed the one-variable consistency parameters, the average operating speed was one of the best indicators. In addition, we have shown in this chapter that it is also highly related to the average deceleration rate.

8.2.3.2. Speed reduction threshold

The consistency model considers all speed transitions produced by the operating speed models. Some of the speed transitions are almost negligible. This is why an analysis of its influence on the final result was performed.

Several models were tried only considering speed reductions higher than 0 (original situation), 1, 2, 3, 4 and 5 kph. The consistency parameter was the selected as the final one. The following AIC values were obtained:

- 0 kph: 693.1170.
- 1 kph: 694.9355.
- 2 kph: 694.3633.
- 3 kph: 694.1007.
- 4 kph: 686.1828.
- 5 kph: 686.4711.

The last two models presented two road segments less than the other cases. This is the reason of their lower AIC, not the better accuracy of the models. Therefore, the 0 kph threshold was selected, since it is easier to calculate, considers the maximum number of road segments, and provides the best adjustment. Figure 153 shows the distribution of speed reductions of all road segments.

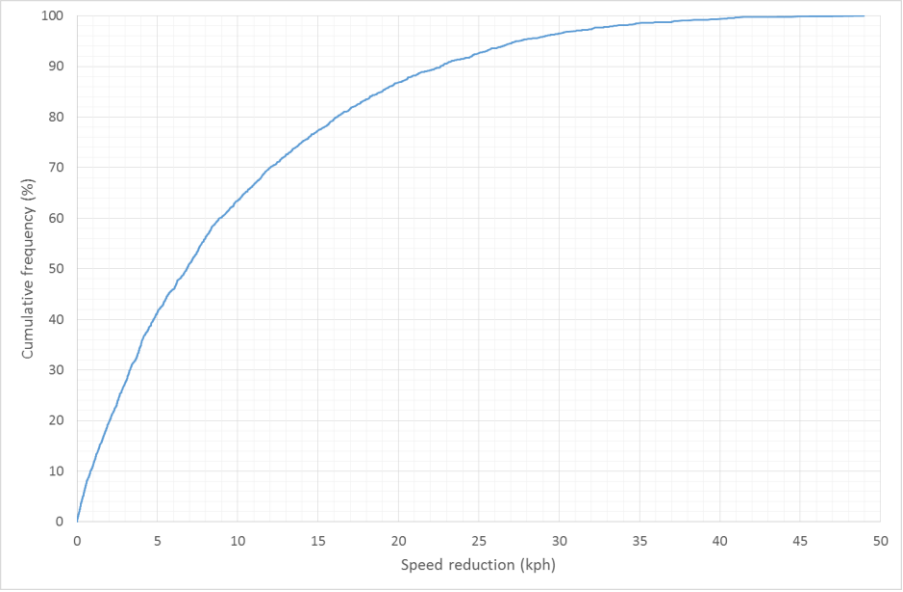

Figure 153. Distribution of speed reductions (kph).

8.2.3.3. Design consistency thresholds

Three consistency zones were identified. Figure 154 shows the estimated number of accidents as a function of the exposure and for the three consistency thresholds. The overall consistency ranges from $C = 1.5$ to $C = 4.2$, which have been the extreme values observed. Thresholds for good and poor consistency are $C = 3.25$ and $C = 2.55$, respectively.

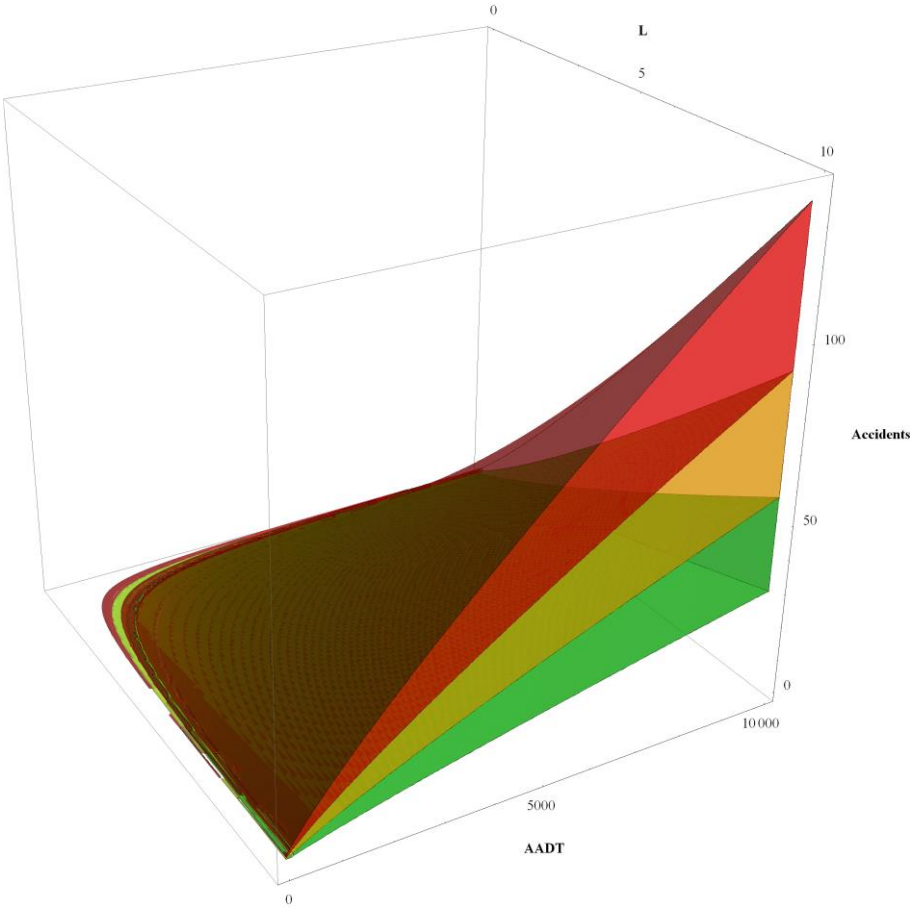

Figure 154. Estimated accidents with victims (10 years) for the three consistency ranges.

Table 52 indicates the changes of average crash rate and crash rate dispersion.

Consistency level	Range	Mean Crash Rate	Crash Rate dispersion
Good	$C \geq 3.25$	0.1241	0.0729
Fair	$2.55 \leq C < 3.25$	0.2080	0.1677
Poor	$C < 2.55$	0.4152	0.3547

Table 52. Crash rate behavior for all consistency thresholds.

Table 52 shows how dramatically changes the expected crash rate behavior depending on the consistency range. As a simple rule, it can be seen that both the

average and the dispersion double when going from good to fair, and double again when going to poor consistency. As a result, a poorer consistency is linked to a worse outcome in terms of crash rates and a higher uncertainty on that estimation.

8.3. Validation of the consistency model

In order to check the validity of the consistency model, a validation test was performed with six road sections. Those sections were not considered in the calibration step.

Those road sections are summarized in Table 53.

Code	Road	Begin	End	Initial station	Final station
V1	CV-370	Roundabout	Roundabout	8+500	12+000
V2	CV-401	Roundabout	Intersection	0+300	6+300
V3	CV-376	Roundabout	Intersection	0+000	10+900
V4	CV-310	Roundabout	Urban	9+300	14+800
V5	CV-315	Roundabout	Roundabout	12+900	17+900
V6	CV-660	Intersection	Roundabout	0+000	26+640

Table 53. Road sections for validation.

The horizontal alignment was extracted for all of them. The operating speed profiles were afterwards calculated. All road sections were divided into homogeneous sections, by applying the methodology exposed in this document. As a result, 23 homogeneous road segments were identified. The AADT, operational parameters, consistency and accidents were estimated. They were compared to the observed accidents, as shown in Table 54.

Segment	Road	Segment type	Length (km)	AADT (vpd)	C	Accidents	
						Estimated	Observed
V1.1	CV-370	Constrained	3.489	20053	2.98	35	33
V2.1	CV-401	Constrained	1.856	4878	2.77	6	10
V2.2	CV-401	Free	0.859	4878	2.43	4	10
V2.3	CV-401	Free	1.945	4878	2.83	7	3
V2.4	CV-401	Constrained	1.383	4878	2.65	5	3
V3.1	CV-376	Constrained	2.904	3284	2.70	8	8
V3.2	CV-376	Free	1.809	3284	2.51	5	15
V3.3	CV-376	Free	2.767	3284	3.35	5	15
V3.4	CV-376	Constrained	3.353	3284	3.15	7	13
V4.1	CV-310	Constrained	5.278	6030	2.85	24	30
V5.1	CV-315	Constrained	1.676	6892	2.99	6	4
V5.2	CV-315	Free	2.129	6892	3.01	10	2
V5.3	CV-315	Constrained	1.105	6892	3.19	3	2
V6.1	CV-660	Constrained	2.803	1213	2.56	4	1

V6.2	CV-660	Free	5.654	1213	2.56	6	13
V6.3	CV-660	Free	1.557	1213	2.37	2	3
V6.4	CV-660	Free	3.68	1213	3.06	3	4
V6.5	CV-660	Free	3.193	1213	2.82	3	1
V6.6	CV-660	Free	1.477	1213	3.02	1	0
V6.7	CV-660	Free	3.726	762	3.15	2	3
V6.8	CV-660	Free	0.811	762	2.03	1	1
V6.9	CV-660	Free	1.844	762	2.61	1	0
V6.10	CV-660	Constrained	1.186	762	2.13	1	1

Table 54. Homogeneous road segments (validation). Estimated and observed accidents.

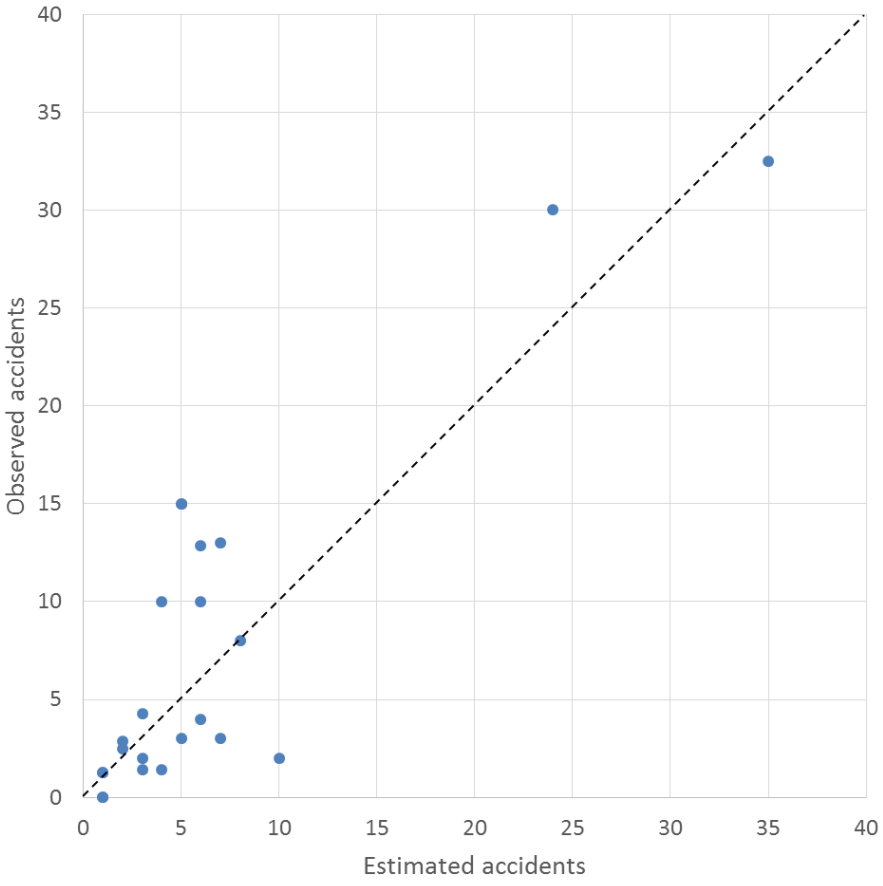

Figure 155. Observed vs. estimated accidents with victims for the validation road segments.

Figure 155 shows the comparison between the observed and predicted accidents for all validation road segments. As it can be seen, the model gives an indicative estimation of the number of accidents with the consistency model.

Figure 156 shows the relationship between the consistency value and the crash rate for those road segments. One can see how a lower value of the consistency is generally linked to a higher crash rate.

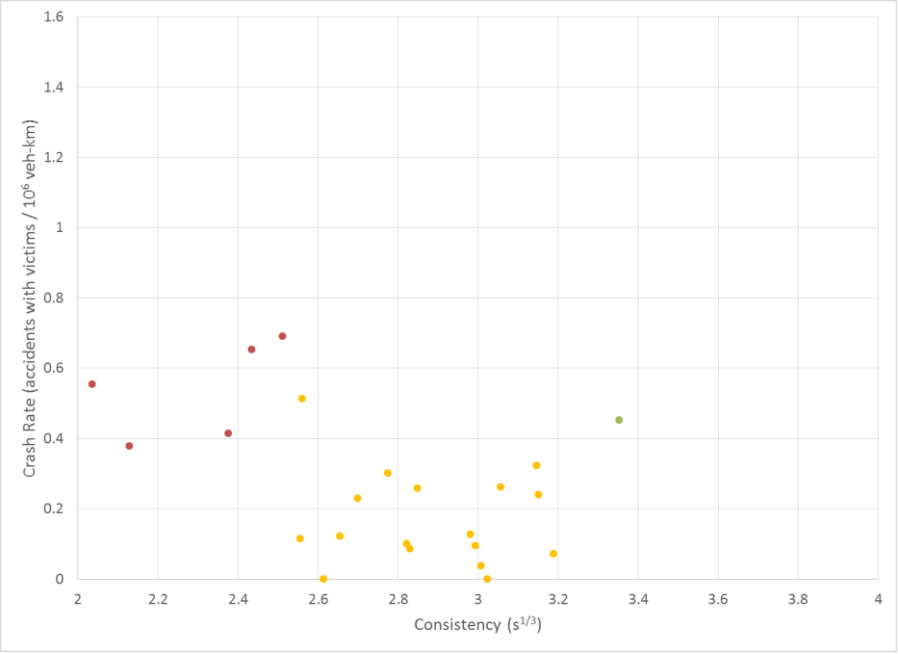

Figure 156. Evolution of the crash rate as a function of the consistency value. Validation road segments.

Figure 157 shows the comparison between the estimated accidents and the observed accidents for two different safety performance functions. The blue small dots represent the original SPF. On the contrary, the red, big dots represent the safety performance function without the influence of the consistency. One can see how the second SPF gives a lower number of accidents, far away from reality. This also indicates that the consistency influence is not negligible in the estimation of the number of crashes.

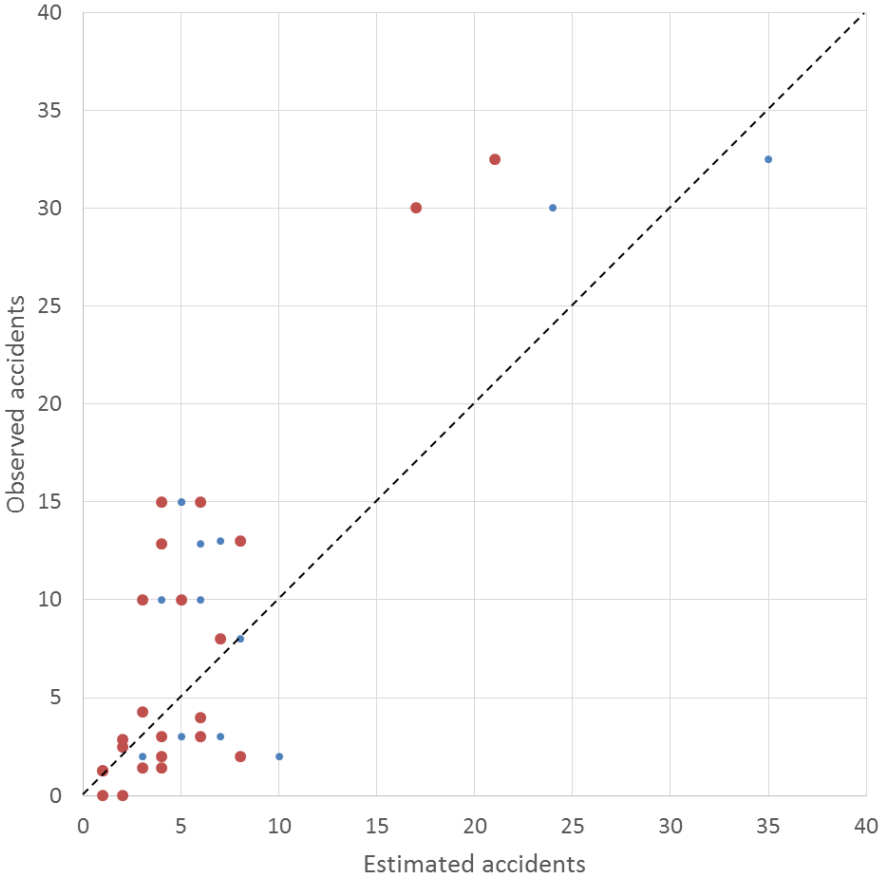

Figure 157. Estimated vs. observed accidents considering the consistency (blue dots) and not considering it (red dots). Validation road segments.

8.4. Comparison to other global consistency models

The proposed consistency model has been compared to other global consistency models. All these models present different functional forms, so the estimates cannot be directly compared. Instead, the comparison is performed by examining the predicted number of accidents with victims by the different models. This comparison was performed for all road segments, including both calibration and validation.

Figure 158 shows the comparison for the developed consistency model, while Figure 159 and Figure 160 are focused on the Polus' consistency model. As it can be seen,

the proposed model produces a better estimation of the number of accidents, especially for large outcomes.

The global consistency model proposed by Polus and Mattar-Habib (2004) clearly overestimates the number of accidents. Their safety performance function, however, was developed for Israeli and German roads. A particular adjustment of their model to Spanish roads was later developed by García and Camacho-Torregrosa (2009) (Figure 160). The adjustment of the safety performance function provided by Laura Garach (2013) is also provided (Figure 161). These adjustments fit better than the first proposed by Polus and Mattar-Habib (2004), but they are still worse than the proposed in this Doctoral Thesis.

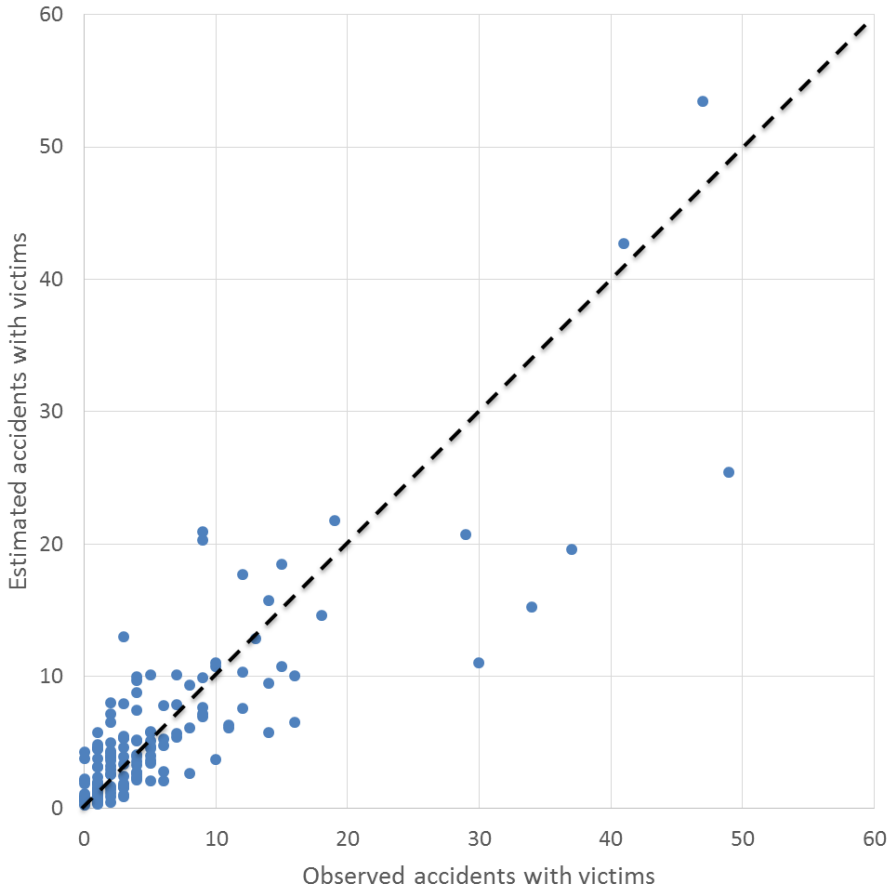

Figure 158. Observed vs. Predicted accidents with victims. Proposed consistency model. Free and constrained road segments are considered, although they are not distinguished here.

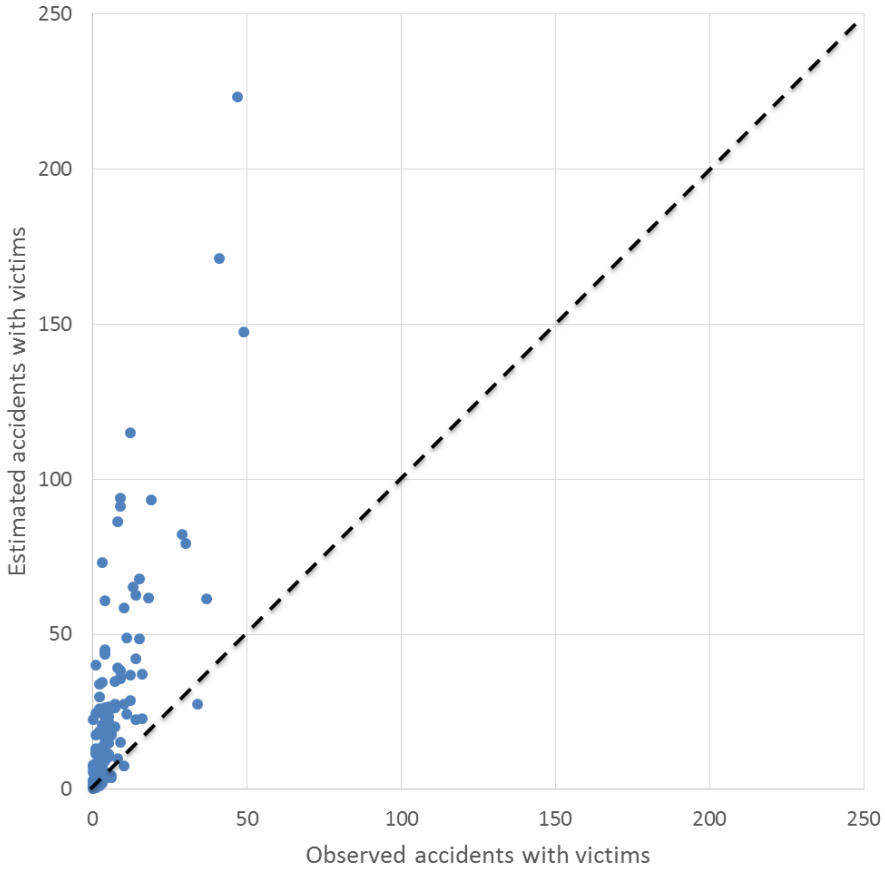

Figure 159. Observed vs. Predicted accidents with victims. Polus consistency model.

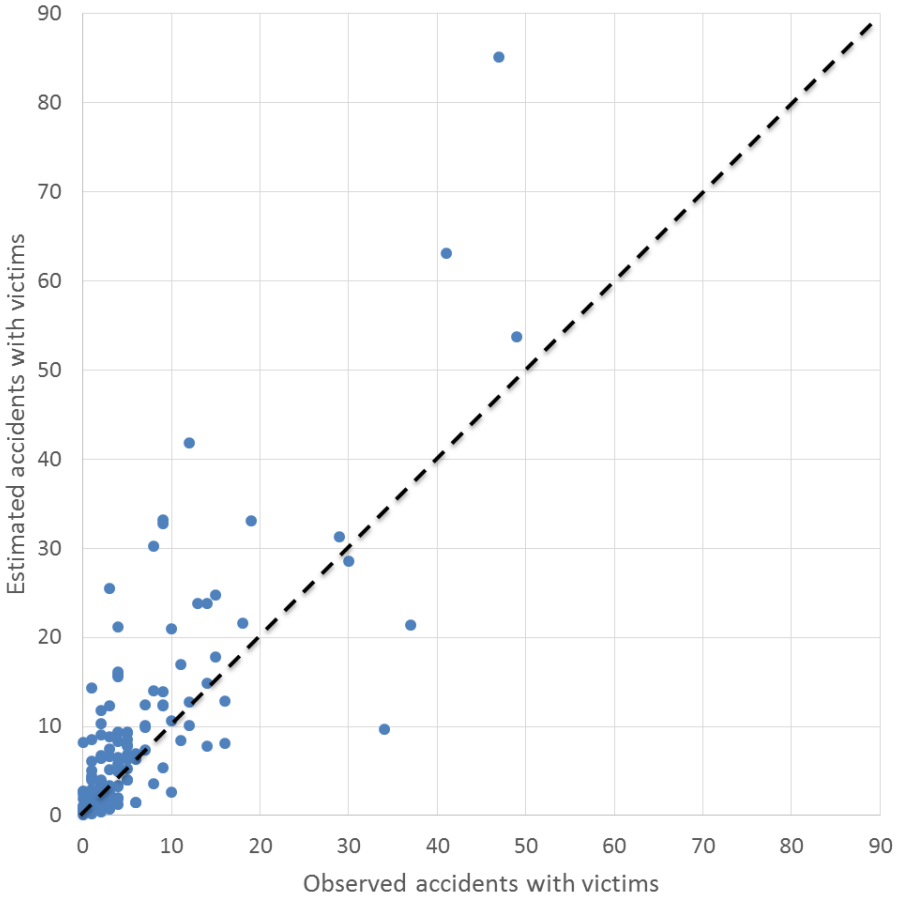

Figure 160. Observed vs. Predicted accidents with victims. Polus consistency model adjusting the crash rate to the Valencian roads.

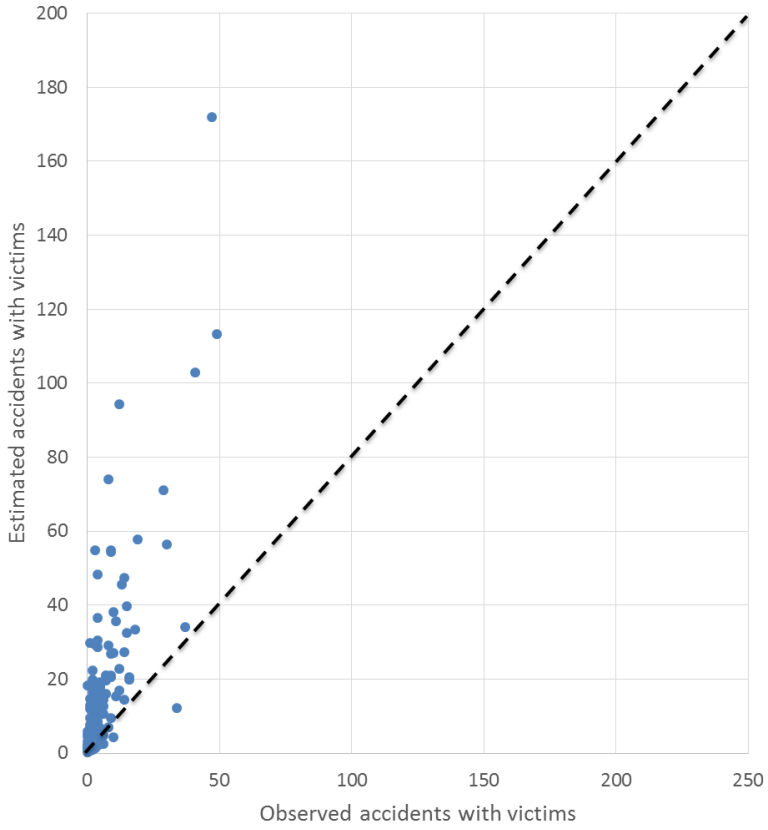

Figure 161. Observed vs. Predicted accidents with victims. Laura Garach consistency model.

It was also indicated that the exposure terms explains most variability. Figure 162 shows the expected vs. observed accidents while considering the Safety Performance Function only with exposure (big red dots). The small blue dots represent the estimated number of accidents for the final consistency model. We can see that adding the consistency parameter allows us to more accurately estimate the number of accidents.

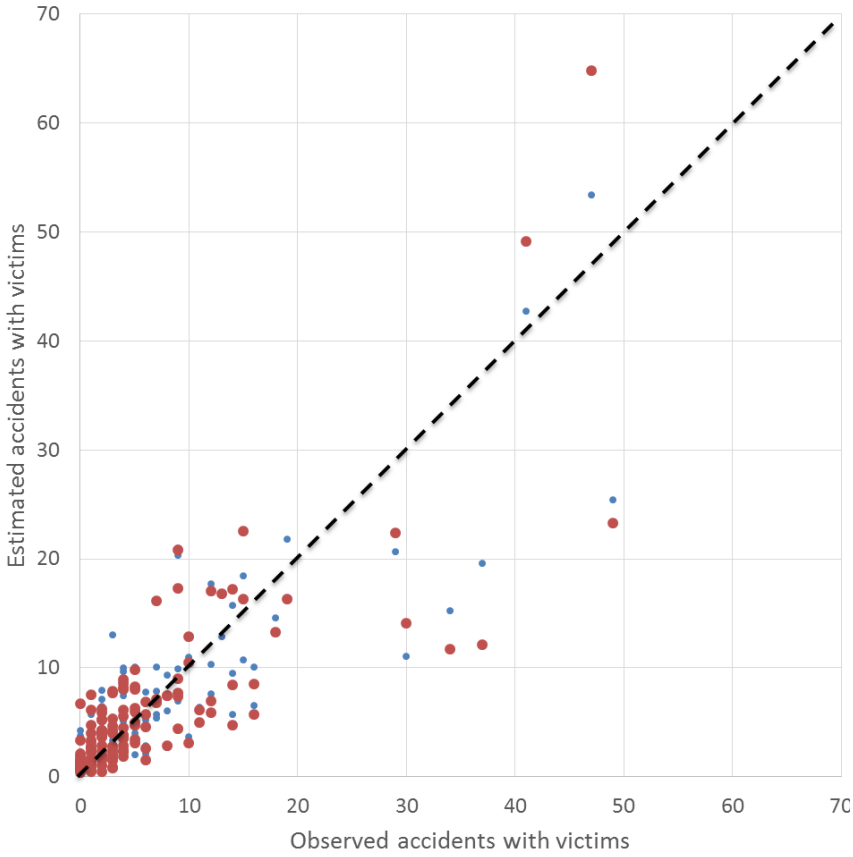

Figure 162. Observed vs. estimated accidents with victims considering the consistency (blue dots) and not considering it (red dots).

Polus, Garach and the proposed consistency models can also be compared in terms of the consistency thresholds. All three consistency models were applied to all road segments. A close-to-linear relationship was expected, but the results show a near-random relationship (Figure 163 and Figure 164). The Polus and Garach consistency models and thresholds were established exclusively considering operating speed variations, not considering the number of accidents. This may be one of the reasons why the thresholds provided by both consistency models differ so much.

The problem of the thresholds given by Polus and Garach is that several good and fair consistent segments are classified as poor, and otherwise. This might lead engineers to redesign already good road segments or to leave without changes poor consistent segments.

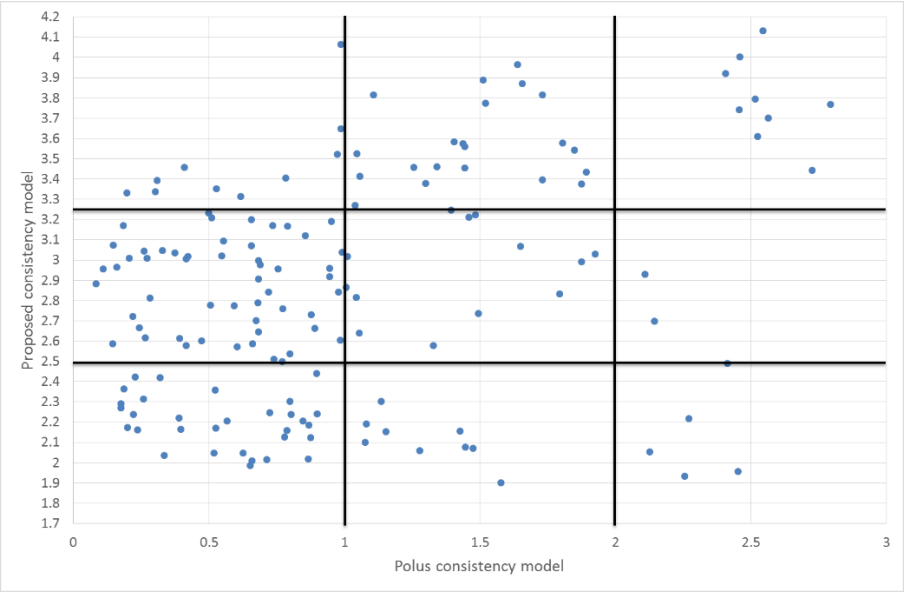

Figure 163. Comparison of the consistency thresholds for the proposed model and Polus consistency model.

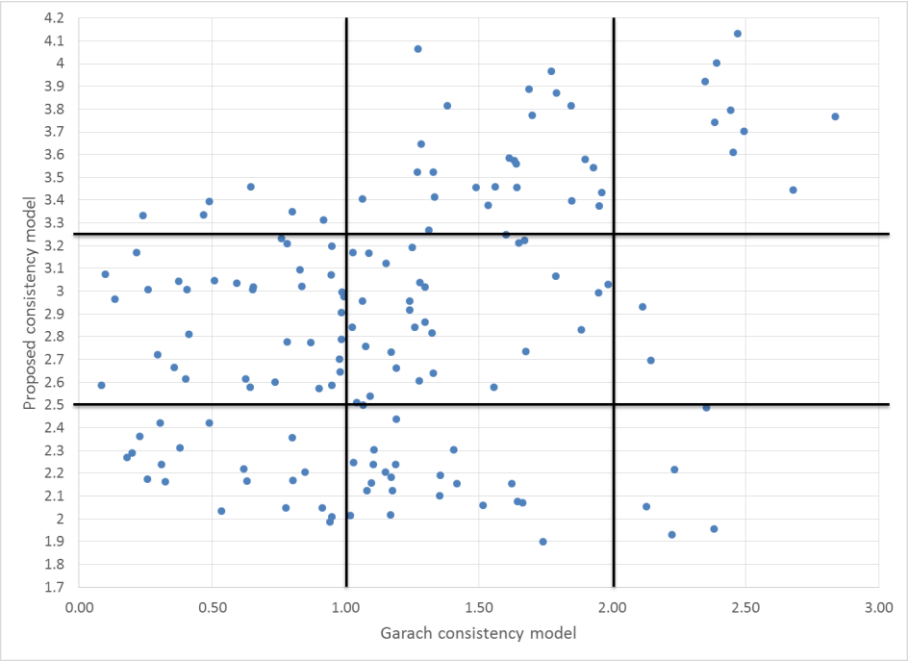

Figure 164. Comparison of the consistency thresholds for the proposed model and Garach consistency model.

Figure 165 and Figure 166 add to the previous comparison the observed crash rate (diameter of the bubbles). We can observe how the proposed model – and the corresponding thresholds – provide a better approach to the crash phenomena than Polus' and Garach's global consistency models.

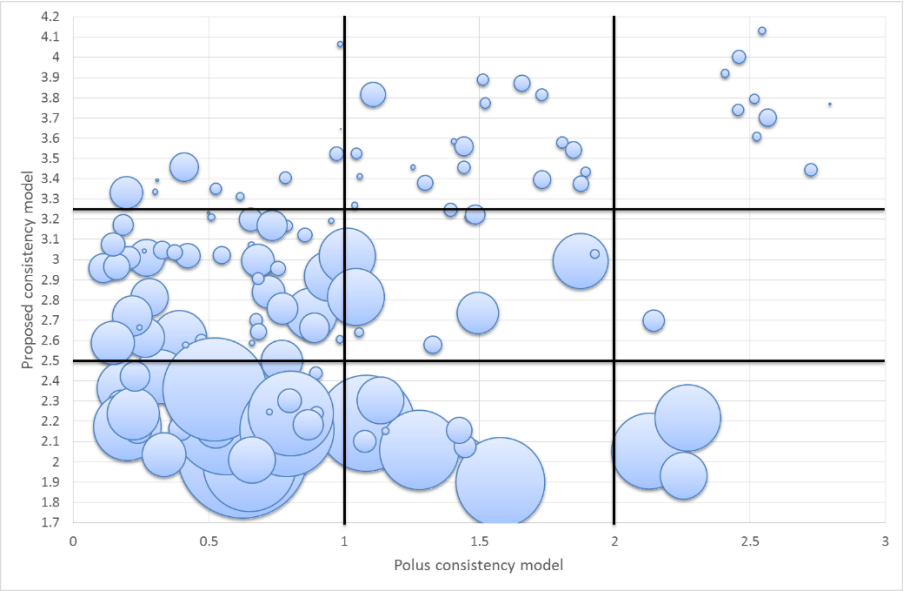

Figure 165. Comparison of the proposed and Polus consistency models. The diameter of the bubbles represent the crash rate for each road segment.

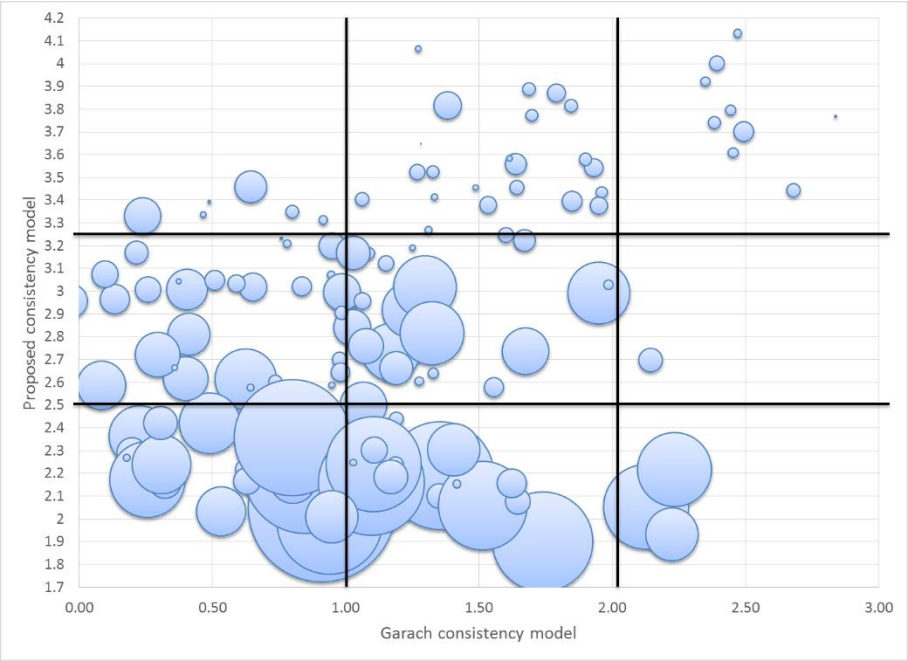

Figure 166. Comparison of the proposed and Garach consistency models. The diameter of the bubbles represent the crash rate for each road segment.

8.5. Road segmentation

Road segmentation is required for determining homogeneous road segments. The presented methodology uses three kinds of parameters:

- Traffic data.
- Geometric data (CCR).
- Operational data (inertial operating speed).

Traffic and CCR have been widely used, but this is not the case with the inertial operating speed. A distance of 1000 m has been selected as appropriate for determining the inertial operating speed, but no evidence of this distance has been given yet.

In the previous development of this parameter, a set of distances were proposed as suitable for determining the inertial operating speed, such as 500 and 1500 m (Figure 167 and Figure 168).

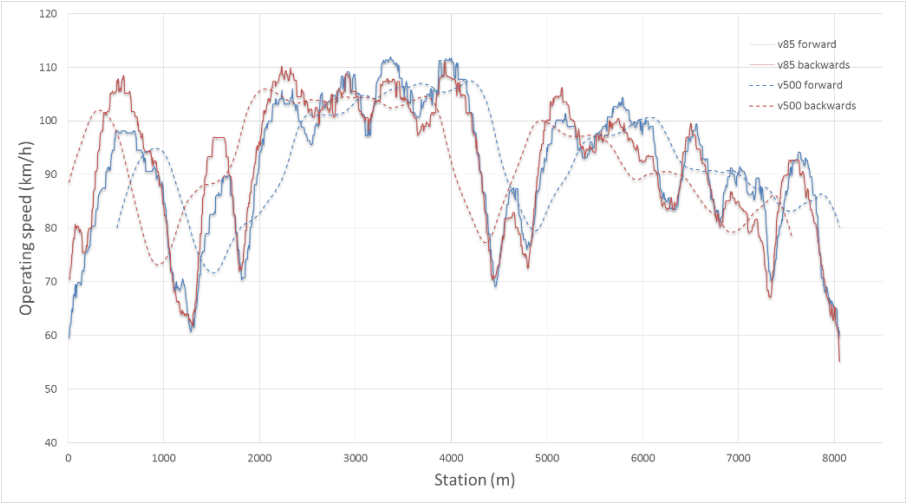

Figure 167. Inertial operating speed profiles considering 500 m.

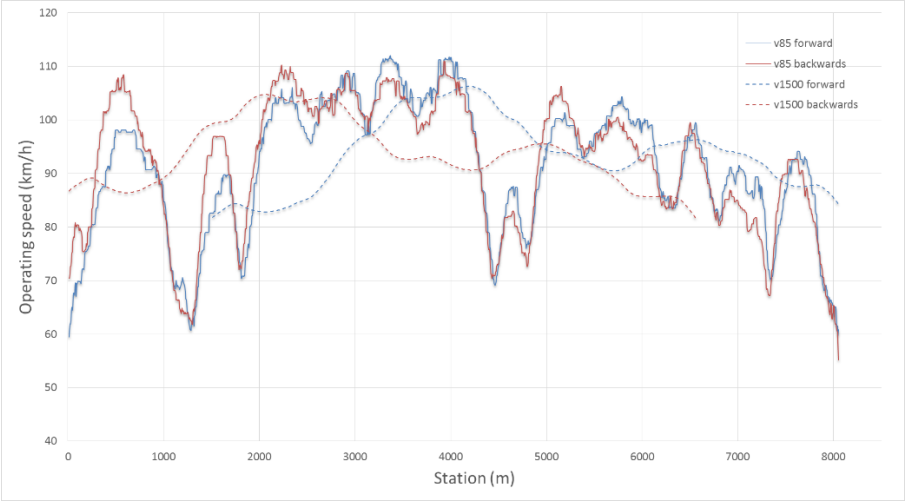

Figure 168. Inertial operating speed profiles considering 1500 m.

The inertial operating speed calculated with a range of 500 m is too similar to the operating speed profile, thus producing too short road segments. Intuitively, one can guess that driver's expectancies are based considering a longer distance. Because of the shorter length, this diagram cannot be used for determining homogeneous behaviors. On the contrary, the inertial operating speed profile created integrating

1500 m was considered to be not enough precise. Thus, a distance of 1000 m was proposed, since it merges the global behavior of drivers with enough precision.

The calibration of the consistency model, as well as the differences found between free and constrained road segments, have produced additional data about driver expectancies that could be used for this purpose.

Figure 169 represents the crash rate depending on the length (front axis) and the AADT, for a very low consistency level. We can see how the crash rate for free road segments is higher for a low length (the drivers are not aware of the change of the characteristics of the road segment). When the drivers readapt their expectations to the current road segment, the crash rate gets similar than for constrained road segments. Figure 169 shows that the required length to do this is from 1 to 4 km, depending on the AADT. However, this conclusion is not entirely valid; a more specified study should be performed.

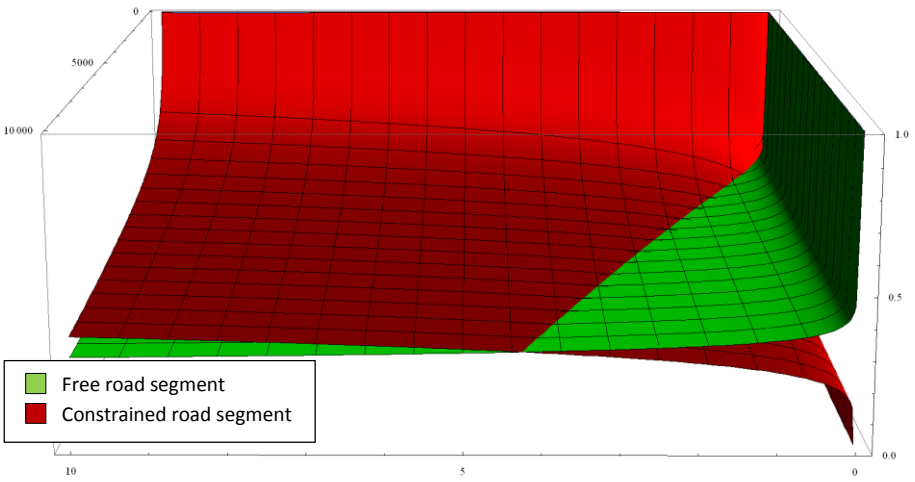

Figure 169. Crash rates for free and constrained road segments (bad consistency). The length where both functions estimate the same number of accidents ranges from 1 to 4 km.

Figure 170 shows the same graphic for high consistency levels. In this case, both crash rates are quite smaller. In addition, the intersection between both surfaces takes place at a longer distance. This means that it is more difficult for drivers to notice all the behavioral changes of the road when the consistency level is high. This agrees with the previous assumptions.

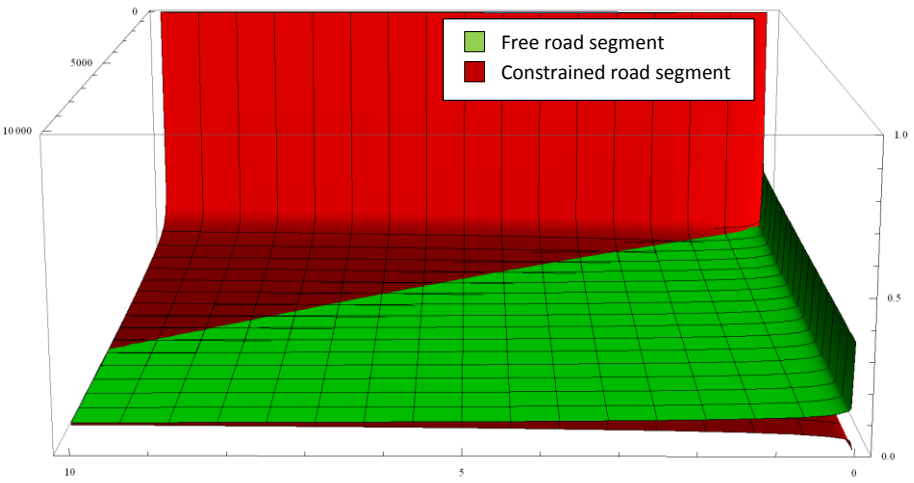

Figure 170. Crash rates for free and constrained road segments (good consistency). Both estimators produce roughly the same outcome.

The previous findings highlight the fact that drivers need different distances for adapting their expectancies to the road behavior, depending on the consistency of the road segment. Hence, the distance should not always be the same, varying depending on the workload demand imposed to the drivers. Complex geometries impose a higher workload, and drivers adapt their behavior sooner than otherwise.

In addition, distance is not important for drivers while acquiring new expectancies, but time is. For a driver, it is not the same travelling 1 km at 120 kph than at 60 kph. In the second case, they will spend twice as much time, thus leading to a better learning of the road. This remarks the importance of considering time instead of distance while dealing with driver experience and behavior. The inertial consistency index should be reformulated accordingly.

In addition, the effect of the previous road segment, regardless of its length, is not homogeneous. Some previous research remarked that drivers take more into account the most recent portion of the road rather than the distant ones. Therefore, some weighting patterns should be added in determining the inertial operating speed parameter.

Two road sections (sections 2 and 3) were divided into homogeneous road segments according to three different methodologies:

- Methodology 1: only using traffic data.
- Methodology 2: using traffic and CCR data.
- Methodology 3: using traffic, CCR and inertial operating speed data.

Road sections 2 and 3 were selected, due to their length and variability of their geometric and operational properties. Both sections provided 16 homogeneous road segments. Figure 171 shows the observed and estimated accidents with victims for both road sections, exclusively according to their traffic and major intersections division. The proposed consistency model estimates a number of accidents (blue) clearly higher than the observed one (green). That difference could be explained as a consequence of two different issues:

- The proposed consistency model is biased.
- The segmentation methodology 1 is biased.

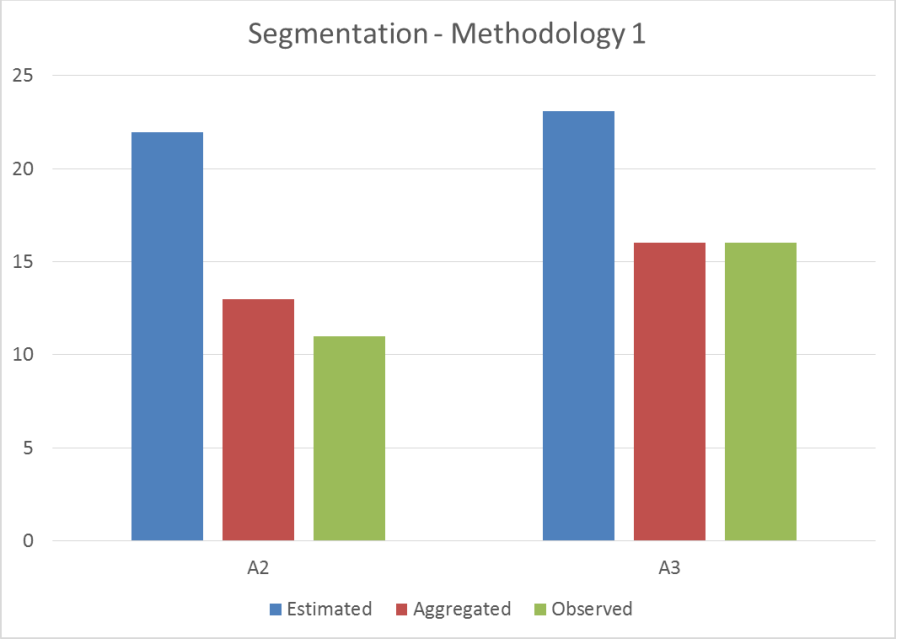

Figure 171. Comparison of estimated and observed accidents according to segmentation methodology 1.

Figure 172 provides a better approach to the actual phenomena. In this case, homogeneous road segments were obtained considering traffic, major junctions and CCR (geometry). We can see how in most cases the estimated number of accidents is really close to the observed number of accidents. This rejects the abovementioned

possibility of a biased proposed consistency model. Moreover, in the case the problem was the consistency model, the estimates should have resulted even worse than for Methodology 1, since we are examining deeper data. As a result, we can affirm that the second methodology is clearly better than the first one.

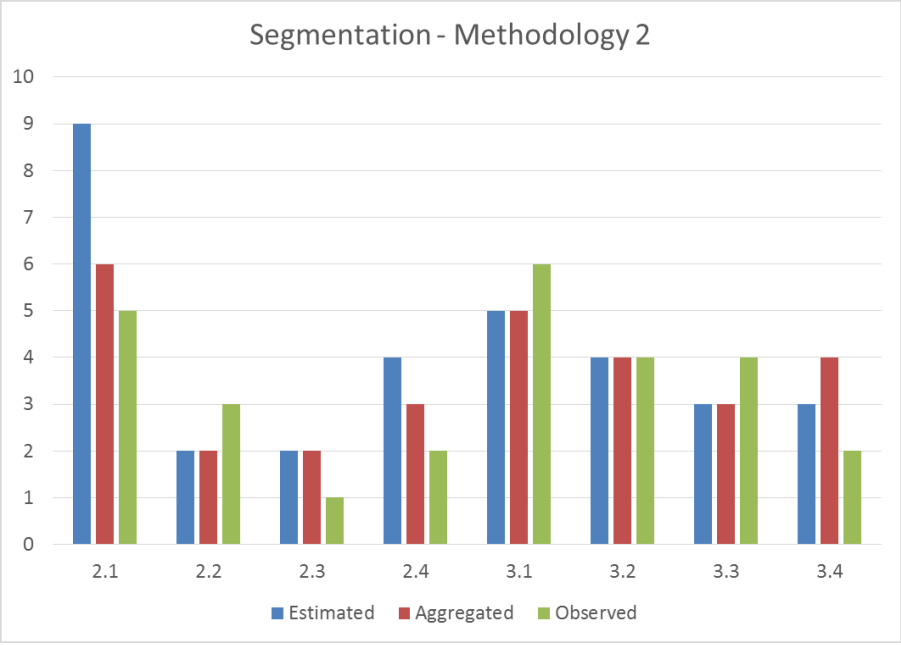

Figure 172. Comparison of estimated and observed accidents according to segmentation methodology 2.

We can, however, provide a better approach to the problem. When adding the third condition for determining homogeneous road segments (inertial operating speed), we can see how the results improve (Figure 173).

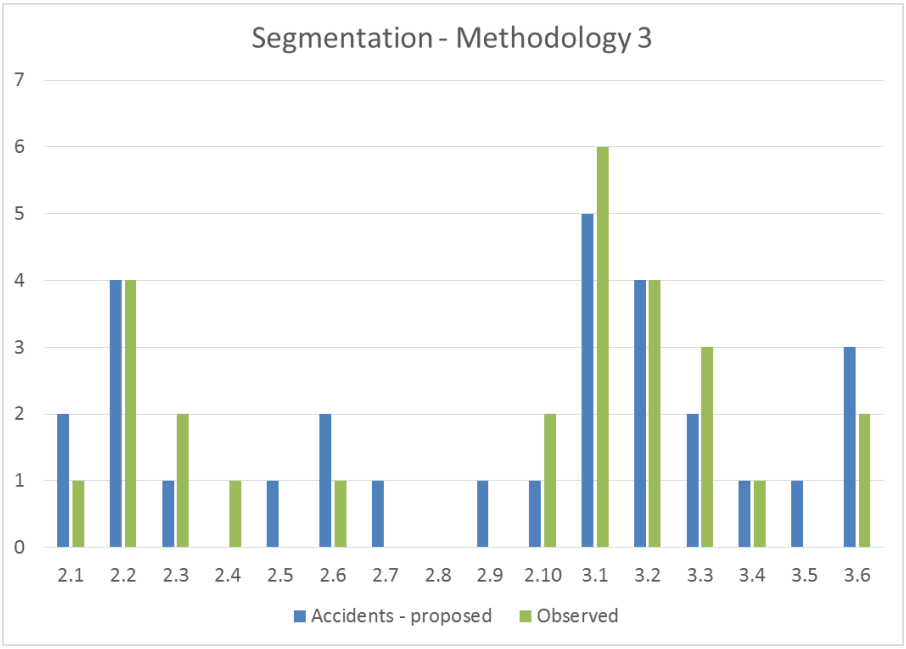

Figure 173. Comparison of estimated and observed accidents according to segmentation methodology 3.

The addition of the operating speed provides a more detailed approach. We can see how segment 2.1 for Methodology 2 is now divided into road segments 2.1 and 2.2 for Methodology 3. There are some other cases, but this was the most dramatic. The inclusion of the operational parameter in the segmentation process adds the possibility of getting a better knowledge about the location of the most hazardous road segments. The highest difference is 1 accident, which is quite good, having into account that we are dealing with count data. In fact, we can merge the estimations for all road segments (column 'Aggregate' for Figure 171 and Figure 172). We can see how the aggregated number of accidents using the proposed consistency model and the proposed segmentation procedure is clearly similar (and even the same in some cases) than the observed number of accidents. This validates both methodologies. This also remarks the necessity of having homogeneous road segments when applying a global consistency model. Otherwise, results might be biased.

Figure 174 shows the relationship between observed and aggregated estimated road accidents for the initial road sections.

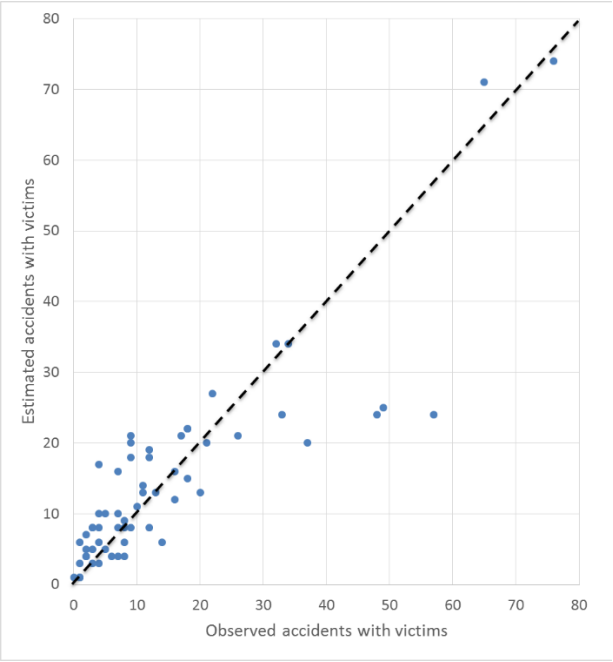

Figure 174. Observed vs. estimated accidents with victims. Aggregated values for original road sections.

8.6. Implications for road design

8.6.1. Clustering of types of roads according to their operating/crash rate behavior

Considering the distribution of average operating speed and average deceleration rate, two types of roads can be distinguished. Two cluster analysis were performed, according to the average operating speed and the average deceleration in the first case, and to both variables as well as the crash rate in the second one. The result was the same in both cases (Figure 175).

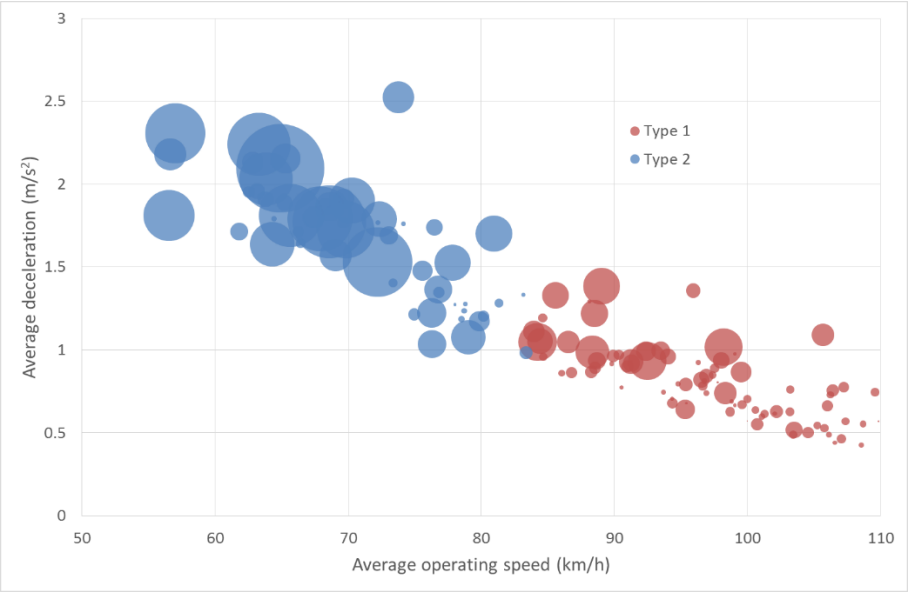

Figure 175. Types of road segments according to their deceleration – operating speed behavior.

Those two groups present a different behavior according to their speed-deceleration relationship. This relationship is also reflected in the crash rates. The roads that belong to Type 1 can be seen as roads that present a general good performance. Drivers reach higher speeds and the average deceleration rate is controlled. A small change in the road design (for instance, smoothing certain radii) that provide a slight reduction of the average deceleration rate will have an important effect on the average operating speed.

Road segments belonging to Type 2 present higher deceleration rates. The operating speeds are indeed quite lower. The operating speed controls are very strong, so a change of the average deceleration rate has a low effect on the average operating speed.

Both operational parameters (average operating speed and average deceleration rate) can be explained as a consequence of the CCR. Figure 176 shows the evolution of the average operating speed in terms of the CCR. We can see how type 1 roads present a CCR lower than 150-200 gon/km. However, in this zone a slight change of the CCR has a high effect on the average operating speed. The limit between type 1 and type 2 roads is set at 83.5 kph. Type 2 roads present quite higher CCR values. However, in this case the operating speed is less affected by CCR variations. This

relationship can be used for road designers for defining a design speed depending on the CCR of the road.

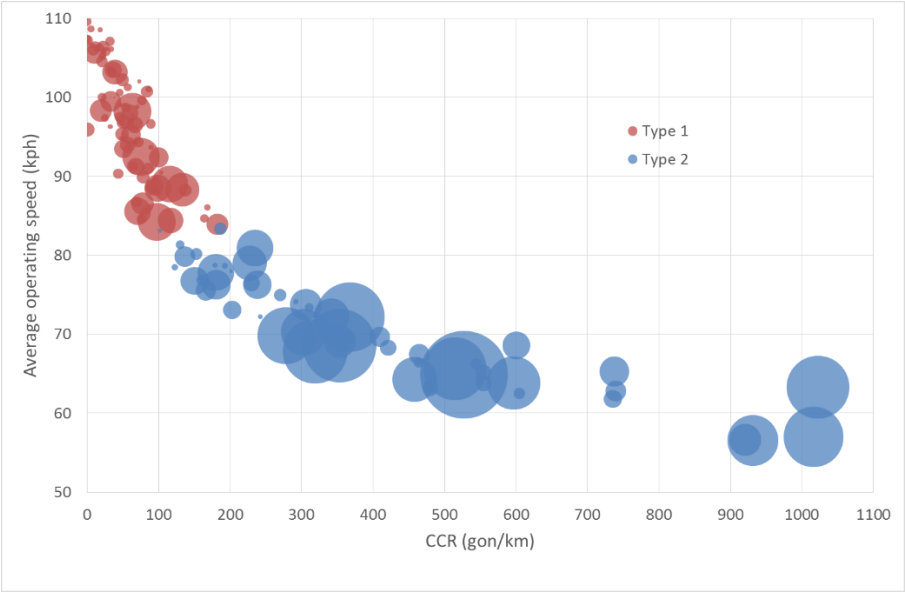

Figure 176. Relationship between the average operating speed and the CCR value.

The other component of the consistency parameter is the average deceleration rate. It is also related to the CCR. A higher CCR leads to higher decelerations. However, for a certain CCR threshold different average deceleration values may appear (see Figure 177, range 0-200 CCR). This is the result of the way horizontal curves are combined. If there is a series of consecutive curves with no intermediate tangents, decelerations might not exist, so the average deceleration is lower. On the contrary, if they are more dispersed, drivers can accelerate and thus there are more decelerations. The last case provides a lower consistency.

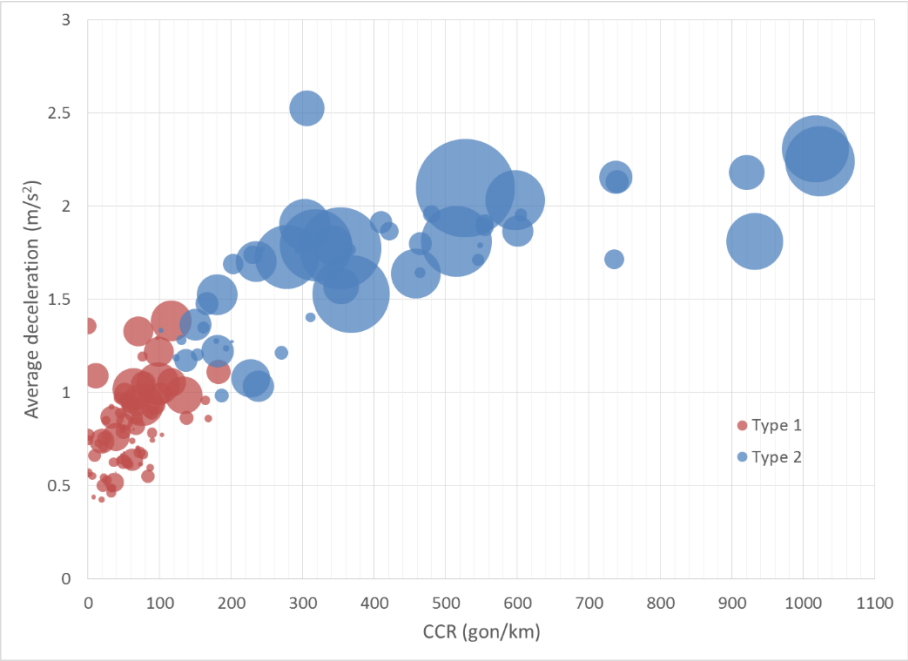

Figure 177. Average deceleration rate as a function of the CCR.

8.6.2. Analysis of the operating speed and surrogate measures

Several parameters present interesting interactions that can be used for road design. For instance, the relationship between the average operating speed and its dispersion. Those two variables are slightly correlated, but a clear trend can be distinguished (Figure 178). Free and constrained road segments are spread randomly. We can see an inverse 'U'-shaped relationship, in which the left and right sides behave completely different according to road crashes.

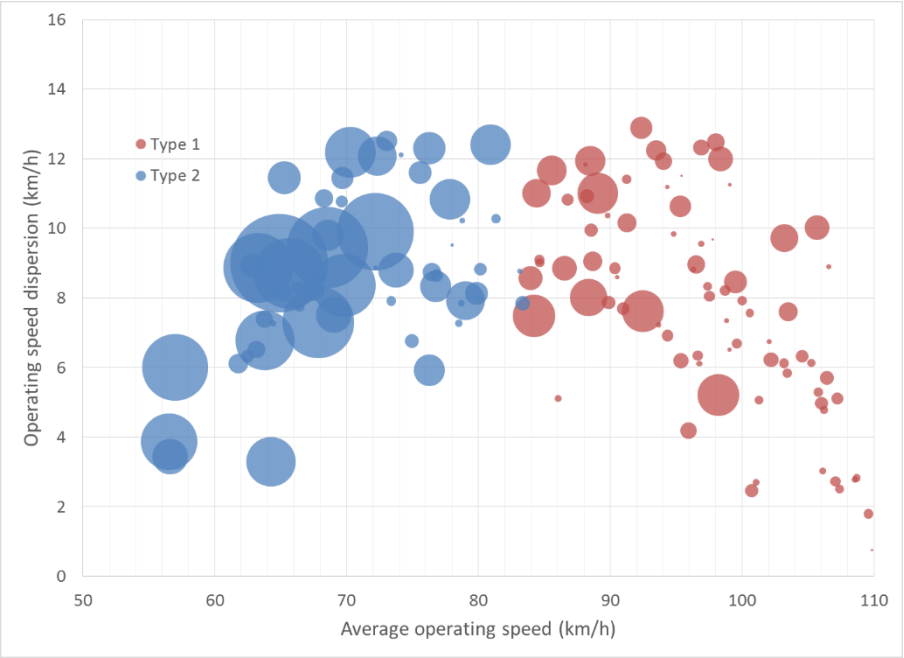

Figure 178. Operating speed dispersion vs. average operating speed.

Higher speed dispersions are reached for medium average operating speeds. This agrees with the conclusions provided by Garber and Gadiraju (1989), who indicated that the speed dispersion decreases as the speed increases for average speeds from 40 to 112.5 kph.

Crash rates are also depicted. The most hazardous road segments are located at the left side of the curve (type 2 roads, low average operating speeds). In fact, in this side an increase of the CCR allows the road users to reach a higher operating speed. However, the higher operating speed for type 2 segments is normally caused by sudden speed variations, which negatively affects road safety. This is also the reason of the higher operating speed dispersion.

On the contrary, the right part of the graph is composed by the type 1 homogeneous segments. They are composed by smooth curves, thus leading to a lower CCR. A reduction of the CCR produces less speed variations since there are fewer speed controls. Thus, a reduction of the CCR makes the average operating speed to increase and the operating speed dispersion to decrease. Crash rates are minimum for this type of road segments.

Some previous local consistency criteria, such as those presented by Lamm et al. focus on the analysis of the speed reduction in order to detect local inconsistencies.

Although Lamm's criterion II is good for detecting where safety issues may appear, the speed reduction average or speed reduction dispersion parameters have not been resulted relevant as a global consistency model. Instead, the deceleration rate results as a good indicator of the safety level or a road segment, itself or combined with the average operating speed.

Figure 179 shows the relationship between the average speed reduction and the average operating speed. It is worth to point out that the first parameter is highly dependent on the operating speed profile model (as well as the deceleration rate). The color of the points is the average deceleration rate. We can clearly see how the average deceleration rate has nothing to see with the speed reduction. Looking at the average deceleration rate, we can see how high speed reductions do not correspond to higher decelerations. This statement agrees with the correlation between both parameters (-0.1319).

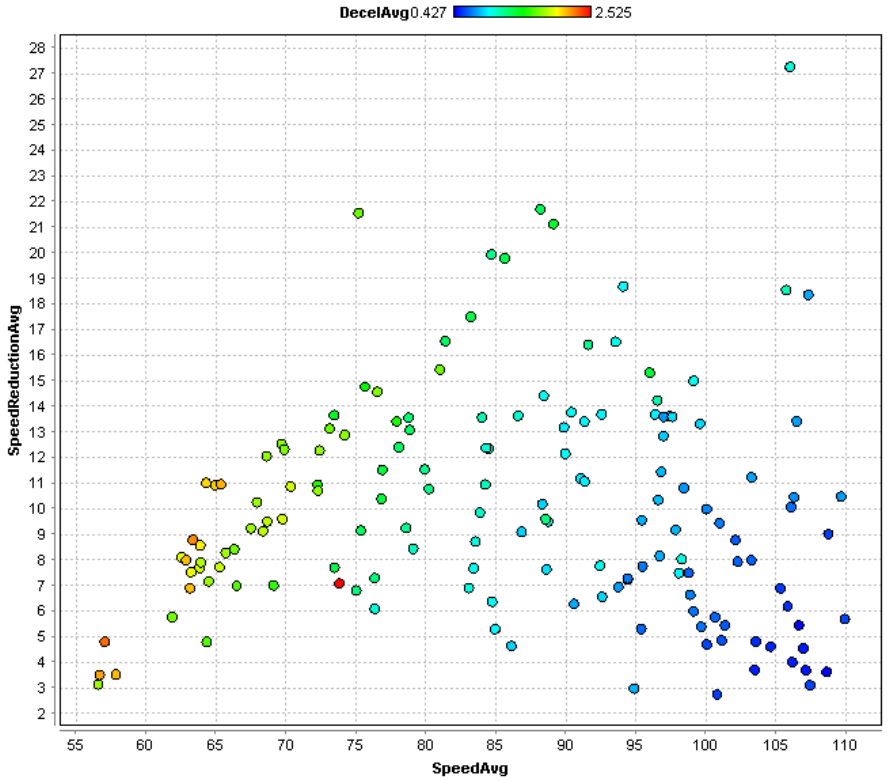

Figure 179 Average speed reduction vs. Average operating speed. The color of the points indicates the average deceleration rate.

This remarks the importance of controlling not only the speed reductions, but also their rate. This can be done through road design by means of establishing smooth speed transitions. This also reflects the importance of creating an entire operating speed profile instead of focusing exclusively on the operating speeds of the individual elements.

The average speed reduction is very low for the extreme operating speed conditions (i.e., low and top high operating speeds). For the first case, closed curves make it impossible to accelerate and reach a higher speed. However, the decelerations are pretty high since drivers tend to reach higher speeds when possible. On the right part of the graph, the road geometry does not impose a control on drivers, so they keep high operating speed, not needing to reduce their speed.

This relationship is confirmed in Figure 180. Road segments with low CCR present a high dispersion of speed reductions, but medium-to-low deceleration rates. Instead, the road segments with high CCR present medium to low speed reductions values, but the deceleration rates are quite noticeable.

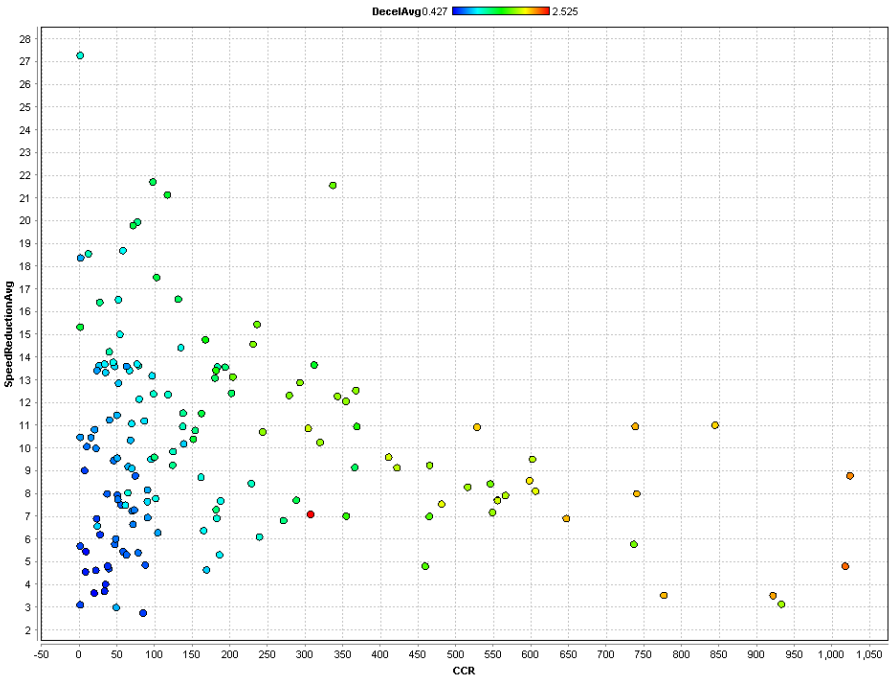

Figure 180. Relationship between the average speed reduction and CCR. The color of the points represent the average deceleration rate.

We can see how the road segments with higher operating speeds present a higher dispersion of the portion of road segment under deceleration conditions (Figure 181). This is because of the lower deceleration rates. If a high speed reduction is required, the speed transition is performed along a longer distance.

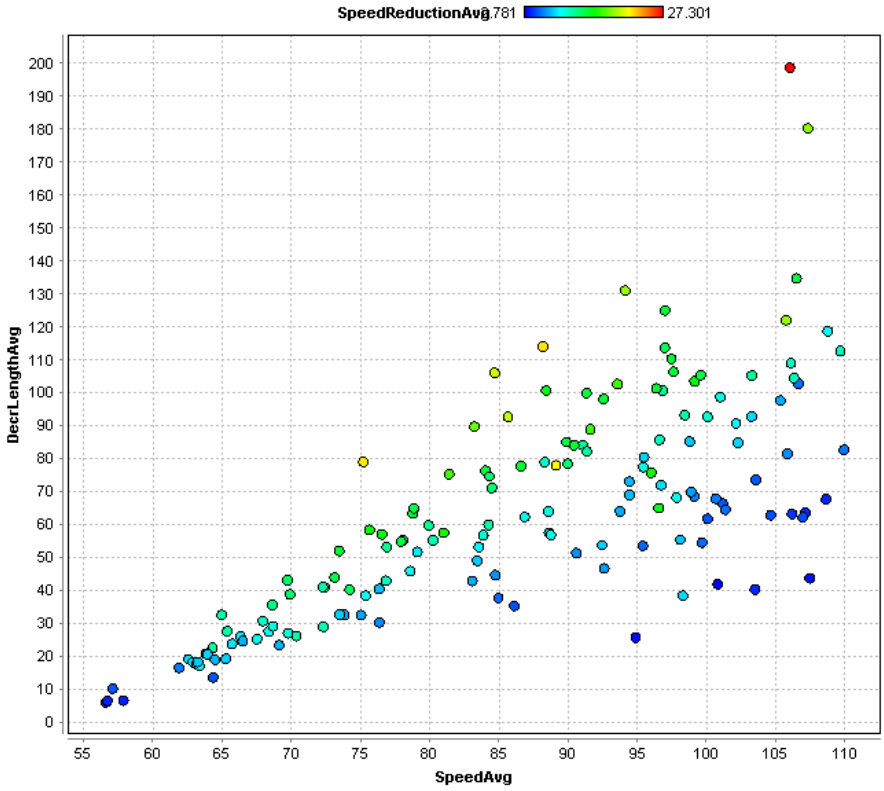

Figure 181. Relationship between the average length under deceleration conditions and the average operating speed. The color of the points represent the average speed reduction.

8.6.3. Application to the Spanish guidelines

Some of the presented innovations can be applied to existing guidelines. Some of them are summarized as follows.

8.6.3.1. General design

The presented methodology allows us to design better, more consistent roads. This is a global model, so no recommendations for the specific radii of curves, or lengths of the different elements are suggested. Instead, general recommendations are provided, such as the use of a global consistency parameter for estimating the number of accidents depending on the road design.

Constrained road segments present lower crash rates, since drivers generally pay more attention to the road. As their length increases, their crash rates become similar to the free ones. Free road segments experience the opposite behavior. Drivers are not aware of the change of the road behavior, so the road design should facilitate them the driving task. Thus, no intersections or complex situations should be nearby the zones where the road design changes.

Both the average operating speed and the average deceleration rate are strongly related to road crashes. In order to achieve the best consistency, smooth speed transitions should be provided. When there is a sequence of several circular curves, their radii should vary uniformly or remain almost the same. Therefore, there will be only one smooth speed transition and the average deceleration rate will be lower. Local consistency is also benefitted from this design rule.

8.6.3.2. Operating speed

The Spanish guidelines do not have specific operating speed models. The general vehicular stability equation is used instead. Thus, no speed approach is provided for tangents. As a result, engineers cannot estimate how drivers will behave through the road under design. This also makes it impossible to apply consistency criteria.

In the recent draft of the new Spanish guidelines, the concept of operating speed is introduced for first time. Road designers are encouraged to estimate how drivers will behave through their road design. However, no operating speed models are provided, so there is no guidance about this important point.

Some operating speed models, as well as construction rules, should be provided. Some examples are those indicated in this document, previously developed by the Highway Engineering Research Group.

8.6.3.3. Design speed

The design speed should be carefully selected for all homogeneous road segments, in order to prevent local inconsistencies. Some parameters, such as the sight distance, are related to the design speed. Spanish guidelines consider that the design speed for a road segment is the minimum of the inferred design for all their geometric elements. This leads to an underestimation of several geometric parameters, such as the sight distance, which may be hazardous. Thus, a new definition of design speed should be provided. According to previous research, and based on the presented results, the design speed should be estimated as the average

operating speed through a homogeneous road segment. This definition implies a relationship between design and operation, and would provide a good way to design self-explaining, less hazardous roads.

It was previously demonstrated that the average operating speed is highly correlated to some geometric parameters such as the CCR. Type 1 road segments present a linear relationship between the CCR and the average operating speed, while type 2 road segments behave in a parabolic way. The frontier between both behaviors is 83.5 km/h of average operating speed.

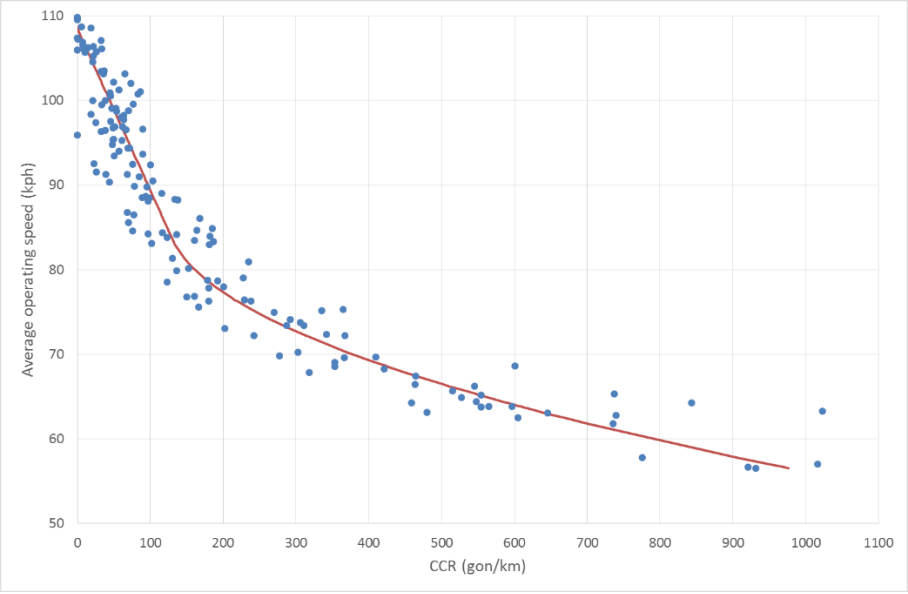

Figure 182. Relationship between the CCR and the average operating speed.

If the average operating speed is selected as design speed, Equations 363 (type 2 road segments) and 364 (type 1) can assist designers in determining the design speed in terms of the CCR, in an iterative approach.

$$CCR = 0.9677 \cdot v_d^2 - 166.85 \cdot v_d + 7316 \quad (363)$$

$$CCR = -5.24 \cdot v_d + 569 \quad (364)$$

8.6.3.4. Stopping Sight distance

Spanish guidelines propose that the stopping sight distance should be calculated with the design speed. However, the design speed is the one calculated for the

sharpest curve. Therefore, this speed is clearly lower than the speed selected by drivers.

This issue would be fixed if operating speed models were included in the guidelines. In addition, the stopping sight distance should be calculated for the local operating speed for all stations along the road segment.

8.6.3.5. Consistency

The current Spanish guidelines do not include the consistency concept. Instead, some geometrical limitations between consecutive elements are provided.

The draft of the new Spanish guidelines include the consistency concept for first time. There are several local consistency criteria, based on Lamm's research. Two of them are Safety Criteria I and II. There is also the possibility of calculating the consistency as a function of the difference of CCRs for each curve and the average CCR for the whole road segment. This global CCR does not consider the tangent sections.

8.7. Proposal of a new road design process

Some new concepts of consistency and road safety have been introduced. Road segmentation processes have been studied and a new criterion has been developed. Thus, a better knowledge of driver behavior and its consequences has been achieved. This allows us to define a new road design process that overcomes the most important issues of the current one. The new design process considers the user behavior in order to adapt them to the road design.

8.7.1. Design of a new road

The new design process starts with the choice of an anticipated target speed, which is the basis for the design speed. This target speed should be based on the expectations that drivers may have according to the road function within the highway network, the orography, urban development, and other factors. This design speed will let the engineers to create a first road layout, determine the geometric controls, sight distances and cross-section. The next step is to determine whether this design is safe or needs to be changed.

This checking is based on the comparison of the road behavior and the drivers' expectancies. Thus, the operating speed profiles have to be modeled. These

operating speed profiles (one per direction) will be used for determining the operating speed design consistency. Several consistency models are recommended:

- Models focusing on the difference between the design speed and the operating speed. Lamm's Criterion I might be applied.
- Local consistency models, based on the operating speed variation. One example is Lamm's Criterion II.
- Inertial consistency models. This is a mixture of both previous models. One example is García et al.'s ICI. These models will allow us to find large discrepancies between operating speeds and driver's expectations.
- Global models which focus on the variability of the operating speed. In this first step, the entire road segment is an undivided road. Thus, global models are applied to the whole road.

If all the consistency models produce a result classified as "good", the road design is validated. Otherwise, it should be redesigned in an iterative process. The first step is to determine whether the road section can be considered as a homogeneous segment or should be divided. In the first case, the not-good consistency may be due either to a bad design speed selection or to a poor geometric design. In the former event the design speed should be redefined. In the latter, the design should be improved.

In the case that the original road section can be split into several homogeneous road segments, a design speed should be defined for each one. After that, every road segment should be redesigned according to that design speed. The designer should keep in mind that no speed shifts larger than 20 km/h should be allowed between different homogeneous segments.

For each road segment, the operating speed profiles and the consistency should be calculated. If a good consistency is not obtained for all criteria, the road segment should be redesigned as aforementioned.

Only when all the homogeneous road segments present a good consistency, the operating speed profiles will be calculated for the entire road, and some final consistency evaluations will be performed. Those evaluations are the inertial consistency index and the local criteria in the boundary zones between two different homogeneous segments. If those criteria do not lead to a good consistency value, the engineer should reconsider the road design.

Once the road is built, some measurements of the actual operating speed and the available sight distances should be taken. According to these conditions, more accurate speed limits can be established. Thus, the harmony of the different speeds will be achieved, leading to a non-hazardous road.

The whole process is shown in Figure 183.

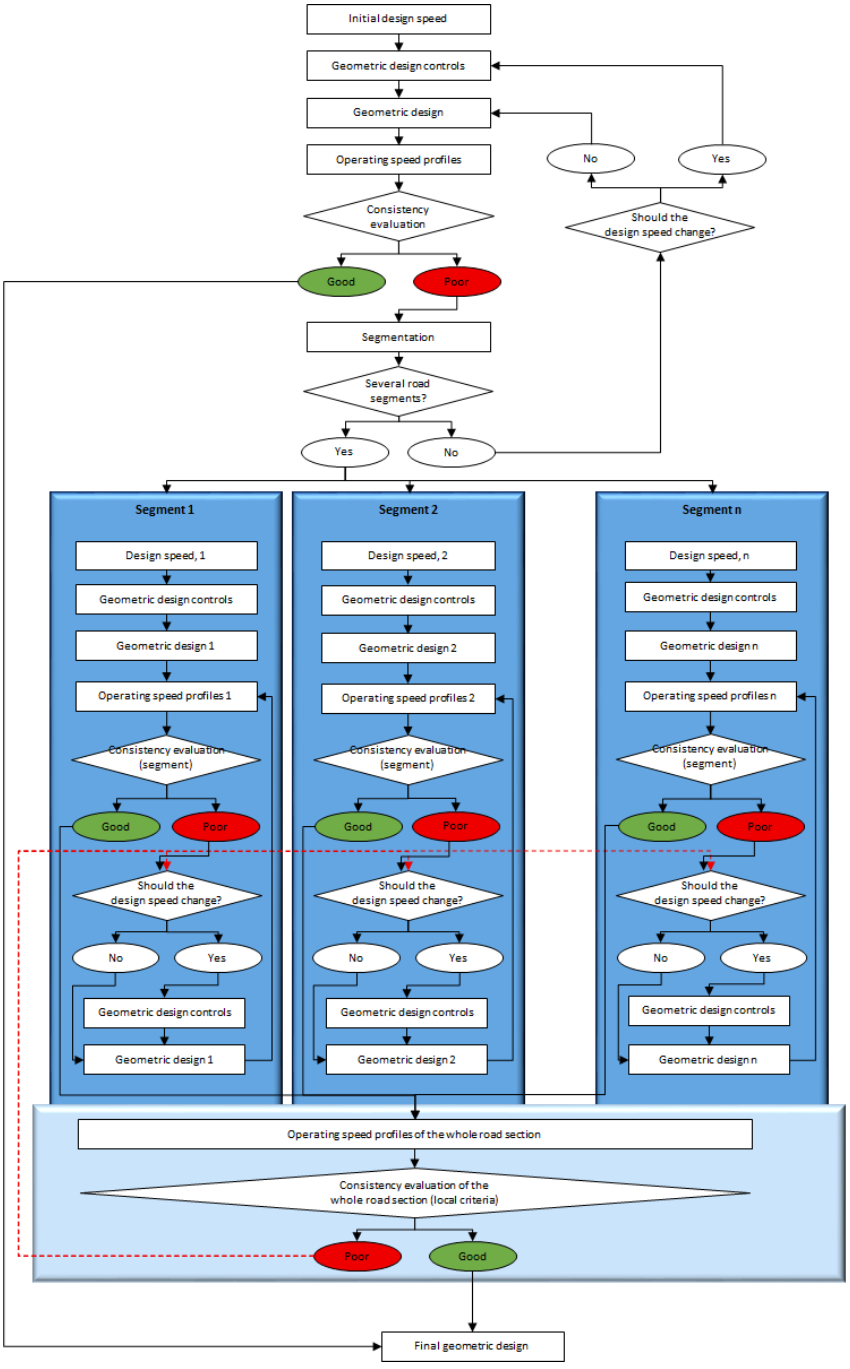

Figure 183. Process for designing a new road.

8.7.2. Redesign of an existing road

This is a similar process than the previous one, but in this case the road is already built. This has some advantages and disadvantages.

The most important advantage is that we will normally have accident data, letting us to better know where the safety problems are located. In addition, we can obtain the operating speed profile from actual drivers, instead of estimating it.

However, some other aspects such as the road geometry and the design speed remain unknown. The road geometry can be estimated by using the presented methodology. This allows us to accurately know the different design parameters. Later, a detailed fitting of the road should be done by means of a computer application, considering the *(x, y)* coordinates.

The design speed has to be inferred from the geometry, visibility and cross-section, which is not easy since it requires a large data collection.

Once we know all the information, the design process can begin. It presents a similar layout than the general one, but in this case a fair consistency is required instead of good. The reason is that a redesign process should be performed only changing small parts of the road layout. Depending on the initial road conditions, this is not always possible.

Figure 184 shows the entire process.

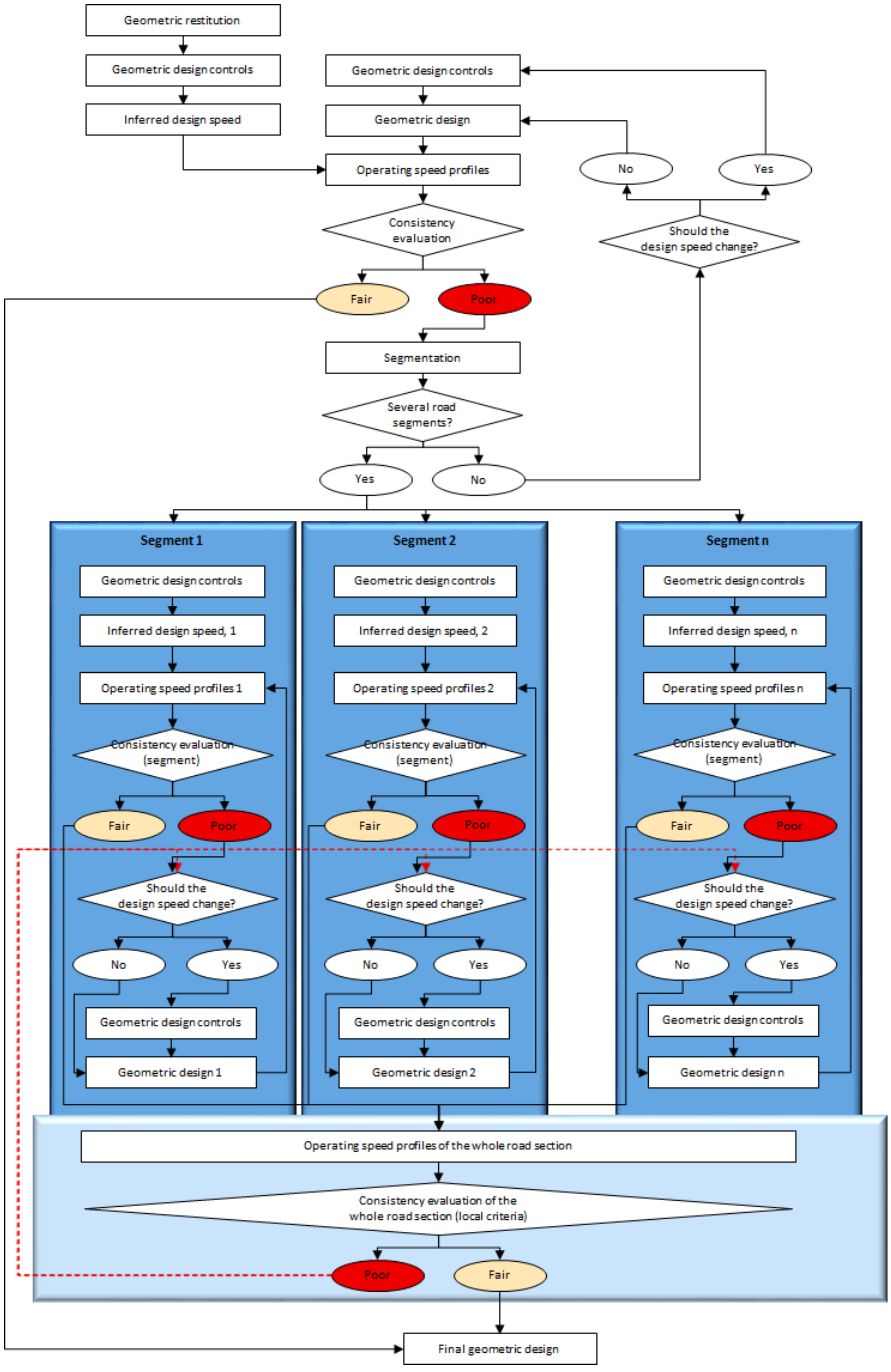

Figure 184. Process for redesigning an existing road.

8.7.3. Planning stage

The proposed methodology can be adapted to the planning stage, in order to add a criterion to select among all the alternatives for a certain road. In this case, no detailed design is produced, so the process is simpler than before.

The first step is the development of a set of different alternatives, including the selection of the design speed. A segmentation process is recommended if different design speed zones can be established. All the road segments with good consistency are kept as definitive. On the contrary, a different segmentation, design speeds or road layout should be considered. This is not a detailed design, con other consistency criteria, such as ICI and Lamm's Criterion II should not be applied.

Only when all the alternatives present a good consistency with the global models, the number of accidents can be estimated for each alternative. Therefore, there is an objective indicator of the road safety for each alternative that should be taken into account as well as other aspects.

9. Applications

This research has provided several tools and results that can be implemented in different fields. The most important ones are briefly mentioned here.

9.1. Geometric recreation of the alignment of a road segment

A new methodology for recreating the horizontal alignment of road sections has been introduced. It consists on a semi-analytic process in which the heading parameter is examined, instead of the curvature. This overcomes most of the existing issues for performing this task.

This methodology can use data extracted from several sources, including GPS and direct image depiction. The effect of the noise introduced by the users has also been analyzed, concluding that the presented method can directly handle raw data without filtering need or artificial thresholds.

The accuracy of this methodology is 1 m. This is good enough for determining the length and parameters of the different road geometric elements, but cannot be used for redesigning a road section. However, this methodology can be used as a first step in order to determine which elements compose the horizontal alignment, as well as their geometric properties. In the next step, those parameters should be introduced into a road design application, thus producing a valid design.

This methodology is also valid for research purposes. For instance, it can be used for determining the geometric elements that compose drivers' behavior and relate them to the road layout.

9.2. Segmentation of existing and planned road sections

A procedure for determining homogeneous road segments has been presented. This methodology can be used for research, and road design or redesign. As an improvement over most existing segmentation methodologies, the presented one includes some operational effects as well as geometry and traffic influence.

Homogeneous road segments are necessary for applying global consistency models and safety performance functions. Otherwise, conclusions may be biased. This can

be used by practitioners and researchers for estimating the number of accidents on road sections.

Homogeneous road segments should also be considered for establishing some global parameters, such as design speed, sight distance, etc. Therefore, this methodology can be used in an iterative way together with the road design process in order to determine those homogeneous road segments.

9.3. Development of operating speed profiles

A computer application was developed in order to perform the calculations through all the process. One of the most important features is the ability of depicting operating speed profiles for road segments as a function of their horizontal alignment. Several operating speed models can be implemented, so the users can adapt the outcome to their local behavioral parameters.

The knowledge of the operating speed profile of a planned road is very useful, since it allows designers to estimate drivers' behavior and to introduce it into the road design process. Aspects such as design consistency, estimation of road accidents, duration of the trip, etc. can now be included in the design stage.

Moreover, some indicators from the operating speed profiles have also been examined and compared. Hence, some conclusions that relate road design to drivers' operation have been extracted.

9.4. Calculation of the design consistency of existing and planned road segments

The consistency model presented allows road designers to develop safer roads. It is based on some operating speed indicators, and the result is directly linked to the number of road accidents.

Although the objective of the parameter is the estimation of the number of accidents, several thresholds have been identified in order to assist road designers in the decision-taking process. Three consistency zones have been identified:

- Good consistency. Road segments tend to produce a low number of accidents. According to geometry, the road segment is well designed.

- Fair consistency. The number of expected accidents is medium. Some geometric improvements could be applied, but a further study should be performed in order to take decisions.
- Poor consistency. The geometric features of the road segment are the cause of a high number of accidents. No road segment should be designed with this consistency level.

The consistency evaluation can be used both for existing and non-existing roads. In the first case, the consistency evaluation can suggest whether a high number of accidents might be due to the road geometry or not. In the second case, the consistency evaluation can be introduced in the design stage in order to determine if a road design is good enough or should be improved. It can also be used for choosing the best alternative.

9.5. Safety Performance Function for two-lane rural road segments

The consistency model has been calibrated based on the number of accidents with victims. Thus, a Safety Performance Function was also developed, allowing designers to estimate the number of accidents for a certain horizontal layout.

The estimation of the number of accidents can be used in order to compare different alternatives. The number of accidents can be converted to a monetary value, and thus be compared to other criteria.

This parameter can also substitute the consistency parameter, in order to compare different solutions from a set of alternatives.

9.6. Introduction of a new process for road design, redesign and planning

Considering all the contributions by this research, a new road design process has also been introduced. The suggested design process is valid for planning, designing and redesigning, with small changes.

The underlying aspect of the new design process is the division of the road into homogeneous road segments and the iterative enhancement to each. Designers could use this methodology in order to design roads that better reflect driver behavior. This would reduce the number of discrepancies between drivers' expectations and road layout.

The proposed process does not invalidate the current guidelines. Moreover, it complements them and fills some existing gaps. Thus, a good road segment could comply with the guidelines and also be modeled using this methodology. At some points, this process could objective explain why some aspects of a solution do not comply with the guidelines.

10. Conclusions

10.1. Development of a methodology to recreate the horizontal alignment

A methodology for recreating the horizontal alignment of two-lane rural roads is presented. It is based on the use of the heading direction instead of the curvature, which overcomes the most important issues to existing methodologies.

The heading profile is quite less sensitive to measurement errors, so it can handle data directly from the source, with no need of additional filtering processes. This avoids the possibility of adding spiral transitions, caused from smoothing algorithms that other methodologies need.

Moreover, the use of the heading direction allowed us to use additional data between consecutive road geometric elements, which is not possible when constraining conditions do not exist between boundary points.

Some analytical solutions have been developed for simple sequences of geometric elements. All solutions are unique, although the boundary points between geometric elements have to be determined in advance. In order to perform that task, heuristic processes were introduced for each analytic solution.

A computer program was developed, in order to facilitate the user to distinguish the different road geometric elements and to fit the geometry. The user has almost no role in the process, since they only have to detect where the different tangents are located.

This procedure has been validated comparing the recreated and the project geometry of a road segment. It has also been compared to some other methodologies.

10.2. Development and validation of a segmentation methodology for existing and planned road sections

Homogeneous road segments are crucial for applying global consistency methods. Segmentation methodologies take an original road section and split it into different, homogeneous road segments. The different segmentation methodologies differ in the aspects they consider for determining those homogeneous road segments.

A segmentation methodology was presented in this research, considering three different sources of information:

- Traffic and major junctions.
- Geometric parameters (considered by means of the CCR, applying the German methodology).
- Operational behavior of drivers.

The most innovative point here was the introduction of operational aspects into the segmentation process. It was demonstrated how in most cases, a geometric change resulted in an operational change. However, there were some other cases where an operational change was observed with no relevant geometric changes. Thus, this third criterion could detect that.

The inertial operating speed was selected as an indicator of driver expectancies. It was calculated as the moving average of the operating speed, considered 1000 m of data. Shorter and longer distances were also tested, but 1000 m was selected as the optimum for this parameter.

The segmentation process was proved to be necessary for accurately estimating the number of accidents, together with the consistency parameter.

10.3. Development and analysis of operating speed parameters

153 homogeneous road segments were finally selected for the research. The horizontal alignment was determined for all, and the operating speed profile in both directions was depicted in all cases. This was carried out with a computer program exclusively created for that purpose.

In order to include the operational behavior in the consistency model, 14 parameters were extracted. Some of those parameters were of a global nature, while others were centered on local behavior. Some operational parameters were found to be correlated to road accidents, such as the average operating speed or the average deceleration rate.

In addition, some interactions between the most important parameters were examined. Two types of road segments were distinguished according to their average operating speed – average deceleration behavior. Both groups presented a very different behavior according to crash rates. This is important, since it allows the designers to expect one or the other road segment type according to the functionality of the road and the environment.

Both types of road segments were found to be highly correlated to the CCR. The evolution of the operating speed, and its relationship to the speed dispersion were further examined. As a result of all those parameters, some suggestions were given in order to produce smoother speed transitions and hence better roads.

10.4. Development of a consistency model for road segments

A consistency model was developed on the basis of traffic, crash, geometric and operational data of 153 homogeneous road segments. This consistency model was calibrated as a part of a safety performance function, in which the length and the AADT were considered as elastic parameters.

The road segments were classified as free or constrained, considering their boundary conditions to the rest of the road network. This allowed us to perform a more specific calibration depending on how drivers acquired the expectancies.

AADT and length were found to influence in an opposite way to free and constrained road segments. For free road segments, the number of crashes decreased as the road segment lengthened. The effect was the opposite for constrained road segments. This was explained based on the hypothesis that drivers noticed where constrained road segments appeared, contrary to free ones. For long road segments, both crash rates tend to be very similar.

The consistency model was established as the cubic root of the average operating speed over the average deceleration rate. This model was selected because of its relative simplicity and easiness to interpret. Faster roads with lower deceleration rates tend to produce less accidents, which appears to be coherent.

A cluster analysis was performed in order to determine three consistency zones (good, fair and poor). This allows designers to take decisions looking for the best road design.

Several Safety Performance Functions were developed for all, free and constrained road segments. This is very useful while selecting between different alternatives.

10.5. Development of a new road design process that gathers all improvements provided by the research

Considering the proposed contributions, a new road design process was presented. This new procedure addresses some of the existing flaws by some guidelines.

The process is based on an iterative design/consistency checking the developed road. The user has to select a first reference design speed and generate the road alignment. If that alignment produces some inconsistencies, then a segmentation process will be required. For each homogeneous segment, a new design speed is suggested (based on the estimated operating speed profile) and new designs and consistency checks are performed. The road design is validated when all road segments produce a good consistency level.

This methodology is valid for new designs, but it was also particularized for redesigns and the planning stage. In all cases, this procedure does not invalidate the application of the design standards.

11. Further research

This document has presented a wide research on how to estimate road crashes according to traffic, geometric and operational characteristics. Although a strong relationship has been found, some further research can be performed.

11.1. Segmentation process

An operational segmentation process has been introduced. This methodology aims to complement the functional and geometrical methodologies for road segmentation. The inertial operating speed has been established with a basis of 1000 m. However, the process for selecting this distance was uncertain. Additional insights were provided in the Discussion section. Considering the distance where the Safety Performance Functions for free and constrained road segments coincided, we suggested that the distance was a function of the AADT.

However, this distance should be further studied. More distances should be considered, as well as different aggregation patterns for creating the inertial operating speed. This could be performed through examining which criteria produces the best estimation of crashes through a consistency index, due to their relationship.

11.2. New design process

A new design process has been introduced, as a result of all contributions in this document. More details can be added to this process, in order to facilitate engineers to design safer roads. One example is the proposed design speed as a function of the average operating speed. Some additional recommendations could be added as a function of the environmental constraints.

In addition, more detailed design rules can be established, based on their influence on the final consistency value.

11.3. Recreation of the road geometry

A new process for recreating the horizontal alignment has been proposed. This is a major contribution, compared to previous research. However, this methodology is still not valid for some cases. One example is the recreation of a detailed horizontal geometry for road redesign. In this case, an *x, y*–based methodology should be developed. The accuracy of the proposed methodology is 1 m. Therefore, almost

negligible errors are accumulated, thus producing a bigger error at the end of the road alignment. This issue would be addressed considering the coordinates in the recreation process.

The hypothesis for the new methodology is that all geometric elements are determined, and slight changes in their parameters or lengths would give the more accurate solution. This could be achieved through artificial intelligence, like genetic algorithms. The seed solution should be obtained with the proposed methodology. The objective function should be established based on the comparison with the actual and the output coordinates.

The proposed methodology only fits the horizontal geometry. This was enough for our research, since the operating speed models are exclusively valid for level geometries. However, the methodology could be enhanced by considering the vertical alignment. The vertical alignment is composed by a series of tangents (grades) and parabolic variations (vertical curves). The stitching points must keep continuity in value (height) and the first derivative (grade). Therefore, this is similar to the curve-to-curve case of the horizontal alignment.

11.4. Development of new and better operating speed models

Several operating speed models have been used for determining the operational performance through all road segments. Those models were based on data from actual drivers, so they reflect well drivers' performance. On the other hand, only the horizontal alignment was considered in their calibration. Therefore, they are only valid for roads with limited grades. Enhanced models should be developed for non-level roads. These models should include the vertical curvature and the longitudinal grade.

As a result of the recreation of the horizontal alignment, it has also been observed that the same curve can be recreated with different combinations transition-circular curve-transition. The radii of these combinations may substantially differ. The operating speed models for curves are based on the curve radius. As a result, different operating speeds could be estimated depending on the recreated alignment. New operating speed models for curves should be developed. Those models should be estimated as a function of the curvature change rate, since this parameter is quite more stable regardless of how the geometry is recreated.

Some additional operating speed models should be developed for complex layouts. Some examples are the presence of intersections or low-deflection angle curves.

11.5. Analysis of the operating speed dispersion and its relationship to road crashes

Local consistency models can also be developed considering operating speeds. Some examples are the inertial consistency models. The operating speed dispersion is known to be different depending on the curve features. It is also known that a higher speed dispersion is linked to higher accident rates. The operating speed dispersion variation from tangents to curves should be examined, looking for relationships to road crashes. As a result, detailed design rules could be provided.

11.6. Analysis of the curve negotiation by drivers

The recreation of the horizontal alignment provides detailed information on the configuration of the horizontal layout. It is well known that drivers do not perfectly follow the road layout. Slight differences may appear, especially in low-deflection angle curves.

By means of GPS devices, individual drivers' paths could be determined, and their horizontal alignment recreated. This operational alignment can be compared to the road layout, in order to identify where strange geometries are induced, thus increasing the crash risk.

11.7. Development of enhanced safety performance functions

Some safety performance functions have been proposed to estimate the number of accidents with victims for two-lane rural roads. Some aspects have not been covered by the research, such as accident severity, vertical alignment, etc.

The accident severity could be based on the existing safety performance function. A parameter that reflects the overall severity for each road segment should be included, thus producing an ordered model.

The vertical alignment should be included as a part of the operating speed models. This would increase the availability of the model for a larger set of roads. However, effects such a higher operating speed dispersion may be induced. Therefore,

additional parameters should be included in the safety performance functions. The segmentation process might also include vertical changes.

12. Acknowledgements

The presented Doctoral thesis has been developed following an existing research field of the Highway Engineering Research Group (HERG) of the Universitat Politècncia de València (UPV).

The author would like to thank the Center for Studies and Experimentation of Public Works (CEDEX) of the Spanish Ministry of Public Works, that partially subsidized the data collection process for obtaining the empirical operating speed profiles used in the validation process.

Also thank to the General Directorate of Public Works of the Infrastructure and Transportation Department of Valencian Government; Valencian Province Council; and to the General Directorate of Traffic of the Ministry of the Interior of the Spanish Government, for their cooperation in data gathering.

13. References

AASHTO, 2011. *A Policy on Geometric Design of Highways and Streets* 6th ed.,

Abdel-Aty, M., 2003. Analysis of driver injury severity levels at multiple locations using ordered probit models. *Journal of Safety Research*, 34(5), pp.597–603. Available at: http://linkinghub.elsevier.com/retrieve/pii/S0022437503000811 [Accessed January 31, 2014].

Abdel-Aty, M.A. & Radwan, A.E., 2000. Modeling Traffic Accident Occurrence and Involvement. *Accident Analysis & Prevention*, 32(5), pp.633–642.

AGVS, 1980. *Traffic Safety by Night. Traffic-Engineering-Related Improvements to the Highway Infrastructure*, Berne.

Ajzen, I., 1991. The Theory of Planned Behavior. *Organizational Behavior and Human Decision Processes*, 50, pp.179–211.

Alexander, G.J. & Lunenfeld, H., 1990. *A Users' Guide to Positive Guidance*, Washington, D.C.

Al-Masaeid, H.R. et al., 1995. Consistency of Horizontal Alignment for Different Vehicle Classes. *Transportation Research Record: Journal of the Transportation Research Board*, 1500, pp.178–183.

Al-Masaeid, H.R., 1997. Impact of pavement condition on rural road accidents. *Canadian Journal of Civil Engineering*, 24(4), pp.523–531. Available at: http://www.nrc.ca/cgi-bin/cisti/journals/rp/rp2_abst_e?cjce_l97-009_24_ns_nf_cjce24-97.

Amundsen, A.H. & Bjørnskau, T., 2003. *Utrygghet og risikokompensasjon i transportsystemet*, Oslo (Norway).

Andersen, G.J. et al., 2011. Limits of spatial attention in three-dimensional space and dual-task driving performance. *Accident; analysis and prevention*, 43(1), pp.381–90. Available at: http://www.pubmedcentral.nih.gov/articlerender.fcgi?artid=2991164&tool=pmcentrez&rendertype=abstract [Accessed June 20, 2012].

Anderson, I.. B. et al., 1999. Relationship to Safety of Geometric Design Consistency Measures for Rural Two-Lane Highways. *Transportation Research Record: Journal of the Transportation Research Board*, 1658, pp.43–51.

Anderson, I.B. & Krammes, R.A., 2000. Speed Reduction as a Surrogate for Accident Experience at Horizontal Curves on Rural Two-Lane Highways. *Transportation Research Record: Journal of the Transportation Research Board*, 1701, pp.86–94.

Babkov, V.F., 1975. *Road Conditions and Traffic Safety*, Moscow: Mir Publishers.

Babkov, V.F., 1968. Road Design and Traffic Safety. *Traffic Engineering and Control*, 9, pp.236–239.

Baffour, R.A., 2002. Collecting Roadway Cross Slope Data Using Multi Antenna-Single Receiver GPS Configuration. In *Proceeding of the International Conference on Applications of Advanced Technology in Transportation Engineering*. pp. 354–361.

Baffour, R.A., 1997. Global Positioning System with an Attitude, Method for Collecing Roadway Grade and Superelevation Data. *Transportation Research Record: Journal of the Transportation Research Board*, 1592, pp.144–150.

Baruya, A., 1998. *Speed-Accident Relationships on Different Kinds of European Roads. Deriveable D7*,

Ben-arieh, D. et al., 2004. Geometric modeling of highways using Global Positioning System data and B-Spline approximation. *Journal of Transportation Engineering*, 130(5), pp.632–636.

Berger, W.J., 1996. *Informationaufnahme im Strassenverkehr - Grundlagen und Konsequenzen für die Praxis*. Universität für Bodenkultur Wien.

Biedermann, B., 1984. *Strassentrassierung auf der Grundlage von Geschwindigkeiten aus Sehfelduntersuchungen*. Fakultät für Wasser und Verkehr.

Bonneson, J.A., 2000. *NCHRP Report 439: Superelevation Distribution Methods and Transition Designs*, Washington, D.C.

Borowsky, A., Shinar, D. & Oron-Gilad, T., 2010. Age, skill, and hazard perception in driving. *Accident; analysis and prevention*, 42(4), pp.1240–9. Available at: http://www.ncbi.nlm.nih.gov/pubmed/20441838 [Accessed June 28, 2012].

Buddhavarapu, P. et al., 2012. Influence of Pavement Condition on Crash-Injury Severity. In *TRB 91st Annual Meeting*. p. 12.

Cafiso, S. et al., 2006. A Procedure to Improve Safety Inspections Effectiveness and Reliability on Rural Two-Lane Highways. *The Baltic Journal of Road and Bridge Engineering*, 1(3), pp.143–150.

Cafiso, S. et al., 2010. Development of comprehensive accident models for two-lane rural highways using exposure, geometry, consistency and context variables. *Accident; analysis and prevention*, 42(4), pp.1072–9. Available at: http://www.ncbi.nlm.nih.gov/pubmed/20441815 [Accessed June 28, 2012].

Cafiso, S., 2000. Experimental Survey of Safety Condition on Road Stretches with Alignment Inconsistencies. In *2nd International Symposium on Highway Geometric Design*. Mainz (Germany), pp. 377–387.

Cafiso, S. & la Cava, G., 2009. Driving Performance, Alignment Consistency, and Road Safety. *Transportation Research Record: Journal of the Transportation Research Board*, 2102(-1), pp.1–8. Available at: http://trb.metapress.com/openurl.asp?genre=article&id=doi:10.3141/2102-01 [Accessed May 11, 2012].

Cafiso, S., La Cava, G. & Montella, A., 2007a. Safety evaluation process for two-lane rural highways. In *4th International SIIV Congress*. Palermo.

Cafiso, S., La Cava, G. & Montella, A., 2007b. Safety Index for Evaluation of Two-Lane Rural Highways. In *TRB 86th Annual Meeting*. Washington, D.C., p. 21.

Cafiso, S., D'Agostino, C. & Persaud, B., 2013. Investigating the influence of segmentation in estimating safety performance functions for roadway sections. In *TRB 92nd Annual Meeting*. Washington, D.C., p. 15.

Cafiso, S. & Di Graziano, A., 2008. Automated in-vehicle data collection and treatment for existing roadway alignment. In *4th International Gulf Conference on Roads*. Doha (Qatar).

Cafiso, S., Di Graziano, A. & La Cava, G., 2005. Actual Driving Data Analysis for Design Consistency Evaluation. *Transportation Research Record*, 1912(1),

pp.19–30. Available at: http://trb.metapress.com/openurl.asp?genre=article&id=doi:10.3141/1912-03.

Cai, H. & Rasdorf, W., 2008. Modeling Road Centerlines and Predicting Lengths in 3-D Using LIDAR Point Cloud and Planimetric Road Centerline Data. *Computer-Aided Civil and Infrastructure Engineering*, 23(3), pp.157–173.

Camacho-Torregrosa, F.J. et al., 2013. New geometric design consistency model based on operating speed profiles for road safety evaluation. *Accident; analysis and prevention*, 61, pp.33–42. Available at: http://www.ncbi.nlm.nih.gov/pubmed/23176754 [Accessed December 19, 2013].

Castro, M. et al., 2008. Automated GIS-Based System for Speed Estimation and Highway Safety Evaluation. *Journal of Computing in Civil Engineering*, 22(5), pp.325–331.

Castro, M. et al., 2006. Geometric modelling of highways using global positioning system (GPS) data and spline approximation. *Transportation Research Part C: Emerging Technologies*, 14(4), pp.233–243. Available at: http://linkinghub.elsevier.com/retrieve/pii/S0968090X06000532 [Accessed May 7, 2012].

Castro, M. et al., 2011. Operating Speed and Speed Differential for Highway Design Consistency. *Journal of Transportation Engineering*, 137(November), pp.837–840.

Ceder, A. & Livneh, M., 1982. Relationships between Road Accidents and Hourly Traffic Flow - I: Analysis and Interpretation. *Accident Analysis & Prevention*, 14(1), pp.19–34.

Chapman, P.R. & Underwood, G., 1998. Visual Search of Driving Situations: Danger and Experience. *Perception*, 27, pp.951–964.

Cirillo, J.A., 1968. Interstate System Accident Research: Study II, Interim Report II. *Public Roads*, 35, pp.71–75.

Collins, K.M. & Krammes, R.A., 1996. Preliminary validation of a speed-profile model for design consistency evaluation. *Transportation Research Record*, 1523, pp.11–21.

Crisman, B. et al., 2007. Deceleration Model for Two-Lane Rural Roads. *Advances in Transportation Studies: An International Journal*, 11, pp.19–32.

Crisman, B. et al., 2004. Operating Speed Prediction Model for Two-Lane Rural Roads.

Dietze, M. et al., 2008. *Road Geometry, Driving Behaviour and Road Safety*,

Dong, H., Easa, S.M. & Li, J., 2007. Approximate Extraction of Spiralled Horizontal Curves from Satellite Imagery. *Journal of Surveying Engineering*, 133(1), pp.36–40. Available at: http://ascelibrary.org/doi/abs/10.1061/(ASCE)0733-9453(2007)133:1(36).

Donnell, E.T., Gross, F., et al., 2009. Appraisal of the Interactive Highway Safety Design Model's Crash Prediction and Design Consistency Modules: Case Studies from Pennsylvania. *Journal of Transportation Engineering*, 135(2), pp.62–73.

Donnell, E.T., Himes, S.C., et al., 2009. *Speed Concepts : Informational Guide*,

Easa, S.M., 1999. Discussion of Superelevation, Side Friction, and Roadway Consistency, by Alan Nicholson. *Journal of Transportation Engineering*, 124(5), pp.411–418.

Easa, S.M., 2003a. Distributing Superelevation to Maximize Highway Design Consistency. *Journal of Transportation Engineering*, 129(2), pp.127–133.

Easa, S.M., 2003b. Improved Speed-Profile Model for Two-Lane Rural Highways. *Canadian Journal of Civil Engineering*, 30, pp.1055–1065.

Easa, S.M., Dong, H. & Li, J., 2007. Use of Satellite Imagery for Establishing Road Horizontal Alignments. *Journal of Surveying Engineering*, 133(1), pp.29–35.

Easa, S.M. & He, W., 2006. Modeling Driver Visual Demand on Three-Dimensional Highway Alignments. *Journal of Transportation Engineering*, 132(5), pp.357–365. Available at: http://ascelibrary.org/doi/abs/10.1061/(ASCE)0733-947X(2006)132:5(357).

Easa, S.M. & Mehmood, A., 2007. Establishing highway horizontal alignment to maximize design consistency. *Canadian Journal of Civil Engineering*, 34, pp.1159–1168.

Echaveguren, T., 2012. Two-Lane Rural Highways Consistency Analysis Using Continuous Operating Speed Measurements Obtained with GPS. *Revista Ingeniería de Construcción*, 27(2), pp.55–70.

Elvik, R., 2010. An exploratory study of mechanisms by which exposure influences accident occurrence. In *TRB 89th Annual Meeting*. Washington, D.C., p. 17.

Elvik, R., 2006. Laws of accident causation. *Accident; analysis and prevention*, 38(4), pp.742–7. Available at: http://www.ncbi.nlm.nih.gov/pubmed/16533493 [Accessed June 28, 2012].

Elvik, R., 2004. To what extent can theory account for the findings of road safety evaluation studies? *Accident; analysis and prevention*, 36(5), pp.841–9. Available at: http://www.ncbi.nlm.nih.gov/pubmed/15203361 [Accessed April 9, 2012].

Elvik, R. & Borger Mysen, A., 1999. Incomplete Accident Reporting. Meta-Analysis of Studies Reported in Thirteen Countries. *Transportation Research Record: Journal of the Transportation Research Board*, 1665, pp.133–140.

Elvik, R., Christensen, P. & Amundsen, A., 2004. *TOI Report 740: Speed and Road Accidents*, Oslo (Norway).

Elvik, R., Erke, A. & Christensen, P., 2009. Elementary Units of Exposure. *Transportation Research Record: Journal of the Transportation Research Board*, 2103, pp.25–31.

Elvik, R. & Vaa, T., 2004. *The Handbook of Road Safety Measures*, Elsevier Ltd.

Evans, L., 1990. An Attempt to Categorize the Main Determinants of Traffic Safety. *Health Education Research*, 5, pp.111–124.

Evans, L., 2004. *Traffic Safety*, Science Serving Society, Bloomfield Hills, MI.

Evans, L., 1991. *Traffic Safety and the Driver*, New York: Van Nostrand Reinhold.

Figueroa Medina, A.M. & Tarko, A.P., 2007. Speed Changes in the Vicinity of Horizontal Curves on Two-Lane Rural Roads. *Journal of Transportation Engineering*, 133(4), pp.215–222.

Fitzpatrick, K., Wooldridge, M.D., et al., 2000. *Alternative Design Consistency Rating Methods for Two-Lane Rural Highways*,

Fitzpatrick, K., Elefteriadou, L., et al., 2000. *Speed Prediction for Two-Lane Rural Highways*,

Fitzpatrick, K. & Collins, J.M., 2000. Speed-Profile Model for Two-Lane Rural Highways. *Transportation Research Record*, 0145, pp.42–49.

Friedinger, C., 1980. *Information and Driver Behavior while Passing through Curves*. ETH, Zurich.

Fuller, R., 2005. Towards a general theory of driver behaviour. *Accident; analysis and prevention*, 37(3), pp.461–72. Available at: http://www.ncbi.nlm.nih.gov/pubmed/15784200 [Accessed March 27, 2012].

Garach, L., 2013. *Medida de la Consistencia en Carreteras Convencionales y su Relacion con la Seguridad Vial. Aplicación a la Provincia de Granada*.

Garach, L., de Oña, J. & Pasadas, M., 2014. Mathematical formulation and preliminary testing of a spline approximation algorithm for the extraction of road alignments. *Automation in Construction*, 47, pp.1–9.

Garber, N.J. & Ehrhart, A.A., 2000. *The Effect of Speed, Flow and Geometric Characteristics on Crash Rates for Different Types of Virginia Highways*, Charlottesville, Va.

Garber, N.J. & Gadiraju, R., 1989. Factors Affecting Speed Variance and Its Influence on Accidents. *Transportation Research Record: Journal of the Transportation Research Board*, 1213, pp.64–71.

García, A. et al., 2013. Consistency Index based on Inertial Operating Speed. In *TRB 92nd Annual Meeting*. Washington, D.C.

García, A. & Camacho-Torregrosa, F.J., 2009. Evaluación de la Seguridad Vial de Carreteras Convencionales mediante la Determinación de la Consistencia Global de su Diseño Geométrico. *Revista Carreteras*, 163, pp.21–32.

Gibreel, G.M., Easa, S.M. & El-Dimeery, I.A., 2001. Prediction of operating speed on three-dimensional highway alignments. *Journal of Transportation Engineering*, 127(1), pp.21–30.

Gibreel, G.M., Easa, S.M. & Hassan, Y., 1999. State of the Art of highway geometric design consistency. *Journal of Transportation Engineering*, 125(4), pp.305–313.

Gikas, V. & Stratakos, J., 2012. A Novel Geodetic Engineering Method for Accurate and Automated Road/Railway Centerline Geometry Extraction Based on the Bearing Diagram and Fractal Behavior. *IEEE Transactions on Intelligent Transportation Systems*, 13(1), pp.115–126. Available at: http://ieeexplore.ieee.org/lpdocs/epic03/wrapper.htm?arnumber=6003789.

Goldenbeld, C., Levelt, P.B.M. & Heidstra, J., 2000. Psychological perspectives on changing driver attitude and behaviour. *Recherche Transports Sécurité*, 67.

Hakamies-Blomqvist, L., Raitanen, T. & O'Neill, D., 2002. Driver Ageing Does Not Cause Higher Accident Rates per Km. *Transportation Research Part F*, 5, pp.271–274.

Harwood, D.W. (Midwest R.I., Council, F.M., et al., 2000. *Prediction of the Expected Safety Performance of Rural Two-Lane Highways*,

Harwood, D.W. (Midwest R.I., Neuman, T.R. & Leisch, J.P., 2000. Summary of Design Speed , Operating Speed , and Design Consistency Issues. *Transportation Research Record*, 1701, pp.116–120.

Hassan, Y., 2004. Highway Design Consistency: Refining the State of Knowledge and Practice. *Transportation Research Record*, 1881, pp.63–71. Available at: http://trb.metapress.com/openurl.asp?genre=article&id=doi:10.3141/1881-08.

Hassan, Y., Gibreel, G.M. & Easa, S.M., 2000. Evaluation of Highway Consistency and Safety: Practical Application. *Journal of Transportation Engineering*, 126(3), pp.193–201.

Hassan, Y., Sayed, T. & Tabernero, V., 2001. Establishing Practical Approach for Design Consistency Evaluation. *Journal of Transportation Engineering*, 127(4), pp.295–302.

Hauer, E. et al., 2002. Estimating Safety by the Empirical Bayes Method: A Tutorial. *Transportation Research Record*, 784, pp.126–131.

Hauer, E., 2006. The frequency-severity indeterminacy. *Accident; analysis and prevention*, 38(1), pp.78–83. Available at: http://www.ncbi.nlm.nih.gov/pubmed/16122689 [Accessed June 28, 2012].

Heger, R., 1995. Driving Behavior and Driver Mental Workload as Criteria of Highway Geometric Design Quality.

Himes, S.C., Donnell, E.T. & Porter, R.J., 2011. Some New Insights on Design Consistency Evaluations for Two-Lane Highways. In *TRB 90th Annual Meeting*. Washington, D.C., p. 21.

Hirsh, M., 1987. Probabilistic Approach to Consistency in Geometric Design. *Journal of Transportation Engineering*, 113(3), pp.268–276.

Hummer, J.E. et al., 2010. An Examination of Horizontal Curve Collisions Characteristics and Corresponding Countermeasures. In *TRB 89th Annual Meeting*. Washington, D.C., p. 17.

Hydén, C., 1987. *The Development of a Method for Traffic Safety Evaluation: the Swedish Traffic Conflict Technique*. Lund University, Sweden.

Imran, M., Hassan, Y. & Patterson, D., 2006. GPS – GIS-Based Procedure for Tracking Vehicle Path on Horizontal Alignments. *Computer-Aided Civil and Infrastructure Engineering*, 21, pp.383–394.

Ivan, J.N., Wang, C. & Bernardo, N.R., 2000. Explaining Two-Lane Highway Crash Rates using Land Use and Hourly Exposure. *Accident Analysis & Prevention*, 32(6), pp.787–795.

Janssen, W.H., 1979. *Routeplanning en geleiding: Een literatuurstudie. Report IZF 1979 C-13*, Soesterberg (The Netherlands).

Jessen, D.R. et al., 2001. Operating Speed Prediction on Crest Vertical Curves of Rural Two-Lane Highways in Nebraska. *Transportation Research Record: Journal of the Transportation Research Board*, 1751, pp.67–75.

Kanellaidis, G., Golias, J. & Efstathiadis, S., 1990. Driver's Speed Behavior on Rural Road Curves. *Traffic Engineering and Control*, 31(7/8), pp.414–415.

Kockelke, W. & Steinbrecher, J., 1987. *Driving behavior investigations with respect to traffic safety in the area of community entrances. Report of the Research*

Project 8363 of the German Federal Research Institute, Bergisch Gladbach, Germany.

Kockelman, K.M. & Ma, J., 2007. Freeway Speeds and Speed Variations Preceding Crashes within and Across Lanes. *Journal of the Transportation Research Forum*, 46(1).

Kopits, E. & Cropper, M., 2005. Traffic Fatalities and Economic Growth. *Accident Analysis & Prevention*, 37(1), pp.169–178.

Krammes, R.A., 2000. Design Speed and Operating Speed in Rural Highway Alignment Design. *Transportation Research Record*, 1701, pp.68–75.

Krammes, R.A. et al., 1995. *Horizontal Alignment Design Consistency for Two-Lane Highways*,

Krammes, R.A. & Hayden, C., 2003. Making two-rural roads safer. *Public Roads*, 66(4), pp.16–21.

Lamm, R. et al., 2007. *How to Make Two-Lane Rural Roads Safer*, Southampton, Boston: WITPress.

Lamm, R. et al., 1988. Possible Design Procedure to Promote Design Consistency in Highway Geometric Design on Two-Lane Rural Roads. *Transportation Research Record: Journal of the Transportation Research Board*, 1195, pp.111–121.

Lamm, R. & Choueiri, E.M., 1987. Recommendations for Evaluating Horizontal Design Consistency based on Investigations in the State of New York. *Transportation Research Record: Journal of the Transportation Research Board*, 1122.

Lamm, R. & Choueiri, E.M., 1995. The Relationship between Highway Safety and Geometric Design Consistency: A Case Study. In *Road Safety in Europe and Strategic Highway Research Program (SHRP)*. pp. 133–151.

Lamm, R., Guenther, A.K. & Choueiri, E.M., 1995. Safety Module for Highway Geometric Design. *Transportation Research Record: Journal of the Transportation Research Board*, 1512, pp.7–15.

Lamm, R., Hayward, J.C. & Cargin, J.G., 1986. Comparison of Different Procedures for Evaluating Speed Consistency. *Transportation Research Record: Journal of the Transportation Research Board*, 1100, pp.10–20.

Lamm, R., Psarianos, B. & Cafiso, S., 2002. Safety Evaluation Process of Two-Lane Rural Roads: A Ten Year Review. In *TRB 81st Annual Meeting*. Washington, D.C., p. 23.

Lamm, R., Psarianos, B. & Mailaender, T., 1999. *Highway Design and Traffic Safety Engineering Handbook*, New York: McGraw-Hill.

Laureshyn, A., Svensson, A. & Hydén, C., 2010. Evaluation of traffic safety, based on micro-level behavioural data: theoretical framework and first implementation. *Accident; analysis and prevention*, 42(6), pp.1637–46. Available at: http://www.ncbi.nlm.nih.gov/pubmed/20728612 [Accessed March 21, 2012].

Lee, S., Lee, D. & Choi, J., 2000. Validation of the 10 mph Rule in Highway Design Consistency Procedure. In *2nd International Symposium on Highway Geometric Design*. Mainz (Germany), pp. 364–376.

Leisch, J.E. & Leisch, J.P., 1977. New Concepts in Design-Speed Application. *Transportation Research Record: Journal of the Transportation Research Board*, 631, pp.5–14.

Leutner, R., 1974. *Fahrraum und Fahrverhalten*, Karlsruhe (Germany).

Lindeman, H.P. & Ranft, B., 1978. *Speed on Curves*, Zurich.

Lipar, P. et al., 2011. Estimation of Road Centerline Curvature from Raw GPS Data. *The Baltic Journal of Road and Bridge Engineering*, 6(3), pp.163–168.

Lippold, C., 1997. *Weiterentwicklung ausgewählter Entwurfsgrundlagen von Landstraßen*.

Lord, D., Manar, A. & Vizioli, A., 2005. Modeling crash-flow-density and crash-flow-V/C ratio relationships for rural and urban freeway segments. *Accident Analysis & Prevention*, 37(1), pp.185–199. Available at: http://www.ncbi.nlm.nih.gov/pubmed/15607290 [Accessed January 31, 2014].

Lord, D. & Mannering, F., 2010. The statistical analysis of crash-frequency data: A review and assessment of methodological alternatives. *Transportation Research Part A: Policy and Practice*, 44(5), pp.291–305. Available at: http://linkinghub.elsevier.com/retrieve/pii/S0965856410000376 [Accessed March 9, 2012].

Mason-Dixon, 2005. *Drive for Life: Annual National Driver Survey*, Washington, D.C.: Mason-Dixon Polling & Research Inc.

Mattar-Habib, C., Polus, A. & Farah, H., 2008. Further Evaluation of the Relationship between Enhanced Consistency Model and Safety of Two-Lane Rural Roads in Israel and Germany. *EJTIR*, 8(4), pp.320–332.

Mcfadden, J. & Elefteriadou, L., 2000. Evaluating Horizontal Alignment Design Consistency of Two-Lane Rural Highways. *Transportation Research Record*, 1737, pp.9–17.

McLean, J., 1979. An ALternative to the Design Speed Concept for Low Speed Alignment Design. *Transportation Research Record: Journal of the Transportation Research Board*, 702, pp.55–63.

Messer, C.J., 1980. Methodology for Evaluating Geometric Design Consistency. *Transportation Research Record: Journal of the Transportation Research Board*, 757, pp.7–14.

Miaou, S.P., Song, J.J. & Mallick, B.K., 2003. Roadway Traffic Crash Mapping: A Space-Time Modeling Approach. *Journal of Transportation Statistics, Bureau of Transportation Statistics*, 6(1), pp.33–57.

Milton, J. & Mannering, F., 1998. The relationship among highway geometrics, traffic-related elements and motor-vehicle accident frequencies. *Transportation*, 25, pp.395–413.

Misaghi, P. & Hassan, Y., 2005. Modeling Operating Speed and Speed Differential on Two-Lane Rural Roads. *Journal of Transportation Engineering*, 131(6), pp.408–417.

Morrall, J. & Talarico, R.J., 1994. Side Friction Demanded and Margins of Safety on Horizontal Curves. *Transportation Research Record: Journal of the Transportation Research Board*, 1435, pp.145–152.

Munden, J.W., 1967. *The Relation between a Driver's Speed and His Accident Rate (Report LR 88)*, Crowthorne, Berkshire, England.

Näätänen, R. & Summala, H., 1976. *Road User Behaviour and Traffic Accidents*, Amsterdam, The Nederlands and New York, N.Y.: North-Holland and American Elsevier.

Nehate, G. & Rys, M., 2006. 3D Calculation of Stopping-Sight Distance from GPS Data. *Journal of Transportation Engineering*, 132(9), pp.691–698.

Ng, J.C.W. & Sayed, T., 2004. Effect of geometric design consistency on road safety. *Canadian Journal of Civil Engineering*, 31, pp.218–227.

Ng, J.C.W. & Sayed, T., 2003. Quantifying Relationships between Geometric Design COnsistency and Road Safety. In *TRB 82nd Annual Meeting*.

Nicholson, A., 1998. Superelevation, side friction, and roadway consistency. *Journal of Transportation Engineering*, 124(5), pp.411–418.

Ogden, K.W., 1996. *Safer Roads, a Guide to Road Safety Engineering*, Cambridge, United Kingdom: Averbury Technical.

Oh, J. et al., 2003. Validation of FHWA Crash Models for Rural Intersections: Lessons learned. *Transportation Research Record: Journal of the Transportation Research Board*, 3883, pp.41–49.

Othman, S., Thomson, R. & Lannér, G., 2013. Safety Analysis of Horizontal Curves Using Real Traffic Data. *Journal of Transportation Engineering*, p.130904224903007. Available at: http://ascelibrary.org/doi/abs/10.1061/(ASCE)TE.1943-5436.0000626 [Accessed November 30, 2013].

Ottesen, J.L. & Krammes, R.A., 2000. Speed-Profile Model for a Design-Consistency Evaluation Procedure in the United States. *Transportation Research Record*, 1701, pp.76–85.

Pardillo Mayora, J.M. & Llamas Rubio, R., 2003. Relevant Variables for Crash Rate Prediction in Spain´s Two Lane Rural Roads. In *TRB 82nd Annual Meeting*. Washington, D.C., p. 24.

De Pauw, E. et al., 2013. The Magnitude of the Regression to the Mean Effect in Traffic Crashes. In *TRB 92nd Annual Meeting*. Washington, D.C., p. 12.

Perco, P., 2006. Desirable Length of Spiral Curves for Two-Lane Rural Roads. *Transportation Research Record*, 1961, pp.1–8. Available at: http://trb.metapress.com/openurl.asp?genre=article&id=doi:10.3141/1961-01.

Pérez-Zuriaga, A.M. et al., 2013. Application of GPS and Questionnaires Data for the Study of Driver Behavior on Two-Lane Rural Roads. *IET Intelligent Transport Systems*, 7(2), pp.182–189.

Pérez-Zuriaga, A.M., 2012. *Caracterización y Modelización de la Velocidad de Operación en Carreteras Convencionales a partir de la Observación Naturalística de la Evolución de Vehículos Ligeros*. Universitat Politècnica de València.

Pérez-Zuriaga, A.M. et al., 2010. Modeling Operating Speed and Deceleration on Two-Lane Rural Roads with Global Positioning System Data. *Transportation Research Record: Journal of the Transportation Research Board*, 2171, p.11+20.

PIARC, 2003. *Road Safety Manual. Recommendations from the World Road Association (PIARC)*, Québec: World Road Association.

Pignataro, L.J., 1973. *Traffic Engineering Theory and Practice*, Englewood Cliffs, N.J.: Prentice-Hall.

Polus, A. et al., 2005. Comprehensive Consistency Model and its Impact on Safety. In *3rd International Symposium on Highway Geometric Design*. Chicago, p. 16.

Polus, A., 1980. The Relationship of Overall Geometric Characteristics to the Safety Level of Rural Highways. *Traffic Quarterly*, 34, pp.575–585.

Polus, A., Fitzpatrick, K. & Fambro, D.B., 2000. Predicting Operating Speeds on Tangent Sections of Two-Lane Rural Highways. *Transportation Research Record*, 1737, pp.50–57.

Polus, A. & Mattar-Habib, C., 2004. New Consistency Model for Rural Highways and Its Relationship to Safety. *Journal of Transportation Engineering*, 130(3), pp.286–293.

Pratt, M.P. & Bonneson, J. a., 2008. Assessing Curve Severity and Design Consistency Using Energy- and Friction-Based Measures. *Transportation Research Record*, 2075, pp.8–15. Available at:

http://trb.metapress.com/openurl.asp?genre=article&id=doi:10.3141/2075-02 [Accessed June 28, 2012].

Reason, J. et al., 1990. Errors and Violations on the Roads: A Real Distinction? *Ergonomics*, 33(10/11), pp.1315–1332.

Resende, P.T. V. & Benekohal, R.F., 1997. Effects of Roadway Section Length on Accident Moeling. In *Proceedings of Traffic Congestion and Traffic Safety in the 21st Century*. p. 8.

Robertson, L.S., 2002. Does Risk Homeostasis Theory Have Implications for Road Safety: Against. *British Medical Journal*, 324, pp.1151–1152.

Roh, T.H., Seo, D.J. & Lee, J.C., 2003. An Accuracy Analysis for Horizontal Alignment of Road by the Kinematic GPS/GLONASS Combination. *KSCE Journal of Civil Engineering*, 7(1), pp.73–79.

Rothengatter, T., 1997. Psychological Aspects of Road User Behaviour. *Applied Psychology*, 46(3), pp.223–234. Available at: http://doi.wiley.com/10.1111/j.1464-0597.1997.tb01227.x.

Rowan, N.J. et al., 1980. *Safety Design and Operational Practices for Streets and Highways*, Washington, D.C.

Sagberg, F., 1998. Month-by-Month Changes in Accident Risk among Novice Drivers. In *24th International Congress of Applied Psychology*. San Francisco.

Said, D., Abd El Halim, A.O. & Hassan, Y., 2009. Desirable Spiral Length Based on Driver Steering Behavior. *Transportation Research Record*, 2092, pp.28–38. Available at: http://trb.metapress.com/openurl.asp?genre=article&id=doi:10.3141/2092-04 [Accessed June 28, 2012].

Said, D., Hassan, Y. & Abd El Halim, A.O., 2007. Quantification and Utilization of Driver Path in Improving the Design of Highway Horizontal Curves. In *TRB 86th Annual Meeting*. p. 17.

Schneider, W.H. & Shifrin, R.M., 1977. Controlled and Automatic Human Information Processing: I. Detection, Search and Attention. *Psychological Review*, 84(1), pp.1–66.

Seneviratne, P.N. & Islam, M.N., 1994. Optimum Curvature for Simple Horizontal Curves. *Journal of Transportation Engineering*, 120(5), pp.773–786.

Shankar, V., Mannering, F.L. & Barfield, W., 1996. Statistical Analyis of Accident Severity on Rural Freeways. *Accident Analysis & Prevention*, 28(3), pp.391–401.

Shinar, D., 2007. *Traffic Safety and Human Behavior*,

Silyanov, V.V., 1973. Comparison of the Pattern of Accident Rates on Roads of Different Countries. *Traffic Engineering and Control*, 14, pp.432–435.

Sivak, M., 2002. How Common Sense Fails Us on the Road: Contribution of Bounded Rationality to the Annual Worldwide Toll of One Million Traffic Fatalities. *Transportation Research Part F*, 5, pp.259–269.

Solomon, D., 1964. Accidents on Main Rural Highways Related to Speed, Driver and Vehicle. *Bureau of Public Roads*.

Spacek, P., 2005. Track Behavior in Curve Areas : Attempt at Typology. , (September), pp.669–676.

Summala, H., 1988. Risk Control is not Risk Adjustment: The Zero-Risk Theory of Driver Behavior and Its Implications. *Ergonomics*, 31, pp.491–506.

Svensson, A., 1998. *A Method for Analysing the Traffic Process in a Safety Perspective*. University of Lund (Sweden).

Taylor, M.C., Baruya, A. & Kennedy, J. V., 2002. *TRL Report 211: The relationship between speed and accidents on rural single-carriageway roads*, Crowthorne, Berkshire.

Taylor, M.C., Lynam, D.A. & Baruya, A., 2000. *The Effects of Drivers' Speed on the Frequency of Road Accidents*, Crowthorne, Berkshire.

Tom, G., 1995. Accidents on Spiral Transition Curves. *ITE Journal*, September, pp.49–53.

Treat, J. et al., 1979. *Tri-Level Study of the Causes of Traffic Accidents. Executive Summary*,

Veneziano, D., Hallmark, S. & Souleyrette, R.R., 2004. Accuracy of Light Detection and Ranging Derived Terrain Data for Highway Location. *Computer-Aided Civil and Infrastructure Engineering*, 19(2), pp.130–143.

Wang, C., Quddus, M.A. & Ison, S.G., 2012. Factors affecting road safety : a review and future research direction. In *TRB 91st Annual Meeting*. Washington, D.C., p. 17.

Wickens, C.D., 1992. *Engineering Psychology and Human Performance* 2nd Editio., New York: Harper-Collins.

Wilde, G.J.S., 1998. Risk Homeostasis Theory: an Overview. *Injury Prevention*, 4, pp.89–91.

Wooldridge, M.D., 1994. Design Consistency and Driver Error. *Transportation Research Record: Journal of the Transportation Research Board*, 1445, pp.148–155.

Wooldridge, M.D. et al., 2000. Effects of Horizontal Curvature on Driver Visual Demand. *Transportation Research Record*, 1737, pp.71–77.

Wu, K. et al., 2013. Exploring the Association between Traffic Safety and Geometric Design Consistency Based on Vehicle Speed Metrics. *Journal of Transportation Engineering*, 139(7), pp.738–748.

Young, S.E. & Miller, R., 2005. High Accuracy Geometric Highway Model Derived from Multi-Track Messy GPS Data. In *Proceedings of the 2005 Mid-Continent Transportation Research Symposium*. Ames, Iowa.

Zegeer, C. V., 1990. *Cost-Effective Geometric Improvements for Safety Upgrading of Horizontal Curves*,

Zegeer, C. V. et al., 1988. Safety Effects of Cross-Section Design for Two-Lane Roads. *Transportation Research Record: Journal of the Transportation Research Board*, 1195.

Zegeer, C. V. et al., 1992. Safety Effects of Geometric Improvements in Horizontal Curves. *Transportation Research Record: Journal of the Transportation Research Board*, 1356.

Zegeer, C. V. et al., 1991. Safety Effects of Geometric Improvements on Horizontal Curves. In *TRB 80th Annual Meeting*. p. 32.

Zhang, C. & Ivan, J.N., 2005. Effects of Geometric Characteristics on Head-On Crash Incidence on Two-Lane Roads in Connecticut. *Transportation Research Record: Journal of the Transportation Research Board*, 1908, pp.159–164.

Zhou, M. & Sisiopiku, V., 1997. Relationship between Volume-to-Capacity Ratios and Accident Rates. *Transportation Research Record: Journal of the Transportation Research Board*, 1581, pp.47–52.

14. Conclusion

This Doctoral Thesis is divided into three main sections. The first one covers the literature review, focusing on the infrastructure, human factors, recreation of the road geometry, and road design consistency. The second part of the document is composed by objectives, hypotheses and methodology. This section explains the scope of this research, as well as it establishes the foundations of the analysis that will be performed. Finally, the last main section obtains and discuss the results. Further research is also exposed in this section.

Therefore, the objectives of this Doctoral Thesis have all been satisfactorily achieved. A practical tool for estimating the road safety level has also been developed. Road designers can use this tool for both the design and the operation stages.

This document also indicates some needs of further research. Some of them would enhance the presented results; while some others are new research fields.

On the basis of the abovementioned last remarks, the current Doctoral Thesis is hereby concluded by the doctoral student Mr. Francisco Javier Camacho Torregrosa.

Valencia, November 25th, 2014

Mr. Francisco Javier Camacho Torregrosa

I. Published and accepted papers

Here are the most relevant scientific publications of the student related to the topic of the presented Doctoral Thesis.

I.1. Indexed Scientific Journals

Paper 1. Pérez Zuriaga, A.M., García García, A., Camacho Torregrosa, F.J. y D'Attoma, P. (2010). *Modeling operating speed and deceleration on two-lane rural roads with global positioning system data*. Transportation Research Record, vol. 2171, pp. 11-20.

Paper 2. Camacho Torregrosa, F.J., Pérez Zuriaga, A.M y García, A. (2013). *New geometric design consistency model based on operating speed profiles for road safety evaluation.* Accident Analysis and Prevention, vol. 61, pp. 33-42.

Paper 3. Ana M. Pérez-Zuriaga, F. Javier Camacho-Torregrosa, José M. Campoy-Ungría and Alfredo García (2013). *Application of GPS and Questionnaires Data for the Study of Driver Behaviour on Two-Lane Rural Roads*. IET Intelligent Transport Systems, vol. 7(2), pp. 182-189.

Paper 4. Ana M. Pérez-Zuriaga, F. Javier Camacho-Torregrosa, Alfredo García (2013). *Tangent-to-curve transition on two-lane rural roads based on continuous speed profiles*. Journal of Transportation Engineering – ASCE, vol. 139-11, pp. 1048-1057.

Paper 5. Alfredo García, David Llopis-Castelló, F. Javier Camacho-Torregrosa, Ana M. Pérez-Zuriaga (2013). *New consistency index based on inertial operating speed*. Transportation Research Record, vol. 2694, pp. 105-112.

Paper 6. F. Javier Camacho-Torregrosa, Ana M. Pérez-Zuriaga, José M. Campoy-Ungría, Alfredo García and Andrew P. Tarko (2014). *Use of Heading Direction for Recreating the Horizontal Alignment of an Existing Road*. Computer-Aided Civil and Infrastructure Engineering. *(Accepted, publication pending).*

I.2. Spanish Scientific Journals

- García García, A. y Camacho Torregrosa, F.J. (2009). *Evaluación de la seguridad vial de carreteras convencionales mediante la determinación de la consistencia global de su diseño geométrico*. Revista Carreteras, vol. 163, pp. 21-32.
- Alfredo García, David Llopis, F. Javier Camacho Torregrosa y Ana M. Pérez Zuriaga (2013). *Nuevo índice de consistencia basado en la velocidad de operación inercial*. Revista Rutas, vol. 154, pp. 19-27.
- Ana M. Pérez Zuriaga, F. Javier Camacho Torregrosa, Alfredo García, José M. Campoy Ungría (2013). *Metodología de toma de datos para el estudio naturalístico del comportamiento de los conductores*. Revista Rutas, vol. 156, pp. 28-36.
- Alfredo García, F. Javier Camacho Torregrosa, Ana M. Pérez Zuriaga, E. Manuel López Porta (2013). *Innovative two-lane rural road safety geometric design process*. Revista Carreteras, vol. 191, pp. 31-46.

I.3. International Conferences

- Pérez Zuriaga, A.M., García García, A., Camacho Torregrosa, F.J. y D'Attoma, P. (2010). *Use of GPS data to model operating speed and deceleration on two-lane rural roads.* 89th Annual Meeting of Transportation Research Board. Washington, D.C., EEUU.
- Camacho Torregrosa, F.J., Pérez Zuriaga, A.M. y García García, A. (2010). *Mathematical model to determine road geometric consistency in order to reduce road crashes.* Mathematical models of addictive behavior, medicine & engineering. Valencia, España.
- Camacho Torregrosa, F.J., Pérez Zuriaga, A.M y García, A. (2011). *New geometric design consistency model based on operating speed profiles for road safety evaluation.* Proceedings of the 3rd Road Safety and Simulation Conference. Indianapolis, USA
- Pérez Zuriaga, A.M., García García, A. y Camacho Torregrosa, F.J. (2011). *Study of tangent-to-curve transition on two-lane rural roads with*

continuous speed profiles. 90th Annual Meeting of Transportation Research Board. Washington, D.C., EEUU.

- Camacho Torregrosa, F.J., Pérez Zuriaga, A.M., Campoy Ungría, J.M. y García García, A. (2012). *Data collection methodology for studying driver behaviour from free flow speed profiles on rural roads*. European Conference on Human Centered Design for Intelligent Transport Systems. Valencia, España.
- García, A., Llopis Castelló, D., Pérez Zuriaga, A.M. y Camacho Torregrosa, F.J. (2012). *Un nuevo indicador de la consistencia del diseño geométrico de carreteras*. III Congreso Iberoamericano de Seguridad Vial. Bogotá, Colombia.
- Alfredo García, David Llopis-Castelló, F. Javier Camacho-Torregrosa, Ana M. Pérez-Zuriaga (2013). *Consistency Index based on Inertial Operating Speed*. 92nd Annual Meeting of the Transportation Research Board. Washington D.C., USA.
- Alfredo García, David Llopis-Castelló, Ana M. Pérez-Zuriaga, F. Javier Camacho-Torregrosa (2013). *Homogeneous Road Segment Identification Based on Inertial Operating Speed*. 92nd Annual Meeting of the Transportation Research Board. Washington D.C., USA.
- Camacho Torregrosa, F.J., Pérez Zuriaga, A.M., Campoy Ungría, J. M. and García, Alfredo (2013). *Enhanced geometric design consistency model based on operating speed profiles.* Proceedings of the 4th Road Safety and Simulation Conference. Rome, Italy.

I.4. Spanish Conferences

- Pérez Zuriaga, A.M., García García, A., Romero Rojas, M. y Camacho Torregrosa, F.J. (2007). *Utilización de equipos GPS de seguimiento pasivo en la obtención de la geometría de la vía y en la evaluación de la seguridad vial.* VII Congreso Español sobre Sistemas Inteligentes de Transporte. Valencia, España.
- Pérez Zuriaga, A.M., García García, A., Romero Rojas, M. y Camacho Torregrosa, F.J. (2008). *Aplicación de rastreadores GPS para la restitución de la geometría de la vía.* VIII Congreso de Ingeniería del Transporte. A Coruña, España.

- Camacho Torregrosa, F.J., García García, A., Romero Rojas, M. y Pérez Zuriaga, A.M. (2008). *Empleo de un modelo global de consistencia en el estudio de la siniestralidad de carreteras convencionales.* VIII Congreso de Ingeniería del Transporte. A Coruña, España.
- Pérez Zuriaga, A.M., García García, A. y Camacho Torregrosa, F.J. (2010). *Estudio de la transición recta-curva a partir de perfiles continuos de velocidad empíricos*. IX Congreso de Ingeniería del Transporte. Madrid, España.
- Pérez Zuriaga, A.M., García, A. y Camacho Torregrosa, F.J. (2012). *Análisis de los factores que condicionan la velocidad elegida por los conductores en rectas de carreteras convencionales*. X Congreso de Ingeniería del Transporte. Granada, España.
- Camacho Torregrosa, F.J., García, A. y Pérez Zuriaga, A.M (2012). *Modelo global de consistencia del diseño geométrico de carreteras convencionales*. X Congreso de Ingeniería del Transporte. Granada, España.
- Camacho Torregrosa, F.J., Pérez Zuriaga, A.M, López Porta, E.M y García, A. (2014). *Restitución geométrica en planta de carreteras mediante el empleo de métodos analíticos basados en el azimut*. XI Congreso de Ingeniería del Transporte. Santander, España.

I.5. Books and Book Chapters

- Pérez Zuriaga, A.M., García García, A. y Camacho Torregrosa, F.J. (2011). *La velocidad de operación y su aplicación en el análisis de la consistencia de carreteras para la mejora de la seguridad vial.* Cuaderno Tecnológico de la PTC. ISBN: 978-84-615-3971-0. Plataforma Tecnológica de la Carretera.
- Alfredo García, F. Javier Camacho Torregrosa, Ana M. Pérez Zuriaga, Ana T. Moreno Chou, Carlos Llorca García (2013). *Nuevo proceso de diseño geométrico para unas carreteras convencionales más seguras*. Cuaderno Tecnológico de la PTC. ISBN: 978-84-695-8771-3. Plataforma Tecnológica de la Carretera.

USE OF GPS DATA TO MODEL OPERATING SPEED AND DECELERATION ON TWO-LANE RURAL ROADS

Ana Mª Pérez Zuriaga
PhD Candidate
Department of Transportation
Polytechnic University of Valencia
Camino de Vera, s/n. 46022 – Valencia
Tel: (34) 96 3877374
Fax: (34) 96 3877379
E-mail: anpezu@tra.upv.es

Alfredo García García
Professor
Department of Transportation
Polytechnic University of Valencia
Camino de Vera, s/n. 46022 – Valencia
Tel: (34) 96 3877374
Fax: (34) 96 3877379
E-mail: agarciag@tra.upv.es

Francisco Javier Camacho Torregrosa
PhD Candidate
Department of Transportation
Polytechnic University of Valencia
Camino de Vera, s/n. 46022 – Valencia
Tel: (34) 96 3877374
Fax: (34) 96 3877379
E-mail: fracator@posgrado.upv.es

Pierangelo D'Attoma
Civil Engineering Student
Department of Transportation
Polytechnic University of Valencia
Camino de Vera, s/n. 46022 – Valencia
Tel: (34) 96 3877374
Fax: (34) 96 3877379
E-mail: dattomap@libero.it

Submission Date: March 15th, 2010

Word count:	Manuscript	5302 words
	2 Tables (*250)	500 words
	6 Figures (*250)	1500 words
	TOTAL	**7302 words**

ABSTRACT

In the road design process the speed variation along the road segment is an important issue to consider in order to adapt the road geometry to drivers' expectancies. To achieve this objective, speed criteria are used to evaluate road consistency. Therefore, being able to estimate the operating speed in the design phase can lead to a safer road alignment.

With this objective, several research have developed operating speed models. Most of these models are based on collected speed spot-data. They assume constant speed on curves and therefore deceleration occurs entirely on the approach tangent. According to these assumptions, speed spot-data are collected at the center of the horizontal curve and at the midpoint of the preceding tangent in order to obtain operating speed models.

This paper presents a new methodology based on the use of GPS devices that allow collecting and processing speed continuous data. By means of this new methodology, not only new and more accurate operating speed models can be developed, but also cited hypotheses can be checked. Observed speed continuous profiles allow new studies than previously couldn't be done, specially relating to deceleration and speed variations.

New speed models have been calibrated in this research, including three for horizontal curves with radius curve and CCR of a single curve as a variable explanatory, and one for tangents that incorporates the curve speed model. Moreover, tangent-curve speed variations have been evaluated, comparing $\Delta_{85}V$ and ΔV_{85}, analyzing the deceleration length occurring on curve, and developing two deceleration models.

KEYWORDS: operating speed, GPS, speed model, deceleration rate, speed profile.

INTRODUCTION

Road safety is dependent of several factors; being the design consistency one of the most important, because it refers to the conformance of highway's geometry to driver expectancy. The design consistency verification is aimed to avoiding road alignment configurations which might surprise drivers and lead to anomalous behavior and possible collisions. A technique to evaluate the consistency of a design is to evaluate changes in operating speeds as a function of the roadway geometry. The operating speed V_{85} is defined as the 85th percentile of the distribution of speeds selected by drivers in free-flow conditions on a location of the road alignment. The estimation of V_{85} on the geometric elements of the alignment make possible to associate every location of the alignment to a value of V_{85} and to verify the design consistency.

Several models have been developed to predict the operating speed at curved sections. However, the model format, independent variables, and regression coefficients are substantially different from one model to the other. This might have been the result of differences in driver behavior from one region to others, and it highlights the fact that no single model is universally accepted.

In addition, the data collection device used to record vehicle speed was, in most cases, a manually operated radar gun or similar. The utilization of radar guns has three important problems: human error, cosine error and effect on driver behavior. Other methods to collect speed data are pavement sensors. However, they require the researcher to carry more equipment and require more time to install and remove the equipment. This method might also affect drivers' behavior.

By using these methods the speed data can only be collected in one location, usually the middle of the curve. Thus, operating speed models based in this data collection method have to assume a constant operating speed on curve, such as the model developed by Lamm *(1)*. It estimates the operating speed on the curve from linear regression equations, using only the curvature change rate (CCR) of a single circular curve as the explanatory variable. The operating speed on tangent was assumed to be constant and estimated from the predicting model for speeds in curves, assuming CCR equal to zero. The acceleration and deceleration were assumed to occur only on tangent sections without validation, and their rates to be equal in magnitude (0.85 m/s^2).

Another model was developed by Ottesen and Krammes *(2)* based essentially on the same assumptions as Lamm. Spot-speed data were collected with radar guns at a sample of horizontal curves and their approach tangents on two-lane rural highways. The speeds of free-flowing passenger cars were measured only at the midpoint of the selected curves and on long tangent sections where desired speeds were believed to be attained.

Fitzpatrick and Collins *(3)* also developed a model based on spot-speed data, recorded at the center of the horizontal curve and at the midpoint of the preceding tangent *(4)*. A family of speed models was developed with the curve radius or the rate of vertical curvature as explanatory variables for selected combinations of horizontal and vertical alignment conditions. However, a model for tangent speeds was not developed, using a value of 100 km/h as an estimate of the speed on long tangents.

They also developed two models, to predict deceleration and acceleration rates as a function of radius. The models developed provide a maximum deceleration rate of 1 m/s^2 and a maximum acceleration rate of 0.54 m/s^2.

Estimation of speeds on curves may be easier than prediction of speeds on tangent sections. Few studies have dealt with this issue because a considerable database is necessary to identify any significant trends and substantial modeling effort is required. Polus et al. *(5)* analyzed the variability of the operating speeds on 162 tangent sections of two-lane rural highways where speed data were collected by using radar meters and on-pavement piezoelectric sensors connected to traffic counter-classifiers. Speeds were measured on the curve and on the preceding tangent. Several models were developed for prediction of operating speed based on the geometric characteristics available.

Concerning deceleration and acceleration rates, Collins and Krammes *(6)* tested the validity of speed-profile model for design consistency evaluation, including the speed reduction estimation ability of the model and the assumptions about deceleration and acceleration characteristics approaching and

departing horizontal curves. It was found that the assumed 0.85 m/s^2 value is reasonable for deceleration rates approaching curves that require speed reductions but may overestimate acceleration rates departing curves. The model's assumptions that deceleration occurs entirely on the approach tangent and that speeds are constant throughout a curve were not confirmed by observed speed behavior.

On the other hand, there are models based on data collected at different sites along the curve and the preceding tangent.

Gibreel et al. *(7)* developed operating speed models for two-lane rural highways that account for the 3D nature of highways. Regression analysis was used to develop the operating speed models based on data collected for each highway section at five points along each travel direction to establish the effect of the 3D alignment combination on the trend of operating speed of the traveling vehicles.

Another study based on speed data collected at five different points on each curve was carried out by Misaghi and Hassan *(8)*. In this case, the speed data were collected using electronic counter/classifiers to observe the vehicle speed change along 20 curves. They developed two models to estimate 85^{th} percentile speed at middle of curve with the radius as the explanatory variable and recommended 103.0 km/h for independent tangents and 95.8 km/h for nonindependent ones. Although relatively weak relationships were developed for the operating speed on horizontal curves, stronger relationships were found for the 85^{th} percentile speed differential from a tangent to a curve.

Figueroa and Tarko *(9)* evaluated driver behavior before and after horizontal curves in order to develop speed models for transition sections. Speeds were measured in each site at several spots distributed along estimated deceleration and acceleration segment. The results indicated that 66% of the speed reduction and 72 % of the speed increase occurs on the tangents preceding and following the curves, respectively. In addition, the mean deceleration rate and the mean acceleration rate are 0.732 and 0.488 m/s^2, respectively, for a 16.1 km/h reduction.

There are also models that predict the expected 85^{th} percentile of the deceleration and acceleration rates based on data collected on the tangent-curve-tangent transition in a driving simulator, such as Bella *(10)*. In this study, the author found out that the mean value of the differences of speed of each driver between the beginning and the midpoint of the curve was not significantly different from zero, while that between the midpoint and the end was significantly different from zero. However, considering the low values of the differences of speed between the midpoint and the end of the curve, the simplified assumption of the constant speed on the circular curve was considered admissible. Furthermore, different average distances of deceleration and acceleration were found. That highlights the correctness of assuming different values of deceleration and acceleration rate.

The most important limitation of the models based on speed spot-data is that data are not collected at the beginning and the ending deceleration/acceleration points. It derives into acceleration and deceleration profiles that not represent the actual driver behavior. Besides, deceleration and acceleration length cannot be determined, so the actual acceleration and deceleration rates cannot be accurately obtained.

To avoid these deficiencies in data collection, there are other methods based on continuous speed tracking, such as instrumented test vehicles or different methods based on digital video recording and processing. Each one are designed to different situations, i.e. digital video processing is only suitable for local studies in a reduced road segment.

Yang and Hassan *(11)* and Hu and Donnell *(12)* studied drivers' behavior from speed data collected using instrumental vehicle. However, the results and the possible developed speed models may be conditioned by the vehicle equipment and the number of observations. Moreover, the sample is not representative enough of the actual driver behavior because volunteers research participants knowing the research objectives.

That's why the data used in this study were from a field experiment based on GPS tracking devices. The main advantage of this method is the huge amount of continuous speed data collected without significant influence over the drivers. This new methodology lets the researchers, for the first time, to develop operating speed models on curves and tangents and to evaluate the speed differential on tangent-curve transitions, developing also deceleration and acceleration models.

OBJECTIVES

The objective of this study is to develop operating speed prediction models for curves and tangents for two-lane rural roads, including geometric characteristics as explanatory variables. Furthermore, the research comprises the evaluation of speed variations from tangent to curve sections. To evaluate this phenomenon, several variables, such as the 85th percentile speed differential ($\Delta_{85}V$), the differential of 85th percentile speed (ΔV_{85}), deceleration length and deceleration length inside the curve, have been studied and a deceleration rate model has also been developed.

The research is not based on speed spot-data, but on continuous data. Consequently, models and results obtained, based on the same sample size, may be more accurate than the previous ones.

Therefore, the aim of this paper is not only to explain the obtained results and models but rather a new methodology to collect and process continuous speed data.

FIELD STUDY

In order to obtain the necessary speed continuous data for the analysis, a new methodology has been developed. The first step consists in data collection using GPS devices. The second step is the data reduction, including filtering and processing data. The results of this step are the horizontal alignment restitution, plotted as curvature diagram, and the individual operating speed continuous profiles.

Data collection

The speed data were collected between February 2008 and July 2008 during morning period between 8:30 a.m. and 2:00 p.m., in a working day and under dry weather conditions.

Speed data were collected using a pocket-sized GPS device. The available passive GPS trackers have an internal computer that accurately determines the GPS location of the device and records detailed travel data every second, such as time and position. Data stored on the GPS device can be accessed by inserting the unit directly into a personal computer via USB port for further processing.

Four two-lane rural road segments, with no main intersections and with a high lateral clearance, were selected for data collection phase. All the roads selected are characterized by low traffic volume to reduce the potential for restricted vehicle flow but enough to guarantee a significant sample size, and by low heavy traffic volume. The longitudinal grade never exceeded ± 4.0 % because the analysis was limited to the horizontal alignment. The general road segments characteristics and the number of observations for each one are summarized in table 1.

At each end of road segment, drivers' cooperation was asked in order to install the GPS device on their vehicles thanks to its strong magnetic mounts. The drivers were encouraged to drive as they usually do, telling them that data were going to be used for a University research, not for enforcement. The device was finally collected at the other road control located at the segment end.

A survey was conducted both at the beginning and at the end of the road segment. While at the beginning control road the questions were about age, gender, number of occupants, driving experience, knowledge of the particular road segments, travel purpose, vehicle type; at the end control road the drivers were asked about posted speed, desirable speed and whether they had been influenced or not in their speed by another vehicle. The first survey lasted for two minutes. Thus, road segments were chosen with a maximum length of 9 km to avoid that a vehicle was caught up by the next one in order to guarantee free-flow conditions. Operating speed must be measured for the vehicles in the traffic stream under free-flow conditions to avoid the effect of traffic flow on vehicle speed. In this study, it is considered that the data representing the free-flow conditions are those of isolated vehicles with a minimum headway of at least 5 seconds.

This data collection method allows to obtain continuous speed data along a road segment and a great number of drivers' individual data. Nevertheless, this method might affect drivers' behavior. To guarantee the results' quality, it is necessary to check whether the operating speed during the data collection is significantly different from the normal operating speed.

Along three of the data collection road segments, two camcorders were installed away from the drivers' sight in order to record the vehicles passing across a tangent section and across a curve section on each site. This process was carried out at the data collection day (with GPS) and a week before (without GPS). After the digital video processing, the statistical equality of both populations, with GPS and without GPS, was confirmed thanks to LSD (Least Significant Differences) intervals. The corresponding LSD intervals are presented in figure 1. As the intervals overlap, the population means are no significantly different from each other at the 95% confidence level.

Data reduction

Data collected by the GPS devices are presented in a latitude-longitude-altitude-compass bearing-time-date format, providing it in a 1–second interval. The data-processing program, developed for the present research, uses UTM (Universal Transverse Mercator) coordinates, so it was necessary to develop a program module to make the coordinate conversion. Occasionally, GPS devices stored anomalous data, so it was necessary to detect and take them out by another program module.

Once the GPS data conversion and debugging were carried out, the processing could begin. The first step was to define the starting and ending point for each one of the road segments. From these points, the program combines all individual paths in order to obtain the average operating trajectory.

From this average path it is possible to determine its curvature diagram and use it to obtain the horizontal alignment. The figure 2 shows an example of curvature diagram.

Considering each one of the drivers' trajectories it is possible to determine their individual operating speeds along the entire road segment. Thus, different speed percentiles can be obtained by considering all the individual speeds.

In order to guarantee free-flow conditions, a study by using speed percentiles was carried out, removing all the trajectories which presented abnormal speed behaviors. This study consisted in plotting several percentile speed profiles and comparing each individual trajectory with them. An example of an abnormal individual speed profile is the one that shows a located speed reduction much higher than the speed reduction of the percentile speed profiles at that point.

By means of these diagrams, it is not difficult to identify maximum and minimum speeds, deceleration points and speed variations. Therefore, this methodology might become a powerful tool for investigation.

MODELS DEVELOPMENT

Considering the curvature diagram developed by the data reduction process, the representative variables of the horizontal alignment of the road segment were obtained. The most important variables are the curve radii, curve length, deflection angle and tangent length. The curve radii varies from 80 m to 930 m, the curve length from 55 m to 205 m, the deflection angle from 4.5º to 38.7º and the tangent length from 25 m to 2590 m.

A sight index was defined as the percentage of curve length that can be seen from the beginning point of the curve. Thus, when the index value is 1, the whole curve length can be seen from the beginning of the curve. The sight distance index varies from 0.1 to 1.6.

Finally, considering that the curvature change rate has already been extensively investigated and that the results of the statistical analysis showed a good correlation between this index and the operating speed, the curvature change rate (CCR) of a single curve, including circular curve and transition curves, was selected as a variable.

$$CCR = \frac{|\gamma_i|}{L_{Ci}} \quad (1)$$

Where,

CCR = curvature change rate (degree/km). In this study, CCR varied from 55.62 degree/km to 485.37 degree/km.

γ_i = deflection angle of the curve (degrees)

L_{Ci} = curve length (km)

The relation between these variables and operating speed, deceleration rate and speed variation was studied in order to develop the different models.

Operating speed model on curves

In order to develop the operating speed models on curves, the minimum speed at each curve was used, taken from the 85th percentile speed profiles obtained in data reduction.

A preliminary ANOVA analysis among the horizontal alignment variables (curvature change rate, radius, etc) and operating speed on curves was performed. From this analysis, it was found that previous tangent length and sight distance index had a p-value of 0.3050 and 0.1428, respectively. Therefore, these variables have not a statistically significant relationship with operating speed at the 90% confidence level. The variables with lowest p-value were radius, curve length and CCR, so those were used in different regression analysis. However, the model obtained with curve length does not explain accurately the operating speed behavior, so the radius and the CCR were the explanatory variables used in the final models.

The regression analysis yield the model showed in figure 3 with radius as explanatory variable, having a R^2 equal to 0.76. This model is valid for a range of radii between 80 m and 930 m.

The model presents a high slope for small radius, decreasing as radius gets larger. It indicates that for large radii curves, the radius is not as significant in the speed choice as for sharp curves. In fact, for radius higher than 500 m the model is consistently overpredicting the observed speeds.

Considering the trend of data, an operating speed model for curves with radius lower than 400 m will represent drivers' behavior more accurately for this range. Thus, another model was developed to estimate the operating speed on curves with those radii. This model, depending on 1/R (figure 3), presents a R^2 equal to 0.84. Its coefficient of determination is higher than the obtained for the global model, but lower than the one obtained for the linear model. However, this model fits better the phenomenon.

On the other hand, based on the CCR as explanatory variable, another global model was obtained by the regression analysis, with a R^2 equal to 0.79. This model is also presented at figure 3 with the data used on its development.

Operating speed model on tangents

On short tangents speed cannot be fully developed because of the influence of the adjacent curves. Therefore, for the model development the tangents used were those with enough length to be independent. These tangents were identified in the speed profiles as the tangents that presented a segment at which constant speed was attained. In all cases, the length of independent tangent was higher than 90 m.

This model was developed by using, as tangent speed data, the mean of the 85th percentile speeds presented in the tangent segment where the speed was approximately constant. These data might not coincide with the speed data corresponding to the middle point of the tangents.

Before stating the model expression, the drivers' behavior along a tangent must be taken into account. Along a tangent the speed increases with the length until the desired speed is reached. Therefore, the model must be asymptotical. Besides, the speed increment is smaller for large previous curve radius. Consequently, the slope of the model curve must be variable, depending on previous curve radius. These considerations led to the model presented in figure 4 with a R^2 equal to 0.52.

The proposed model includes:

- V_{85} (km/h) is defined as the estimated 85th percentile speed on tangents obtained from the model.
- λ has been calibrated minimizing the MSE.
- $V_{85\ c}$ (km/h) is defined as 85th percentile speed on previous curves obtained from the proposed speed model for curves.
- V_{des} (km/h) is the desired speed. The desired speed is defined as the speed at which drivers choose to travel under free-flow conditions when they are not constrained by alignment features. In this

research its value has been assumed equal to 110 km/h corresponding to the speed data registered in the longest tangents.

- L (m) is the tangent length.

Tangent–curve speed variations

The current approach to evaluate design consistency is based on calculating the operating speed of the drivers on both the curved and the tangent sections and, then, subtracting these two values and naming it as the speed differential value. However, according to Hirsh *(13)* and McFadden and Elefteriadou *(14)*, speed distributions at the curved and tangent sections are not the same, and thus the simple subtraction of the operating speed values should not be performed. Also, even if the speed distributions are the same, the 85th percentile driver does not need to be the same in the two locations. Moreover, most previous research based these calculations on data collected at two sections, without verification whether these data correspond to the speed at the beginning and end points of deceleration.

Thanks to the continuous speed profile obtained by the methodology presented in this paper, the beginning and end points of deceleration and the associated speeds, both the 85th percentile and the individual ones have been determined. Thus, in present research speed differential (ΔV_{85}) was calculated for each individual vehicle using their individual speed at beginning and end points of its deceleration. Besides, the statistic $\Delta_{85}V$ (85th percentile speed differential) was calculated. It is defined as the differential speed not exceeded by 85% of the drivers traveling under free-flow conditions.

Figure 5 shows the representation of $\Delta_{85}V$ in relationship with ΔV_{85}.

Based on the observations of this study, it can be concluded that the simple subtraction of operating speed underestimates the actual values of speed differential. This conclusion is similar to the conclusions carried out by McFadden and Elefteriadou *(14)* and Misaghi and Hassan *(8)*.

Deceleration model

Deceleration model tries to complete the operating speed profile model, reflecting as accurate as possible the drivers' behavior in a tangent-to-curve transition. This problem is generally solved by using deceleration rates, obtained by the equation (2).

$$d = \frac{V_{85\,(i)}^2 - V_{85(i+1)}^2}{2D} \quad (2)$$

Where,

$V_{85\,(i)}$ and $V_{85\,(i+1)}$ = operating speeds in the locations (i) and (i+1)

D = the distance between the locations (i) and (i+1)

However, according to Bella *(10)* the deceleration rate calculated on the basis of the individual driver behavior is significantly higher than the one obtained from the operating speed profiles. Consequently, the methodology for the determination of the deceleration rate on the basis of the operating speeds leads to an underestimation of the deceleration and acceleration rates effectively experienced by the drivers.

Taking into account these considerations, the value of the deceleration rate in the tangent-to-curve transition was calculated based on individual driver speed profile by the equation (3).

$$d_i = \frac{V_{T\,(i)}^2 - V_{C(i)}^2}{2D} \quad (3)$$

Where,

$V_{T\,(i)}$ = individual speed at the beginning point of deceleration in the tangent

$V_{C\,(i)}$ = individual speed at the end point of deceleration in the curve

D = the distance between the beginning and the end point of deceleration

Once the decelerations of the individual drivers have been obtained, the value of the 85th percentile (d_{85}) was determined for every configuration and a correlation analysis was performed in order

to determine which independent variables are correlated with this rate. An ANOVA analysis revealed that a positive and strong correlation exists between d_{85} and inverse of radius (p-value = 0.00) and the CCR of the single curve (p-value = 0.00).

Based on the values of d_{85} calculated from the individual speed profiles and on the results of the correlation analysis, models that predict the expected deceleration were developed. The regression analysis yield the model shown in figure 6 with radius as explanatory variable, having a R^2 equal to 0.70.

Since the model estimates the deceleration rate when a vehicle enters a horizontal curve that increases as radius decreases, the models appears to be congruent.

The curve radius was not the only significant variable, but a strong correlation between the deceleration rate and the CCR was also confirmed. Therefore, another alternative model to predict the deceleration from CCR data has been developed. This model is shown in figure 6.

In the study of deceleration phenomenon it is not only important to consider the deceleration rates, but also the deceleration length. Several research assumed that the speed remains constant throughout a curve and that the deceleration occurs entirely on the approach tangent.

Thanks to the continuous observed speed profiles these assumptions have been invalidated. The study of collected data found out that at least the 7% of the deceleration transition length occurs on the curve. The average deceleration transition length that occurs on the curve is 47.34%. There are values even higher than 89%.

Moreover, the average percentage of curve length affected by deceleration is 45%, and in the 58% of sites deceleration finishes before curve's midpoint.

MODELS COMPARISON

The developed models have been compared to others existing in the literature. All models were applied to the geometric elements obtained from the curvature diagram developed for different road segments than those ones used for calibrating the models, estimating the operating speed on curves and tangents and the deceleration rates. After that, the minimum square error (MSE) and root minimum square error (RMSE) have been calculated for each model. In table 2 all the results are summarized.

Concerning to operating speed on curves, the three models developed in this research fit better to the drivers' behavior in the studied roads, presenting less MSE and RMSE than the others.

Tangent models present a lower MSE difference. However, the current operating speed model for tangents includes in its equation the operating speed model for curves. This issue is important in order to develop continuous speed profiles.

Previous deceleration models were calibrated by using speed spot-data. Therefore, rates obtained with those models do not consider the correct speed variation length. Besides, they use a unique length value to calculate decelerations, dealing to non-accurate results. Moreover, most of them calculate the deceleration rate considering the V_{85} variations, instead of the individual speed differences.

These limitations are avoided by considering the individual continuous speed profiles. It implies that the results obtained with this new methodology lead to a more accurate estimations. In fact, the MSE and MRSE obtained with the proposed models are considerably lower.

CONCLUSIONS

This paper presents a new data collection methodology that allows developing continuous speed profiles. By using these data, it is possible to study accurately drivers' behavior and to develop accurate operating speed and deceleration models.

Three operating speed models for curves have been calibrated. Several variables have been studied for this purpose, such as: radius; CCR; curve length; and previous tangent length. After a preliminary ANOVA evaluation, radius and CCR have been chosen as explanatory variables in two alternative models. Another lineal model has been proposed for curve with $R < 400$ m.

In order to obtain the operating speed model expression for curves, a regression analysis has been carried out. However, in the case of tangents, considering drivers' behavior is necessary to establish

previously a model expression. As a result, the proposed model is asymptotical and shows a decreasing speed increment as curve radius increases.

The speed variation on tangent-curve transitions was also studied. To evaluate this phenomenon several variables, such as $\Delta_{85}V$, ΔV_{85}, deceleration length and deceleration length inside the curve, have been studied and two deceleration rate models have been developed.

From the study of the $\Delta_{85}V$ and $\Delta V85$, it can be concluded that the simple subtraction of operating speed underestimates the actual values of speed differential. Its evaluation can be done accurately thanks to the observed individual continuous speed profiles.

From these profiles, the deceleration lengths occurring in the curve have also been studied, refusing the assumption that the deceleration process occurs entirely in the approach tangent.

Finally, two deceleration models have been presented. While the first one depends on the inverse of radius, the second have the CCR of the individual curve as explanatory variable. These models have been calibrated by using the 85^{th} percentile of deceleration, calculated based on individual driver speed profile.

These models have been compared with the models developed by other authors, resulting in a better fit to actual operating speed for the geometric characteristics of the examined roads.

All these results can be achieved by means of the individual continuous speed profiles obtained from data collection. Applying them, it is not difficult to identify maximum and minimum speeds, deceleration points and speed variations. Therefore, this methodology becomes as a promise and powerful tool for driver behavior investigation.

ACKNOWLEDGEMENTS
Authors would like to thank Center for Studies and Experimentation of Public Works (CEDEX) of the Spanish Ministry of Public Works that partially subsidizes the research. Also thank to the Infrastructure and Transportation Department, General Directorate of Public Works, Valencian Government, Spain, Valencian Provincial Council and to the Ministry of the Interior, General Directorate of Traffic, Spain, for their cooperation in field data gathering.

REFERENCES

1. Lamm, R., Psarianos, B. and Mailaender, T. *Highway design and Traffic Safety Engineering Handbook*. McGraw-Hill, New York, 1999.
2. Ottesen, J.L. and Krammes, R.A. Speed profile model for a design consistency evaluation procedure in the United States. In *Transportation Research Record: Journal of the Transportation Research Board,* No. 1701, Transportation Research Board of the National Academies, Washington, D.C., 2000, pp. 76-85.
3. Fitzpatrick, K. and Collins, J. Speed-profile model for two-lane rural highways. In *Transportation Research Record: Journal of the Transportation Research Board*, No. 1737, Transportation Research Board of the National Academies, Washington, D.C., 2000, pp. 42-49.
4. Fitzpatrick, K., Elefteriadou, L., Harwood, D. W., Collins, J. M., McFadden, J., Anderson, I., Krammes, R. A., Irizarry, N., Parma, K. D., Bauer, K. M. and Passetti. K. Speed Prediction for Two-Lane Rural Highways. *Draft Report FHWA-RD-99-171. FHWA*, U.S. Department of Transportation, 1999.
5. Polus, A., Fitzpatrick, K. and Fambro, D. Predicting operating speeds on tangent sections of two-lane rural highways. In *Transportation Research Record: Journal of the Transportation Research Board*, No. 1737, Transportation Research Board of the National Academies, Washington D.C., 2000, pp. 50-57.
6. Collins, K.M. and Krammes, R.A. Preliminary validation of a speed-profile model for design consistency evaluation. In *Transportation Research Record: Journal of the Transportation Research Board*, No. 1523, Transportation Research Board of the National Academies, Washington D.C., 1996, pp. 11 - 21.
7. Gibreel, G. M, Easa, S. M. and El-Dimeery, I.A. Prediction of operating speed on three-dimensional highway alignments. *Journal of Transportation Engineering, ASCE*, Vol. 127, 2001, pp. 21-30.
8. Misaghi, P. y Hassan, Y. Modeling Operating Speed and Speed Differential on Two-Lane Rural Roads. *Journal of Transportation Engineering, ASCE*, Vol. 131, No. 6, 2005, pp. 408-417.
9. Figueroa, A.M. and Tarko, A.P. Speed changes in the vicinity of horizontal curves on two-lane rural roads. *Journal of Transportation Engineering, ASCE*, Vol. 133, No. 4, 2007, pp. 215-222.
10. Bella, F. Assumptions of operating speed-profile models on deceleration and acceleration rates: verification in the driving simulator. *87th Annual Meeting Transportation Research Board*, Washington D.C., 2008.
11. Yang, L. and Hassan, Y. Driver Speed and Acceleration Behavior on Canadian Roads. *87th Annual Meeting of the Transportation Research Board*, Washington, D.C., 2008.
12. Hu, W. and Donnel, E.T. Models of Acceleration and Deceleration Rates on a Complex Two-Lane Rural Highway: Results from a Nighttime Driving Experiment. *87th Annual Meeting of the Transportation Research Board*, Washington, D.C., 2008.
13. Hirsh, M. Probabilistic approach to consistency of highway alignment. *Journal of Transportation Engineering, ASCE*, Vol. 113, No. 3, 1987, pp. 268-276.
14. McFadden, J. and Elefteriadou, L. Evaluating horizontal alignment design consistency of two-lane rural highways: Development of new procedure. In *Transportation Research Record: Journal of the Transportation Research Board*, No. 1737, Transportation Research Board of the National Academies, Washington, D.C., 2000, pp. 9-17.

LIST OF TABLES AND FIGURES

TABLE 1 Summary of Road Segments Characteristics

		ROAD SEGMENT			
		CV-333	CV-370	CV-401	CV-376
Road segment length		5.1 km	8.3 km	6 km	6.7 km
Number of curves		4	21	18	38
Number of tangents		5	21	16	11
Number of tangent-curve sections		4	8	10	6
Lane width		3.35 m	3.13 m – 3.33 m	3.55 m – 4.03 m	3.25 m
Shoulder width		1 m	0 m – 1 m	0 m – 0.4 m	0 m – 0.80 m
Observations*	Forward direction	110	65	87	26
	Backward direction	88	74	86	46

*number of observations after removal of non-free-flow vehicles.

TABLE 2 Models Comparison

OPERATING SPEED MODELS ON CURVES			
MODEL	EQUATION	MSE	RMSE
Lamm et al (1999)	$V_{85} = 95.594 - 1.597 \cdot DC$	341.01	18.47
Fitzpatrick and Collins (2000) Grade -4% ≤ G < 0%	$V_{85} = 105.98 - 3709.90/R$	73.20	8.56
Fitzpatrick and Collins (2000) Grade 0% ≤ G < 4%	$V_{85} = 104.82 - 3574.51/R$	89.98	9.49
Ottesen and Krammes (2000)	$V_{85} = 103.66 - 1.95 \cdot DC$	73.36	8.56
Ottesen and Krammes (2000)	$V_{85} = 102.44 - 1.57 \cdot DC - 0.012 \cdot L_C - 0.01 \cdot DC \cdot L_C$	57.87	7.60
Pérez et al (2010)	$V_{85} = 97.4254 - 3310.94/R$	30.45	5.52
Pérez et al (2010)	$V_{85} = 1/(0.00948323 + 0.0000136809 \cdot CCR)$	15.34	3.92
Pérez et al (2010) R < 400 m	$V_{85} = 102.048 - 3990.26/R$	35.04	5.91
OPERATING SPEED MODELS ON TANGENTS			
Polus et al (2000) G1	$V_{85} = 101.11 - 3420/GM$	87.38	9.34
Polus et al (2000) G2	$V_{85} = 105 - 28.107/e^{0.00108 \cdot GM}$	79.18	8.89
Polus et al (2000) G3	$V_{85} = 97.73 - 0.00067 \cdot GM$	98.08	9.90
Polus et al (2000) G4	$V_{85} = 105 - 22.953/e^{0.00012 \cdot GM}$	84.32	9.18
Pérez el al (2010)	$V_{85} = V_{85C} + (1 - e^{-\lambda L}) \cdot (V_{des} - V_{85c})$	77.52	8.80
DECELERATION MODELS			
Fitzpatrick et al (2000)	$d_{85} = 0.6794 - 295.14/R$	0.35	0.59
Pérez et al (2010)	$d_{85} = 0.263571 + 67.7999/R$	0.0084	0.092
Pérez et al (2010)	$d_{85} = 0.242186 + 0.00150693/CCR$	0.0084	0.091

Where,
DC = degree of curvature (degrees per 100 ft of arc)
L_C = curve length (m)
GM = geometric measure (Polus et al., 2007)

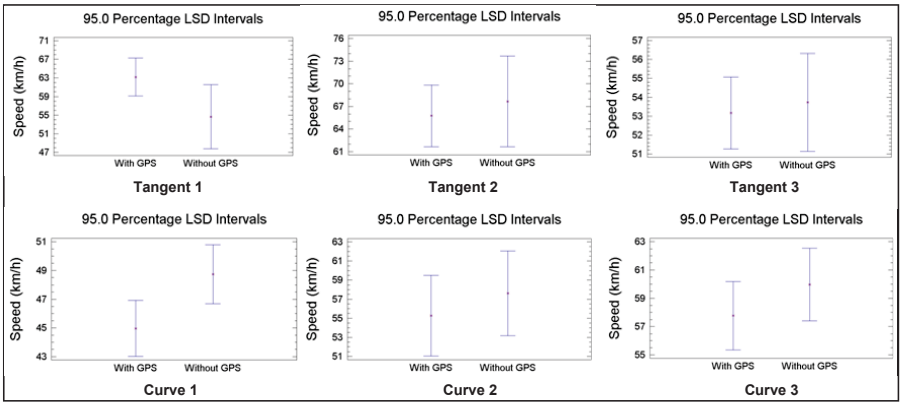

FIGURE 1 LSD Intervals for Methodology Validation.

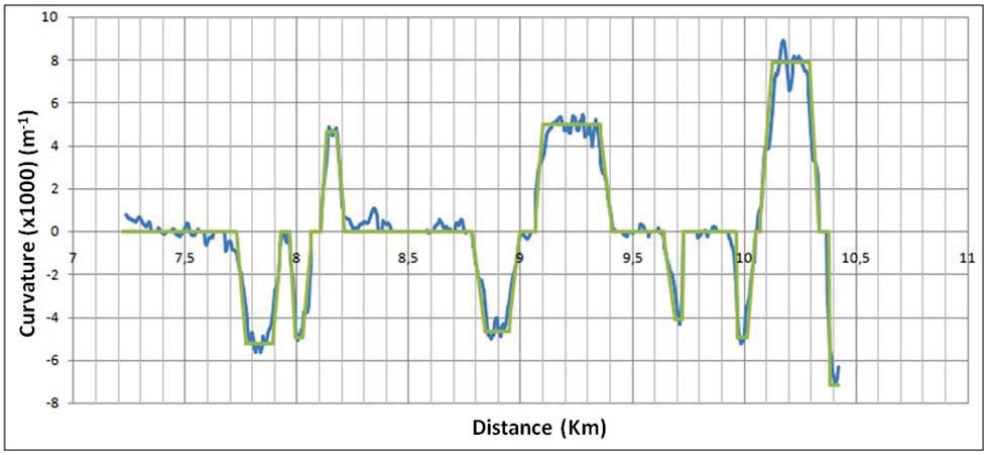

FIGURE 2 Curvature Diagram.

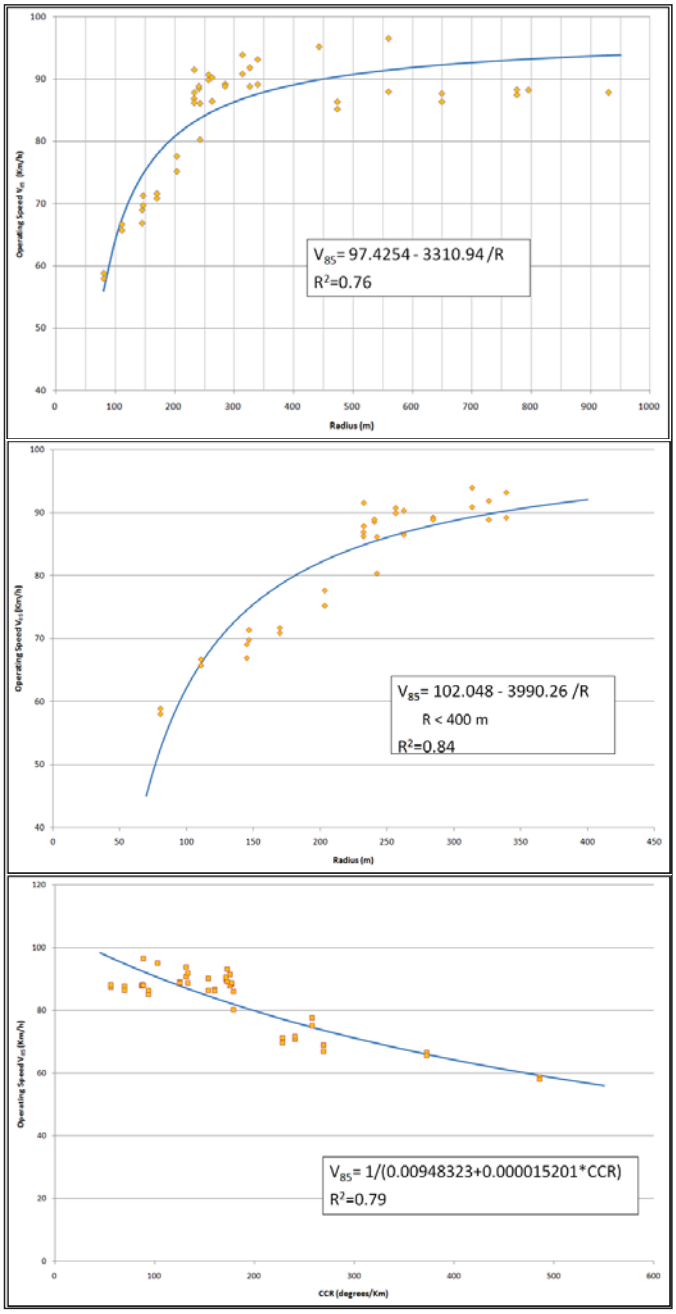

FIGURE 3 Operating speed model for curves.

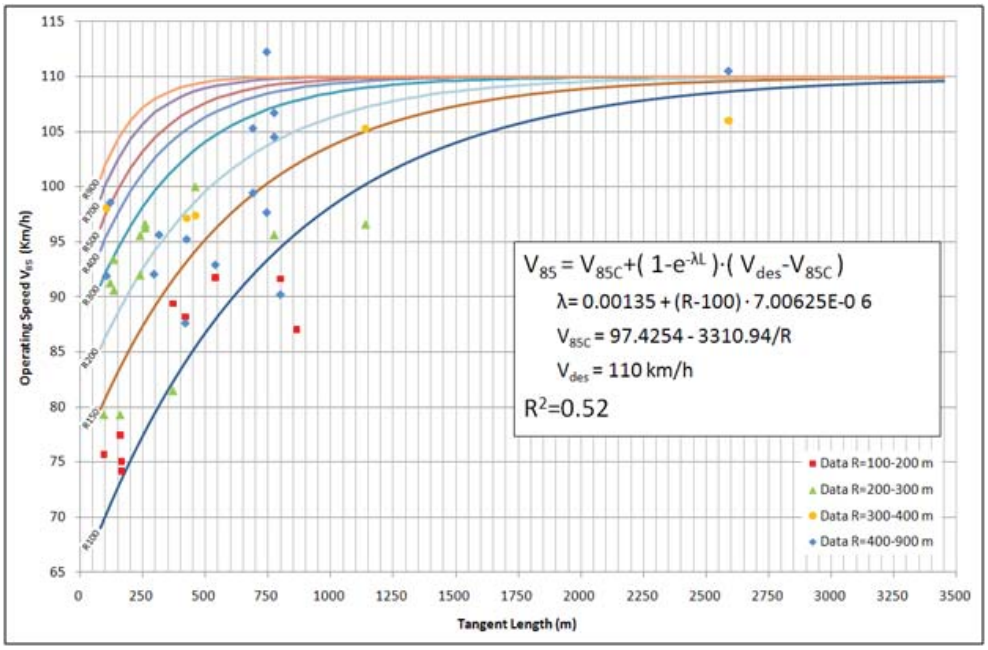

FIGURE 4 Operating speed model for tangents.

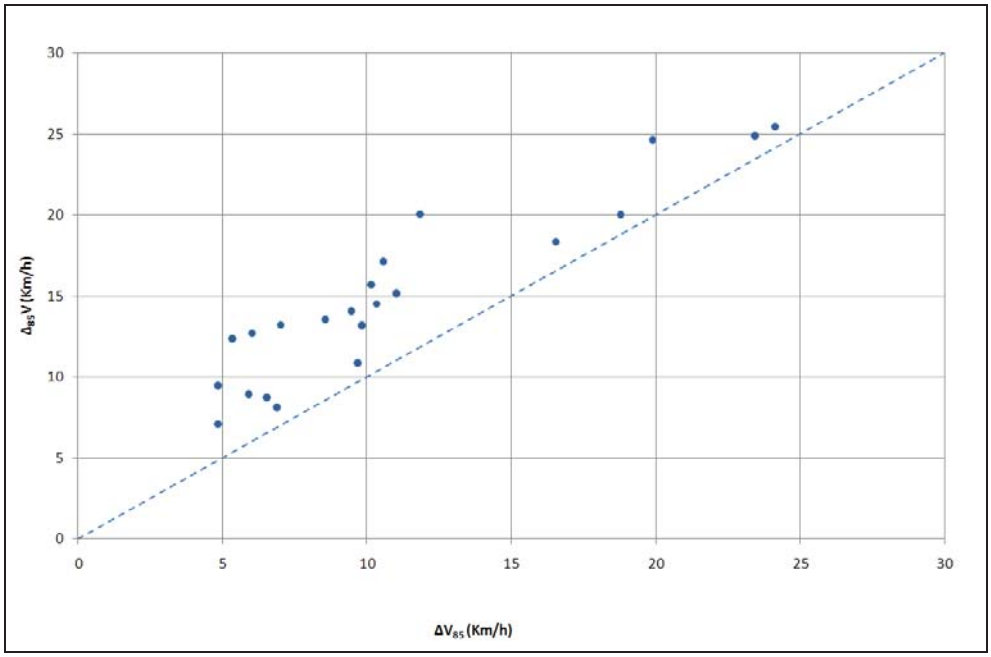

FIGURE 5 $\Delta_{85}V$ vs ΔV_{85}.

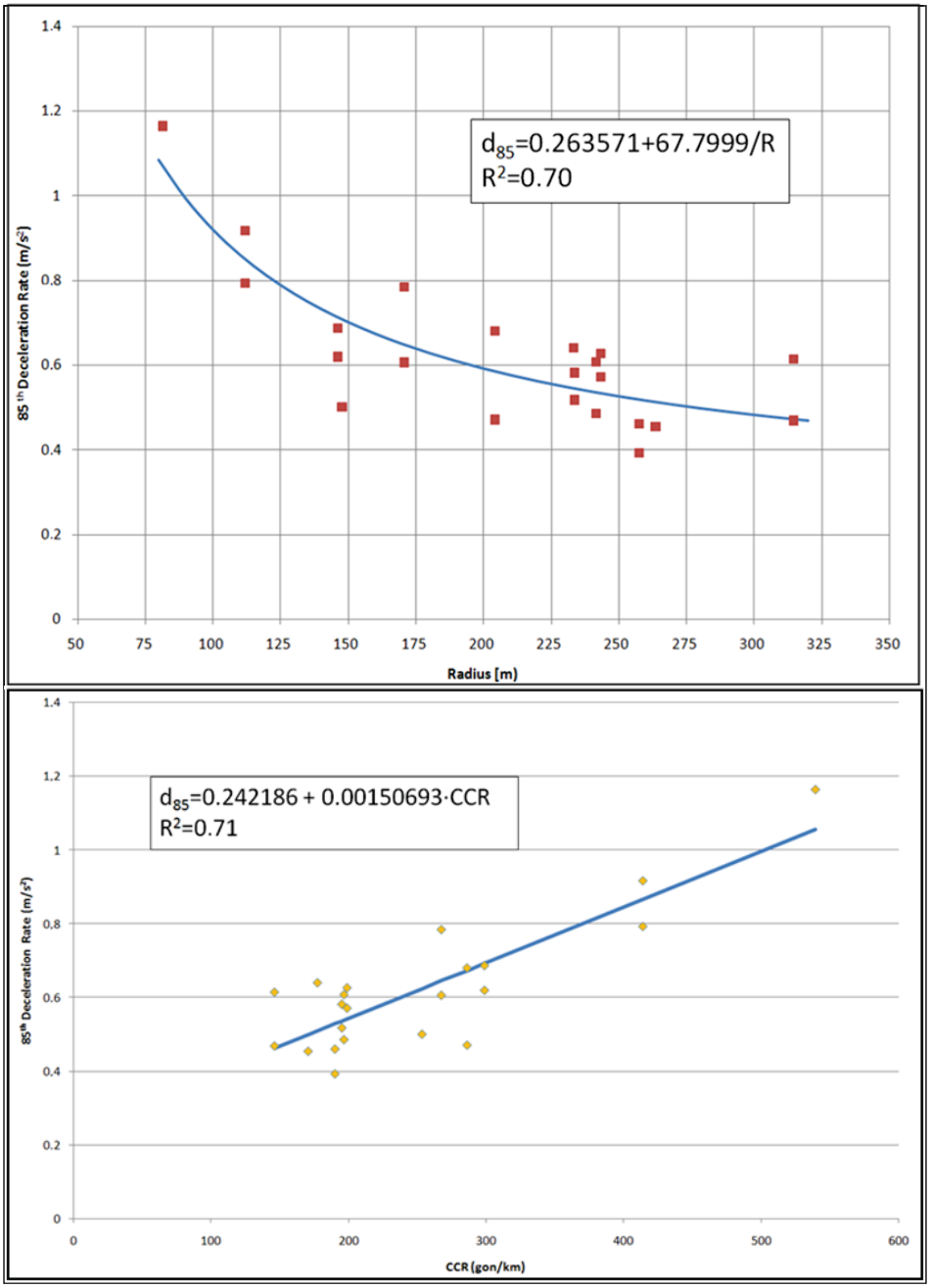

FIGURE 6 Deceleration model.

NEW GEOMETRIC DESIGN CONSISTENCY MODEL BASED ON OPERATING SPEED PROFILES FOR ROAD SAFETY EVALUATION

Francisco Javier Camacho Torregrosa
PhD Candidate, Department of Transportation, Universitat Politècnica de València
Valencia, Spain, email: fracator@tra.upv.es

Ana María Pérez Zuriaga
PhD Candidate, Department of Transportation, Universitat Politècnica de València
Valencia, Spain, email: anpezu@tra.upv.es

Alfredo García García
Professor, Department of Transportation, Universitat Politècnica de València
Valencia, Spain, email: agarciag@tra.upv.es

ABSTRACT

In order to reduce road fatalities as maximum as possible, this paper presents a new methodology to evaluate road safety in both design and redesign stages of two-lane rural highways. This methodology is based on the evaluation of road geometric design consistency, determining one value which will be a surrogate measure of the safety level of a two-lane rural road segment. The consistency model presented in this paper is based on the consideration of continuous operating speed profiles. The models used for their construction have been obtained by using an innovative GPS-data collecting method, based on continuous operating speed profiles recorded from individual drivers. This new methodology allowed the researchers to observe the actual behavior of drivers and to develop more accurate operating speed models than those which are based on spot-speed data collection. That means a more accurate approximation to the real phenomenon, and thus a better consistency measurement.
Operating speed profiles were built for 33 Spanish two-lane rural road segments, and several consistency measurements based on the global and local operating speed were checked. The final consistency model takes into account not only the global dispersion of the operating speed, but also some indexes that consider both local speed decelerations and speeds over posted speeds.
For the development of the consistency model, the crash frequency for all sites was considered, obtaining a model directly related to safety. This allows estimating the number of crashes of a road segment by means of the calculation of its geometric design consistency. Consequently, the present consistency evaluation method becomes an innovative tool that can be used as a surrogate measure to estimate road safety of a road segment even before its construction.

Keywords: road safety, surrogate measures, design consistency, operating speed, crash estimation.

INTRODUCTION

Road crashes are one of the most important problems in our society. Every year 1.2 million of people are killed and between 20 and 50 million people are injured due to road accidents. If current trends continue road traffic injures are predicted to be the third leading contributor to the global burden of disease and injury by 2020. In Spain approximately 60% of rural road accident fatalities occur on two-lane rural roads.

Three factors may have influence on the occurrence of a road accident: human factor, vehicle and road infrastructure. Some studies pointed out that the infrastructure factor is behind over 30% of road crashes (Treat et al., 1979). In fact, previous research has shown that collisions tend to concentrate at certain road segments, indicating that besides driver's error, road characteristics play a major role in collision occurrence. One of the main reasons for accident occurrence can be lack of geometric design consistency. This concept can be defined as how drivers' expectancies and road behavior fit. Thus, a road with a good consistency level is the one in which its behavior and what drivers expect are very similar, so drivers will not be surprised while driving along them. A poor consistency means bad fitting, surprising events and also high speed variability along different road segments and among different drivers, which may increase the likelihood of crash occurrence.

Most of the research and development of design consistency measures focuses on four main areas: operating speed, vehicle stability, alignment indices and driver workload (Ng and Sayed, 2004; Awata and Hassan, 2002).

A simpler approach to evaluate design consistency can be based on the alignment indices (Hassan, 2004), which are quantitative measures of the general character of an alignment in a section of road. Examples of alignment indices include average radius (*AR*), ratio of maximum to minimum radius (*RR*), average rate of vertical curvature (*AVC*) and the *CRR* that is defined as the ratio of radius of a single horizontal curve to the average radius of the entire section. Analyses of collisions on the two-lane rural highways have shown that a significant relationship exists between collision frequency and alignment indices.

Other method to evaluate design consistency is the study of vehicle stability. When insufficient side friction is provided at a horizontal curve, vehicles may skid out, rollover or be involved in head-on accidents. According to this statement, locations that do not guaranty enough vehicle stability can be considered as geometric design inconsistencies.

In this sense, Lamm et al. (1999) presented a design consistency criterion which includes the difference between the assumed side friction of the road and the side friction demanded by the driver. The difference between side friction assumed (f_{RA}, that depends on the design speed) and demanded (f_{RD}, that depends on the operating speed), denoted as Δf_R, was used to represent vehicle stability at Lamm's criterion III. According to this criterion, consistency is considered good when Δf_R is higher than or equal to 0.01, fair when its value is between 0.01 and -0.014, and poor when Δf_R is lower than -0.04.

A third approach for evaluating design consistency is by means of drivers' workload. Driver workload is defined as the time rate at which drivers must perform a given amount of driving tasks that increases with the increase of the complexity in highway geometric features (Gibreel et al., 1999). Driver workload may be a more appealing approach for identifying inconsistencies than operating speed because it represents the effort that the roadway requires

from drivers, while operating speed is only one of the observable outputs of the driving task (Ng and Sayed, 2004). Several methods and approaches have been tried to model driver workload including visual demand (*VD*) and workload rating (Hassan, 2004). However, compared with the other consistency evaluation measures, evaluation of drivers' workload, is much more complex, so it is less used.

The most commonly used criteria to evaluate highway design consistency are based on operating speed evaluation (Gibreel et al., 1999), often defined as the 85th percentile speed (v_{85}) of a sample of vehicles, and obtained by using operating speed prediction models. This specific measure of speed can be used in consistency evaluation by examining disparities between design speed (v_d) and v_{85} or examining the differences in v_{85} between successive elements of the road (Δv_{85}). Tangent-to-curve transitions are the most critical locations when considering safety measures. In fact, it is estimated that more than 50% of the total fatalities on rural highways take place on curved sections (Lamm et al., 1992).

Leisch and Leisch (1977) recommended a revised design speed concept that included guidelines on both operating speed reductions and differentials between design and operating speeds. In the same way, Kanellaidis et al. (1990) suggested that a good design can be achieved when the difference between v_{85} on the tangent and the following curve does not exceed 10 km/h.

However, the most commonly used method to evaluate road consistency was developed by Lamm et al. (1999) based on mean accident rates. They presented two design consistency criteria related to operating speed, which include the difference between design and operating speed and the difference between operating speeds on successive elements.

The difference between operating speed and design speed $|v_{85} - v_d|$ is a good indicator of the inconsistency at one single element, while the speed reduction between two successive elements (Δv_{85}) indicates the inconsistency experienced by drivers when traveling from one element to the next one. On Table 1, consistency thresholds for Criteria I and II are summarized.

Table 1 Thresholds for a determination of design consistency quality. Lamm's criteria I & II.

Consistency rating	Criterion I (km/h)	Criterion II (km/h)
Good	$\lvert v_{85} - v_d \rvert \leq 10$	$\lvert v_{85_i} - v_{85_{i+1}} \rvert \leq 10$
Fair	$10 < \lvert v_{85} - v_d \rvert \leq 20$	$10 < \lvert v_{85_i} - v_{85_{i+1}} \rvert \leq 20$
Poor	$\lvert v_{85} - v_d \rvert > 20$	$\lvert v_{85_i} - v_{85_{i+1}} \rvert > 20$

Although most consistency criteria give thresholds for good, fair and poor design consistency, other authors (Hassan, 2004) suggest continuous functions as a better tool for designers.

The consistency criteria previously presented allow evaluating the design consistency and estimating road safety only in a road element (the horizontal curve). Other studies, such as the one carried out by Polus and Mattar-Habib (2004), used continuous speed profiles to determine the global speed variation along a road segment, and determining a single consistency value for the whole road segment. Moreover, their design consistency index is a continuous function instead of being based on ranges.

They developed two new consistency measures. The first was the relative area bounded between the operating speed profile and the line of average weighted speed by length (*Ra*).

The second was the standard deviation of operating speed in each design element along the whole section investigated (σ). It was necessary to use this additional measure to complement the first measure because the *Ra* measure by itself provided similar results for somewhat different geometric characteristics in a few cases.

Based on the two independent measures, a consistency model was developed; and thresholds for good, acceptable, and poor design consistency of any section were proposed (Table 2). The *Ra* and σ on several test sections provided a similar assessment of consistency as Lamm's measures.

Table 2 Thresholds for a determination of design consistency quality.

Design consistency quality $C = e^{-0.278 \cdot [Ra \cdot (\sigma/3.6)]}$		
Good	**Acceptable**	**Poor**
$\boldsymbol{C > 2\ (m/s)}$	$1 < C \leq 2\ (m/s)$	$C \leq 1\ (m/s)$

The geographic environment at which consistency variables and their relationships to crash rates are obtained is also important. Extrapolation must be carried out carefully. For example, further test for the applicability of Lamm's criteria revealed that a 20 km/h limit for poor design is applicable to Korea (Lee et al., 2000), but a different limit was recommended for Italy (Cafiso, 2000).

Several research have studied the effect of geometric design consistency on road safety. Anderson et al. (1999) have investigated the relationship between design consistency and safety using loglinear regression models. Two models have been developed that relate accident frequency to traffic volume, curve length, and speed reduction (Δv_{85}). A separate model has been developed that relates accident frequency to curve length and *CRR*.

Ng and Sayed (2004) investigated the effects of several design consistency measures on safety and developed models that incorporate the measures to quantify their effects on safety. The design consistency measures mentioned were $v_{85} - v_d$, Δv_{85}, Δf_R, *CRR* and visual demand.

Finally, it is worthy highlighting the study carried out by Cafiso et al. (2007). They presented a methodological approach for the safety evaluation of two-lane rural highway segments that uses both analytical procedures referring to alignment design consistency models and safety inspection processes.

They developed a safety index (SI) that quantitatively measures the relative safety performance of a road segment. The SI is formulated by combining three components of risk: the exposure of road users to road hazards, the probability of a vehicle being involved in an accident and the resulting consequences should an accident occur.

To test the procedure, comparisons were carried out between SI scores and EB (Empirical Bayes) safety estimates. The results showed that ranking of segments gives comparable results in terms of SI or accident frequency.

Different studies show that improving design consistency leads to safer roads. The present paper shows a new geometric design consistency model based on continuous operating speed profiles. Its relationship to safety is also obtained, so it can be used as a surrogate measure for road safety evaluation.

OBJECTIVES

The objective of this study is to develop a design consistency model that may be used as a surrogate measure for road safety evaluation for two-lane rural roads. Several measures will be obtained based on operating speed profiles, with the aim of obtaining a single consistency value for the whole road segment instead of focusing only on individual or consecutive road geometric elements.

The design consistency parameter will be based on continuous operating speed models, developed in previous research through an innovative technique that uses GPS devices for monitoring actual drivers. Thus, operating speed profiles are more accurate, reflecting better the actual behavior of drivers.

The crash frequency will also be considered in the development of the model. Consequently, a relationship between consistency and crash rate will be obtained, being an important tool to assist engineers to design safer roads.

DATA COLLECTION

The consistency measure that will be developed in this research is based on the analysis of the operating speed profiles of two-lane rural road segments. For its calibration, some speed profile surrogate measures will be compared to crash data, in order to obtain a consistency model useful for designing safer roads. Thus, three main databases are necessary for this research: geometry characteristics, traffic volume and crash data. Those data were obtained for 65 two-lane rural road segments of the Valencian Community (Spain), so a high volume of data has been analyzed for the development of this investigation.

Data description: road segments characteristics, traffic volume, crash data

The purpose of the geometry data is, by means of some models, to develop their operating speed profiles. 65 road segments of the Valencian Community (Spain) were chosen, presenting a length between 2 and 5 km, longitudinal grades lower than 5% and without important intersections.

The availability of traffic volume data for those road segments is public, so it was downloaded from the official website. The database consisted on all crash data during last 15 years for all road segments. Having this large database is important for research, but it also has to be handled with care, because of possible changes at conditions or road geometry of some segments during this long period of time. In order to prevent this problem, traffic volume values were examined in order to determine irregular variations of the *AADT* through years; and also was the history for all road segments, checking for redesigns. Depending on each particular case, some specific years or road segments were no longer considered in the analysis.

Accident data was provided by the local Administration. It consisted on a list of all accidents reported on those roads during last 13 years. Accidents are characterized by location, day and hour, daylight conditions, severity, vehicle type, driver characteristics, external factors, causes and other conditions. Considering all data, a filtering process was done, deleting accidents that presented at least one of the following issues:

- Crashes that took place during the years that are not considered in the traffic volume data.
- Property Damage Only (PDO) accidents. In Spain, some of these accidents are reported and some are not, so the crash database does not show the accidents occurred, but the accidents reported. In order to not add external variation on crash data, there were only considered accidents with victims (they are always reported).
- The causes for all accidents were examined, taking out from the analysis those related to external factors (e.g. due to previous illness of the driver, or animals crossing the road), or minor intersections (because the consistency model does not consider this factor).

Operating speed models

The operating speed profiles were developed by means of two types of operating speed models: one for horizontal curves and other for tangents, and some construction keys. For developing the final operating speed profile, acceleration and deceleration rates are also calculated depending on geometric features. These models have been obtained and calibrated on previous research (Pérez et al., 2010) by using continuous operating speed profiles. Those profiles were obtained by means of GPS devices from individual drivers. The drivers used for calibration are actual drivers of the road, using their individual vehicles. Road characteristics and geographic region are similar than those used for calibration.

The main advantages of these operating speed models is that they are not based on speed-spot data collection, but calibrated based on continuous data. Thus, they reflect better the behavior of actual drivers.

The operating speed model for curves was developed by Pérez et al. (2010) and uses radius as the explanatory variable.

In that research, a big change in driver behavior was appreciated when radius of curves was higher or lower than 400 m. Thus, two models were developed: one for all curves and other for curves with radius lower than 400 m. Also, for curves with a radius lower than 70 m, the specific model underestimates the actual operating speed, so it needs to be replaced by the speed calculated by the side-friction expression. In this research, only a few number of curves had to consider this other model.

$$v_{85} = 97.4254 - \frac{3310.94}{R} \qquad 400\ \text{m} < R \leq 950\ \text{m} \tag{1}$$

$$v_{85} = 102.048 - \frac{3990.26}{R} \qquad 70\ \text{m} < R \leq 400\ \text{m} \tag{2}$$

$$v_{85}^2 = 127 \cdot R \cdot \left(f_t + \frac{e}{100}\right) \qquad R \leq 70\ \text{m} \tag{3}$$

where:
v_{85}: operating speed on curve (km/h)

R: radius (m)
f_t: side friction
e: superelevation rate (%)

An operating speed model for tangents was also developed, considering the length of the tangent and the speed of the previous curve. It was noticed that all drivers tended to reach a desired speed, which was set to 110 km/h. However, depending on the length of the tangent they could accelerate more or less departing from the operating speed of the previous curve. Thus, the higher the length of the tangent, the closer its operating speed will be to the desired speed.

$$v_{85T} = v_{85C} + \left(1 - e^{-\lambda \cdot L}\right) \cdot (v_{des} - v_{85C}) \quad (4)$$

where:
$\lambda = 0.00135 + (R - 100) \cdot 7.00625 \cdot 10^{-6}$
v_{85C}: operating speed on previous curve (km/h)
v_{85T}: operating speed on tangent (km/h)
v_{des}: desired speed (110 km/h)
R: horizontal curve radius (m)
L: length of the tangent (m)

The difference of this model compared to previous models is that the individual reached speed for each driver is accurately determined, regardless of the location where it was reached, based on the examination of their individual speed profiles. Previous models were based on spot-speed location methods, without considering whether the speed recorded for each driver was the maximum speed at the tangent or was not.

In order to plot the operating speed profile, acceleration and deceleration rates were obtained. Deceleration rates were obtained by Pérez et al. (2011), while acceleration rates being obtained for this research using the same methodology. Both of them are based on the radius of the curve. It is an important improvement compared to other operating speed profile models, since it depends on the curve radius, instead of using constant acceleration or deceleration rates.

$$d_{85} = 0.313 + \frac{114.436}{R} \quad (5)$$

$$a_{85} = 0.41706 + \frac{65.93588}{R} \quad (6)$$

where:
d_{85}: deceleration rate (m/s^2)
a_{85}: acceleration rate (m/s^2)
R: radius (m)

These deceleration and acceleration rates have been obtained by considering each driver individually, selecting the specific points at which each driver starts and ends speed variations, instead of considering the same speed transition length for all drivers. Thus, the acceleration and deceleration rates reflect better drivers' behavior. In this operating speed profile model, the 85th percentile of acceleration and deceleration rates are used.

Operating speed profiles construction

Considering the previous models, a computer program was developed in order to calculate the operating speed profile for each road segment, both in forward and backward directions. It is done in two steps: determination of the horizontal alignment for each road segment, and calculation of the operating speed profiles based on the previous models.

As previously mentioned, the geometry was not directly available for all road segments. We only had the GPS coordinates of all road segments. The calculation of the horizontal alignment is based on the determination of the curvature diagram for each road segment. This calculation is based on two steps:

- The first one takes the succession of points of the axis and calculates the local curvature. In this calculation, not only three points are considered, the process is much more accurate. The result is an unprocessed curvature diagram, which allows to know the general behavior of the road, but still not composed by tangents, circular and spiral curves.
- The second step takes the previous curvature diagram and transforms it into a final diagram, composed by straight lines that represent the succession of tangents, spiral and circular curves that compose the horizontal alignment.

After processing all road segments, some of them were found to show errors in their coordinates, so they were removed from the analysis, establishing the number of road segments at this point in 43.

Once the horizontal alignment is determined for all road segments, their operating speed profiles can be determined. The same computer program performed the calculations, in two steps:

- Calculation and graphical representation of the operating speed for constant curvature elements (circular curves and tangents). It is based on the previous models.
- Development of the operating speed profile. Based on the acceleration and deceleration expressions and construction rules.

It is necessary to point out that each road segment presents two operating speed profiles: one for each direction of travel.

CONSISTENCY MODELS

For developing the design consistency parameter, the following process was carried out: in first place, crash rates were estimated for each road segment. Also, all operating speed profiles were determined, and by means of them, several variables were calculated. After this calculation, correlations among all variables were examined, and five of them were selected for calibrating the consistency model.

The consistency model was calibrated by means of examining its relationship to safety, selecting one model that could be easily used for designing the road and it was related to safety.

Number of accidents

For almost all road segments, accident data was available for 13 years. In order to improve the accuracy of the model, a Safety Performance Function for estimating the number of accidents in 10 years was developed. For its calibration, a logistic, negative binomial regression was carried out, considering exposure units (length and *AADT*) and an alignment index (Table 3).

Several Four alignment indices were obtained based on the developed geometry for all road segments: Average Radius (AR), Curvature Change Ratio (CCR), Ratio between maximum and minimum radius of the road segment (RR), and ratio between the minimum radius and the average radius of the road segment (Rmin/AR). Different regressions were made considering the exposure and each one of the alignment indices. Finally, only the last one had a significant effect over safety, so it was included in the final form of the Safety Performance Function.

$$Y_{i,10} = e^{-4.9462} \cdot L^{0.8645} \cdot \overline{AADT}^{0.7683} \cdot e^{-0.7285 \cdot \frac{R_{\min}}{AR}} \quad (7)$$

Where:
$Y_{i,10}$: Estimated number of crashes in 10 years for the road segment.
L: Length of the road segment (km).
$\overline{AADT}$: mean value of Average Annual Daily Traffic for 10 years (veh/day).
$R_{\min}$: Minimum radius of the road segment (m).
AR: Average Radius of the road segment (m).

Table 3 Negative binomial model of accident frequency

Independent Variable	Coefficient	t-statistics
Intercept	-4.9462	<.0001
Log of the length **of road segment (km)**	0.8645	0.0021
Log of $\overline{AADT}$ per lane	0.7683	<.0001
R_{min}/AR	-0.7285	0.0842
Overdispersion	0.1519	
Number of sections	43	
Log Likelihood at zero	167.8662	
Log Likelihood at convergence	-94.5553	
Pearson χ^2	38.9802	
AIC	199.1107	

Considering the expected number of accidents by the SPF and the occurred number of accidents, the Empirical Bayes method was used to estimate the final number of accidents expected for each site. With them, crash rates (accidents with victims by 10^6 veh-km) were

obtained for each road segment. The overdispersion parameter of the Safety Performance Function is $\mu = 0.1519$. Then, $k = 1/\mu = 6.5832$.

Finally, the Empirical Bayes Method calculates the estimated number of accidents:

$$E(\lambda/r) = \alpha \cdot \lambda + (1 - \alpha) \cdot r \quad (8)$$

where:
$\alpha = \frac{1}{1+\frac{\lambda}{k}}$
λ: number of accidents estimated by the Safety Performance Function
r: number of observed crashes for the specific site

Correlation among variables

The operating speed profiles were developed in both directions for all road segments considered. By means of them, some measures of the speed dispersion and deceleration were obtained and processed. The speed limits for all road segments were also examined, and some variables considering the speed dispersion and the speed limit were checked. The total amount of examined variables was 14.

Considering the operating speed profiles, the average operating speed ($\bar{v}_{85}$) and the standard deviation of the operating speed (σ_{85}) are directly obtained. The first one is obtained in order to be an indicator of the road segment, while the second one is for determining the global dispersion of the operating speed. The higher the dispersion is, the more inconsistent the road segment is expected to be.

Considering the operating speed profile, the average speed and posted speed, some other measures were tried:

- R_a (m/s). First introduced by Polus and Mattar-Habib (2004), it measures the sum of the area between the operating speed profile and the average speed of each road segment, divided by its length. Thus, it measures the global variability of the speed, presenting higher values as the speed variability increases.
- $E_{a,10}$ (m/s). It is also a measurement of the speed dispersion. As the previous measure, it is the sum of the areas between the operating speed profile and the average operating speed profile plus and minus 10 km/h. Finally, it is divided by its length.
- $E_{a,20}$ (m/s). As the previous index, but considering 20 km/h.
- L_{10}. Rate (in %) between the total length of the road segment at which the absolute difference between the operating speed and the average operating speed is more than 10 km/h and the length of the road segment.
- L_{20}. As the previous variable, but using 20 km/h.

By means of the operating speed profiles, it is also easy to determine all the speed decrement transitions. They were detected for all road segments, calculating the speed differential (km/h) in absolute value (Δv_{85}), and the distance (m) used for each speed transition ($L_{\Delta v_{85}}$). After that, all decelerations lower than 1 km/h were not considered, because their low value might not be perceived by users. After that, some road segments presented a very low number of decelerations. In order to not influence further calculations, those road segments were also taken out from the analysis, because they behaved in a very different way than others. Thus,

the final number of road segments was 33. Table 4 shows the main characteristics of alignment, traffic volume and crash data for each road segment.

Table 4 Characteristics of the road segments used on consistency model

Road Segment	Length (km)	Mean *AADT* (veh/day)	Observed crashes in 10 years
1	3.42	824	2
2	2.105	802	3
3	1.805	908	1
4	2.42	4546	5
5	2.565	2511	3
6	3.205	2511	3
7	4.84	985	6
8	2.24	918	1
9	2.31	403	1
10	4.035	2895	9
11	2.53	486	2
12	2.285	486	0
13	3.895	486	2
14	4.13	2750	6
15	1.41	425	2
16	3.925	1216	2
17	1.695	272	0
18	3.365	3292	8
19	3.04	2958	5
20	2.595	4550	3
21	4.675	1215	3
22	2.145	2522	8
23	3.825	3108	23
24	1.88	789	3
25	4.415	513	4
26	2.325	2231	3
27	1.865	577	1
28	1.42	577	1
29	1.805	7442	2
30	2.495	8252	22
31	1.32	6553	1
32	3.89	209	3
33	1.72	922	3

Considering all deceleration processes for each road segment in both directions, the following variables were obtained:

- Average speed reduction ($\overline{\Delta v_{85}}$). Average value of all speed reduction processes in each road segment. The higher this variable is, the more dramatic the speed reductions in the road segment will be, so the road segment will be more inconsistent.

- Standard deviation of the speed reductions ($\sigma_{\Delta v_{85}}$). It measures the standard deviation of the speed reduction value for each road segment. It is supposed that the higher the standard deviation is, the more disperse the drivers' behavior will be, so the road segment is more inconsistent.
- Deceleration average distance ($\bar{L}_{\Delta v_{85}}$). Average value of the distances used for deceleration in a road segment. Due to acceleration and deceleration rates are obtained from geometry relationships, similar speed differentials could be achieved by means of different distances. Thus, this measure could add more variability to the average deceleration value in its relationship to crash rates.
- Speed reduction intensity ($\bar{d}_{\Delta v_{85}}$). For all individual speed reduction processes, their magnitude were divided by the length used, determining the individual speed reduction intensity (km/h/m). This value represents the average value for each road segment.
- Deceleration length rate of each road segment (L_d). It is an index of the distance at which the road segment's speed profile is under deceleration conditions. It is obtained by adding the individual deceleration lengths on a road segment and dividing it into its total length.

All previous values are determined by considering the operating speed profile by itself for each road segment. Also considering the speed limits, two new variables were determined:

- Difference between the average operating speed and the speed limit (Δv_{85-l}). This value of speed limit has been calculated as the average of posted speed limits weighted by length. The difference has not been calculated in absolute value. It is intended to be an auxiliary variable for helping other variables to add correlation to the final model. For this consideration, the global speed limit has been selected for each road segment.
- $E_{a,l}$ (m/s). As $E_{a,10}$ and $E_{a,20}$, this variable is the sum of the areas between the operating speed and the speed limit for the road segment. Finally, it is divided by its length.

Some variables are correlated among them, showing some interesting relationships. The average speed reduction and its standard deviation are highly correlated: higher speed reduction values are combined with higher variability.

In Figure 1, the average standard deviation of all road segments are plotted against their average value. In that figure the values have been distinguished by different color taking into account their estimated crash rates. Those values have been obtained by dividing the total number of estimated accidents in each individual road segment by its total exposure (calculated from its length and its traffic volume for ten years).

R_a also presents a high correlation with the average operating speed. On road segments composed by sharp curves and short tangents, drivers are constrained by the road geometry and they cannot develop their desired speed, usually leading to low operating speeds and deviations. Thus, the R_a variable, which measures the speed variability, is low. At road segments where the geometry does not constraint drivers as in the previous segments, operating speeds are higher, resulting into lower speed variability and thus, into lower R_a values. So, the maximum values of R_a are reached with medium operating speeds. A graphical representation is shown on Figure 2.

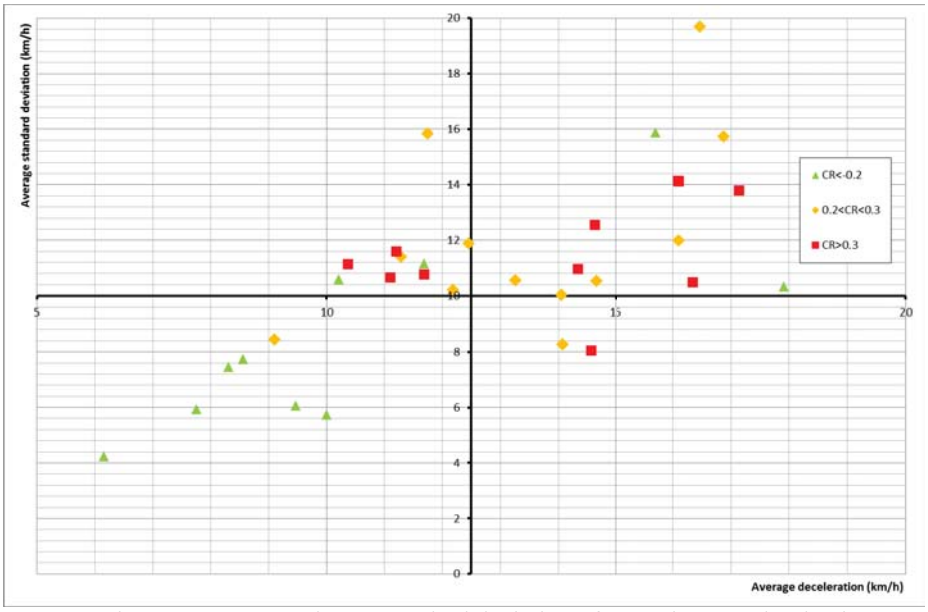

Figure 1 Average value vs standard deviation of operating speed reductions

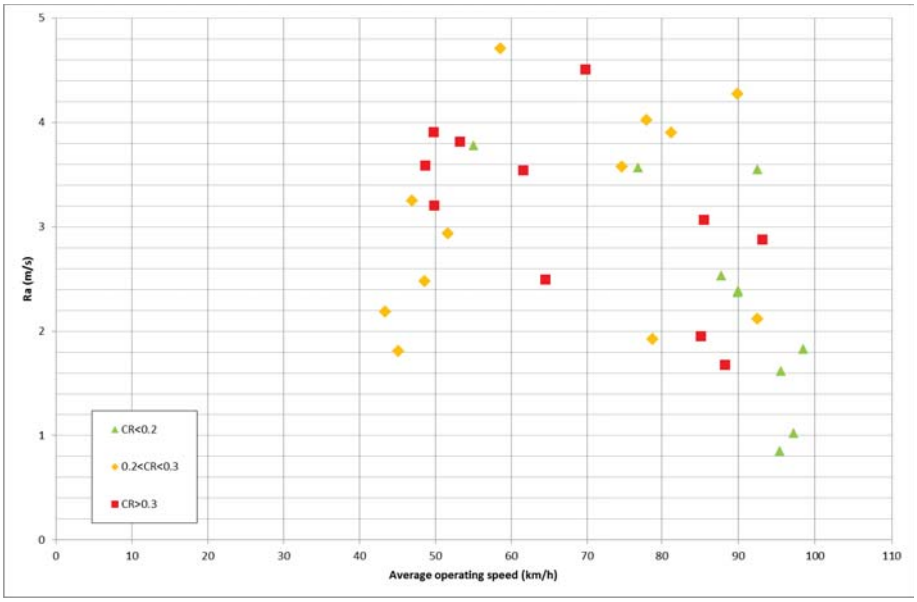

Figure 2 R_a vs average operating speed

Considering all 14 variables, an analysis of correlation was carried out in order to determine the final variables to consider in the model. The correlation matrix is shown on Table 5. High correlations are highlighted in dark grey, while medium correlations are in light grey.

Table 5 Correlation among independent variables

	$\bar{v}_{85}$	σ_{85}	R_a	L_{10}	L_{20}	$E_{a,10}$	$E_{a,20}$	$\overline{\Delta v_{85}}$	$\sigma_{\Delta v_{85}}$	$\bar{L}_{\Delta v_{85}}$	L_d	$\bar{d}_{\Delta v_{85}}$	Δv_{85-l}	$E_{a,l}$
$\bar{v}_{85}$		-0.391	-0.380	-0.377	-0.305	-0.338	-0.258	-0.372	-0.445	0.902	0.381	-0.975	0.691	0.453
σ_{85}	-0.391		0.992	0.942	0.955	0.980	0.839	0.645	0.765	-0.400	-0.201	0.447	-0.067	0.212
R_a	-0.380	0.992		0.955	0.953	0.970	0.806	0.615	0.746	-0.396	-0.166	0.437	-0.048	0.228
L_{10}	-0.377	0.942	0.955		0.869	0.89	0.636	0.593	0.627	-0.372	-0.207	0.415	-0.031	0.266
L_{20}	-0.305	0.955	0.953	0.869		0.977	0.871	0.595	0.734	-0.334	-0.045	0.369	0.004	0.247
$E_{a,10}$	-0.338	0.980	0.970	0.890	0.977		0.902	0.594	0.767	-0.377	-0.134	0.409	0.001	0.263
$E_{a,20}$	-0.258	0.839	0.806	0.636	0.871	0.902		0.538	0.741	-0.283	-0.090	0.356	0.003	0.174
$\overline{\Delta v_{85}}$	-0.372	0.645	0.615	0.593	0.595	0.594	0.538		0.673	-0.102	-0.157	0.402	-0.230	-0.150
$\sigma_{\Delta v_{85}}$	-0.445	0.765	0.746	0.627	0.734	0.767	0.741	0.673		-0.438	-0.190	0.459	-0.172	0.010
$\bar{L}_{\Delta v_{85}}$	0.902	-0.400	-0.396	-0.372	-0.334	-0.377	-0.283	-0.102	-0.438		0.353	-0.862	0.555	0.285
L_d	0.381	-0.201	-0.166	-0.207	-0.045	-0.134	-0.090	-0.157	-0.190	0.353		-0.419	0.207	-0.023
$\bar{d}_{\Delta v_{85}}$	-0.975	0.447	0.437	0.415	0.369	0.409	0.356	0.402	0.459	-0.862	-0.419		-0.634	-0.378
Δv_{85-l}	0.691	-0.067	-0.048	-0.031	0.004	0.001	0.003	-0.230	-0.172	0.555	0.207	-0.634		0.874
$E_{a,l}$	0.453	0.21	0.228	0.266	0.247	0.263	0.174	-0.150	0.010	0.285	-0.023	-0.378	0.874	

As can be seen in the correlation matrix, the following correlations are found:

- σ_{85}, R_a, L_{10}, L_{20}, $E_{a,10}$, $E_{a,20}$ and $\sigma_{\Delta v_{85}}$ present high correlation values. Considering that R_a was previously used by Polus and Mattar-Habib (2004), it was recommended for consideration in the following stages of the analysis.
- $\bar{L}_{\Delta v_{85}}$, $\bar{d}_{\Delta v_{85}}$ and $\bar{v}_{85}$. They present high correlation values, so only the operating speed average value is considered for further analysis.
- $\overline{\Delta v_{85}}$. It is medium-correlated with other variables, represented all of them by R_a in the models. As the correlation is medium, it is suggested to be maintained for further research.
- L_d. This variable is not correlated to any other variable.
- Those variables, under the influence of limit speeds, are correlated between them, and also a medium correlation is found with the average operating speed. Then, $E_{a,l}$ is suggested for consideration in the further research.

So, the variables that will be chosen for the next step are the following:

- R_a
- Average operating speed ($\bar{v}_{85}$)
- Percentage of road segment under deceleration conditions (L_d).
- Average speed reduction ($\overline{\Delta v_{85}}$).
- $E_{a,l}$

It is important to point out that the Global Consistency Model developed by Polus and Mattar-Habib (2004) consists on a combination of R_a and σ, variables which have been demonstrated here to have a high correlation. Then, it is suggested to use only one of them and combine with another variable, probably obtaining higher statistical significance.

Relationship to safety

Considering the previous variables, several models were checked in order to analyze the relationship between the Estimated Crash Rate (*ECR*) and all variables separately. Those models are shown on Table 6.

Table 6 Calibrated models for *ECR* by individual variable

Variable	Model	R^2
R_a	$ECR = \frac{1}{2.22562 + \frac{5.46248}{R_a}}$	30.9%
	$ECR = e^{-1.00383} \cdot e^{-\frac{0.988661}{R_a}}$	24.9%
	$ECR = e^{-1.89911} \cdot R_a^{0.497538}$	24.4%
$\bar{v}_{85}$	$ECR = \frac{1}{2.00006 + 0.000429405 \cdot \bar{v}_{85}^2}$	31.7%
	$ECR = e^{-0.915549} \cdot e^{-0.0000860305 \cdot \bar{v}_{85}^2}$	31.3%
	$ECR = e^{1.81969} \cdot \bar{v}_{85}^{-0.75763}$	25.8%
L_d	$ECR = \frac{1}{3.16716 + 27.9187 \cdot L_d^2}$	10.6%
	$ECR = e^{-1.23859} \cdot e^{-3.65402 \cdot L_d^2}$	4.5%
	$ECR = e^{-1.70654} \cdot L_d^{-0.186688}$	1.5%
$\overline{\Delta v_{85}}$	$ECR = \frac{1}{0.524925 + \frac{46.9038}{\overline{\Delta v_{85}}}}$	30.9%
	$ECR = e^{-0.675934} \cdot e^{-8.72905 \cdot \overline{\Delta v_{85}}}$	26.3%
	$ECR = e^{0.407621} \cdot \overline{\Delta v_{85}}^{-4.51153}$	25.9%
$E_{a,l}$	$ECR = 0.292265 - 0.0196406 \cdot E_{a,l}$	5.7%
	$ECR = e^{-1.31034} \cdot e^{-0.0692368 \cdot E_{a,l}}$	4.7%
	$ECR = e^{-1.42202} \cdot E_{a,l}^{0.0448093}$	2.7%

As can be seen on Table 6 variables with better fitting to Crash Rate are R_a, $\bar{v}_{85}$ and $\overline{\Delta v_{85}}$. The other variables had a very low correlation coefficient, so they did not fit to Crash Rate and they were only used for trying to improve the final model.

Considering only the best variables, additional models were checked, always combining them into a single index. Those models are presented on Table 7.

Table 7 Final calibrated models for ECR

Model number	Expression	R^2
1	$ECR = \frac{1}{2.65897 + \frac{0.0570069}{\frac{R_a}{\bar{v}_{85}}}}$	39.8%
2	$ECR = \frac{1}{3.00826 + \frac{0.00056031}{\frac{R_a}{\bar{v}_{85}^2}}}$	42.3%
3	$ECR = e^{0.00516932} \cdot \left(\frac{R_a}{\bar{v}_{85}}\right)^{0.431919}$	35.8%
4	$ECR = \frac{1}{3.18601 + \frac{33.4686}{R_a \cdot \bar{v}_{85}}}$	32.8%
5	$ECR = \frac{1}{3.11287 + 0.0273507 \cdot \left(\frac{\bar{v}_{85}}{\Delta v_{85}}\right)^2}$	45.7%
6	$ECR = e^{-0.866762} \cdot e^{-0.085472 \cdot \frac{\bar{v}_{85}}{\Delta v_{85}}}$	40.1%
7	$ECR = \frac{1}{3.36708 + 0.0000029176 \cdot \left(\frac{\bar{v}_{85}^2}{\Delta v_{85}}\right)^2}$	48.2%
8	$ECR = \frac{1}{2.40939 + 0.00403287 \cdot \left(\frac{\bar{v}_{85}^2}{\Delta v_{85}}\right)}$	46.3%

The strongest correlation to the crash rate is given by the division of the squared average operating speed and the average speed reduction value. Once the main expression was obtained, several attempts were made to add any of the two variables that were taken out from this analysis, but no good results were obtained.

Thus, the proposed design consistency index is the following:

$$C = \frac{\bar{v}_{85}^2}{\overline{\Delta v_{85}}} \quad (9)$$

Both speeds are in km/h, so the final index is also in km/h.

Analyzing its composition, road segments with lower average speed reduction value will lead to higher consistency values, due to the more uniform speed. Higher operating speed average values are associated to better, more consistent roads.

It is worth to highlight that this model considers both the average speed and its variability. As a difference to other consistency indices, the model only considers decelerations in its determination, instead of both acceleration and decelerations, represented in the standard deviation of the operating speed.

Estimation of Crash Rates

After determining the composition of the consistency model, it is turn to determine its relationship to safety. Since the consistency model has been fitted according to the crash rates, the expressions are already obtained (models 7 and 8). As can be seen in Table 6, the model 7 has a bit more correlation to data than model 8, but for low-consistent road segments model 8 behaves slightly better. Both models are plotted on Figure 3, but model 8 is finally chosen for estimating crash rates.

On Figure 3, the estimated crash rates for all road segments are plotted as a function of their consistency index.

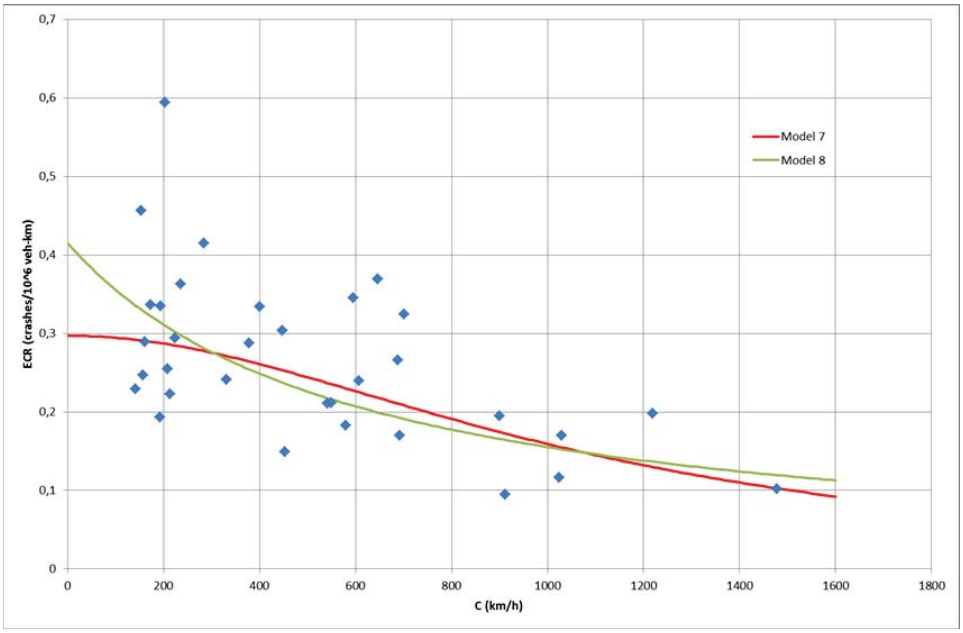

Figure 3 Estimated crash rate estimation models

CONCLUSIONS

Road fatalities are one of the most important problems in our society, causing thousands of victims every year. To contribute with the improvement of the road safety, this paper presents a new design consistency model that may be used as a surrogate measure for road safety evaluation of two-lane rural roads.

The consistency model has been developed from the regression analysis between several speed-measures variables and crash data.

The used speed-measures include not only variables related to operating speed but also related to deceleration and posted speed. All of them have been obtained from operating speed profiles built with the operating speed and deceleration/acceleration speed models developed in previous research. Those models were calibrated with continuous speed data recorded by an innovative technique that uses GPS devices for monitoring actual drivers' behavior. Thus, operating speed profiles are more accurate, presenting better approximation to the actual behavior of drivers.

The used crash data were not directly the observed accidents. With these accidents, a Safety Performance Function was calibrated showing an overdispersion of 0.1519. Then, based on this parameter and the observed accidents, the Empirical Bayes methodology was applied to estimate more accurately the number of accidents and thus the crash frequencies.
14 operating-speed-related variables were obtained from analyzing the operating speed profiles, crash data and speed limits for all road segments. A correlation analysis was made in order to reduce the final amount of parameters, reducing the final number of variables to five, being candidates to be used in the final consistency model form. Also, some interesting relationships were found among variables, such as the higher crash rates reached when operating speed variability presents a medium value, or the high correlation between this parameter and the operating speed deviation.

After the statistical analysis, the proposed model for relating crash data to road geometry is the following:

$$ECR = \frac{1}{2.40939+0.00403287 \cdot C} \tag{10}$$

Where C is the design consistency index, calculated as:

$$C = \frac{\bar{v}_{85}^2}{\Delta v_{85}} \tag{11}$$

The development of the new model and consistency index leads to a new design consistency measure for a whole road segment. Moreover, since the model presents the relationship between consistency and crash rate, it is possible to use that parameter as a surrogate measure to evaluate road safety. Consequently, the results of this study can be an innovative tool for assisting engineers' decision. In fact, according to this methodology, the engineers may evaluate the consistency and road safety of several possible solutions and chose the safest one. Besides, the presented model can be also applied to the estimation of crash rates of an existing road where accident data are not available.

Further research is proposed to consist mainly on the determination of the consistency thresholds. Once the consistency model and the consistency index are defined, the thresholds for the consistency measure should be proposed after detailed crash data observation. Thus, taking into account the relationship between this index and the estimated crash rate, the adequacy of the road to drivers' expectancies will be able to be measured also from the value of this road safety parameter.

ACKNOWLEDGEMENTS

Authors would like to thank Center for Studies and Experimentation of Public Works (CEDEX) of the Spanish Ministry of Public Works that partially subsidized the research. We also wish to thank to the Infrastructure and Transportation Department of the General Directorate of Public Works of the Valencian Government, to the Valencian Provincial Council and to the Ministry of the Interior, specially to General Directorate of Traffic of Spain, for their cooperation in field data gathering.

REFERENCES

Anderson, I.B., Bauer, K.M., Harwood, D.W., and Fitzpatrick, K. (1999). "Relationship to safety of geometric design consistency measures for rural two-lane highways". *Transportation Research Record: Journal of the Transportation Research Board,* Vol. 1658, Transportation Research Board, National Research Council, Washington, D.C., pp. 43–51.

Anderson, I. B., and Krammes, R. A.(2000). "Speed Reduction as a Surrogate for Accident Experience at Horizontal Curves on Rural Two-Lane Highways". *Transportation Research Record: Journal of the Transportation Research Board*, Vol. 1701, pp. 86-94.

Awata, M. and Hassan, Y. (2002). *"Towards Establishing an Overall Safety-Based Geometric Design Consistency Measure"*. 4th Transportation Specialty Conference of the Canadian Society for Civil Engineering.

Babkov, V. F. (1968). "Road design and traffic safety". *Traffic Engineering and Control*, Vol. 9, pp. 236–239.

Cafiso, S. (2000). *"Experimental Survey of Safety Condition on Road Stretches with Alignment Inconsistencies"*. Proc., 2nd International Symposium on Highway Geometric Design, Mainz, Germany, pp. 377–387.

Cafiso, S., La Cava, G. and Montella, A. (2007). "Safety Index for Evaluation of Two-Lane Rural Highways". *Transportation Research Record: Journal of the Transportation Research Board*, Vol. 2019, pp. 136-156.

Cafiso, S., Di Graziano, A., Di Silvestro, G., La Cava, G. and Persaud, B. (2010). "Development of Comprehensive Accident Models for Two-Lane Rural Highways using Exposure, Geometry, Consistency and Context Variables". *Accident Analysis and Prevention*, Vol. 42, No. 4, pp. 1072-1079.

Fitzpatrick, K., L. Elefteriadou, D. W. Harwood, J. M. Collins, J. McFadden, I. B. Anderson, R. A. Krammes, N. Irizarry, K. D. Parma, K. M. Bauer, and K. Passetti.(2000). *"Speed Prediction for Two-Lane Rural Highways"*. Report FHWA-RD-99–171. FHWA, U.S. Department of Transportation.

Gibreel, G. M., Easa, S.M., Hassan, Y. and El-Dimeery, I.A. (1999). "State of the Art of Highway Geometric Design Consistency". *Journal of Transportation Engineering*, Vol. 125, pp. 305-313.

Hassan, Y. (2004). "Highway Design Consistency: Refining the State of Knowledge and Practice". *Transportation Research Record: Journal of the Transportation Research Board*, Vol. 1881, pp. 63-71.

Kanellaidis, G., Golias, J., and Efstathiadis, S. (1990*).* "Driver's speed behaviour on rural road curves". *Traffic Engineering and Control*, Vol. 31(7/8), pp. 414–415.

Lamm, R., Choueiri, E. M., Hayward, J. C., and Paluri, A.(1988). "Possible Design Procedure to Promote Design Consistency in Highway Geometric Design on Two-Lane Rural Roads". *Transportation Research Record: Journal of the Transportation Research Board,* Vol. 1195, TRB, National Research Council, Washington, D.C., pp. 111–122.

Lamm, R., Choueiri, E. M., and Mailaender, T. (1992). *"Traffic safety on two continents—a ten year analysis of human and vehicular involvements"*. Proc., Strategic Highway Research Program (SHRP) and Traffic Safety on Two Continents, 18–20.

Lamm, R., Psarianos, B., and Mailaender, T. (1999). *"Highway design and traffic safety engineering handbook"*. McGraw-Hill Companies, Inc., New York, N.Y.

Lee, S., D. Lee, and J. Choi. (2000*). "Validation of the 10 MPH Rule in Highway Design Consistency Procedure"*. Proc., 2nd International Symposium on Highway Geometric Design, Mainz, Germany, pp. 364–376.

Leisch, J. E., and Leisch, J. P. (1977). "New Concepts in Design-Speed Application". *Transportation Research Record: Journal of the Transportation Research Board*, Vol. 631, TRB, National Research Council, Washington, D.C., pp. 4–14.

Ng, J. C. W. and Sayed, T. (2004). "Effect of Geometric Design Consistency on Road Safety". *Canadian Journal of Civil Engineering*, Vol. 31, No. 2, pp. 218.

Pérez Zuriaga, A.M., García García, A., Camacho Torregrosa, F.J. and D'Attoma, P. (2010). "Modeling operating speed and deceleration on two-lane rural roads with global positioning system data". *Transportation Research Record: Journal of Transportation Research Board,* Vol. 2171, TRB, National Research Council, Washington, D.C., pp. 11-20.

Pérez Zuriaga, A.M., García García, A. and Camacho Torregrosa, F.J. (2011). *"Study of tangent-to-curve transition on two-lane rural roads with continuous speed profiles"*. Transportation Research Board 90th Annual Meeting, Washington, D.C.

Polus, A. and Mattar-Habib, C. (2004). "New Consistency Model for Rural Highways and its Relationship to Safety". *Journal of Transportation Engineering*, Vol. 130, No. 3, pp. 286-293.
Treat, J.R, Tumbas, N.S., McDonald, S.T., Shinar, D., Hume, R.D., Mayer, R.E., Stansifer, R.L. and Castellan, N.J. (1979). *"Tri-level study of the causes of traffic accidents: Final report – Executive summary"*. Bloommington. Institute for Research in Public Safety. [REPORT No. DOT-HS-034-3-535-79-TAC(S)].

APPLICATION OF GPS AND QUESTIONNAIRES DATA FOR THE STUDY OF DRIVER BEHAVIOUR ON TWO-LANE RURAL ROADS

Ana María Pérez-Zuriaga, Ph.D., anpezu@tra.upv.es

Francisco Javier Camacho-Torregrosa, Ph.D. Candidate, fracator@tra.upv.es

José Manuel Campoy-Ungría, Ph.D. Candidate, jocamun@trr.upv.es

Alfredo García, Professor, agarciag@tra.upv.es

Highway Engineering Research Group, Universitat Politècnica de València

Camino de Vera s/n, 46022 Valencia - Spain

ABSTRACT:

Methodologies based on naturalistic observation provide the most accurate data for studying drivers' behaviour. This paper presents a new methodology to obtain naturalistic data related to drivers' behaviour in a road segment. It is based on the combination of using global positioning system data and drivers' questionnaires. The continuous speed profiles along a road segment and the characteristics of drivers, of their trips and the type of their vehicles can be obtained for a great amount of drivers. It has already been successfully used for several studies, such as the development of models to estimate operating speed profile in two-lane rural road segments; or the characterization of driving styles. These operating speed models have been the key for the development of a new geometric design consistency model, allowing an easier road safety evaluation. Besides, knowledge on the human factors that influence speed choice may be useful for road safety media campaigns and education programs designers, and also for the improvement of intelligent driver assistance systems.

1 INTRODUCTION

Multiple factors typically combine to produce circumstances that lead a vehicle to crash. The main concurrent factors are human factors, roadway environment factors, and vehicle factors. According to the research by Treat et al. [1], human factors are the most prevalent contributing factor of crashes, being present on the 93 % of crashes; followed by roadway (34 %) and vehicle factors (13 %). However, due to its characteristics, it is also the most complicated factor to study. The best results in this area have been achieved by using data collection methodologies based on naturalistic observation. This kind of methodologies is based on subjects driving the way they usually do, in their own vehicles and without any specific instructions or interventions. Projects such as *100-Cars Naturalistic Driving Study [2]*, *SHRP2 Naturalistic Driving Study* [3] and *2 Be Safe* [4] use this data collection methodology.

The first one tracked the behaviour of the drivers of 100 vehicles equipped with video and sensor devices over an 18-month period of time. Its main objective was to provide a high level of detail concerning driver performance, behaviour, environment, driving context and other factors that were associated with critical incidents, near crashes and crashes.

Whereas *100-Cars Naturalistic Driving Study* was focused on drivers' behaviour at crash situations, the central goal of *SHRP2 Naturalistic Driving Study* is the study of how the driver interacts with and adapts to the vehicle, traffic environment, roadway characteristics, traffic control devices, and the environment. It also includes assessing the changes in collision risk associated with each of these factors and interactions.

This research is involving more than 3000 volunteer drivers, who are monitored for a three year period, beginning in 2010.

Both previous research mainly study passenger car drivers' behaviour. *2 Be Safe* aims to understand and characterize powered two wheeler (PTW) rider behaviour. This is the world's first naturalistic riding study involving instrumented PTWs.

In most of that kind of studies, drivers are volunteers who know the scope of the research project, so their behaviour may be biased. Besides, they mainly focus on drivers' behaviour at crash situations, which are rare events.

In traffic psychology, some measures, called ‘intermediate measures’, are used in order to study drivers’ behaviour and understand drivers’ perceptions of risk [5]. Those measures characterize changes in behaviour that correlate with objective changes in the driving context. Some examples of those measures are: vehicle speed, headway, overtaking frequency, hand-held cell phone use, and lane-changing frequency.

For characterizing drivers’ behaviour, the most studied variable is the speed at which they drive at different road alignment elements (curves, tangents and spiral transitions) and its variations. In order to deal with this issue, it is necessary to collect data from a huge sample of people driving along a sample of elements. Speed data can be obtained by using either spot or continuous collection methodologies.

In most cases, data collection device is a manually operated radar gun or similar [6]. The use of radar gun has three important problems: human error, cosine error and drivers’ behaviour affection. Pavement sensors are also used for collecting speed data [7]. Although they address those problems, they only collect data in one location, as well. However, they require the researcher to carry more equipment, require more time to install and remove and may also affect driver behaviour.

Since those methodologies allow only spot speed data collection, the study of deceleration and acceleration phenomenon is not possible. Therefore, several research projects [7] complemented data collection by using lidar guns. This way, speed data is collected in several spots within a road segment. However, even with the use of lidar guns, starting and ending points of deceleration/acceleration cannot be accurately determined.

These deficiencies in data collection may be avoided with other methods based on continuous speed tracking, such as instrumented test vehicles, driving simulators or different methods based on digital video recording and processing. Last one is only suitable for local studies at short road segments.

Some researchers [8, 9] studied the influence of the road geometric characteristics on drivers’ behaviour from speed data collected using instrumented vehicles. However, the results may be conditioned by the equipment of the vehicle and the number of observations. Moreover, the sample may be biased, not enough representative of the actual driver’s behaviour because volunteers knew the research objectives and they were not used to drive the instrumented vehicle.

Drivers’ behaviour may also be biased at driving simulators studies. In fact, the higher speeds in

simulator may be due to a lower perception of risk in the simulated road than in the actual road. However, the lower risk in simulator does not restrain the tendency to adopt higher speed on simple road alignments than on complex ones. In order to use a driving simulator as a tool for drivers' behavioural studies, it must be correctly validated [10], though.

The results of those studies may be the key for improving Intelligent Speed Adaptation (ISA) and speed limit credibility. Both of them significantly improve speed behaviour, i.e. they are effective measures to reduce speeding [11, 12].

ISA is an advanced driver assistance system that addresses driving speeding, and it leaves higher-order task control, manoeuvring and navigation to the driver. ISA can be informative, interactive or intervening. Informative ISA only displays the current speed limit continuously and prompts the driver if the speed limit is exceeded. When designing these new devices, the goal is to make them as effective as possible in reducing speed, while at the same time accepted by drivers. To achieve this, it is of great importance that the focus is on the drivers and why they make the decision to speed during their everyday driving [13].

On the other hand, speed limits should provide information to the driver about the speed he/she can drive safely in average conditions [14]. However, setting a limit does not automatically result in the required speed behaviour. One of the reasons for drivers to exceed a speed limit is considered to relate to the credibility of the speed limit. Credibility means that drivers consider a speed limit as logical or appropriate in the light of the characteristics of the road and its immediate surroundings. This is why it is important the study of the relationship between road characteristics and speed choice and the credibility of a speed limit.

This measure especially affects non-ISA users who appear to be more sensitive for the credibility of speed limits than ISA users [12].

2 OBJECTIVES

Considering the shown deficiencies on speed data collection for drivers' behaviour studies, a new data collection methodology has been developed, as an adaptation of usual naturalistic methodologies.

The main objective is getting naturalistic data in order to study drivers' behaviour in a road segment.

The researchers should be able to get enough sample size of drivers along road segments.

Collected data should be both drivers' individual continuous speed profile along a road segment and data related to their social conditions, trip characteristics and vehicle type.

Besides, data collection should not be the cause of drivers' behavioural change, so that it may be considered as naturalistic data collection methodology.

3 METHODOLOGY

This section describes the application of developed data collection methodology on ten two-lane rural road segments located in the region of Valencia (Spain). Data about the path and the continuous speed profile of actual drivers, their social characteristics, their trip characteristics and the type of their vehicles were obtained.

3.1 Data collection

For data collection, two checkpoints were located at the beginning and at the end of each road segment, controlling both directions. Two or three people controlled each checkpoint. At each one, two members were at the starting point, while the other one was at the final point. The general diagram of the data collection system is presented in figure 1.

When there was an incoming vehicle, one member of the checkpoint team stopped it and asked the driver about collaboration in the research project, emphasizing that he/she was part of the University. In order to avoid data biasing, the scope of the research was not explained at the beginning. After driver's agreement, he/she was asked about some general questions about his/her driving experience, previous knowledge of the road segment and the purpose and length of the trip. Another member of the group placed a 1 Hz GPS device on the vehicle and wrote down some data, such as the number of passengers or the type of vehicle. Driver was also encouraged to not change his/her usual driving behaviour.

This process took around 1-2 minutes. After this time period, driver was allowed to continue along the road segment.

When the vehicle arrived to the final checkpoint, a member of the team took the GPS device out of the vehicle and asked the driver some questions about his/her perception of the road segment. At this

point, the driver was informed about the research project, by means of a leaflet, in order to be as fast as possible and not slow the traffic down.

This data collection methodology was implemented on ten two-lane rural road segments with no main intersections and with high lateral clearance. The general road segment characteristics are summarized in Table 1.

All the selected roads are characterized by traffic volumes low enough to reduce the potential for restricted vehicle flow but sufficient to ensure a significant sample size. On average, 180 drivers were considered for each road segment. The total data sample of the research project was 11877 vehicles·km.

The data collection was carried out during working days, between approximately 8:30 a.m. and 2:00 p.m. under dry weather conditions. The duration of each data collection depended on the AADT of the corresponding road segment and the amount of data needed. It was also needed to consider at least one hour before and after the test in order to set and pick up all the equipment placed on the road.

A provision of GPS devices was always needed at both checkpoints. Depending on the traffic flow balance by direction, at some moments it was needed to transport devices between checkpoints, in case of lack of devices at one checkpoint.

Some additional equipment was needed in order to perform the test, besides of GPS devices. Some traffic sign and guidance elements had to be used for warning drivers about the presence of the checkpoints. A safe area was created at each checkpoint for allowing their members to work safely. They also wore safety vests.

3.2 Naturalistic data test

GPS devices contain the information about position and speed of all drivers along the road segment under study. The main goal of this field data collection is to obtain accurate, naturalistic and disaggregated data from actual drivers. Thus, it is important to ensure that drivers perform their driving task without being influenced by the presence of GPS devices, by means of a naturalistic data test.

The test was carried out during the first two field data collections, comparing data obtained from drivers who were driving the day of the experiment and drivers who were driving the day before the

experiment. Speed data from both types of drivers was obtained at the same spots. Those locations were a sharp curve and a long tangent at each road segment. A sharp curve is a control element where road geometric characteristics have great influence over driver speed choice; whereas a long tangent is an element where driver may reach his/her desired speed. So, speed at those locations may be assumed as speed boundaries.

Some video cameras were set closed to the roadside, hidden from driver's vision. They were recording the traffic flow in order to calculate the speed of individual drivers. In order to perform speed calculation, two pairs of references were located at each control element (Figure 2). Those references were spaced a known distance. Thus, knowing the distance between references and the time the vehicle spent on going from one to the other, it was possible to calculate vehicles' individual speeds.

Individual operating speeds of drivers involved and not involved in the field data collection was compared, for checking if they were influenced by the presence of GPS devices. The analysis was performed by means of least significant difference (LSD) intervals. As the intervals overlap, the population means are not significantly different from each other at the 95 % confidence level. Consequently, no statistical difference was found between people driving the data collection day (with GPS) and other day (without GPS) [15].

Recorded traffic was also used for determining the operating speed at those spots. By comparing speeds obtained from video cameras and GPS devices at the same moment, data obtained from last ones was validated.

3.3 Free-flow conditions test

In order to analyse the influence of the infrastructure over drivers' behaviour and to characterize driver groups from their speed choice, involved vehicles are supposed to drive at free-flow conditions. This study defines free-flow conditions as those of isolated vehicles with a minimum headway of at least 5 seconds. It is assumed that vehicles with shorter headways might be constrained by a lead vehicle.

During data collection, vehicles were released from the initial point of the road segment at free flow conditions, but they might be disturbed by other vehicles along the road segment. In this case, there was not a simple way for determining if the registered data was under free or non-free flow conditions. Thus, a methodology was developed in order to determine the road segment where a driver drove under non-free flow conditions.

From GPS data treatment different continuous speed profiles are available: individual speed profile for each single driver and every continuous profile corresponded to every percentile of speed distribution. The free-flow conditions test consists on those profiles comparison.

It is supposed that each single driver behaves in a particular way, approaching his/her individual speed profile to certain operating speed percentiles. This behaviour was observed under free-flow conditions, but the difference between profiles increased when the driver was disturbed due to traffic flow. Therefore, for each individual speed profile, a non-free flow road section may be identified by means of comparing different aggregated speed percentiles profiles and individual speed profiles.

Figure 3 shows an example of a vehicle constrained by a lead one. It is clear that around the point station 4000 m the vehicle suddenly changed its behaviour, driving at an unusual speed. This road segment of the individual speed profile was therefore not considered in the study.

4 APPLICATIONS

Described data collection methodology allows us to obtain data on several road segments of vehicle paths, individual continuous speed profiles, social characteristics of drivers, of their trips and the type of their vehicles. These data are the base for performing new and more accurate research.

4.1 Operating speed profile models for geometric design consistency evaluation

Geometric design consistency has an important influence over road safety because it refers to the conformance of highway geometry to driver expectancies. The main technique for design consistency evaluation is the examination of the operating speed, defined as the 85^{th} percentile of speed distribution, and its variations. A continuous operating speed profile is needed. However, during road design phase operating speed can only be estimated as a function of the roadway geometric characteristics.

Several models have been developed to predict operating speed at curve and tangent sections, and some research has been carried out to study deceleration and acceleration phenomena. Most of them were based on spot speed data collection [16, 17, 18, 19]. Therefore, some hypotheses had to be made in order to develop operating speed profiles construction rules, such as considering constant speed at curves. Besides, spot speed data collection is only able to determine the speed at two

previously located spots. Thus, for determining deceleration and acceleration rates, the length of the transition zone is unknown and it had to be assumed constant for all drivers.

This new methodology addresses these problems. The continuous operating speed profiles help the researchers to check the behaviour of all drivers at different alignment elements, so the previous hypotheses can be considered or rejected based on naturalistic data consideration. Also, deceleration and acceleration lengths are known for all individual drivers, so more accurate analysis can be done.

Taking into account these considerations, it can be concluded that operating speed and deceleration/acceleration rates models calibrated from continuous naturalistic speed data fit better drivers' behaviour than those based on spot data do.

According to this assumption, operating speed models for tangent and curve sections have been developed based on operating speed profiles. Besides, other models have been calibrated for estimating the 85^{th} percentile of deceleration/acceleration rates, instead of the deceleration/acceleration rate from 85^{th} percentile speed profile [5].

Those models have been the key for the development of a new geometric design consistency model [20]. It allows the estimation of the crash rate of a road segment. Thus, this data collection methodology has turn into a tool for road safety evaluation on both road design phase and operation phase.

4.2 Human factors analysis

As a result of data collection and treatment, individual continuous speed profile is available for each single vehicle and for each road segment. Besides, the different questions asked to drivers before and after the test allow the characterization of some variables, such as: driver's characteristics (age, gender, driving experience); characteristics of the trip (distance, regular or not, number and type of passengers); and vehicle type.

Therefore, it is possible to study the relationship between both types of variables, instead of performing an aggregated analysis. The obtained results may be used for studying: drivers' speed perception; driving styles characterization; and consistency of drivers' behaviour among elements, among road segments and along the time. It may also be the base for the validation of driving simulators that have the purpose of drivers' behaviour study.

The analysis about the influence of those variables over the developed speed on tangent sections has already performed, based on a sample of 78 tangents and 6133 driver·tangents, since one driver might drive along several tangents. This analysis consisted on a multifactor ANOVA, e.g. a multifactor analysis of variance, for the variable *Speed*, considering:

- *Driver Age*: this variable was divided into 5 years intervals.
- *Driver Sex*: it was divided into man and women.
- *Driver Experience*: it measured the amount of kilometres driven by each driver in the last year.
- *Passenger*: this variable considered the presence of passenger inside the vehicle, taking into account if they were children, adult or elderly people.
- *Trip Frequency*: it identified whether the trip was regular or not.
- *Trip Length*: the trip length was classified into short, medium and long distance trip. It was also included if the trip was a professional route.
- *Trip Purpose: it identified whether the purpose of the trip was work or not.*
- *Vehicle Type*: the considered vehicle types were light truck, van, minivan, all-terrain and passenger car.

The ANOVA analysis decomposed the variability of the variable *Speed* into the contributions due to the different factors. It measured the contribution of each factor having removed the effects of all other factors. The ANOVA results showed that all factors, apart from *Trip Purpose*, presented p-values less than 0.05, so those factors had a statistically significant effect on *Speed* at the 95 % confidence level.

In order to characterize the effect of each factor on the developed speed on tangents, several LSD intervals were performed. They allowed significant differences identification among variables at the 95 % confidence level, and forming groups of means within which there were no statistically significant differences.

Figure 4 shows the plotted LSD intervals for the study of the effect of the driver related factors on the developed speed on tangents.

Considering the age of the drivers, 5 groups can be identified: 18-21, 21-25, 26-55, 56-75, >76. Drivers tend to increase their speed after getting the driving licence and they tend to gradually

decrease it after being 26 years old.

On the other hand, men tend to drive faster than women, and also do it drivers with higher driving experience.

Figure 5 shows the plotted LSD intervals for the study of the effect of the trip related factors on the developed speed on tangents. Drivers tend to drive faster when their trips are regular. It is probably due to the fact that they know the road characteristics. Higher speeds have also been found out when the driven distance was long.

The factor related to the amount of passengers inside the vehicle has also been identified as significant. Drivers develop higher speeds when they drive alone than when they are accompanied, especially by elderly people (Figure 6).

The *Vehicle Type* factor, as well as *Driver Age*, presented different groups (Figure 7). Three groups can be detected: light truck, van and the group consisted of minivan, passenger car and all-terrain. The recorded speed was higher for the last group.

In summary, men drive faster than women, and the older the driver is the slower he/she drives. Driver's experience is also a significant variable, so people with less driving experience drive slower. Besides, people drive faster in a regular trip and/or when they are alone in the car. These conclusions are similar to those obtained by previous studies [21, 22, 23].

This is an initial approach to drivers' behaviour on tangents. An additional multivariate analysis is necessary because of correlations among the independent variables which may give rise to confounding of effects.

Other developed research focused the study of drivers' behaviour on the variations of deceleration and acceleration [24, 25]. With data obtained from the proposed data collection methodology it has also been performed the analysis about the influence of the variables non related to the infraestructure over the deceleration and acceleration. In that case, almost none variable was significant, so, according to the results, deceleration and acceleration may not be considered as a variable for drivers' behaviour characterization.

The knowledge of the influence of those data about drivers' behaviour may be useful for road safety media campaigns and education programs designers, but also for the improvement of intelligent

driver assistance systems.

5 CONCLUSIONS

An adaptation of previous naturalistic data collection methodology has been developed for studying drivers' behaviour on two-lane rural roads. This methodology consists on getting continuous speed profiles of actual drivers by placing on their vehicles GPS devices. Besides, data related to the social characteristics of the driver, the purpose of his/her trip and the type of his/her vehicles are obtained from questionnaires taken during the test.

This data collection methodology was implemented on ten two-lane rural road segments, involving an average of 180 volunteers per test, considering both road directions. The total data sample of the research project was 11877 vehicles·km.

In order to test if this data collection can be considered as naturalistic, a comparison analysis was carried out between spot speed data registered a day before data collection and spot speed data recorded during data collection. Results showed that there are no significant differences between both data.

With data obtained from the new data collection methodology, aggregated (speed percentiles) and disaggregated (driver individual data) analysis may be performed. In fact, it was successfully used in order to calibrate the models and construction rules for getting continuous operating speed profile of a two-lane rural road segment. Those models, based on aggregated data, allow road design consistency evaluation and road safety improvement.

For this kind of analysis it is necessary to ensure free flow conditions. Therefore, a procedure was developed in order to remove from the collected data all individual speed-constrained sections. This procedure is based on the comparison of individual speed profiles and percentiles speed profiles.

On the other hand, disaggregated data were used for studying the influence of driver's characteristics and the characteristics of trip and the vehicle on chosen speed and deceleration/acceleration rates.

Therefore, this data collection methodology turns into a new tool for drivers' behaviour and road design evaluation.

6 AKNOWLEDGEMENTS

Authors would like to thank “Centre for Studies and Experimentation of Public Works (CEDEX)” of the “Spanish Ministry of Public Works” that partially subsidizes the research. We also wish to thank to the “General Directorate of Public Works, Urban Projects and Housing” of the “Infrastructure, Territory and Environment Department” of the “Valencian Government”, to the “Valencian Provincial Council” and to the “General Directorate of Traffic” of the “Ministry of the Interior” for their cooperation in field data gathering.

7 REFERENCES

1. Treat, J. R., Tumbas, N. S., McDonald, S. T., Dhinar, D., Hume, R. D., Mayer, R. E., Stansifer, R. L., and Castellan, N. J.: ‘Tri-level Study of the Causes of Traffic Crashes: Final report—Executive Summary’, Report No. DOT-HS-034-3-535-79-TAC(S). Institute for Research in Public Safety, Bloomington, IN, 1979.
2. Dingus, T. A., Klauer, S.G., Neale, V. L., Petersen, A., Lee, S. E., Sudweeks, J., Perez, M. A., Hankey, J., Ramsey, D., Gupta, S., Bucher, C., Doerzaph, Z. R., Jermeland, J., and Knipling, R.R.: ’The 100-car naturalistic driving study; Phase II- Results of the 100-car field experiment’, Report No. DOT HS 810 593. Virginia Tech Transportation Institute, Blacksburg, VA, 2004.
3. http://www.trb.org/StrategicHighwayResearchProgram2SHRP2/Public/Pages/The_SHRP_2_Naturalistic_Driving%20Study_472.aspx, accessed September 2012.
4. http://www.2besafe.eu/, accessed September 2012.
5. Fourie, M., Walton, D., and Thomas, J.A.: ‘Naturalistic observation of drivers’ hands, speed and headway’, Transportation Research Part F: Traffic Psycology and Behaviour, vol. 14, 2011, pp. 413-421.
6. Gibreel, G. M, Easa, S. M., and El-Dimeery, I.A.: ‘Prediction of operating speed on three-dimensional highway alignments’, Journal of Transportation Engineering, 2001, pp. 21-30.
7. Fitzpatrick, K., and Collins, J.: ‘Speed-profile model for two-lane rural highways’, Transportation Research Record, vol. 1737, 2000, pp. 42-49.
8. Yang, L., and Hassan, Y.: ‘Driver speed and acceleration behavior on Canadian roads’, 87th Annual Meeting of the Transportation Research Board, Washington, D.C., USA, 2008.
9. Hu, W., and Donnel, E.T.: ‘Models of acceleration and deceleration rates on a complex two-lane rural highway: results from a nighttime driving experiment’, 87th Annual Meeting of the

Transportation Research Board, Washington, D.C., USA, 2008.

10. Bella, F.: 'Driving simulator for speed research on two-lane rural roads', Accident Analysis and Prevention, vol. 40, 2008, pp. 1078-1087.
11. Van Nes, N., Houtenbos, M., and Van Schagen, I.: 'Improving speed behaviour: the potential of in-car speed assistance and speed limit credibility', IET Intelligent Transport Systems, Special Issue – selected papers from HCD 2008.
12. Van Nes, N., and Van Schagen, I.: 'Opportunities to improve speed behavior: Credibility of speed limits and the use of ISA', Advances in Transportation Studies, vol. 20, 2010, pp. 39-46.
13. Warner, H.W., and Aberg, L.: 'Drivers' decision to speed: A study inspired by the theory of planned behavior', Transportation Research Part F: Traffic Psycology and Behaviour, vol. 9, 2006, pp. 427-433.
14. Goldenbeld, C., and Van Schagen, I.: 'the credibility of speed limits on 80 km/h rural roads: The effects of road and person(ality) characteristics', Accident Analisys and Prevention, vol. 39, 2007, pp. 1121-1130.
15. Pérez-Zuriaga, A.M, García García, A., Camacho-Torregrosa, F.J. and D'Attoma, P. "Modelling operating speed and deceleration on two-lane rural roads with global positioning system data". Transportation Research Record, vol. 2171, 2010, pp. 11-20.
16. Lamm, R., Psarianos, B., and Mailaender, T.: 'Highway design and traffic safety engineering handbook'. McGraw-Hill, New York, 1999.
17. Ottesen, J.L., and Krammes, R.A.: 'Speed profile model for a design consistency evaluation procedure in the United States', Transportation Research Record: Journal of the Transportation Research Board, vol. 1701, 2000, pp. 76-85.
18. Fitzpatrick, K., and Collins, J.M.: 'Speed-profile model for two-lane rural highways', Transportation Research Record: Journal of the Transportation Research Board, vol. 1737, 2000, pp. 42-49.
19. Park, P.Y., Miranda-Moreno, L.F., and Saccomanno, F.F.: 'Estimation of speed differentials on rural highways using hierarchical linear regression models', Canadian Journal of Civil Engineering, vol. 37 (4), 2010, pp. 624-637.
20. Camacho-Torregrosa, F.J., Pérez-Zuriaga, A.M, and García García, A. "New geometric design consistency model based on operating speed profiles for road safety evaluation". 3rd Road

Safety and Simulation Conference, Indianapolis, USA, 2011.

21. Wasielewski, P.: ‘Speed as a measure of driver risk: observed speeds versus driver and vehicle characteristics’, Accidents Analysis and Prevention, vol. 16 (2), 1984, pp. 89-103.
22. Jorgensen, F., and Polak, J.: ‘The effect of personal characteristics on drivers’ speed selection. An economic approach’, Journal of Transport Economics and Policy, 1993, pp. 237-252.
23. Williams, A.F., Kyrychencko, S.Y, and Retting, R.A.: ‘Characteristics of speeders’, Journal of Safety Research, Vol. 37, 2006, pp. 227-232.
24. Lajunen, T., Karola, J., and Summala, H.: ‘Speed and acceleration as measures of driving style in young male drivers’, Perceptual and Motor Skills, vol. 85, 1997, pp. 3-16.
25. Wahlberg, A.E.: ‘Speed choice versus celeration behavior as traffic accident predictor’, Journal of Safety Research, vol. 37, 2006, pp. 43-51.

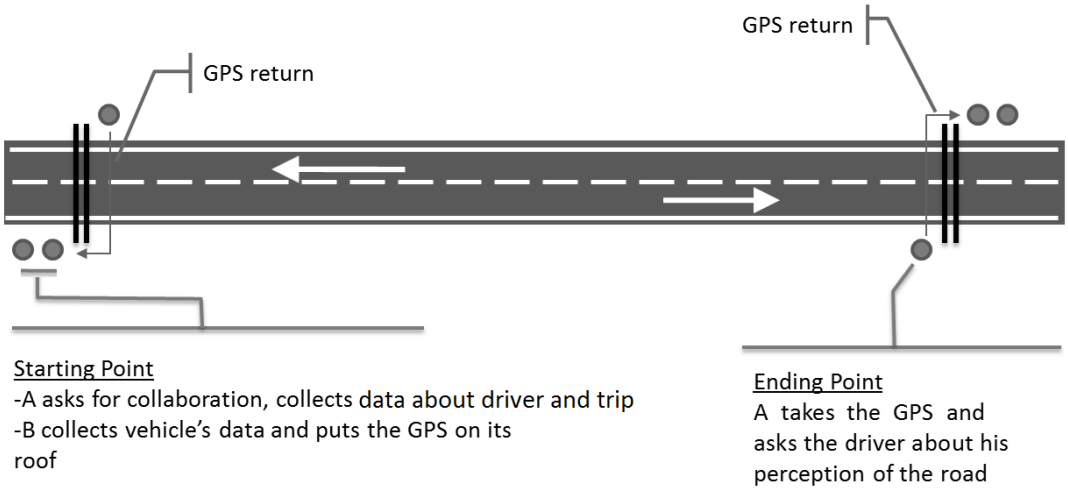

Figure 1. Data collection diagram

Figure 2. References for naturalistic data test

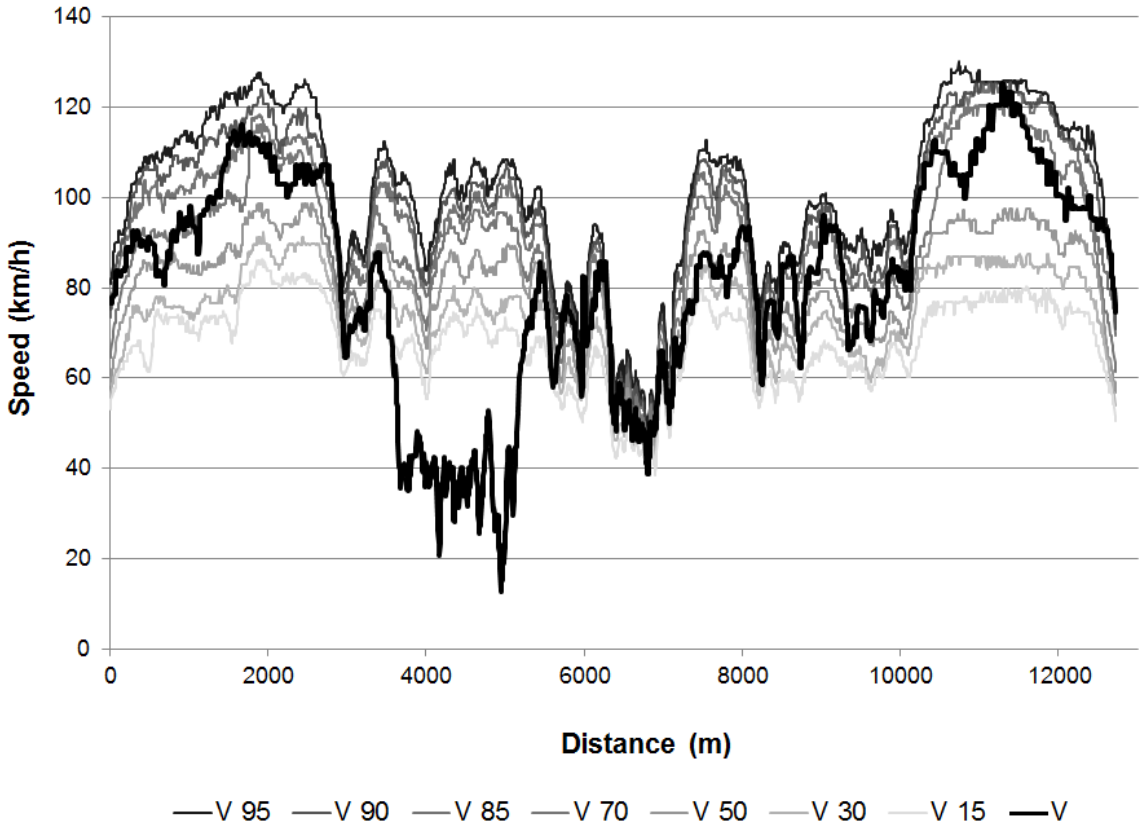

Figure 3. Free-flow conditions test

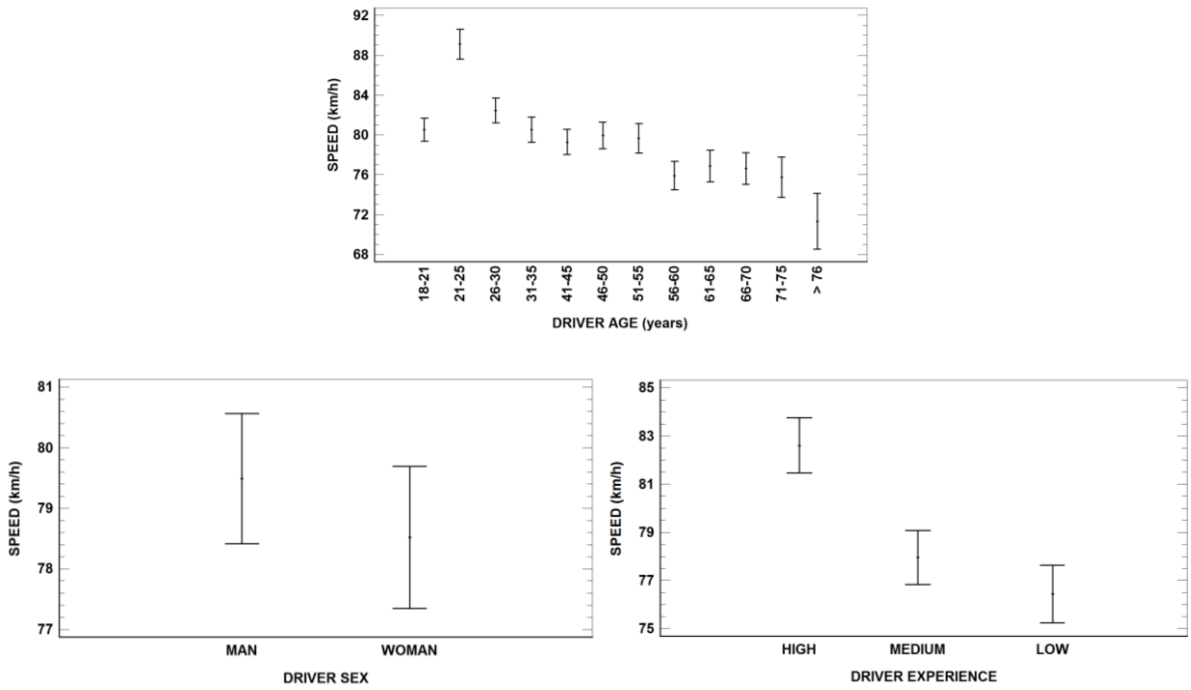

Figure 4. Means and 95 % LSD intervals. *Driver Age, Driver Sex* and *Driver Experience*

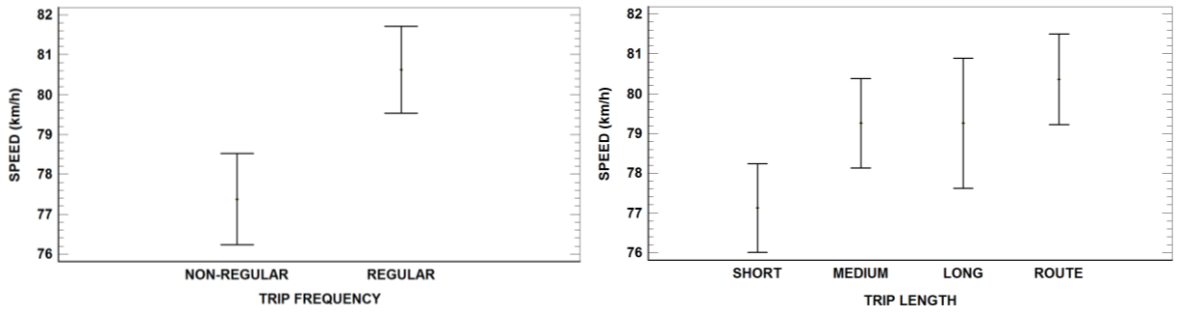

Figure 5. Means and 95 % LSD intervals. *Trip Frequency* and *Trip Length*

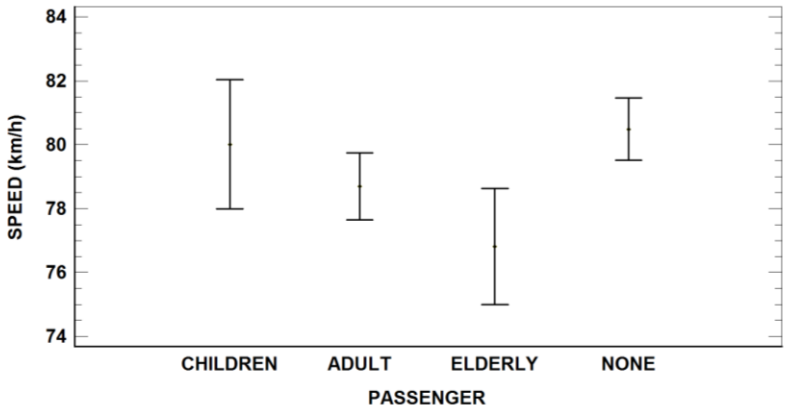

Figure 6. Means and 95 % LSD intervals. *Passenger*

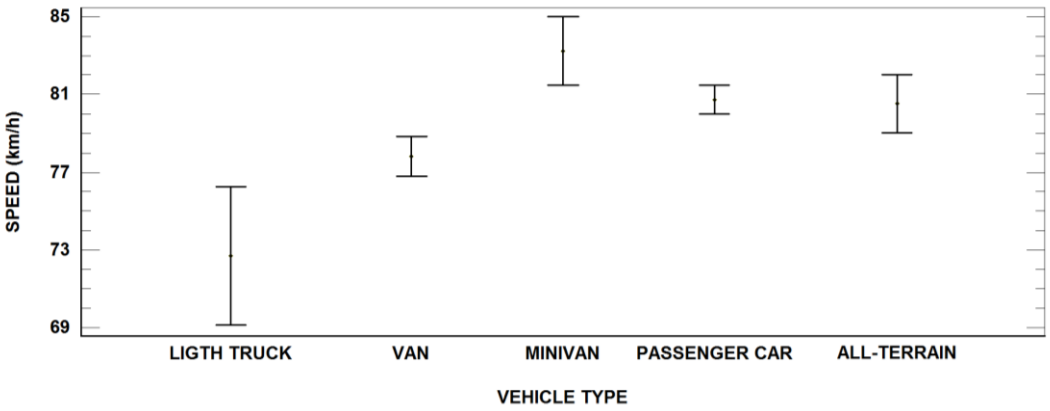

Figure 7. Means and 95 % LSD intervals. *Vehicle Type*

ID	Road segment	Road segment length (km)	Estimated AADT (vpd)	Forward direction observations	Backward direction observations
1	CV-35	13.40	860	70	90
2	CV-35	8.20	2257	121	120
3	CV-333	5.10	2419	101	89
4	CV-50	5.70	4852	116	96
5	CV-372	4.50	4149	77	117
6	CV-305	4.40	6086	112	105
7	CV-370	8.30	2523	61	79
8	CV-401	6.00	5292	102	91
9	CV-376	6.70	2656	58	53
10	CV-310	4.70	6809	74	58

Table 1. Summary of road segment characteristics

TE1351
TANGENT-TO-CURVE TRANSITION ON TWO-LANE RURAL ROADS BASED ON CONTINUOUS SPEED PROFILES

Ana M. Pérez-Zuriaga[1], Francisco J. Camacho-Torregrosa[2], Alfredo García[3]

Abstract

In road geometric design process, speed variation along the road segment is one of the most popular criteria to evaluate road consistency. Hence, the importance of estimating operating speed and its variations. Most of the estimation models are based on speed spot data collection, usually assuming some hypotheses like operating speed remains constant at curves and speed variations take place entirely at preceding tangent. This paper presents the results of the study of the deceleration phenomenon using a new methodology based on data collection by GPS devices. By means of this new methodology, not only new and more accurate models can be developed, but also the previous hypotheses can be checked and new studies can be carried out. Tangent-to-curve speed variations have been evaluated, comparing the 85th percentile speed differential ($\Delta_{85}V$) and the differential of 85th percentile operating speed (ΔV_{85}), analyzing the percentage of deceleration length which takes place at curves, and developing two deceleration models with radius of horizontal curve and parameter of transition curve as explanatory variables.

Subject headings: traffic speed, highways and roads, mathematical models, regression models, global positioning systems

INTRODUCTION

Road safety depends on several factors; design consistency being one of the most important because it refers to the conformance of highway geometry to driver expectancies. A consistent road design does not give rise to surprises to drivers, thus avoiding anomalous behavior and possible collisions. A technique to evaluate design consistency is by means of examining changes on the operating speed (V_{85}) as a function of the roadway geometry and, specially, the speed differential at tangent-to-curve transitions.

Several models have been developed for predicting operating speed at curves and tangents. Some research has also been focused on the tangent-to-curve transition. However, most studies were based on speed data collected by radar guns, pavement sensors or similar spot speed collecting devices. Therefore, the developed operating speed models had to assume important hypotheses, such as constant operating speeds throughout horizontal curves or acceleration and deceleration transitions fully developed on tangents. Both statements are known to be false, as some

[1]PhD, Highway Engineering Research Group, Universitat Politècnica de València
Camino de Vera, s/n, Valencia, 46071, Spain, e-mail: anpezu@tra.upv.es
[2]PhD Candidate, Highway Engineering Research Group, Universitat Politècnica de València
Camino de Vera, s/n, Valencia, 46071, Spain, e-mail: fracator@tra.upv.es
[3]Professor, Highway Engineering Research Group, Universitat Politècnica de València
Camino de Vera, s/n, Valencia, 46071, Spain, e-mail: agarciag@tra.upv.es

other studies have confirmed. The models that focused on the tangent-to-curve transition were developed by using spot speed data collected at several locations along the transition, but no accurate results were obtained.

Lamm et al. (1988) presented a model without validation derived from a car-following test. In this model, acceleration and deceleration were assumed to occur only on tangent sections. A rate of 0.85 m/s^2 (2.8 ft/s^2) was estimated for both acceleration and deceleration. They also found that the speed at the end of the curve was on average 6.4–8 km/h (4–5 mph) higher than at the beginning. This confirms that drivers vary their speed at horizontal curves. Another model for two-lane rural roads was developed by Ottesen and Krammes (2000), based on the same assumptions as Lamm. Speed data were collected with radar guns at the midpoint of horizontal curves. For the approaching tangents, the speed was collected at a point that was considered to be constant. A speed profile model was developed, considering Lamm's acceleration and deceleration rates, locating the entire speed transition on the tangent.

Collins and Krammes (1996) tested the validity of a speed-profile model for design consistency evaluation. They also studied the speed reduction of the model and the assumptions on deceleration and acceleration characteristics approaching and departing horizontal curves. The rate of 0.85 m/s^2 was valid for deceleration but not for acceleration. The assumption that deceleration occurs entirely on the approaching tangent (and also that the operating speed is constant all along the horizontal curve) was not confirmed by observing the speed behavior.

Fitzpatrick and Collins (2000) also developed a model based on spot speed data, recorded at the center of the horizontal curve and at the midpoint of the approaching tangent (Fitzpatrick et al. 1999). The developed model predicts deceleration rates depending on the radius (Table 1), providing a maximum deceleration rate of 1 m/s^2. They also assumed that the entire speed transition occurred on the approaching tangent.

Park et al. (2010) also used spot speed data for estimating speed differentials. They analyzed 18 tangent-to-curve transitions (speeds were measured 200 m ahead of the curve section and at the midpoint of the curve for each individual vehicle). Two linear models and two multilevel models were developed from disaggregated data.

On the other hand, there are models based on data collected at different sites along the curve and the approaching tangent. From this, Marchionna and Perco (2007) developed a deceleration model depending on curve radius (Table 1) based on data collected using a Lidar gun along tangents before 18 curves of 19 two-lane rural roads in level and hilly terrain.

Misaghi and Hassan (2005) developed another research based on speed collected at five points. In this case, the speed data were collected using electronic counter/classifiers to observe the vehicle speed change along 20 horizontal curves. Although relatively weak relationships were developed for operating speed on curves, stronger relationships were found for 85^{th} percentile speed differential on tangent-to-curve transitions (Table 2).

Figueroa and Tarko (2007) evaluated driver's behavior before and after horizontal curves in order to develop operating speed models for transition sections. Speeds were measured in each site at several spots distributed along the estimated speed variation length. The results indicated that 66% of the speed reduction and 72 % of the speed increase occur on the tangents preceding and following the curves, respectively. In addition, the mean deceleration rate and the mean acceleration rate were 0.732 and 0.488 m/s^2, respectively, for a 16.1 km/h reduction.

In the same way, in order to study roadway users' approach curve and departure curve movements, Dell'Acqua (2010) placed a laser detector in three different positions at the beginning and ending segments of the circular element. The study of transitions showed how the mean deceleration rate was equal to 0.70 m/s^2, and the mean acceleration rate equaled to 0.68 m/s^2, occurring the 40% of the deceleration length and the 49% of the acceleration length on the circular element.

Castro et al. (2011) presented a study of vehicle speeds on tangents and curves of two-lane rural highways, carried out in Colombia. Car speeds were measured by radar meters at the beginning, at the midpoint, and at the end of 22 curves, and on the approaching tangent at points located 200 m, 140 m, and 70 m from the beginning of the curve. The developed model for estimating $\Delta_{85}V$ is shown on table 2.

The most important limitation of the models based on spot speed data is that data are not collected at the beginning and the ending points of the speed transitions, because those points cannot be *a priori* determined. Therefore, the acceleration and deceleration patterns do not reflect drivers' actual behavior. Moreover, the speed transition lengths are unknown, so the actual acceleration and deceleration rates cannot be accurately obtained. Continuous operating speed recording methods should be used in order to avoid these deficiencies, such as instrumented test vehicles or digital video recording and processing. Each one is designed for different situations, i.e. digital video processing is only suitable for local studies in a reduced road segment.

Yang and Hassan (2008) and Hu and Donnell (2010) used an instrumented vehicle to collect speed data for studying drivers' behavior. However, the results may be biased because of the vehicle equipment. The number of

observations is also limited in this methodology. In addition, the sample used is not representative enough of the actual drivers' behavior because the participants knew the research objectives. This issue also exists when using driving simulators.

Bella (2007) describes the results of a study performed with an interactive fixed-base driving simulator. Thirty people drove the driving simulator on a two-lane rural road with 16 different tangent-curve configurations. On the basis of measured speeds, the parameters were calculated for the 85th-percentile of the distribution of maximum speed reduction experienced by each driver (85MSR) as well as the differential speed not exceeded by 85 % of the drivers traveling under free-flow conditions ($\Delta_{85}V$). The proposed models are shown on table 2.

Bella (2008) calibrated a model to predict the 85th percentile of the deceleration based on data collected on the tangent-curve-tangent transition in a driving simulator. In this study, the author found that the mean value of the speed differences of each driver between the beginning and the midpoint of the curve did not differ significantly from zero. However, the difference of the speeds between the midpoint and the final point of the curve was significantly different from zero. This difference was very small, so the simplified hypothesis of assuming a constant speed along the circular curve was admitted. The acceleration and deceleration distances were also found to be different, highlighting the need for different rates for both phenomena. The developed deceleration model is shown on table 1.

All these issues can be addressed by using GPS tracking devices for obtaining continuous operating speed data from actual drivers. The main advantage of this method is the huge amount of continuous operating speed data collected without significant influence over the drivers (Pérez-Zuriaga et al. 2010). This new methodology allows researchers, for the first time, to study the tangent-to-curve transition, evaluating the speed differential and the length and location of the deceleration, and also to develop deceleration models.

OBJECTIVES

The objective of this study is the evaluation of speed variation in tangent-to-curve transitions for two-lane rural roads. To analyze this phenomenon, several variables, such as the 85th percentile speed differential ($\Delta_{85}V$) and the differential of 85th percentile operating speed (ΔV_{85}) have been studied and a deceleration rate model, including geometric characteristics as explanatory variables, has also been developed.

Moreover, this paper presents a discussion on some hypotheses assumed by previous researchers such as the fully development of the deceleration on the tangent section. The deceleration length has been examined, as well as the portion within the different geometric elements.

In this research, continuous operating speed data has been used instead of spot speed data, obtained by means of GPS devices placed on passenger cars. Consequently, the attained models and conclusions are much better supported than the ones obtained in previous research, considering the same sample size.

DATA COLLECTION

Continuous data collection was performed by means of GPS devices placed on the passenger cars of actual drivers (Pérez-Zuriaga et al. 2010). All collected data were filtered and reduced. The coordinates were used for composing the horizontal alignment of the road (Camacho-Torregrosa et al. 2010), while the speed data were used for obtaining the individual operating speed profiles.

Speed data were collected between February 2008 and July 2008 during periods between 8:30 a.m. and 2:00 p.m., in a working day and under dry weather conditions. Data was obtained from ten two-lane rural road segments, with no main intersections and with a high lateral clearance. All road segments presented a low to medium traffic volume in order to reduce the impact on traffic conditions as well as ensuring a significant sample size. Heavy traffic volume was also low. Longitudinal grades ranged from -6.3% to +5.7%. Lane widths varied from 3.4 m to 3.65 m, shoulder widths from 0.15 m to 1.5 m and posted speed limits varied from 60 km/h to 80 km/h.

The data collection process consisted on determining a road segment by means of two checkpoints, separated by several kilometers. Drivers entering the road segment were asked to participate in the project. In such case, a 1 Hz GPS device was placed on the vehicle and the vehicle was released in order to get to the other checkpoint. Drivers were also told that the collected data was going to be used for researching purposes, not for enforcement, and thus they were encouraged to drive as they usually do. The device was later removed at the second checkpoint.

To ensure drivers' unbiasedness due to the data collection, it was necessary to check whether the operating speed differed significantly during the test and at normal conditions. Therefore, at three road segments, two spot speed measurements were taken, during the test and a few days before. Those speed measurements were obtained by means

of video recording, far away from drivers' line of sight. Results showed that drivers were no biased by the presence of GPS devices (Pérez-Zuriaga et al. 2010 and Pérez-Zuriaga et al. 2013).

37 tangent-to-curve transitions were identified from those ten road segments. Only clear transitions were selected, discarding all cases where the desired speed might not have being fully developed. This selection was carried out after an in-depth analysis of the operating speed profiles for all drivers. Vehicles travelling at non-free-flow conditions were also discarded from the analysis (Pérez-Zuriaga et al. 2013). The number of vehicles at each tangent-to-curve transition ranged from 24 to 102. Totally, 2479 vehicles were part of the study.

At the selected transitions the curve radii varied from 52 m to 519 m; the curve length from 93 m to 333 m (including circular curve and transition curves); the deflection angle from 11.41 grad to 122.64 grad (10.269 degrees to 110.376 degrees); and the approaching tangent length from 6 m (with a previous curve with large radius) to 1548 m. In all cases, there exists a spiral transition between the tangent and the circular curve. Those transition curves are the Euler spiral, which is also known as clothoid. The parameters of the clothoids ranged from 49 m and 231 m.

ΔV_{85} vs $\Delta_{85}V$

One of the most used methods for determining design consistency is based on the calculation of drivers' operating speed on both the curve and the tangent sections, being its subtraction the speed differential value. However, according to Hirsh (1987) and McFadden and Elefteriadou (2000), speed distributions differ from the curve to the tangent. Thus, the simple subtraction of the operating speed values is not valid. Even before considering the previous assumption, the driver corresponding to the "85th percentile behavior" may not remain the same for both elements.

Continuous speed profile allow to clearly determine the initial and final points of the speed transitions, as well as their corresponding speeds. It was performed for all drivers and transitions. The 85th percentile of the operating speed was also obtained. Thus, in the present research, the speed differential (ΔV_{85}**)** was calculated for each transition as the 85th percentile of the difference between the operating speed on the preceding tangent and the operating speed on the curve. Besides, ΔV was calculated for each individual vehicle using their individual speed at beginning and ending points of its deceleration. Then, the parameter $\Delta_{85}V$ (85th percentile speed differential) was calculated as the differential speed not exceeded by 85% of the drivers traveling under free-flow conditions. The relationship between

both parameters can be determined by Equation 1 (R^2=0.90), from data shown in Fig. 1. The statistical analysis results are shown at table 3.

$$\Delta_{85}v = 5.3072 + 0.9092 \cdot \Delta v_{85} \quad (1)$$

Based on the observations performed in this study, it can be concluded that the simple subtraction of operating speeds underestimates the actual values of the speed differential. The difference between both indicators remains almost constant, about 5 km/h. This conclusion is similar to those obtained by McFadden and Elefteriadou (2000) and Misaghi and Hassan (2005).

Besides, the individual operating speed difference was calculated for all vehicles, and the speed differential not exceeded by the 85% of the drivers was determined for all transitions. A model depending on the curve radius has been determined (Equation 2, R^2=0.63), with the statistics shown at table 3.

$$\Delta_{85}v = 9.051 + \frac{1527.328}{R} \quad (2)$$

As can be seen (Fig. 2), the 85th percentile of the speed reduction in a tangent-to-curve transition behaves asymptotically, being higher for sharper curves. At this figure, an outlier was identified. This point was not considered in the developed speed model because of its anomalous behavior, which is thought to be influenced by other variables not considered in the research.

We can observe some issues:

- In all the cases examined, the minimum 85th percentile of the operating speed reduction in the transition is higher than 10 km/h. Considering Lamm's Consistency Criterion II (Lamm et al. 1995), the classification for all curves would be fair or poor. It doesn't mean that all isolated curves are inconsistent. Those results are owing to the fact that, in this study, only curves with radii lower than 600 m and long approaching tangents have been considered, in order to better study the deceleration phenomenon.
- As stated above, the difference between the 85th percentile of the speed reduction and the reduction of operating speeds is around 5 km/h. Hence, if we consider the operating speed reduction, a high number of curves would change their classification from fair to good consistency (according to Lamm's Criterion II).

DECELERATION STUDY

The study of the deceleration process includes not only the development of a model to estimate the deceleration rates through geometric parameters, but also the evaluation of the deceleration length.

Deceleration model

The deceleration model tries to complete the operating speed profile model, reflecting as accurately as possible the drivers' behavior in a tangent-to-curve transition. This problem is generally solved by using deceleration rates, obtained by Equation (3).

$$d = \frac{V_{85(i)}^2 - V_{85(i+1)}^2}{2D} \quad (3)$$

where $V_{85\,(i)}$ and $V_{85\,(i+1)}$ - operating speeds in locations (i) and (i+1); D - distance between locations (i) and (i+1).

However, according to Bella (2008) the deceleration rate calculated on the basis of the individual driver behavior is significantly higher than the one obtained from the operating speed profiles. Consequently, the methodology for the determination of the deceleration rate on the basis of the operating speeds leads to an underestimation of the deceleration and acceleration rates effectively experienced by the drivers.

Taking into account these considerations, the value of the deceleration rate in the tangent-to-curve transition was calculated based on individual driver speed profile by Equation (4).

$$d_i = \frac{V_{T(i)}^2 - V_{C(i)}^2}{2D} \quad (4)$$

where $V_{T\,(i)}$ – individual speed at the beginning point of deceleration, usually in the tangent; $V_{C\,(i)}$ – individual speed at the ending point of deceleration, usually in the curve; D - distance between the beginning and the ending point of deceleration. Normally, the operating speed profiles behave sharply, sometimes making the deceleration starting and ending points difficult to be found. A 20 meters moving average operating speed profile was used in order to better determine when the driver clearly performed the speed transition. This was visually determined for all drivers and transitions. In almost all cases, speed transitions behaved in a linear way, making it easy for the researcher to identify both the initial and final points of the speed transitions.

Once the decelerations of individual drivers have been obtained, the value of the 85th percentile (d_{85}) was determined for each configuration and a correlation analysis was performed in order to determine which independent variables are correlated to this rate. An ANOVA analysis revealed that a positive and strong correlation exists between d_{85} and the inverse of radius (p-value = 0.00).

Based on the values of d_{85} calculated from the individual speed profiles and on the results of the correlation analysis, a model that predicts the expected deceleration rate was developed. The regression analysis yielded the model shown in Fig. 3, which considers radius as the explanatory variable, being R^2 equal to 0.68 (Table 3, Equation 5).

Since the model estimates the deceleration rate when a vehicle enters a horizontal curve that increases as radius decreases, the model appears to be congruent.

$$d_{85} = 0.447 + \frac{90.472}{R} \quad (5)$$

As can be seen, deceleration rates for sharp curves are higher, showing that drivers tend to reduce their speed by a steeper braking maneuver than for smoother curves. As stated above, the 85th percentile of the individual operating speed reduction behaves in a similar way, being the speed reduction for sharp curves higher than for smooth curves.

Other variables such as CCR (Curvature Change Rate), deflection angle, tangent length or curve length were discarded because of their low regression coefficients, compared to the radius' coefficient (Table 4). This indicates that the most important geometric variable related to the deceleration rate is the curve radius.

The influence of the posted speed limit on the deceleration rate was also examined, but no relationship was found.

However, the parameter of the transition curve (*A*) also presents a high correlation to deceleration rate. This parameter is defined as the square root of the product between the length of the transition curve and the radius of the adjacent circular curve. This model is shown in Fig. 4, being R^2 equal to 0.70 (Table 3, Equation 6).

$$d_{85} = 0.173 + \frac{86.401}{A} \quad (6)$$

Deceleration length

In the study of deceleration phenomenon it is not only important to consider the deceleration rates, but the deceleration length and its location as well. Thanks to the continuous speed profiles observed for each individual trajectory, the individual deceleration length has been obtained. This analysis produced the different types of deceleration showed in Table 5 with the corresponding percentage of appearance on the collected data (the percentage of appearance for the rest of cases is less than 1%). In most cases, the deceleration is developed in both the tangent and the curve. In fact, the most common behavior is starting on the tangent and finishing inside the curve (77.23% of all cases). Only in 1.12% of the cases the deceleration begins after the first spiral curve.

The deceleration length distribution was seen to have a lot of variation regardless of the geometric characteristics of the horizontal curve. Several variables, such as curve radius, curve length, deflection angle, tangent length, tangent operating speed, and their combinations were studied, but accurate models were not found. It seems that decelerating behavior depends more on driver characteristics (such as age, gender, purpose of the trip, distance traveled, etc.) rather than on the tangent-to-curve transition design.

However, the study of individual decelerations found out that the average percentage of deceleration length that takes place in the tangent is 45.7%; 42.7% in the first spiral curve; 7.4% in the circular curve; 3.3% in the second spiral curve; and 0.7% in the next tangent. By considering only the individual decelerations that begin in the previous tangent or in the first spiral curve, the last percentages decrease considerably.

The same study has been carried out only for the driver that presents the 85^{th} higher deceleration rate (85^{th} percentile of deceleration) for each transition. In that case, the average percentage of deceleration length that takes place in the tangent is 44.8%; 48.3% in the first spiral curve; 4.3% in the circular curve; 2.5% in the second spiral curve; and 0% in the next tangent.

According to these results, it can be assumed that the 45% of deceleration takes place in the approaching tangent and 55% in the curve. These results should be considered for further development of operating speed profiles.

DISCUSSION

Previous research assumed that the operating speed remains constant throughout the circular curve and that the deceleration occurs entirely on the approaching tangent. Thanks to the observed continuous speed profiles these assumptions have been checked.

Fitzpatrick et al. (1999) stated that in estimating average acceleration or deceleration rates, two possible approaches emerged, related to the distances across which these rates are to be measured. The first approach estimates the average acceleration and deceleration rates occurring outside the limits of the curve and for 200 m on either side of it. This approach is consistent with the assumption that the speed through the horizontal curve is constant; however, it does not consider the possibility that acceleration and/or deceleration may occur over different distances and locations at each site. The second approach would be to estimate the maximum acceleration and deceleration rates for each site, regardless of the distance over which these occurred.

According to that, both approaches were examined for all trajectories, and the following four tests were carried out:

- Test whether the rate of deceleration calculated with speed data 200 m before the beginning of the curve, the speed data at the beginning of the curve, and 200 m deceleration length ($d_{200start}$) is significantly different from the deceleration obtained from the continuous speed profiles (d).
- Test whether the rate of deceleration calculated with speed data at 200 m before the beginning of the curve, the speed data at the curve's midpoint, and the distance between these points as deceleration length ($d_{200middle}$) is significantly different from the deceleration obtained from the continuous speed profiles (d).
- Test whether the rate of deceleration calculated with speed data at 100 m before the beginning of the curve, the speed data at the beginning of the curve, and 100 m deceleration length ($d_{100start}$) is significantly different from the deceleration obtained from the continuous speed profiles (d).
- Test whether the rate of deceleration calculated with speed data at 100 m before the beginning of the curve, speed data at the curve's midpoint, and the distance between these points as deceleration length ($d_{100middle}$) is significantly different from the deceleration obtained from the continuous speed profiles (d).

A two-tail t-test with 95 % level of significance was performed for each case and for each trajectory. The results of these t-test (Tables 6 and 7) showed that the deceleration rates obtained from the four aforementioned approaches were significantly lower than those directly obtained from the operating speed profiles. That occurs for all the tangent-to-curve transitions except the case that estimates the rate of deceleration from 100 m before the beginning of the

curve to the beginning of the curve and from 100 m before the beginning of the curve to the curve's midpoint in the transition with the radius of the curve of 519 m. This curve is the one which has been identified as an outlier in the study of speed reductions.

So, it can be concluded that those approaches result in lower average deceleration rates than the actual one.

A similar analysis was also carried out for the evaluation of the location of the point where deceleration finishes. The aim is to compare it to the singular points of the transition, so that the location of the speed data collector would be defined for further research, if there is no possibility of obtaining continuous speed profiles. Five tests have been performed:

a. Test whether the end of deceleration point is significantly different from the beginning of the first transition curve.
b. Test whether the end of deceleration point is significantly different from the midpoint of the first transition curve.
c. Test whether the end of deceleration point is significantly different from the beginning of the circular curve.
d. Test whether the end of deceleration point is significantly different from the midpoint of the circular curve.
e. Test whether the end of deceleration point is significantly different from the end of the circular curve.

A t-test was performed for each case and for each single trajectory. The results of these t-tests (Table 8) showed that all were significantly different. Some important conclusions were obtained:

- The difference of the location between the end of deceleration point and the midpoint of the curve is statistically different from 0 m, which indicates that from a statistical point of view, they are located at different places. Therefore, the research on the deceleration phenomenon where the data collection takes place at the midpoint of the curve is inaccurate.
- The difference of the location between the end of deceleration point and the beginning point of transition curve is significantly positive. The same conclusion has been observed in the comparison between the end of deceleration point and the midpoint of transition curve. Besides, the differences of the location between the end of deceleration point and the beginning point of circular curve, the

midpoint of circular curve and the end point of circular curve, are significantly negative. Therefore, the end of deceleration appears at the second half of the transition curve. Thus, in case of spot data collection, the location of the data collector to get the speed at the end of deceleration should be between the midpoint of transition curve and the beginning point of circular curve.

- However, the corresponding standard deviation presents a high value. It indicates that, although, considering all the trajectories, the average behavior could be assumed similar, there is a high dispersion, indicating that there may be a large difference between the speeds on that point.

A similar study has been carried out regarding the beginning point of the deceleration. The performed tests are:

a. Test whether the beginning of deceleration point is significantly different from the point placed 100 m before the beginning of the first transition curve.
b. Test whether the beginning of deceleration point is significantly different from the point placed 70 m before the beginning of the first transition curve.
c. Test whether the beginning of deceleration point is significantly different from the point placed 50 m before the beginning of the first transition curve.

The results of these t-tests (Table 9) showed that the beginning of deceleration point is significantly higher than the point placed 100 m before the beginning of the first transition curve and significantly lower than the point placed 50 m before the beginning of the first transition curve, so the beginning of deceleration takes place between those points. However, the beginning of deceleration point is not significantly different from the point placed 70 m before the beginning of the first transition curve. Thus, in case of spot data collection, the location of the data collector to obtain the speed at the beginning of deceleration should be 70 m before the beginning of the first transition curve. Despite this result, it has to be considered that, in this case, the corresponding standard deviation also presents a high value.

Finally, the speed profiles of the drivers corresponding to the 85^{th} percentile of deceleration rate have been drawn for some tangent-to-curve transitions, from 200 m before the beginning point of transition curves. Fig. 5a represents the speed profile for some studied curve with a radius lower than 200 m, while Fig. 5b shows the speed profile for some studied curve with a radius higher than 200 m.

As can be seen, at curves with radius lower than 200 m the minimum speed in the curve is maintained only in a reduced section. At the speed profiles for curves with radius higher than 200 m, speeds are higher and the speed transitions are smoother, as expected. In this case, the lowest speed is maintained during a higher length in the curve.

CONCLUSIONS

This paper presents the results of the analysis of the operating speed variation along 37 tangent-to-curve transitions. A large sample size was obtained by setting some GPS devices on passenger cars, by means of a methodology presented by Pérez-Zuriaga et al. (2010). In all the transitions, the desired speed was reached in the tangent section.

The operating speed reduction was examined, not only considering the operating speed profiles, but also all the individual trajectories. As previous researchers stated, the 85% of the speed reduction not exceeded by drivers is higher than the operating speed difference obtained by considering only the tangent and curve operating speed. Two models were obtained: one comparing both indicators, which stated that the $\Delta_{85}v$ was about 5 km/h higher than Δv_{85}, and another one which estimated $\Delta_{85}v$ depending on the curve radius. Considering this variable, all the analyzed transitions showed speed reductions higher than 10 km/h, leading to fair or poor consistency (considering Lamm's Consistency Criterion II). These inconsistencies may not be detected by considering the variable Δv_{85}, because it underestimates the speed reduction about 5 km/h.

By considering all decelerations obtained individually for all drivers, the 85th percentile of all of them was determined, ranging between 0.3 and 1.7 m/s^2, and two regression models were calibrated. The first model has the radius of circular curve as explanatory variable, while the second model depends on the shape of the transition curve represented by the parameter A. Both models behave asymptotically.

The deceleration length and the position of the minimum speed point in the curve were studied. It was found that the hypothesis that the speed reduction takes place only before the curve is only true in 8.35% of the cases. The deceleration lengths were compared to the transition geometric characteristics, but no significant results were found, which leads to the conclusion that behavior depends more on driver's characteristics than on transition geometry.

Finally, a discussion in order to identify the validity of some assumptions made by previous research was carried out.

It has been proven that the calculation of deceleration rate from 100 m or 200 m before the beginning of the curve to the beginning of the curve or the curve's midpoint results in lower deceleration rate than the actual one.

The analysis of the location of the beginning and the end of deceleration shows that the best approach for the location of speed spot data collectors is 70 m before the beginning of the first transition curve, as beginning of deceleration, and at the second half of the first transition curve, as end of deceleration. However, the high value of the corresponding standard deviation has to be taken into account.

Acknowledgments

Authors would like to thank Center for Studies and Experimentation of Public Works (CEDEX) of the Spanish Ministry of Public Works that partially subsidizes the research. We also wish to thank to the Infrastructure and Transportation Department, General Directorate of Public Works, Valencian Government, Spain, Valencian Provincial Council and to the Ministry of the Interior, General Directorate of Traffic, Spain, for their cooperation in field data gathering.

References

Bella, F. (2007). "Parameters for evaluating speed differential: contribution using driving simulator." *86th Annual Meeting of the Transportation Research Board*, Washington D.C., U.S.A.

Bella, F. (2008). "Assumptions of operating speed-profile models on deceleration and acceleration rates: verification in the driving simulator." *87th Annual Meeting of the Transportation Research Board*, Washington D.C., U.S.A.

Camacho-Torregrosa, F.J., Pérez-Zuriaga, A.M., and García, A. (2010). "Mathematical model to determine road geometric consistency in order to reduce road crashes." *Proc., Mathematical Models of Addictive Behaviour, Medicine & Engineering,* Valencia, Spain.

Castro, M., Sánchez, J.F., Sánchez, J.A., and Iglesias, L. (2011). "Operating speed and speed differential for highway design consistency." *Journal of Transportation Engineering*, *ASCE* 137 (11), 837-840.

Collins, K.M., and Krammes, R.A. (1996). "Preliminary validation of a speed-profile model for design consistency evaluation." *Transportation Research Record: Journal of the Transportation Research Board,* 1523, 11 - 21.

Dell'Acqua, G., and Russo, F. (2010). "Speed factors on low-volume roads for horizontal curves and tangents." *The Baltic Journal of Road and Bridge Engineering,* 5(2), 89-97.

Figueroa, A.M., and Tarko, A.P. (2007). "Speed changes in the vicinity of horizontal curves on two-lane rural roads." *Journal of Transportation Engineering, ASCE,* 133(4), 215-222.

Fitzpatrick, K., Elefteriadou, L., Harwood, D. W., Collins, J. M., McFadden, J., Anderson, I., Krammes, R. A., Irizarry, N., Parma, K. D., Bauer, K. M., and Passetti. K. (1999). "Speed prediction for two-lane rural highways." *Draft Report FHWA-RD-99-171. FHWA*, U.S. Department of Transportation.

Fitzpatrick, K., and Collins, J. (2000). "Speed-profile model for two-lane rural highways." *Transportation Research Record: Journal of the Transportation Research Board,* 1737, 42-49.

Hirsh, M. (1987). "Probabilistic approach to consistency of highway alignment." *Journal of Transportation Engineering, ASCE,* 113(3), 268-276.

Hu, W., and Donnel, E.T. (2010). "Models of acceleration and deceleration rates on a complex two-lane rural highway: results from a nighttime driving experiment", *Transportation Research Part F: Traffic Psychology and Behaviour,* 13(6), 397-408.

Lamm, R., Choueiri, E. M., and Hayward, J. C. (1988). "Tangent as an independent design element." *Transportation Research Record: Journal of the Transportation Research Board,* 1195, 123-131.

Lamm, R., Guenther, A. K., and Choueiri, E. M. (1995). "Safety module for highway geometric design." *Transportation Research Record: Journal of the Transportation Research Board,* 1512, 7-15.

Marchionna, A., and Perco, P. (2007). "Operating speed-profile prediction model for two-lane rural roads in the Italian context." *International Conference Road Safety and Simulation,* Rome, Italy.

McFadden, J., and Elefteriadou, L. (2000). "Evaluating horizontal alignment design consistency of two-lane rural highways: Development of new procedure." *Transportation Research Record: Journal of the Transportation Research Board,* 1737, 9-17.

Misaghi, P., and Hassan, Y. (2005). "Modeling operating speed and speed differential on two-lane rural roads." *Journal of Transportation Engineering, ASCE,* 131(6), 408-417.

Ottesen, J.L., and Krammes, R.A. (2000). "Speed profile model for a design consistency evaluation procedure in the United States." *Transportation Research Record: Journal of the Transportation Research Board,* 1701, 76-85.

Park, P.Y., Miranda-Moreno, L.F., and Saccomanno, F.F. (2010). "Estimation of speed differentials on rural highways using hierarchical linear regression models." *Canadian Journal of Civil Engineering,* 37 (4), 624-637.

Pérez-Zuriaga, A. M., García García, A., Camacho-Torregrosa, F. J., and D'Attoma, P. (2010). "Modeling operating speed and deceleration on two-lane rural roads with Global Positioning System data." *Transportation Research Record: Journal of the Transportation Research Board,* 2171, 11-20.

Pérez-Zuriaga, A. M., Camacho-Torregrosa, F. J., Campoy-Ungría, J.M. , and García García, A. (2013). "Application of GPS and questionnaires data for the study of driver behaviour on two-lane rural roads." *IET Intelligent Transport Systems,* in press.

Yang, L., and Hassan, Y. (2008). “Driver speed and acceleration behavior on Canadian roads.” *87th Annual Meeting of the Transportation Research Board*, Washington, D.C., U.S.A.

Figure captions:

Fig 1: Relationship between $\Delta_{85}V$ and ΔV_{85}.

Fig 2: $\Delta_{85}V$ model with radius of horizontal curve as independent variable.

Fig 3: Deceleration model with radius of horizontal curve as independent variable.

Fig 4: Deceleration model with parameter of transition curve as independent variable.

Fig 5: Speed profiles of the drivers corresponding to the 85^{th} percentile of deceleration rate, for curves with radius lower than 200 m (a) and higher than 200 m (b).

Table captions:

Table 1. Deceleration models with curve radius as independent variable.

Table 2. Speed differential models.

Table 3. Statistical analysis results for developed models.

Table 4. Statistical analysis results for rejected deceleration models.

Table 5. Different types of deceleration, classified depending on their beginning and ending points.

Table 6. Statistical results for t-test analysis of deceleration rate approaches, considering the beginning point of the deceleration 200 m before the beginning of the curve ($d\text{-}d_{200start}$ and $d\text{-}d_{200middle}$).

Table 7. Statistical results for t-test analysis of deceleration rate approaches, considering the beginning point of the deceleration 100 m before the beginning of the curve ($d\text{-}d_{100start}$ and $d\text{-}d_{100middle}$).

Table 8. Statistical results for t-test analysis of end point of deceleration.

Table 9. Statistical results for t-test analysis of beginning point of deceleration.

Table 1. Deceleration models with curve radius as independent variable

Author(s)	Models	
Fitzpatrick and Collins (2000)	$R \geq 436$	$d = 0.00$
	$175 \leq R \leq 436$	$d = 0.6794 - \frac{295.14}{R}$
	$R < 175$	$d = 1.00$
Marchionna and Perco (2007)	$d = 1.757 - 0.222 \cdot Ln(R)$	
Bella (2008)	$85dec = -1.316 + \frac{148}{R} + 0.015 \cdot V_{85\,\max at}$	

Note: d: deceleration rate (m/s^2); R: curve radius (m); $V_{85\ max\ at}$: maximum operating speed on approach tangent (km/h)

Table 2. Speed differential models

Author(s)	Models
Misaghi and Hassan (2005)	$\Delta_{85}V = -83.63 + 0.93 \cdot V_T + e^{-8.93+\frac{3507.10}{R}}$
	$\Delta_{85}V = -198.74 + 21.42 \cdot \sqrt{V_T} + 0.11 \cdot DFC - 4.55 \cdot SW - 5.36 \cdot (curve\_dir) + 1.30 \cdot G + 4.22 \cdot (drv\_flag)$
Castro et al. (2011)	$\Delta_{85}V = -82.359 + 0.009 \cdot R + 9.946 \cdot \sqrt{V_T} + e^{-8.232+0.223 \cdot \Omega}$
Bella (2007)	$85MSR_{t-c} = -0.198 + 0.037 \cdot L + \frac{7929.37}{R}$
	$85MSR_{t-c} = -77.74 + 0.711V_{85P200} + 0.01 \cdot L + \frac{6113.89}{R}$
	$85MSR_{t-c} = -83.48 + 0.782 \cdot V_{85P200} + \frac{6016.15}{R}$

Note: R: curve radius (m); V_T: approach tangent speed (km/h); V_{85P200}: 85th percentile of speed at 200 m prior to the beginning of the curved section (km/h); DFC: deflection angle of circular curve (degrees); SW: shoulder width (m); curve_dir: curve direction (right-turn: curve_dir=1; left-turn: curve_dir=0); G: vertical grade (%); drv_flag: driveway flag (intersection on curve: drv_flag=1; otherwise: drv_flag=0); L: tangent length (m); Ω: deflection angle of the curve (degrees)

Table 3. Statistical analysis results for developed models

	Parameter	Estimate	Standard Error	t Statistic	P-Value
Equation 1	Constant	5.3071	0.8284	6.4059	0.0000
	Δv_{85}	0.9092	0.0493	18.4353	0.0000
Equation 2	Constant	9.0513	1.4742	6.1397	0.0000
	1/R	1527.3280	197.358	7.7388	0.0000
Equation 5	Constant	0.4469	0.0766	5.8327	0.0000
	1/R	90.4721	10.3912	8.7065	0.0000
Equation 6	Constant	0.1735	0.0992	1.7476	0.0893
	1/A	86.4012	9.3715	9.2195	0.0000

Table 4. Statistical analysis results for rejected deceleration models

Parameter	Estimate	Standard Error	t Statistic	P-Value	R^2
Constant	0.5527	0.0763	7.2429	0.0000	0.613
CCR	0.0019	0.0002	7.4460	0.0000	
Constant	0.6341	0.0994	6.3793	0.0000	0.382
Deflection angle	0.0099	0.00213	4.6584	0.0000	
Constant	1.0745	0.1154	9.30465	0.0000	0.009
Tangent length	-0.0001	0.0001	-0.5762	0.5681	
Constant	1.6321	0.2024	8.0622	0.0000	0.222
Curve length	-0.0035	0.0011	-3.1659	0.0032	

Table 5. Different types of deceleration, classified depending on their beginning and ending points.

Case	T1	SC1	CC	SC2	T2	%
1 – Starts before curve and ends at first spiral curve	X	X				37.55%
2 – Starts before curve and ends at circular curve	X	X	X			24.68%
3 – Starts before curve and ends at second spiral curve	X	X	X	X		15.00%
4 – Totally at tangent before curve	X					8.35%
5 – Starts at first spiral curve and ends at second spiral curve		X	X	X		4.55%
6 – Starts at first spiral curve and ends at circular curve		X	X			4.47%
7 – Totally at spiral curve before circular curve		X				2.78%

Note: T1: Tangent before curve; SC1: Spiral curve before circular curve; CC: Circular curve; SC2: Spiral curve after circular curve; T2: Tangent after curve.

Table 6. Statistical results for t-test analysis of deceleration rate approaches, considering the beginning point of the deceleration 200 m before the beginning of the curve (d-$d_{200start}$ and d-$d_{200middle}$).

		d-$d_{200start}$				d-$d_{200middle}$			
	Radius (m)	sample mean	Simple std. deviation	t statistic	p-value	sample mean	Simple std. deviation	t statistic	p-value
1	102	0.625	0.552	9.193	0	0.442	0.399	9.006	0
2	158	0.566	0.345	13.346	0	0.534	0.297	14.585	0
3	100	0.795	0.461	13.997	0	0.757	0.410	15.003	0
4	52	0.903	0.418	17.269	0	0.818	0.357	18.307	0
5	142	0.580	0.387	12.075	0	0.562	0.347	13.049	0
6	275	0.483	0.346	11.765	0	0.518	0.336	12.971	0
7	76	0.986	0.436	20.730	0	0.910	0.384	21.703	0
8	328	0.395	0.314	12.444	0	0.416	0.313	13.159	0
9	324	0.466	1.095	4.304	0.0000	0.465	1.103	4.261	4.5E-05
10	297	0.204	0.152	12.840	0	0.195	0.132	14.137	0
11	256	0.141	0.168	7.795	2.7E-07	0.134	0.112	11.102	0
12	297	0.173	0.179	8.981	3.3E-07	0.153	0.184	7.703	2.5E-07
13	256	0.196	0.277	6.340	2.5E-07	0.207	0.266	6.960	2.6E-07
14	443	0.221	0.198	10.570	0	0.200	0.196	9.667	0
15	242	0.363	0.340	9.197	0	0.343	0.247	11.937	0
16	97	0.545	0.452	9.405	0	0.479	0.378	9.876	0
17	87	0.719	0.614	9.515	0	0.646	0.555	9.456	0
18	194	0.426	0.392	7.537	1.2E-09	0.415	0.346	8.321	8.4E-11
19	97	0.697	0.482	13.561	0	0.642	0.456	13.201	0
20	327	0.155	0.136	10.648	0	0.150	0.111	12.639	0
21	519	-0.291	0.266	-10.317	0	0.268	0.191	13.278	0
22	409	0.465	0.760	4.538	3.2E-05	0.447	0.728	4.558	2.9E-05
23	236	0.490	0.452	9.333	0	0.558	0.445	10.783	0
24	105	0.752	0.472	10.685	0	0.753	0.445	11.350	0
25	83	0.542	0.493	9.454	0	0.538	0.456	10.148	0
26	105	0.466	0.522	4.378	0.0002	0.463	0.445	5.094	3.6E-05
27	138	0.269	0.272	5.400	8.3E-06	0.261	0.236	6.062	1.3E-06
28	125	0.595	0.273	15.373	0	0.472	0.209	15.923	0
29	151	0.780	0.464	11.875	0	0.702	0.385	12.879	0
30	484	0.056	0.107	3.454	0.0012	0.120	0.172	4.591	0.00003
31	260	0.376	0.361	8.510	3.2E-12	0.369	0.306	9.870	0
32	208	0.445	0.354	10.511	0	0.428	0.338	10.610	0
33	189	0.341	0.334	7.970	5.5E-11	0.353	0.280	9.861	0
34	149	0.509	0.266	14.699	0	0.489	0.253	14.844	0
35	260	0.466	0.364	9.064	4.7E-12	0.421	0.344	8.656	1.9E-11
36	208	0.466	0.287	11.722	0	0.434	0.236	13.239	0
37	189	0.356	0.199	11.684	0	0.366	0.182	13.148	0

Table 7. Statistical results for t-test analysis of deceleration rate approaches, considering the beginning point of the deceleration 100 m before the beginning of the curve ($d\text{-}d_{100start}$ and $d\text{-}d_{100middle}$).

		$d\text{-}d_{100start}$				$d\text{-}d_{100middle}$			
	Radius (m)	**sample mean**	**Simple std. deviation**	**t statistic**	**p-value**	**sample mean**	**Simple std. deviation**	**t statistic**	**p-value**
1	102	0.723	0.540	10.880	0	0.586	0.470	10.115	0
2	158	0.470	0.354	10.784	0	0.417	0.293	11.569	0
3	100	0.448	0.374	9.724	0	0.567	0.336	13.729	0
4	52	0.563	0.395	11.402	0	0.550	0.309	14.235	0
5	142	0.390	0.334	9.407	0	0.466	0.281	13.343	0
6	275	0.409	0.331	10.403	0	0.462	0.328	11.854	0
7	76	0.769	0.469	14.996	0	0.556	0.310	16.408	0
8	328	0.360	0.313	11.389	0	0.402	0.310	12.845	0
9	324	0.312	0.926	3.407	0.0009	0.380	1.014	3.790	0.0002
10	297	0.118	0.170	6.657	2.2E-07	0.146	0.139	10.0723	0
11	256	0.061	0.203	2.786	0.0065	0.082	0.128	5.972	2.9E-07
12	297	0.088	0.202	4.076	0.0001	0.089	0.169	4.870	5.2E-06
13	256	0.110	0.234	4.200	6.9E-05	0.159	0.231	6.176	2.4E-07
14	443	0.157	0.248	6.016	2.6E-07	0.146	0.201	6.928	2.8E-07
15	242	0.262	0.283	7.960	3.6E-07	0.279	0.226	10.609	0
16	97	0.493	0.463	8.324	1.3E-11	0.478	0.372	10.047	0
17	87	0.523	0.538	7.905	3.5E-07	0.478	0.471	8.246	1.0E-11
18	194	0.267	0.344	5.375	2.6E-06	0.303	0.287	7.331	2.5E-09
19	97	0.423	0.431	9.204	3.7E-07	0.438	0.395	10.408	0
20	327	0.059	0.162	3.399	0.0010	0.088	0.103	7.941	6.9E-12
21	519	-1.105	0.367	-28.342	0	0.142	0.187	7.175	2.1E-10
22	409	0.419	0.761	4.080	0.0001	0.406	0.723	4.164	0.0001
23	236	0.393	0.541	6.250	3.0E-07	0.539	0.441	10.513	0
24	105	0.685	0.453	10.132	0	0.551	0.357	10.352	0
25	83	0.345	0.414	7.167	2.6E-07	0.402	0.381	9.067	0
26	105	0.342	0.537	3.123	0.0047	0.377	0.401	4.609	0.0001
27	138	0.177	0.247	3.925	0.0004	0.193	0.184	5.760	3.0E-06
28	125	0.319	0.289	7.817	3.6E-10	0.211	0.186	8.032	1.7E-10
29	151	0.597	0.400	10.545	0	0.519	0.305	12.033	0
30	484	-0.003	0.152	-0.134	0.8935	0.121	0.203	3.929	0.0003
31	260	0.226	0.450	4.123	0.0001	0.278	0.305	7.477	2.2E-10
32	208	0.358	0.388	7.733	3.5E-07	0.356	0.350	8.493	2.5E-12
33	189	0.328	0.320	8.014	4.6E-11	0.352	0.292	9.405	0
34	149	0.355	0.450	6.053	1.1E-07	0.398	0.278	10.987	0
35	260	0.383	0.369	7.329	2.0E-09	0.330	0.340	6.867	3.6E-07
36	208	0.348	0.298	8.427	3.1E-11	0.339	0.230	10.618	0
37	189	0.240	0.211	6.754	3.2E-08	0.301	0.1928	10.2534	0

Table 8. Statistical results for t-test analysis of end point of deceleration.

	sample mean	sample standard deviation	t statistic	p-value
$PS_{\text{end deceleration}} - PS_{\text{start transition curve}}$	64.7185	64.8454	49.662	0
$PS_{\text{end deceleration}} - PS_{\text{middle point of transition curve}}$	29.2118	62.239	23.3545	0
$PS_{\text{end deceleration}} - PS_{\text{start circular curve}}$	-6.2948	61.5375	-5.090	3.59E-07
$PS_{\text{end deceleration}} - PS_{\text{middle point of circular curve}}$	-24.414	60.5508	-20.0629	0
$PS_{\text{end deceleration}} - PS_{\text{end circular curve}}$	-42.6393	64.5093	-32.8899	0

Table 9. Statistical results for t-test analysis of beginning point of deceleration.

	sample mean	sample standard deviation	t statistic	p-value
$PS_{\text{start deceleration}} - PS_{\text{100m before curve}}$	29.1652	81.482	17.8106	0
$PS_{\text{start deceleration}} - PS_{\text{70m before curve}}$	-0.8348	81.482	-0.5098	0.6101
$PS_{\text{start deceleration}} - PS_{\text{50m before curve}}$	-20.8348	81.482	-12.7234	0.00E+00

NEW CONSISTENCY INDEX BASED ON INERTIAL OPERATING SPEED

Corresponding Author:

Alfredo García
Professor
Highway Engineering Research Group, Universitat Politècnica de València
Camino de Vera, s/n. 46022 – Valencia. Spain
Tel: (34) 96 3877374
Fax: (34) 96 3877379
E-mail: agarciag@tra.upv.es

Other Authors:

David Llopis-Castelló
Ph.D. Candidate
Highway Engineering Research Group, Universitat Politècnica de València
Camino de Vera, s/n. 46022 – Valencia. Spain
Tel: (34) 96 3877374
Fax: (34) 96 3877379
E-mail: dallocas@cam.upv.es

Francisco Javier Camacho-Torregrosa
Ph.D. Candidate
Highway Engineering Research Group, Universitat Politècnica de València
Camino de Vera, s/n. 46022 – Valencia. Spain
Tel: (34) 96 3877374
Fax: (34) 96 3877379
E-mail: fracator@cam.upv.es

Ana María Pérez-Zuriaga
Ph.D.
Highway Engineering Research Group, Universitat Politècnica de València
Camino de Vera, s/n. 46022 – Valencia. Spain
Tel: (34) 96 3877374
Fax: (34) 96 3877379
E-mail: anpezu@tra.upv.es

Submission date: March 7th, 2013

Word count:		
	Abstract:	250
	Manuscript:	3960
	Figures: 9 x 250 =	2250
	Tables: 2 x 250 =	500
	TOTAL:	**6960**

Key words: Road safety, design consistency, operating speed, geometric design, inertial operating speed, inertial consistency index.

ABSTRACT

Road crashes occurrence depends on several factors, being the design consistency one of the most important. It refers to the conformance of highway geometry to drivers' expectations.

A new consistency model for evaluating the performance of tangent-to-curve transitions on two-lane rural roads is presented. It is based on the Inertial Consistency Index (ICI), defined for each transition. It is calculated at the beginning point of the curve, as the difference between the average operating speed of the previous 1 km road segment (inertial operating speed) and the operating speed at this point.

88 road segments, which included 1,686 tangent-to-curve transitions, were studied in order to calibrate ICI and its thresholds. The relationship between those results and the crash rate associated to each transition has been analyzed. It has been pointed out that the higher the ICI is, the higher the crash rate is, thus increasing the probability of accidents to take place. Similar results were obtained from the study of the relationship between ICI and the weighted average crash rate of the corresponding group of transitions.

A graphical and statistical analysis established that road consistency may be considered good when ICI is lower than 10 km/h; poor when ICI is higher than 20 km/h; and fair otherwise.

A validation process has been carried out considering 20 road segments. The obtained ICI values were highly correlated to the number of crashes which had occurred at the analyzed transitions. Hence, the Inertial Consistency Index (ICI) and its consistency thresholds resulted in a new approach for consistency evaluation.

INTRODUCTION

Road crashes have three general categories of contributing factors: human factor, vehicle factor and road infrastructure factor. Previous research *(1)* pointed out that the infrastructure factor is responsible for over 30% of road crashes. In fact, collisions tend to concentrate on certain road segments, highlighting that road characteristics play a major role in some accidents.

The influence of road geometric characteristics increases when the geometric design consistency level is low. Road geometric consistency may be defined as how drivers' expectations and road behavior fit. An inconsistent road design surprises drivers, leading to anomalous behavior and possible collisions.

Most of the related research and developed design consistency models focus on four main areas: operating speed and its variations, vehicle stability, alignment indexes and driver workload *(2, 3)*. Among them, the most worldwide used criteria for road design consistency evaluation are based on the operating speed evaluation *(4)*. Operating speed is often defined as the 85th percentile speed (V_{85}) of the distribution of speeds selected by drivers in free-flow conditions. This specific measure of speed can be used in consistency evaluation by examining differences between design speed (V_d) and V_{85} or examining the differences in V_{85} between successive road elements, especially between horizontal curves and previous tangents. In fact, tangent-to-curve transitions are considered the most critical locations since it is estimated that more than 50% of the total fatalities on rural highways take place on curved sections *(5)*.

Leisch and Leisch *(6)* recommended a revised design speed concept that included guidelines on both operating speed reductions and differentials between design and operating speed. In the same way, Kanellaidis et al. *(7)* suggested that a good design can be achieved when the difference between V_{85} on the tangent and on the following curve does not exceed 10 km/h.

However, the most commonly used method to evaluate road consistency was developed by Lamm et al. *(8)*, based on mean accident rates observed at several alignment configurations. They presented two design consistency criteria related to operating speed, which included the difference between design and operating speed (criterion I) and the difference between operating speeds on successive elements (criterion II).

The difference between operating speed and design speed ($|V_{85} - V_d|$) allows the identification of road alignment elements whose design does not fit the general road alignment. It is a good indicator of the consistency on one single element.

The operating speed reduction between two successive elements (ΔV_{85}) indicates the surprises experienced by drivers, making them to reduce their speed, when traveling from one element to the next.

Table 1 summarized the consistency thresholds for criteria I and II. Those thresholds are an approach to the thresholds that determine the need for redesign. However, other authors *(9)* suggested continuous functions instead of consistency thresholds, as a better tool for designers.

The consistency criteria previously presented allow design consistency evaluation on a single road element (the horizontal curve) or at tangent-to-curve transitions. They are usually called local consistency models.

Local consistency models try to identify road inconsistencies by considering that drivers' expectations are failed when operating speed is much higher than design speed; or by assuming that drivers are surprised when the operating speed in a road element is much lower than the previous one.

Hence, drivers' expectations are assumed to be characterized as the design speed of the whole road segment or as the operating speed in the previous element. While in the first case the road segment immediately preceding the inconsistency is not taken into account; in the second one only the previous element is considered.

However, there is no previous research which determines the road segment length necessary for producing *ad hoc* expectations, which may be compared to road design geometry.

Other studies, such as the one carried out by Polus and Mattar-Habib *(10)*, Cafiso et al. *(11)* and Camacho-Torregrosa et al. *(12)*, are based on continuous speed profiles. They studied the global speed variation along a road segment, as a function of several indexes, and determined a single consistency value for the whole road segment. Moreover, their design consistency index is a continuous function instead of being based on ranges.

Those global consistency models are less used than local ones due to the difficulty of continuous operating speed estimation.

Finally, it is important to highlight that each consistency model was calibrated at a specific geographic environment and that drivers' behavior may change from one region to other. Therefore, the extrapolation of those models or thresholds should be carefully carried out. In fact, further test for the applicability of Lamm's criteria revealed that a 20 km/h limit for poor design is applicable to Korea *(13)*, but a different limit was recommended for Italy *(14)*.

Taking into account the previous considerations, this paper presents a new model for consistency evaluation of two-lane rural roads. It is based on the comparison of *ad hoc* drivers' expectations and road design geometry, since it is the definition of road consistency.

OBJECTIVES AND HYPOTHESES

The main objective of this study is the development of a new index for two-lane rural road design consistency evaluation that allows including drivers' expectations within the analysis.

This development is based on the hypothesis that drivers' expectations at one point station can be estimated as the average operating speed at the previous road segment. This speed parameter is called inertial operating speed ($V_{85\ inertial}$). According to this hypothesis, the difference between inertial operating speed and operating speed shows the discordance between drivers' expectations and road alignment.

DATA DESCRIPTION

Tangent-to-curve transitions are the most conflictive points of a road alignment. In fact, Lamm et al. *(5)* estimated that more than 50 % of fatal accidents occur on rural roads on those locations. This is why the proposed consistency model is focused on those transitions.

For its development, 88 two-lane rural road segments from the Valencian region (Spain) were evaluated, identifying 1,686 tangent-to-curve transitions. The length of the road segments ranged from 2.0 km to 15.5 km, being their longitudinal grades between -3 % and 3 %. None of the selected road segments presented important intersections that could significantly vary traffic volumes, operating speeds and number of crashes.

Traffic volume

Traffic volume data was downloaded from the official website of the Valencian local road administration. It consisted on AADT data for the last 15 years, but only data from 2001 to 2010 were used in order to avoid considering of data belonging to road segments that were redesigned or improved during that period of time. The highest traffic volume considered was 25,015 vpd, while the road segment with the lowest AADT presented only 363 vpd.

Crash data

Crash data were also provided by the Valencian local road administration. It consisted on a list of all reported crashes during those years, characterized by point station, date and time, lighting conditions, crash severity, type of vehicle, characteristics of the driver, external factors, causes and other conditions. Considering all data, a filtering process was performed, discarding all property damage only accidents in order to prevent bias due to underreporting problems. Accidents caused by external factors, such as previous illness of the driver or animals crossing the road, were also removed from the analysis.

Thanks to data characterization, crash locations and driving directions were identified. However, the accuracy of crash locations was one hectometer, so relating the crashes to their corresponding tangent-to-curve transition could not be directly performed. It was considered that each accident could have been produced within a range [-50 m, +50 m] from its reported location. An accident is considered to be transition-related if its actual location yields within the curve or 100 beyond, due to kinematic effects. Considering the uncertainty of the accident location, an accident was considered to be transition-related if its reported location is somewhere between 50 m before and 150 m after the corresponding curve.

Continuous operating speed profiles

The operating speed profiles were based on operating speed models developed by Pérez-Zuriaga et al. *(15)*. The operating speed model for curves uses the radius as explanatory variable (Eq. 1 and 2).

$$V_{85\,C} = 97.4254 - \frac{3310.94}{R}; \quad 400m < R \leq 950m \tag{1}$$

$$V_{85\,C} = 102.048 - \frac{3990.26}{R}; \quad 70m < R \leq 400m \tag{2}$$

Where:
$V_{85\,C}$: operating speed on curve (km/h)
R: horizontal curve radius (m)

This model does not consider radius lower than 70 m. However, it was not necessary since none of the road segments presented any curve with radius lower than 70 m.

The developed model for estimating operating speed on tangents considers the length of the tangent and the estimated operating speed of the preceding curve (Eq. 3).

$$V_{85\,T} = V_{85\,C} + \left(1 - e^{-\lambda \cdot L}\right) \cdot (V_{des} - V_{85\,C}) \tag{3}$$

Where:
$V_{85\,T}$: operating speed on tangent (km/h)
$V_{85\,C}$: operating speed on previous curve (km/h)
V_{des}: desired speed (110 km/h)
L: tangent length (m)
$\lambda = 0.00135 + (R - 100) \cdot 7.00625 \cdot 10^{-6}$
R: horizontal curve radius (m)

Considering these models, the operating speed profiles were built, both in forward and backward directions, for all road segments. Some construction rules and deceleration and acceleration rates estimated by Equation 4 and 5 had also to be considered in their construction. Those models were calibrated by Pérez-Zuriaga et al. *(15)* and Camacho-Torregrosa et al. *(12)*, respectively.

$$d_{85} = 0.313 + \frac{114.436}{R} \tag{4}$$

$$a_{85} = 0.41706 + \frac{65.93588}{R} \tag{5}$$

Where:
d_{85}: deceleration rate (m/s^2)
a_{85}: acceleration rate (m/s^2)
R: horizontal curve radius (m)

DEVELOPMENT

Road safety is highly correlated with road design consistency, so every design consistency model should be calibrated considering its relationship to crashes.

The representative index of the proposed model is the difference between inertial operating speed ($V_{85\,\text{inertial}}$), as an estimation of drivers' expectations, and operating speed (V_{85}), as an estimation of road geometry performance. The new index is called inertial consistency index (ICI).

$V_{85\,\text{inertial}}$ was defined as the average operating speed of the previous road segment for each point of the road. It was first necessary to identify which length should be used for constructing this index. This was carried out by means of a sensitivity analysis. The aim of this study was to determine

which road segment length better reflects drivers' behavior. Several road segment lengths were evaluated. The use of road segment lengths lower than 1,000 m led to an inertial operating speed profile slightly smoother than the corresponding operating speed profile, without significant contributions compared to the operating speed profile. At the other extreme, road segment lengths higher than 1,000 m resulted in a too smooth profile, hiding the significant speed variations.

After this evaluation, it was concluded that the most suitable road segment length for this kind of study was 1,000 m. Hence, $V_{85\ inertial}$ was finally defined as the 1,000 m moving average value of the operating speed. Figure 1 shows an example of inertial operating speed profile, both in forward and backward directions.

The next step was to calibrate the relationship between the new consistency index and the corresponding crash rate. The consistency index was determined at the beginning of the curve of each tangent-to-curve transition. In order to establish consistency thresholds, the ICI was also grouped into several intervals and the average crash rates were obtained for all of them.

Crash rate vs ICI

The crash rate of each tangent-to-curve transition was calculated as the quotient between the number of crashes and the total traffic volume in each transition. ICI was also determined for each tangent-to-curve transition. The relationship between those variables is shown in Figure 2.

Figure 2 shows a clear relationship between crash rate and ICI. The higher the ICI is, the higher the crash rate is. However, it was not possible to obtain general conclusions from this graph because of the large amount of data without crashes that may bias results and conclusions.

Weighted average crash rate vs ICI

The second analysis was based on considering the relationship between the ICI and the weighted average crash rate (WACR). Two kinds of graphs were used in this part of the analysis. The first one is shown in Figure 3. ICI values were put into groups of 5 km/h. For each group, the weighted average crash rate was calculated as the quotient between the total number of crashes with a certain interval of ICI, and the total traffic volume of them.

Grey columns reflect the calculated WACR considering all the curves and the black ones correspond to the WACR, previously removing the transitions with no accidents. This data treatment was carried out because of the high amount of data without crashes that could have a serious influence on the results of the analysis.

From the statistical point of view, crashes are rare, random and discrete events. This is why they should be adjusted to a Poisson or a negative binomial distribution. However, this one does not correctly fit to data when there is a high amount of zeros. In this case, zero-crash tangent-to-curve transitions may be associated to a safe transition or to the randomness of the crash phenomenon. There are some methodologies, such as Bayesian analyses, that differentiate between both data groups, improving the results of the analysis.

Nevertheless, this analysis is only useful when a large data sample is available. In this case, data set was not enough to perform this calculation, so a different methodology was carried out. Two different calculations, with and without consideration of blank transitions, were carried out. The real result was assumed to be between both solutions.

A similar graph was plotted setting ICI into groups of 10 km/h intervals (Figure 4). Both graphs showed that WACR increases as ICI does.

Since there is a high proportion of curves without crashes (blank transitions), it was studied, for each interval, its percentage compared to the total number of transitions (Figures 5 and 6).

Figures 5 and 6 show a decreasing trend of the percentage of blank transitions with the ICI. This result points out that the proportion of curves with accidents increases as the difference between inertial operating speed and operating speed does. According to that, it can be concluded that the ICI presents a strong relationship with road safety. Therefore, the increase of the ICI is related to a higher probability of crash occurrence in the tangent-to-curve transition.

Thresholds analysis

Once the relationship between the ICI and road safety was demonstrated, it was necessary to establish the intervals of values of this index where the influence of the road design consistency index on road safety can be considered the same.

So, weighted average crash rate represented in Figure 3 clearly shows a general increasing trend, divided in two minor trends. The first one ranges from -2.5 km/h to 12.5 km/h, while the second one is from 12.5 km/h to 27.5 km/h.

The differences between trends are shown clearer in Figure 4. As can be seen, the trend almost remains horizontal from -10 km/h to 10 km/h and dramatically increases up in the [10; 20] km/h interval. The [20; 30] km/h interval shows even a higher increase.

A statistical analysis was carried out in order to confirm those thresholds. This process was carried out by means of least significant difference (LSD) intervals (Figure 7), comparing different ICI intervals. It can be assumed that two ICI ranges belong to different populations (i.e., different tangent-to-curve behavior) when their intervals do not overlap.

This analysis pointed out that there are statistical significant differences with a 95 % confidence level between tangent-to-curve transitions with ICI between [0; 10] km/h and those with ICI between [10; 20] km/h, and between [0; 10] km/h and [20; 30] km/h as well. Both results were obtained taking into account all the curves, as well as not considering blank curves.

However, the tangent-to-curve transitions where ICI ranges from 10 to 20 km/h and from 20 to 30 km/h seem to belong to the same population. This result is due to small data sample for this interval (15 not-blank tangent-to-curve transitions). This also causes higher crash rate dispersion. It is suggested to increase this sample for further research.

PROPOSED GEOMETRIC DESIGN CONSISTENCY MODEL

As stated previously, the Inertial Consistency Index (ICI) is related to safety and may be used for analyzing safety at tangent-to-curve transitions. Threshold values are defined in Table 2, as obtained before.

As demonstrated above, a higher difference between inertial operating speed (i.e. drivers' expectations) and operating speed (i.e. road geometric design) results in a lower consistency and therefore, a higher crash probability.

VALIDATION

The validation of the proposed model for geometric design consistency evaluation was carried out applying it to other 20 two-lane rural road segments, including 370 tangent-to-curve transitions. Empirical operating speed profiles were used for validation. The corresponding empirical operating speed profiles were obtained by the application of the data collection methodology developed by Pérez-Zuriaga et al. *(15)*. This methodology consisted on asking drivers to install a GPS device, which has strong magnetic points, between two checkpoints belonging to each road segment. Drivers were encouraged to drive as they usually do. This method allowed collection of continuous speed data along a road segment from a great number of individual drivers. Additional tests were performed in order to ensure that drivers were not biased by the presence of the checkpoints or the device *(15)*.

As was expected, tangent-to-curve transitions identified as inconsistent by the ICI model presented a higher crash concentration than the rest within the same road segment. Figure 8 shows the road consistency evaluation and crash locations for one road segment.

In order to improve the validation analysis, a graph comparing ICI with weighted average crash rate (WACR) was performed (Figure 9), including all tangent-to-curve transitions located at the 20 road segments used in this process. Grey columns correspond to WACR considering all the transitions and the black ones correspond to WACR considering only transitions with accidents.

Figure 9 shows an increasing trend of the weighted average crash rate with the difference between the inertial operating speed and the operating speed. In fact, the WACR differences between the intervals of ICI values are even higher than in the model calibration process. The inflection points clearly correspond to the thresholds identified for the consistency model.

CONCLUSIONS

Road safety and, specially, fatal crashes are one of the most important problems in our society. The infrastructure factor is found in 30 % of road crashes occurring on two-lane rural roads. In fact, collisions tend to concentrate on certain road segments, road characteristics playing a major role at some accidents. Besides, tangent-to-curve transitions are considered the most conflictive points as more than 50 % of crashes are located on those sections.

In order to improve road geometric design and road safety evaluation, this paper presents a new design consistency model for evaluating the quality of tangent-to-curve transitions on two-lane rural roads. The proposed model is based on the hypothesis that design consistency may be defined as the difference between drivers' expectations and road alignment behavior.

The road alignment behavior on one station may be estimated by means of the operating speed at that point. Drivers' expectations may be estimated by the inertial operating speed on the same point, defined as the average operating speed of the previous 1 km road segment. The difference between both parameters, called Inertial Consistency Index (ICI), results in a new approach for road consistency evaluation.

The ICI and the associated consistency thresholds were developed studying the operating speed profiles of 44 two-lane rural road segments considering both driving directions, which included 1,686 tangent-to-curve transitions. $V_{85\ \mathrm{inertial}} - V_{85}$ was calculated at the beginning point of the curve of each transition. The relationship between those results and the crash rate associated to each transition from 2001 to 2010 was examined. This relationship pointed out that higher crash rates corresponded to higher ICI values. Therefore, a high ICI is linked to a higher crash probability.

A graphical and a statistical analysis were carried out in order to establish the thresholds of the consistency model. According to these analyses, road alignment consistency at every location may be considered good when ICI is lower than 10 km/h; fair when it is between 10 km/h and 20 km/h; and poor when ICI is higher than 20 km/h.

The proposed consistency model was validated with its application to the empirical operating speed profiles of 20 road segments, which included 370 tangent-to-curve transitions. The obtained ICI values were correlated to the number of crashes occurred at the studied transitions. The validation process pointed out that the transitions with higher ICI value presented more collisions.

ACKNOWLEDGEMENTS

Authors would like to thank Center for Studies and Experimentation of Public Works (CEDEX) of the Spanish Ministry of Public Works that partially subsidizes the data collection for obtaining the empirical operating speed profiles used in the validation process.

Also thank to the General Directorate of Public Works of the Infrastructure and Transportation Department of Valencian Government; Valencian Province Council; and to the General Directorate of Traffic of the Ministry of the Interior of the Government of Spain, for their cooperation in data gathering.

REFERENCES

1. Treat, J.R, Tumbas, N.S., McDonald, S.T., Shinar, D., Hume, R.D., Mayer, R.E., Stansifer, R.L. and Castellan, N.J. *Tri-level study of the causes of traffic accidents: Final report – Executive summary*. Publication DOT-HS-034-3-535-79-TAC(S). Bloommington. Institute for Research in Public Safety, 1979.
2. Ng, J. C. W. and Sayed, T. Effect of Geometric Design Consistency on Road Safety. In *Canadian Journal of Civil Engineering, Vol. 31, No. 2*, National Research Council of Canada, Canada, 2004, pp. 218-227.
3. Awata, M. and Hassan, Y. Towards Establishing an Overall Safety-Based Geometric Design Consistency Measure. Presented at 4th Transportation Specialty Conference of the Canadian Society for Civil Engineering, 2002.
4. Gibreel, G. M., Easa, S.M., Hassan, Y. and El-Dimeery, I.A. State of the Art of Highway Geometric Design Consistency. In *Journal of Transportation Engineering, Vol. 125, No. 4*, American Society of Civil Engineers (ASCE), U.S.A., 1999, pp. 305-313.

5. Lamm, R., Choueiri, E. M. and Mailaender, T. *Traffic safety on two continents—a ten year analysis of human and vehicular involvements*. Proceedings of the Strategic Highway Research Program (SHRP) and Traffic Safety on Two Continents, 1992, pp. 18–20.
6. Leisch, J. E., and Leisch, J. P. New Concepts in Design-Speed Application. In *Transportation Research Record: Journal of the Transportation Research Board, No. 631*, Transportation Research Board of the National Academies, Washington, D.C., 1977, pp. 4–14.
7. Kanellaidis, G., Golias, J., and Efstathiadis, S. Driver's speed behaviour on rural road curves. In *Traffic Engineering and Control*, *Vol. 31(7/8)*, Hemming Group, Greece, 1990, pp. 414–415.
8. Lamm, R., Psarianos, B. and Mailaender, T. *Highway design and traffic safety engineering handbook*. McGraw-Hill Companies, Inc., 1999.
9. Hassan, Y. Highway Design Consistency: Refining the State of Knowledge and Practice. In *Transportation Research Record: Journal of the Transportation Research Board, Vol. 1881*, Transportation Research Board of the National Academies, Washington, D.C., 2004, pp. 63-71.
10. Polus, A. and Mattar-Habib, C. New Consistency Model for Rural Highways and its Relationship to Safety. In *Journal of Transportation Engineering, Vol. 130, No. 3*, American Society of Civil Engineers (ASCE), U.S.A., 2004, pp.286-293.
11. Cafiso, S., Di Graziano, A., Di Silvestro, G., La Cava, G. and Persaud, B. Development of comprehensive accident models for two-lane rural highways using exposure, geometry, consistency and context variables. In *Accident Analysis and Prevention, Vol. 42, No. 4*, Elsevier, 2010, pp. 1072-1079.
12. Camacho-Torregrosa, F. J., Pérez-Zuriaga, A. M., Campoy-Ungría, J.M, and García García, A. New Geometric Design Consistency Model Based on Operating Speed Profiles for Road Safety Evaluation. In *Accident, Analysis and Prevention*, *accepted DOI: 10.1016/j.aap.2012.10.001*, Elsevier Limited, 2012.
13. Lee, S., D. Lee, and J. Choi. *Validation of the 10 MPH Rule in Highway Design Consistency Procedure*. Proceedings of 2nd International Symposium on Highway Geometric Design, Mainz, Germany, 2000, pp. 364–376.
14. Cafiso, S. *Experimental Survey of Safety Condition on Road Stretches with Alignment Inconsistencies*. Proceedings of 2nd International Symposium on Highway Geometric Design, Mainz, Germany, 2000, pp. 377–387.
15. Pérez-Zuriaga, A.M., García, A., Camacho-Torregrosa, F.J. and D'Attoma, P. Modeling operating speed and deceleration on two-lane rural roads with global positioning system data. *Transportation Research Record: Journal of the Transportation Research Board, Vol. 2171*, Transportation Research Board of the National Academies, Washington, D.C., 2010, pp.11-20.

LIST OF TABLES AND FIGURES

1 **TABLE 1 Thresholds for design consistency quality determination. Lamm's criteria I & II.**

Consistency rating	Criterion I (km/h)	Criterion II (km/h)
Good	$\lvert V_{85} - V_d \rvert \leq 10$	$\lvert V_{85\,i} - V_{85\,i+1} \rvert \leq 10$
Fair	$10 < \lvert V_{85} - V_d \rvert \leq 20$	$10 < \lvert V_{85\,i} - V_{85\,i+1} \rvert \leq 20$
Poor	$\lvert V_{85} - V_d \rvert > 20$	$\lvert V_{85\,i} - V_{85\,i+1} \rvert > 20$

2

1 **TABLE 2 Thresholds design consistency evaluation. Proposed model.**

Good	Fair	Poor
$V_{85\ inertial} - V_{85} \leq 10\ km/h$	$10 < V_{85\ inertial} - V_{85} \leq 20\ km/h$	$V_{85\ inertial} - V_{85} > 20\ km/h$

2

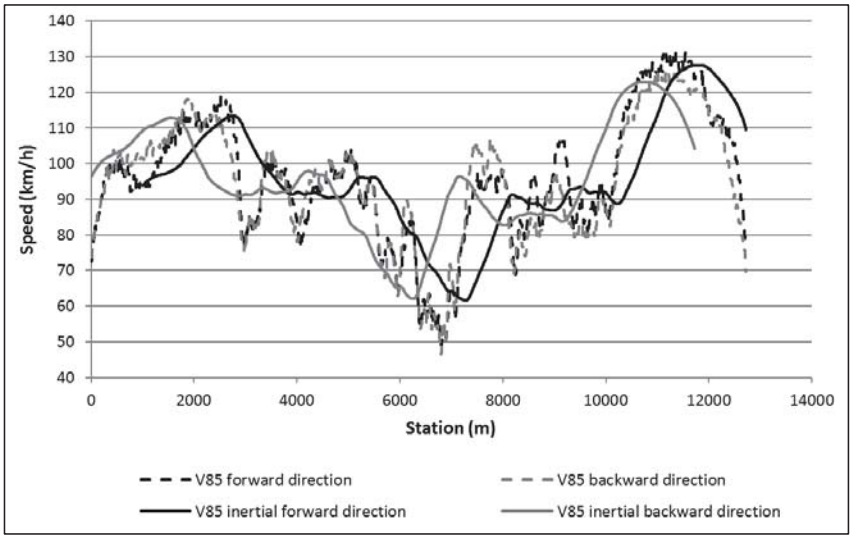

FIGURE 1 Example of inertial operating speed profile

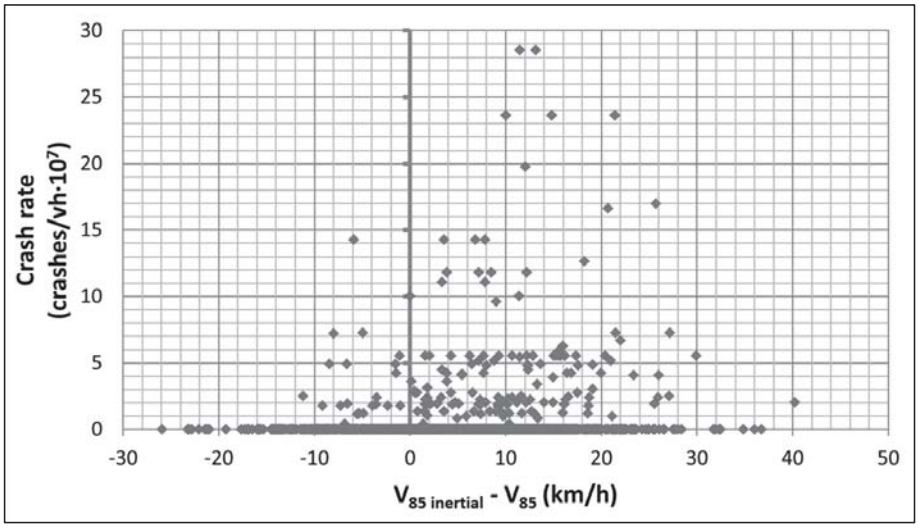

FIGURE 2 Crash rate vs ICI

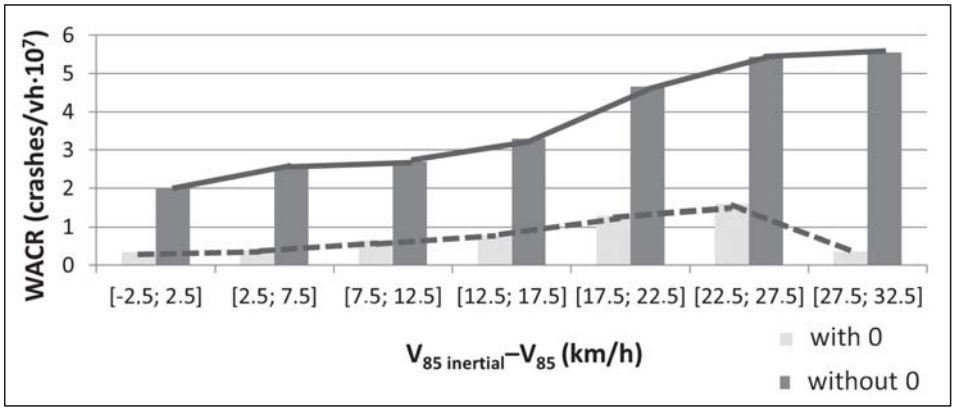

FIGURE 3 Weighted average crash rate vs ICI (5 km/h intervals)

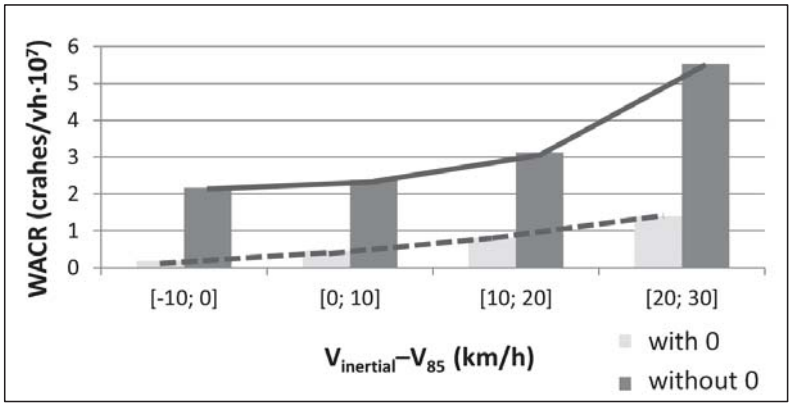

FIGURE 4 Weighted average crash rate vs ICI (10 km/h intervals)

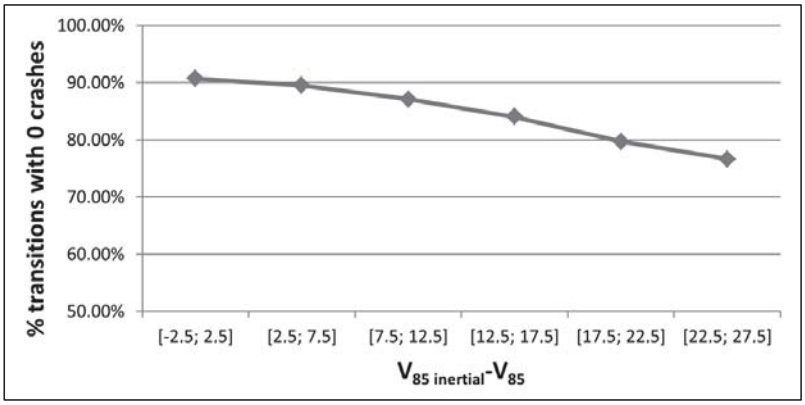

FIGURE 5 Percentage of blank transitions vs ICI (5 km/h intervals)

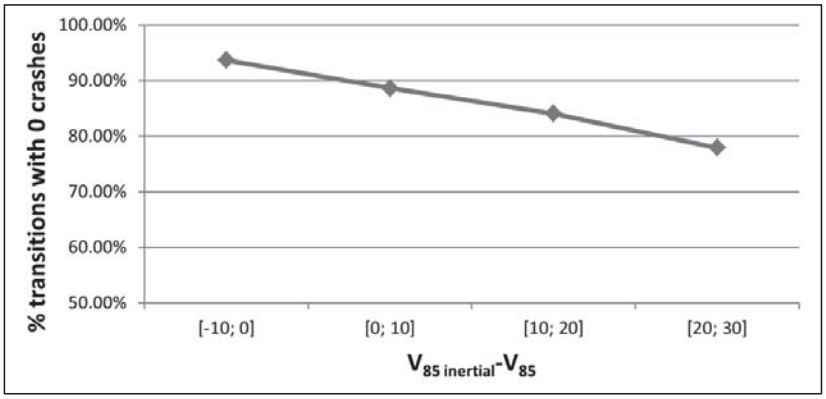

FIGURE 6 Percentage of blank transitions vs ICI (10 km/h intervals)

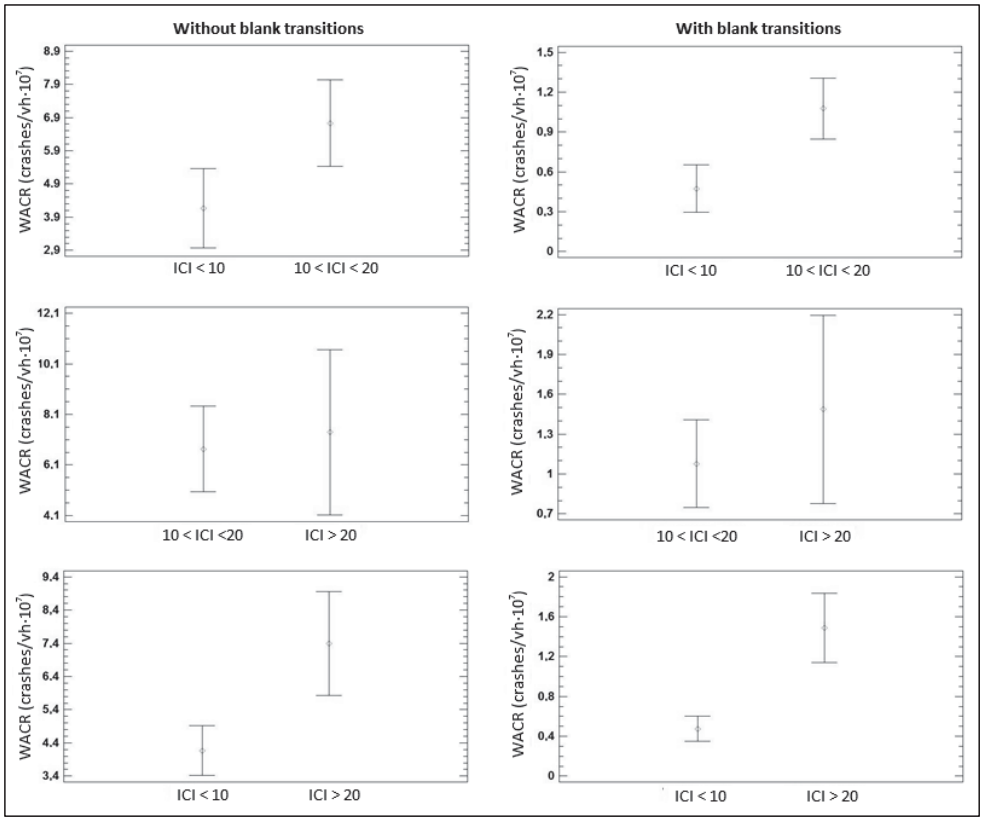

FIGURE 7 LSD intervals (95.0 percentage) for model thresholds determination

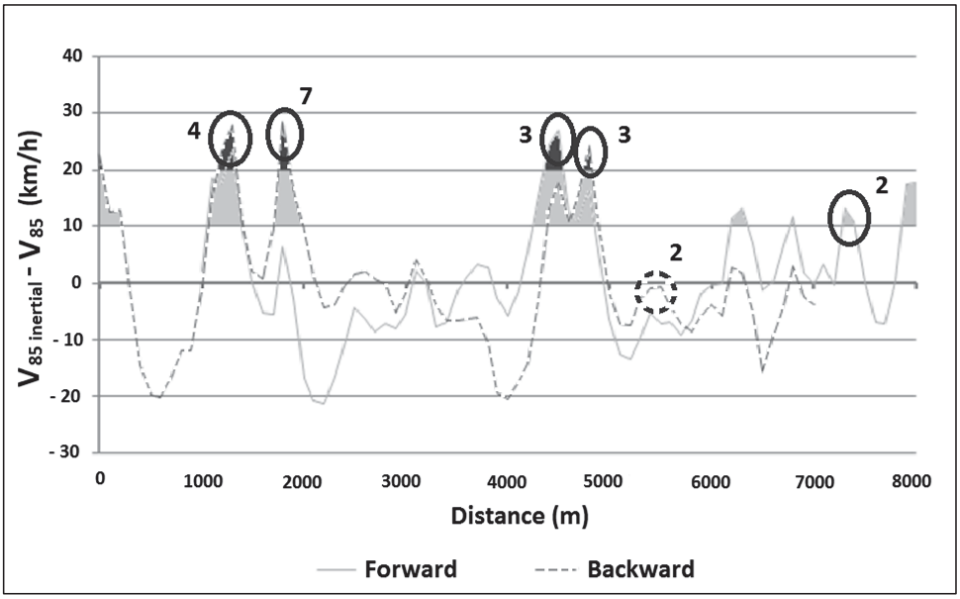

FIGURE 8 Validation road segment example. Inconsistencies identification and crashes location

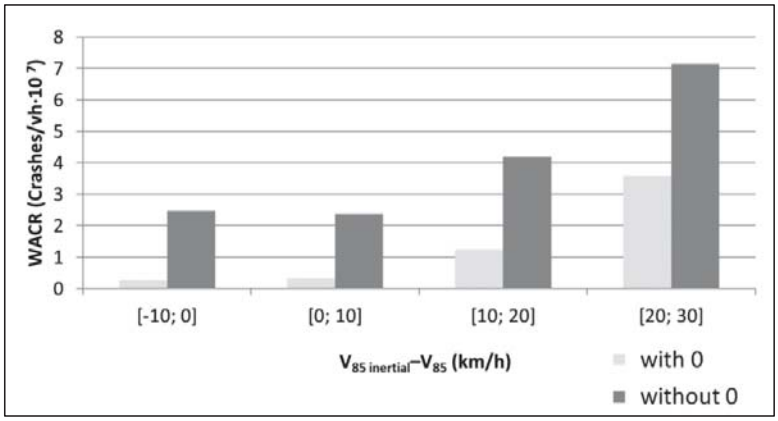

FIGURE 9 Weighted average crash rate vs ICI (10 km/h intervals) for validation road segments

Use of Heading Direction for Recreating the Horizontal Alignment of an Existing Road

Francisco J. Camacho-Torregrosa, Ana M. Pérez-Zuriaga, José M. Campoy-Ungría, Alfredo García*

Highway Engineering Research Group (HERG), Universitat Politècnica de València, Spain

&

Andrew P. Tarko

Center for Road Safety, School of Civil Engineering, Purdue University, West Lafayette, Indiana, USA

Abstract: *This paper proposes a new method for fitting the horizontal alignment of a road to a set of (x, y) points. Those points can be obtained from digital imagery or GPS-data collection. Unlike current methods that represent road alignment through its curvature, the proposed method describes the horizontal alignment as a sequence of headings. An analytic-heuristic approach is introduced. The proposed method produces unique solutions even for complex horizontal alignments. Some examples and a case study are presented.*

This solution may not be accurate enough for road redesign, but it allows researchers and departments of transportation to obtain accurate geometric features.

1 INTRODUCTION

Road alignment recreation can be viewed as the process of fitting horizontal alignment curves to a sequence of points that represent the road centerline. The locations of points are typically measured with errors. Also, the design consistency of a road is evaluated with operating speed profiles estimated from the horizontal alignment parameters (e.g., the radii of circular curves). It sometimes becomes necessary to recreate the horizontal alignment of a road, for example, checking the design consistency of an existing road when its design documentation is not available or redesigning an existing road where a safety issue has been detected.

Although the points of the alignment can be known with relatively high accuracy, it may be necessary to recreate the components of the horizontal alignment (i.e., the parameters that represent the road's geometry in the design process that are subject to design decisions). The horizontal alignment of a road is composed of the following three types of geometric components typically used by designers, which are subject to the existing standards:

- Tangents – straight segments with a zero curvature,
- Circular curves with a non-zero but constant curvature, and
- Clothoids (spiral transitions) that smoothly vary the curvature between the tangents and/or circular curves.

Some authors, such as Bosurgi and D'Andrea (2012) have investigated about the use of different curves instead of clothoids, due to better vehicle performance.

The process of recreating the road horizontal alignment is frequently conducted in two phases:

1. Measuring at certain frequency the locations of points along the road alignment and
2. Determining the geometric components of the alignment from the collected data points.

Several methods are available for the first step. Field surveying is one of the most accurate methods, but it is a high cost and time-consuming procedure, which limits its use for the mentioned applications. Another approach involves aerial imagery. Easa et al. (2007) and Dong et al. (2007) used IKONOS imagery for determining simple horizontal configurations of geometric elements. They first converted images from color to grayscale and then used the Canny edge detector to identify the road edges by detecting changes in the brightness level. This method is not as resource-demanding as topographic restitution, but it is less accurate and its accuracy depends on the quality of the images used. A different approach was performed by Tsai et al. (2010), who extracted roadway curvature data from photographic images. They proposed an algorithm that also used the Canny edge detector, thus automatically determining the location of

the centerline points of the road. They later were able to determine the radii of the different curves, although they were limited to horizontal curves with no spiral transitions.

GPS devices are also used for collecting road data points. Baffour et al. (1997) combined different GPS systems with vehicle data to obtain the road alignment, the longitudinal grades, and the superelevation rates. Roh et al. (2003) recreated several road alignments based on RTK DGPS (Real Time Kinematic Differential GPS) and GLONASS and studied their accuracy. Young and Miller (2005) developed methods capable of processing millions of data points collected by the Kansas Department of Transportation in the U.S. They also demonstrated that data points collected with GPS devices include an error term composed of constant and random components. The random error was found to be small, and the collected data were concluded to be useful for road geometry recreation.

Castro et al. (2006) presented another GPS-based technique of collecting road geometric data useful for recreating the geometry of the road centerline. They used a one-Hertz GPS receiver installed in a vehicle driven at 80 km/h. Pérez et al. (2010) used GPS devices placed on vehicles driven by regular drivers. They developed a method to determine the average vehicle path; and the results represent the average path followed by the drivers and not the road centerline. Such a horizontal line can be defined as the "operational alignment," which is different from the designed alignment. The average behavior of both directions of travel should be considered. Its knowledge is also very useful due to its relationships to safety. Othman et al. (2012) also used a GPS-based naturalistic data collection method for developing a new procedure to identify horizontal curves.

Geographical Information System (GIS) maps are an efficient and fast way to deal with the horizontal alignment of roads (Shafahi and Bagherian, 2013). This is why several methods have been developed for working with GIS systems. Imran et al. (2006) used GPS and GIS systems for studying vehicle paths and recreating the horizontal alignment of roads. Cai and Rasdorf (2008) proposed a GIS- and LIDAR-based method for determining the centerlines of roads instead of using satellite imagery or GPS technology.

In the second phase of recreating the horizontal alignment, the sequence of the geometric components of the alignment that best fits the given set of points is determined. As the three types of geometric components are characterized by their curvature, most techniques analyze the profile of the road curvature. The curvature can be locally estimated by fitting a circle to three consecutive points. This procedure usually leads to a noisy and inconvenient curvature profile. Smoothing with user-defined thresholds is frequently required.

Cubic B-splines are often used to represent horizontal alignments; the continuity of these curves and their first derivatives make them convenient for that purpose. Ben-Arieh et al. (2004) and Castro et al. (2006) are among the authors who fitted cubic B-splines to alignment data points. Cafiso and Di Graziano (2008) presented a method that deploys low-cost equipment to fit smoother splines to data points and to determine the road alignment parameters. However, there is a weakness in their approach, which is revealed if one attempts to use it to fit complex geometries. The splines-based approach seems to be applicable only to isolated curves or easy road geometry layouts. As demonstrated later in this paper, the curvature profile is also susceptible to errors caused by limited locations that sometimes make identification of the road geometric elements difficult.

Another approach to recreating road alignment involves user-defined thresholds for determining the break points between geometric components. Imran et al. (2006) used this approach, but they applied it to headings instead of curvatures. Their method first determines the heading direction for each point and assumes that the points that belong to a tangent section should have an "almost constant" heading direction. Thus, the difference between the heading directions of two consecutive points exceeding a certain threshold indicates the end of the tangent and the beginning of a different geometric component (e.g., a spiral transition or a circular curve). A horizontal curve is determined with the assumption that at least half of the points between two already identified consecutive tangents belong to a circular curve. A circular curve is fitted to these points and the fitting error is estimated. Then, two new adjacent points are added to the central section, and the circular curve is re-fitted with the corresponding error estimated. Expanding the circular curve is stopped when adding new points does not lead to a better solution. Next, the radius of the circular curve and the parameters of the spiral transitions are determined. Although finding the tangent sections by means of the heading direction is a good approach, a user-defined threshold must be used. Moreover, some curves may include fewer than half the points between two tangents, leading to a biased solution. This method works well if the geometry is relatively simple and composed of isolated curves. Othman et al. (2012) developed another procedure to determine the radius and the initial and final points of horizontal curves by using headings. They showed that headings lead to less noisy profiles than curvature-based profiles, such as the yaw rate. The radii of horizontal curves are estimated with a regression equation while the break points are determined based on thresholds established by the user.

There are some other methods that recreate the horizontal alignment from the *(x, y)* coordinates instead of using an indicator such as curvature or heading. The advantage of these approaches is that a better solution is normally achieved. On the other hand, only very simple geometries can be fitted, since the problem becomes very complex.

Easa et al. (2007) applied imagery data to recreate the horizontal alignment for circular curves and reverse curves without intermediate tangents. Based on some geometric

relationships, they were able to fit the best solution to the existing data by applying Hough's transformation. This method was applied on raster images and identified the pixels belonging to each element. This method was further improved by Dong et al. (2007), adding the possibility of determining the radii and parameters for circular curves with symmetric transition curves. These methodologies produced a very high level of accuracy, but its applications are limited to the geometric cases included in their research.

There are some additional methods for calculating curve radii based on few points. These methodologies are very useful when data is extracted from GIS, but they are normally limited to circular curves with no spiral transitions (Hummer et al., 2010). Price (2010) proposed a method for determining the curve radii from GIS data by means of using the Middle Ordinate (i.e., the perpendicular distance from the chord to the maximum curve extent). Li (2012) proposed a method and an add-in tool in ArcMap for identifying simple curves from GIS data. However, both approaches were only valid for simple geometries with no spiral transitions.

Hans et al. (2012) developed a GIS-based horizontal alignment recreation method for determining the radii of horizontal curves and their relationship to safety. Their method was based on determining the properties of the circular curves by means of comparing the results of two techniques: circular regression and Newton iteration of the modified circular curve equation. However, this was also limited to circular curves with no spiral transitions.

Camacho et al. (2010) developed a method for obtaining an improved curvature profile for the alignment passing a set of points collected with the low-cost data collection technique applied by Pérez et al. (2010). The method considers more than three points for estimating curvature; and additional smoothing processes were introduced to improve the accuracy. Compared to other methods, the alignment components are easily distinguishable in the obtained "raw curvature profile." The final sequence of tangents, circular curves, and spiral transitions are produced with a user-defined thresholds procedure. Figure 1a shows a raw curvature profile and several results obtained for different thresholds. The smoothing process may have slightly affected the alignments. Figure 1b shows the final adjusted profile.

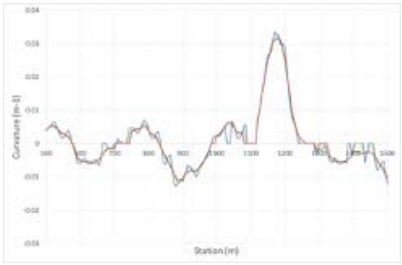

Selected Road Segment (st. 500 - 1500 m)

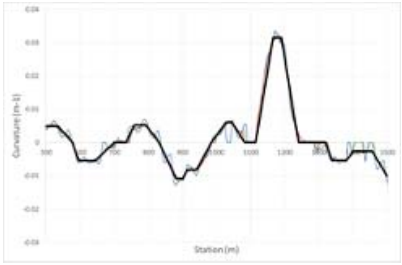

Estimated Alignment of the Selected Road Segment

Figure 1 Curvature-based fitting of a horizontal alignment.

2 OBJECTIVES AND PAPER ORGANIZATION

A new low-cost method of fitting horizontal alignment to a set of 2D points (orthogonal projection of 3D data points on a horizontal plane) is presented in this paper. The proposed method addresses some of the most important problems of the current methods discussed above. This new method uses the heading direction to represent the horizontal alignment of the road.

The "Basic Considerations" section discusses the effect of the point location error on the "noisiness" of the road alignment representation via curvatures and headings. Then, a representation of the design curves (tangent, circular curve, and spiral transition) as a sequence of headings is described and a formulation of the general optimization problem is presented. The advantages of the heading method also are discussed.

The "Heuristic Approximation" section considers the theoretical fundamentals of the method and proposes several heuristic algorithms for fitting different sequences of horizontal geometric elements. A computer program including all the algorithms also is introduced.

The advantages of the proposed method with examples are presented in the "Discussion" section; and the paper then concludes with a summary the method and identification of further research needs.

The computer program in the proposed method was developed with Visual Basic for Applications embedded in Microsoft Office Excel. All the examples shown were obtained using this program.

3 BASIC CONSIDERATIONS

3.1. Data source

The initial set of point locations must be in the Cartesian system (x, y coordinates), which may be obtained in several ways. GPS-equipped vehicles can be used for determining

the typical vehicle paths, called sometimes "operating paths." Nowadays, the locations of designed and existing roads are typically available on electronic maps and orthogonal images with embedded geo-coordinates. Therefore, the geo-coded locations of the centerline road point sequence can be obtained by the user manually from such maps and aerial imagery. In many cases of existing roads, design documentation does not exist or retrieving the paper-based design documentation is not practical when an alternative of high quality orthogonal and geo-coded images are available. Therefore, a method of estimating the curvature profile is needed and, more specifically, such a method should estimate a complete set of design parameters from the (x, y) data extracted from images. In a general case, a sequence of (x, y) data points may follow the centerline of the road, the centerline of a selected traffic lane, or the edge of a lane. Some advanced methods, such as those presented in the literature review can also be used for determining the road centerline.

3.2 Consideration of the location error

Determining the geometric elements that compose the horizontal alignment of a road from a set of data points is not easy. As revealed by our literature review, the first approach to this task utilized an initial curvature profile estimated from the points. A curvature profile (s, κ) is used in road designing to depict the rate κ at which the road changes its direction per the unit distance (curvature κ=1/R) at any point along the road at distance s from the beginning (station s). Unlike the (x, y) road alignment, the curvature profile (s, κ) is not smooth and even may not be continuous. It is composed of horizontal lines with κ=0 that represent tangents, horizontal lines with κ≠0 that represent circular curves, and sloped straight lines that represent spiral transitions. Such a profile was meant to help identify the presence of spirals and compound circular curves.

The proposed heading profile is related to curvature in the following way:

$$\kappa = \frac{d\theta}{ds} \tag{1}$$

where:
κ: Curvature (m^{-1}),
θ: Heading (rad),
s: Distance (m).

The following section discusses the level of noise (random error) expected in the curvature and headings profiles under certain assumptions to demonstrate which profile is a more convenient representation of the road alignment. The noise level is measured with the standard deviation of the random error compared to the minimum changes in the profile values that ought to be detectable.

An extraction of point location data from the alignment yields a sequence of (x, y) coordinates. These coordinates can be converted to the corresponding initial heading profile (s, θ) by calculating Δs and θ with the following equations:

$$\Delta s_i = \sqrt{\Delta x_i^2 + \Delta y_i^2} \tag{2}$$

$$\theta_i = \begin{cases} \arctan\left(\dfrac{\Delta y_i}{\Delta x_i}\right) & ;\Delta x_i \neq 0 \\ \pm\dfrac{\pi}{2} & ;\Delta x_i = 0 \end{cases} \tag{3}$$

where:
coordinates (x_i, y_i) represent point i located at distance s_i from the beginning of the alignment
$\Delta x_i = x_{i+1} - x_i$,
$\Delta y_i = y_{i+1} - y_i$.

The initial curvature profile (s, κ) can be determined by estimating the radius R of a circular curve that passes through three consecutive points and calculating the corresponding curvature κ=1/R assigned to the middle point with station s. Another option, used here, is to calculate curvature κ with Equation 1. The increment of road length ds is approximated with the length of a short segment calculated with Equation 2, and the change of the heading dθ is approximated with the change in the headings of the two consecutive short segments. The latter method leads to the following calculation of the curvature at station s_i:

$$\kappa_i = \frac{\theta_{i+1} - \theta_i}{\Delta s_i} \tag{4}$$

The primary objective when extracting location data is reducing the lateral error to the maximum extent while keeping the longitudinal separation of points constant. Thus, it is more relevant and convenient to discuss the data location errors in terms of longitudinal and lateral errors. Let us assume that the longitudinal separations along the alignment are, on average, m_s with a limited standard deviation of these separations σ_s. The lateral error e_l is the distance between the estimated location of a point and the actual road alignment. Their mean value is zero and their standard deviation is σ_l.

A successful identification of individual curves, or more precisely, changes in the curvature caused by the presence of these curves is possible if the error in the curvature estimates is considerably lower than these changes. To test this condition, let us consider the standard estimation error $\sigma_{\Delta\theta}$ of changes in θ and $\sigma_{\Delta\kappa}$ in κ. The standard deviation of separation is kept much smaller than its mean value m_s. This assumption allows stating that $e_\theta \cong e_l/m_s$. Another assumption is that the lateral error e_l is i.i.d. (independent and identically distributed) and normally distributed. This assumption is valid if the point data are collected by human observers from paper documentation or from digital renderings of the alignment. Although GPS data may exhibit serial correlation and the i.i.d. assumption does not hold in this case, the findings from the following analysis should also be applicable also to GPS data.

Table 1
Location error versus ability to identify curves in horizontal alignments.

Lateral standard error (m)	Alignment points interval Δs (m)	Headings profile		Curvature profile	
		Std. error of θ change estimate (rad)	Minimum detectable change in heading (°)	Std. error of κ change estimate (1/m)	Largest radius of detectable isolated curve (m)
0.02	2	0.0141	1.6	0.01000	50 x
0.02	5	0.0057	0.64	0.00160	312 x
0.02	10	0.0028	0.3	0.00040	1250
0.05	2	0.0354	4.1 x	0.02500	20 x
0.05	5	0.0141	1.6	0.00400	124 x
0.05	10	0.0071	0.83	0.00100	500 ?

Notes: Symbol ? indicates profiles that are noisy enough to make identifying flat horizontal curves difficult.
Symbol x indicates profiles so noisy that identifying most of horizontal curves is quite difficult.

The approximation $e_\theta \cong e_l/m_s$ and the assumption of i.i.d. for the e_l error allow calculating the standard error of the change in the heading as

$$\sigma_{\Delta\theta} = \frac{\sqrt{2}}{m_s} \cdot \sigma_l \qquad (5)$$

Equation 4 can be approximated with $\kappa = \Delta\theta/m_s$, thus the standard error of κ estimate is $\sigma_\kappa = \sigma_{\Delta\theta}/m_s$ or $\sigma_\kappa = \sqrt{2}e_l/m_s^2$. Using the i.i.d. assumption again, this time for the e_κ error, the following can be stated for the standard error of the curvature change:

$$\sigma_{\Delta\kappa} = \frac{2}{m_s^2} \cdot \sigma_l \qquad (6)$$

Table 1 presents the standard errors in the estimates of the headings changes and curvature changes calculated for any two consecutive points of the horizontal alignment. The corresponding detectable changes in the headings and curvature profiles are also provided. They are assumed to be twice the estimation standard error. The table clearly indicates that, in the majority of cases, the curvature profiles are too "noisy" to allow convenient identification and estimation of curves. On the other hand, the heading profile is less "noisy," and even small changes in the headings can be conveniently detected.

Another consideration of the location error is its impact on the accuracy of s in the estimated curvature and heading profile. Since the Δs calculated with Equation 2 is not measured exactly along the alignment but rather along a line that tends to be at a slight skew to the alignment due to the lateral errors e_l, the distance s is overestimated and this overestimation is growing with distance. Fortunately, the longitudinal error e_s is negligible when evaluating the driving convenience and safety. For example, a statistical simulation that followed the stated earlier assumptions has shown that a point one kilometer away from the beginning is expected to be shifted by approximately 0.35 m if the data points on the alignment are separated by two meters and the lateral location accuracy is 0.02 m (standard deviation). This overestimation may require adjustments if the reconstructed location of the alignment is important.

It can be concluded that, to produce good results, the alignment points separated by two meters (Δs=2 m) should not have the standard measurement error exceeding 0.02 meter. This paper shows how to utilize heading profiles to fit horizontal alignments to data points obtained from manual image-based data collection. Another data collection method previously discussed uses drivers' paths. Camacho et al. (2010) developed a method that combines different paths followed by drivers into a single one called the "average path" with the alignment points separated at 1 m.

3.3 Components of horizontal alignment

The horizontal curvature of a road strongly affects the safety and comfort of travel, and that is why curvature profiles are widely used in road design and road alignment analysis. Three kinds of geometric elements are used in designing the horizontal alignment of roads: tangents, circular curves, and spiral transitions. These are the components that closely follow the natural vehicle paths, and the existing design standards apply to the parameters of these curves. Each type of curve has a distinct curvature profile shape.

A horizontal alignment is normally composed of a series of tangents separated by curves. These curves may or may not present spiral transitions. The proposed new method covers all these situations, but does not consider curve-to-curve transitions (with or without spiral transitions). The last case has also been developed, but it is not presented due to the brevity required here and because it is rare in that it is mainly used in loops and odd geometries. However, it will be presented in further publications.

Table 2
Curvature-heading correspondences.

Geometric element	Curvature	Heading
Tangent	$\kappa = 0$	$\theta = \int 0 \cdot ds = \theta_k$
Circular curve	$\kappa = c_k$	$\theta = \int c_k \cdot ds = c_k \cdot s + \theta_k$
Spiral transition	$\kappa = \frac{s + d_o}{A^2}$	$\theta = \int \frac{s + d_o}{A^2} \cdot ds = \frac{1}{A^2} \cdot \left[\frac{s^2}{2} + d_0 \cdot s + \theta_k\right]$

κ: Curvature (m^{-1}), θ: Heading (centesimal degrees),
s: Distance measured from the beginning of the geometric element (m),
A: Parameter of the spiral transition (m), d_0, c_k, θ_k: Constants

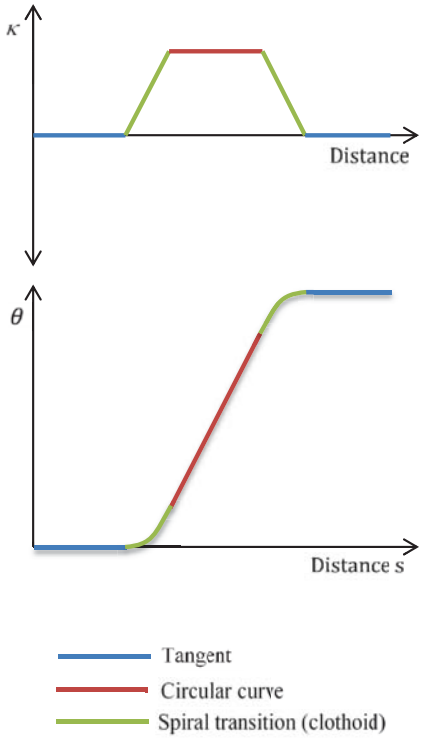

Figure 2 A horizontal curve expressed in terms of curvature κ and heading direction θ

Analyzing the horizontal alignment based on the heading profile instead of the curvature profile presents two important advantages:

- As demonstrated above, the heading profile is considerably less sensitive to measurement error, which allows the alignment components to be easily identifiable, even including visual inspection by the user. This benefit is clear when comparing the heading profile to the curvature profile.
- The road heading must always be continuous. This means that the heading value presented by a geometric element at its final point must always be the same as the initial heading value of the following geometric element. Consequently, fitting the alignment in this way allows sharing some information longitudinally, thereby addressing some issues produced by the randomness of the data. Moreover, in most cases the heading's first derivative is also continuous (except when a large radius of the circular curve eliminates the necessity of using spiral transitions), meaning that a continuity in the heading's slope profile must also be satisfied, thus adding more information. The curvature profile does not present this property, and the different geometric elements must be independently fitted, producing less accurate solutions.

For the reasons previously explained, the heading profile will be used to represent the horizontal alignment. Table 2 shows the relationships between the station s and the curvature κ and heading θ for tangents, circular curves, and spiral transitions. Figure 2 shows example profiles of curvature (Figure 2a) and heading (Figure 2b) for a single horizontal curve with spiral transitions and tangent sections and a heading direction. Tangents, circular curves, and spiral transitions are horizontal, sloped, and parabolic lines on the heading profile, respectively.

3.4 General formulation and solution of the problem

The horizontal alignment recreation problem can be described in general terms as fitting the three types of alignment components by minimizing the square-mean error of heading estimates while preserving the continuity of the heading at the stitching points between the geometric elements. The continuity of the heading's first derivative (curvature) must also be preserved if the transition curves are used. The decision variables include the parameters of the alignment curves and the stitching points. The continuity conditions are the constraints of the problem. Table 2 shows that a tangent heading curve has one parameter, a circular curve – two, and a transition curve – three.

To simplify the problem, it is assumed that the number and type of curves of the sequence are known. This

requirement can be partly relaxed by assuming that at least the number of tangents is known, and only one circular curve between two consecutive tangents is allowed (no compound curves), which is valid for the vast majority of horizontal geometric layouts. The presence of transition curves at the end of each circular curve is also assumed.

The problem is a mixed integer optimization problem. There are a limited number of discrete positions for the stitching points. On the other hand, knowing the stitching points allows fitting individual heading curves that are continuous functions. The general strategy is to separate the integer and continuous problems by solving them interchangeably until the solution converges. Fortunately, when the stitching points are known (or solved), the number of constraints and decision variables can be made equal in all cases. Thus, only one set of curves exists that meets the continuity and smoothness conditions. These curves can be easily calculated from the system of linear equations that represents the continuity and smoothness conditions at the stitching points.

The overall solving strategy includes:

(1) Balancing the number of curve parameters with the number of continuity/smoothness conditions.

(2) Solving the system of linear equations to obtain feasible curves for the current stitching points.

(3) Finding the best stitching points for the current set of curves.

(4) Repeating steps 2 and 3 until the solution converges.

Decomposition of the entire problem by dividing the alignment into shorter pieces is another strategy used to simplify and speed up the search for the solution. The midpoints of tangent segments are the natural choice, which reduces the number of tangents in each sub-problem to two and the number of circular curves to one (no compound curves). After solving all the sub-problems, the entire alignment can be obtained by combining the solutions of sub-problems.

The following section discusses selected cases in a more specific and analytical manner. A heuristic procedure of finding the best stitching points is also presented and demonstrated with examples.

4 HEURISTIC APPROXIMATION

This section develops the methodology for different geometric sequences, considering the equations, the continuity conditions, and the heuristic process. Although the analytical solution is always valid, the heuristic process has been programmed to work with a set of points regularly separated at a one meter interval ($\Delta s = 1$ m).

4.1 A single circular curve with spiral transitions

Figure 3 shows the particular solution to an isolated curve, composed of tangent T_1 – spiral transition Cl_1 – circular curve C – spiral transition Cl_2 – tangent T_2. The user has to detect two points belonging to the initial and final tangents (it does not matter where they are located as long as they belong to the corresponding tangent). These points are known as x_0 and x_5. There are more x_i stitching points (with i ranging from 1 to 4) between each one of the different road geometric elements.

Tangent T_1: $\theta_{T_1} = c_1$ (7)

Spiral transition Cl_1: $\theta_{Cl_1} = a_2 \cdot s^2 + b_2 \cdot s + c_2$ (8)

Circular curve C: $\theta_C = b_3 \cdot s + c_3$ (9)

Spiral transition Cl_2: $\theta_{Cl_2} = a_4 \cdot s^2 + b_4 \cdot s + c_4$ (10)

Tangent T_2: $\theta_{T_2} = c_5$ (11)

At all stitching points, the heading and curvature continuity must be satisfied:

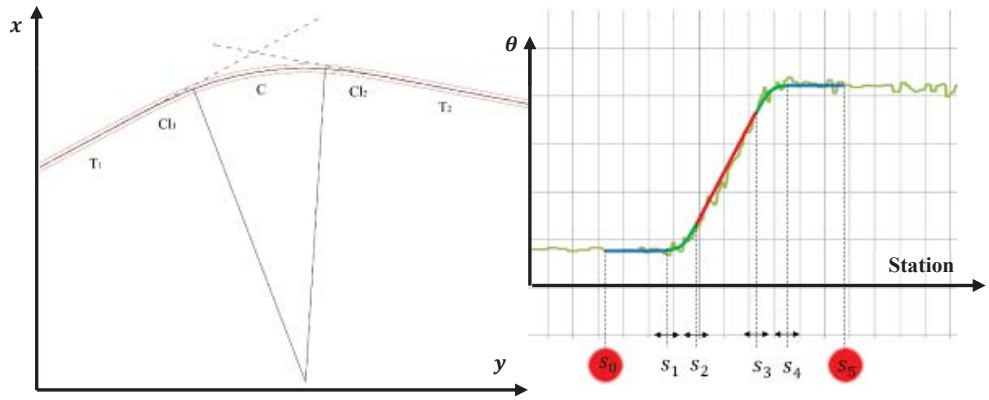

Figure 3 Geometric layout and heading profile for an isolated curve.

$$\begin{cases} \lim_{s\to s_i^-} \theta(s_i) = \lim_{s\to s_i^+} \theta(s_i) \\ \lim_{s\to s_i^-} \theta'(s_i) = \lim_{s\to s_i^+} \theta'(s_i) \end{cases} \quad (12)$$

Being s_i the stitching points, where $i = 1$ to 4.

Hence, eight conditions can be obtained:

- Point s_1:

Heading: $\theta_{T_1}(s_1) = \theta_{Cl_1}(s_1) \rightarrow c_1 = a_2 \cdot s_1^2 + b_2 \cdot s_1 + c_2$ (13)

Curvature: $\theta'_{T_1}(s_1) = \theta'_{Cl_1}(s_1) \rightarrow 0 = 2 \cdot a_2 \cdot s_1 + b_2$ (14)

- Point s_2:

Heading: $\theta_{Cl_1}(s_2) = \theta_C(s_2) \rightarrow a_2 \cdot s_2^2 + b_2 \cdot s_2 + c_2 = b_3 \cdot s_2 + c_3$ (15)

Curvature: $\theta'_{Cl_1}(s_2) = \theta'_C(s_2) \rightarrow 2 \cdot a_2 \cdot s_2 + b_2 = b_3$ (16)

- Point s_3:

Heading: $\theta_C(s_3) = \theta_{Cl_2}(s_3) \rightarrow b_3 \cdot s_3 + c_3 = a_4 \cdot s_3^2 + b_4 \cdot s_3 + c_4$ (17)

Curvature: $\theta'_C(s_3) = \theta'_{Cl_2}(s_3) \rightarrow b_3 = 2 \cdot a_4 \cdot s_3 + b_4$ (18)

- Point s_4:

Heading: $\theta_{Cl_2}(s_4) = \theta_{T_2}(s_4) \rightarrow a_4 \cdot s_4^2 + b_4 \cdot s_4 + c_4 = c_5$ (19)

Curvature: $\theta'_{Cl_2}(s) = \theta'_{T_2}(s_4) \rightarrow 2 \cdot a_4 \cdot s_4 + b_4 = 0$ (20)

There is a lack of two equations since the system is composed by eight equations and there are ten unknown parameters. The OLS (Ordinary Least Squares) estimation of the headings is sufficient if the lateral location errors el are indeed i.i.d. and normally distributed. This is not a problem because θ_{T_1} and θ_{T_2} (heading direction of the initial and final tangents) can be determined from the simple calculation of the average values within the currently tangent ranges (Equations 21 and 22). No weighting is needed if the separations between points are approximately equal.

$$\theta_{T_1} = \frac{\sum_{s=s_0}^{s=s_1} \theta(s)}{(s_1 - s_0)} \quad (21)$$

$$\theta_{T_2} = \frac{\sum_{s=s_4}^{s=s_5} \theta(s)}{(s_5 - s_4)} \quad (22)$$

Thus, there are eight unknown variables and eight equations. The system can now be solved. Equations 23 to 30 show the expressions for each one of the corresponding coefficients.

$$a_2 = \frac{\theta_{T_1} - \theta_{T_2}}{\big((s_1 + s_2) - (s_3 + s_4)\big)(s_2 - s_1)} \quad (23)$$

$$b_2 = \frac{2\big(\theta_{T_2} - \theta_{T_1}\big)s_1}{\big((s_1 + s_2) - (s_3 + s_4)\big)(s_2 - s_1)} \quad (24)$$

$$c_2 = \theta_{T_1} + \frac{\big(\theta_{T_1} - \theta_{T_2}\big)s_1^2}{\big((s_1 + s_2) - (s_3 + s_4)\big)(s_2 - s_1)} \quad (25)$$

$$b_3 = \frac{2\big(\theta_{T_1} - \theta_{T_2}\big)}{(s_1 + s_2) - (s_3 + s_4)} \quad (26)$$

$$c_3 = \frac{\theta_{T_2}(s_1 + s_2) - \theta_{T_1}(s_3 + s_4)}{(s_1 + s_2) - (s_3 + s_4)} \quad (27)$$

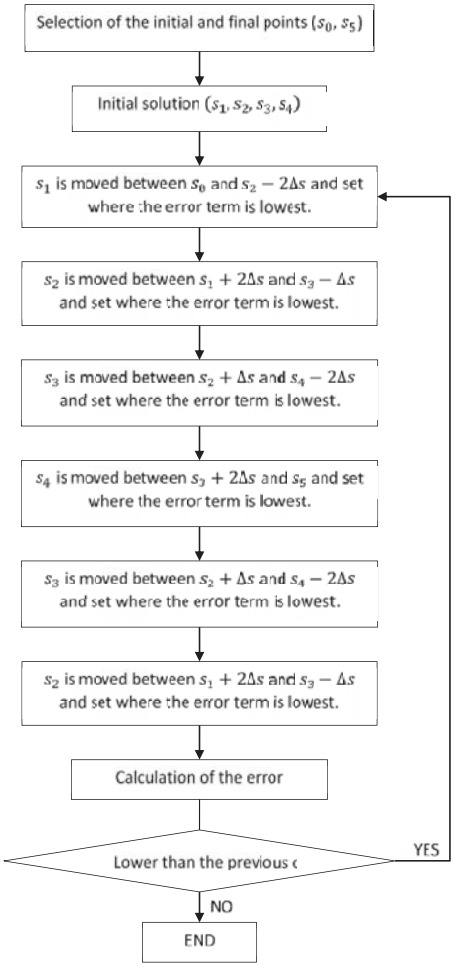

Figure 4 Flowchart for fitting an isolated curve.

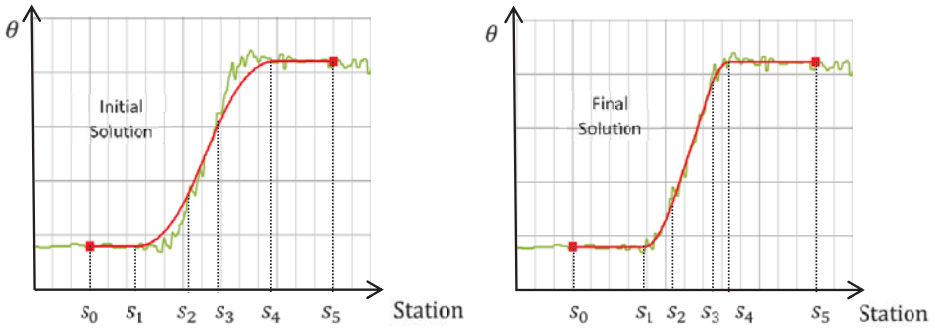

Figure 5 Isolated curve adjustment: initial and final solutions.

$$a_4 = \frac{\theta_{T_1} - \theta_{T_2}}{((s_1 + s_2) - (s_3 + s_4))(s_3 - s_4)} \quad (28)$$

$$b_4 = \frac{2(\theta_{T_2} - \theta_{T_1})s_4}{((s_1 + s_2) - (s_3 + s_4))(s_3 - s_4)} \quad (29)$$

$$c_4 = \theta_{T_2} + \frac{(\theta_{T_1} - \theta_{T_2})s_4^2}{((s_1 + s_2) - (s_3 + s_4))(s_3 - s_4)} \quad (30)$$

A heuristic approximation is now required to determine the $s_1 \dots s_4$ combination that gives the best solution to the problem. For each individual solution, the error term (E) between the initial heading profile (θ_0) and the fitted one (θ) is given by Equation 31.

$$E = \frac{\sum_{s=s_0}^{s=s_5} (\theta(s) - \theta_0(s))^2}{s_5 - s_0} \quad (31)$$

The final location of each stitching point will be the one which leads to the general solution with the lowest error. This solution depends on the position of all these points; therefore, they cannot be fitted one by one. A heuristic method was developed in order to obtain the final solution. Figure 4 summarizes this process.

The stitching points must be ordered and keep some distance for computing purposes (no distance needed for tangents, Δs for circular curves and $2\Delta s$ for spiral transitions). These conditions for the heuristic process are:

- s_1 varies from s_0 to $s_2 - 2\Delta s$.
- s_2 varies from $s_1 + 2\Delta s$ to $s_3 - \Delta s$
- s_3 varies from $s_2 + \Delta s$ to $s_4 - 2\Delta s$
- s_4 varies from $s_3 + 2\Delta s$ to s_5

After a number of iterations, the best solution is reached.

Figure 5 shows one of the initial solutions and the final one. Note that the user only had to select two points belonging to the consecutive tangents. It is not required that these points coincide with the beginning (or ending) of the tangents. Furthermore, it is recommended that the user select a large portion of the tangents in order to get a better approximation to their actual heading directions. Since the tangent heading is easy to estimate, any reasonable selection of tangent points used in the estimation produces a good result. Both spiral transitions are not forced to be similar.

4.2 A single circular curve without spiral transitions

Flat circular curves do not require spiral transitions. In this case, the previous solution for curves with spirals can be used if one assumes spirals with minimal lengths (each $2\Delta s$ long). This approximation is acceptable for a practical purpose. An exact solution with no spiral transitions can be obtained if the number of equations and the parameters remain the same. In this case, there is continuity of the heading direction, but not for its first derivative. Hence, the number of equations for each stitching point is reduced to one. On the other hand, the number of stitching points is reduced to two (preceding tangent to circular curve and circular curve to following tangent).

The heading direction for each one of the road geometric elements is:

$$\text{Tangent } T_1\text{: } \theta_{T_1} = c_1 \quad (32)$$

$$\text{Circular curve } C\text{: } \theta_C = b_2 \cdot s + c_2 \quad (33)$$

$$\text{Tangent } T_2\text{: } \theta_{T_2} = c_3 \quad (34)$$

In this case, only the continuity condition has to be satisfied at the stitching points (s_1 and s_2):

$$\lim_{s \to s_i^-} \theta(s_i) = \lim_{s \to s_i^+} \theta(s_i) \quad (35)$$

Two conditions must be satisfied:

- Point s_1:

$$\text{Heading: } \theta_{T_1}(s_1) = \theta_C(s_1) \rightarrow c_1 = \mathrm{b}_2 \cdot \mathrm{s}_1 + c_2 \quad (36)$$

- Point s_2:

$$\text{Heading: } \theta_C(s_2) = \theta_{T_2}(s_2) \rightarrow b_2 \cdot s_2 + c_2 = c_3 \quad (37)$$

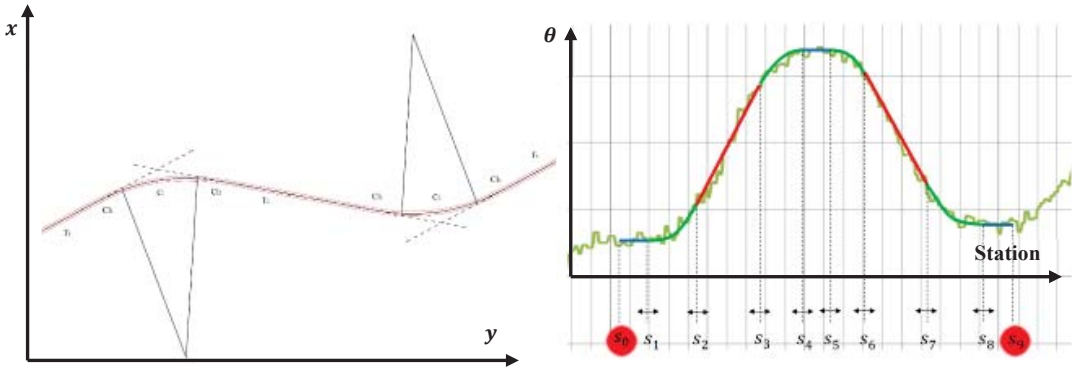

Figure 6 Geometric layout and heading profile for reverse and broken back curves (n=2).

Again, parameters c_1 and c_3 are already known since they are the fitted heading direction of the preceding (θ_{T_1}) and the following (θ_{T_2}) tangents, respectively. The solution of the system is:

$$b_2 = \frac{c_3 - \theta_{T_1}}{s_2 - s_1} \tag{38}$$

$$c_2 = \theta_{T_1} - \frac{\theta_{T_2} - \theta_{T_1}}{s_2 - s_1} \cdot s_1 \tag{39}$$

The proposed procedure starts with fitting an isolated curve with spirals to the alignment points. If the solution converges to the minimum spirals of with the minimum length, the case without spirals is solved next. Out of the two obtained solutions, the solution with a smaller estimation error calculated with Equation 31 is selected as the final one.

4.3 Sequence of circular curves

The previously discussed cases require distinguishable tangent segments that separate the curves from each other. Sometimes, the horizontal alignment is composed of a series of several curves with almost negligible tangents. In this case, it is not easy for the user to identify points that belong to tangents.

The previous cases can be expanded in order to fit several curves at the same time if the number of equations (constraints) equals the number of parameters to be estimated. The main advantage of this procedure, compared to fitting each curve separately, is that the program converges to the most accurate position of the intermediate tangents, even if their lengths are short. The case of no tangent between curves is also included as a feasible solution.

The general approach is the same as in the previous cases, although the heuristic process has to consider $4n$ boundary points, n being the number of circular curves (Figure 6). The number of resulting equations from the boundary points is $8n$ (two for each point). With i being each one of the circular curves, ranging from 1 to n, the expressions of the corresponding geometric elements can be expressed in a matrix form (Equation 40).

The stitching points for a curve i are the following:

- Tangent T_i: from s_{4i-4} to s_{4i-3}.
- Spiral transition Cl_{2i-1}: from s_{4i-3} to s_{4i-2}.
- Circular curve C_i: from s_{4i-2} to s_{4i-1}.
- Spiral transition Cl_{2i}: from s_{4i-1} to s_{4i}.

$$\begin{pmatrix} \theta_{T_1} \\ \theta_{Cl_1} \\ \theta_{C_1} \\ \theta_{Cl_2} \\ \theta_{T_2} \\ \theta_{Cl_3} \\ \theta_{C_2} \\ \theta_{Cl_4} \\ \dots \\ \theta_{T_i} \\ \theta_{Cl_{2i-1}} \\ \theta_{C_i} \\ \theta_{Cl_{2i}} \\ \dots \\ \theta_{T_n} \\ \theta_{Cl_{2n-1}} \\ \theta_{C_n} \\ \theta_{Cl_{2n}} \\ \theta_{T_{n+1}} \end{pmatrix} = \begin{pmatrix} 0 & 0 & c_1 \\ a_2 & b_2 & c_2 \\ 0 & b_3 & c_3 \\ a_4 & b_4 & c_4 \\ 0 & 0 & c_5 \\ a_6 & b_6 & c_6 \\ 0 & b_7 & c_7 \\ a_8 & b_8 & c_8 \\ \dots & \dots & \dots \\ 0 & 0 & c_{4i-3} \\ a_{4i-2} & b_{4i-2} & c_{4i-2} \\ 0 & b_{4i-1} & c_{4i-1} \\ a_{4i} & b_{4i} & c_{4i} \\ \dots & \dots & \dots \\ 0 & 0 & c_{4n-3} \\ a_{4n-2} & b_{4n-2} & c_{4n-2} \\ 0 & b_{4n-1} & c_{4n-1} \\ a_{4n} & b_{4n} & c_{4n} \\ 0 & 0 & c_{4n+1} \end{pmatrix} \cdot \begin{pmatrix} s^2 \\ s \\ 1 \end{pmatrix} \tag{40}$$

Each curve adds nine unknown variables, and the last tangent adds an additional one. Hence, the number of unknown parameters is $9n + 1$. However, the tangent-related parameters are known since they can be directly obtained once the position of their stitching points is defined. This eliminates $n + 1$ parameters of the equation system and the final number of unknowns being $8n$, which is the same

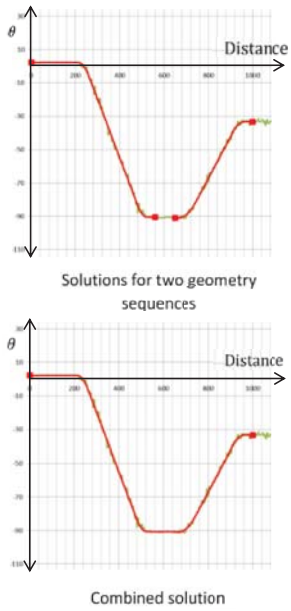

Figure 7 Combining solutions by removing gaps between fitted alignments inside tangents.

as the number of equations. This allows us to generate a system to solve the parameters. The solution to the problem is shown in the following equations, for i from 1 to n:

$$a_{4i-2} = \frac{\theta_{T_i} - \theta_{T_{i+1}}}{\left((s_{4i-3} + s_{4i-2}) - (s_{4i-1} + s_{4i})\right)(s_{4i-2} - s_{4i-3})} \quad (41)$$

$$b_{4i-2} = \frac{2\left(\theta_{T_{i+1}} - \theta_{T_i}\right)s_{4i-3}}{\left((s_{4i-3} + s_{4i-2}) - (s_{4i-1} + s_{4i})\right)(s_{4i-2} - s_{4i-3})} \quad (42)$$

$$c_{4i-2} = \theta_{T_i} + \frac{\left(\theta_{T_i} - \theta_{T_{i+1}}\right)s_{4i-3}^2}{\left((s_{4i-3} + s_{4i-2}) - (s_{4i-1} + s_{4i})\right)(s_{4i-2} - s_{4i-3})} \quad (43)$$

$$b_{4i-1} = \frac{2\left(\theta_{T_i} - \theta_{T_{i+1}}\right)}{(s_{4i-3} + s_{4i-2}) - (s_{4i-1} + s_{4i})} \quad (44)$$

$$c_{4i-1} = \frac{\theta_{T_{i+1}}(s_{4i-3} + s_{4i-2}) - \theta_{T_i}(s_{4i-1} + s_{4i})}{(s_{4i-3} + s_{4i-2}) - (s_{4i-1} + s_{4i})} \quad (45)$$

$$a_{4i} = \frac{\theta_{T_i} - \theta_{T_{i+1}}}{\left((s_{4i-3} + s_{4i-2}) - (s_{4i-1} + s_{4i})\right)(s_{4i-1} - s_{4i})} \quad (46)$$

$$b_{4i} = \frac{2\left(\theta_{T_{i+1}} - \theta_{T_i}\right)s_{4i}}{\left((s_{4i-3} + s_{4i-2}) - (s_{4i-1} + s_{4i})\right)(s_{4i-1} - s_{4i})} \quad (47)$$

$$c_{4i} = \theta_{T_{i+1}} + \frac{\left(\theta_{T_i} - \theta_{T_{i+1}}\right)s_{4i}^2}{\left((s_{4i-3} + s_{4i-2}) - (s_{4i-1} + s_{4i})\right)(s_{4i-1} - s_{4i})} \quad (48)$$

As can be seen, the structure of the equations is similar to the equations corresponding to the isolated curve. The heuristic process is also very similar, but more stitching points are considered.

4.4 Obtaining the final solution

As explained in Section 3.3, the entire section of the road is divided into smaller segments and the proposed method is use to obtain a sequence of curves for each segment separately. In the last step, all the individual solutions must be assembled to obtain the entire section. This can be easily done since consecutive individual solutions share the same tangent. Thus, the heading if this tangent is calculated by averaging the headings obtained for the two consecutive solutions. Figure 7 shows this step. All the initial and final points of the individual adjustments were initially marked with a spot. After the merging process was carried out, the intermediate tangent was merged and the spots were removed.

4.5 Computer program

A computer program was developed for the proposed method in Visual Basic for Applications. This program determines the initial heading profile and also assists the user in detecting and fitting all the geometric sequences. Finally, it merges all the individual pieces and shows the horizontal alignment.

5 DISCUSSION

The results obtained by the proposed method are considerably more accurate than the results obtained by other methods, such as the curvature-based one. The heading parameter allows the use of certain relationships between geometric features that are not available when other parameters are used.

5.1 Estimating the horizontal alignment for complex geometries

The heading profile is much more readable than the curvature profile and it does not require any smoothing. The proposed method can be applied to some geometric layouts that could not be fitted with other methods. Figure 10 shows one example. This horizontal layout is composed of a sequence of several curves without tangents. Several previous methodologies were not able to find a solution while other methods needed smoothing, which might lead to hiding short geometric elements or to introducing non-existent spiral transitions. The new method does not require smoothing; all the geometry elements, even short ones, can be identified.

As discussed in Section 3.2, flat circular curves have small curvatures that can be easily overlooked in the presence of noisy data – particularly if the curve has a small deflection angle. The opposite may also happen when the noise of the

Figure 8 Example of a curve with a low deflection angle. This curve is hardly detected by other methodologies, but easily found with the one presented in this paper.

curvature profile is confused with a small curvature. As the result, a non-existing curve may be added or an existing one removed.

Use of headings mitigates and in many cases eliminates the above difficulty. A curve, regardless of its radius or its length, always introduces a visible change in the heading direction. Figure 8 shows an example of a low-deflection angle curve. Although the horizontal curve is hardly detected, the change in the heading direction is obvious. Figure 9 shows the curvature and heading profiles for a sequence of tangent-circular curves. The radius of the circular curve is 200 m, which is a medium value. The initial data set of points was configured to simulate data collection by a human user, so it displays some random error. Points are separated at a 1 m interval, while the standard error of all points is considered to be 1 cm. As can be seen, the noise of the curvature profile considerably masks the change of curvature introduced by the circular curve. Hence, a curvature-based methodology would not detect this geometric element. On the other hand, the noise level of the heading profile is similar to the curvature profile, but the change in the heading direction is considerably higher. Thus, both the geometric elements are easily discernible.

One of the most important advantages of the proposed method is that it detects the number of geometry components and estimates their parameters. The obtained solution is much more accurate than the solutions obtained by other methods. Figure 10 shows the horizontal alignment obtained by two different methods: the curvature-based method presented by Camacho et al. (2010) and the proposed method. The primary cause of the poor performance of the

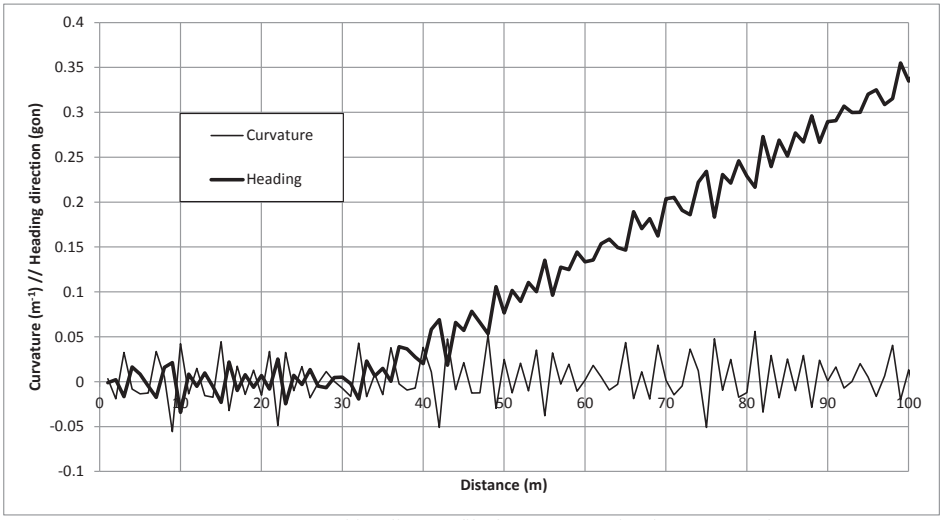

Figure 9 Curvature and heading profile for a tangent-circular curve section.

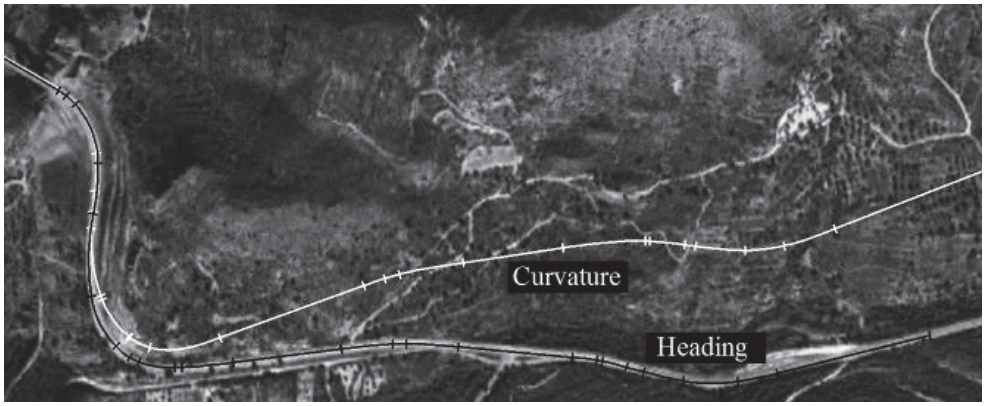

Figure 10 Horizontal alignment fitted by means of the curvature (white) and the heading profile (black).

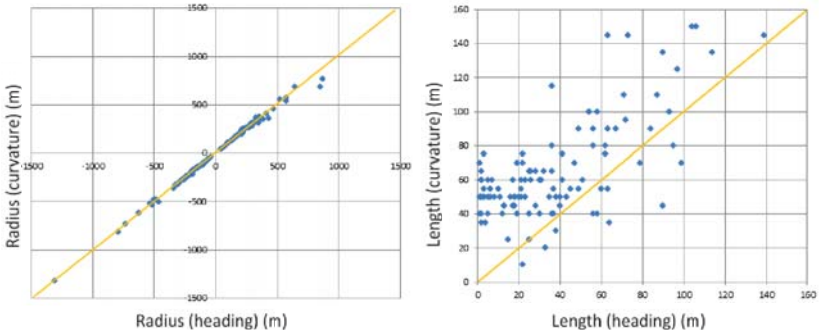

Figure 11 Comparison of the radii and lengths estimated for circular curves with the proposed and curvature-based methods.

other method is incorrect number of geometric elements that leads to accumulation of the location error.

5.2 Comparison to a previous method

Several curvature-based methodologies employ user-defined thresholds for detecting the existence and position of different geometric elements. The resulted solutions may depend on these thresholds. Moreover, it is common than the user-defined thresholds are suitable for a certain range of geometry characteristics and are not suitable for other cases leading to incorrect solutions.

A comparison of radii and lengths of circular curve obtained with the curvature-based method presented by Camacho et al. (2010) and the proposed method was performed. A set of 200 isolated, horizontal curves were randomly extracted from 10 two-lane rural highways in Spain. Figure 11 shows the comparison of the results from the two methods (estimated radii and lengths of the selected curves). As can be seen, the radii obtained with the two methodologies are almost identical, while their lengths are significantly different. In this case, the lengths estimated with the curvature-based method tend to be higher than those obtained with the proposed method. This discrepancy is caused primarily due to an error in estimating the curve lengths with the curvature-based method.

5.3 Accuracy of the results

The heuristic process used for determining the best location of s_i stitching points evaluates all possible solutions before the final solution is selected based on minimizing the fitting error. The average distance between data points - one meter - is sufficiently precise to obtain accurate estimates of the horizontal alignment. Figure 12 shows the comparison between the estimated and actual geometry of the road alignment. The horizontal curves were correctly detected except one curve composed of two consecutive curves and a very short intermediate tangent. The estimated geometry is sufficiently close to the actual geometry for the purpose of evaluating local curvature from the safety point of view.

The accuracy of the results depends on selected Δs. In this case, $\Delta s = 1$ m, is acceptable for safety and mobility-related analysis that requires curve radius and length. A lower Δs

should be used, such as 1 mm if the estimated alignment is need for the road redesign. Additional steps are needed to accomplish a higher accuracy of results are discussed in the next section where the needed future research is postulated.

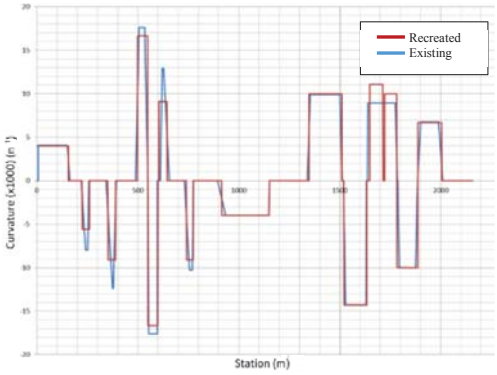

Figure 12 Comparison between the road horizontal alignment obtained by the heading method and the actual alignment obtained from the project.

6 PRACTICAL APPLICATION

In order to show the performance of this methodology, the horizontal alignment of an existing road (CV-35) was obtained. The section goes from station 68+100 to station 86+740.

The road section was manually depicted by one person with Google Earth, thus producing a polyline 18,245 m long, composed by 2530 points. The user spent 57 minutes on it. Thus, the average distance between points is slightly higher than 7 m. This distance is higher on zones with less curvature, and lower otherwise.

The next step was to transform the polyline into a homogeneous-spaced, (x, y) one. This was performed by a computer program developed by the HERG (Camacho et al., 2010), being immediate. This polyline was introduced in the program to calculate the heading and the horizontal alignment. This process took 92 minutes, performed on a quad-core computer, with 4 GB of RAM. The amount of time is highly dependent on the average curvature of the alignment.

The horizontal alignment is composed by 62 tangents, 85 circular curves and 139 spiral transitions. The largest detected radius was 2242 m, while the sharpest one was only 36 m. It also presented a series of more than 10 consecutive curves. The final road segment length is 18,241 m long, which is only 4 m difference from the original one.

Figure 13 shows the orthoimage of the existing road. Figure 14 shows the intermediate and final results including the initial heading profile, the fitted, and the curvature profile, which is directly related to the horizontal alignment.

7 CONCLUSIONS AND FURTHER RESEARCH

A new method for fitting the horizontal alignment of a road segment was proposed in this paper. Instead of using the curvature as the main input, it uses the heading direction. Abandoning the curvature alleviates the problems caused by noisy measurements and eliminates the necessity of smoothing the profiles before fitting the alignment

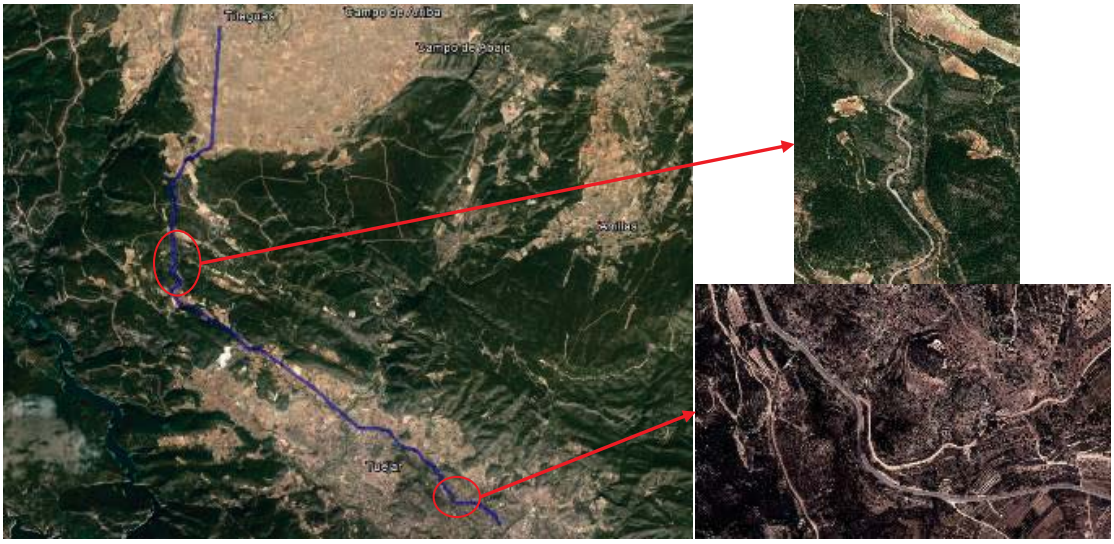

Figure 13 Orthoimage of the road of the case study. Some examples of successions of several curves and flat curves are shown.

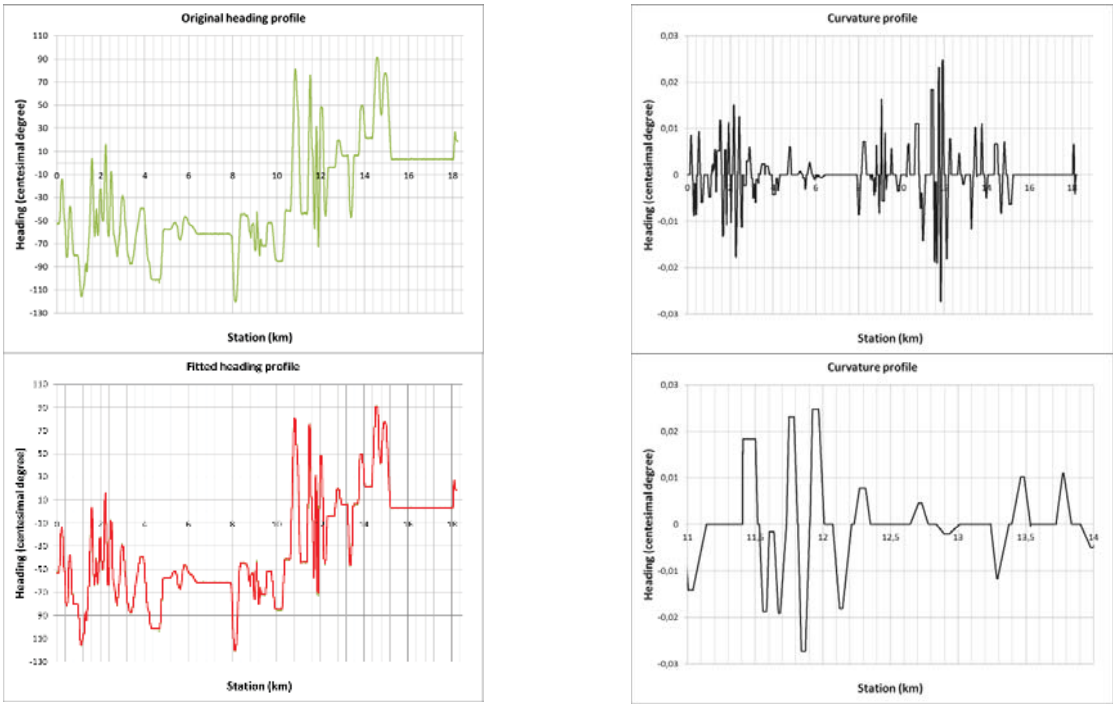

Figure 14 Recreated alignment of the case study. Original heading (top left), fitted heading (bottom left), resulting curvature profile (top right) and a detail of some curves belonging to the most complex zone (bottom right).

component curves. The fitting method uses the geometric properties of the road geometric elements and their relationships. The obtained solution is unique since the user-defined thresholds are eliminated. This new method is practical for complex road alignments. This method is valid for a (x, y) polyline that represents the road centerline. It can be obtained by several methods, highlighting field surveillance, aerial image extraction, GPS-based data collection or automated photographic analysis.

First, the relationship between the curvature and the heading direction was demonstrated, and the most important advantages of this method were explained. These advantages then were used in the paper to fully develop the method and examples were provided.

In the proposed method, each geometric element can be defined by means of the heading direction as a polynomial function: a 0-degree function for tangents, a 1-degree function for horizontal curves and a 2-degree polynomial function for spiral transitions. The most important advantage of the proposed method compared to previous methods is the possibility of using the stitching relationships between consecutive geometric elements. Every point of a road segment must present continuity in its heading direction and in its first derivative (which represents the curvature). Thus, a set of equations can be set out for each stitching point, leading to an analytical solution to the problem instead of a threshold-based solution. This implies an almost null involvement of the user in the process and that the proposed method would be a powerful tool for very complex horizontal geometries.

A computer application written in Microsoft Visual Basic was developed for the proposed method, and evaluation of the method was conducted. The results confirmed that the proposed method produces the same solution regardless of the assumptions made by different users. Thus, the results generated by this method closely fit the actual road layout.

The proposed method is sufficiently accurate for research and study purposes (i.e., curve negotiation analysis, crash risk determination on curves, operating speed modeling, etc.). On the contrary to most previous methodologies, spiral transitions are not a problem, and complex geometries can be recreated with a minimal involvement of the user. However, the horizontal alignment determined with this methodology is not valid for horizontal alignment redesign. An improvement of the algorithm is needed in order to enhance its accuracy based on the solution presented in this paper. The authors are exploring this topic by adding a Genetic Algorithm that fits the geometry to a set of *(x, y)*

points. In this case, the solution provided by this methodology is used as the seed solution.

This methodology can also be used for recreating the "operational geometry," defined as the path followed by actual vehicles. In this case, the initial data set of points may be provided by GPS devices. A polyline that represents the road centerline should be produced by considering the average path of both directions of travel.

Complex horizontal geometries such as compound curves were not discussed here for the sake of brevity. The proposed approach is suitable for such more complex cases and a separate paper is in preparation to discuss them. Vertical alignment was discussed neither. A method with a corresponding algorithm for estimating the vertical alignment should be developed in the future. The proposed methodology is centered on a certain kind of spiral transitions. Some guidelines use different forms of spiral transitions. In such case, the proposed methodology would not be valid. However, the approach might be accurate enough in some cases.

However, the methodology provided does not intend to substitute the previously existing ones, but adding a new tool that may be of interest for some cases where high accuracy at a low effort has to be achieved.

REFERENCES

Baffour, R. (1997). Global positioning system with an attitude, method for collecting roadway grade and superelevation data. *Transportation Research Record 1592*, 144-150.

Ben-Arieh, D., Chang, S., Rys, M., and Zhang, G. (2004). Geometric modeling of highways using global positioning system data and B-spline approximation. *Journal of Transportation Engineering 130-5*, 632-636.

Bosurgi, G. and D'Andrea, A (2012). A Polynomial Parametric Curve (PPC-Curve) for the Design of Horizontal Geometry of Highways. *Computer-Aided Civil and Infrastructure Engineering* 27, 303-312.

Cafiso, S. and Di Graziano, A. (2008). Automated in-vehicle data collection and treatment for existing roadway alignment. *4th International Gulf Conference on Roads Compendium of Papers* CD-ROM. Doha (Qatar)

Cai, H. and Rasdorf, W. (2008). Modeling road centerlines and predicting lengths in 3-D using LIDAR point cloud and planimetric road centerline data. *Computer-Aided Civil and Infrastructure Engineering* 23, 157-173.

Camacho Torregrosa, F., Pérez Zuriaga, A., and García García, A. (2010). Mathematical model to determine road geometric consistency in order to reduce road crashes. *Mathematical Models of Addictive Behavior, Medicine, and Engineering*. Valencia (Spain).

Castro, M., Iglesias, L., Rodríguez-Solano, R., and Sánchez, J. (2006). Geometric modeling of highways using global positioning system (GPS) data and spline approximation. *Transportation Research Part C 14-4,* pp 233-243.

Dong, H., Easa, S., and Li, J. (2007). Approximate extraction of spiralled horizontal curves from satellite imagery. *Journal of Surveying Engineering 133-1*, pp. 36-40.

Easa, S., Dong, H., and Li, J. (2007). Use of satellite imagery for establishing road horizontal alignments. *Journal of Surveying Engineering 133-1*, pp. 29-35.

Hans, Z., Souleyrette, R., and Bogenreif, C. (2012). Horizontal Curve Identification and Evaluation. *Iowa State University*

Hummer, J.E., Rasdorf, W.J., Findley, D.J., Zegeer, C.V. and Sundstrom, C.A. (2010). Procedure for Curve Warning Signing, Delineation, and Advisory Speeds for Horizontal Curves. *Report No. FHWA/NC/2009-07, available at http://ntl.bts.gov/lib/38000/38400/38476/2009-07finalreport.pdf*.

Imran, M., Hassan, Y., and Patterson, D. (2006). GPS-GIS-based procedure for tracking vehicle path on horizontal alignments. *Computer-Aided Civil and Infrastructure Engineering* 21, 383-394.

Li, Z., Chitturi, M.V., Bill, A.R. and Noyce, D.A. (1997). Automated Identification and Extraction of Horizontal Curve Information from Geographic Information System Roadway Maps. *Transportation Research Record 2291*, 80-92.

Othman, S., Thomson, R., and Lannér, G. (2012). Using naturalistic field operational test data to identify horizontal curves. *Journal of Transportation Engineering*, pp. 1151-1160

Pérez Zuriaga, A., García García, A., Camacho Torregrosa, F., and D'Attoma, P. (2010). Modeling operating speed and deceleration on two-lane rural roads with global positioning system data. *Transportation Research Record* 2171, pp. 11-20.

Price, M. (2010). Under Construction: Building and Calculating Turn Radii. *ArcUser Magazine,* Winter 2010, 50-56.

Roh, T., Seo, D., and Lee, J. (2003). An accuracy analysis for horizontal alignment of road by the kinematic GPS/GLONASS combination. *KSCE Journal of Civil Engineering* 7-1, 73-79.

Safahi, Y. and Bagherian, M. (2013). A Customized Particle Swarm Method to Solve Highway Alignment Optimization Problem. *Computer-Aided Civil and Infrastructure Engineering* 28, 52-67

Tsai, Y., Wu, J. and Wang, Z. (2010). Horizontal Roadway Curvature Computation Algorithm Using Vision Technology. *Computer-Aided Civil and Infrastructure Engineering* 25, 78-88

Young, S. and Miller, R. (2005). High accuracy geometric highway model derived from multi-track messy GPS data. *Proceedings of the 2005 Mid-Continent Transportation Research Symposium. Ames, Iowa (EEUU).*

II. Road sections

ROAD SECTION 1

Road:	CV-11	
Initial station:	0+710	Urban
Final station:	10+550	Intersection

AADT:	1801	vpd
Length:	9885	m

OPERATING SPEED

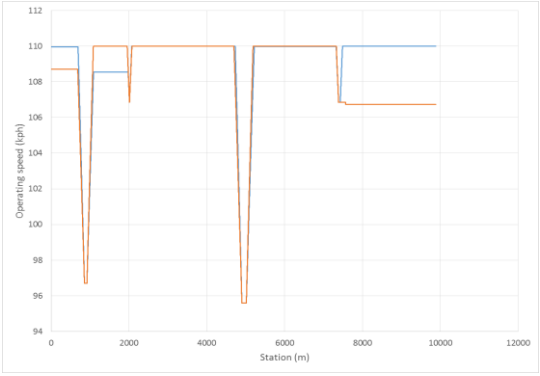

HOMOGENEOUS ROAD SEGMENTS

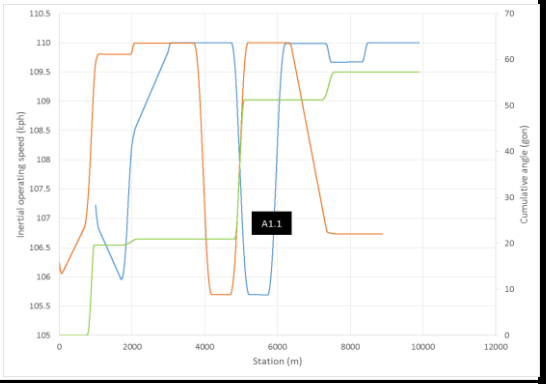

CRASHES

Observed:	7

Exposure	16
Polus (2004)	14
Camacho (2009)	10
Garach (2013)	20
Camacho (2014)	10

ROAD SECTION 2

Road:	CV-12	
Initial station:	0+050	Intersection
Final station:	23+790	Intersection

AADT:	859	vpd
Length:	20845	m

OPERATING SPEED

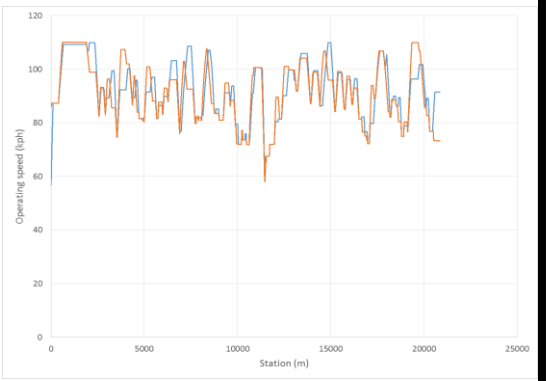

HOMOGENEOUS ROAD SEGMENTS

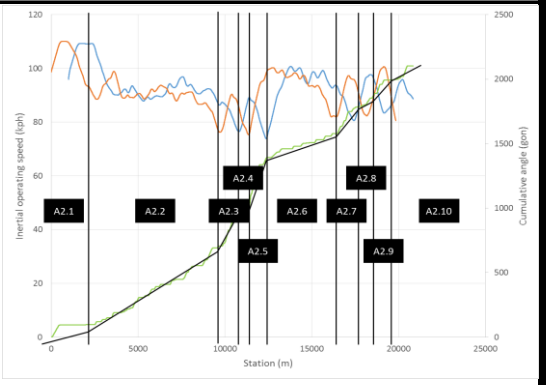

CRASHES

Observed:	11

Exposure	17
Polus (2004)	22
Camacho (2009)	18
Garach (2013)	30
Camacho (2014)	13

ROAD SECTION 3

Road:	CV-14	
Initial station:	0+230	Intersection
Final station:	19+600	Urban

AADT:	1286	vpd
Length:	19335	m

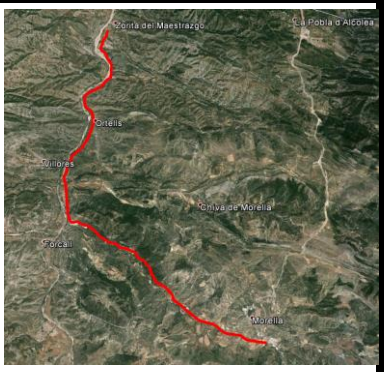

OPERATING SPEED

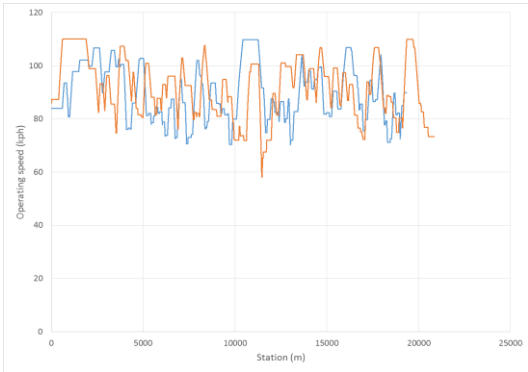

HOMOGENEOUS ROAD SEGMENTS

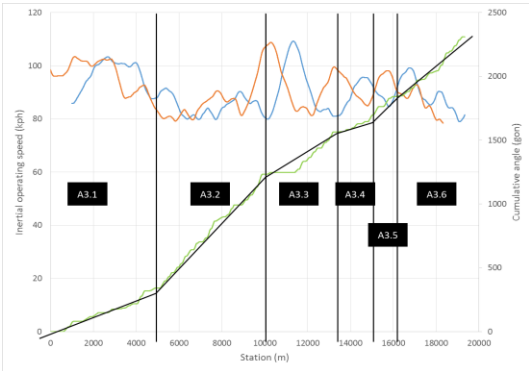

CRASHES

Observed:	16	Exposure	19
		Polus (2004)	29
		Camacho (2009)	20
		Garach (2013)	33
		Camacho (2014)	16

ROAD SECTION 4

Road:	CV-15	
Initial station:	55+670	Free
Final station:	64+840	Urban

AADT:	1036	vpd
Length:	9145	m

OPERATING SPEED

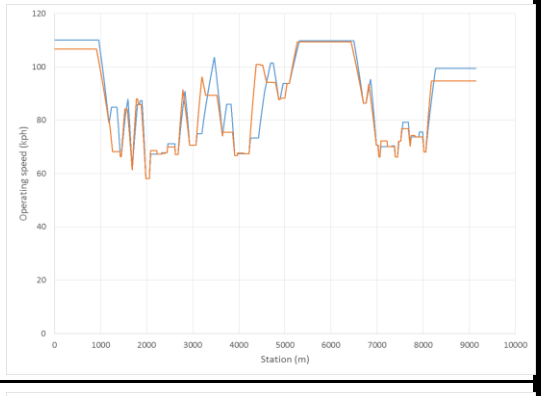

HOMOGENEOUS ROAD SEGMENT

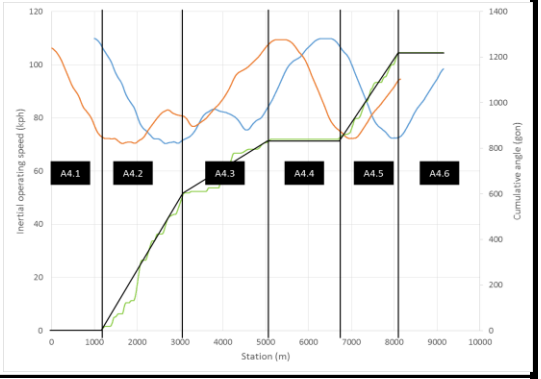

CRASHES

Observed:	7	Exposure	8
		Polus (2004)	13
		Camacho (2009)	8
		Garach (2013)	18
		Camacho (2014)	8

ROAD SECTION 5

Road:	CV-15	
Initial station:	68+510	Urban
Final station:	72+460	Free

AADT:	1012	vpd
Length:	3925	m

OPERATING SPEED

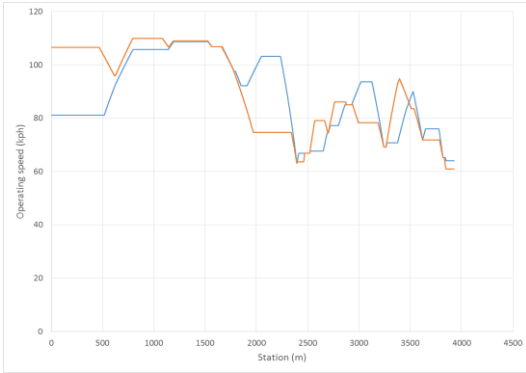

HOMOGENEOUS ROAD SEGMENT

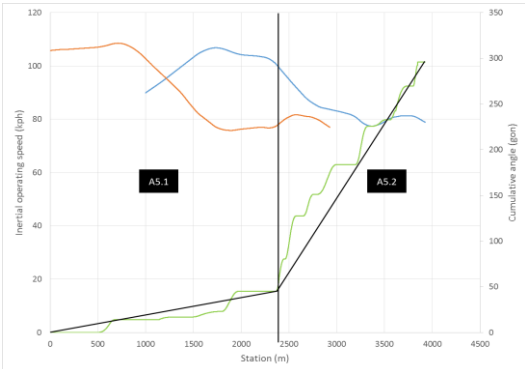

CRASHES

Observed:	4	Exposure	4
		Polus (2004)	6
		Camacho (2009)	5
		Garach (2013)	8
		Camacho (2014)	3

ROAD SECTION 6

Road:	CV-25	
Initial station:	15+850	Urban
Final station:	19+770	Urban

AADT:	407	vpd
Length:	3893	m

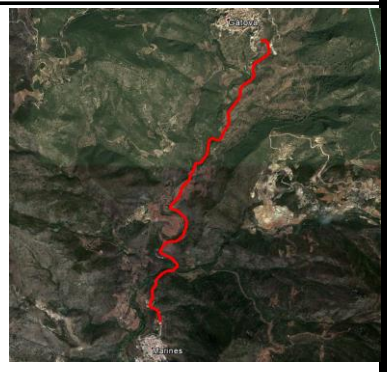

OPERATING SPEED

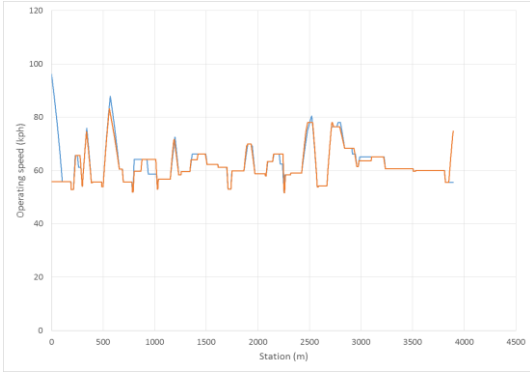

HOMOGENEOUS ROAD SEGMENT

CRASHES

Observed:	1		Exposure	3
			Polus (2004)	2
			Camacho (2009)	1
			Garach (2013)	2
			Camacho (2014)	3

ROAD SECTION 7

Road:	CV-60	
Initial station:	0+090	Roundabout
Final station:	22+680	Free

AADT:	9714	vpd
Length:	22616	m

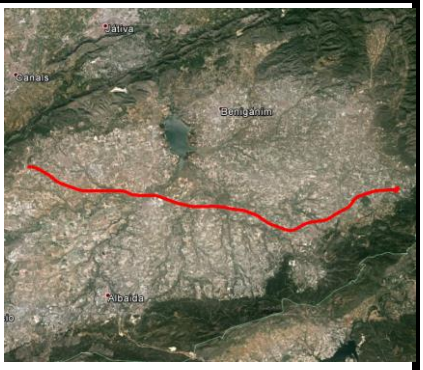

OPERATING SPEED

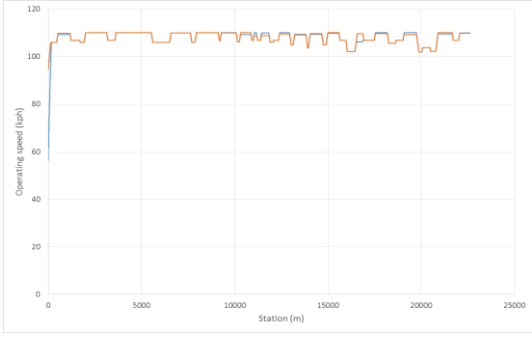

HOMOGENEOUS ROAD SEGMENTS

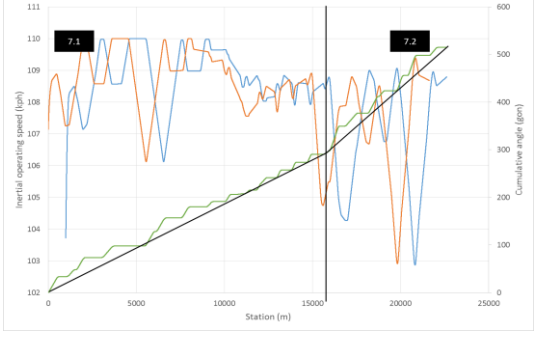

CRASHES

Observed:	76	Exposure	87
		Polus (2004)	159
		Camacho (2009)	116
		Garach (2013)	243
		Camacho (2014)	75

ROAD SECTION 8

Road:	CV-700	
Initial station:	21+760	Roundabout
Final station:	26+270	Urban

AADT:	506	vpd
Length:	4533	m

OPERATING SPEED

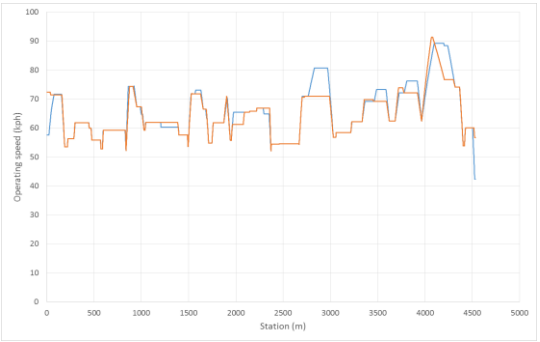

HOMOGENEOUS ROAD SEGMENTS

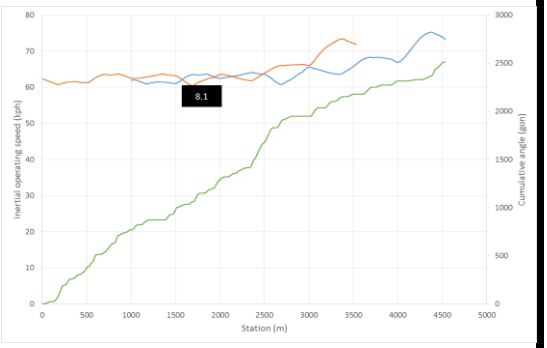

CRASHES

Observed:	2

Exposure	4
Polus (2004)	3
Camacho (2009)	2
Garach (2013)	3
Camacho (2014)	4

ROAD SECTION 9

Road:	CV-700	
Initial station:	27+520	Urban
Final station:	38+610	Urban

AADT:	506	vpd
Length:	11102	m

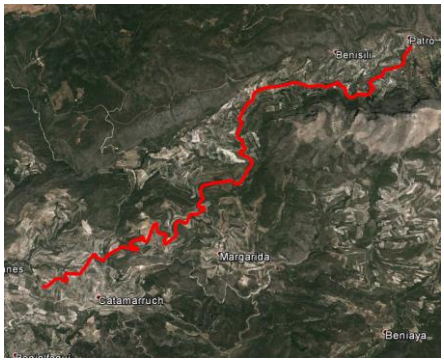

OPERATING SPEED

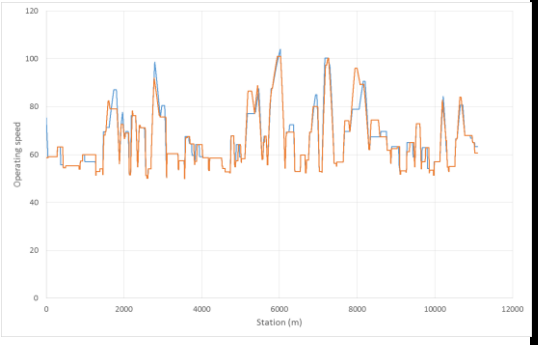

HOMOGENEOUS ROAD SEGMENTS

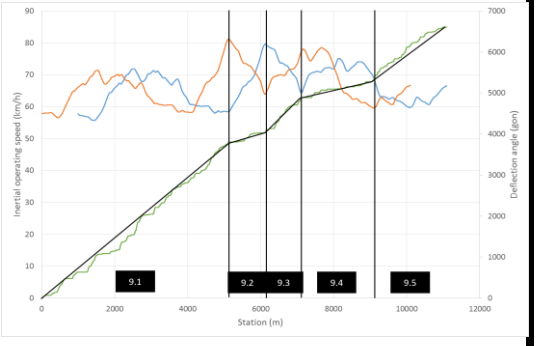

CRASHES

Observed:	5	Exposure	9
		Polus (2004)	9
		Camacho (2009)	7
		Garach (2013)	10
		Camacho (2014)	10

ROAD SECTION 10

Road:	CV-700	
Initial station:	44+390	Urban
Final station:	52+770	Urban

AADT:	506	vpd
Length:	8382	m

OPERATING SPEED

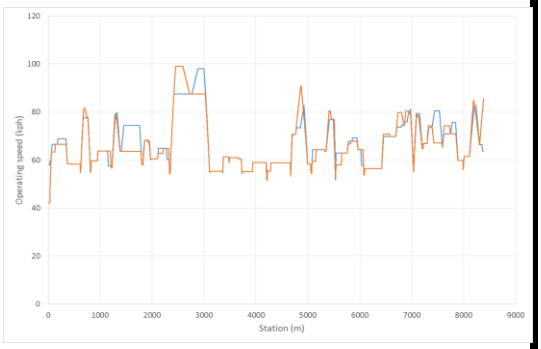

HOMOGENEOUS ROAD SEGMENT

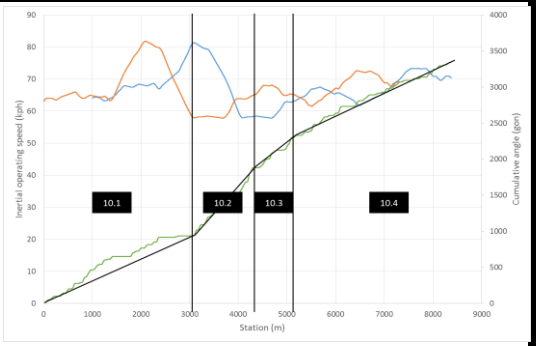

CRASHES

Observed:	12	Exposure	7
		Polus (2004)	6
		Camacho (2009)	4
		Garach (2013)	8
		Camacho (2014)	8

ROAD SECTION 11

Road:	CV-715	
Initial station:	10+390	Urban
Final station:	16+290	Urban
AADT:	2925	vpd
Length:	5904	m

OPERATING SPEED

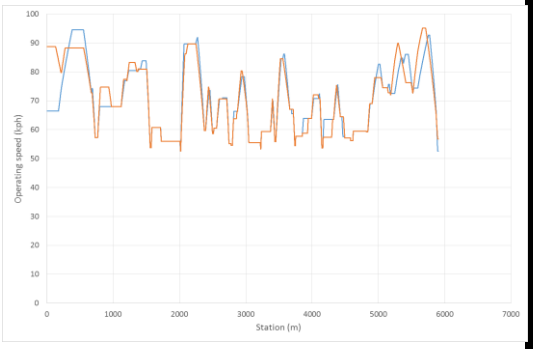

HOMOGENEOUS ROAD SEGMENTS

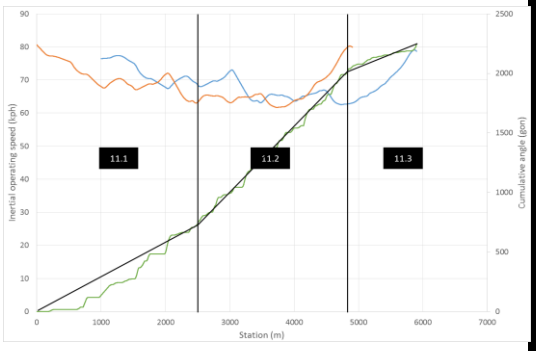

CRASHES

Observed:	9	Exposure	12
		Polus (2004)	26
		Camacho (2009)	18
		Garach (2013)	36
		Camacho (2014)	18

ROAD SECTION 12

Road:	CV-715	
Initial station:	40+280	Urban
Final station:	46+440	Urban

AADT:	427	vpd
Length:	6172	m

OPERATING SPEED

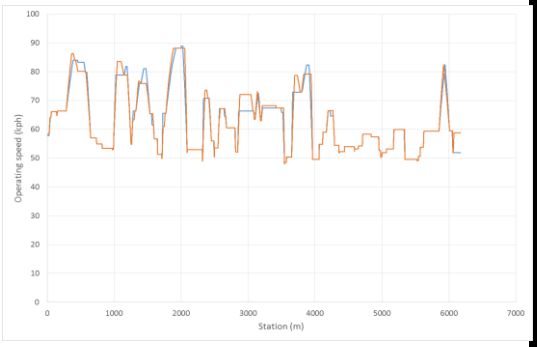

HOMOGENEOUS ROAD SEGMENT

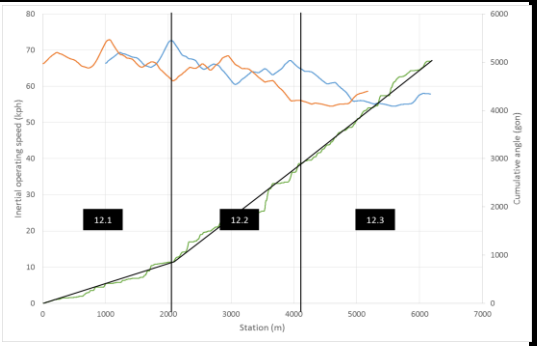

CRASHES

Observed:	7	Exposure	5
		Polus (2004)	4
		Camacho (2009)	3
		Garach (2013)	5
		Camacho (2014)	5

ROAD SECTION 13

Road:	CV-83	
Initial station:	14+270	Roundabout
Final station:	23+530	Urban

AADT:	5581	vpd
Length:	9068	m

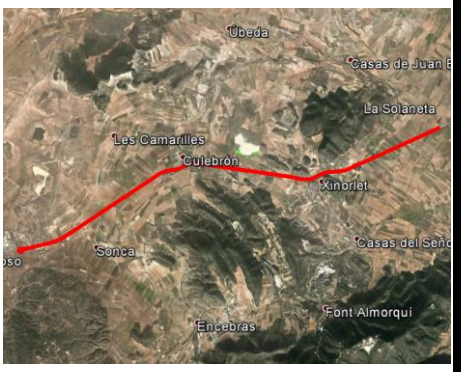

OPERATING SPEED

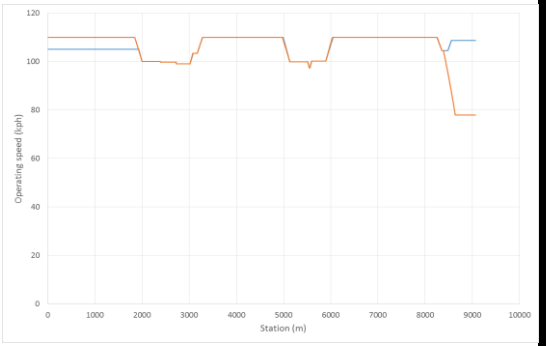

HOMOGENEOUS ROAD SEGMENTS

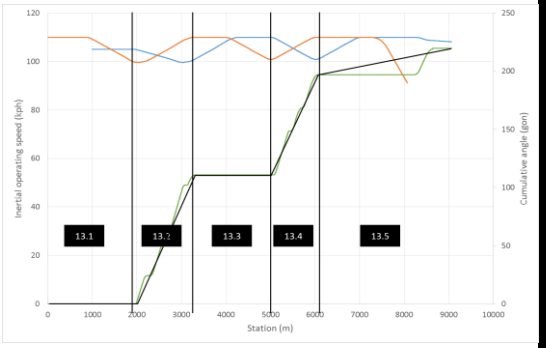

CRASHES

Observed:	17

Exposure	30
Polus (2004)	48
Camacho (2009)	34
Garach (2013)	85
Camacho (2014)	21

ROAD SECTION 14

Road:	CV-840	
Initial station:	20+688	Urban
Final station:	11+437	Urban

AADT:	3129	vpd
Length:	9211	m

OPERATING SPEED

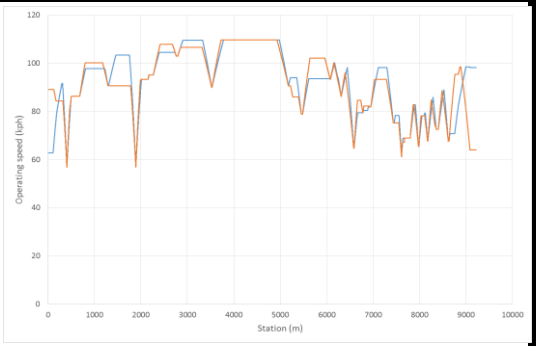

HOMOGENEOUS ROAD SEGMENTS

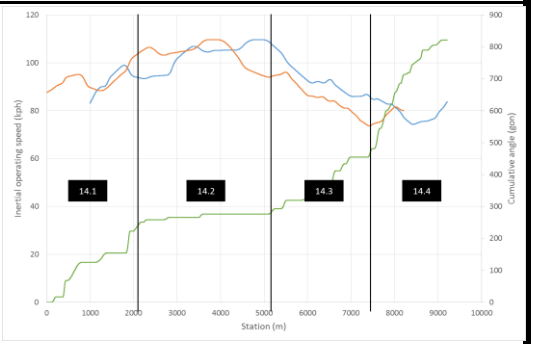

CRASHES

Observed:	26

Exposure	20
Polus (2004)	39
Camacho (2009)	28
Garach (2013)	55
Camacho (2014)	21

ROAD SECTION 15

Road:	CV-860	
Initial station:	0+090	Roundabout
Final station:	4+640	Roundabout

AADT:	4980	vpd
Length:	4536	m

OPERATING SPEED

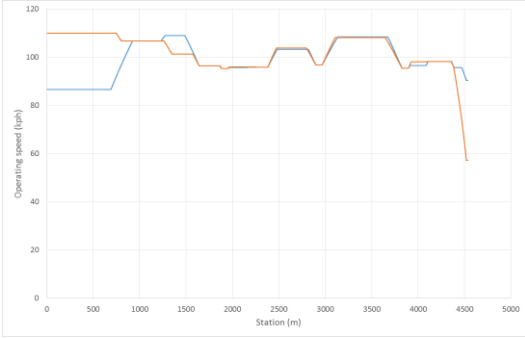

HOMOGENEOUS ROAD SEGMENT

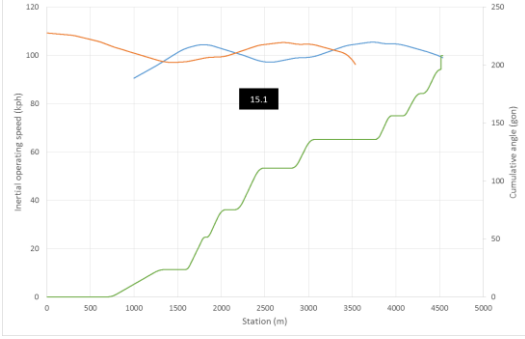

CRASHES

Observed:	10	Exposure	13
		Polus (2004)	30
		Camacho (2009)	21
		Garach (2013)	38
		Camacho (2014)	11

ROAD SECTION 16

Road:	CV-925	
Initial station:	14+190	Intersection
Final station:	24+930	Roundabout

AADT:	1285	vpd
Length:	10688	m

OPERATING SPEED

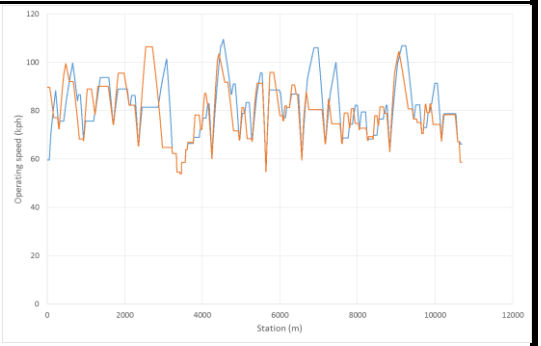

HOMOGENEOUS ROAD SEGMENTS

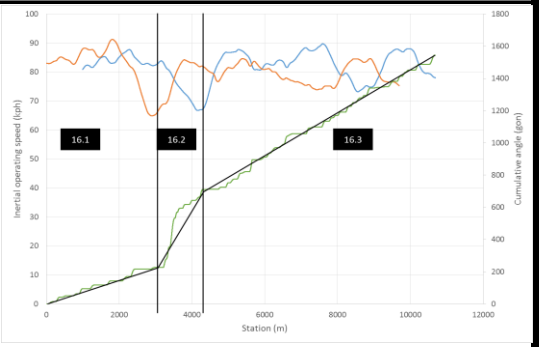

CRASHES

Observed:	7

Exposure	15
Polus (2004)	22
Camacho (2009)	15
Garach (2013)	24
Camacho (2014)	16

ROAD SECTION 17

Road:	CV-935	
Initial station:	6+000	Roundabout
Final station:	9+910	Intersection

AADT:	2588	vpd
Length:	3906	m

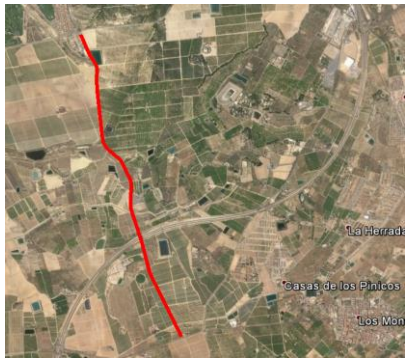

OPERATING SPEED

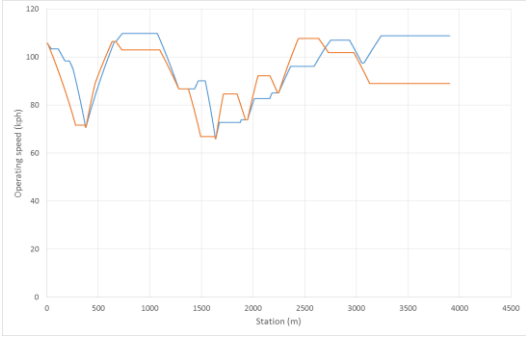

HOMOGENEOUS ROAD SEGMENT

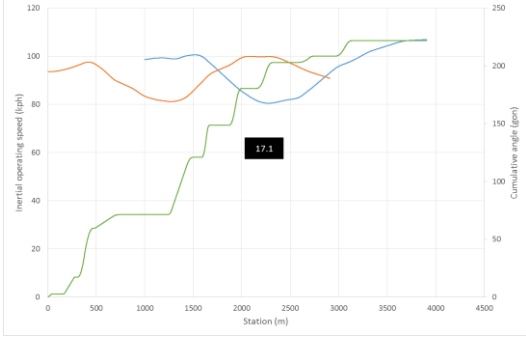

CRASHES

Observed:	9	Exposure	8
		Polus (2004)	18
		Camacho (2009)	12
		Garach (2013)	21
		Camacho (2014)	8

ROAD SECTION 18

Road:	CV-941	
Initial station:	1+190	Roundabout
Final station:	6+390	Roundabout

AADT:	3472	vpd
Length:	5202	m

OPERATING SPEED

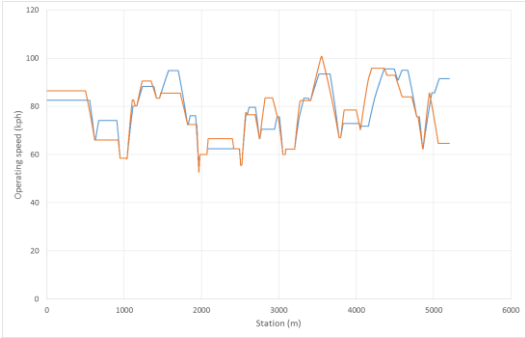

HOMOGENEOUS ROAD SEGMENT

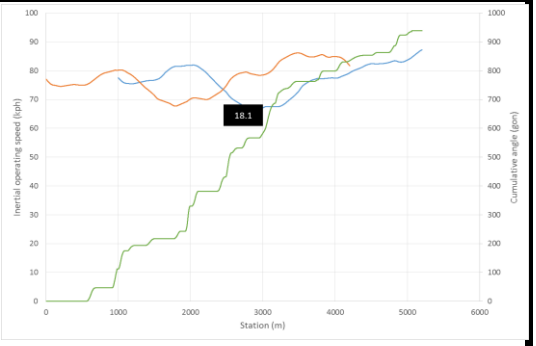

CRASHES

Observed:	37	Exposure	12
		Polus (2004)	31
		Camacho (2009)	21
		Garach (2013)	34
		Camacho (2014)	20

ROAD SECTION 19

Road:	CV-949	
Initial station:	0+020	Intersection
Final station:	6+980	Free

AADT:	813	vpd
Length:	6898	m

OPERATING SPEED

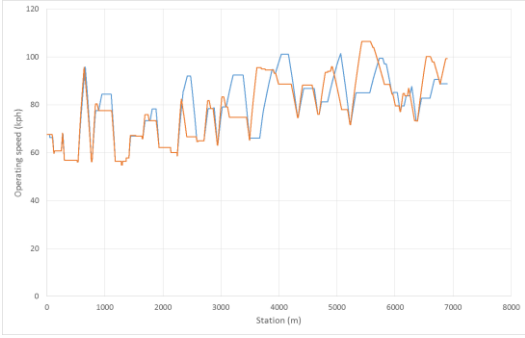

HOMOGENEOUS ROAD SEGMENT

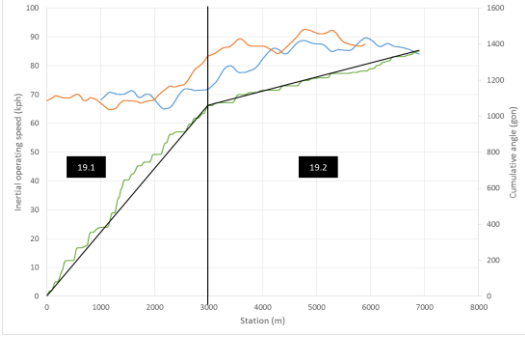

CRASHES

Observed:	14		Exposure	5
			Polus (2004)	9
			Camacho (2009)	6
			Garach (2013)	9
			Camacho (2014)	6

ROAD SECTION 20

Road:	CV-25	
Initial station:	10+280	Urban
Final station:	15+110	Urban

AADT:	528	vpd
Length:	4768	m

OPERATING SPEED

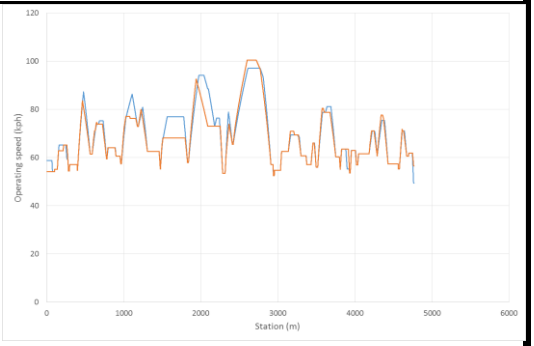

HOMOGENEOUS ROAD SEGMENT

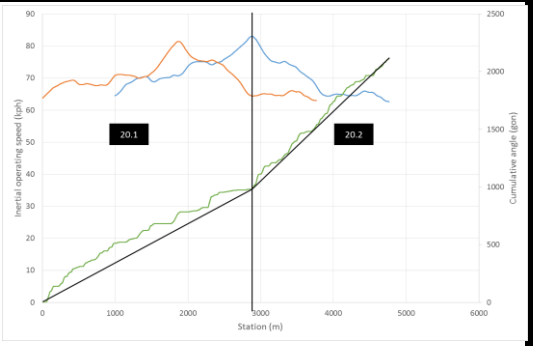

CRASHES

Observed:	6	Exposure	4
		Polus (2004)	4
		Camacho (2009)	3
		Garach (2013)	5
		Camacho (2014)	4

ROAD SECTION 21

Road:	CV-35	
Initial station:	87+120	Urban
Final station:	95+910	Urban

AADT:	520	vpd
Length:	8605	m

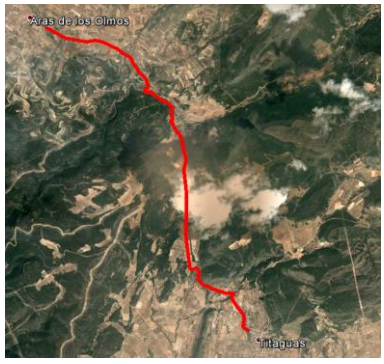

OPERATING SPEED

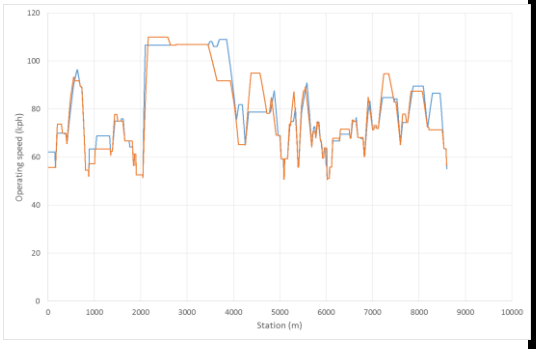

HOMOGENEOUS ROAD SEGMENTS

CRASHES

Observed:	4	Exposure	6
		Polus (2004)	8
		Camacho (2009)	5
		Garach (2013)	8
		Camacho (2014)	6

ROAD SECTION 22

Road:	CV-41	
Initial station:	5+780	Roundabout
Final station:	7+050	Roundabout

AADT:	9202	vpd
Length:	1451	m

OPERATING SPEED

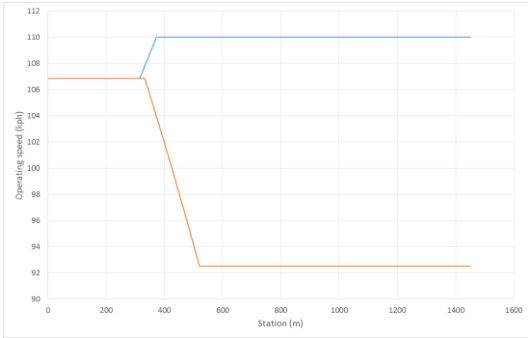

HOMOGENEOUS ROAD SEGMENT

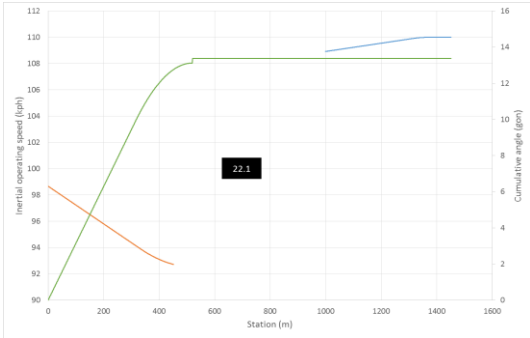

CRASHES

Observed:	8	Exposure	6
		Polus (2004)	9
		Camacho (2009)	7
		Garach (2013)	21
		Camacho (2014)	

ROAD SECTION 23

Road:	CV-41	
Initial station:	9+750	Roundabout
Final station:	11+910	Roundabout

AADT:	6690	vpd
Length:	2265	m

OPERATING SPEED

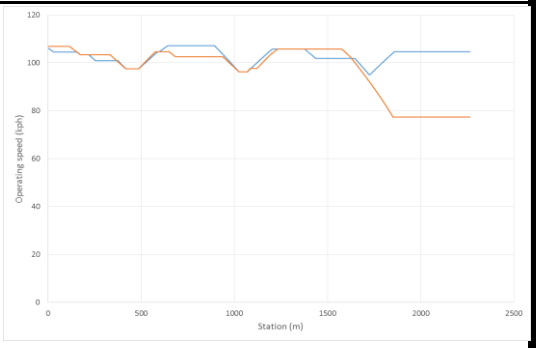

HOMOGENEOUS ROAD SEGMENT

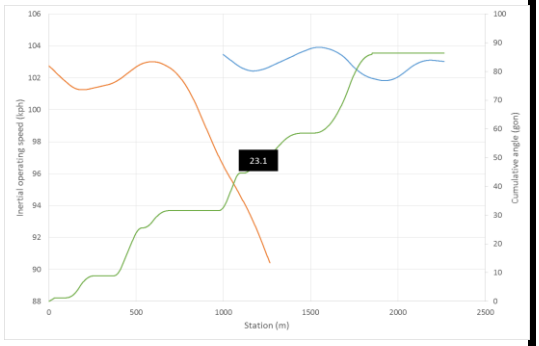

CRASHES

Observed:	1	Exposure	8
		Polus (2004)	20
		Camacho (2009)	14
		Garach (2013)	30
		Camacho (2014)	6

ROAD SECTION 24

Road:	CV-41	
Initial station:	12+100	Roundabout
Final station:	18+420	Roundabout

AADT:	8472	vpd
Length:	6316	m

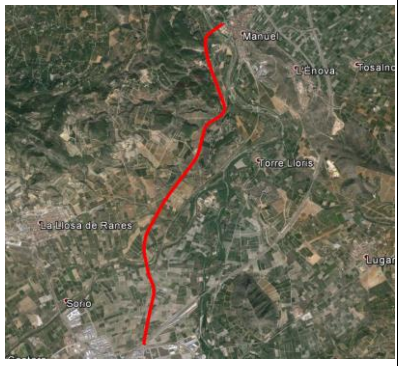

OPERATING SPEED

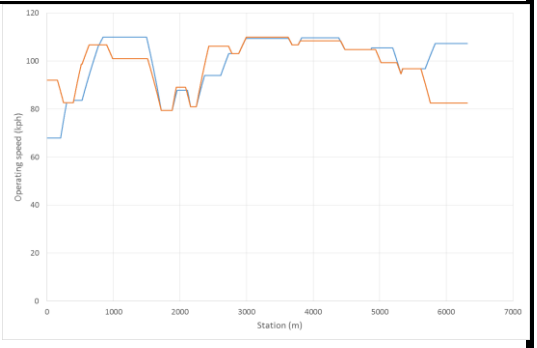

HOMOGENEOUS ROAD SEGMENTS

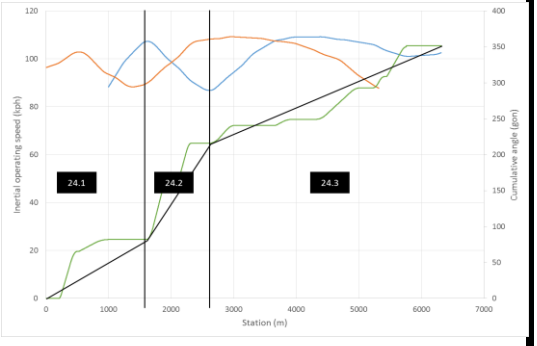

CRASHES

Observed:	57	Exposure	26
		Polus (2004)	75
		Camacho (2009)	54
		Garach (2013)	112
		Camacho (2014)	24

ROAD SECTION 25

Road:	CV-42	
Initial station:	1+870	Roundabout
Final station:	3+060	Roundabout

AADT:	6943	vpd
Length:	1254	m

OPERATING SPEED

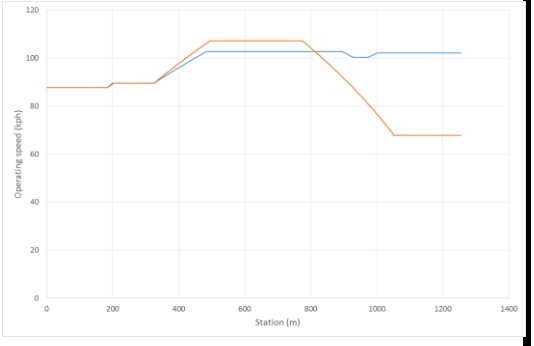

HOMOGENEOUS ROAD SEGMENT

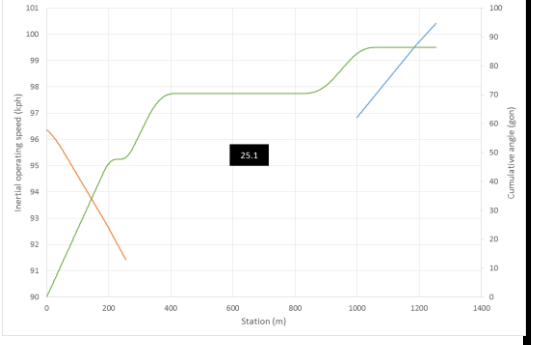

CRASHES

Observed:	2	Exposure	4
		Polus (2004)	15
		Camacho (2009)	10
		Garach (2013)	22
		Camacho (2014)	4

ROAD SECTION 26

Road:	CV-42	
Initial station:	3+260	Roundabout
Final station:	4+990	Roundabout

AADT:	6943	vpd
Length:	1735	m

OPERATING SPEED

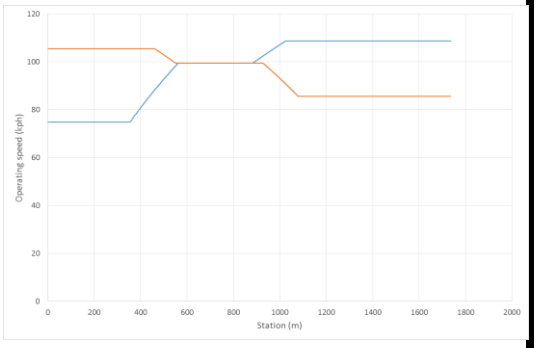

HOMOGENEOUS ROAD SEGMENTS

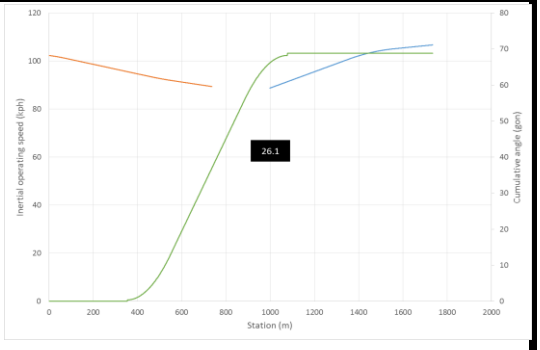

CRASHES

Observed:	3	Exposure	6
		Polus (2004)	8
		Camacho (2009)	6
		Garach (2013)	18
		Camacho (2014)	

ROAD SECTION 27

Road:	CV-42	
Initial station:	5+150	Roundabout
Final station:	7+370	Roundabout

AADT:	6544	vpd
Length:	2254	m

OPERATING SPEED

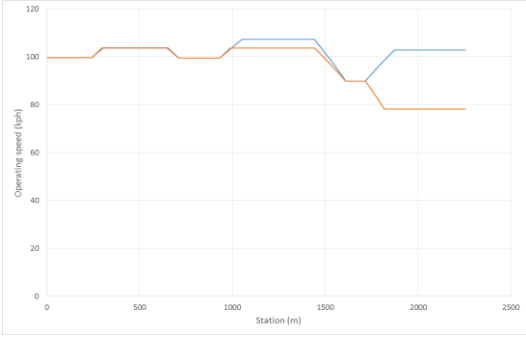

HOMOGENEOUS ROAD SEGMENT

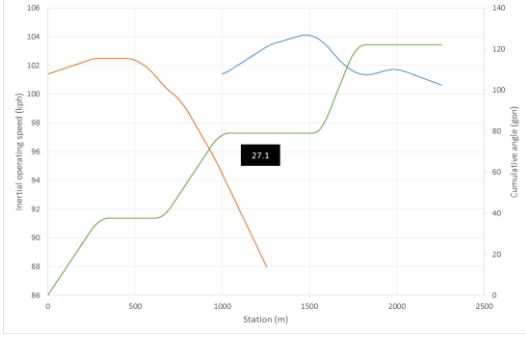

CRASHES

Observed:	8	Exposure	7
		Polus (2004)	20
		Camacho (2009)	14
		Garach (2013)	29
		Camacho (2014)	6

ROAD SECTION 28

Road:	CV-811	
Initial station:	0+800	Roundabout
Final station:	4+490	Roundabout

AADT:	875	vpd
Length:	3788	m

OPERATING SPEED

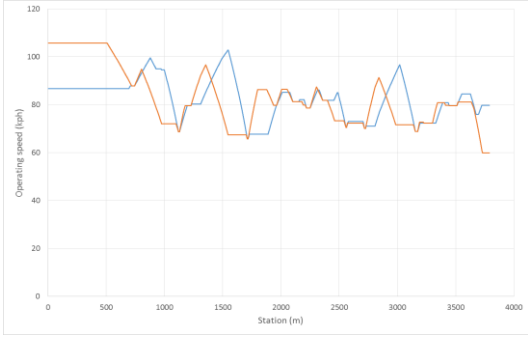

HOMOGENEOUS ROAD SEGMENTS

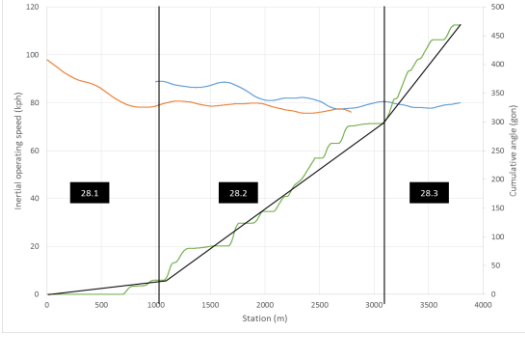

CRASHES

Observed:	3	Exposure	4
		Polus (2004)	4
		Camacho (2009)	4
		Garach (2013)	6
		Camacho (2014)	3

ROAD SECTION 29

Road:	CV-900	
Initial station:	10+270	Roundabout
Final station:	11+070	Roundabout

AADT:	7143	vpd
Length:	841	m

OPERATING SPEED

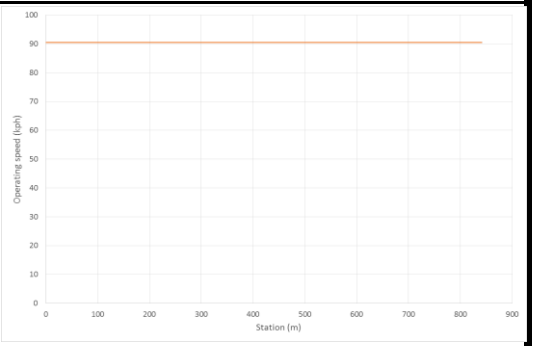

HOMOGENEOUS ROAD SEGMENTS

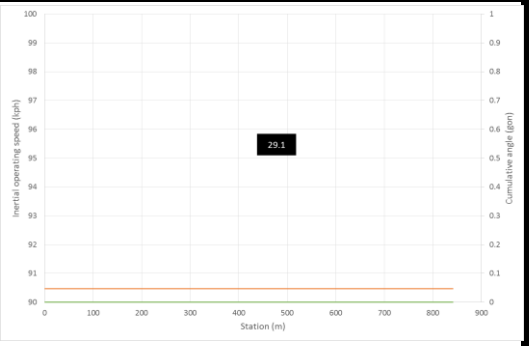

CRASHES

Observed:	2	Exposure	3
		Polus (2004)	4
		Camacho (2009)	3
		Garach (2013)	10
		Camacho (2014)	

ROAD SECTION 30

Road:	CV-15	
Initial station:	0+080	Roundabout
Final station:	7+560	Roundabout

AADT:	8891	vpd
Length:	7407	m

OPERATING SPEED

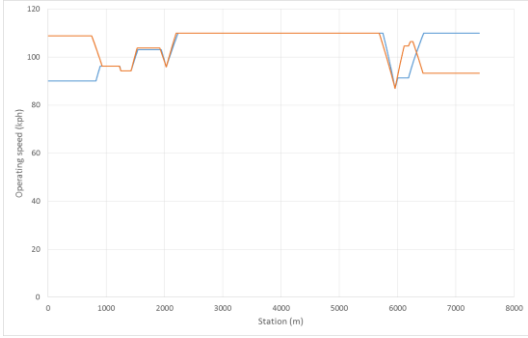

HOMOGENEOUS ROAD SEGMENT

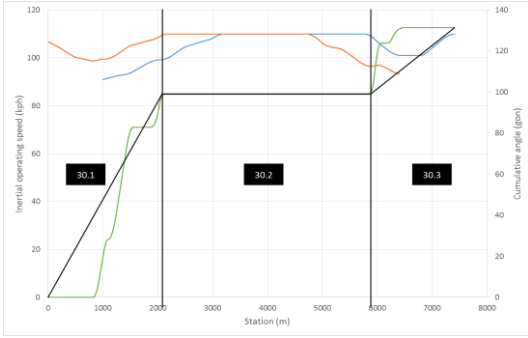

CRASHES

Observed:	18	Exposure	24
		Polus (2004)	49
		Camacho (2009)	35
		Garach (2013)	82
		Camacho (2014)	22

ROAD SECTION 31

Road:	CV-820	
Initial station:	12+320	Roundabout
Final station:	12+320	Roundabout

AADT:	4476	vpd
Length:	3396	m

OPERATING SPEED

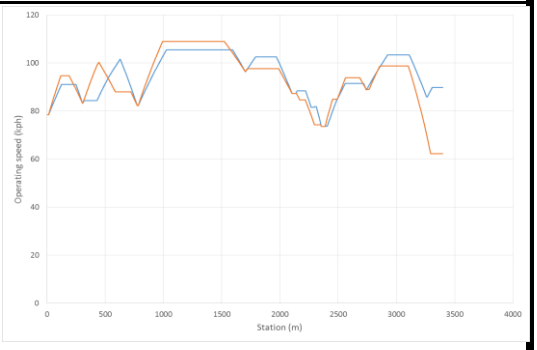

HOMOGENEOUS ROAD SEGMENT

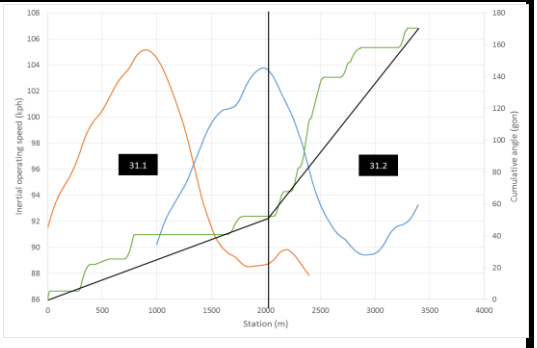

CRASHES

Observed:	8	Exposure	10
		Polus (2004)	22
		Camacho (2009)	15
		Garach (2013)	33
		Camacho (2014)	8

ROAD SECTION 32

Road:	CV-20	
Initial station:	12+200	Urban
Final station:	27+070	Urban

AADT:	4541	vpd
Length:	14797	m

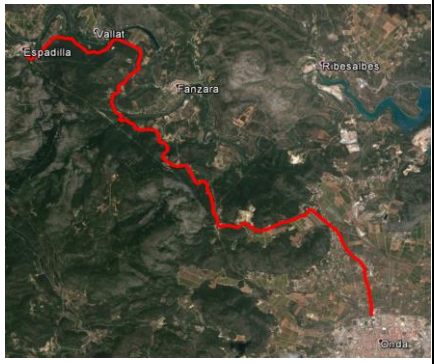

OPERATING SPEED

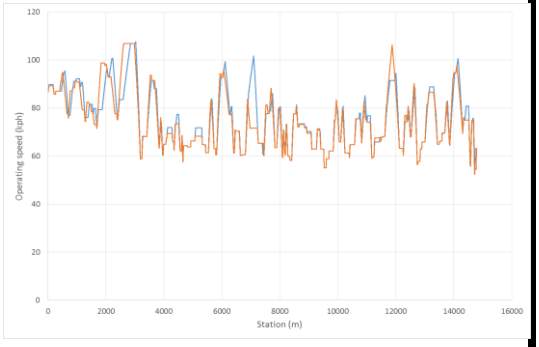

HOMOGENEOUS ROAD SEGMENT

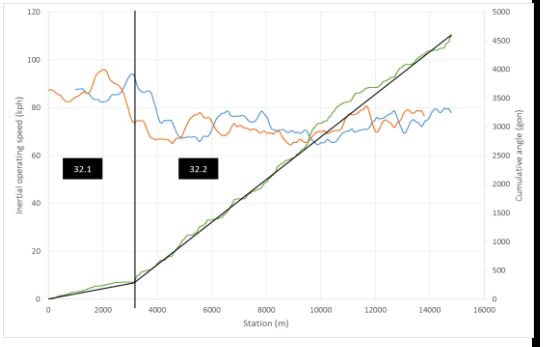

CRASHES

Observed:	48	Exposure	20
		Polus (2004)	35
		Camacho (2009)	25
		Garach (2013)	39
		Camacho (2014)	25

ROAD SECTION 33

Road:	CV-50	
Initial station:	50+740	Urban
Final station:	74+510	Roundabout

AADT:	1296	vpd
Length:	22856	m

OPERATING SPEED

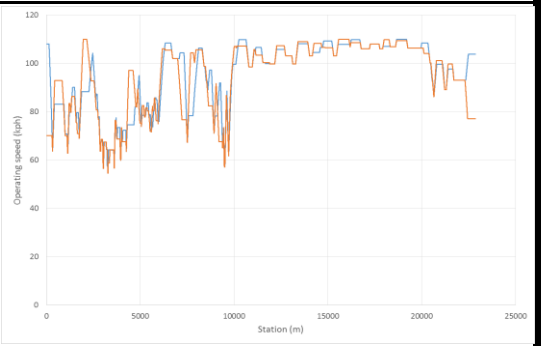

HOMOGENEOUS ROAD SEGMENTS

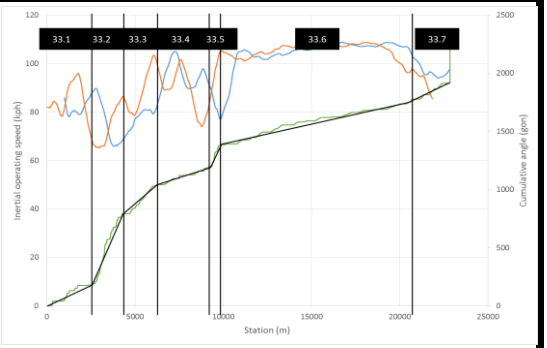

CRASHES

Observed:	34

Exposure	36
Polus (2004)	71
Camacho (2009)	50
Garach (2013)	98
Camacho (2014)	34

ROAD SECTION 34

Road:	CV-805	
Initial station:	2+070	Interchange with freeway
Final station:	13+090	Interchange with freeway

AADT:	2903	vpd
Length:	10832	m

OPERATING SPEED

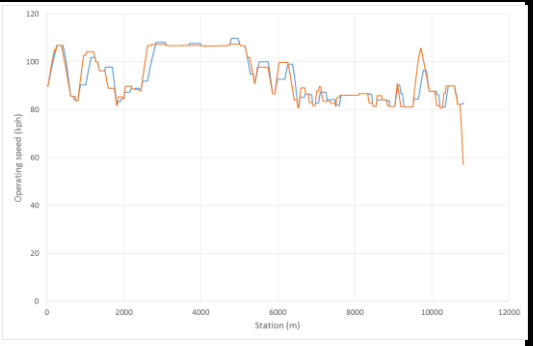

HOMOGENEOUS ROAD SEGMENT

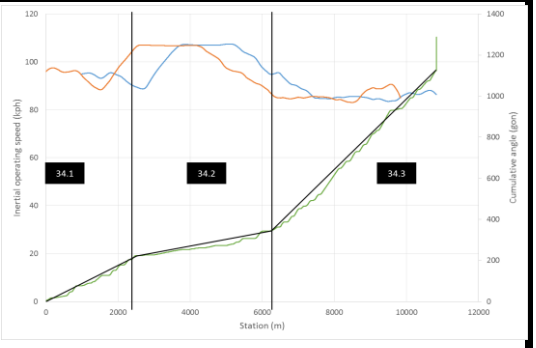

CRASHES

Observed:	12	Exposure	21
		Polus (2004)	34
		Camacho (2009)	24
		Garach (2013)	49
		Camacho (2014)	20

ROAD SECTION 35

Road:	CV-10	
Initial station:	48+230	Roundabout
Final station:	80+510	Roundabout

AADT:	5013	vpd
Length:	32164	m

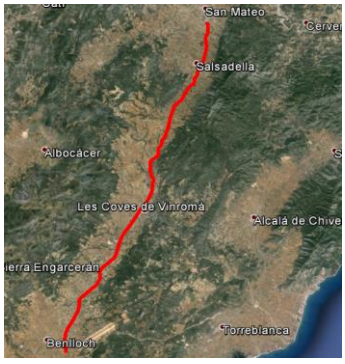

OPERATING SPEED

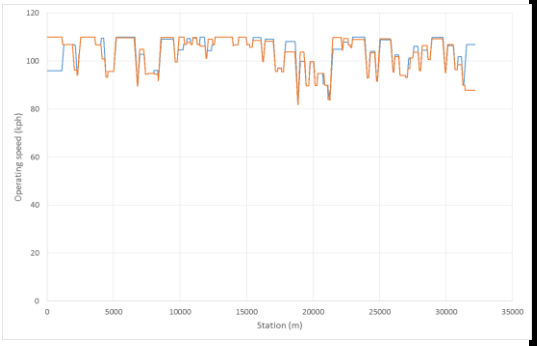

HOMOGENEOUS ROAD SEGMENT

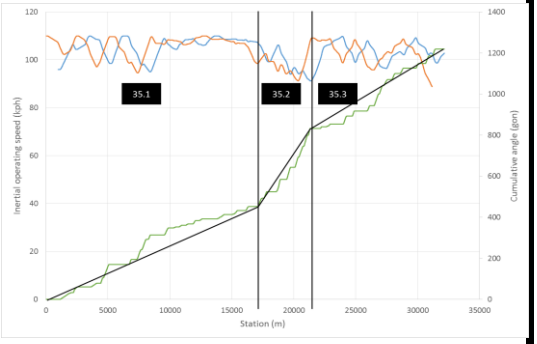

CRASHES

Observed:	65	Exposure	81
		Polus (2004)	142
		Camacho (2009)	102
		Garach (2013)	170
		Camacho (2014)	74

ROAD SECTION 36

Road:	CV-15	
Initial station:	9+630	Roundabout
Final station:	15+550	Urban

AADT:	4754	vpd
Length:	5911	m

OPERATING SPEED

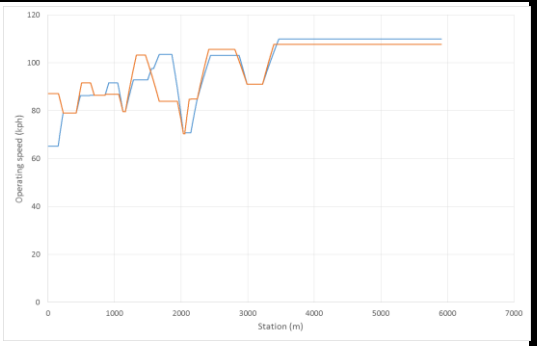

HOMOGENEOUS ROAD SEGMENT

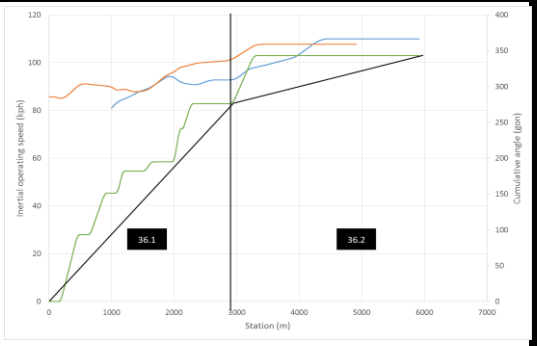

CRASHES

Observed:	11	Exposure	15
		Polus (2004)	33
		Camacho (2009)	23
		Garach (2013)	45
		Camacho (2014)	14

ROAD SECTION 37

Road:	CV-18	
Initial station:	1+220	Roundabout
Final station:	2+310	Roundabout

AADT:	25015	vpd
Length:	1089	m

OPERATING SPEED

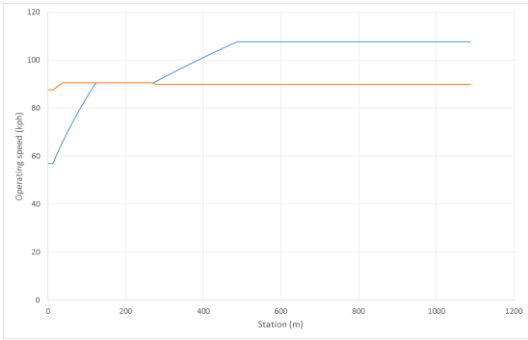

HOMOGENEOUS ROAD SEGMENT

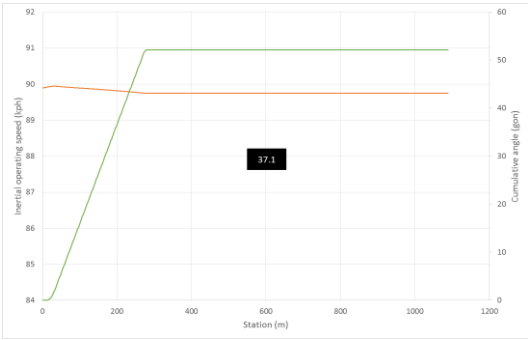

CRASHES

Observed:	8	Exposure	7
		Polus (2004)	43
		Camacho (2009)	30
		Garach (2013)	74
		Camacho (2014)	9

ROAD SECTION 38

Road:	CV-50	
Initial station:	33+890	Urban
Final station:	39+660	Roundabout

AADT:	5243	vpd
Length:	5750	m

OPERATING SPEED

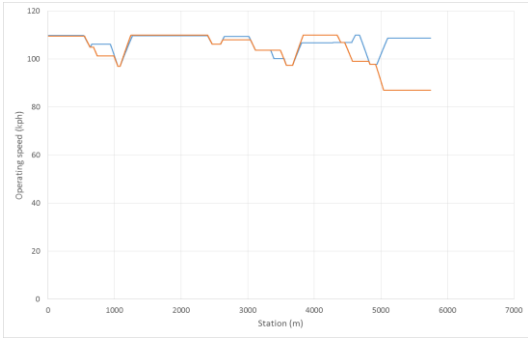

HOMOGENEOUS ROAD SEGMENT

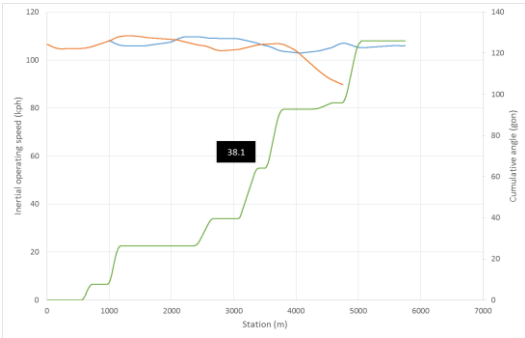

CRASHES

Observed:	13	Exposure	17
		Polus (2004)	33
		Camacho (2009)	24
		Garach (2013)	46
		Camacho (2014)	13

ROAD SECTION 39

Road:	CV-720	
Initial station:	2+500	Urban
Final station:	8+780	Urban
AADT:	363	vpd
Length:	6311	m

OPERATING SPEED

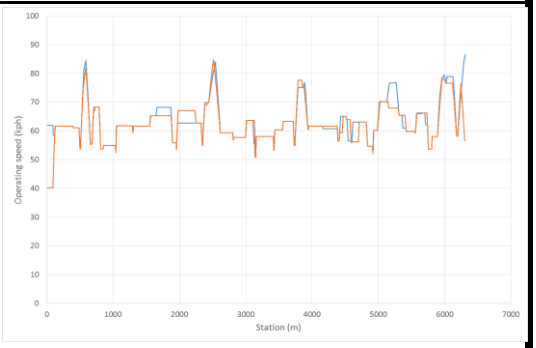

HOMOGENEOUS ROAD SEGMENT

CRASHES

Observed:	2	Exposure	4
		Polus (2004)	3
		Camacho (2009)	2
		Garach (2013)	3
		Camacho (2014)	5

ROAD SECTION 40

Road:	CV-806	
Initial station:	0+790	Urban
Final station:	6+680	Roundabout

AADT:	5390	vpd
Length:	5826	m

OPERATING SPEED

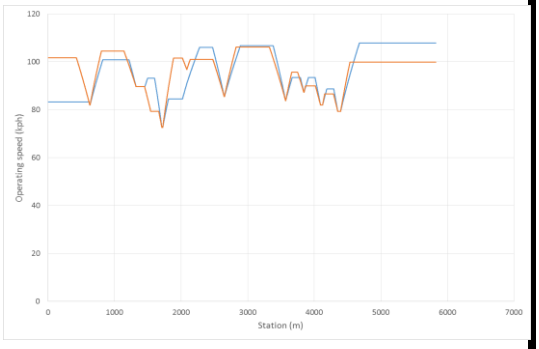

HOMOGENEOUS ROAD SEGMENT

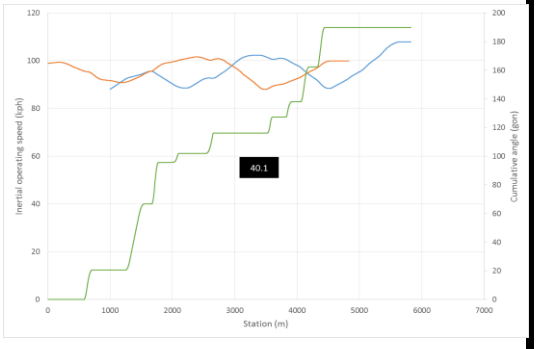

CRASHES

Observed:	9	Exposure	17
		Polus (2004)	47
		Camacho (2009)	33
		Garach (2013)	55
		Camacho (2014)	21

ROAD SECTION 41

Road:	CV-840	
Initial station:	14+550	Roundabout
Final station:	20+590	Interchange with

AADT:	3129	vpd
Length:	6032	m

OPERATING SPEED

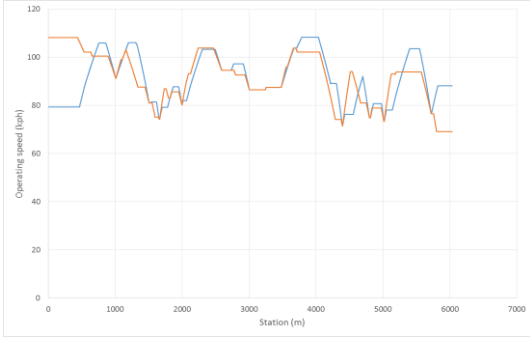

HOMOGENEOUS ROAD SEGMENTS

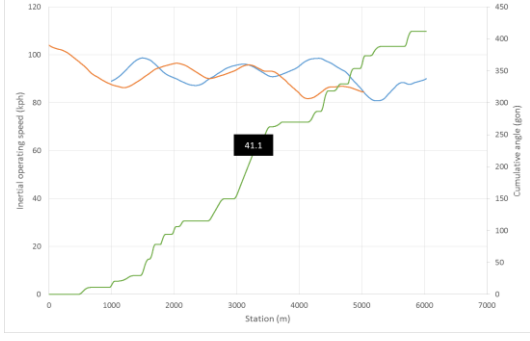

CRASHES

Observed:	18	Exposure	13	
		Polus (2004)	31	
		Camacho (2009)	22	
		Garach (2013)	33	
		Camacho (2014)	15	

ROAD SECTION 42

Road:	CV-827	
Initial station:	0+180	Roundabout
Final station:	9+890	Urban

AADT:	384	vpd
Length:	9470	m

OPERATING SPEED

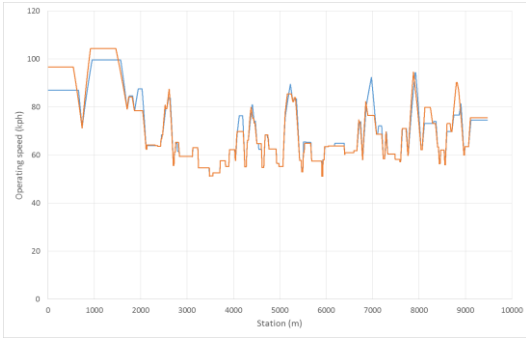

HOMOGENEOUS ROAD SEGMENT

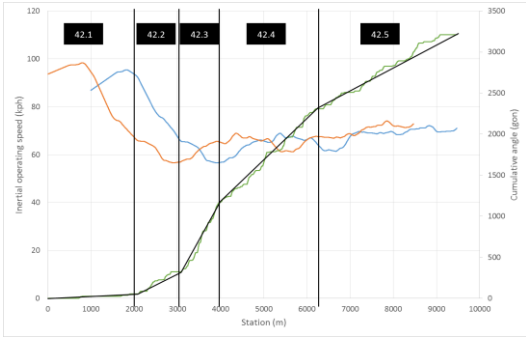

CRASHES

Observed:	12	Exposure	4
		Polus (2004)	4
		Camacho (2009)	3
		Garach (2013)	6
		Camacho (2014)	4

ROAD SECTION 43

Road:	CV-35	
Initial station:	68+340	Urban
Final station:	86+640	Urban

AADT:	1958	vpd
Length:	18240	m

OPERATING SPEED

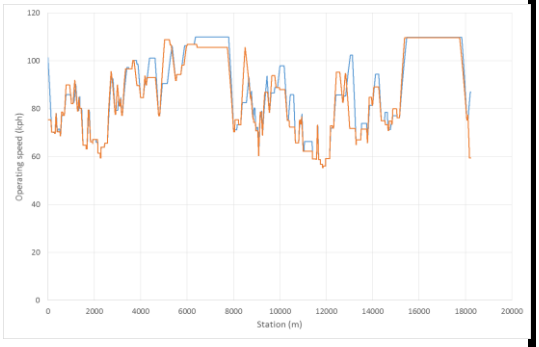

HOMOGENEOUS ROAD SEGMENTS

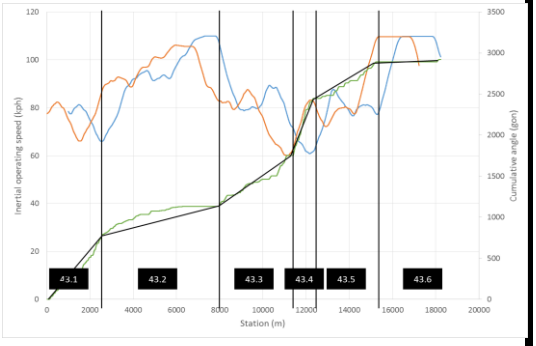

CRASHES

Observed:	18	Exposure	19
		Polus (2004)	37
		Camacho (2009)	25
		Garach (2013)	43
		Camacho (2014)	22

ROAD SECTION 44

Road:	CV-35	
Initial station:	53+510	Urban
Final station:	67+050	Roundabout

AADT:	2258	vpd
Length:	13571	m

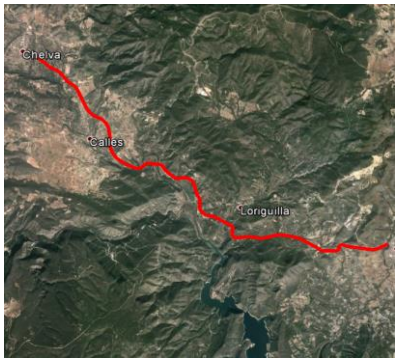

OPERATING SPEED

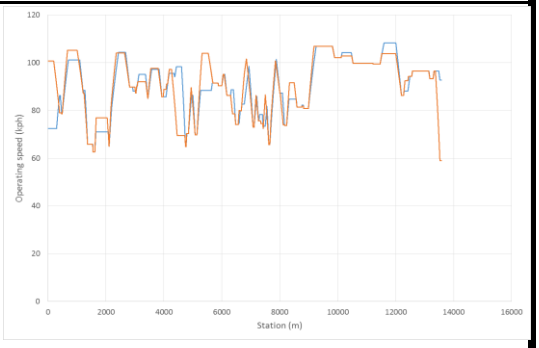

HOMOGENEOUS ROAD SEGMENTS

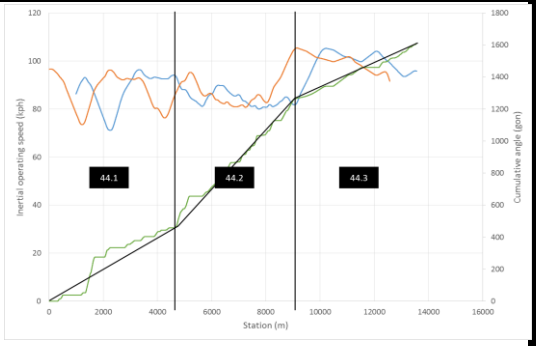

CRASHES

		Exposure	23
Observed:	33	Polus (2004)	43
		Camacho (2009)	31
		Garach (2013)	52
		Camacho (2014)	23

ROAD SECTION 45

Road:	CV-333	
Initial station:	3+850	Roundabout
Final station:	8+390	Roundabout

AADT:	4076	vpd
Length:	4583	m

OPERATING SPEED

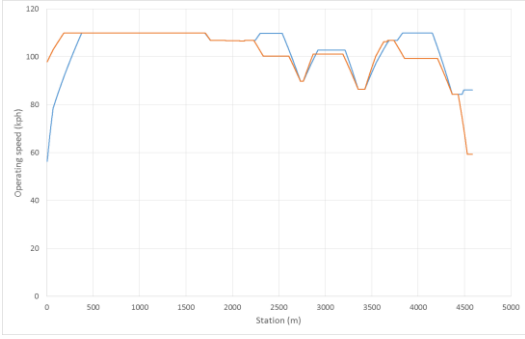

HOMOGENEOUS ROAD SEGMENTS

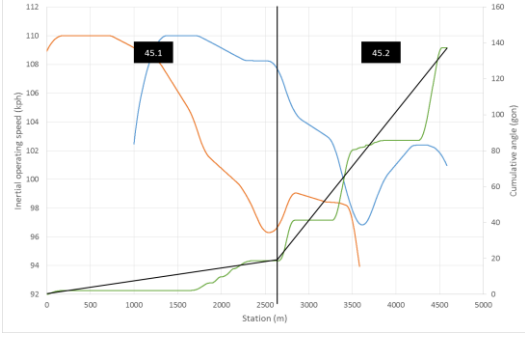

CRASHES

Observed:	2	Exposure	11
		Polus (2004)	20
		Camacho (2009)	14
		Garach (2013)	30
		Camacho (2014)	7

ROAD SECTION 46

Road:	CV-801	
Initial station:	0+420	Urban
Final station:	9+070	Intersection

AADT:	547	vpd
Length:	8477	m

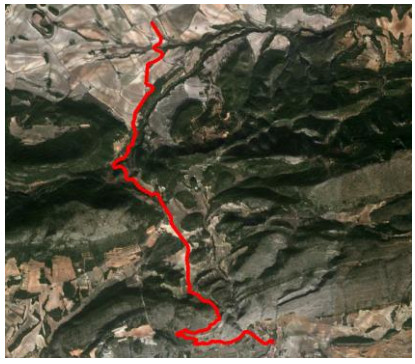

OPERATING SPEED

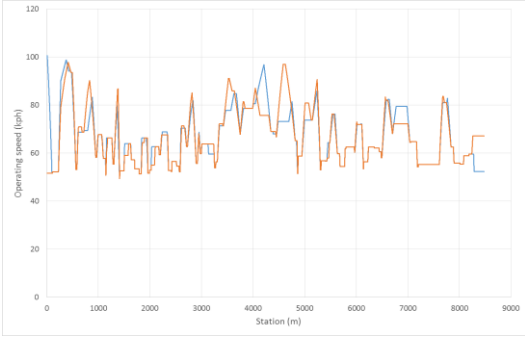

HOMOGENEOUS ROAD SEGMENTS

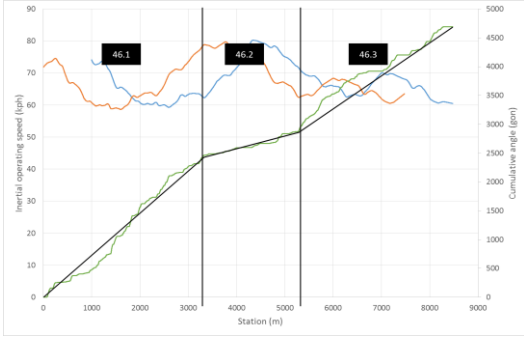

CRASHES

Observed:	4	Exposure	7
		Polus (2004)	9
		Camacho (2009)	6
		Garach (2013)	9
		Camacho (2014)	8

ROAD SECTION 47

Road:	CV-820	
Initial station:	8+950	Urban
Final station:	10+860	Roundabout

AADT:	4476	vpd
Length:	1791	m

OPERATING SPEED

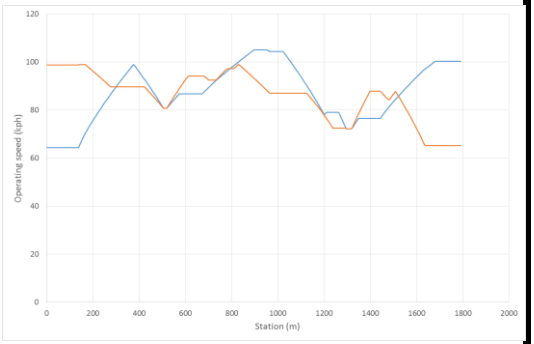

HOMOGENEOUS ROAD SEGMENTS

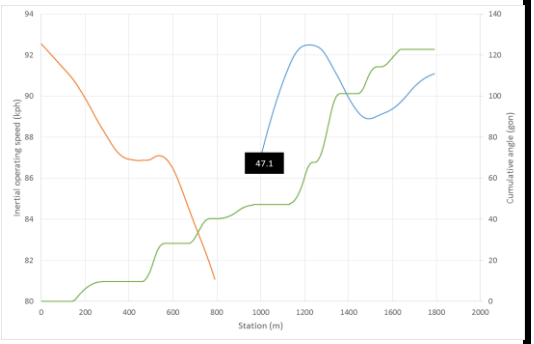

CRASHES

Observed:	5	Exposure	5
		Polus (2004)	13
		Camacho (2009)	9
		Garach (2013)	18
		Camacho (2014)	5

ROAD SECTION 48

Road:	CV-755	
Initial station:	0+000	Urban
Final station:	0+650	Urban

AADT:	871	vpd
Length:	642	m

OPERATING SPEED

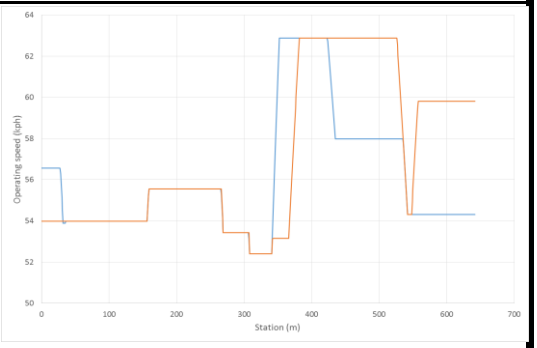

HOMOGENEOUS ROAD SEGMENTS

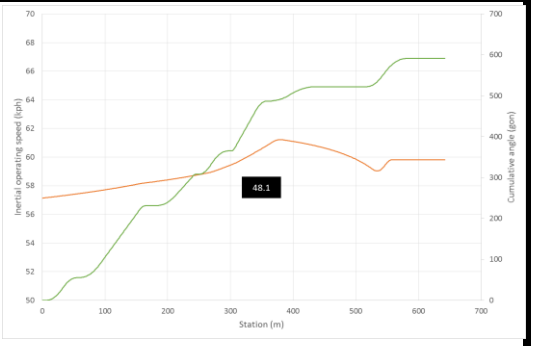

CRASHES

Observed:	1	Exposure	1
		Polus (2004)	0
		Camacho (2009)	0
		Garach (2013)	1
		Camacho (2014)	1

ROAD SECTION 49

Road:	CV-50	
Initial station:	42+210	Urban
Final station:	48+830	Urban

AADT:	2676	vpd
Length:	6599	m

OPERATING SPEED

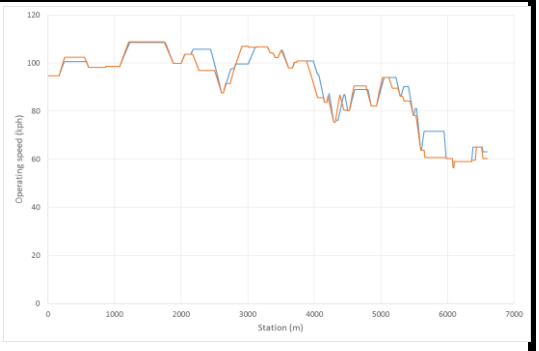

HOMOGENEOUS ROAD SEGMENT

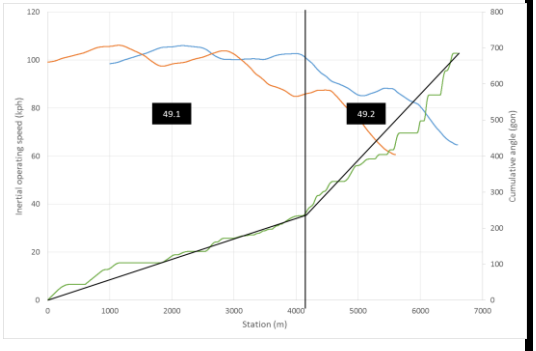

CRASHES

Observed:	16	Exposure	13
		Polus (2004)	23
		Camacho (2009)	16
		Garach (2013)	31
		Camacho (2014)	12

ROAD SECTION 50

Road:	CV-15	
Initial station:	17+850	Urban
Final station:	38+020	Free

AADT:	2703	vpd
Length:	20117	m

OPERATING SPEED

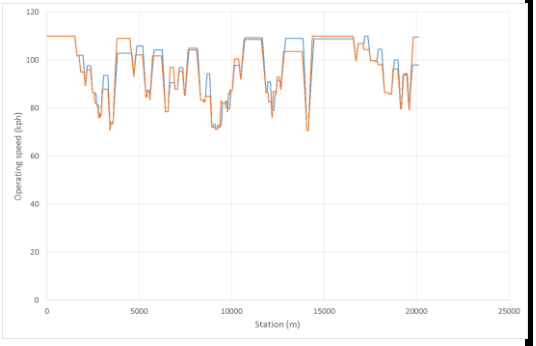

HOMOGENEOUS ROAD SEGMENTS

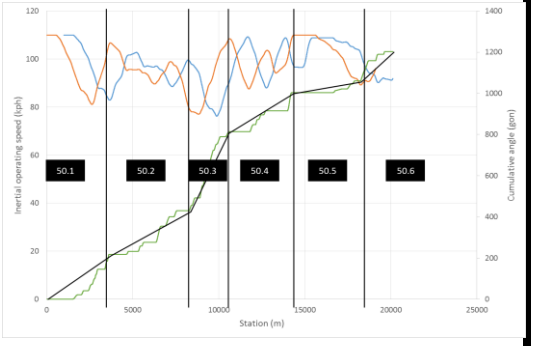

CRASHES

Observed:	32	Exposure	32
		Polus (2004)	74
		Camacho (2009)	52
		Garach (2013)	81
		Camacho (2014)	32

ROAD SECTION 51

Road:	CV-50	
Initial station:	76+240	Urban
Final station:	83+740	Roundabout

AADT:	4722	vpd
Length:	7509	m

OPERATING SPEED

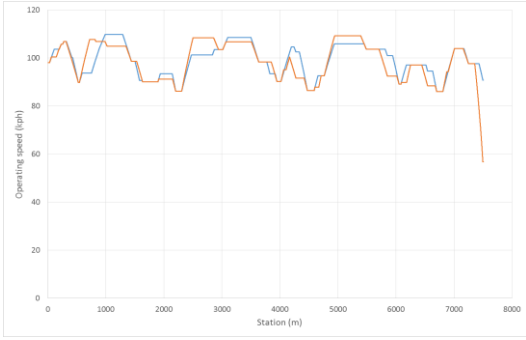

HOMOGENEOUS ROAD SEGMENT

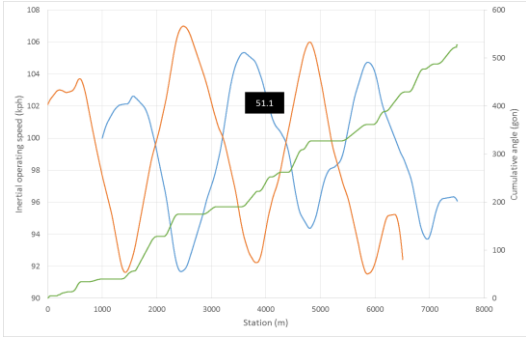

CRASHES

Observed:	9	Exposure	21
		Polus (2004)	46
		Camacho (2009)	33
		Garach (2013)	54
		Camacho (2014)	20

ROAD SECTION 52

Road:	CV-16	
Initial station:	8+890	Roundabout
Final station:	10+050	Roundabout

AADT:	10325	vpd
Length:	1252	m

OPERATING SPEED

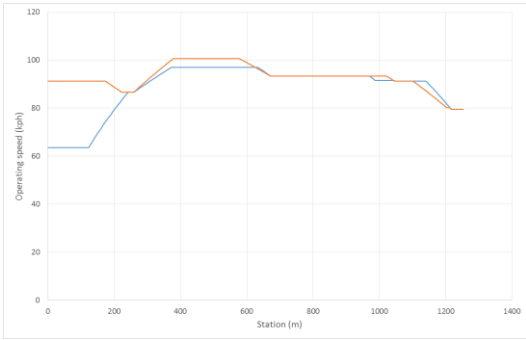

HOMOGENEOUS ROAD SEGMENT

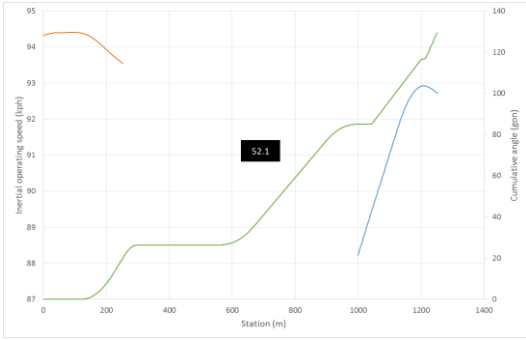

CRASHES

Observed:	3	Exposure	5
		Polus (2004)	17
		Camacho (2009)	12
		Garach (2013)	29
		Camacho (2014)	6

ROAD SECTION 53

Road:	CV-18	
Initial station:	3+350	Roundabout
Final station:	8+000	Roundabout

AADT:	14640	vpd
Length:	4522	m

OPERATING SPEED

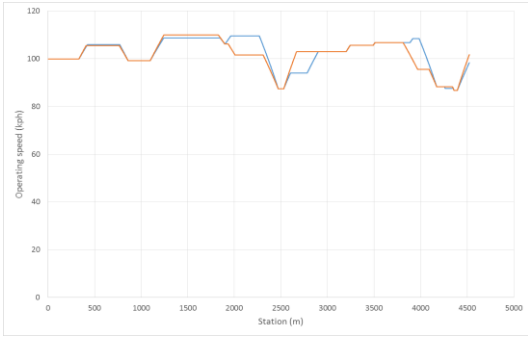

HOMOGENEOUS ROAD SEGMENT

CRASHES

Observed:	49	Exposure	23
		Polus (2004)	75
		Camacho (2009)	54
		Garach (2013)	113
		Camacho (2014)	26

ROAD SECTION 54

Road:	CV-18	
Initial station:	2+570	Roundabout
Final station:	3+100	Roundabout

AADT:	14640	vpd
Length:	520	m

OPERATING SPEED

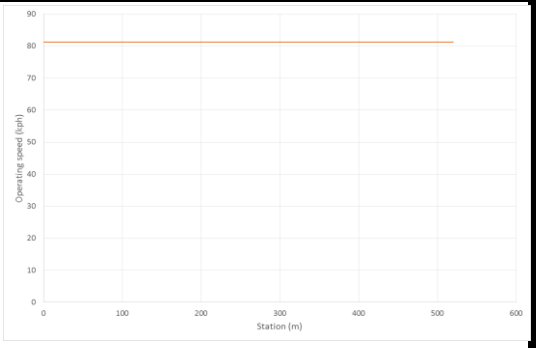

HOMOGENEOUS ROAD SEGMENTS

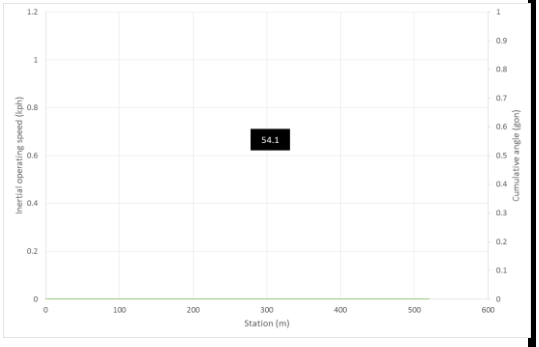

CRASHES

		Exposure	3	
Observed:	2	Polus (2004)	5	
		Camacho (2009)	4	
		Garach (2013)	15	
		Camacho (2014)		

ROAD SECTION 55

Road:	CV-439	
Initial station:	0+270	Roundabout
Final station:	12+590	Free

AADT:	371	vpd
Length:	11992	m

OPERATING SPEED

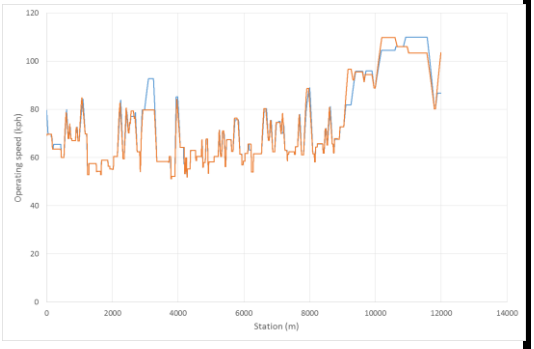

HOMOGENEOUS ROAD SEGMENTS

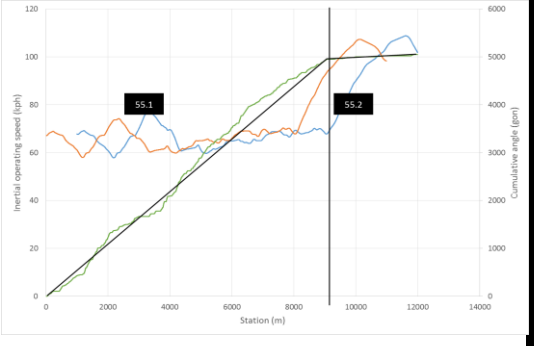

CRASHES

Observed:	3	Exposure	7
		Polus (2004)	6
		Camacho (2009)	4
		Garach (2013)	5
		Camacho (2014)	8

ROAD SECTION 56

Road:	CV-222	
Initial station:	0+530	Roundabout
Final station:	6+450	Roundabout

AADT:	6549	vpd
Length:	5871	m

OPERATING SPEED

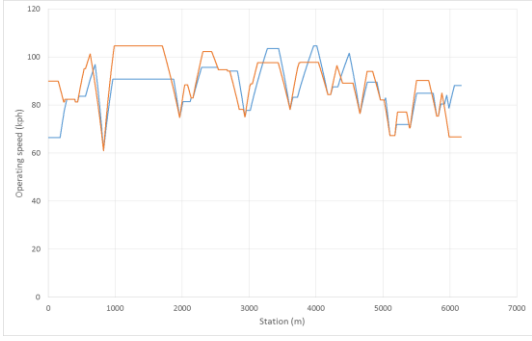

HOMOGENEOUS ROAD SEGMENT

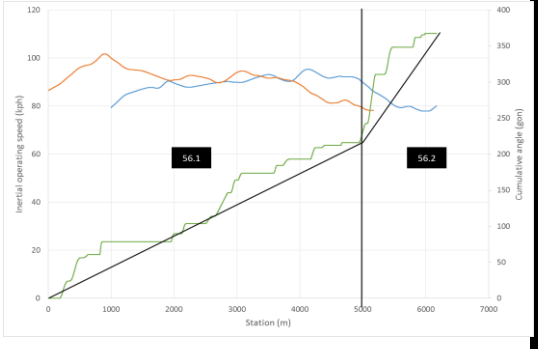

CRASHES

Observed:	22	Exposure	20
		Polus (2004)	58
		Camacho (2009)	40
		Garach (2013)	76
		Camacho (2014)	28

ROAD SECTION 57

Road:	CV-245	
Initial station:	0+620	Urban
Final station:	3+270	Urban

AADT:	209	vpd
Length:	2352	m

OPERATING SPEED

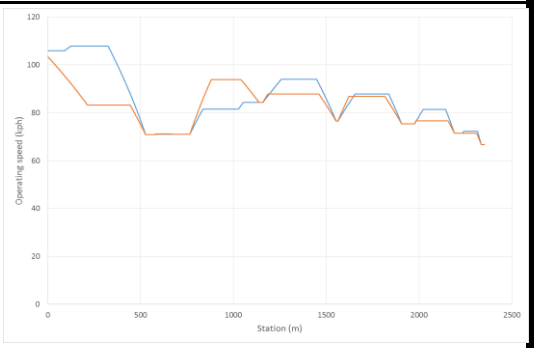

HOMOGENEOUS ROAD SEGMENT

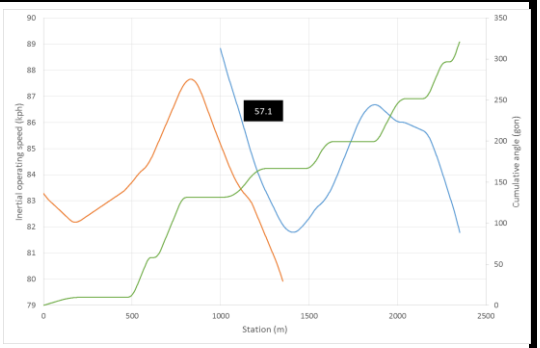

CRASHES

Observed:	0	Exposure	1
		Polus (2004)	1
		Camacho (2009)	1
		Garach (2013)	1
		Camacho (2014)	1

ROAD SECTION 58

Road:	CV-245	
Initial station:	3+770	Urban
Final station:	6+690	Roundabout

AADT:	209	vpd
Length:	3082	m

OPERATING SPEED

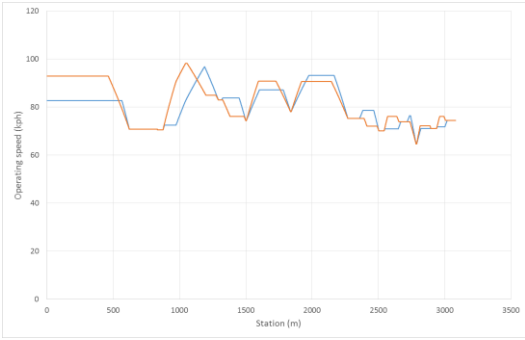

HOMOGENEOUS ROAD SEGMENTS

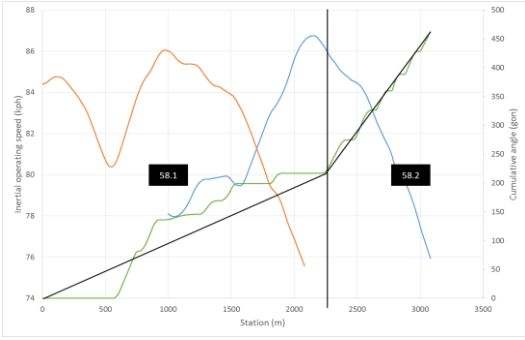

CRASHES

Observed:	1	Exposure	1
		Polus (2004)	1
		Camacho (2009)	0
		Garach (2013)	1
		Camacho (2014)	1

ROAD SECTION 59

Road:	CV-585	
Initial station:	0+160	Roundabout
Final station:	5+980	Roundabout

AADT:	3555	vpd
Length:	5807	m

OPERATING SPEED

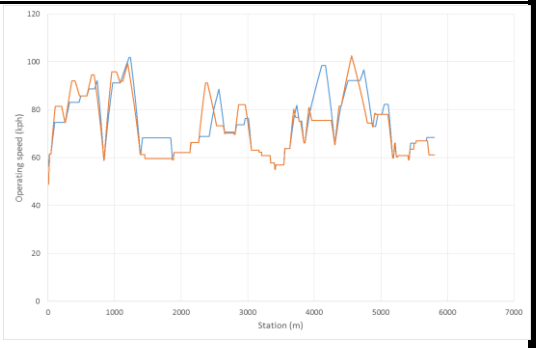

HOMOGENEOUS ROAD SEGMENTS

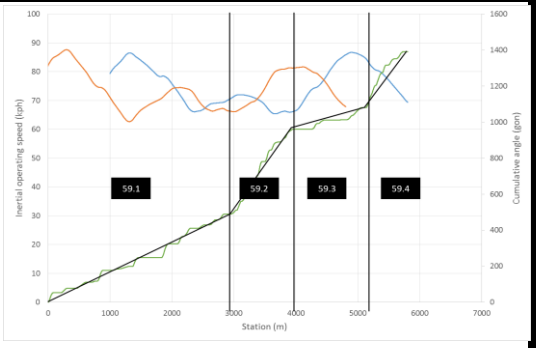

CRASHES

Observed:	21	Exposure	15
		Polus (2004)	31
		Camacho (2009)	22
		Garach (2013)	45
		Camacho (2014)	21

ROAD SECTION 60

Road:	CV-790	
Initial station:	0+020	Intersection
Final station:	5+890	Roundabout

AADT:	1966	vpd
Length:	5874	m

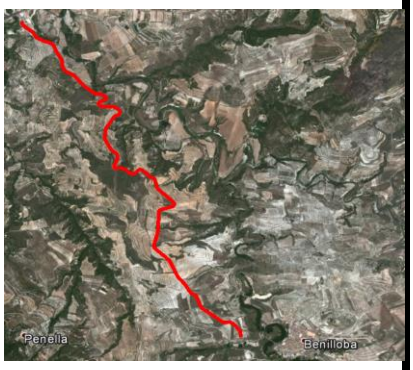

OPERATING SPEED

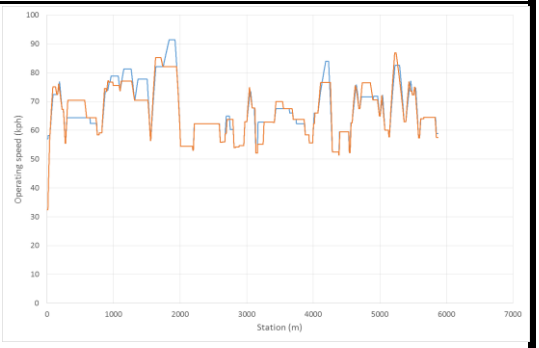

HOMOGENEOUS ROAD SEGMENT

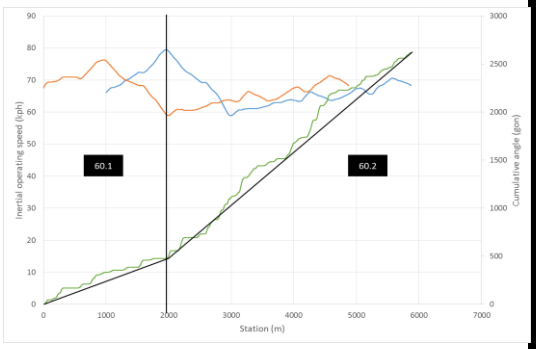

CRASHES

Observed:	4	Exposure	11
		Polus (2004)	19
		Camacho (2009)	13
		Garach (2013)	24
		Camacho (2014)	18

ROAD SECTION 61

Road:	CV-11	
Initial station:	10+660	Urban
Final station:	19+320	Roundabout

AADT:	3267	vpd
Length:	8608	m

OPERATING SPEED

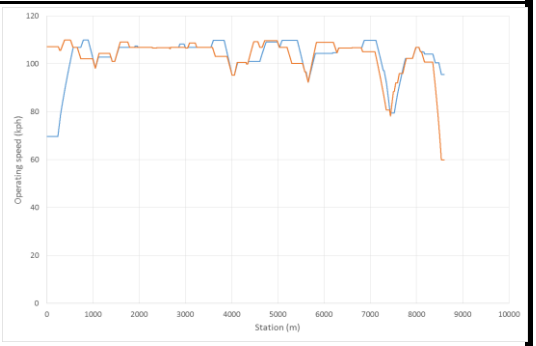

HOMOGENEOUS ROAD SEGMENTS

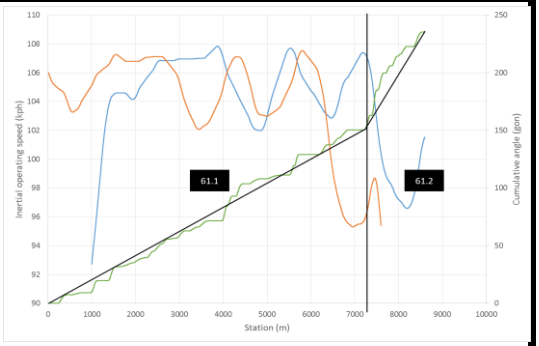

CRASHES

Observed:	20		Exposure	19
			Polus (2004)	32
			Camacho (2009)	23
			Garach (2013)	44
			Camacho (2014)	14

ROAD SECTION 62

Road:	CV-17	
Initial station:	0+230	Roundabout
Final station:	3+370	Roundabout

AADT:	16339	vpd
Length:	3117	m

OPERATING SPEED

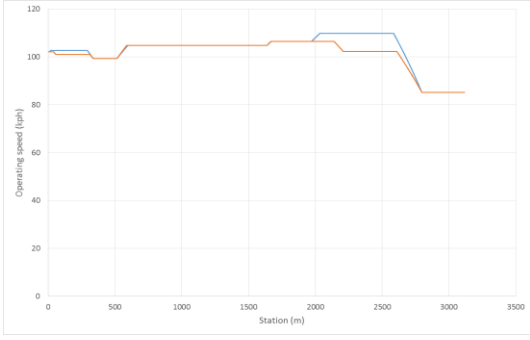

HOMOGENEOUS ROAD SEGMENTS

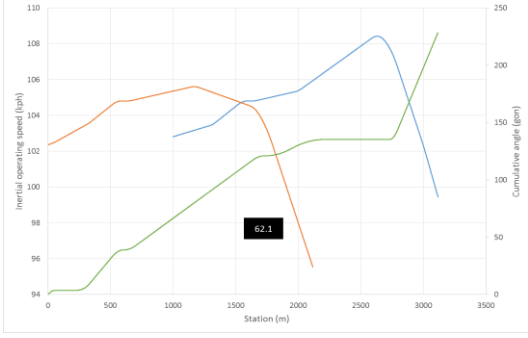

CRASHES

Observed:	12		Exposure	17
			Polus (2004)	59
			Camacho (2009)	42
			Garach (2013)	94
			Camacho (2014)	18

ROAD SECTION 63

Road:	CV-403	
Initial station:	2+050	Roundabout
Final station:	3+320	Roundabout

AADT:	14176	vpd
Length:	1228	m

OPERATING SPEED

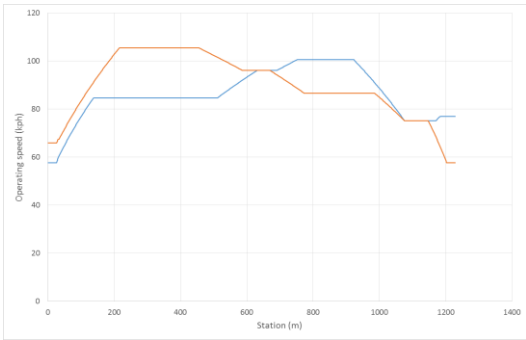

HOMOGENEOUS ROAD SEGMENT

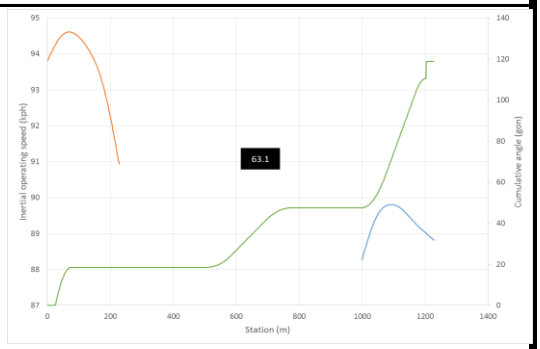

CRASHES

Observed:	4	Exposure	6
		Polus (2004)	30
		Camacho (2009)	21
		Garach (2013)	48
		Camacho (2014)	10

ROAD SECTION 64

Road:	CV-407	
Initial station:	0+500	Urban
Final station:	2+160	Roundabout

AADT:	13149	vpd
Length:	1633	m

OPERATING SPEED

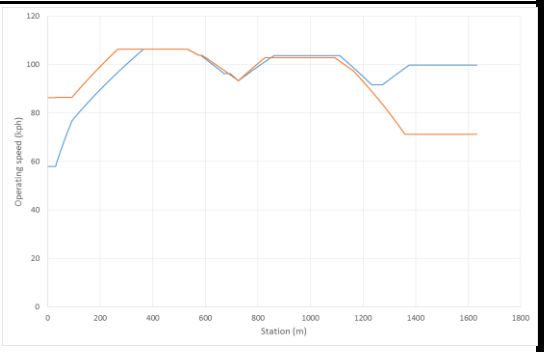

HOMOGENEOUS ROAD SEGMENTS

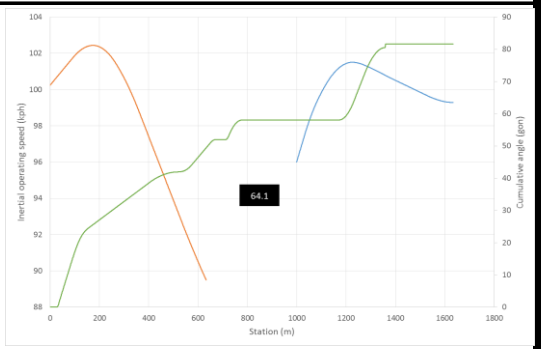

CRASHES

Observed:	3

Exposure	8
Polus (2004)	37
Camacho (2009)	25
Garach (2013)	55
Camacho (2014)	8

ROAD SECTION 65

Road:	CV-720	
Initial station:	0+020	Urban
Final station:	2+380	Urban

AADT:	363	vpd
Length:	2367	m

OPERATING SPEED

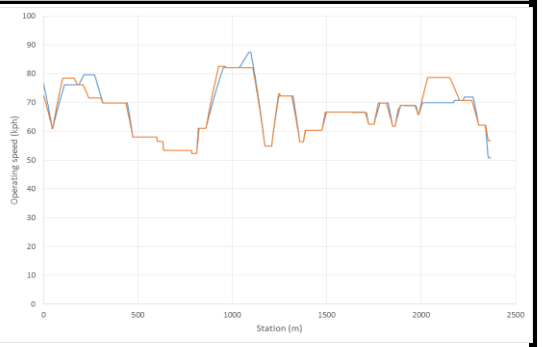

HOMOGENEOUS ROAD SEGMENTS

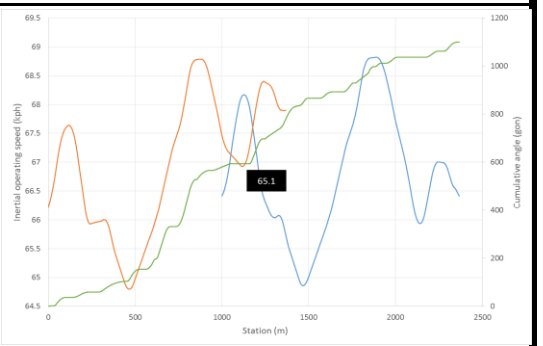

CRASHES

Observed:	1

Exposure	2
Polus (2004)	1
Camacho (2009)	1
Garach (2013)	1
Camacho (2014)	2

III. Road homogeneous segments

ROAD SEGMENT: 1.1

Road:	CV-11	
Initial station:	0+710	Town
Final station:	10+550	Intersection
		Constrained

AADT:	1801 vpd
Length:	9885 m

OPERATIONAL CHARACTERISTICS

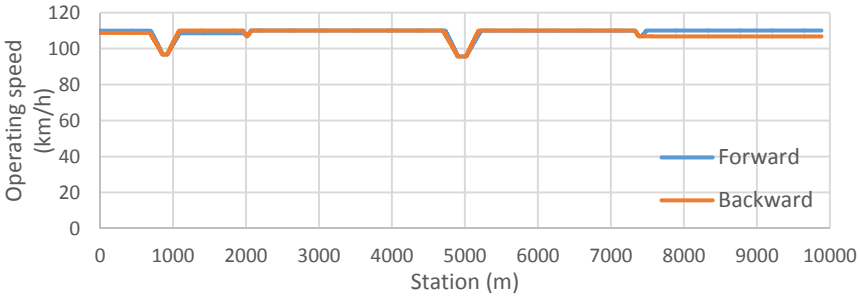

CCR	5.797635 gon/km	$\overline{\Delta v_{85}}$	9.0453594 km/h
$\bar{v}_{85}$	108.6807 km/h	d_{85}	0.552366 m/s^2
$\sigma_{v_{85}}$	2.829634 km/h	$\sigma_{\Delta v_{85}}$	6.0170673 km/h
R_a	0.503504 m/s	$\sigma_{d_{85}}$	0.1246488 m/s^2
$E_{a,10}$	0.1042 m/s	$\bar{L}_{\Delta v_{85}}$	119 m
$E_{a,20}$	0 m/s	L_d	4.21%
L_{10}	0.030956 m	N	7
L_{20}	0 m		

CONSISTENCY

Polus (2004)	2.51545
Garach (2013)	2.44474
Camacho (2014	3.79496

CRASHES

Observed:	7
Estimated:	
Exposure	16
Polus (2004)	14
Camacho (2009)	10
Garach (2013)	20
Camacho (2014)	10

ROAD SEGMENT: 2.1

Road:	CV-12	
Initial station:	0+050	Intersection
Final station:	2+570	Free
		Constrained

AADT:	859 vpd
Length:	2504 m

OPERATIONAL CHARACTERISTICS

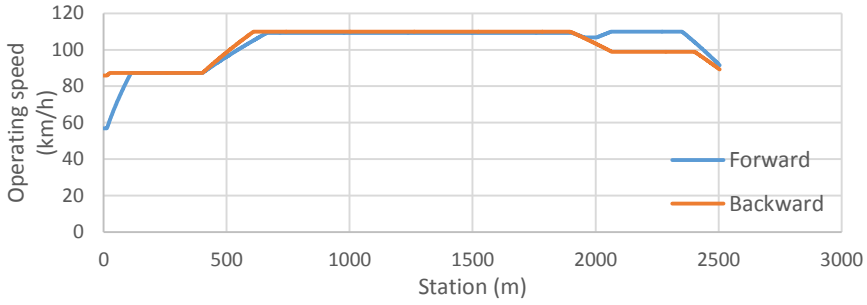

CCR	38.99146 gon/km	$\overline{\Delta v_{85}}$	11.267728 km/h
$\bar{v}_{85}$	103.1851 km/h	d_{85}	0.7620057 m/s^2
$\sigma_{v_{85}}$	9.717697 km/h	$\sigma_{\Delta v_{85}}$	10.835079 km/h
R_a	2.229069 km/h	$\sigma_{d_{85}}$	0.2315275 m/s^2
$E_{a,10}$	0.924185 km/h	$\bar{L}_{\Delta v_{85}}$	105.5 m
$E_{a,20}$	0.182417 km/h	L_d	8.43%
L_{10}	0.19389 m	N	4
L_{20}	0.019169 m		

CONSISTENCY

Polus (2004)	0.52715
Garach (2013)	0.80125
Camacho (2014	3.35057

CRASHES

Observed:	1
Estimated:	
Exposure	3
Polus (2004)	3
Camacho (2009)	2
Garach (2013)	4
Camacho (2014)	2

ROAD SEGMENT: 2.2

Road:	CV-12	
Initial station:	2+570	Free
Final station:	9+760	Free
		Free

AADT:	859 vpd
Length:	7151 m

OPERATIONAL CHARACTERISTICS

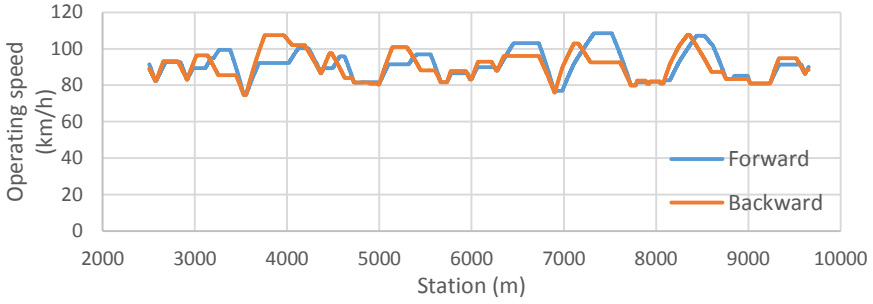

CCR	85.13764 gon/km	$\overline{\Delta v_{85}}$	11.90533 km/h
$\bar{v}_{85}$	90.96252 km/h	d_{85}	0.9075072 m/s^2
$\sigma_{v_{85}}$	7.699005 km/h	$\sigma_{\Delta v_{85}}$	9.4554022 km/h
R_a	1.751929 km/h	$\sigma_{d_{85}}$	0.1220181 m/s^2
$E_{a,10}$	0.651851 km/h	$\bar{L}_{\Delta v_{85}}$	89.451613 m
$E_{a,20}$	0 km/h	L_d	19.39%
L_{10}	0.175989 m	N	31
L_{20}	0 m		

CONSISTENCY

Polus (2004)	0.99093
Garach (2013)	1.27927
Camacho (2014	3.03089

CRASHES

Observed:	4
Estimated:	
Exposure	4
Polus (2004)	8
Camacho (2009)	6
Garach (2013)	9
Camacho (2014)	4

ROAD SEGMENT: 2.3

Road:	CV-12	
Initial station:	9+760	Free
Final station:	10+960	Free
		Free

AADT:	859 vpd
Length:	1192 m

OPERATIONAL CHARACTERISTICS

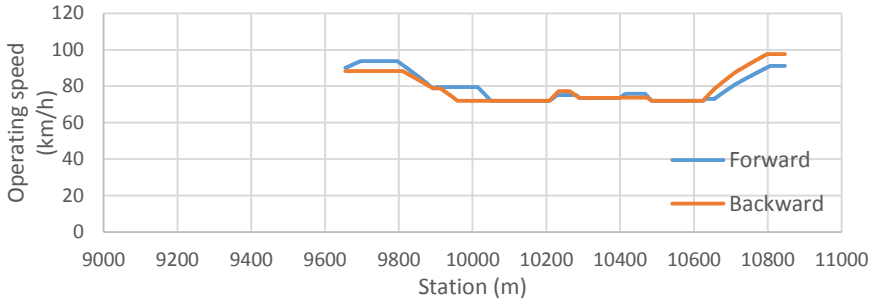

CCR	227.5114 gon/km	$\overline{\Delta v_{85}}$	9.8603354 km/h
$\bar{v}_{85}$	79.0199 km/h	d_{85}	1.1118991 m/s^2
$\sigma_{v_{85}}$	7.921178 km/h	$\sigma_{\Delta v_{85}}$	9.0240243 km/h
R_a	1.89923 km/h	$\sigma_{d_{85}}$	0.1016922 m/s^2
$E_{a,10}$	0.596396 km/h	$\bar{L}_{\Delta v_{85}}$	60.5 m
$E_{a,20}$	0 km/h	L_d	15.23%
L_{10}	0.150587 m	N	6
L_{20}	0 m		

CONSISTENCY

Polus (2004)	0.87874
Garach (2013)	1.17187
Camacho (2014	2.70265

CRASHES

Observed:	2
Estimated:	
Exposure	1
Polus (2004)	1
Camacho (2009)	1
Garach (2013)	2
Camacho (2014)	1

ROAD SEGMENT: 2.4

Road:	CV-12	
Initial station:	10+960	Free
Final station:	11+510	Free
		Free

AADT:	859 vpd
Length:	553 m

OPERATIONAL CHARACTERISTICS

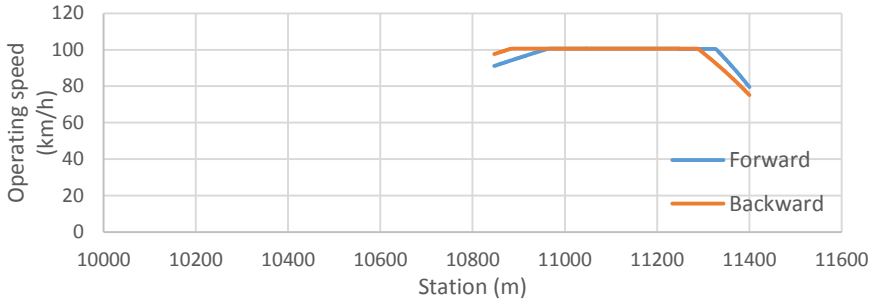

CCR	63.39914 gon/km	$\overline{\Delta v_{85}}$	11.952243 km/h
$\bar{v}_{85}$	98.19766 km/h	d_{85}	1.2986656 m/s^2
$\sigma_{v_{85}}$	5.217057 km/h	$\sigma_{\Delta v_{85}}$	12.593147 km/h
R_a	1.003205 km/h	$\sigma_{d_{85}}$	0.968658 m/s^2
$E_{a,10}$	0.322635 km/h	$\bar{L}_{\Delta v_{85}}$	55.5 m
$E_{a,20}$	0.064901 km/h	L_d	10.04%
L_{10}	0.074141 m	N	2
L_{20}	0.01085 m		

CONSISTENCY

Polus (2004)	1.87444
Garach (2013)	1.95009
Camacho (2014	2.7591

CRASHES

Observed:	1
Estimated:	
Exposure	1
Polus (2004)	0
Camacho (2009)	0
Garach (2013)	1
Camacho (2014)	0

ROAD SEGMENT: 2.5

Road:	CV-12	
Initial station:	11+510	Free
Final station:	12+560	Free
		Free

AADT:	859 vpd
Length:	1042 m

OPERATIONAL CHARACTERISTICS

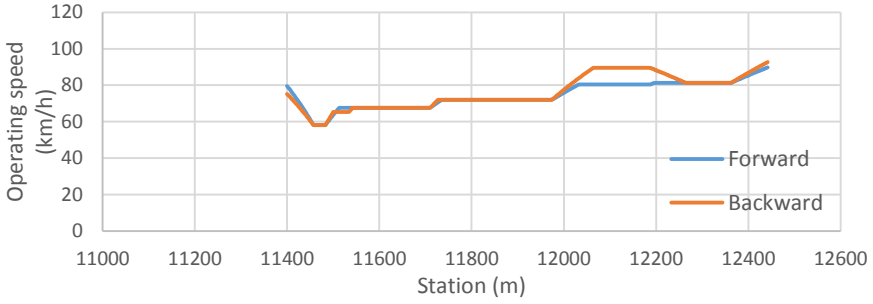

CCR	364.9956 gon/km	$\overline{\Delta v_{85}}$	10.703772 km/h
$\bar{v}_{85}$	75.28562 km/h	d_{85}	1.4630194 m/s^2
$\sigma_{v_{85}}$	8.191584 km/h	$\sigma_{\Delta v_{85}}$	7.5751339 km/h
R_a	1.987813 km/h	$\sigma_{d_{85}}$	0.3999193 m/s^2
$E_{a,10}$	0.817449 km/h	$\bar{L}_{\Delta v_{85}}$	45 m
$E_{a,20}$	0 km/h	L_d	12.96%
L_{10}	0.216411 m	N	6
L_{20}	0 m		

CONSISTENCY

Polus (2004)	0.79855
Garach (2013)	1.09294
Camacho (2014	2.42691

CRASHES

Observed:	0
Estimated:	
Exposure	1
Polus (2004)	1
Camacho (2009)	1
Garach (2013)	2
Camacho (2014)	1

ROAD SEGMENT: 2.6

Road:	CV-12	
Initial station:	12+560	Free
Final station:	16+340	Free
		Free

AADT:	859 vpd
Length:	3765 m

OPERATIONAL CHARACTERISTICS

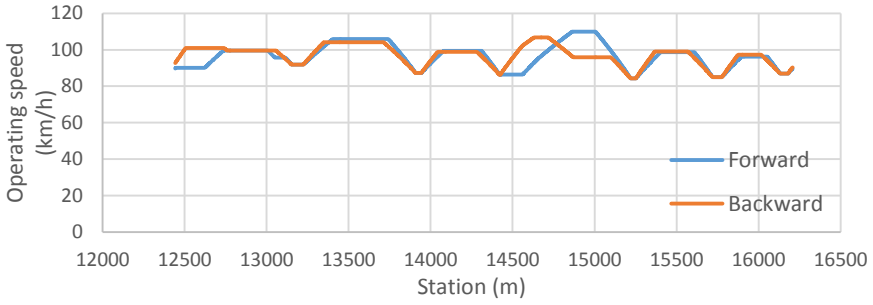

CCR	48.99551 gon/km	$\overline{\Delta v_{85}}$	11.477595 km/h
$\bar{v}_{85}$	96.74531 km/h	d_{85}	0.8116337 m/s^2
$\sigma_{v_{85}}$	6.117022 km/h	$\sigma_{\Delta v_{85}}$	6.1880463 km/h
R_a	1.385465 km/h	$\sigma_{d_{85}}$	0.1110395 m/s^2
$E_{a,10}$	0.334151 km/h	$\bar{L}_{\Delta v_{85}}$	100.93333 m
$E_{a,20}$	0 km/h	L_d	20.11%
L_{10}	0.104914 m	N	15
L_{20}	0 m		

CONSISTENCY

Polus (2004)	1.45939
Garach (2013)	1.65043
Camacho (2014	3.21111

CRASHES

Observed:	1
Estimated:	
Exposure	2
Polus (2004)	4
Camacho (2009)	3
Garach (2013)	5
Camacho (2014)	2

ROAD SEGMENT: 2.7

Road:	CV-12	
Initial station:	16+340	Free
Final station:	17+550	Free
		Free

AADT:	859 vpd
Length:	1205 m

OPERATIONAL CHARACTERISTICS

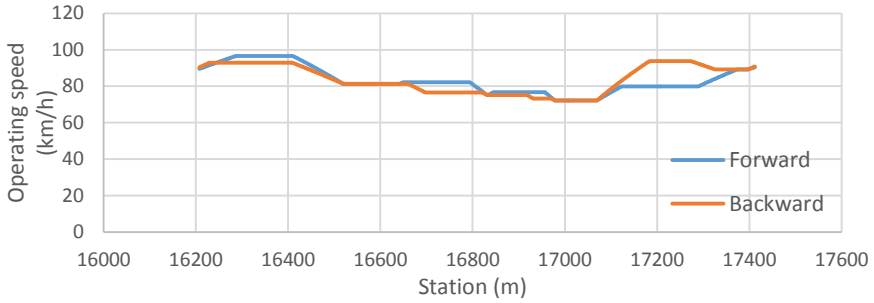

CCR	160.5563 gon/km	$\overline{\Delta v_{85}}$	8.7538749 km/h
$\bar{v}_{85}$	83.47257 km/h	d_{85}	1.0088025 m/s^2
$\sigma_{v_{85}}$	7.505263 km/h	$\sigma_{\Delta v_{85}}$	7.962221 km/h
R_a	1.819745 km/h	$\sigma_{d_{85}}$	0.1729464 m/s^2
$E_{a,10}$	0.699446 km/h	$\bar{L}_{\Delta v_{85}}$	53.5 m
$E_{a,20}$	0 km/h	L_d	13.32%
L_{10}	0.220332 m	N	6
L_{20}	0 m		

CONSISTENCY

Polus (2004)	0.97804
Garach (2013)	1.26038
Camacho (2014	2.84323

CRASHES

Observed:	0
Estimated:	
Exposure	1
Polus (2004)	1
Camacho (2009)	1
Garach (2013)	2
Camacho (2014)	1

ROAD SEGMENT: 2.8

Road:	CV-12	
Initial station:	17+550	Free
Final station:	18+270	Free
		Free

AADT:	859 vpd
Length:	717 m

OPERATIONAL CHARACTERISTICS

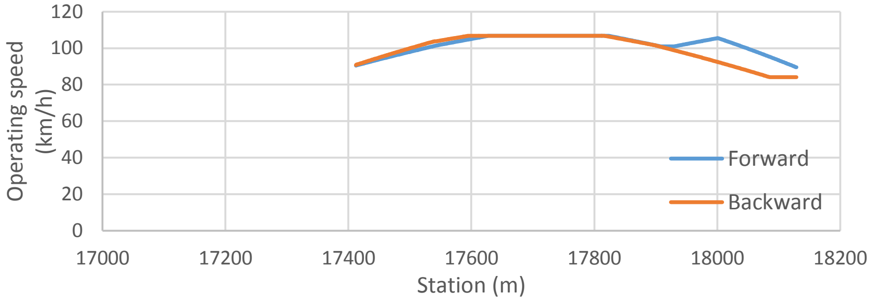

CCR	44.57772 gon/km
$\bar{v}_{85}$	100.9074 km/h
$\sigma_{v_{85}}$	6.458111 km/h
R_a	1.482777 km/h
$E_{a,10}$	0.356051 km/h
$E_{a,20}$	0 km/h
L_{10}	0.090656 m
L_{20}	0 m

$\overline{\Delta v_{85}}$	9.4785879 km/h
d_{85}	0.67727 m/s^2
$\sigma_{\Delta v_{85}}$	6.0561181 km/h
$\sigma_{d_{85}}$	0.2155034 m/s^2
$\bar{L}_{\Delta v_{85}}$	99 m
L_d	27.62%
N	4

CONSISTENCY

Polus (2004)	1.34044
Garach (2013)	1.5607
Camacho (2014	3.45902

CRASHES

Observed:	0
Estimated:	
Exposure	1
Polus (2004)	1
Camacho (2009)	1
Garach (2013)	1
Camacho (2014)	0

ROAD SEGMENT: 2.9

Road:	CV-12	
Initial station:	18+270	Free
Final station:	19+320	Free
		Free

AADT:	859 vpd
Length:	1051 m

OPERATIONAL CHARACTERISTICS

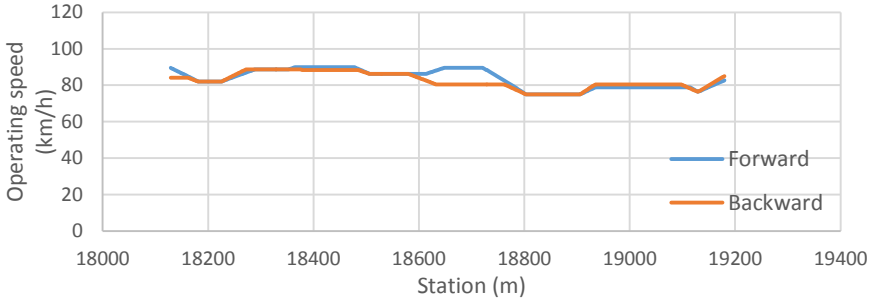

CCR	181.4654 gon/km	$\overline{\Delta v_{85}}$	6.9406743 km/h
$\bar{v}_{85}$	82.99592 km/h	d_{85}	1.0148058 m/s^2
$\sigma_{v_{85}}$	4.836563 km/h	$\sigma_{\Delta v_{85}}$	3.9642595 km/h
R_a	1.19819 km/h	$\sigma_{d_{85}}$	0.1022435 m/s^2
$E_{a,10}$	0 km/h	$\bar{L}_{\Delta v_{85}}$	43.142857 m
$E_{a,20}$	0 km/h	L_d	14.37%
L_{10}	0 m	N	7
L_{20}	0 m		

CONSISTENCY

Polus (2004)	1.79492
Garach (2013)	1.88546
Camacho (2014	2.8322

CRASHES

Observed:	0
Estimated:	
Exposure	1
Polus (2004)	1
Camacho (2009)	1
Garach (2013)	2
Camacho (2014)	1

ROAD SEGMENT: 2.10

Road:	CV-12	
Initial station:	19+320	Free
Final station:	23+790	Intersection
		Constrained

AADT:	859 vpd
Length:	1665 m

OPERATIONAL CHARACTERISTICS

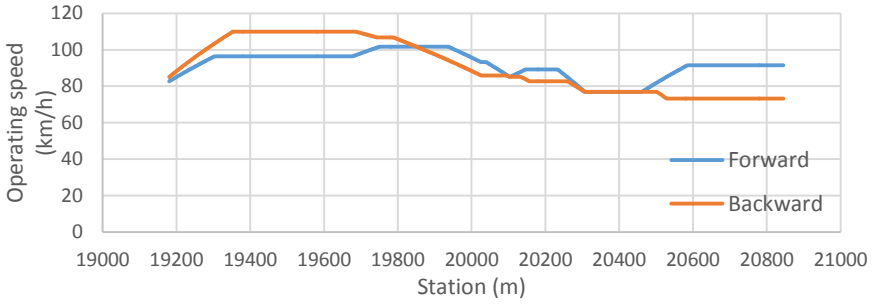

CCR	65.44732 gon/km	$\overline{\Delta v_{85}}$	13.44131 km/h
$\bar{v}_{85}$	91.24581 km/h	d_{85}	0.9310364 m/s^2
$\sigma_{v_{85}}$	11.41586 km/h	$\sigma_{\Delta v_{85}}$	7.8886597 km/h
R_a	2.65157 km/h	$\sigma_{d_{85}}$	0.1794318 m/s^2
$E_{a,10}$	2.009412 km/h	$\bar{L}_{\Delta v_{85}}$	100.25 m
$E_{a,20}$	0 km/h	L_d	12.04%
L_{10}	0.466366 m	N	4
L_{20}	0 m		

CONSISTENCY

Polus (2004)	0.27116
Garach (2013)	0.40548
Camacho (2014	3.00825

CRASHES

Observed:	2
Estimated:	
Exposure	2
Polus (2004)	2
Camacho (2009)	2
Garach (2013)	3
Camacho (2014)	1

ROAD SEGMENT: 3.1

Road:	CV-14	
Initial station:	0+230	Intersection
Final station:	5+380	Free
		Constrained

AADT:	1286 vpd
Length:	5112 m

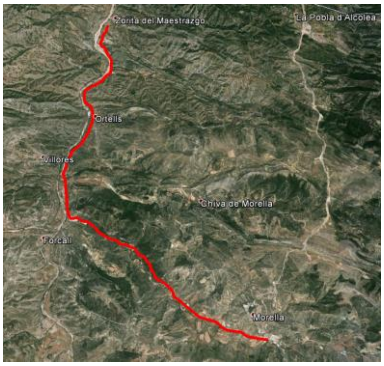

OPERATIONAL CHARACTERISTICS

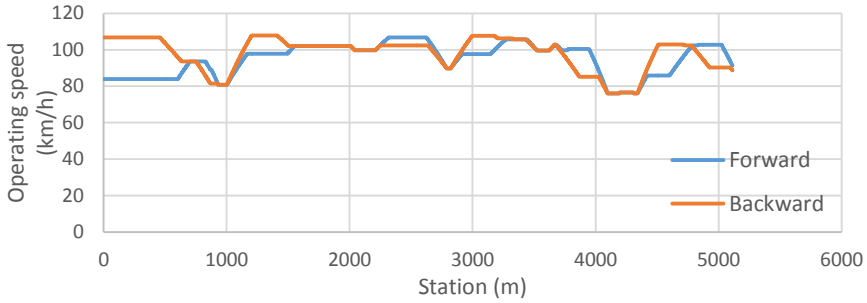

CCR	66.85797 gon/km	$\overline{\Delta v_{85}}$	11.900696 km/h
$\bar{v}_{85}$	96.51999 km/h	d_{85}	0.7943113 m/s^2
$\sigma_{v_{85}}$	8.962456 km/h	$\sigma_{\Delta v_{85}}$	9.6032787 km/h
R_a	2.101293 km/h	$\sigma_{d_{85}}$	0.2072998 m/s^2
$E_{a,10}$	1.199385 km/h	$\bar{L}_{\Delta v_{85}}$	98.769231 m
$E_{a,20}$	0.153167 km/h	L_d	12.56%
L_{10}	0.327954 m	N	13
L_{20}	0.026995 m		

CONSISTENCY

Polus (2004)	0.65584
Garach (2013)	0.94962
Camacho (2014	3.23178

CRASHES

Observed:	6
Estimated:	
Exposure	7
Polus (2004)	10
Camacho (2009)	7
Garach (2013)	11
Camacho (2014)	5

ROAD SEGMENT: 3.2

Road:	CV-14	
Initial station:	5+380	Free
Final station:	10+150	Free
		Free

AADT:	1177 vpd
Length:	4771 m

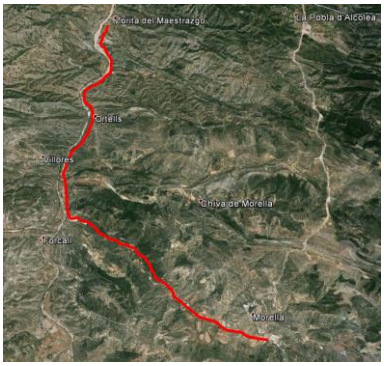

OPERATIONAL CHARACTERISTICS

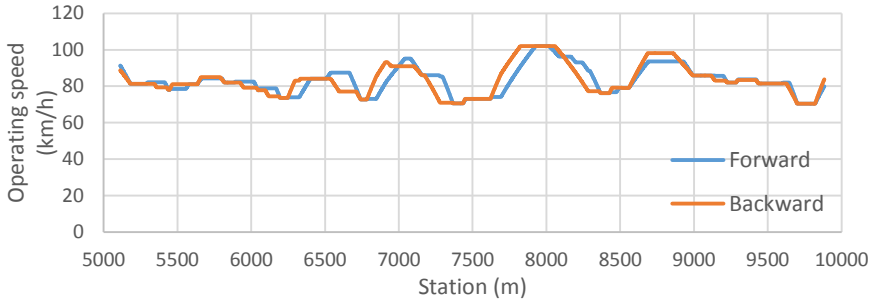

CCR	186.5491 gon/km	$\overline{\Delta v_{85}}$	8.2484653 km/h
$\bar{v}_{85}$	83.346 km/h	d_{85}	1.0003073 m/s^2
$\sigma_{v_{85}}$	7.851347 km/h	$\sigma_{\Delta v_{85}}$	6.8734213 km/h
R_a	1.690678 km/h	$\sigma_{d_{85}}$	0.1680667 m/s^2
$E_{a,10}$	0.920876 km/h	$\bar{L}_{\Delta v_{85}}$	52.666667 m
$E_{a,20}$	0 km/h	L_d	14.90%
L_{10}	0.253616 m	N	27
L_{20}	0 m		

CONSISTENCY

Polus (2004)	1.00744
Garach (2013)	1.29767
Camacho (2014	2.84981

CRASHES

Observed:	4
Estimated:	
Exposure	4
Polus (2004)	7
Camacho (2009)	5
Garach (2013)	9
Camacho (2014)	4

ROAD SEGMENT: 3.3

Road:	CV-14	
Initial station:	10+150	Free
Final station:	13+480	Free
		Free

AADT:	804 vpd
Length:	3318 m

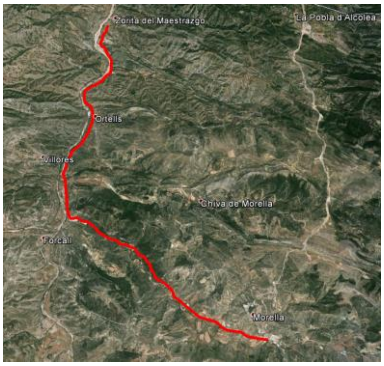

OPERATIONAL CHARACTERISTICS

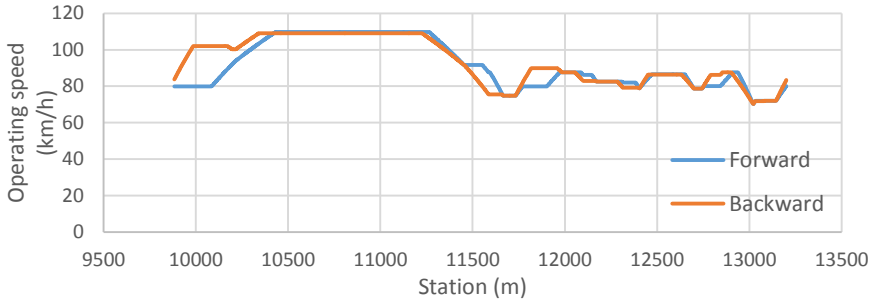

CCR	100.2608 gon/km	$\overline{\Delta v_{85}}$	8.7461935 km/h
$\bar{v}_{85}$	92.3642 km/h	d_{85}	0.9941378 m/s^2
$\sigma_{v_{85}}$	12.88741 km/h	$\sigma_{\Delta v_{85}}$	6.1341791 km/h
R_a	3.253037 km/h	$\sigma_{d_{85}}$	0.2052202 m/s^2
$E_{a,10}$	2.540448 km/h	$\bar{L}_{\Delta v_{85}}$	60.5 m
$E_{a,20}$	0.236989 km/h	L_d	14.59%
L_{10}	0.586197 m	N	16
L_{20}	0.041441 m		

CONSISTENCY

Polus (2004)	0.11026
Garach (2013)	-0.02932
Camacho (2014	2.95519

CRASHES

Observed:	3
Estimated:	
Exposure	2
Polus (2004)	5
Camacho (2009)	3
Garach (2013)	5
Camacho (2014)	2

ROAD SEGMENT: 3.4

Road:	CV-14	
Initial station:	13+480	Free
Final station:	15+100	Free
		Free

AADT:	804 vpd
Length:	1635 m

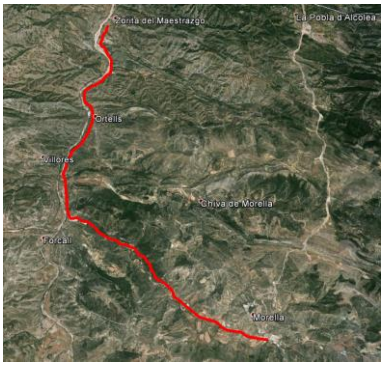

OPERATIONAL CHARACTERISTICS

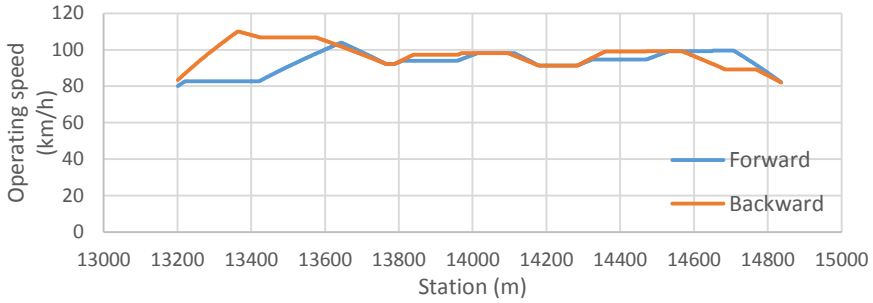

CCR	49.18635 gon/km	$\overline{\Delta v_{85}}$	10.938814 km/h
$\bar{v}_{85}$	95.34756 km/h	d_{85}	0.822169 m/s^2
$\sigma_{v_{85}}$	6.193947 km/h	$\sigma_{\Delta v_{85}}$	8.637805 km/h
R_a	1.332743 km/h	$\sigma_{d_{85}}$	0.1986518 m/s^2
$E_{a,10}$	0.592157 km/h	$\bar{L}_{\Delta v_{85}}$	88.571429 m
$E_{a,20}$	0 km/h	L_d	18.96%
L_{10}	0.175535 m	N	7
L_{20}	0 m		

CONSISTENCY

Polus (2004)	1.4844
Garach (2013)	1.6713
Camacho (2014	3.18187

CRASHES

Observed:	1
Estimated:	
Exposure	1
Polus (2004)	1
Camacho (2009)	1
Garach (2013)	2
Camacho (2014)	1

ROAD SEGMENT: 3.5

Road:	CV-14	
Initial station:	15+100	Free
Final station:	16+080	Free
		Free

AADT:	804 vpd
Length:	987 m

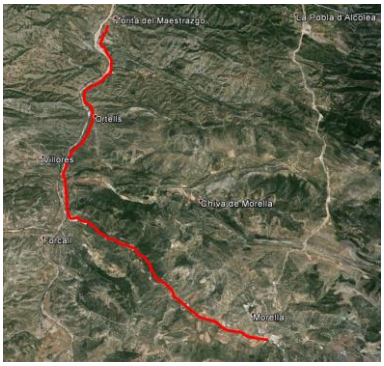

OPERATIONAL CHARACTERISTICS

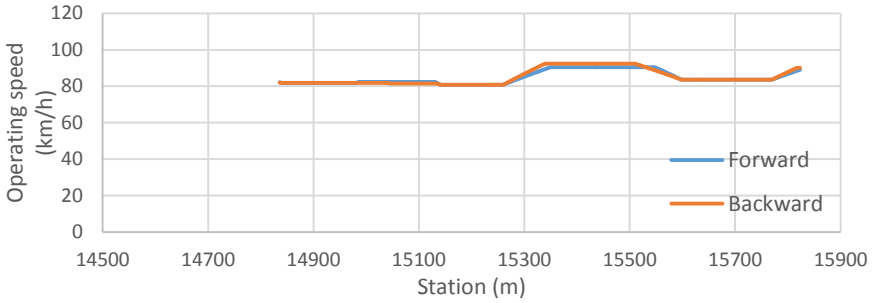

CCR	185.1201 gon/km	$\overline{\Delta v_{85}}$	6.5909696 km/h
$\bar{v}_{85}$	84.87408 km/h	d_{85}	0.9326885 m/s^2
$\sigma_{v_{85}}$	3.91864 km/h	$\sigma_{\Delta v_{85}}$	4.1367544 km/h
R_a	0.946647 km/h	$\sigma_{d_{85}}$	0.0337746 m/s^2
$E_{a,10}$	0 km/h	$\bar{L}_{\Delta v_{85}}$	47 m
$E_{a,20}$	0 km/h	L_d	9.52%
L_{10}	0 m	N	4
L_{20}	0 m		

CONSISTENCY

Polus (2004)	2.10857
Garach (2013)	2.11305
Camacho (2014	2.9348

CRASHES

Observed:	0
Estimated:	
Exposure	1
Polus (2004)	1
Camacho (2009)	1
Garach (2013)	1
Camacho (2014)	1

ROAD SEGMENT: 3.6

Road:	CV-14	
Initial station:	16+080	Free
Final station:	19+600	Town
		Constrained

AADT:	804 vpd
Length:	3512 m

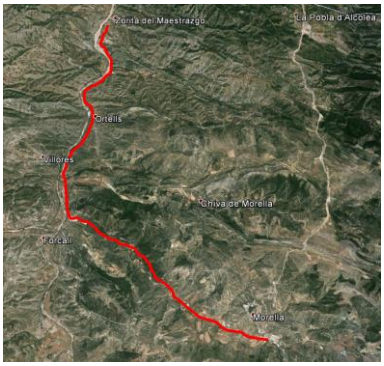

OPERATIONAL CHARACTERISTICS

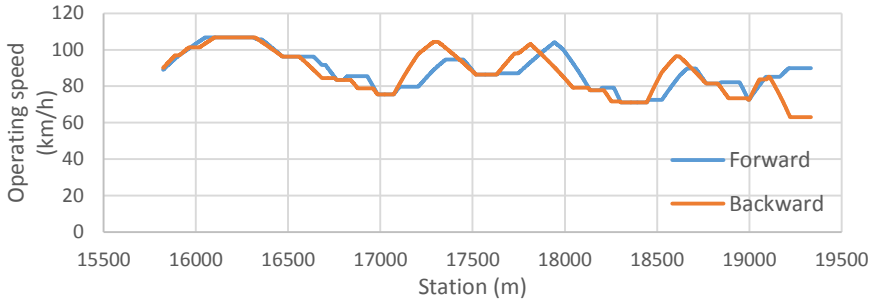

CCR	137.5097 gon/km	$\overline{\Delta v_{85}}$	10.218814 km/h
$\bar{v}_{85}$	88.23372 km/h	d_{85}	0.8658107 m/s^2
$\sigma_{v_{85}}$	10.92578 km/h	$\sigma_{\Delta v_{85}}$	7.9576603 km/h
R_a	2.543604 km/h	$\sigma_{d_{85}}$	0.2332103 m/s^2
$E_{a,10}$	1.716197 km/h	$\bar{L}_{\Delta v_{85}}$	79.210526 m
$E_{a,20}$	0.134164 km/h	L_d	21.43%
L_{10}	0.403474 m	N	19
L_{20}	0.019505 m		

CONSISTENCY

Polus (2004)	0.32837
Garach (2013)	0.50899
Camacho (2014	3.04768

CRASHES

Observed:	2
Estimated:	
Exposure	4
Polus (2004)	5
Camacho (2009)	3
Garach (2013)	5
Camacho (2014)	3

ROAD SEGMENT: 4.1

Road:	CV-15	
Initial station:	55+670	Free
Final station:	56+840	Free
		Free

AADT:	1036	vpd
Length:	1159	m

OPERATIONAL CHARACTERISTICS

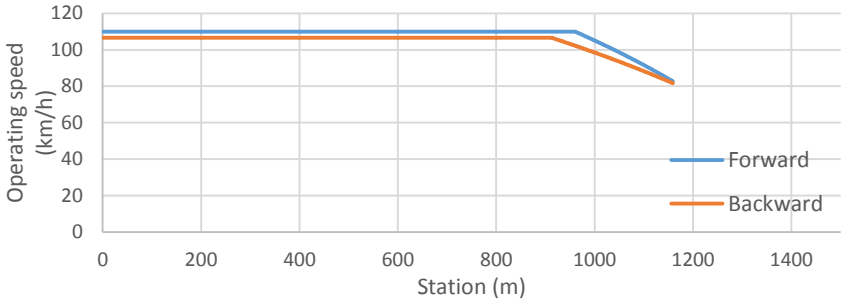

CCR	0.018249	gon/km
$\bar{v}_{85}$	105.9365	km/h
$\sigma_{v_{85}}$	6.192619	km/h
R_a	1.112532	km/h
$E_{a,10}$	0.448652	km/h
$E_{a,20}$	0.155383	km/h
L_{10}	0.096204	m
L_{20}	0.025453	m

$\overline{\Delta v_{85}}$	27.300822	km/h
d_{85}	1.0198997	m/s^2
$\sigma_{\Delta v_{85}}$	0	km/h
$\sigma_{d_{85}}$	0	m/s^2
$\bar{L}_{\Delta v_{85}}$	199	m
L_d	8.58%	
N	1	

CONSISTENCY

Polus (2004)	1.64946
Garach (2013)	1.7888
Camacho (2014	3.0671

CRASHES

Observed:	0
Estimated:	
Exposure	1
Polus (2004)	1
Camacho (2009)	1
Garach (2013)	2
Camacho (2014)	1

ROAD SEGMENT: 4.2

Road:	CV-15	
Initial station:	56+840	Free
Final station:	58+790	Free
		Free

AADT:	1036 vpd
Length:	1946 m

OPERATIONAL CHARACTERISTICS

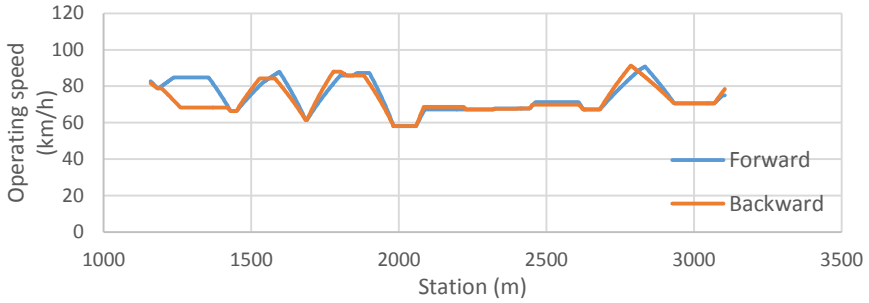

CCR	310.7112 gon/km	$\overline{\Delta v_{85}}$	15.927635 km/h
$\bar{v}_{85}$	73.37331 km/h	d_{85}	1.4742531 m/s^2
$\sigma_{v_{85}}$	7.912935 km/h	$\sigma_{\Delta v_{85}}$	9.8394469 km/h
R_a	1.867961 km/h	$\sigma_{d_{85}}$	0.3007115 m/s^2
$E_{a,10}$	0.88942 km/h	$\bar{L}_{\Delta v_{85}}$	60.75 m
$E_{a,20}$	0 km/h	L_d	18.73%
L_{10}	0.245632 m	N	12
L_{20}	0 m		

CONSISTENCY

Polus (2004)	0.89677
Garach (2013)	1.19078
Camacho (2014	2.40005

CRASHES

Observed:	1
Estimated:	
Exposure	2
Polus (2004)	3
Camacho (2009)	2
Garach (2013)	4
Camacho (2014)	2

ROAD SEGMENT: 4.3

Road:	CV-15	
Initial station:	58+790	Free
Final station:	60+800	Free
		Free

AADT:	1036	vpd
Length:	2011	m

OPERATIONAL CHARACTERISTICS

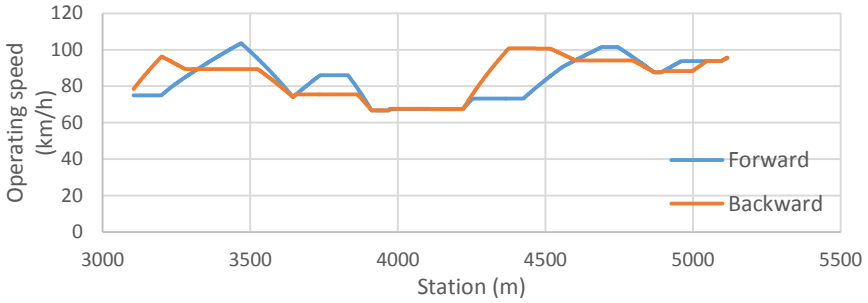

CCR	116.6652	gon/km	$\overline{\Delta v_{85}}$	15.288587	km/h
$\bar{v}_{85}$	84.40787	km/h	d_{85}	1.0747947	m/s^2
$\sigma_{v_{85}}$	11.00468	km/h	$\sigma_{\Delta v_{85}}$	12.076402	km/h
R_a	2.703466	km/h	$\sigma_{d_{85}}$	0.276383	m/s^2
$E_{a,10}$	1.679854	km/h	$\bar{L}_{\Delta v_{85}}$	88	m
$E_{a,20}$	0	km/h	L_d	17.50%	
L_{10}	0.404774	m	N	8	
L_{20}	0	m			

CONSISTENCY

Polus (2004)	0.28225
Garach (2013)	0.41205
Camacho (2014	2.79416

CRASHES

Observed:	3
Estimated:	
Exposure	2
Polus (2004)	4
Camacho (2009)	2
Garach (2013)	4
Camacho (2014)	2

ROAD SEGMENT: 4.4

Road:	CV-15	
Initial station:	60+800	Free
Final station:	62+390	Free
		Free

AADT:	1036 vpd
Length:	1584 m

OPERATIONAL CHARACTERISTICS

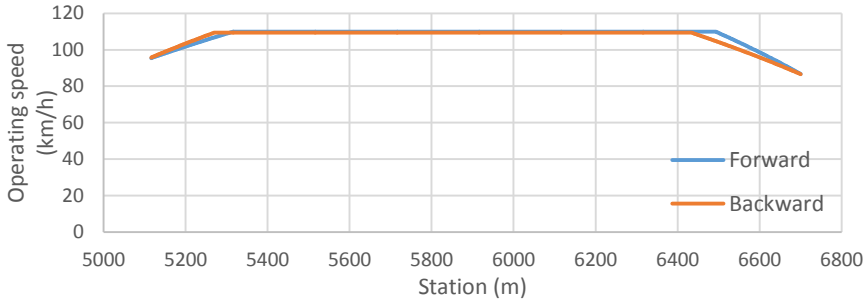

CCR	0.522527 gon/km	$\overline{\Delta v_{85}}$	18.39577 km/h
$\bar{v}_{85}$	107.2357 km/h	d_{85}	0.7748015 m/s^2
$\sigma_{v_{85}}$	5.119606 km/h	$\sigma_{\Delta v_{85}}$	6.6881086 km/h
R_a	1.021068 km/h	$\sigma_{d_{85}}$	0.1083538 m/s^2
$E_{a,10}$	0.311123 km/h	$\bar{L}_{\Delta v_{85}}$	180.5 m
$E_{a,20}$	0.019586 km/h	L_d	11.40%
L_{10}	0.077336 m	N	2
L_{20}	0.003472 m		

CONSISTENCY

Polus (2004)	1.87535
Garach (2013)	1.95101
Camacho (2014	3.37507

CRASHES

Observed:	1
Estimated:	
Exposure	1
Polus (2004)	2
Camacho (2009)	1
Garach (2013)	3
Camacho (2014)	1

ROAD SEGMENT: 4.5

Road:	CV-15	
Initial station:	62+390	Free
Final station:	63+800	Free
		Free

AADT:	1036 vpd
Length:	1402 m

OPERATIONAL CHARACTERISTICS

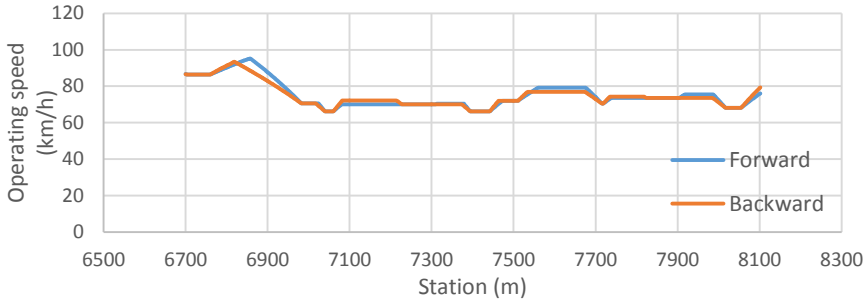

CCR	270.2902 gon/km	$\overline{\Delta v_{85}}$	8.0378156 km/h
$\bar{v}_{85}$	74.94774 km/h	d_{85}	1.2736077 m/s^2
$\sigma_{v_{85}}$	6.767489 km/h	$\sigma_{\Delta v_{85}}$	5.9462645 km/h
R_a	1.431992 km/h	$\sigma_{d_{85}}$	0.1709472 m/s^2
$E_{a,10}$	0.559103 km/h	$\bar{L}_{\Delta v_{85}}$	38.363636 m
$E_{a,20}$	0.012 km/h	L_d	15.05%
L_{10}	0.142653 m	N	11
L_{20}	0.00214 m		

CONSISTENCY

Polus (2004)	1.32858
Garach (2013)	1.55618
Camacho (2014	2.53789

CRASHES

Observed:	1
Estimated:	
Exposure	1
Polus (2004)	2
Camacho (2009)	1
Garach (2013)	3
Camacho (2014)	1

ROAD SEGMENT: 4.6

Road:	CV-15	
Initial station:	63+800	Free
Final station:	64+840	Town
		Constrained

AADT:	1158	vpd
Length:	1043	m

OPERATIONAL CHARACTERISTICS

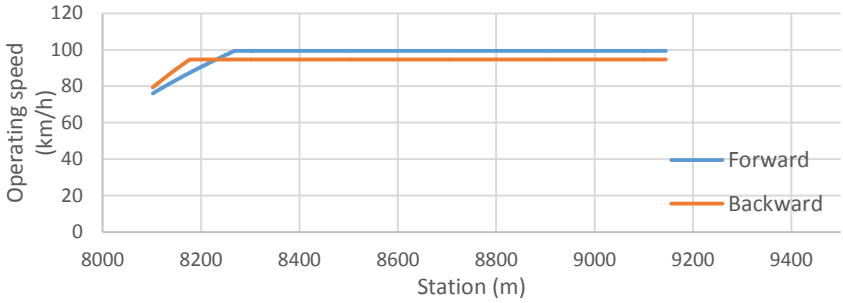

CCR	0 gon/km	$\overline{\Delta v_{85}}$	15.355335 km/h
$\bar{v}_{85}$	95.91594 km/h	d_{85}	1.357303 m/s^2
$\sigma_{v_{85}}$	4.193715 km/h	$\sigma_{\Delta v_{85}}$	0 km/h
R_a	0.831913 km/h	$\sigma_{d_{85}}$	0 m/s^2
$E_{a,10}$	0.183289 km/h	$\bar{L}_{\Delta v_{85}}$	76 m
$E_{a,20}$	0 km/h	L_d	3.64%
L_{10}	0.046021 m	N	1
L_{20}	0 m		

CONSISTENCY

Polus (2004)	2.14483
Garach (2013)	2.14465
Camacho (2014	2.69756

CRASHES

Observed:	1
Estimated:	
Exposure	1
Polus (2004)	1
Camacho (2009)	1
Garach (2013)	2
Camacho (2014)	1

ROAD SEGMENT: 5.1

Road:	CV-15	
Initial station:	68+510	Town
Final station:	70+900	Free
		Constrained

AADT:	1012	vpd
Length:	2369	m

OPERATIONAL CHARACTERISTICS

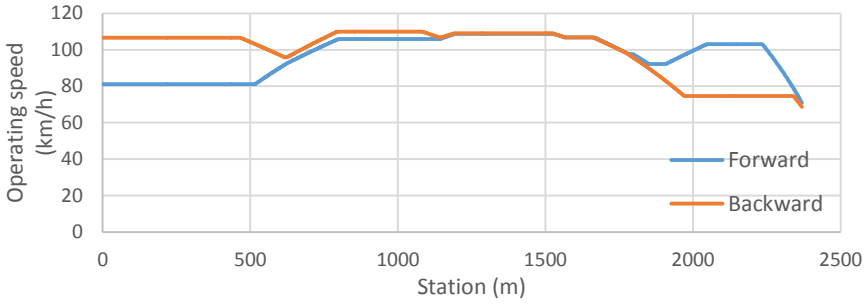

CCR	19.06739	gon/km	$\overline{\Delta v_{85}}$	10.845749	km/h
$\bar{v}_{85}$	98.34256	km/h	d_{85}	0.7389129	m/s^2
$\sigma_{v_{85}}$	12.00153	km/h	$\sigma_{\Delta v_{85}}$	11.405124	km/h
R_a	2.867246	km/h	$\sigma_{d_{85}}$	0.4419608	m/s^2
$E_{a,10}$	1.976452	km/h	$\bar{L}_{\Delta v_{85}}$	93.5	m
$E_{a,20}$	0.630745	km/h	L_d	11.84%	
L_{10}	0.465386	m	N	6	
L_{20}	0.09561	m			

CONSISTENCY

Polus (2004)	0.19694
Garach (2013)	0.23912
Camacho (2014	3.33131

CRASHES

Observed:	3
Estimated:	
Exposure	3
Polus (2004)	4
Camacho (2009)	3
Garach (2013)	5
Camacho (2014)	2

ROAD SEGMENT: 5.2

Road:	CV-15	
Initial station:	70+900	Free
Final station:	72+460	Free
		Free

AADT:	1012	vpd
Length:	1556	m

OPERATIONAL CHARACTERISTICS

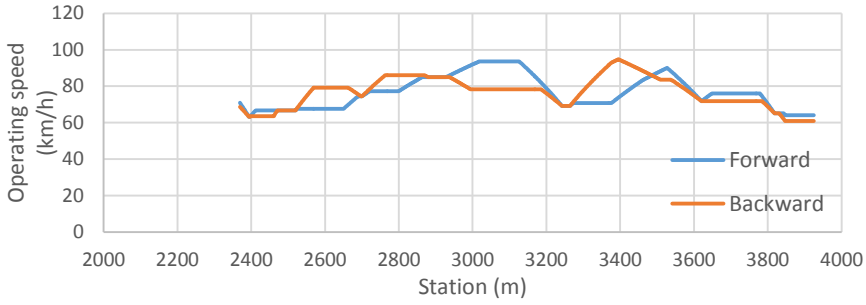

CCR	161.1333	gon/km	$\overline{\Delta v_{85}}$	12.787089	km/h
$\bar{v}_{85}$	76.8162	km/h	d_{85}	1.3627709	m/s^2
$\sigma_{v_{85}}$	8.65268	km/h	$\sigma_{\Delta v_{85}}$	8.5669428	km/h
R_a	1.994442	km/h	$\sigma_{d_{85}}$	0.1494868	m/s^2
$E_{a,10}$	1.06841	km/h	$\bar{L}_{\Delta v_{85}}$	59.222222	m
$E_{a,20}$	0	km/h	L_d	17.13%	
L_{10}	0.291774	m	N	9	
L_{20}	0	m			

CONSISTENCY

Polus (2004)	0.74069
Garach (2013)	1.04236
Camacho (2014	2.50174

CRASHES

Observed:	1
Estimated:	
Exposure	1
Polus (2004)	2
Camacho (2009)	2
Garach (2013)	3
Camacho (2014)	1

ROAD SEGMENT: 6.1

Road:	CV-25	
Initial station:	15+850	Town
Final station:	19+770	Town
		Constrained

AADT:	407 vpd
Length:	3893 m

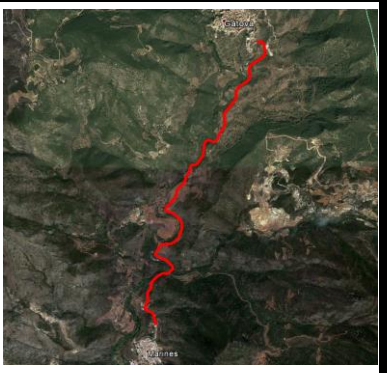

OPERATIONAL CHARACTERISTICS

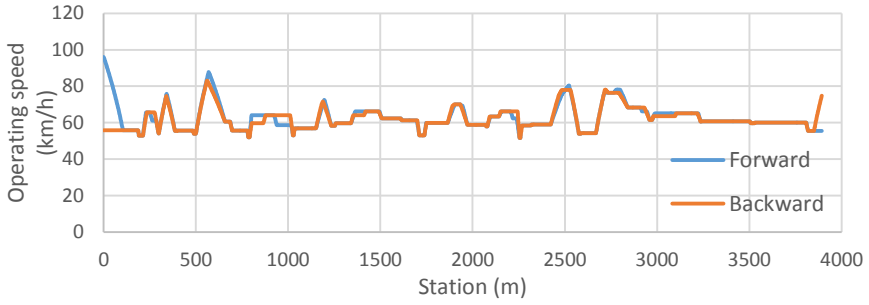

CCR	604.8879 gon/km	$\overline{\Delta v_{85}}$	9.7046686 km/h
$\bar{v}_{85}$	62.48768 km/h	d_{85}	2.0956764 m/s^2
$\sigma_{v_{85}}$	6.323289 km/h	$\sigma_{\Delta v_{85}}$	9.0485067 km/h
R_a	1.318672 km/h	$\sigma_{d_{85}}$	0.482845 m/s^2
$E_{a,10}$	0.370038 km/h	$\bar{L}_{\Delta v_{85}}$	23 m
$E_{a,20}$	0.070841 km/h	L_d	13.00%
L_{10}	0.087208 m	N	44
L_{20}	0.010275 m		

CONSISTENCY

Polus (2004)	1.47487
Garach (2013)	1.66524
Camacho (2014	2.02328

CRASHES

Observed:	1
Estimated:	
Exposure	3
Polus (2004)	2
Camacho (2009)	1
Garach (2013)	2
Camacho (2014)	3

ROAD SEGMENT: 7.1

Road:	CV-60	
Initial station:	0+090	Roundabout
Final station:	15+730	Free
		Constrained

AADT:	9714 vpd
Length:	15645 m

OPERATIONAL CHARACTERISTICS

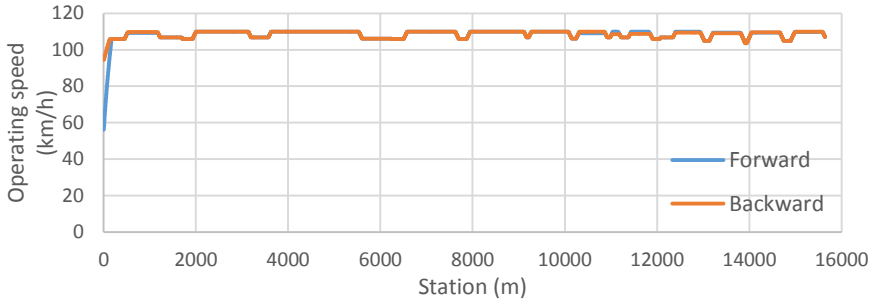

CCR	18.55668 gon/km	$\overline{\Delta v_{85}}$	4.0000645 km/h
$\bar{v}_{85}$	108.5544 km/h	d_{85}	0.4351776 m/s^2
$\sigma_{v_{85}}$	2.782243 km/h	$\sigma_{\Delta v_{85}}$	1.8394335 km/h
R_a	0.458796 km/h	$\sigma_{d_{85}}$	0.0518334 m/s^2
$E_{a,10}$	0.042188 km/h	$\bar{L}_{\Delta v_{85}}$	74.259259 m
$E_{a,20}$	0.031855 km/h	L_d	6.41%
L_{10}	0.006008 m	N	27
L_{20}	0.003228 m		

CONSISTENCY

Polus (2004)	2.54441
Garach (2013)	2.47089
Camacho (2014	4.10733

CRASHES

Observed:	47
Estimated:	
Exposure	65
Polus (2004)	116
Camacho (2009)	85
Garach (2013)	172
Camacho (2014)	54

ROAD SEGMENT: 7.2

Road:	CV-60	
Initial station:	15+730	Free
Final station:	22+680	Free
		Free

AADT:	7774 vpd
Length:	6971 m

OPERATIONAL CHARACTERISTICS

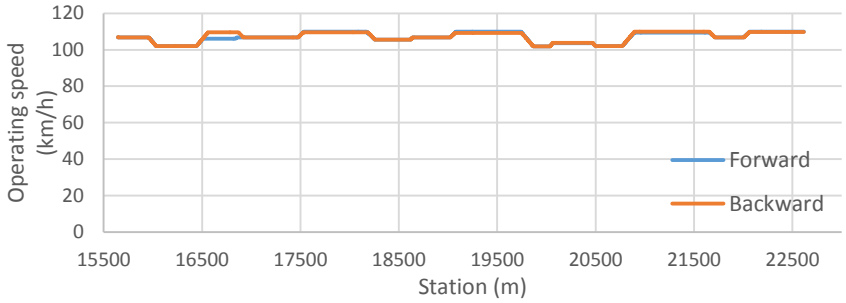

CCR	32.21964 gon/km	$\overline{\Delta v_{85}}$	4.0329589 km/h
$\bar{v}_{85}$	107.062 km/h	d_{85}	0.4673594 m/s^2
$\sigma_{v_{85}}$	2.727299 km/h	$\sigma_{\Delta v_{85}}$	2.513413 km/h
R_a	0.630805 km/h	$\sigma_{d_{85}}$	0.0518786 m/s^2
$E_{a,10}$	0 km/h	$\bar{L}_{\Delta v_{85}}$	69.083333 m
$E_{a,20}$	0 km/h	L_d	5.95%
L_{10}	0 m	N	12
L_{20}	0 m		

CONSISTENCY

Polus (2004)	2.45867
Garach (2013)	2.39234
Camacho (2014	3.99234

CRASHES

Observed:	29
Estimated:	
Exposure	22
Polus (2004)	43
Camacho (2009)	31
Garach (2013)	71
Camacho (2014)	21

ROAD SEGMENT: 8.1

Road:	CV-700	
Initial station:	21+760	Roundabout
Final station:	26+270	Town
		Constrained

AADT:	506 vpd
Length:	4533 m

OPERATIONAL CHARACTERISTICS

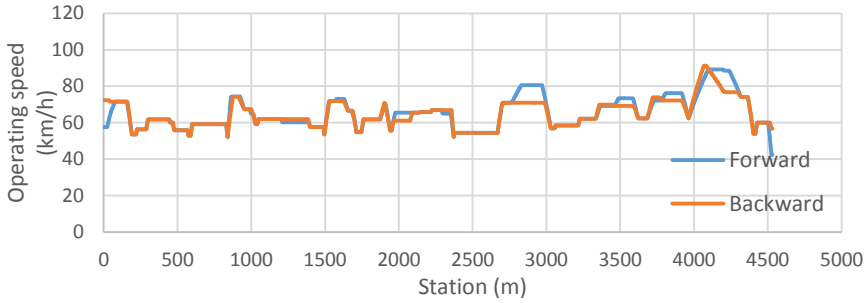

CCR	554.4779 gon/km	$\overline{\Delta v_{85}}$	8.8049226 km/h
$\bar{v}_{85}$	65.1919 km/h	d_{85}	2.0511353 m/s^2
$\sigma_{v_{85}}$	8.16667 km/h	$\sigma_{\Delta v_{85}}$	7.0605188 km/h
R_a	1.847399 km/h	$\sigma_{d_{85}}$	0.5090808 m/s^2
$E_{a,10}$	0.765337 km/h	$\bar{L}_{\Delta v_{85}}$	22 m
$E_{a,20}$	0.208514 km/h	L_d	10.19%
L_{10}	0.197992 m	N	42
L_{20}	0.032098 m		

CONSISTENCY

Polus (2004)	0.87583
Garach (2013)	1.17634
Camacho (2014	2.0668

CRASHES

Observed:	2
Estimated:	
Exposure	4
Polus (2004)	3
Camacho (2009)	2
Garach (2013)	3
Camacho (2014)	4

ROAD SEGMENT: 9.1

Road:	CV-700	
Initial station:	27+520	Town
Final station:	32+690	Free
		Constrained

AADT:	506 vpd
Length:	5141 m

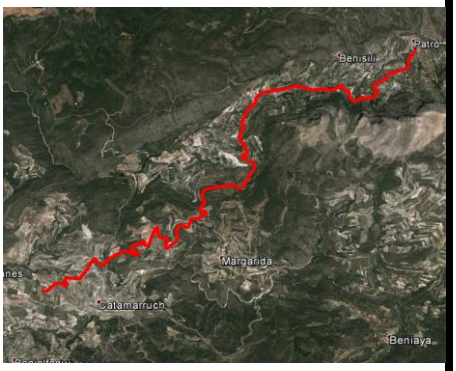

OPERATIONAL CHARACTERISTICS

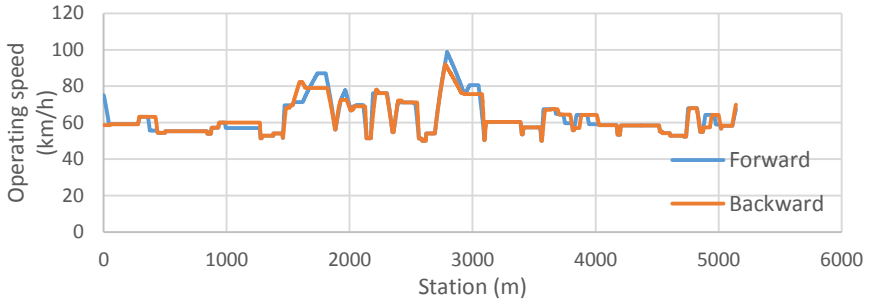

CCR	739.5106 gon/km	$\overline{\Delta v_{85}}$	9.1614618 km/h
$\bar{v}_{85}$	62.80973 km/h	d_{85}	2.2472548 m/s^2
$\sigma_{v_{85}}$	8.944707 km/h	$\sigma_{\Delta v_{85}}$	8.966529 km/h
R_a	1.982498 km/h	$\sigma_{d_{85}}$	0.5514225 m/s^2
$E_{a,10}$	0.791165 km/h	$\bar{L}_{\Delta v_{85}}$	21.056604 m
$E_{a,20}$	0.250625 km/h	L_d	10.85%
L_{10}	0.172535 m	N	53
L_{20}	0.035207 m		

CONSISTENCY

Polus (2004)	0.71398
Garach (2013)	1.01912
Camacho (2014	1.98012

CRASHES

Observed:	3
Estimated:	
Exposure	4
Polus (2004)	4
Camacho (2009)	3
Garach (2013)	4
Camacho (2014)	5

ROAD SEGMENT: 9.2

Road:	CV-700	
Initial station:	32+690	Free
Final station:	33+630	Free
		Free

AADT:	506 vpd
Length:	963 m

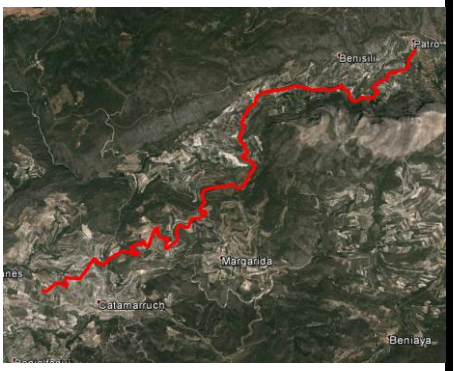

OPERATIONAL CHARACTERISTICS

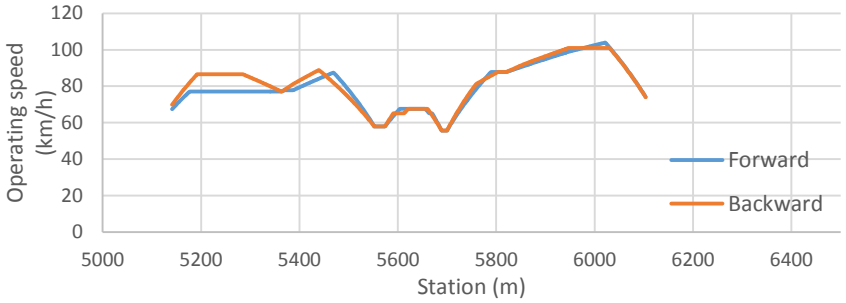

CCR	234.9676 gon/km	$\overline{\Delta v_{85}}$	15.472542 km/h
$\bar{v}_{85}$	80.93588 km/h	d_{85}	1.7019856 m/s^2
$\sigma_{v_{85}}$	12.40069 km/h	$\sigma_{\Delta v_{85}}$	11.253382 km/h
R_a	2.827053 km/h	$\sigma_{d_{85}}$	0.5430598 m/s^2
$E_{a,10}$	2.162833 km/h	$\bar{L}_{\Delta v_{85}}$	57.8 m
$E_{a,20}$	0.873492 km/h	L_d	30.01%
L_{10}	0.455348 m	N	10
L_{20}	0.144341 m		

CONSISTENCY

Polus (2004)	0.18736
Garach (2013)	0.22809
Camacho (2014	2.36389

CRASHES

Observed:	1
Estimated:	
Exposure	1
Polus (2004)	1
Camacho (2009)	1
Garach (2013)	1
Camacho (2014)	1

ROAD SEGMENT: 9.3

Road:	CV-700	
Initial station:	33+630	Free
Final station:	34+660	Free
		Free

AADT:	506 vpd
Length:	1017 m

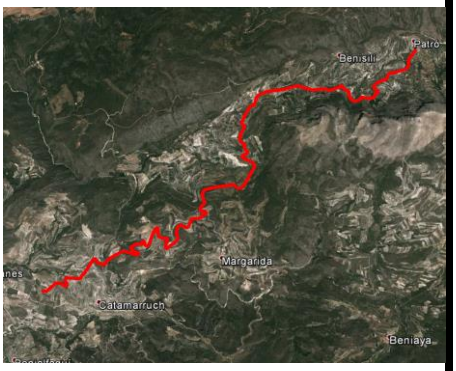

OPERATIONAL CHARACTERISTICS

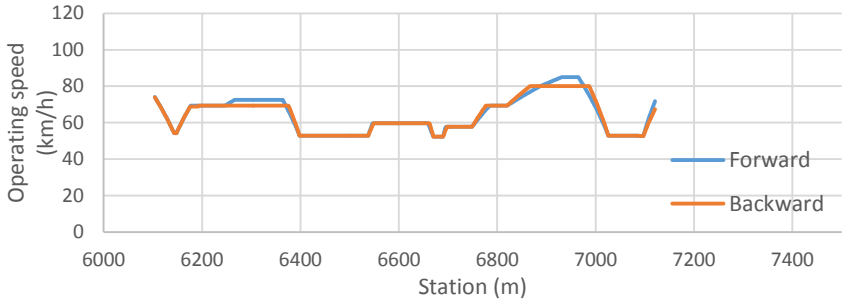

CCR	843.5452 gon/km	$\overline{\Delta v_{85}}$	14.277865 km/h
$\bar{v}_{85}$	64.22957 km/h	d_{85}	2.5200025 m/s^2
$\sigma_{v_{85}}$	9.450017 km/h	$\sigma_{\Delta v_{85}}$	8.0182185 km/h
R_a	2.315931 km/h	$\sigma_{d_{85}}$	0.5051239 m/s^2
$E_{a,10}$	1.396842 km/h	$\bar{L}_{\Delta v_{85}}$	29.2 m
$E_{a,20}$	0.118622 km/h	L_d	14.36%
L_{10}	0.382989 m	N	10
L_{20}	0.020649 m		

CONSISTENCY

Polus (2004)	0.5181
Garach (2013)	0.77716
Camacho (2014	1.92019

CRASHES

Observed:	0
Estimated:	
Exposure	1
Polus (2004)	1
Camacho (2009)	1
Garach (2013)	1
Camacho (2014)	1

ROAD SEGMENT: 9.4

Road:	CV-700	
Initial station:	34+660	Free
Final station:	36+560	Free
		Free

AADT:	506 vpd
Length:	1911 m

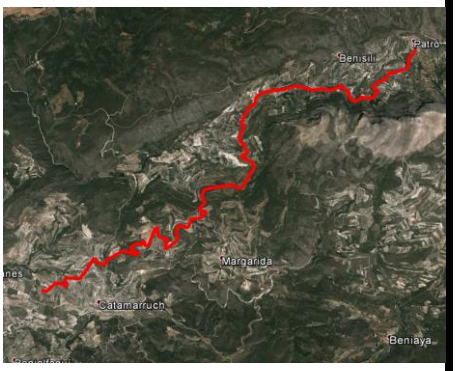

OPERATIONAL CHARACTERISTICS

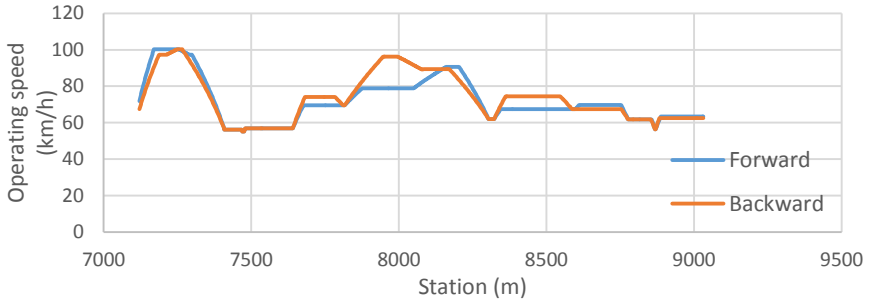

CCR	202.7634 gon/km	$\overline{\Delta v_{85}}$	14.154939 km/h
$\bar{v}_{85}$	73.05089 km/h	d_{85}	1.7772735 m/s^2
$\sigma_{v_{85}}$	12.51223 km/h	$\sigma_{\Delta v_{85}}$	13.25454 km/h
R_a	2.866569 km/h	$\sigma_{d_{85}}$	0.6347535 m/s^2
$E_{a,10}$	2.178394 km/h	$\bar{L}_{\Delta v_{85}}$	47.384615 m
$E_{a,20}$	0.679101 km/h	L_d	16.12%
L_{10}	0.473574 m	N	13
L_{20}	0.099424 m		

CONSISTENCY

Polus (2004)	0.176
Garach (2013)	0.19862
Camacho (2014	2.25176

CRASHES

Observed:	1
Estimated:	
Exposure	1
Polus (2004)	2
Camacho (2009)	1
Garach (2013)	2
Camacho (2014)	1

ROAD SEGMENT: 9.5

Road:	CV-700	
Initial station:	36+560	Free
Final station:	38+610	Town
		Constrained

AADT:	506 vpd
Length:	2070 m

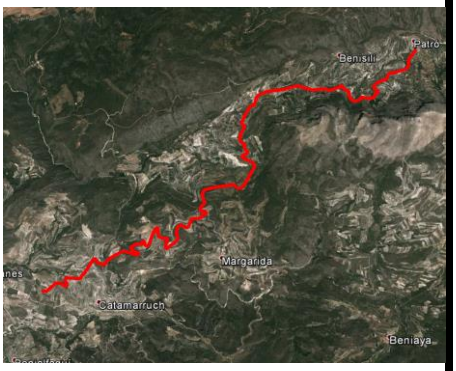

OPERATIONAL CHARACTERISTICS

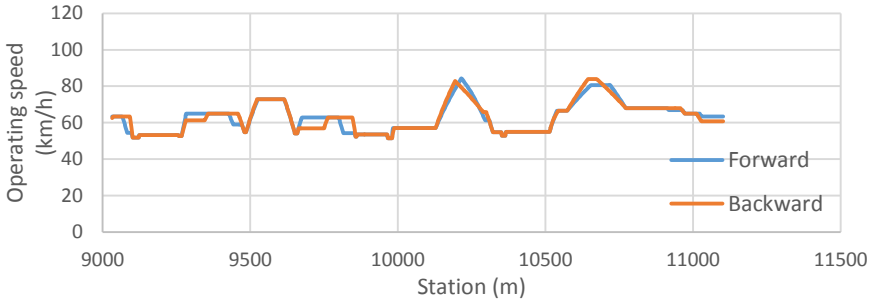

CCR	645.9015 gon/km	$\overline{\Delta v_{85}}$	7.3810012 km/h
$\bar{v}_{85}$	63.07215 km/h	d_{85}	2.1667052 m/s^2
$\sigma_{v_{85}}$	8.174194 km/h	$\sigma_{\Delta v_{85}}$	7.0596288 km/h
R_a	1.860994 km/h	$\sigma_{d_{85}}$	0.5277484 m/s^2
$E_{a,10}$	0.586802 km/h	$\bar{L}_{\Delta v_{85}}$	19 m
$E_{a,20}$	0.069771 km/h	L_d	12.85%
L_{10}	0.143237 m	N	28
L_{20}	0.012077 m		

CONSISTENCY

Polus (2004)	0.86741
Garach (2013)	1.16783
Camacho (2014	2.00714

CRASHES

Observed:	0
Estimated:	
Exposure	2
Polus (2004)	1
Camacho (2009)	1
Garach (2013)	2
Camacho (2014)	2

ROAD SEGMENT: 10.1

Road:	CV-700	
Initial station:	44+390	Town
Final station:	47+490	Free
		Constrained

AADT:	506 vpd
Length:	3089 m

OPERATIONAL CHARACTERISTICS

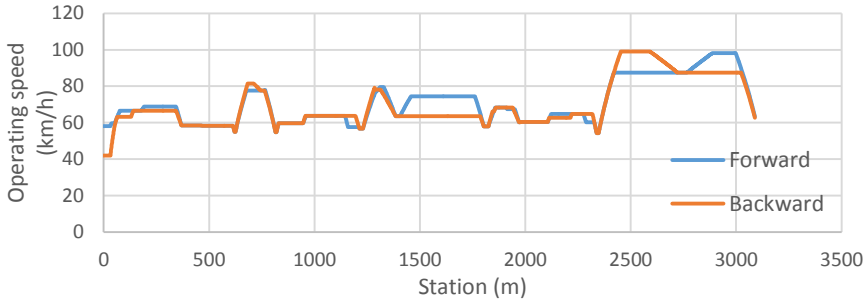

CCR	302.9476 gon/km	$\overline{\Delta v_{85}}$	12.879059 km/h
$\bar{v}_{85}$	70.26889 km/h	d_{85}	2.0117533 m/s^2
$\sigma_{v_{85}}$	12.1821 km/h	$\sigma_{\Delta v_{85}}$	11.979053 km/h
R_a	2.806139 km/h	$\sigma_{d_{85}}$	0.378716 m/s^2
$E_{a,10}$	1.908542 km/h	$\bar{L}_{\Delta v_{85}}$	31.190476 m
$E_{a,20}$	0.63258 km/h	L_d	10.60%
L_{10}	0.417125 m	N	21
L_{20}	0.086274 m		

CONSISTENCY

Polus (2004)	0.20042
Garach (2013)	0.25703
Camacho (2014	2.13286

CRASHES

Observed:	4
Estimated:	
Exposure	2
Polus (2004)	3
Camacho (2009)	2
Garach (2013)	3
Camacho (2014)	3

ROAD SEGMENT: 10.2

Road:	CV-700	
Initial station:	47+490	Free
Final station:	48+720	Free
		Free

AADT:	506 vpd
Length:	1220 m

OPERATIONAL CHARACTERISTICS

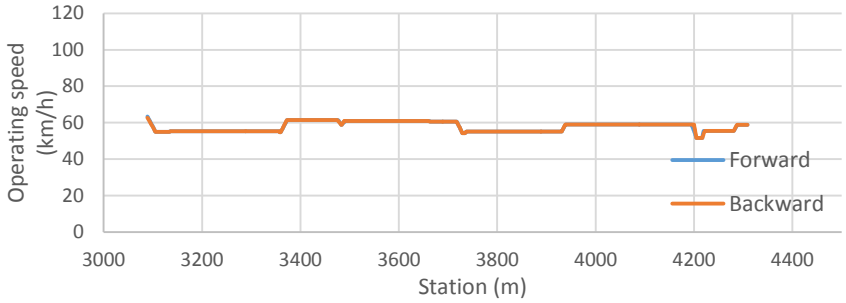

CCR	775.5637 gon/km	$\overline{\Delta v_{85}}$	4.9089728 km/h
$\bar{v}_{85}$	57.78688 km/h	d_{85}	2.3047627 m/s^2
$\sigma_{v_{85}}$	2.591483 km/h	$\sigma_{\Delta v_{85}}$	2.2788355 km/h
R_a	0.676147 km/h	$\sigma_{d_{85}}$	0.448981 m/s^2
$E_{a,10}$	0 km/h	$\bar{L}_{\Delta v_{85}}$	9.3333333 m
$E_{a,20}$	0 km/h	L_d	3.44%
L_{10}	0 m	N	9
L_{20}	0 m		

CONSISTENCY

Polus (2004)	2.45263
Garach (2013)	2.38279
Camacho (2014	1.90971

CRASHES

Observed:	0
Estimated:	
Exposure	1
Polus (2004)	0
Camacho (2009)	0
Garach (2013)	1
Camacho (2014)	1

ROAD SEGMENT: 10.3

Road:	CV-700	
Initial station:	48+720	Free
Final station:	49+530	Free
		Free

AADT:	506 vpd
Length:	800 m

OPERATIONAL CHARACTERISTICS

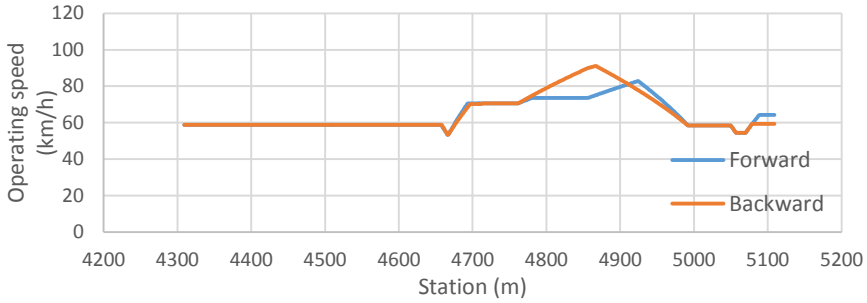

CCR	527.2677 gon/km	$\overline{\Delta v_{85}}$	12.699833 km/h
$\bar{v}_{85}$	64.87965 km/h	d_{85}	2.2315337 m/s^2
$\sigma_{v_{85}}$	9.00142 km/h	$\sigma_{\Delta v_{85}}$	8.9742476 km/h
R_a	2.159855 km/h	$\sigma_{d_{85}}$	0.5625251 m/s^2
$E_{a,10}$	0.776705 km/h	$\bar{L}_{\Delta v_{85}}$	38 m
$E_{a,20}$	0.263541 km/h	L_d	14.25%
L_{10}	0.17375 m	N	6
L_{20}	0.040625 m		

CONSISTENCY

Polus (2004)	0.62571
Garach (2013)	0.91184
Camacho (2014	2.00632

CRASHES

Observed:	2
Estimated:	
Exposure	1
Polus (2004)	1
Camacho (2009)	0
Garach (2013)	1
Camacho (2014)	1

ROAD SEGMENT: 10.4

Road:	CV-700	
Initial station:	49+530	Free
Final station:	52+770	Town
		Constrained

AADT:	506 vpd
Length:	3273 m

OPERATIONAL CHARACTERISTICS

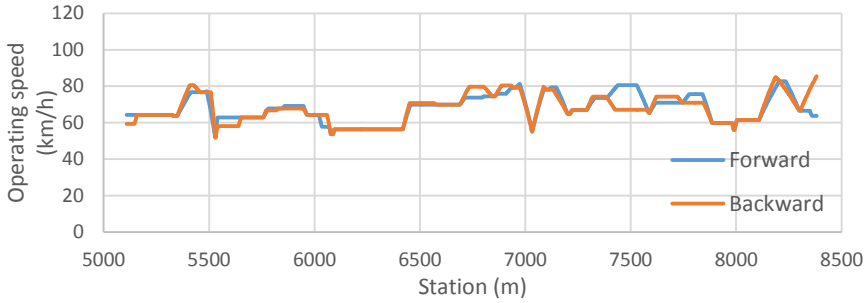

CCR	318.7091 gon/km	$\overline{\Delta v_{85}}$	10.627795 km/h
$\bar{v}_{85}$	67.85998 km/h	d_{85}	1.8174872 m/s^2
$\sigma_{v_{85}}$	7.303358 km/h	$\sigma_{\Delta v_{85}}$	7.857355 km/h
R_a	1.690736 km/h	$\sigma_{d_{85}}$	0.4943488 m/s^2
$E_{a,10}$	0.776842 km/h	$\bar{L}_{\Delta v_{85}}$	32 m
$E_{a,20}$	0 km/h	L_d	13.69%
L_{10}	0.236022 m	N	28
L_{20}	0 m		

CONSISTENCY

Polus (2004)	1.08213
Garach (2013)	1.35526
Camacho (2014	2.18079

CRASHES

Observed:	6
Estimated:	
Exposure	3
Polus (2004)	2
Camacho (2009)	2
Garach (2013)	3
Camacho (2014)	3

ROAD SEGMENT: 11.1

Road:	CV-715	
Initial station:	10+390	Town
Final station:	12+880	Free
		Constrained

AADT:	2925	vpd
Length:	2483	m

OPERATIONAL CHARACTERISTICS

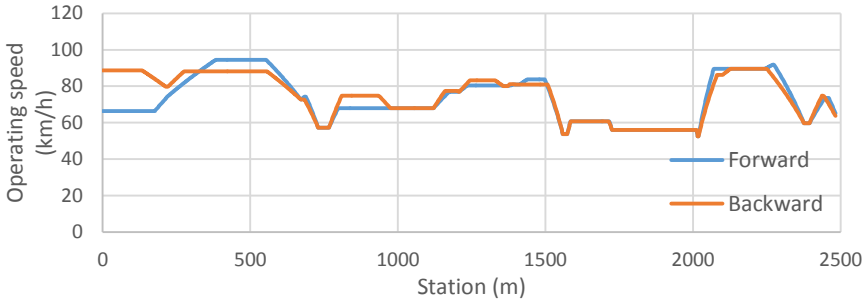

CCR	291.9777	gon/km	$\overline{\Delta v_{85}}$	14.550508	km/h
$\bar{v}_{85}$	74.13088	km/h	d_{85}	1.8754787	m/s^2
$\sigma_{v_{85}}$	12.11474	km/h	$\sigma_{\Delta v_{85}}$	10.547039	km/h
R_a	2.959856	km/h	$\sigma_{d_{85}}$	0.6692176	m/s^2
$E_{a,10}$	2.206125	km/h	$\bar{L}_{\Delta v_{85}}$	45.4	m
$E_{a,20}$	0.254547	km/h	L_d	13.71%	
L_{10}	0.50443	m	N	15	
L_{20}	0.044905	m			

CONSISTENCY

Polus (2004)	0.17613
Garach (2013)	0.18024
Camacho (2014	2.2226

CRASHES

Observed:	2
Estimated:	
Exposure	5
Polus (2004)	13
Camacho (2009)	9
Garach (2013)	16
Camacho (2014)	8

ROAD SEGMENT: 11.2

Road:	CV-715	
Initial station:	12+880	Free
Final station:	15+230	Free
		Free

AADT:	2925	vpd
Length:	2368	m

OPERATIONAL CHARACTERISTICS

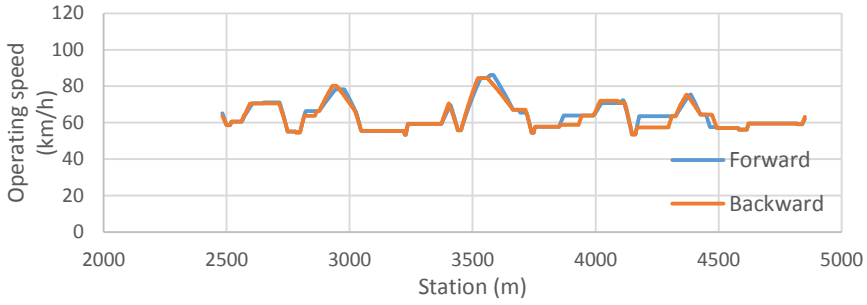

CCR	554.5322	gon/km	$\overline{\Delta v_{85}}$	8.9704512	km/h
$\bar{v}_{85}$	63.7662	km/h	d_{85}	1.9288908	m/s^2
$\sigma_{v_{85}}$	7.393967	km/h	$\sigma_{\Delta v_{85}}$	6.9385981	km/h
R_a	1.67837	km/h	$\sigma_{d_{85}}$	0.3988972	m/s^2
$E_{a,10}$	0.457899	km/h	$\bar{L}_{\Delta v_{85}}$	24.482759	m
$E_{a,20}$	0.137024	km/h	L_d	14.99%	
L_{10}	0.108319	m	N	29	
L_{20}	0.023438	m			

CONSISTENCY

Polus (2004)	1.07698
Garach (2013)	1.35281
Camacho (2014	2.09408

CRASHES

Observed:	6
Estimated:	
Exposure	5
Polus (2004)	9
Camacho (2009)	6
Garach (2013)	13
Camacho (2014)	8

ROAD SEGMENT: 11.3

Road:	CV-715	
Initial station:	15+230	Free
Final station:	16+290	Town
		Constrained

AADT:	2925 vpd
Length:	1053 m

OPERATIONAL CHARACTERISTICS

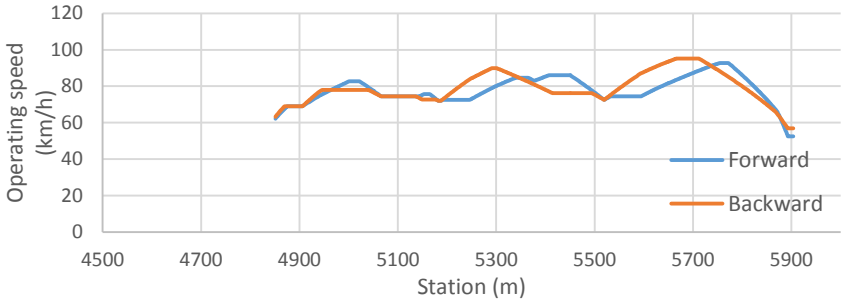

CCR	192.7345 gon/km	$\overline{\Delta v_{85}}$	13.589019 km/h
$\bar{v}_{85}$	78.69533 km/h	d_{85}	1.236304 m/s^2
$\sigma_{v_{85}}$	7.851874 km/h	$\sigma_{\Delta v_{85}}$	12.017773 km/h
R_a	1.728119 km/h	$\sigma_{d_{85}}$	0.301167 m/s^2
$E_{a,10}$	0.727254 km/h	$\bar{L}_{\Delta v_{85}}$	63.666667 m
$E_{a,20}$	0.113954 km/h	L_d	27.21%
L_{10}	0.181387 m	N	9
L_{20}	0.017569 m		

CONSISTENCY

Polus (2004)	0.98476
Garach (2013)	1.27668
Camacho (2014	2.6052

CRASHES

Observed:	1
Estimated:	
Exposure	2
Polus (2004)	4
Camacho (2009)	3
Garach (2013)	7
Camacho (2014)	2

ROAD SEGMENT: 12.1

Road:	CV-715	
Initial station:	40+280	Town
Final station:	42+360	Free
		Constrained

AADT:	427 vpd
Length:	2081 m

OPERATIONAL CHARACTERISTICS

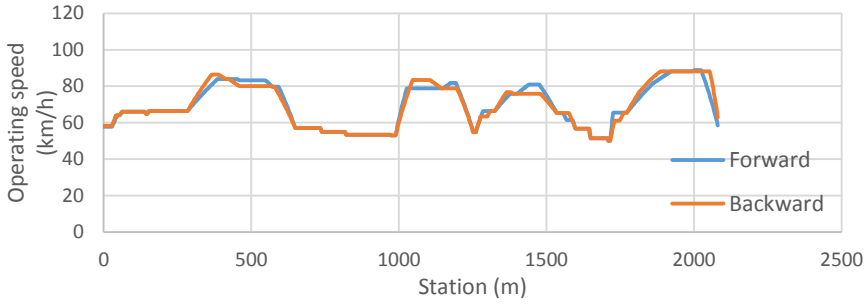

CCR	409.8054 gon/km	$\overline{\Delta v_{85}}$	10.42099 km/h
$\bar{v}_{85}$	69.67957 km/h	d_{85}	1.9737012 m/s^2
$\sigma_{v_{85}}$	11.4422 km/h	$\sigma_{\Delta v_{85}}$	10.058116 km/h
R_a	2.795367 km/h	$\sigma_{d_{85}}$	0.6600366 m/s^2
$E_{a,10}$	2.13893 km/h	$\bar{L}_{\Delta v_{85}}$	29.391304 m
$E_{a,20}$	0 km/h	L_d	16.24%
L_{10}	0.528111 m	N	23
L_{20}	0 m		

CONSISTENCY

Polus (2004)	0.23752
Garach (2013)	0.32374
Camacho (2014	2.14046

CRASHES

Observed:	1
Estimated:	
Exposure	2
Polus (2004)	2
Camacho (2009)	1
Garach (2013)	2
Camacho (2014)	2

ROAD SEGMENT: 12.2

Road:	CV-715	
Initial station:	42+360	Free
Final station:	44+360	Free
		Free

AADT:	427 vpd
Length:	1999 m

OPERATIONAL CHARACTERISTICS

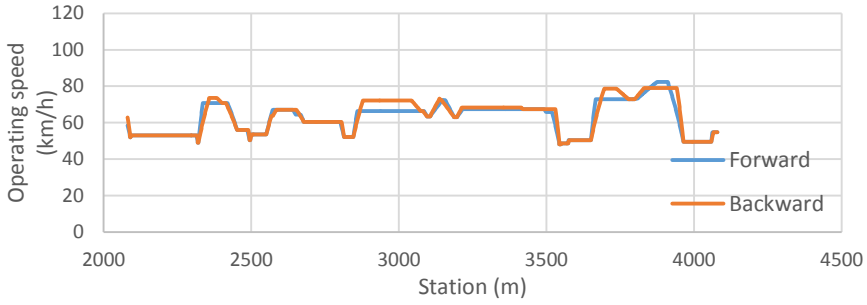

CCR	1022.738 gon/km	$\overline{\Delta v_{85}}$	9.5298298 km/h
$\bar{v}_{85}$	63.27938 km/h	d_{85}	2.3360356 m/s^2
$\sigma_{v_{85}}$	8.86803 km/h	$\sigma_{\Delta v_{85}}$	8.9180169 km/h
R_a	2.133538 km/h	$\sigma_{d_{85}}$	0.7248388 m/s^2
$E_{a,10}$	1.211833 km/h	$\bar{L}_{\Delta v_{85}}$	18.833333 m
$E_{a,20}$	0 km/h	L_d	11.31%
L_{10}	0.345173 m	N	24
L_{20}	0 m		

CONSISTENCY

Polus (2004)	0.65142
Garach (2013)	0.94035
Camacho (2014	1.95957

CRASHES

Observed:	3
Estimated:	
Exposure	1
Polus (2004)	1
Camacho (2009)	1
Garach (2013)	2
Camacho (2014)	1

ROAD SEGMENT: 12.3

Road:	CV-715	
Initial station:	44+360	Free
Final station:	46+440	Town
		Constrained

AADT:	427 vpd
Length:	2092 m

OPERATIONAL CHARACTERISTICS

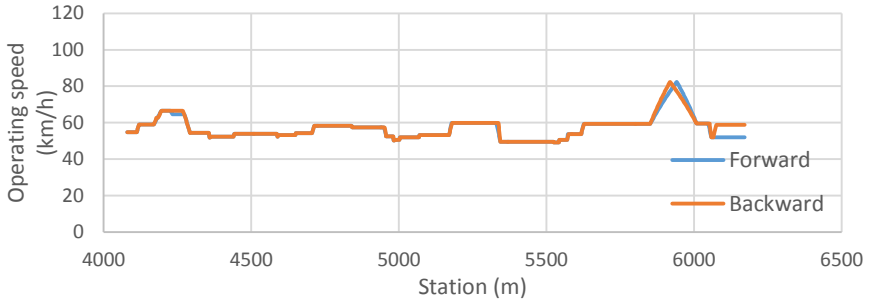

CCR	1016.504 gon/km	$\overline{\Delta v_{85}}$	5.7569219 km/h
$\bar{v}_{85}$	56.99929 km/h	d_{85}	2.4267732 m/s^2
$\sigma_{v_{85}}$	6.008518 km/h	$\sigma_{\Delta v_{85}}$	6.0660084 km/h
R_a	1.242474 km/h	$\sigma_{d_{85}}$	0.4620506 m/s^2
$E_{a,10}$	0.264803 km/h	$\bar{L}_{\Delta v_{85}}$	12.434783 m
$E_{a,20}$	0.123995 km/h	L_d	6.84%
L_{10}	0.053059 m	N	23
L_{20}	0.019598 m		

CONSISTENCY

Polus (2004)	1.57771
Garach (2013)	1.73981
Camacho (2014	1.86858

CRASHES

Observed:	3
Estimated:	
Exposure	2
Polus (2004)	1
Camacho (2009)	1
Garach (2013)	1
Camacho (2014)	2

ROAD SEGMENT: 13.1

Road:	CV-83	
Initial station:	14+270	Roundabout
Final station:	16+320	Free
		Constrained

AADT:	5581 vpd
Length:	1974 m

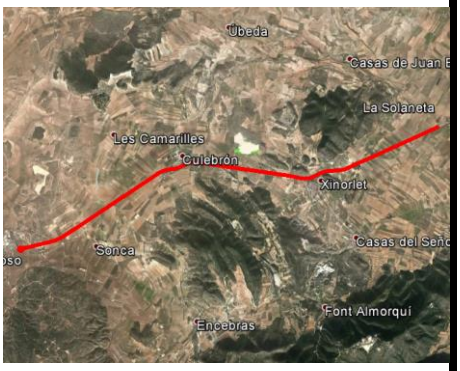

OPERATIONAL CHARACTERISTICS

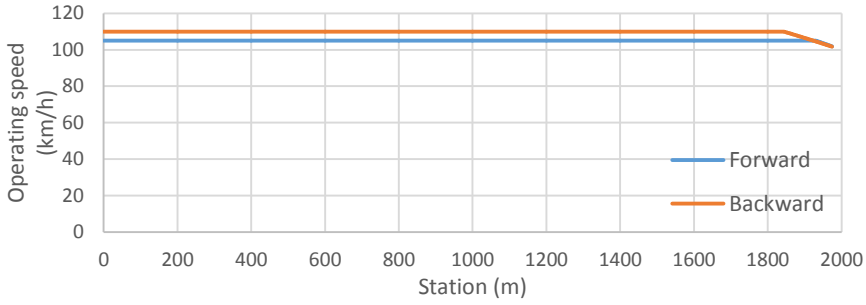

CCR	0.00468 gon/km	$\overline{\Delta v_{85}}$	3.1390725 km/h
$\bar{v}_{85}$	107.3681 km/h	d_{85}	0.569626 m/s^2
$\sigma_{v_{85}}$	2.50986 km/h	$\sigma_{\Delta v_{85}}$	0 km/h
R_a	0.68979 km/h	$\sigma_{d_{85}}$	0 m/s^2
$E_{a,10}$	0 km/h	$\overline{L}_{\Delta v_{85}}$	44 m
$E_{a,20}$	0 km/h	L_d	1.11%
L_{10}	0 m	N	1
L_{20}	0 m		

CONSISTENCY

Polus (2004)	2.4566
Garach (2013)	2.38375
Camacho (2014	3.74106

CRASHES

Observed:	5
Estimated:	
Exposure	6
Polus (2004)	9
Camacho (2009)	6
Garach (2013)	18
Camacho (2014)	4

ROAD SEGMENT: 13.2

Road:	CV-83	
Initial station:	16+320	Free
Final station:	17+690	Free
		Free

AADT:	5486	vpd
Length:	1326	m

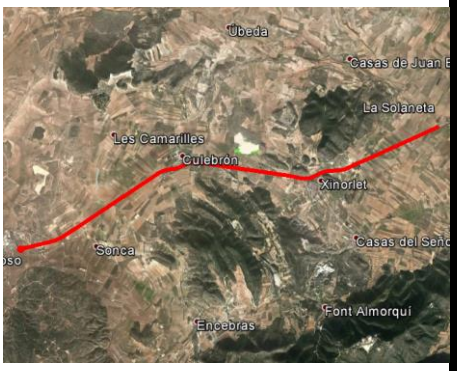

OPERATIONAL CHARACTERISTICS

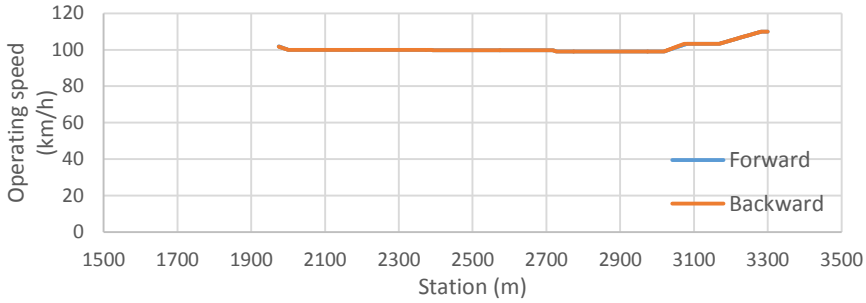

CCR	83.50926	gon/km	$\overline{\Delta v_{85}}$	4.299985	km/h
$\bar{v}_{85}$	100.7277	km/h	d_{85}	0.5470812	m/s^2
$\sigma_{v_{85}}$	2.468914	km/h	$\sigma_{\Delta v_{85}}$	2.3640375	km/h
R_a	0.475388	km/h	$\sigma_{d_{85}}$	0.0558799	m/s^2
$E_{a,10}$	0	km/h	$\bar{L}_{\Delta v_{85}}$	65.666667	m
$E_{a,20}$	0	km/h	L_d	7.43%	
L_{10}	0	m	N	3	
L_{20}	0	m			

CONSISTENCY

Polus (2004)	2.56469
Garach (2013)	2.49349
Camacho (2014	3.71192

CRASHES

Observed:	5
Estimated:	
Exposure	5
Polus (2004)	6
Camacho (2009)	4
Garach (2013)	12
Camacho (2014)	4

ROAD SEGMENT: 13.3

Road:	CV-83	
Initial station:	17+690	Free
Final station:	19+530	Free
		Free

AADT:	5486 vpd
Length:	1772 m

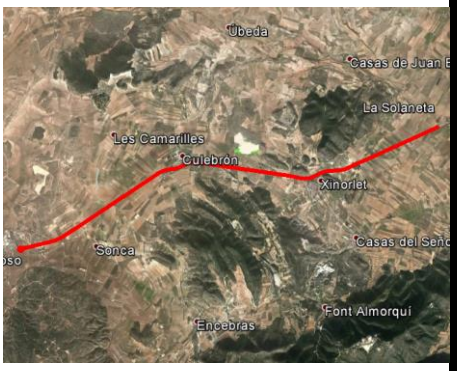

OPERATIONAL CHARACTERISTICS

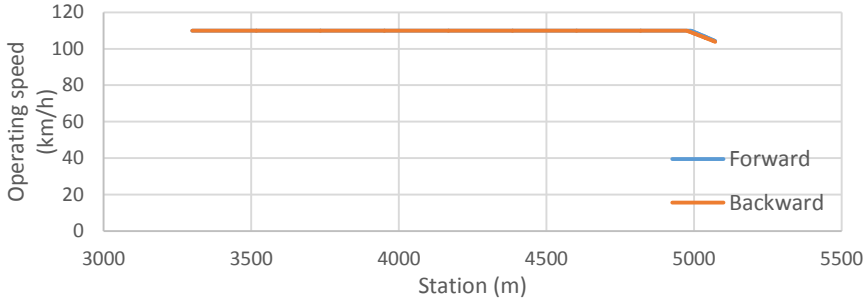

CCR	0.044479 gon/km	$\overline{\Delta v_{85}}$	5.7232298 km/h
$\bar{v}_{85}$	109.8432 km/h	d_{85}	0.5700302 m/s^2
$\sigma_{v_{85}}$	0.758771 km/h	$\sigma_{\Delta v_{85}}$	0 km/h
R_a	0.079618 km/h	$\sigma_{d_{85}}$	0 m/s^2
$E_{a,10}$	0 km/h	$\bar{L}_{\Delta v_{85}}$	83 m
$E_{a,20}$	0 km/h	L_d	2.34%
L_{10}	0 m	N	1
L_{20}	0 m		

CONSISTENCY

Polus (2004)	2.79493
Garach (2013)	2.83743
Camacho (2014	3.76869

CRASHES

Observed:	1
Estimated:	
Exposure	6
Polus (2004)	7
Camacho (2009)	5
Garach (2013)	15
Camacho (2014)	5

ROAD SEGMENT: 13.4

Road:	CV-83	
Initial station:	19+530	Free
Final station:	20+570	Free
		Free

AADT:	5486 vpd
Length:	997 m

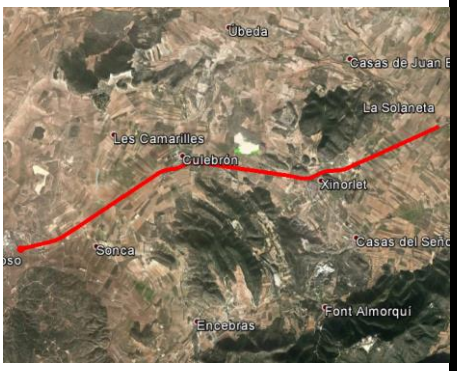

OPERATIONAL CHARACTERISTICS

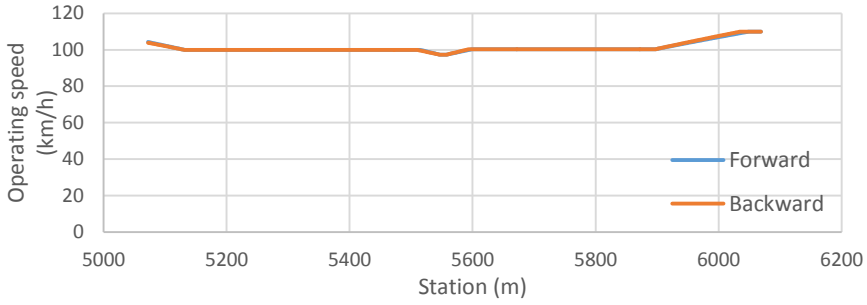

CCR	86.52604 gon/km	$\overline{\Delta v_{85}}$	4.8936627 km/h
$\bar{v}_{85}$	101.0611 km/h	d_{85}	0.597248 m/s^2
$\sigma_{v_{85}}$	2.697307 km/h	$\sigma_{\Delta v_{85}}$	3.3511415 km/h
R_a	0.510639 km/h	$\sigma_{d_{85}}$	0.0341661 m/s^2
$E_{a,10}$	0 km/h	$\bar{L}_{\Delta v_{85}}$	66.75 m
$E_{a,20}$	0 km/h	L_d	13.39%
L_{10}	0 m	N	4
L_{20}	0 m		

CONSISTENCY

Polus (2004)	2.52467
Garach (2013)	2.45426
Camacho (2014	3.60891

CRASHES

Observed:	2
Estimated:	
Exposure	4
Polus (2004)	4
Camacho (2009)	3
Garach (2013)	10
Camacho (2014)	3

ROAD SEGMENT: 13.5

Road:	CV-83	
Initial station:	20+570	Free
Final station:	23+530	Town
		Constrained

AADT:	5486	vpd
Length:	2999	m

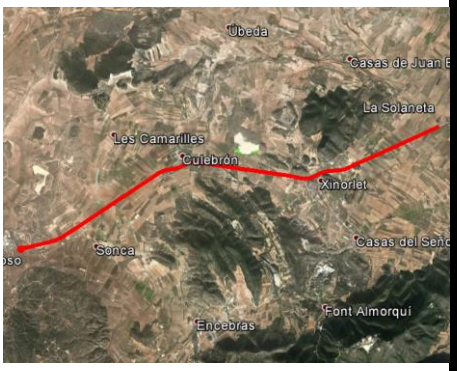

OPERATIONAL CHARACTERISTICS

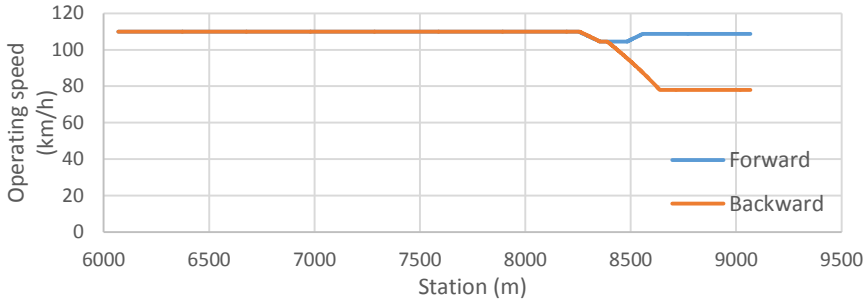

CCR	7.499785	gon/km	$\overline{\Delta v_{85}}$	5.4820872	km/h
$\bar{v}_{85}$	106.559	km/h	d_{85}	0.4404845	m/s^2
$\sigma_{v_{85}}$	8.905674	km/h	$\sigma_{\Delta v_{85}}$	0	km/h
R_a	1.520355	km/h	$\sigma_{d_{85}}$	0	m/s^2
$E_{a,10}$	0.717007	km/h	$\bar{L}_{\Delta v_{85}}$	103	m
$E_{a,20}$	0.651455	km/h	L_d	1.72%	
L_{10}	0.0997	m	N	1	
L_{20}	0.083861	m			

CONSISTENCY

Polus (2004)	0.98699
Garach (2013)	1.27271
Camacho (2014	4.06555

CRASHES

Observed:	4
Estimated:	
Exposure	9
Polus (2004)	22
Camacho (2009)	16
Garach (2013)	30
Camacho (2014)	5

ROAD SEGMENT: 14.1

Road:	CV-840	
Initial station:	20+688	Town
Final station:	18+501	Free
		Constrained

AADT:	3129 vpd
Length:	2165 m

OPERATIONAL CHARACTERISTICS

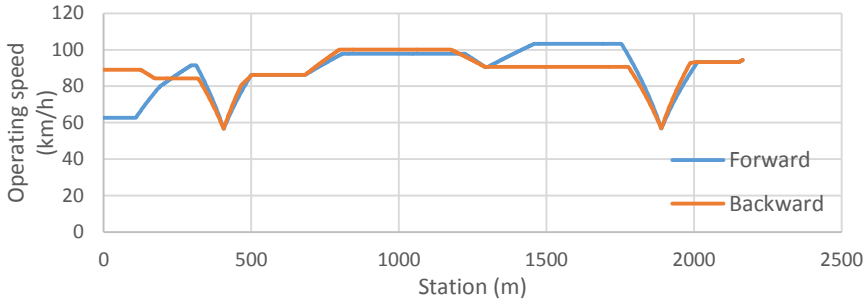

CCR	115.8909 gon/km	$\overline{\Delta v_{85}}$	24.122875 km/h
$\bar{v}_{85}$	89.03915 km/h	d_{85}	1.4844112 m/s^2
$\sigma_{v_{85}}$	11.00921 km/h	$\sigma_{\Delta v_{85}}$	16.806897 km/h
R_a	2.315852 km/h	$\sigma_{d_{85}}$	0.6850941 m/s^2
$E_{a,10}$	1.529182 km/h	$\bar{L}_{\Delta v_{85}}$	88.714286 m
$E_{a,20}$	0.646025 km/h	L_d	14.34%
L_{10}	0.332794 m	N	7
L_{20}	0.089838 m		

CONSISTENCY

Polus (2004)	0.39205
Garach (2013)	0.62488
Camacho (2014	2.55412

CRASHES

Observed:	14
Estimated:	
Exposure	5
Polus (2004)	11
Camacho (2009)	8
Garach (2013)	15
Camacho (2014)	6

ROAD SEGMENT: 14.2

Road:	CV-840	
Initial station:	18+501	Free
Final station:	15+548	Free
		Free

AADT:	3129	vpd
Length:	2948	m

OPERATIONAL CHARACTERISTICS

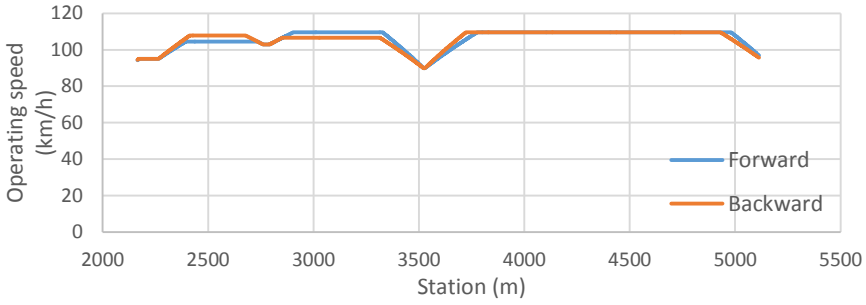

CCR	8.750313	gon/km	$\overline{\Delta v_{85}}$	11.687071	km/h
$\bar{v}_{85}$	106.0097	km/h	d_{85}	0.6603806	m/s^2
$\sigma_{v_{85}}$	4.975345	km/h	$\sigma_{\Delta v_{85}}$	7.6709252	km/h
R_a	1.088963	km/h	$\sigma_{d_{85}}$	0.1397546	m/s^2
$E_{a,10}$	0.284148	km/h	$\bar{L}_{\Delta v_{85}}$	126.5	m
$E_{a,20}$	0	km/h	L_d	12.87%	
L_{10}	0.084294	m	N	6	
L_{20}	0	m			

CONSISTENCY

Polus (2004)	1.84796
Garach (2013)	1.93019
Camacho (2014	3.54609

CRASHES

Observed:	6
Estimated:	
Exposure	6
Polus (2004)	9
Camacho (2009)	7
Garach (2013)	15
Camacho (2014)	5

ROAD SEGMENT: 14.3

Road:	CV-840	
Initial station:	15+548	Free
Final station:	13+266	Free
		Free

AADT:	3129 vpd
Length:	2277 m

OPERATIONAL CHARACTERISTICS

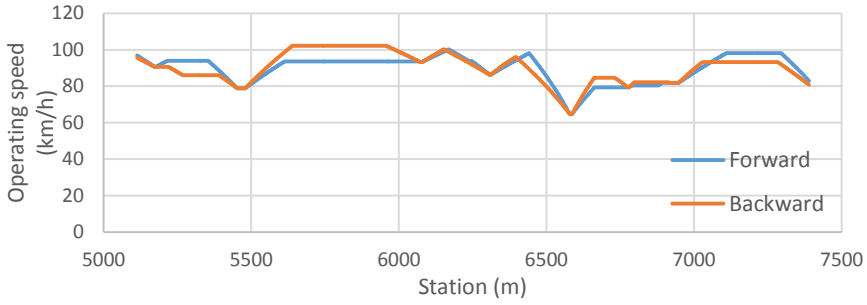

CCR	78.35891 gon/km	$\overline{\Delta v_{85}}$	13.172782 km/h
$\bar{v}_{85}$	89.88312 km/h	d_{85}	0.9917877 m/s^2
$\sigma_{v_{85}}$	7.869536 km/h	$\sigma_{\Delta v_{85}}$	8.7678003 km/h
R_a	1.789687 km/h	$\sigma_{d_{85}}$	0.277657 m/s^2
$E_{a,10}$	0.72912 km/h	$\bar{L}_{\Delta v_{85}}$	84.916667 m
$E_{a,20}$	0.142583 km/h	L_d	22.38%
L_{10}	0.194115 m	N	12
L_{20}	0.022398 m		

CONSISTENCY

Polus (2004)	0.94637
Garach (2013)	1.24006
Camacho (2014	2.9308

CRASHES

Observed:	5
Estimated:	
Exposure	5
Polus (2004)	10
Camacho (2009)	7
Garach (2013)	13
Camacho (2014)	5

ROAD SEGMENT: 14.4

Road:	CV-840	
Initial station:	13+266	Free
Final station:	11+437	Town
		Constrained

AADT:	3129 vpd
Length:	1821 m

OPERATIONAL CHARACTERISTICS

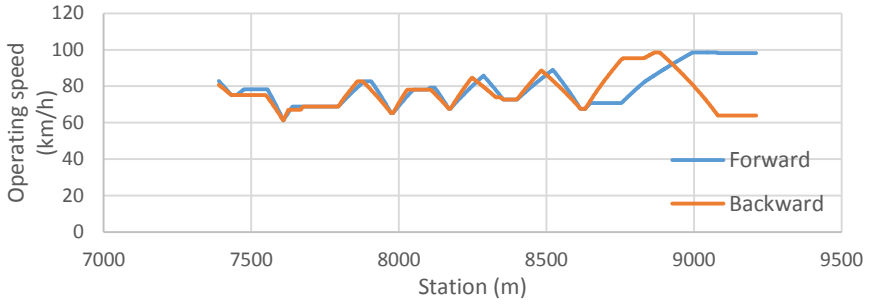

CCR	201.0938 gon/km	$\overline{\Delta v_{85}}$	13.312431 km/h
$\bar{v}_{85}$	77.99701 km/h	d_{85}	1.330028 m/s^2
$\sigma_{v_{85}}$	9.525961 km/h	$\sigma_{\Delta v_{85}}$	7.075652 km/h
R_a	2.088273 km/h	$\sigma_{d_{85}}$	0.2597811 m/s^2
$E_{a,10}$	1.162687 km/h	$\bar{L}_{\Delta v_{85}}$	59.214286 m
$E_{a,20}$	0.385954 km/h	L_d	22.76%
L_{10}	0.269632 m	N	14
L_{20}	0.068369 m		

CONSISTENCY

Polus (2004)	0.60429
Garach (2013)	0.89983
Camacho (2014	2.53496

CRASHES

Observed:	1
Estimated:	
Exposure	4
Polus (2004)	9
Camacho (2009)	6
Garach (2013)	12
Camacho (2014)	5

ROAD SEGMENT: 15.1

Road:	CV-860	
Initial station:	0+090	Roundabout
Final station:	4+640	Roundabout
		Constrained

AADT:	4980 vpd
Length:	4536 m

OPERATIONAL CHARACTERISTICS

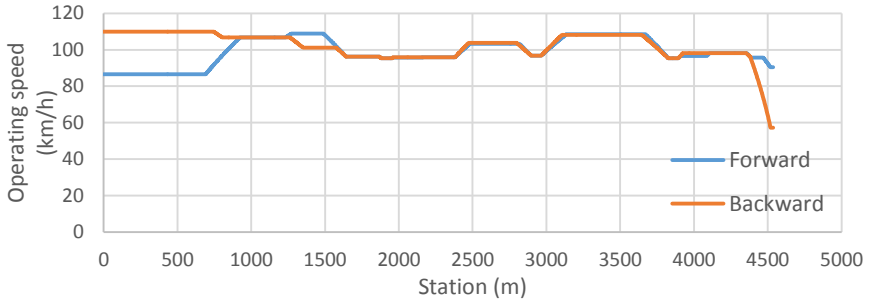

CCR	45.9033 gon/km	$\overline{\Delta v_{85}}$	7.7568058 km/h
$\bar{v}_{85}$	100.5803 km/h	d_{85}	0.6664303 m/s^2
$\sigma_{v_{85}}$	7.565422 km/h	$\sigma_{\Delta v_{85}}$	4.2353915 km/h
R_a	1.688734 km/h	$\sigma_{d_{85}}$	0.0377403 m/s^2
$E_{a,10}$	0.428939 km/h	$\bar{L}_{\Delta v_{85}}$	91.25 m
$E_{a,20}$	0.093928 km/h	L_d	8.05%
L_{10}	0.097443 m	N	8
L_{20}	0.010141 m		

CONSISTENCY

Polus (2004)	1.04695
Garach (2013)	1.32898
Camacho (2014	3.47391

CRASHES

Observed:	10
Estimated:	
Exposure	13
Polus (2004)	30
Camacho (2009)	21
Garach (2013)	38
Camacho (2014)	11

ROAD SEGMENT: 16.1

Road:	CV-925	
Initial station:	14+190	Intersection
Final station:	17+180	Free
		Constrained

AADT:	1285 vpd
Length:	2972 m

OPERATIONAL CHARACTERISTICS

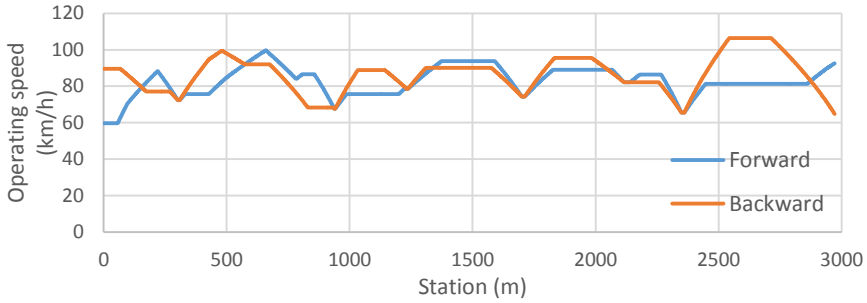

CCR	76.14327 gon/km	$\overline{\Delta v_{85}}$	19.97154 km/h
$\bar{v}_{85}$	84.61129 km/h	d_{85}	1.1925999 m/s^2
$\sigma_{v_{85}}$	9.100536 km/h	$\sigma_{\Delta v_{85}}$	8.8111026 km/h
R_a	2.027591 km/h	$\sigma_{d_{85}}$	0.2099772 m/s^2
$E_{a,10}$	0.99688 km/h	$\bar{L}_{\Delta v_{85}}$	106.36364 m
$E_{a,20}$	0.282421 km/h	L_d	19.68%
L_{10}	0.2357 m	N	11
L_{20}	0.045256 m		

CONSISTENCY

Polus (2004)	0.6754
Garach (2013)	0.97761
Camacho (2014	2.70112

CRASHES

Observed:	2
Estimated:	
Exposure	4
Polus (2004)	6
Camacho (2009)	4
Garach (2013)	7
Camacho (2014)	4

ROAD SEGMENT: 16.2

Road:	CV-925	
Initial station:	17+180	Free
Final station:	18+520	Free
		Free

AADT:	1285 vpd
Length:	1322 m

OPERATIONAL CHARACTERISTICS

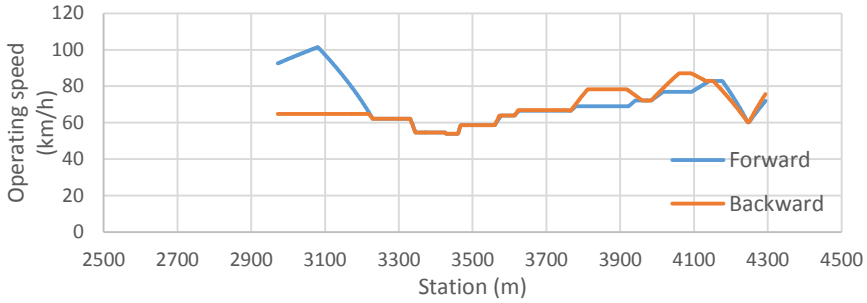

CCR	366.3544 gon/km	$\overline{\Delta v_{85}}$	13.874402 km/h
$\bar{v}_{85}$	69.62735 km/h	d_{85}	1.7840838 m/s^2
$\sigma_{v_{85}}$	10.77278 km/h	$\sigma_{\Delta v_{85}}$	11.424457 km/h
R_a	2.370335 km/h	$\sigma_{d_{85}}$	0.4249229 m/s^2
$E_{a,10}$	1.477149 km/h	$\bar{L}_{\Delta v_{85}}$	48 m
$E_{a,20}$	0.456792 km/h	L_d	16.34%
L_{10}	0.330938 m	N	9
L_{20}	0.060893 m		

CONSISTENCY

Polus (2004)	0.39086
Garach (2013)	0.6189
Camacho (2014	2.2132

CRASHES

Observed:	1
Estimated:	
Exposure	2
Polus (2004)	3
Camacho (2009)	2
Garach (2013)	4
Camacho (2014)	2

ROAD SEGMENT: 16.3

Road:	CV-925	
Initial station:	18+520	Free
Final station:	24+930	Roundabout
		Constrained

AADT:	1285 vpd
Length:	6394 m

OPERATIONAL CHARACTERISTICS

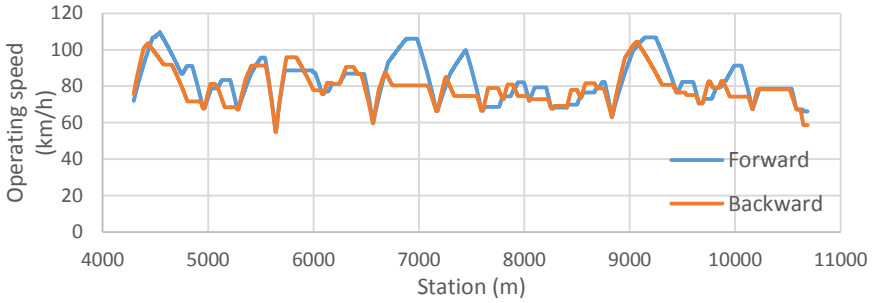

CCR	130.3308 gon/km	$\overline{\Delta v_{85}}$	18.531884 km/h
$\bar{v}_{85}$	81.31861 km/h	d_{85}	1.3419402 m/s^2
$\sigma_{v_{85}}$	10.28363 km/h	$\sigma_{\Delta v_{85}}$	11.816035 km/h
R_a	2.245032 km/h	$\sigma_{d_{85}}$	0.3422209 m/s^2
$E_{a,10}$	1.392822 km/h	$\bar{L}_{\Delta v_{85}}$	84.424242 m
$E_{a,20}$	0.448419 km/h	L_d	21.79%
L_{10}	0.31858 m	N	33
L_{20}	0.068736 m		

CONSISTENCY

Polus (2004)	0.47219
Garach (2013)	0.73595
Camacho (2014	2.56282

CRASHES

Observed:	4
Estimated:	
Exposure	9
Polus (2004)	13
Camacho (2009)	9
Garach (2013)	13
Camacho (2014)	10

ROAD SEGMENT: 17.1

Road:	CV-935	
Initial station:	6+000	Roundabout
Final station:	9+910	Intersection
		Constrained

AADT:	2588 vpd
Length:	3906 m

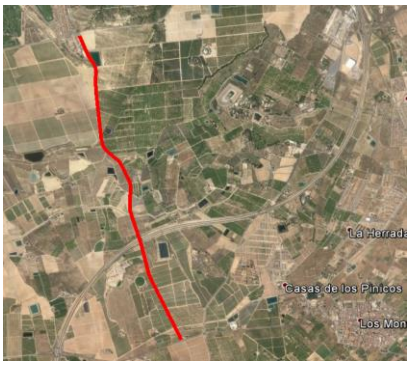

OPERATIONAL CHARACTERISTICS

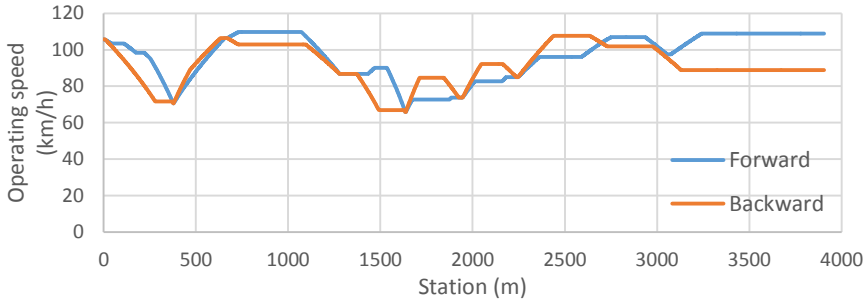

CCR	56.77743 gon/km	$\overline{\Delta v_{85}}$	18.72415 km/h
$\bar{v}_{85}$	94.02704 km/h	d_{85}	0.9590486 m/s^2
$\sigma_{v_{85}}$	11.93395 km/h	$\sigma_{\Delta v_{85}}$	10.404888 km/h
R_a	2.83863 km/h	$\sigma_{d_{85}}$	0.3423746 m/s^2
$E_{a,10}$	1.951406 km/h	$\bar{L}_{\Delta v_{85}}$	131.3 m
$E_{a,20}$	0.613242 km/h	L_d	16.81%
L_{10}	0.44022 m	N	10
L_{20}	0.095878 m		

CONSISTENCY

Polus (2004)	0.20525
Garach (2013)	0.26
Camacho (2014	3.00864

CRASHES

Observed:	9
Estimated:	
Exposure	8
Polus (2004)	18
Camacho (2009)	12
Garach (2013)	21
Camacho (2014)	8

ROAD SEGMENT: 18.1

Road:	CV-941	
Initial station:	1+190	Roundabout
Final station:	6+390	Roundabout
		Constrained

AADT:	3472 vpd
Length:	5202 m

OPERATIONAL CHARACTERISTICS

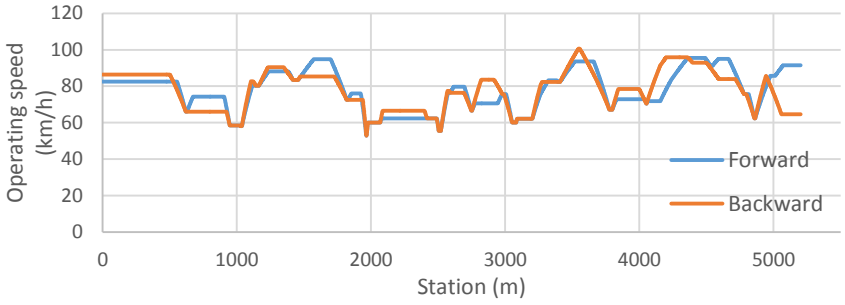

CCR	180.3423 gon/km	$\overline{\Delta v_{85}}$	14.429133 km/h
$\bar{v}_{85}$	77.84264 km/h	d_{85}	1.5479488 m/s^2
$\sigma_{v_{85}}$	10.8372 km/h	$\sigma_{\Delta v_{85}}$	7.9126024 km/h
R_a	2.592412 km/h	$\sigma_{d_{85}}$	0.5388305 m/s^2
$E_{a,10}$	1.798784 km/h	$\bar{L}_{\Delta v_{85}}$	59.115385 m
$E_{a,20}$	0.079923 km/h	L_d	14.77%
L_{10}	0.438677 m	N	26
L_{20}	0.013072 m		

CONSISTENCY

Polus (2004)	0.32077
Garach (2013)	0.4896
Camacho (2014	2.40835

CRASHES

Observed:	37
Estimated:	
Exposure	12
Polus (2004)	31
Camacho (2009)	21
Garach (2013)	34
Camacho (2014)	20

ROAD SEGMENT: 19.1

Road:	CV-949	
Initial station:	0+020	Intersection
Final station:	3+060	Free
		Constrained

AADT:	813 vpd
Length:	2997 m

OPERATIONAL CHARACTERISTICS

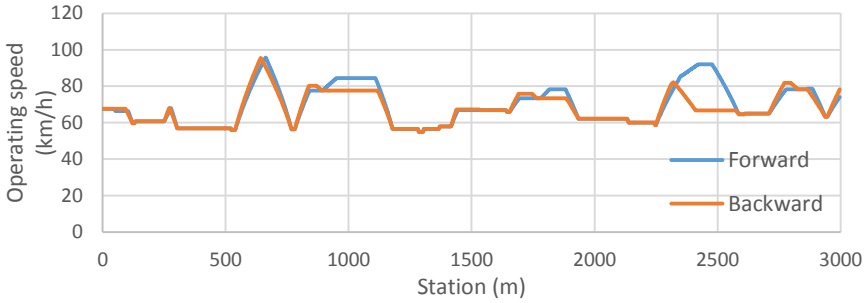

CCR	353.0901 gon/km	$\overline{\Delta v_{85}}$	13.650586 km/h
$\bar{v}_{85}$	68.55914 km/h	d_{85}	1.8090624 m/s^2
$\sigma_{v_{85}}$	9.451916 km/h	$\sigma_{\Delta v_{85}}$	12.187125 km/h
R_a	2.19241 km/h	$\sigma_{d_{85}}$	0.3247777 m/s^2
$E_{a,10}$	1.204632 km/h	$\bar{L}_{\Delta v_{85}}$	40.5 m
$E_{a,20}$	0.225703 km/h	L_d	14.86%
L_{10}	0.311645 m	N	22
L_{20}	0.035202 m		

CONSISTENCY

Polus (2004)	0.56679
Garach (2013)	0.84847
Camacho (2014	2.19164

CRASHES

Observed:	10
Estimated:	
Exposure	3
Polus (2004)	4
Camacho (2009)	3
Garach (2013)	4
Camacho (2014)	4

ROAD SEGMENT: 19.2

Road:	CV-949	
Initial station:	3+060	Free
Final station:	6+980	Free
		Free

AADT:	813 vpd
Length:	3901 m

OPERATIONAL CHARACTERISTICS

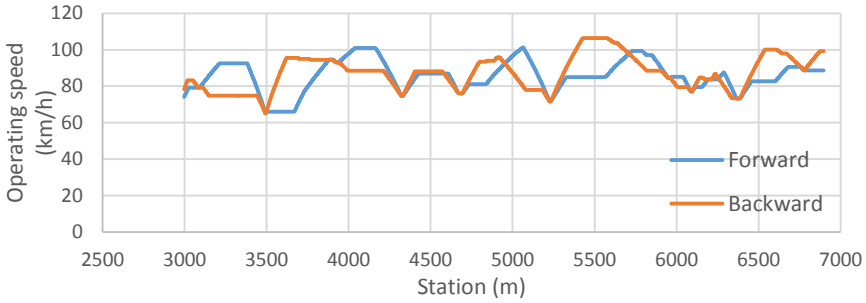

CCR	77.46075 gon/km	$\overline{\Delta v_{85}}$	14.331669 km/h
$\bar{v}_{85}$	86.51722 km/h	d_{85}	1.0658741 m/s^2
$\sigma_{v_{85}}$	8.853569 km/h	$\sigma_{\Delta v_{85}}$	11.077667 km/h
R_a	1.989429 km/h	$\sigma_{d_{85}}$	0.2707881 m/s^2
$E_{a,10}$	1.076123 km/h	$\bar{L}_{\Delta v_{85}}$	81.75 m
$E_{a,20}$	0.144609 km/h	L_d	20.96%
L_{10}	0.27493 m	N	20
L_{20}	0.025378 m		

CONSISTENCY

Polus (2004)	0.72059
Garach (2013)	1.02461
Camacho (2014	2.82508

CRASHES

Observed:	4
Estimated:	
Exposure	2
Polus (2004)	5
Camacho (2009)	3
Garach (2013)	5
Camacho (2014)	2

ROAD SEGMENT: 20.1

Road:	CV-25	
Initial station:	10+280	Town
Final station:	13+200	Free
		Constrained

AADT:	528 vpd
Length:	2868 m

OPERATIONAL CHARACTERISTICS

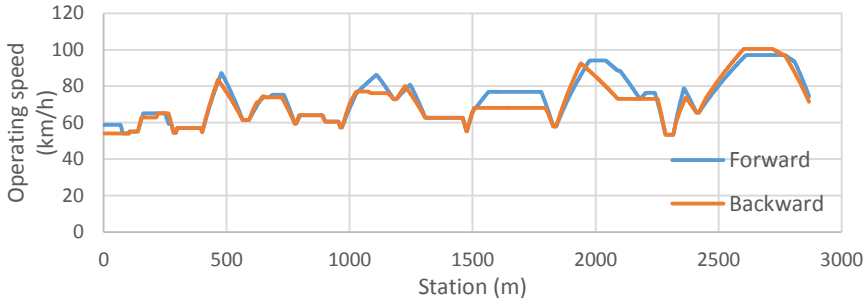

CCR	341.8278 gon/km	$\overline{\Delta v_{85}}$	12.307471 km/h
$\bar{v}_{85}$	72.32733 km/h	d_{85}	1.7893853 m/s^2
$\sigma_{v_{85}}$	12.08459 km/h	$\sigma_{\Delta v_{85}}$	9.8595907 km/h
R_a	2.721516 km/h	$\sigma_{d_{85}}$	0.4470416 m/s^2
$E_{a,10}$	1.863142 km/h	$\bar{L}_{\Delta v_{85}}$	41.21875 m
$E_{a,20}$	0.675793 km/h	L_d	23.00%
L_{10}	0.391736 m	N	32
L_{20}	0.098849 m		

CONSISTENCY

Polus (2004)	0.22152
Garach (2013)	0.30969
Camacho (2014	2.23923

CRASHES

Observed:	3
Estimated:	
Exposure	2
Polus (2004)	3
Camacho (2009)	2
Garach (2013)	3
Camacho (2014)	2

ROAD SEGMENT: 20.2

Road:	CV-25	
Initial station:	13+200	Free
Final station:	15+110	Town
		Constrained

AADT:	528 vpd
Length:	1900 m

OPERATIONAL CHARACTERISTICS

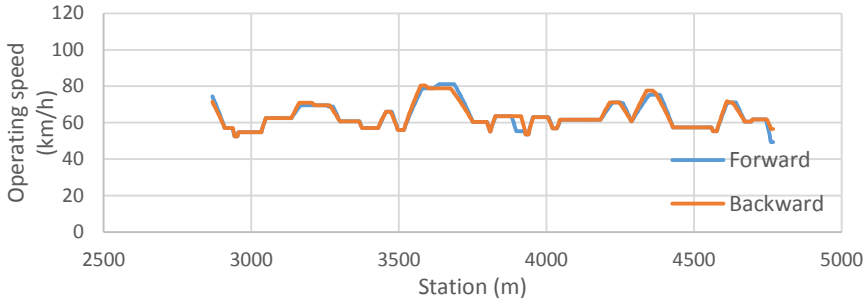

CCR	596.9967 gon/km	$\overline{\Delta v_{85}}$	9.1783693 km/h
$\bar{v}_{85}$	63.81044 km/h	d_{85}	2.0940572 m/s^2
$\sigma_{v_{85}}$	6.782664 km/h	$\sigma_{\Delta v_{85}}$	6.1044221 km/h
R_a	1.502846 km/h	$\sigma_{d_{85}}$	0.3848396 m/s^2
$E_{a,10}$	0.457742 km/h	$\bar{L}_{\Delta v_{85}}$	22.428571 m
$E_{a,20}$	0 km/h	L_d	16.53%
L_{10}	0.118421 m	N	28
L_{20}	0 m		

CONSISTENCY

Polus (2004)	1.27803
Garach (2013)	1.51547
Camacho (2014	2.03798

CRASHES

Observed:	3
Estimated:	
Exposure	2
Polus (2004)	1
Camacho (2009)	1
Garach (2013)	2
Camacho (2014)	2

ROAD SEGMENT: 21.1

Road:	CV-35	
Initial station:	87+120	Town
Final station:	89+200	Free
		Constrained

AADT:	520	vpd
Length:	2080	m

OPERATIONAL CHARACTERISTICS

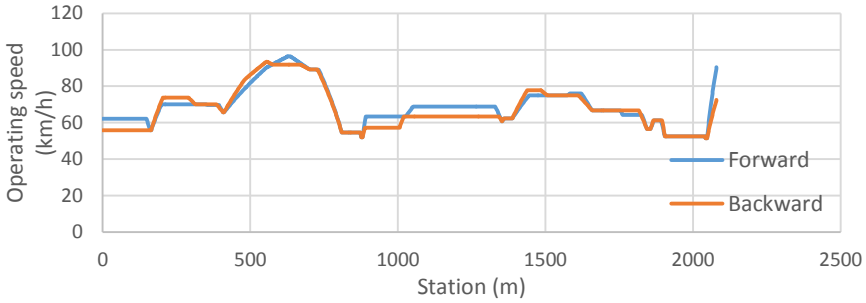

CCR	420.8943	gon/km	$\overline{\Delta v_{85}}$	10.104618	km/h
$\bar{v}_{85}$	68.28231	km/h	d_{85}	1.9913136	m/s^2
$\sigma_{v_{85}}$	10.86774	km/h	$\sigma_{\Delta v_{85}}$	9.2005843	km/h
R_a	2.33106	km/h	$\sigma_{d_{85}}$	0.6092863	m/s^2
$E_{a,10}$	1.578755	km/h	$\bar{L}_{\Delta v_{85}}$	30.526316	m
$E_{a,20}$	0.64426	km/h	L_d	13.94%	
L_{10}	0.340865	m	N	19	
L_{20}	0.099038	m			

CONSISTENCY

Polus (2004)	0.397
Garach (2013)	0.63085
Camacho (2014	2.11977

CRASHES

Observed:	1
Estimated:	
Exposure	2
Polus (2004)	2
Camacho (2009)	1
Garach (2013)	2
Camacho (2014)	2

ROAD SEGMENT: 21.2

Road:	CV-35	
Initial station:	89+200	Free
Final station:	92+240	Free
		Free

AADT:	520 vpd
Length:	2871 m

OPERATIONAL CHARACTERISTICS

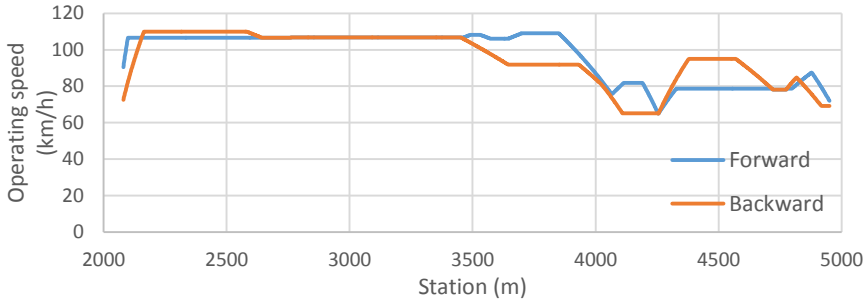

CCR	38.51796 gon/km	$\overline{\Delta v_{85}}$	20.26446 km/h
$\bar{v}_{85}$	96.45595 km/h	d_{85}	1.4247289 m/s^2
$\sigma_{v_{85}}$	13.56601 km/h	$\sigma_{\Delta v_{85}}$	13.568616 km/h
R_a	3.36258 km/h	$\sigma_{d_{85}}$	0.8400805 m/s^2
$E_{a,10}$	3.099367 km/h	$\bar{L}_{\Delta v_{85}}$	91.714286 m
$E_{a,20}$	0.610579 km/h	L_d	11.18%
L_{10}	0.801811 m	N	7
L_{20}	0.081505 m		

CONSISTENCY

Polus (2004)	0.0829
Garach (2013)	-0.12456
Camacho (2014	2.65928

CRASHES

Observed:	0
Estimated:	
Exposure	1
Polus (2004)	3
Camacho (2009)	2
Garach (2013)	3
Camacho (2014)	1

ROAD SEGMENT: 21.3

Road:	CV-35	
Initial station:	92+240	Free
Final station:	93+490	Free
		Free

AADT:	520 vpd
Length:	1226 m

OPERATIONAL CHARACTERISTICS

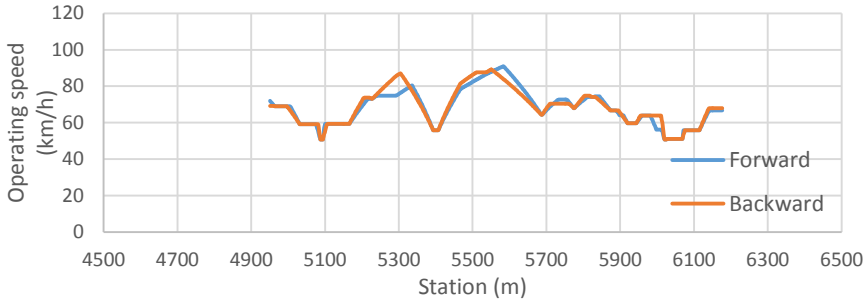

CCR	600.8482 gon/km	$\overline{\Delta v_{85}}$	9.9726876 km/h
$\bar{v}_{85}$	68.59279 km/h	d_{85}	1.86286 m/s^2
$\sigma_{v_{85}}$	9.806474 km/h	$\sigma_{\Delta v_{85}}$	8.2578053 km/h
R_a	2.211969 km/h	$\sigma_{d_{85}}$	0.6287206 m/s^2
$E_{a,10}$	1.289377 km/h	$\bar{L}_{\Delta v_{85}}$	30.714286 m
$E_{a,20}$	0.111865 km/h	L_d	26.31%
L_{10}	0.304649 m	N	21
L_{20}	0.019168 m		

CONSISTENCY

Polus (2004)	0.52592
Garach (2013)	0.80209
Camacho (2014	2.17069

CRASHES

Observed:	1
Estimated:	
Exposure	1
Polus (2004)	1
Camacho (2009)	1
Garach (2013)	1
Camacho (2014)	1

ROAD SEGMENT: 21.4

Road:	CV-35	
Initial station:	93+490	Free
Final station:	95+910	Town
		Constrained

AADT:	520 vpd
Length:	2428 m

OPERATIONAL CHARACTERISTICS

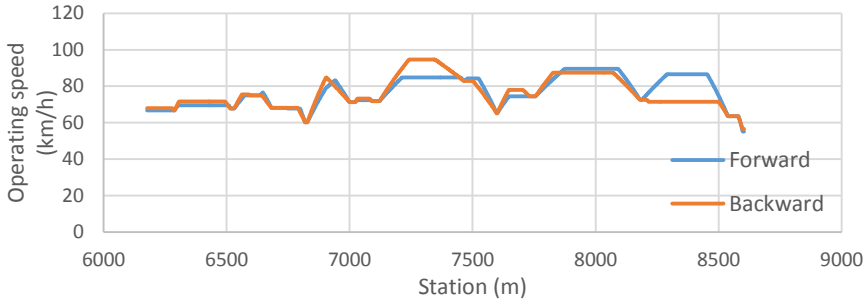

CCR	150.231 gon/km	$\overline{\Delta v_{85}}$	11.671185 km/h
$\bar{v}_{85}$	76.75831 km/h	d_{85}	1.41381 m/s^2
$\sigma_{v_{85}}$	8.334877 km/h	$\sigma_{\Delta v_{85}}$	7.7463926 km/h
R_a	2.007698 km/h	$\sigma_{d_{85}}$	0.3263694 m/s^2
$E_{a,10}$	0.845413 km/h	$\bar{L}_{\Delta v_{85}}$	48.3125 m
$E_{a,20}$	0.019131 km/h	L_d	15.93%
L_{10}	0.236506 m	N	16
L_{20}	0.003296 m		

CONSISTENCY

Polus (2004)	0.77124
Garach (2013)	1.06693
Camacho (2014	2.47065

CRASHES

Observed:	2
Estimated:	
Exposure	2
Polus (2004)	2
Camacho (2009)	1
Garach (2013)	2
Camacho (2014)	2

ROAD SEGMENT: 22.1

Road:	CV-41	
Initial station:	5+780	Roundabout
Final station:	7+050	Roundabout
		Constrained

AADT:	9202 vpd
Length:	1451 m

OPERATIONAL CHARACTERISTICS

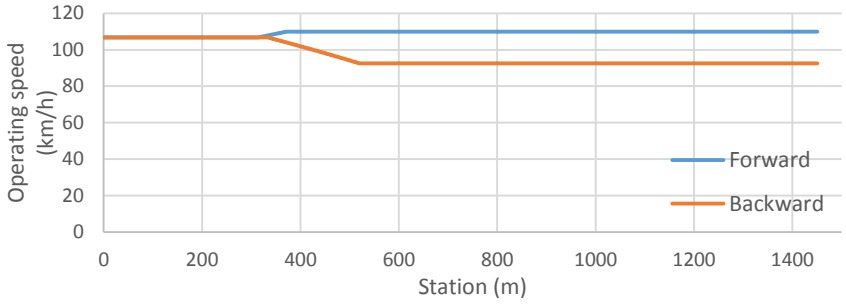

CCR	0 gon/km	$\overline{\Delta v_{85}}$	0 km/h
$\bar{v}_{85}$	0 km/h	d_{85}	0 m/s^2
$\sigma_{v_{85}}$	0 km/h	$\sigma_{\Delta v_{85}}$	0 km/h
R_a	0 km/h	$\sigma_{d_{85}}$	0 m/s^2
$E_{a,10}$	0 km/h	$\bar{L}_{\Delta v_{85}}$	0 m
$E_{a,20}$	0 km/h	L_d	0.00%
L_{10}	0 m	N	0
L_{20}	0 m		

CONSISTENCY

Polus (2004)	2.808
Garach (2013)	2.94029
Camacho (2014	#¡DIV/0!

CRASHES

Observed:	8
Estimated:	
Exposure	6
Polus (2004)	9
Camacho (2009)	7
Garach (2013)	21
Camacho (2014)	#¡DIV/0!

ROAD SEGMENT: 23.1

Road:	CV-41	
Initial station:	9+750	Roundabout
Final station:	11+910	Roundabout
		Constrained

AADT:	6690 vpd
Length:	2265 m

OPERATIONAL CHARACTERISTICS

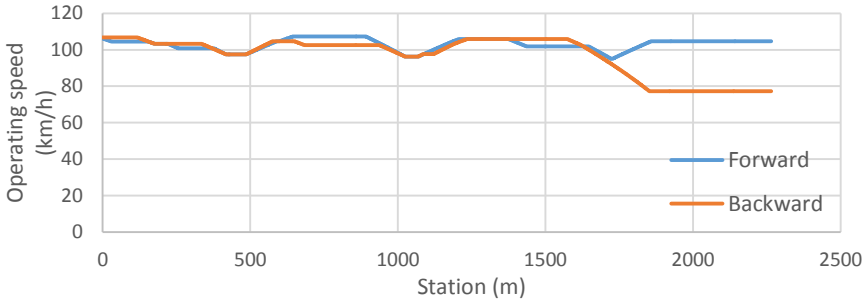

CCR	38.128 gon/km	$\overline{\Delta v_{85}}$	4.7304447 km/h
$\bar{v}_{85}$	99.98955 km/h	d_{85}	0.5723237 m/s^2
$\sigma_{v_{85}}$	8.35813 km/h	$\sigma_{\Delta v_{85}}$	3.3805088 km/h
R_a	1.618362 km/h	$\sigma_{d_{85}}$	0.076816 m/s^2
$E_{a,10}$	0.682133 km/h	$\bar{L}_{\Delta v_{85}}$	62 m
$E_{a,20}$	0.603443 km/h	L_d	13.69%
L_{10}	0.115011 m	N	10
L_{20}	0.096026 m		

CONSISTENCY

Polus (2004)	0.988
Garach (2013)	1.28249
Camacho (2014	3.64757

CRASHES

Observed:	1
Estimated:	
Exposure	8
Polus (2004)	20
Camacho (2009)	14
Garach (2013)	30
Camacho (2014)	6

ROAD SEGMENT: 24.1

Road:	CV-41	
Initial station:	12+100	Roundabout
Final station:	13+720	Free
		Constrained

AADT:	8472	vpd
Length:	1611	m

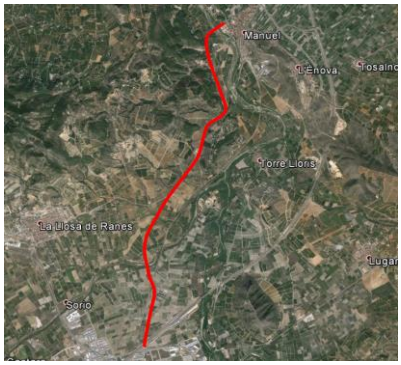

OPERATIONAL CHARACTERISTICS

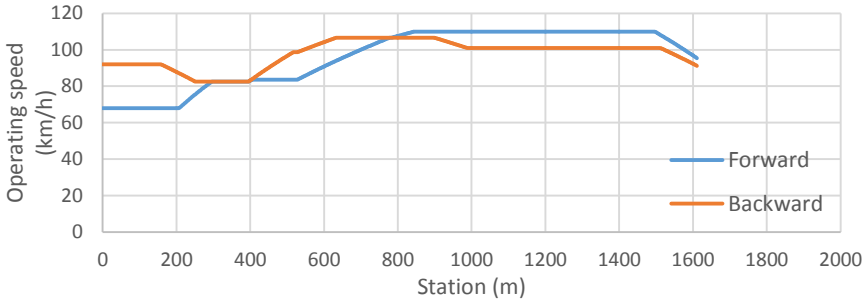

CCR	50.9806	gon/km	$\overline{\Delta v_{85}}$	12.883794	km/h
$\bar{v}_{85}$	96.8958	km/h	d_{85}	0.8438753	m/s^2
$\sigma_{v_{85}}$	12.32978	km/h	$\sigma_{\Delta v_{85}}$	4.2945746	km/h
R_a	2.862248	km/h	$\sigma_{d_{85}}$	0.2161633	m/s^2
$E_{a,10}$	2.059259	km/h	$\bar{L}_{\Delta v_{85}}$	114	m
$E_{a,20}$	0.627198	km/h	L_d	10.61%	
L_{10}	0.469274	m	N	3	
L_{20}	0.080695	m			

CONSISTENCY

Polus (2004)	0.18401
Garach (2013)	0.21554
Camacho (2014	3.17133

CRASHES

Observed:	11
Estimated:	
Exposure	6
Polus (2004)	24
Camacho (2009)	17
Garach (2013)	36
Camacho (2014)	6

ROAD SEGMENT: 24.2

Road:	CV-41	
Initial station:	13+720	Free
Final station:	14+710	Free
		Free

AADT:	8472	vpd
Length:	1000	m

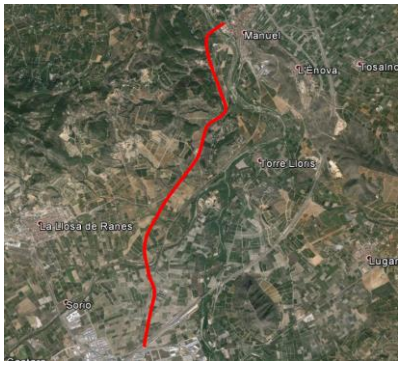

OPERATIONAL CHARACTERISTICS

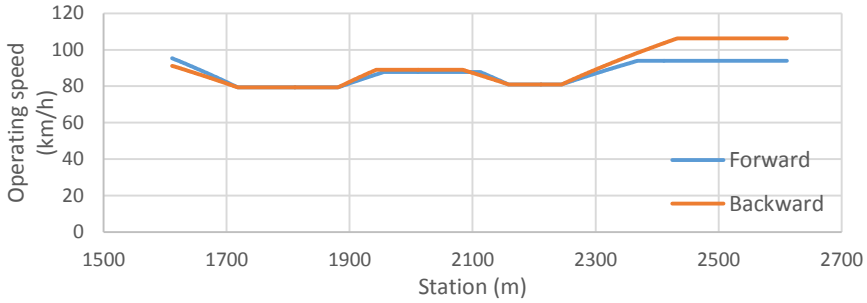

CCR	133.7703	gon/km	$\overline{\Delta v_{85}}$	14.448723	km/h
$\bar{v}_{85}$	88.33616	km/h	d_{85}	0.9872741	m/s^2
$\sigma_{v_{85}}$	8.020788	km/h	$\sigma_{\Delta v_{85}}$	8.1301024	km/h
R_a	1.759141	km/h	$\sigma_{d_{85}}$	0.0248602	m/s^2
$E_{a,10}$	0.568334	km/h	$\bar{L}_{\Delta v_{85}}$	101	m
$E_{a,20}$	0	km/h	L_d	20.20%	
L_{10}	0.1215	m	N	4	
L_{20}	0	m			

CONSISTENCY

Polus (2004)	0.94449
Garach (2013)	1.24145
Camacho (2014	2.91832

CRASHES

Observed:	16
Estimated:	
Exposure	6
Polus (2004)	11
Camacho (2009)	8
Garach (2013)	20
Camacho (2014)	7

ROAD SEGMENT: 24.3

Road:	CV-41	
Initial station:	14+710	Free
Final station:	18+420	Roundabout
		Constrained

AADT:	8472	vpd
Length:	3705	m

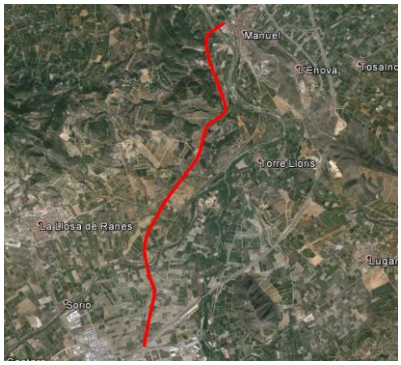

OPERATIONAL CHARACTERISTICS

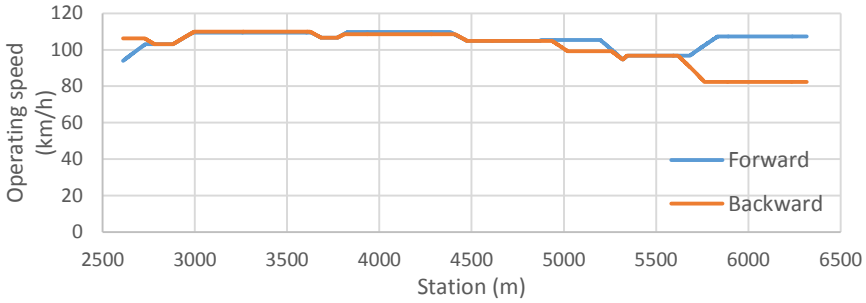

CCR	36.6174	gon/km
$\bar{v}_{85}$	103.4879	km/h
$\sigma_{v_{85}}$	7.60431	km/h
R_a	1.584429	km/h
$E_{a,10}$	0.500475	km/h
$E_{a,20}$	0.445071	km/h
L_{10}	0.089474	m
L_{20}	0.076113	m

$\overline{\Delta v_{85}}$	4.8425993	km/h
d_{85}	0.5174232	m/s^2
$\sigma_{\Delta v_{85}}$	3.4696574	km/h
$\sigma_{d_{85}}$	0.1200046	m/s^2
$\bar{L}_{\Delta v_{85}}$	73.833333	m
L_d	5.98%	
N	6	

CONSISTENCY

Polus (2004)	1.10745
Garach (2013)	1.38289
Camacho (2014	3.81575

CRASHES

Observed:	30
Estimated:	
Exposure	14
Polus (2004)	40
Camacho (2009)	29
Garach (2013)	56
Camacho (2014)	11

ROAD SEGMENT: 25.1

Road:	CV-42	
Initial station:	1+870	Roundabout
Final station:	3+060	Roundabout
		Constrained

AADT:	6943 vpd
Length:	1254 m

OPERATIONAL CHARACTERISTICS

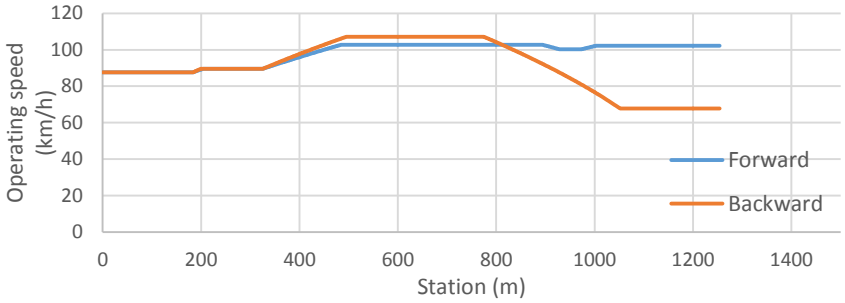

CCR	68.932 gon/km	$\overline{\Delta v_{85}}$	7.2710708 km/h
$\bar{v}_{85}$	94.33507 km/h	d_{85}	0.7058971 m/s^2
$\sigma_{v_{85}}$	11.18819 km/h	$\sigma_{\Delta v_{85}}$	8.9790803 km/h
R_a	2.577033 km/h	$\sigma_{d_{85}}$	0.1243549 m/s^2
$E_{a,10}$	1.259943 km/h	$\bar{L}_{\Delta v_{85}}$	73.333333 m
$E_{a,20}$	0.691797 km/h	L_d	8.77%
L_{10}	0.253589 m	N	3
L_{20}	0.095694 m		

CONSISTENCY

Polus (2004)	0.303
Garach (2013)	0.46665
Camacho (2014	3.33587

CRASHES

Observed:	2
Estimated:	
Exposure	4
Polus (2004)	15
Camacho (2009)	10
Garach (2013)	22
Camacho (2014)	4

ROAD SEGMENT: 26.1

Road:	CV-42	
Initial station:	3+260	Roundabout
Final station:	4+990	Roundabout
		Constrained

AADT:	6943 vpd
Length:	1735 m

OPERATIONAL CHARACTERISTICS

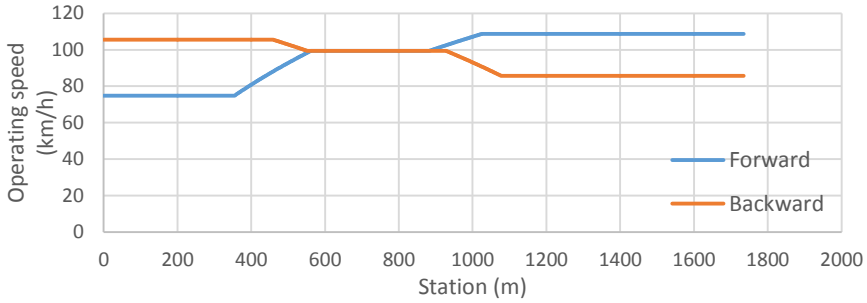

CCR	0 gon/km	$\overline{\Delta v_{85}}$	0 km/h
$\bar{v}_{85}$	0 km/h	d_{85}	0 m/s^2
$\sigma_{v_{85}}$	0 km/h	$\sigma_{\Delta v_{85}}$	0 km/h
R_a	0 km/h	$\sigma_{d_{85}}$	0 m/s^2
$E_{a,10}$	0 km/h	$\bar{L}_{\Delta v_{85}}$	0 m
$E_{a,20}$	0 km/h	L_d	0.00%
L_{10}	0 m	N	0
L_{20}	0 m		

CONSISTENCY

Polus (2004)	2.808
Garach (2013)	2.94029
Camacho (2014	#¡DIV/0!

CRASHES

Observed:	3
Estimated:	
Exposure	6
Polus (2004)	8
Camacho (2009)	6
Garach (2013)	18
Camacho (2014)	#¡DIV/0!

ROAD SEGMENT: 27.1

Road:	CV-42	
Initial station:	5+150	Roundabout
Final station:	7+370	Roundabout
		Constrained

AADT:	6544 vpd
Length:	2254 m

OPERATIONAL CHARACTERISTICS

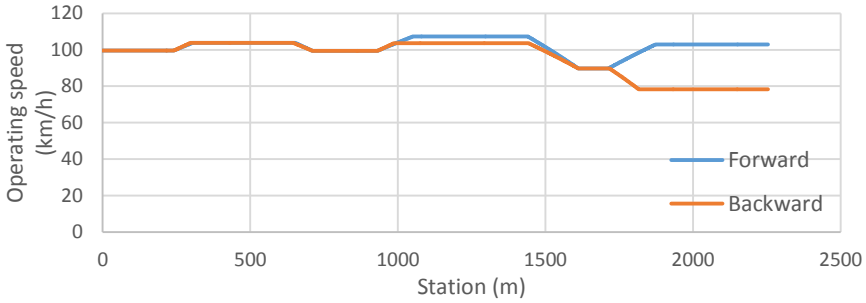

CCR	54.14352 gon/km	$\overline{\Delta v_{85}}$	7.5296966 km/h
$\bar{v}_{85}$	98.69725 km/h	d_{85}	0.6272321 m/s^2
$\sigma_{v_{85}}$	8.212489 km/h	$\sigma_{\Delta v_{85}}$	6.6834352 km/h
R_a	1.671182 km/h	$\sigma_{d_{85}}$	0.1024298 m/s^2
$E_{a,10}$	0.635891 km/h	$\bar{L}_{\Delta v_{85}}$	85.5 m
$E_{a,20}$	0.555975 km/h	L_d	7.59%
L_{10}	0.117125 m	N	4
L_{20}	0.097826 m		

CONSISTENCY

Polus (2004)	0.973
Garach (2013)	1.26971
Camacho (2014	3.52256

CRASHES

Observed:	8
Estimated:	
Exposure	7
Polus (2004)	20
Camacho (2009)	14
Garach (2013)	29
Camacho (2014)	6

ROAD SEGMENT: 28.1

Road:	CV-811	
Initial station:	0+800	Roundabout
Final station:	1+780	Free
		Constrained

AADT:	875 vpd
Length:	1071 m

OPERATIONAL CHARACTERISTICS

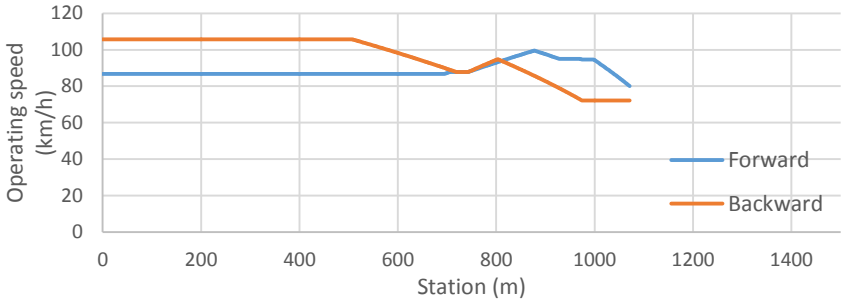

CCR	22.75051 gon/km	$\overline{\Delta v_{85}}$	8.6774449 km/h
$\bar{v}_{85}$	92.52091 km/h	d_{85}	0.9439773 m/s^2
$\sigma_{v_{85}}$	9.457852 km/h	$\sigma_{\Delta v_{85}}$	5.1186324 km/h
R_a	2.223546 km/h	$\sigma_{d_{85}}$	0.3437196 m/s^2
$E_{a,10}$	1.352529 km/h	$\bar{L}_{\Delta v_{85}}$	61.333333 m
$E_{a,20}$	0.262224 km/h	L_d	8.59%
L_{10}	0.34127 m	N	3
L_{20}	0.046218 m		

CONSISTENCY

Polus (2004)	0.55349
Garach (2013)	0.83003
Camacho (2014	3.00833

CRASHES

Observed:	0
Estimated:	
Exposure	1
Polus (2004)	1
Camacho (2009)	1
Garach (2013)	2
Camacho (2014)	1

ROAD SEGMENT: 28.2

Road:	CV-811	
Initial station:	1+780	Free
Final station:	3+760	Free
		Free

AADT:	875 vpd
Length:	1996 m

OPERATIONAL CHARACTERISTICS

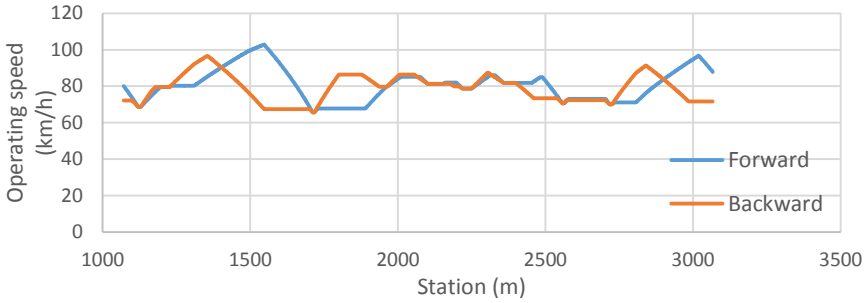

CCR	136.6153 gon/km	$\overline{\Delta v_{85}}$	11.568442 km/h
$\bar{v}_{85}$	79.84125 km/h	d_{85}	1.1735864 m/s^2
$\sigma_{v_{85}}$	8.131177 km/h	$\sigma_{\Delta v_{85}}$	9.4758673 km/h
R_a	1.827642 km/h	$\sigma_{d_{85}}$	0.1940148 m/s^2
$E_{a,10}$	0.849573 km/h	$\bar{L}_{\Delta v_{85}}$	60 m
$E_{a,20}$	0.092856 km/h	L_d	22.55%
L_{10}	0.2252 m	N	15
L_{20}	0.015531 m		

CONSISTENCY

Polus (2004)	0.89126
Garach (2013)	1.19125
Camacho (2014	2.66361

CRASHES

Observed:	2
Estimated:	
Exposure	2
Polus (2004)	2
Camacho (2009)	2
Garach (2013)	3
Camacho (2014)	1

ROAD SEGMENT: 28.3

Road:	CV-811	
Initial station:	3+760	Free
Final station:	4+490	Roundabout
		Constrained

AADT:	875 vpd
Length:	721 m

OPERATIONAL CHARACTERISTICS

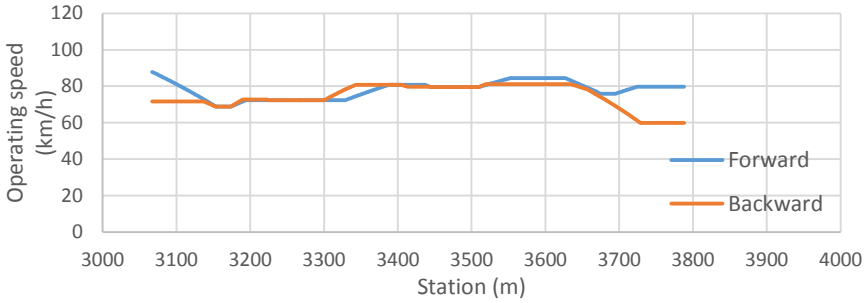

CCR	238.1416 gon/km	$\overline{\Delta v_{85}}$	7.1337029 km/h
$\bar{v}_{85}$	76.27782 km/h	d_{85}	1.1330132 m/s^2
$\sigma_{v_{85}}$	5.921538 km/h	$\sigma_{\Delta v_{85}}$	6.6594904 km/h
R_a	1.377701 km/h	$\sigma_{d_{85}}$	0.1701054 m/s^2
$E_{a,10}$	0.266791 km/h	$\bar{L}_{\Delta v_{85}}$	35.5 m
$E_{a,20}$	0 km/h	L_d	14.77%
L_{10}	0.0638 m	N	6
L_{20}	0 m		

CONSISTENCY

Polus (2004)	1.49554
Garach (2013)	1.67509
Camacho (2014	2.65432

CRASHES

Observed:	1
Estimated:	
Exposure	1
Polus (2004)	1
Camacho (2009)	1
Garach (2013)	1
Camacho (2014)	1

ROAD SEGMENT: 29.1

Road:	CV-900	
Initial station:	10+270	Roundabout
Final station:	11+070	Roundabout
		Constrained

AADT:	7143 vpd
Length:	841 m

OPERATIONAL CHARACTERISTICS

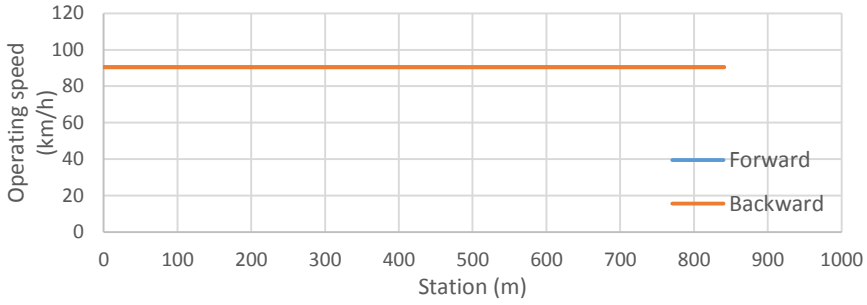

CCR	0 gon/km	$\overline{\Delta v_{85}}$	0 km/h
$\bar{v}_{85}$	0 km/h	d_{85}	0 m/s^2
$\sigma_{v_{85}}$	0 km/h	$\sigma_{\Delta v_{85}}$	0 km/h
R_a	0 km/h	$\sigma_{d_{85}}$	0 m/s^2
$E_{a,10}$	0 km/h	$\bar{L}_{\Delta v_{85}}$	0 m
$E_{a,20}$	0 km/h	L_d	0.00%
L_{10}	0 m	N	0
L_{20}	0 m		

CONSISTENCY

Polus (2004)	2.808
Garach (2013)	2.94029
Camacho (2014	#¡DIV/0!

CRASHES

Observed:	2
Estimated:	
Exposure	3
Polus (2004)	4
Camacho (2009)	3
Garach (2013)	10
Camacho (2014)	#¡DIV/0!

ROAD SEGMENT: 30.1

Road:	CV-15	
Initial station:	0+080	Roundabout
Final station:	2+230	Free
		Constrained

AADT:	8891	vpd
Length:	2095	m

OPERATIONAL CHARACTERISTICS

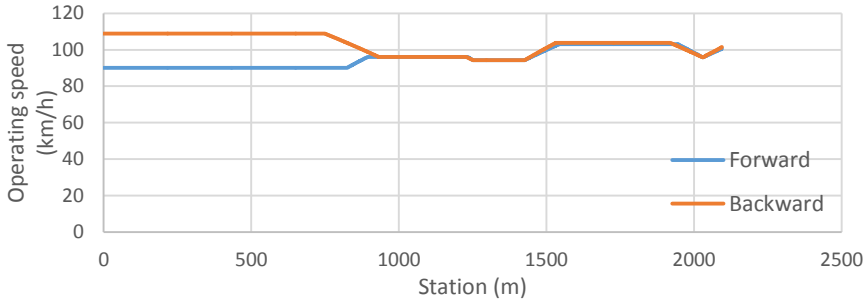

CCR	47.34945	gon/km	$\overline{\Delta v_{85}}$	6.0364522	km/h
$\bar{v}_{85}$	99.04168	km/h	d_{85}	0.6658682	m/s^2
$\sigma_{v_{85}}$	6.51586	km/h	$\sigma_{\Delta v_{85}}$	3.2167878	km/h
R_a	1.600138	km/h	$\sigma_{d_{85}}$	0.0153642	m/s^2
$E_{a,10}$	0	km/h	$\bar{L}_{\Delta v_{85}}$	68.75	m
$E_{a,20}$	0	km/h	L_d	6.56%	
L_{10}	0	m	N	4	
L_{20}	0	m			

CONSISTENCY

Polus (2004)	1.25525
Garach (2013)	1.48834
Camacho (2014	3.45708

CRASHES

Observed:	4
Estimated:	
Exposure	8
Polus (2004)	23
Camacho (2009)	16
Garach (2013)	37
Camacho (2014)	7

ROAD SEGMENT: 30.3

Road:	CV-15	
Initial station:	6+010	Free
Final station:	7+560	Roundabout
		Constrained

AADT:	5328	vpd
Length:	1539	m

OPERATIONAL CHARACTERISTICS

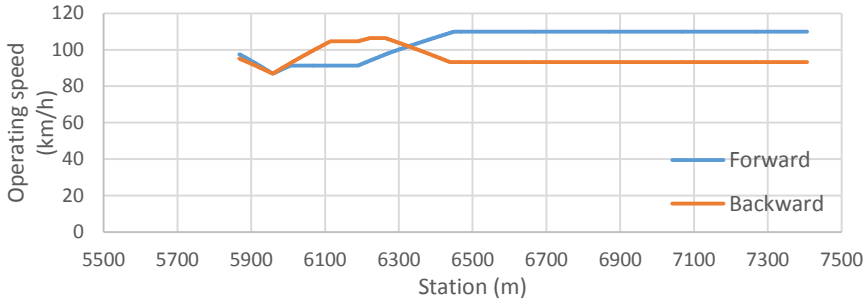

CCR	20.83877	gon/km	$\overline{\Delta v_{85}}$	10.021769	km/h
$\bar{v}_{85}$	99.98784	km/h	d_{85}	0.7039772	m/s^2
$\sigma_{v_{85}}$	7.929556	km/h	$\sigma_{\Delta v_{85}}$	7.985167	km/h
R_a	2.082809	km/h	$\sigma_{d_{85}}$	0.2334733	m/s^2
$E_{a,10}$	0.985204	km/h	$\bar{L}_{\Delta v_{85}}$	93	m
$E_{a,20}$	0	km/h	L_d	9.06%	
L_{10}	0.348603	m	N	3	
L_{20}	0	m			

CONSISTENCY

Polus (2004)	0.78434
Garach (2013)	1.06255
Camacho (2014	3.40431

CRASHES

Observed:	4
Estimated:	
Exposure	5
Polus (2004)	12
Camacho (2009)	8
Garach (2013)	18
Camacho (2014)	4

ROAD SEGMENT: 31.1

Road:	CV-820	
Initial station:	12+320	Roundabout
Final station:	14+400	Free
		Constrained

AADT:	4476 vpd
Length:	2075 m

OPERATIONAL CHARACTERISTICS

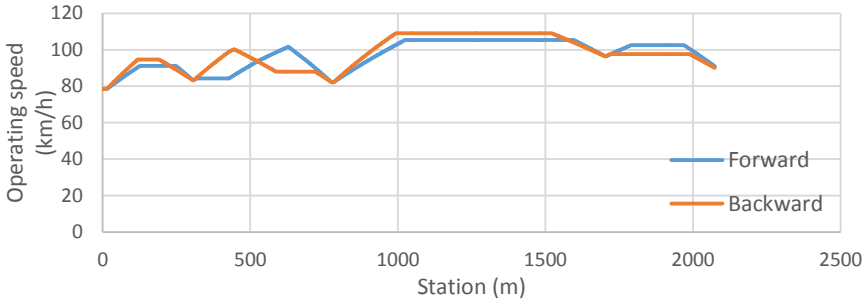

CCR	25.18559 gon/km	$\overline{\Delta v_{85}}$	13.653012 km/h
$\bar{v}_{85}$	97.37399 km/h	d_{85}	0.8506921 m/s^2
$\sigma_{v_{85}}$	8.331751 km/h	$\sigma_{\Delta v_{85}}$	7.8712172 km/h
R_a	1.971717 km/h	$\sigma_{d_{85}}$	0.1449664 m/s^2
$E_{a,10}$	0.974605 km/h	$\bar{L}_{\Delta v_{85}}$	110.625 m
$E_{a,20}$	0 km/h	L_d	21.34%
L_{10}	0.28134 m	N	8
L_{20}	0 m		

CONSISTENCY

Polus (2004)	0.78968
Garach (2013)	1.08812
Camacho (2014	3.16803

CRASHES

Observed:	4
Estimated:	
Exposure	6
Polus (2004)	13
Camacho (2009)	9
Garach (2013)	19
Camacho (2014)	5

ROAD SEGMENT: 31.2

Road:	CV-820	
Initial station:	11+000	Free
Final station:	12+320	Roundabout
		Constrained

AADT:	4476 vpd
Length:	1321 m

OPERATIONAL CHARACTERISTICS

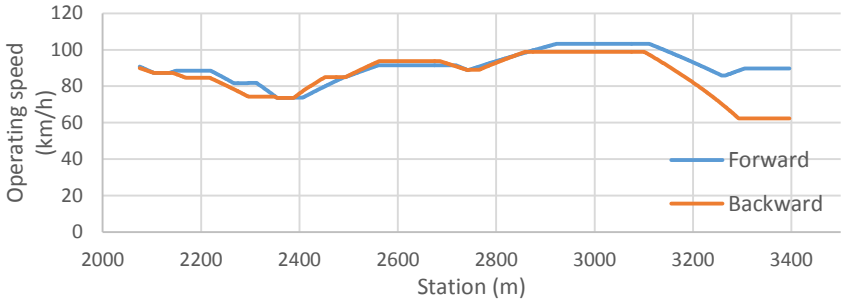

CCR	89.24508 gon/km	$\overline{\Delta v_{85}}$	8.6081775 km/h
$\bar{v}_{85}$	88.53569 km/h	d_{85}	0.9140896 m/s^2
$\sigma_{v_{85}}$	9.956931 km/h	$\sigma_{\Delta v_{85}}$	4.644545 km/h
R_a	2.125001 km/h	$\sigma_{d_{85}}$	0.1450943 m/s^2
$E_{a,10}$	1.493091 km/h	$\bar{L}_{\Delta v_{85}}$	64.75 m
$E_{a,20}$	0.349742 km/h	L_d	19.61%
L_{10}	0.370174 m	N	8
L_{20}	0.049205 m		

CONSISTENCY

Polus (2004)	0.54803
Garach (2013)	0.83517
Camacho (2014	2.99646

CRASHES

Observed:	4
Estimated:	
Exposure	4
Polus (2004)	9
Camacho (2009)	6
Garach (2013)	14
Camacho (2014)	3

ROAD SEGMENT: 30.2

Road:	CV-15	
Initial station:	2+230	Free
Final station:	6+010	Free
		Free

AADT:	5328	vpd
Length:	3773	m

OPERATIONAL CHARACTERISTICS

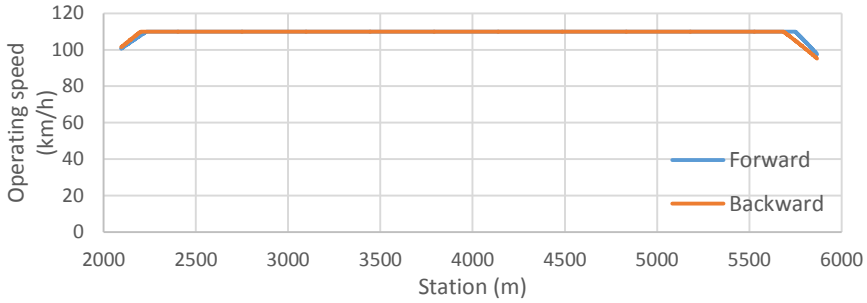

CCR	0.023733	gon/km	$\overline{\Delta v_{85}}$	10.507045	km/h
$\bar{v}_{85}$	109.5805	km/h	d_{85}	0.7453519	m/s^2
$\sigma_{v_{85}}$	1.796311	km/h	$\sigma_{\Delta v_{85}}$	2.7357271	km/h
R_a	0.215955	km/h	$\sigma_{d_{85}}$	0.1298977	m/s^2
$E_{a,10}$	0.031109	km/h	$\bar{L}_{\Delta v_{85}}$	113	m
$E_{a,20}$	0	km/h	L_d	2.99%	
L_{10}	0.009409	m	N	2	
L_{20}	0	m			

CONSISTENCY

Polus (2004)	2.72513
Garach (2013)	2.67969
Camacho (2014	3.44368

CRASHES

Observed:	10
Estimated:	
Exposure	11
Polus (2004)	14
Camacho (2009)	11
Garach (2013)	27
Camacho (2014)	11

ROAD SEGMENT: 32.1

Road:	CV-20	
Initial station:	12+200	Town
Final station:	15+340	Free
		Constrained

AADT:	4541 vpd
Length:	3138 m

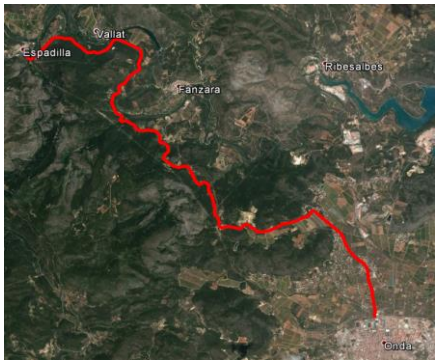

OPERATIONAL CHARACTERISTICS

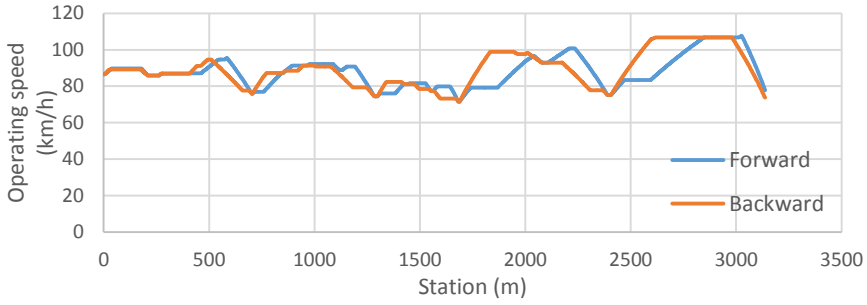

CCR	93.98131 gon/km	$\overline{\Delta v_{85}}$	11.003083 km/h
$\bar{v}_{85}$	88.66492 km/h	d_{85}	1.0097534 m/s^2
$\sigma_{v_{85}}$	9.060529 km/h	$\sigma_{\Delta v_{85}}$	10.603052 km/h
R_a	2.005748 km/h	$\sigma_{d_{85}}$	0.284156 m/s^2
$E_{a,10}$	1.185254 km/h	$\bar{L}_{\Delta v_{85}}$	65.473684 m
$E_{a,20}$	0 km/h	L_d	19.83%
L_{10}	0.300606 m	N	19
L_{20}	0 m		

CONSISTENCY

Polus (2004)	0.69011
Garach (2013)	0.99404
Camacho (2014	2.90009

CRASHES

Observed:	14
Estimated:	
Exposure	8
Polus (2004)	21
Camacho (2009)	15
Garach (2013)	27
Camacho (2014)	10

ROAD SEGMENT: 32.2

Road:	CV-20	
Initial station:	15+340	Free
Final station:	27+070	Town
		Constrained

AADT:	749 vpd
Length:	11659 m

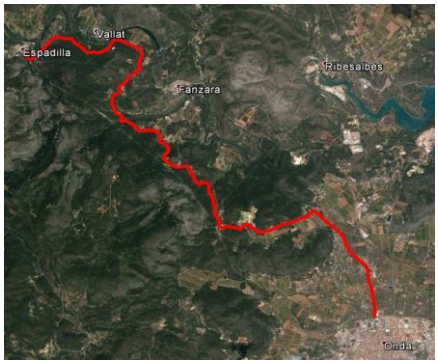

OPERATIONAL CHARACTERISTICS

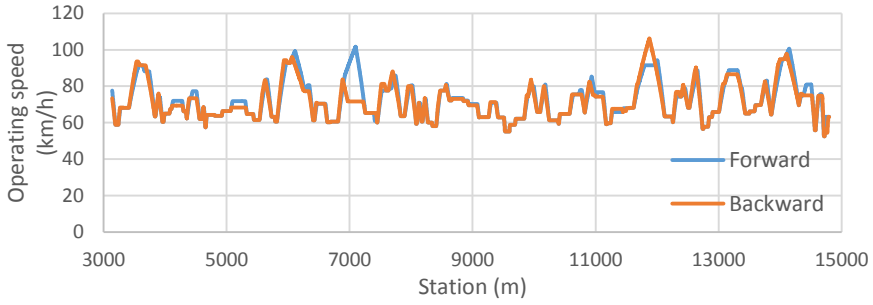

CCR	367.6244 gon/km	$\overline{\Delta v_{85}}$	11.834881 km/h
$\bar{v}_{85}$	72.18654 km/h	d_{85}	1.5593326 m/s^2
$\sigma_{v_{85}}$	9.903686 km/h	$\sigma_{\Delta v_{85}}$	8.6996947 km/h
R_a	2.198525 km/h	$\sigma_{d_{85}}$	0.3878977 m/s^2
$E_{a,10}$	1.247758 km/h	$\bar{L}_{\Delta v_{85}}$	44.636364 m
$E_{a,20}$	0.338711 km/h	L_d	18.95%
L_{10}	0.292263 m	N	99
L_{20}	0.05142 m		

CONSISTENCY

Polus (2004)	0.52261
Garach (2013)	0.79989
Camacho (2014	2.34282

CRASHES

Observed:	34
Estimated:	
Exposure	12
Polus (2004)	14
Camacho (2009)	10
Garach (2013)	12
Camacho (2014)	15

ROAD SEGMENT: 33.1

Road:	CV-50	
Initial station:	50+740	Town
Final station:	53+400	Free
		Constrained

AADT:	1296 vpd
Length:	2557 m

OPERATIONAL CHARACTERISTICS

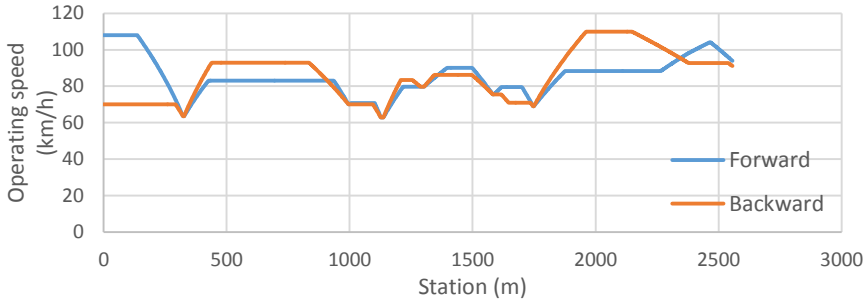

CCR	70.29041 gon/km	$\overline{\Delta v_{85}}$	19.817924 km/h
$\bar{v}_{85}$	85.56878 km/h	d_{85}	1.3286679 m/s^2
$\sigma_{v_{85}}$	11.66639 km/h	$\sigma_{\Delta v_{85}}$	13.770339 km/h
R_a	2.618912 km/h	$\sigma_{d_{85}}$	0.2703873 m/s^2
$E_{a,10}$	1.871593 km/h	$\bar{L}_{\Delta v_{85}}$	93 m
$E_{a,20}$	0.655248 km/h	L_d	18.19%
L_{10}	0.400235 m	N	10
L_{20}	0.103091 m		

CONSISTENCY

Polus (2004)	0.26529
Garach (2013)	0.40081
Camacho (2014	2.61536

CRASHES

Observed:	5
Estimated:	
Exposure	3
Polus (2004)	6
Camacho (2009)	4
Garach (2013)	7
Camacho (2014)	3

ROAD SEGMENT: 33.2

Road:	CV-50	
Initial station:	53+400	Free
Final station:	55+200	Free
		Free

AADT:	1296	vpd
Length:	1728	m

OPERATIONAL CHARACTERISTICS

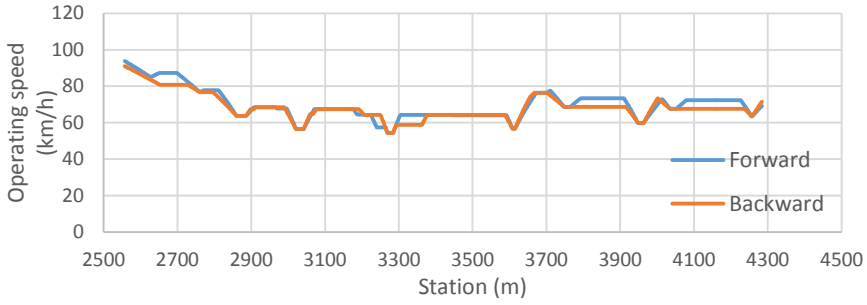

CCR	353.6489	gon/km	$\overline{\Delta v_{85}}$	8.0036393	km/h
$\bar{v}_{85}$	69.04241	km/h	d_{85}	1.6991574	m/s^2
$\sigma_{v_{85}}$	7.508165	km/h	$\sigma_{\Delta v_{85}}$	4.6245051	km/h
R_a	1.56186	km/h	$\sigma_{d_{85}}$	0.4171935	m/s^2
$E_{a,10}$	0.735921	km/h	$\bar{L}_{\Delta v_{85}}$	26.809524	m
$E_{a,20}$	0.104236	km/h	L_d	16.30%	
L_{10}	0.184424	m	N	21	
L_{20}	0.017082	m			

CONSISTENCY

Polus (2004)	1.13532
Garach (2013)	1.40563
Camacho (2014	2.24316

CRASHES

Observed:	4
Estimated:	
Exposure	2
Polus (2004)	3
Camacho (2009)	2
Garach (2013)	4
Camacho (2014)	2

ROAD SEGMENT: 33.3

Road:	CV-50	
Initial station:	55+200	Free
Final station:	57+300	Free
		Free

AADT:	1296	vpd
Length:	2038	m

OPERATIONAL CHARACTERISTICS

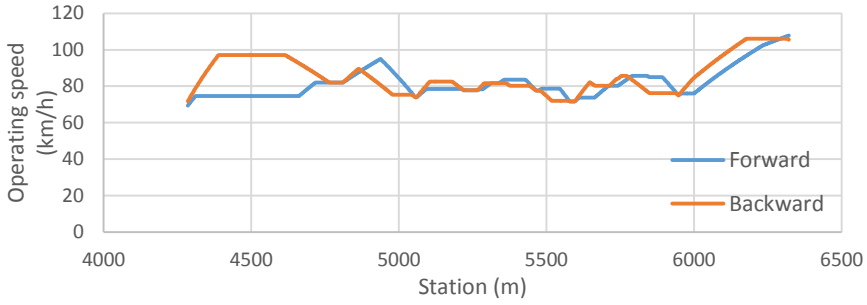

CCR	123.3162	gon/km
$\bar{v}_{85}$	83.78217	km/h
$\sigma_{v_{85}}$	9.122185	km/h
R_a	2.013383	km/h
$E_{a,10}$	0.984113	km/h
$E_{a,20}$	0.3529	km/h
L_{10}	0.231959	m
L_{20}	0.057437	m

$\overline{\Delta v_{85}}$	11.401924	km/h
d_{85}	1.1065708	m/s^2
$\sigma_{\Delta v_{85}}$	9.3260204	km/h
$\sigma_{d_{85}}$	0.1916777	m/s^2
$\bar{L}_{\Delta v_{85}}$	65.666667	m
L_d	19.34%	
N	12	

CONSISTENCY

Polus (2004)	0.67989
Garach (2013)	0.98338
Camacho (2014	2.7603

CRASHES

Observed:	0
Estimated:	
Exposure	2
Polus (2004)	4
Camacho (2009)	3
Garach (2013)	5
Camacho (2014)	2

ROAD SEGMENT: 33.4

Road:	CV-50	
Initial station:	57+300	Free
Final station:	61+400	Free
		Free

AADT:	1296	vpd
Length:	3023	m

OPERATIONAL CHARACTERISTICS

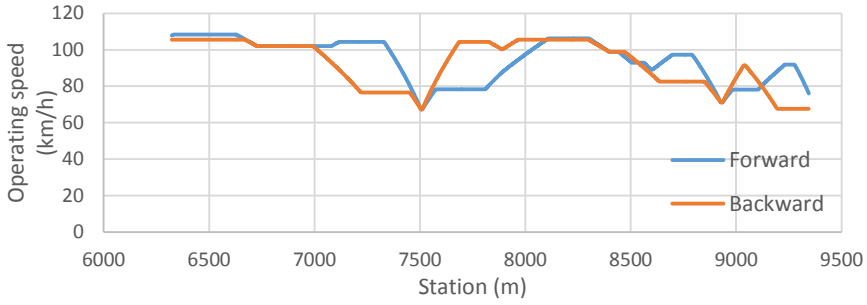

CCR	50.80135	gon/km	$\overline{\Delta v_{85}}$	16.557573	km/h
$\bar{v}_{85}$	93.47977	km/h	d_{85}	0.9965167	m/s^2
$\sigma_{v_{85}}$	12.23569	km/h	$\sigma_{\Delta v_{85}}$	13.059416	km/h
R_a	3.027631	km/h	$\sigma_{d_{85}}$	0.3981329	m/s^2
$E_{a,10}$	2.365378	km/h	$\bar{L}_{\Delta v_{85}}$	102.9	m
$E_{a,20}$	0.41895	km/h	L_d	17.03%	
L_{10}	0.590007	m	N	10	
L_{20}	0.062872	m			

CONSISTENCY

Polus (2004)	0.1607
Garach (2013)	0.13457
Camacho (2014	2.96467

CRASHES

Observed:	4
Estimated:	
Exposure	3
Polus (2004)	7
Camacho (2009)	5
Garach (2013)	8
Camacho (2014)	3

ROAD SEGMENT: 33.5

Road:	CV-50	
Initial station:	61+400	Free
Final station:	62+000	Free
		Free

AADT:	3573 vpd
Length:	567 m

OPERATIONAL CHARACTERISTICS

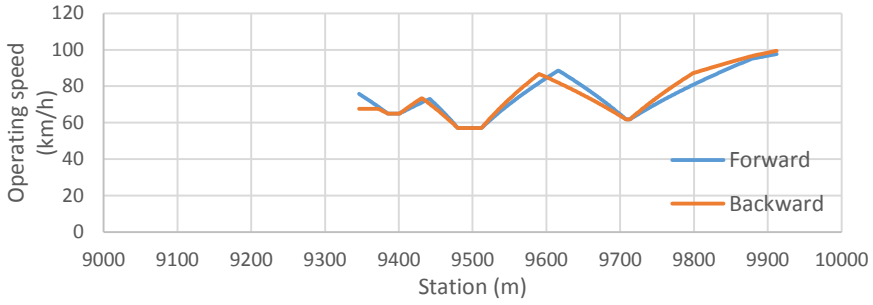

CCR	335.7643 gon/km	$\overline{\Delta v_{85}}$	21.590297 km/h
$\bar{v}_{85}$	75.1231 km/h	d_{85}	1.6861519 m/s^2
$\sigma_{v_{85}}$	11.44322 km/h	$\sigma_{\Delta v_{85}}$	11.577169 km/h
R_a	2.696533 km/h	$\sigma_{d_{85}}$	0.3704904 m/s^2
$E_{a,10}$	1.864496 km/h	$\bar{L}_{\Delta v_{85}}$	79.333333 m
$E_{a,20}$	0.434717 km/h	L_d	42.05%
L_{10}	0.434629 m	N	6
L_{20}	0.071555 m		

CONSISTENCY

Polus (2004)	0.25914
Garach (2013)	0.37845
Camacho (2014	2.31308

CRASHES

Observed:	0
Estimated:	
Exposure	2
Polus (2004)	4
Camacho (2009)	2
Garach (2013)	6
Camacho (2014)	2

ROAD SEGMENT: 33.6

Road:	CV-50	
Initial station:	62+000	Free
Final station:	71+500	Free
		Free

AADT:	3865 vpd
Length:	10478 m

OPERATIONAL CHARACTERISTICS

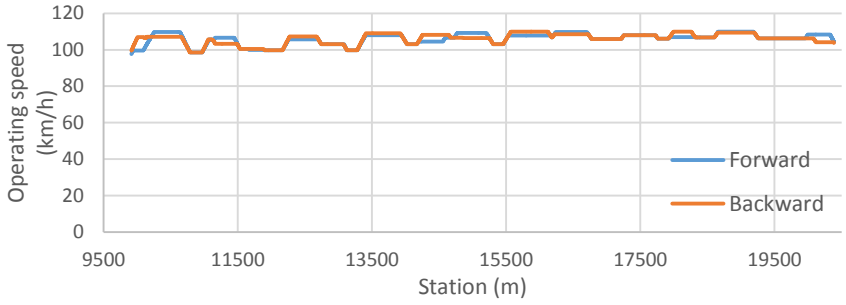

CCR	33.53153 gon/km	$\overline{\Delta v_{85}}$	5.1096715 km/h
$\bar{v}_{85}$	106.1001 km/h	d_{85}	0.5028312 m/s^2
$\sigma_{v_{85}}$	3.030944 km/h	$\sigma_{\Delta v_{85}}$	2.5968384 km/h
R_a	0.657313 km/h	$\sigma_{d_{85}}$	0.075977 m/s^2
$E_{a,10}$	0 km/h	$\bar{L}_{\Delta v_{85}}$	79.75 m
$E_{a,20}$	0 km/h	L_d	7.61%
L_{10}	0 m	N	20
L_{20}	0 m		

CONSISTENCY

Polus (2004)	2.40759
Garach (2013)	2.34945
Camacho (2014	3.88446

CRASHES

Observed:	14
Estimated:	
Exposure	17
Polus (2004)	33
Camacho (2009)	24
Garach (2013)	47
Camacho (2014)	16

ROAD SEGMENT: 33.7

Road:	CV-50	
Initial station:	71+500	Free
Final station:	74+510	Roundabout
		Constrained

AADT:	4722	vpd
Length:	2465	m

OPERATIONAL CHARACTERISTICS

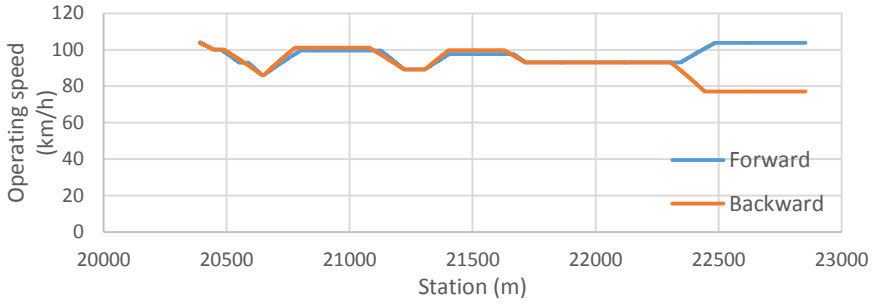

CCR	71.77201	gon/km	$\overline{\Delta v_{85}}$	8.3511898	km/h
$\bar{v}_{85}$	94.34196	km/h	d_{85}	0.7540358	m/s^2
$\sigma_{v_{85}}$	6.922731	km/h	$\sigma_{\Delta v_{85}}$	3.844488	km/h
R_a	1.440666	km/h	$\sigma_{d_{85}}$	0.0999183	m/s^2
$E_{a,10}$	0.443903	km/h	$\bar{L}_{\Delta v_{85}}$	79	m
$E_{a,20}$	0	km/h	L_d	11.23%	
L_{10}	0.095412	m	N	7	
L_{20}	0	m			

CONSISTENCY

Polus (2004)	1.29993
Garach (2013)	1.53486
Camacho (2014	3.2634

CRASHES

Observed:	7
Estimated:	
Exposure	7
Polus (2004)	14
Camacho (2009)	10
Garach (2013)	21
Camacho (2014)	6

ROAD SEGMENT: 34.1

Road:	CV-805	
Initial station:	2+070	Interchange
Final station:	4+560	Free
		Constrained

AADT:	2903	vpd
Length:	2489	m

OPERATIONAL CHARACTERISTICS

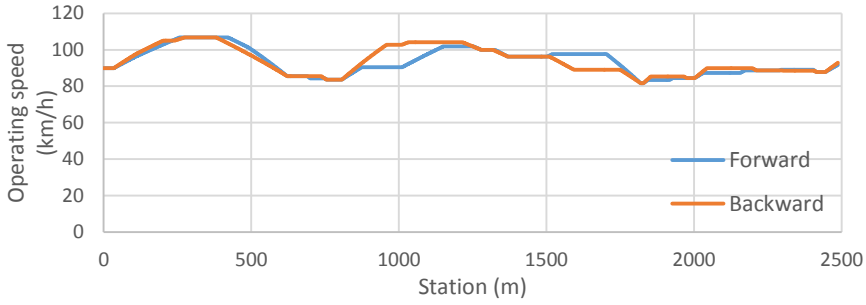

CCR	89.61091	gon/km	$\overline{\Delta v_{85}}$	7.4670655	km/h
$\bar{v}_{85}$	93.66643	km/h	d_{85}	0.7435769	m/s^2
$\sigma_{v_{85}}$	7.229665	km/h	$\sigma_{\Delta v_{85}}$	7.5124031	km/h
R_a	1.77958	km/h	$\sigma_{d_{85}}$	0.1705037	m/s^2
$E_{a,10}$	0.605118	km/h	$\bar{L}_{\Delta v_{85}}$	68.846154	m
$E_{a,20}$	0	km/h	L_d	17.99%	
L_{10}	0.189309	m	N	13	
L_{20}	0	m			

CONSISTENCY

Polus (2004)	1.03972
Garach (2013)	1.3118
Camacho (2014	3.27078

CRASHES

Observed:	2
Estimated:	
Exposure	5
Polus (2004)	9
Camacho (2009)	7
Garach (2013)	13
Camacho (2014)	4

ROAD SEGMENT: 34.2

Road:	CV-805	
Initial station:	4+560	Free
Final station:	8+250	Free
		Free

AADT:	2903	vpd
Length:	3692	m

OPERATIONAL CHARACTERISTICS

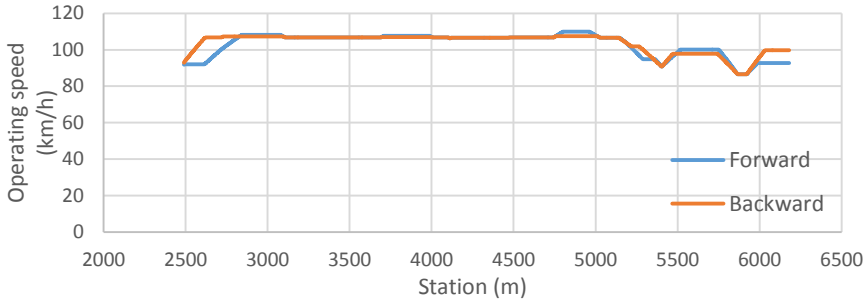

CCR	32.50073	gon/km	$\overline{\Delta v_{85}}$	8.491223	km/h
$\bar{v}_{85}$	103.4186	km/h	d_{85}	0.6830103	m/s^2
$\sigma_{v_{85}}$	5.846467	km/h	$\sigma_{\Delta v_{85}}$	5.1532621	km/h
R_a	1.36945	km/h	$\sigma_{d_{85}}$	0.1742201	m/s^2
$E_{a,10}$	0.38848	km/h	$\bar{L}_{\Delta v_{85}}$	87.875	m
$E_{a,20}$	0	km/h	L_d	9.52%	
L_{10}	0.111081	m	N	8	
L_{20}	0	m			

CONSISTENCY

Polus (2004)	1.51316
Garach (2013)	1.68745
Camacho (2014	3.47768

CRASHES

Observed:	5
Estimated:	
Exposure	6
Polus (2004)	12
Camacho (2009)	8
Garach (2013)	17
Camacho (2014)	6

ROAD SEGMENT: 34.3

Road:	CV-805	
Initial station:	8+250	Free
Final station:	13+090	Interchange
		Constrained

AADT:	2903 vpd
Length:	4651 m

OPERATIONAL CHARACTERISTICS

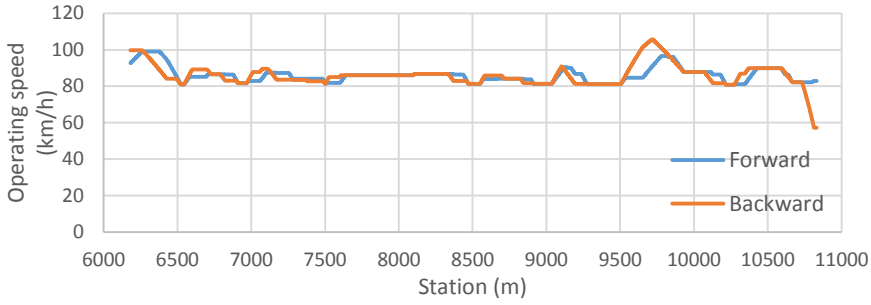

CCR	168.0057 gon/km	$\overline{\Delta v_{85}}$	6.204458 km/h
$\bar{v}_{85}$	86.03885 km/h	d_{85}	0.9017912 m/s^2
$\sigma_{v_{85}}$	5.115957 km/h	$\sigma_{\Delta v_{85}}$	5.4399586 km/h
R_a	0.954663 km/h	$\sigma_{d_{85}}$	0.0614182 m/s^2
$E_{a,10}$	0.29829 km/h	$\bar{L}_{\Delta v_{85}}$	47 m
$E_{a,20}$	0.035255 km/h	L_d	11.12%
L_{10}	0.075468 m	N	22
L_{20}	0.004838 m		

CONSISTENCY

Polus (2004)	1.92575
Garach (2013)	1.98589
Camacho (2014	2.98146

CRASHES

Observed:	5
Estimated:	
Exposure	10
Polus (2004)	13
Camacho (2009)	9
Garach (2013)	19
Camacho (2014)	10

ROAD SEGMENT: 35.1

Road:	CV-10	
Initial station:	48+230	Roundabout
Final station:	65+320	Free
		Constrained

AADT:	5013	vpd
Length:	17085	m

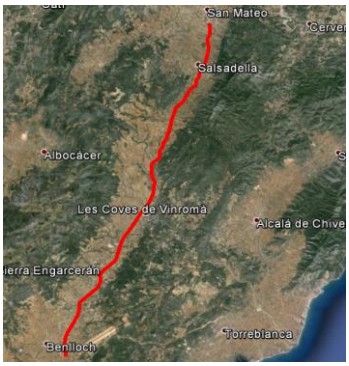

OPERATIONAL CHARACTERISTICS

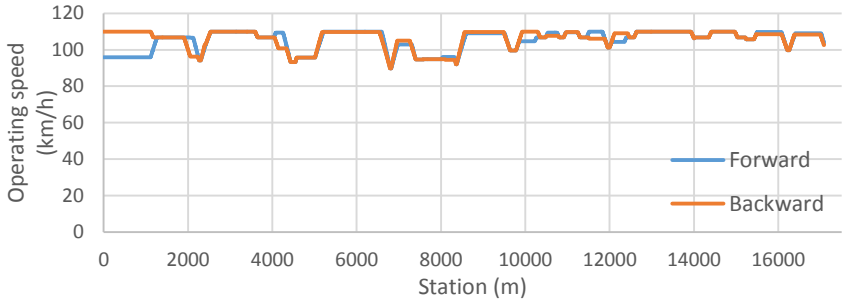

CCR	26.44752	gon/km	$\overline{\Delta v_{85}}$	7.7147863	km/h
$\bar{v}_{85}$	105.7682	km/h	d_{85}	0.5667713	m/s^2
$\sigma_{v_{85}}$	5.294206	km/h	$\sigma_{\Delta v_{85}}$	5.2893861	km/h
R_a	1.183921	km/h	$\sigma_{d_{85}}$	0.1314862	m/s^2
$E_{a,10}$	0.314142	km/h	$\bar{L}_{\Delta v_{85}}$	100.85714	m
$E_{a,20}$	0	km/h	L_d	8.27%	
L_{10}	0.10103	m	N	28	
L_{20}	0	m			

CONSISTENCY

Polus (2004)	1.73057
Garach (2013)	1.84626
Camacho (2014	3.72862

CRASHES

Observed:	41
Estimated:	
Exposure	49
Polus (2004)	88
Camacho (2009)	63
Garach (2013)	103
Camacho (2014)	45

ROAD SEGMENT: 35.2

Road:	CV-10	
Initial station:	65+320	Free
Final station:	69+570	Free
		Free

AADT:	3955	vpd
Length:	4256	m

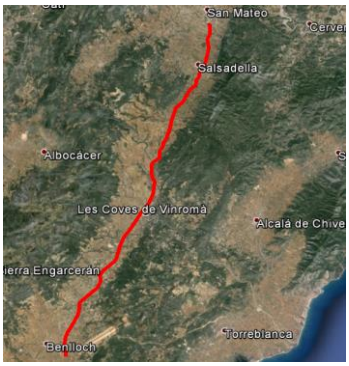

OPERATIONAL CHARACTERISTICS

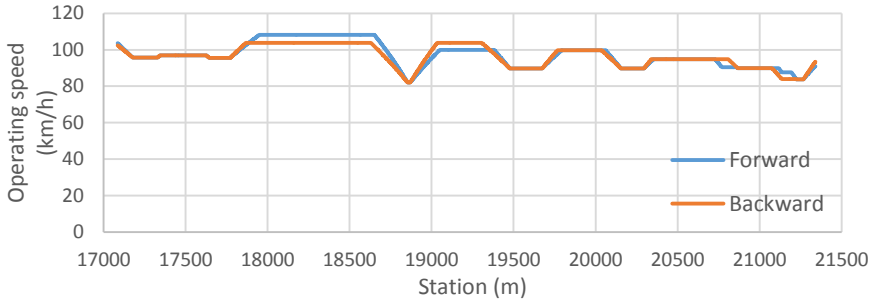

CCR	89.3544	gon/km	$\overline{\Delta v_{85}}$	8.7381017	km/h
$\bar{v}_{85}$	96.62889	km/h	d_{85}	0.7846096	m/s^2
$\sigma_{v_{85}}$	6.342503	km/h	$\sigma_{\Delta v_{85}}$	7.2749277	km/h
R_a	1.430609	km/h	$\sigma_{d_{85}}$	0.1077374	m/s^2
$E_{a,10}$	0.461439	km/h	$\bar{L}_{\Delta v_{85}}$	77.071429	m
$E_{a,20}$	0	km/h	L_d	12.68%	
L_{10}	0.139953	m	N	14	
L_{20}	0	m			

CONSISTENCY

Polus (2004)	1.39345
Garach (2013)	1.60184
Camacho (2014	3.24626

CRASHES

Observed:	9
Estimated:	
Exposure	9
Polus (2004)	19
Camacho (2009)	14
Garach (2013)	27
Camacho (2014)	10

ROAD SEGMENT: 35.3

Road:	CV-10	
Initial station:	69+570	Free
Final station:	80+510	Roundabout
		Constrained

AADT:	2810	vpd
Length:	10823	m

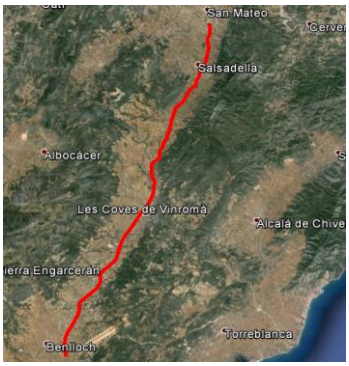

OPERATIONAL CHARACTERISTICS

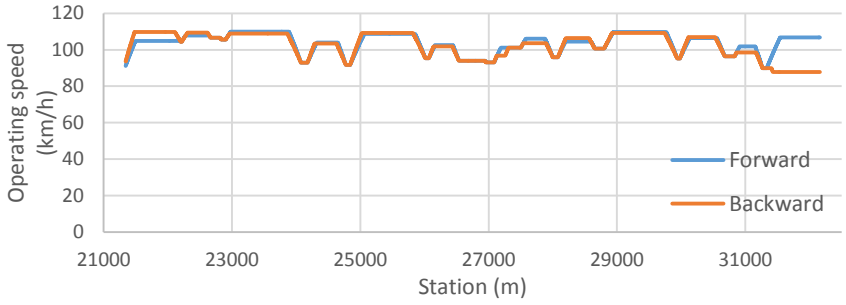

CCR	35.74704	gon/km	$\overline{\Delta v_{85}}$	8.9691283	km/h
$\bar{v}_{85}$	103.1757	km/h	d_{85}	0.6447996	m/s^2
$\sigma_{v_{85}}$	6.123704	km/h	$\sigma_{\Delta v_{85}}$	5.0313114	km/h
R_a	1.415936	km/h	$\sigma_{d_{85}}$	0.115363	m/s^2
$E_{a,10}$	0.293729	km/h	$\bar{L}_{\Delta v_{85}}$	103.65217	m
$E_{a,20}$	0	km/h	L_d	11.01%	
L_{10}	0.081586	m	N	23	
L_{20}	0	m			

CONSISTENCY

Polus (2004)	1.43749
Garach (2013)	1.63284
Camacho (2014	3.54228

CRASHES

Observed:	15
Estimated:	
Exposure	23
Polus (2004)	35
Camacho (2009)	25
Garach (2013)	40
Camacho (2014)	19

ROAD SEGMENT: 36.1

Road:	CV-15	
Initial station:	9+630	Roundabout
Final station:	12+520	Free
		Constrained

AADT:	4754	vpd
Length:	2890	m

OPERATIONAL CHARACTERISTICS

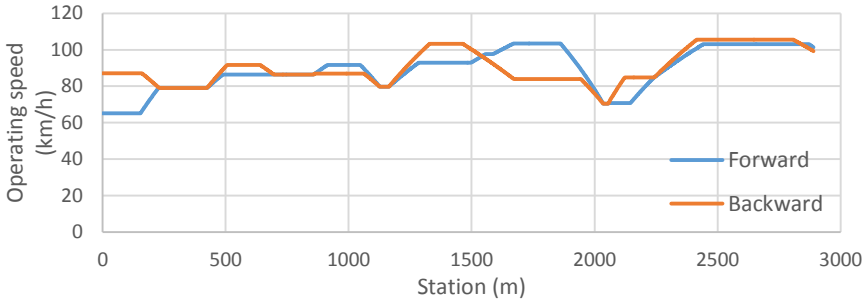

CCR	95.57808	gon/km	$\overline{\Delta v_{85}}$	16.91185	km/h
$\bar{v}_{85}$	89.79411	km/h	d_{85}	1.0245492	m/s^2
$\sigma_{v_{85}}$	10.3756	km/h	$\sigma_{\Delta v_{85}}$	10.001288	km/h
R_a	2.382127	km/h	$\sigma_{d_{85}}$	0.1953384	m/s^2
$E_{a,10}$	1.737282	km/h	$\bar{L}_{\Delta v_{85}}$	109	m
$E_{a,20}$	0.206634	km/h	L_d	13.20%	
L_{10}	0.437024	m	N	7	
L_{20}	0.030623	m			

CONSISTENCY

Polus (2004)	0.41638
Garach (2013)	0.65074
Camacho (2014	2.89826

CRASHES

Observed:	4
Estimated:	
Exposure	8
Polus (2004)	23
Camacho (2009)	16
Garach (2013)	29
Camacho (2014)	9

ROAD SEGMENT: 36.2

Road:	CV-15	
Initial station:	12+520	Free
Final station:	15+550	Town
		Constrained

AADT:	3333	vpd
Length:	3021	m

OPERATIONAL CHARACTERISTICS

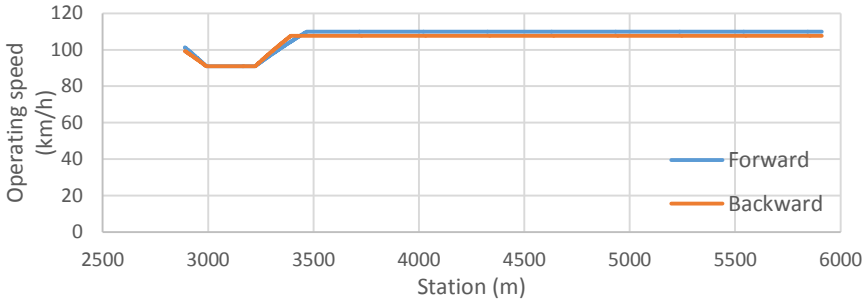

CCR	22.14957	gon/km	$\overline{\Delta v_{85}}$	13.449215	km/h
$\bar{v}_{85}$	106.4173	km/h	d_{85}	0.7546929	m/s^2
$\sigma_{v_{85}}$	5.699826	km/h	$\sigma_{\Delta v_{85}}$	4.4745924	km/h
R_a	1.098004	km/h	$\sigma_{d_{85}}$	0.0015582	m/s^2
$E_{a,10}$	0.4644	km/h	$\bar{L}_{\Delta v_{85}}$	135	m
$E_{a,20}$	0	km/h	L_d	4.47%	
L_{10}	0.115525	m	N	2	
L_{20}	0	m			

CONSISTENCY

Polus (2004)	1.73184
Garach (2013)	1.8494
Camacho (2014	3.3961

CRASHES

Observed:	7
Estimated:	
Exposure	7
Polus (2004)	10
Camacho (2009)	7
Garach (2013)	16
Camacho (2014)	5

ROAD SEGMENT: 37.1

Road:	CV-18	
Initial station:	1+220	Roundabout
Final station:	2+310	Roundabout
		Constrained

AADT:	25015 vpd
Length:	1089 m

OPERATIONAL CHARACTERISTICS

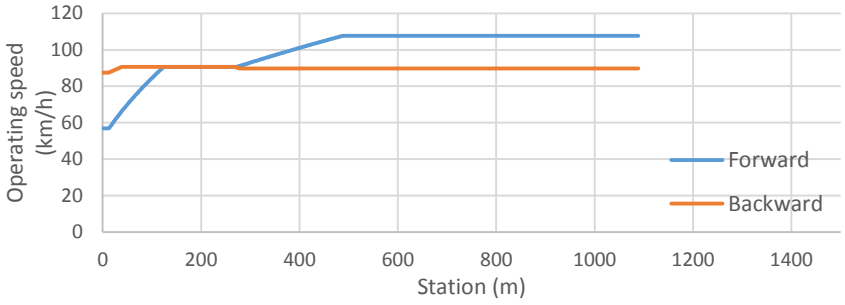

CCR	47.87882 gon/km	$\overline{\Delta v_{85}}$	3.0137114 km/h
$\bar{v}_{85}$	94.79349 km/h	d_{85}	0.7963576 m/s^2
$\sigma_{v_{85}}$	9.838051 km/h	$\sigma_{\Delta v_{85}}$	0 km/h
R_a	2.244408 km/h	$\sigma_{d_{85}}$	0 m/s^2
$E_{a,10}$	1.364347 km/h	$\bar{L}_{\Delta v_{85}}$	26 m
$E_{a,20}$	0.256591 km/h	L_d	1.19%
L_{10}	0.34068 m	N	1
L_{20}	0.030303 m		

CONSISTENCY

Polus (2004)	0.51036
Garach (2013)	0.78066
Camacho (2014	3.20964

CRASHES

Observed:	8
Estimated:	
Exposure	7
Polus (2004)	43
Camacho (2009)	30
Garach (2013)	74
Camacho (2014)	9

ROAD SEGMENT: 38.1

Road:	CV-50	
Initial station:	33+890	Town
Final station:	39+660	Roundabout
		Constrained

AADT:	5243 vpd
Length:	5750 m

OPERATIONAL CHARACTERISTICS

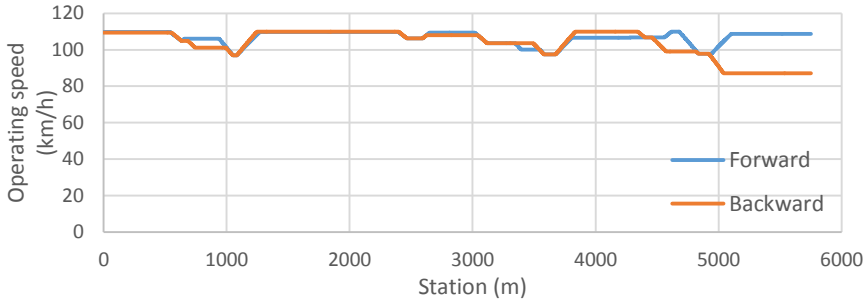

CCR	21.89505 gon/km	$\overline{\Delta v_{85}}$	6.9253456 km/h
$\bar{v}_{85}$	105.2565 km/h	d_{85}	0.5441883 m/s^2
$\sigma_{v_{85}}$	6.132246 km/h	$\sigma_{\Delta v_{85}}$	4.4085361 km/h
R_a	1.293561 km/h	$\sigma_{d_{85}}$	0.0967904 m/s^2
$E_{a,10}$	0.34172 km/h	$\bar{L}_{\Delta v_{85}}$	97.9 m
$E_{a,20}$	0 km/h	L_d	8.51%
L_{10}	0.069478 m	N	10
L_{20}	0 m		

CONSISTENCY

Polus (2004)	1.52183
Garach (2013)	1.69913
Camacho (2014	3.7734

CRASHES

Observed:	13
Estimated:	
Exposure	17
Polus (2004)	33
Camacho (2009)	24
Garach (2013)	46
Camacho (2014)	13

ROAD SEGMENT: 39.1

Road:	CV-720	
Initial station:	2+500	Town
Final station:	8+780	Town
		Constrained

AADT:	363 vpd
Length:	6311 m

OPERATIONAL CHARACTERISTICS

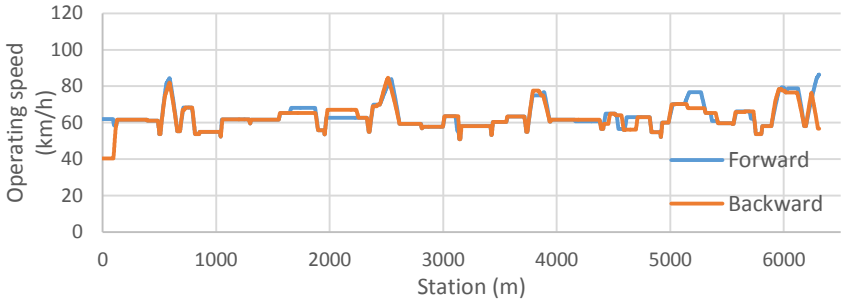

CCR	480.1772 gon/km	$\overline{\Delta v_{85}}$	8.8586974 km/h
$\bar{v}_{85}$	63.16019 km/h	d_{85}	2.1141398 m/s^2
$\sigma_{v_{85}}$	6.516398 km/h	$\sigma_{\Delta v_{85}}$	7.1562655 km/h
R_a	1.31676 km/h	$\sigma_{d_{85}}$	0.4701735 m/s^2
$E_{a,10}$	0.455309 km/h	$\bar{L}_{\Delta v_{85}}$	21.555556 m
$E_{a,20}$	0.0828 km/h	L_d	9.22%
L_{10}	0.109254 m	N	54
L_{20}	0.013469 m		

CONSISTENCY

Polus (2004)	1.44754
Garach (2013)	1.64565
Camacho (2014	2.02458

CRASHES

Observed:	2
Estimated:	
Exposure	4
Polus (2004)	3
Camacho (2009)	2
Garach (2013)	3
Camacho (2014)	5

ROAD SEGMENT: 40.1

Road:	CV-806	
Initial station:	0+790	Town
Final station:	6+680	Roundabout
		Constrained

AADT:	5390 vpd
Length:	5826 m

OPERATIONAL CHARACTERISTICS

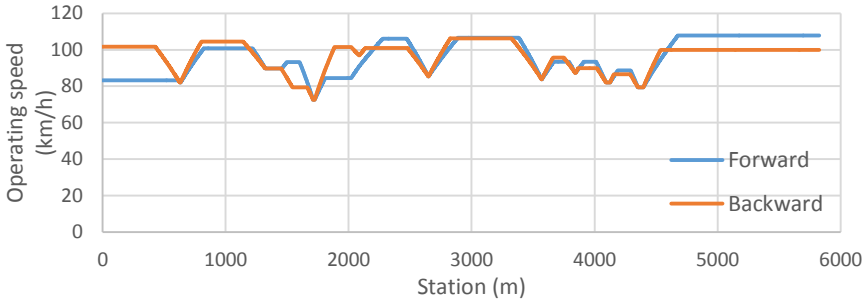

CCR	32.59183 gon/km	$\overline{\Delta v_{85}}$	13.725136 km/h
$\bar{v}_{85}$	96.29608 km/h	d_{85}	0.923298 m/s^2
$\sigma_{v_{85}}$	8.815067 km/h	$\sigma_{\Delta v_{85}}$	8.681212 km/h
R_a	2.133405 km/h	$\sigma_{d_{85}}$	0.1414793 m/s^2
$E_{a,10}$	1.134679 km/h	$\bar{L}_{\Delta v_{85}}$	101.625 m
$E_{a,20}$	0.059468 km/h	L_d	13.95%
L_{10}	0.32149 m	N	16
L_{20}	0.009612 m		

CONSISTENCY

Polus (2004)	0.65719
Garach (2013)	0.94567
Camacho (2014	3.07129

CRASHES

Observed:	9
Estimated:	
Exposure	17
Polus (2004)	47
Camacho (2009)	33
Garach (2013)	55
Camacho (2014)	21

ROAD SEGMENT: 41.1

Road:	CV-840	
Initial station:	14+550	Roundabout
Final station:	20+590	Interchange
		Constrained

AADT:	3129	vpd
Length:	6032	m

OPERATIONAL CHARACTERISTICS

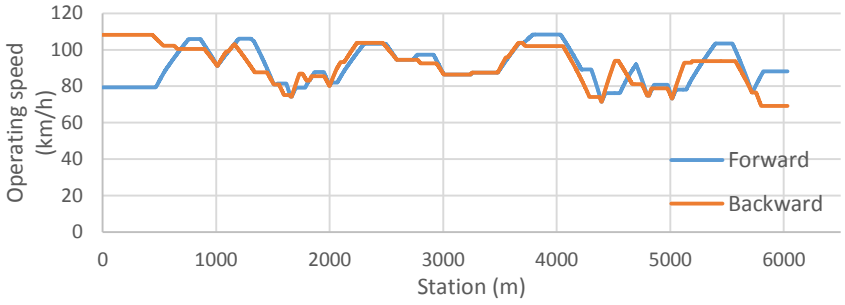

CCR	68.29738	gon/km	$\overline{\Delta v_{85}}$	11.987023	km/h
$\bar{v}_{85}$	91.26933	km/h	d_{85}	0.9360019	m/s^2
$\sigma_{v_{85}}$	10.16272	km/h	$\sigma_{\Delta v_{85}}$	7.0930015	km/h
R_a	2.412175	km/h	$\sigma_{d_{85}}$	0.2024955	m/s^2
$E_{a,10}$	1.690817	km/h	$\bar{L}_{\Delta v_{85}}$	88.869565	m
$E_{a,20}$	0.123984	km/h	L_d	16.94%	
L_{10}	0.443302	m	N	23	
L_{20}	0.020225	m			

CONSISTENCY

Polus (2004)	0.42292
Garach (2013)	0.65393
Camacho (2014	3.00318

CRASHES

Observed:	18
Estimated:	
Exposure	13
Polus (2004)	31
Camacho (2009)	22
Garach (2013)	33
Camacho (2014)	15

ROAD SEGMENT: 42.1

Road:	CV-827	
Initial station:	0+180	Roundabout
Final station:	2+280	Free
		Constrained

AADT:	384 vpd
Length:	2097 m

OPERATIONAL CHARACTERISTICS

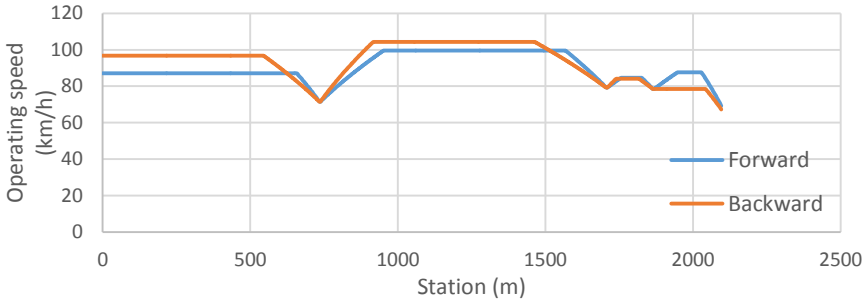

CCR	25.90329 gon/km	$\overline{\Delta v_{85}}$	16.439843 km/h
$\bar{v}_{85}$	91.51987 km/h	d_{85}	1.1910814 m/s^2
$\sigma_{v_{85}}$	9.019331 km/h	$\sigma_{\Delta v_{85}}$	10.278295 km/h
R_a	2.230117 km/h	$\sigma_{d_{85}}$	0.25519 m/s^2
$E_{a,10}$	1.114045 km/h	$\bar{L}_{\Delta v_{85}}$	89.166667 m
$E_{a,20}$	0.048534 km/h	L_d	12.76%
L_{10}	0.299618 m	N	6
L_{20}	0.008111 m		

CONSISTENCY

Polus (2004)	0.59405
Garach (2013)	0.86894
Camacho (2014	2.7739

CRASHES

Observed:	0
Estimated:	
Exposure	1
Polus (2004)	1
Camacho (2009)	1
Garach (2013)	1
Camacho (2014)	1

ROAD SEGMENT: 42.2

Road:	CV-827	
Initial station:	2+280	Free
Final station:	3+270	Free
		Free

AADT:	384 vpd
Length:	993 m

OPERATIONAL CHARACTERISTICS

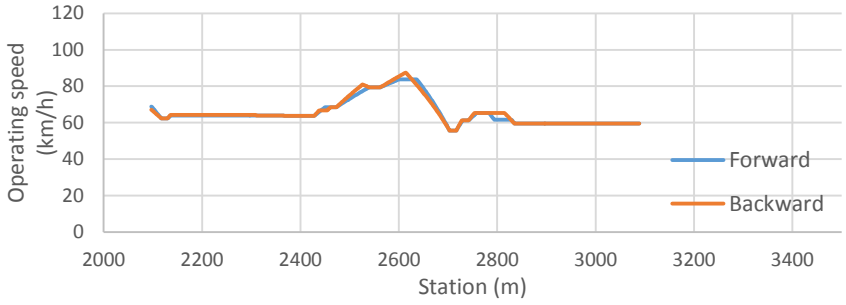

CCR	269.7145 gon/km	$\overline{\Delta v_{85}}$	7.0437321 km/h
$\bar{v}_{85}$	65.66419 km/h	d_{85}	1.629023 m/s^2
$\sigma_{v_{85}}$	7.303549 km/h	$\sigma_{\Delta v_{85}}$	7.6746307 km/h
R_a	1.514163 km/h	$\sigma_{d_{85}}$	0.3752152 m/s^2
$E_{a,10}$	0.630428 km/h	$\bar{L}_{\Delta v_{85}}$	23.181818 m
$E_{a,20}$	0.055594 km/h	L_d	12.85%
L_{10}	0.147177 m	N	11
L_{20}	0.009577 m		

CONSISTENCY

Polus (2004)	1.19541
Garach (2013)	1.45379
Camacho (2014	2.23717

CRASHES

Observed:	4
Estimated:	
Exposure	0
Polus (2004)	0
Camacho (2009)	0
Garach (2013)	1
Camacho (2014)	0

ROAD SEGMENT: 42.3

Road:	CV-827	
Initial station:	3+270	Free
Final station:	4+180	Free
		Free

AADT:	384 vpd
Length:	912 m

OPERATIONAL CHARACTERISTICS

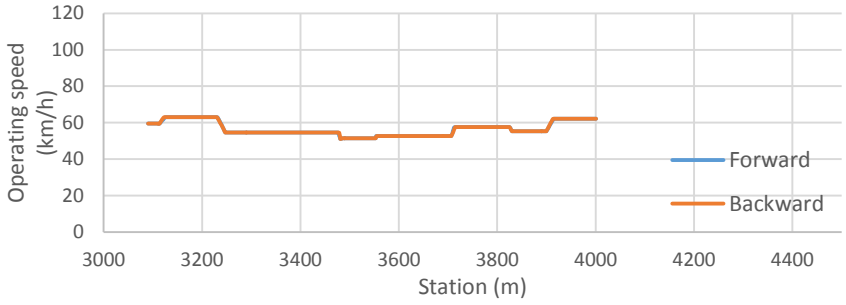

CCR	931.6279 gon/km	$\overline{\Delta v_{85}}$	4.4744872 km/h
$\bar{v}_{85}$	56.52496 km/h	d_{85}	2.3520873 m/s^2
$\sigma_{v_{85}}$	3.864323 km/h	$\sigma_{\Delta v_{85}}$	2.5437068 km/h
R_a	0.929708 km/h	$\sigma_{d_{85}}$	0.3574537 m/s^2
$E_{a,10}$	0 km/h	$\bar{L}_{\Delta v_{85}}$	8.5714286 m
$E_{a,20}$	0 km/h	L_d	3.29%
L_{10}	0 m	N	7
L_{20}	0 m		

CONSISTENCY

Polus (2004)	2.12769
Garach (2013)	2.12738
Camacho (2014	1.8829

CRASHES

Observed:	1
Estimated:	
Exposure	0
Polus (2004)	0
Camacho (2009)	0
Garach (2013)	1
Camacho (2014)	0

ROAD SEGMENT: 42.4

Road:	CV-827	
Initial station:	4+180	Free
Final station:	6+390	Free
		Free

AADT:	384 vpd
Length:	2206 m

OPERATIONAL CHARACTERISTICS

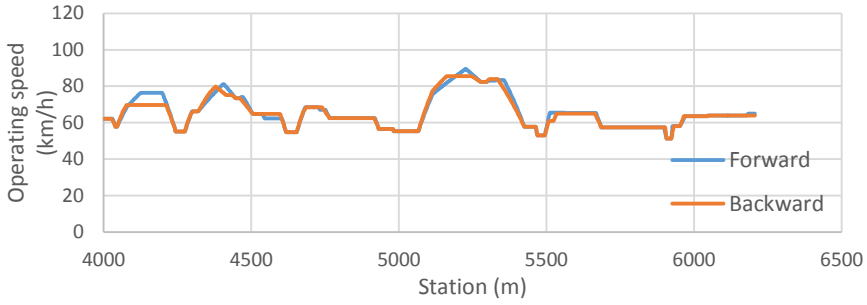

CCR	514.8906 gon/km	$\overline{\Delta v_{85}}$	8.9664527 km/h
$\bar{v}_{85}$	65.63368 km/h	d_{85}	1.887156 m/s^2
$\sigma_{v_{85}}$	8.705948 km/h	$\sigma_{\Delta v_{85}}$	7.2797073 km/h
R_a	1.88885 km/h	$\sigma_{d_{85}}$	0.5401799 m/s^2
$E_{a,10}$	1.025231 km/h	$\bar{L}_{\Delta v_{85}}$	25.92 m
$E_{a,20}$	0.084441 km/h	L_d	14.69%
L_{10}	0.260091 m	N	25
L_{20}	0.013832 m		

CONSISTENCY

Polus (2004)	0.78869
Garach (2013)	1.0966
Camacho (2014	2.1298

CRASHES

Observed:	3
Estimated:	
Exposure	1
Polus (2004)	1
Camacho (2009)	1
Garach (2013)	1
Camacho (2014)	1

ROAD SEGMENT: 42.5

Road:	CV-827	
Initial station:	6+390	Free
Final station:	9+890	Town
		Constrained

AADT:	384 vpd
Length:	3262 m

OPERATIONAL CHARACTERISTICS

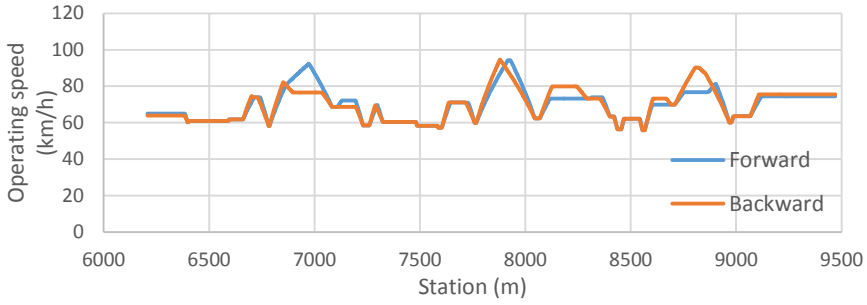

CCR	277.6558 gon/km	$\overline{\Delta v_{85}}$	13.825153 km/h
$\bar{v}_{85}$	69.81274 km/h	d_{85}	1.8006826 m/s^2
$\sigma_{v_{85}}$	8.359409 km/h	$\sigma_{\Delta v_{85}}$	8.874592 km/h
R_a	1.938556 km/h	$\sigma_{d_{85}}$	0.2529171 m/s^2
$E_{a,10}$	0.741374 km/h	$\bar{L}_{\Delta v_{85}}$	43.708333 m
$E_{a,20}$	0.151572 km/h	L_d	16.08%
L_{10}	0.188381 m	N	24
L_{20}	0.024831 m		

CONSISTENCY

Polus (2004)	0.80338
Garach (2013)	1.1044
Camacho (2014	2.20834

CRASHES

Observed:	4
Estimated:	
Exposure	2
Polus (2004)	2
Camacho (2009)	1
Garach (2013)	2
Camacho (2014)	2

ROAD SEGMENT: 43.1

Road:	CV-35	
Initial station:	68+340	Town
Final station:	70+950	Free
		Constrained

AADT:	1958	vpd
Length:	2589	m

OPERATIONAL CHARACTERISTICS

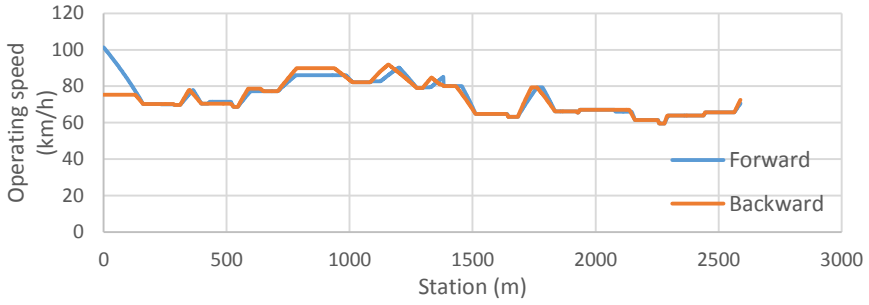

CCR	306.1104	gon/km	$\overline{\Delta v_{85}}$	8.0257377	km/h
$\bar{v}_{85}$	73.75441	km/h	d_{85}	2.7251618	m/s^2
$\sigma_{v_{85}}$	8.7978	km/h	$\sigma_{\Delta v_{85}}$	6.925315	km/h
R_a	2.131956	km/h	$\sigma_{d_{85}}$	6.476556	m/s^2
$E_{a,10}$	0.895575	km/h	$\bar{L}_{\Delta v_{85}}$	37.045455	m
$E_{a,20}$	0.057525	km/h	L_d	15.74%	
L_{10}	0.23793	m	N	22	
L_{20}	0.008691	m			

CONSISTENCY

Polus (2004)	0.65971
Garach (2013)	0.94822
Camacho (2014	1.95898

CRASHES

Observed:	9
Estimated:	
Exposure	4
Polus (2004)	8
Camacho (2009)	5
Garach (2013)	10
Camacho (2014)	7

ROAD SEGMENT: 43.2

Road:	CV-35	
Initial station:	70+950	Free
Final station:	76+290	Free
		Free

AADT:	1440	vpd
Length:	5348	m

OPERATIONAL CHARACTERISTICS

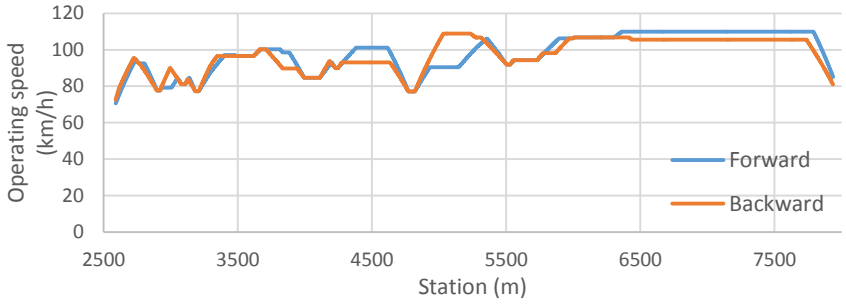

CCR	63.71487	gon/km	$\overline{\Delta v_{85}}$	10.910596	km/h
$\bar{v}_{85}$	97.75583	km/h	d_{85}	0.8817902	m/s^2
$\sigma_{v_{85}}$	9.683365	km/h	$\sigma_{\Delta v_{85}}$	9.1701114	km/h
R_a	2.307884	km/h	$\sigma_{d_{85}}$	0.1936141	m/s^2
$E_{a,10}$	1.300139	km/h	$\bar{L}_{\Delta v_{85}}$	80.428571	m
$E_{a,20}$	0.157676	km/h	L_d	15.79%	
L_{10}	0.336107	m	N	21	
L_{20}	0.026926	m			

CONSISTENCY

Polus (2004)	0.49993
Garach (2013)	0.7595
Camacho (2014	3.13443

CRASHES

Observed:	1
Estimated:	
Exposure	5
Polus (2004)	12
Camacho (2009)	9
Garach (2013)	13
Camacho (2014)	5

ROAD SEGMENT: 43.3

Road:	CV-35	
Initial station:	76+290	Free
Final station:	79+780	Free
		Free

AADT:	1062 vpd
Length:	3472 m

OPERATIONAL CHARACTERISTICS

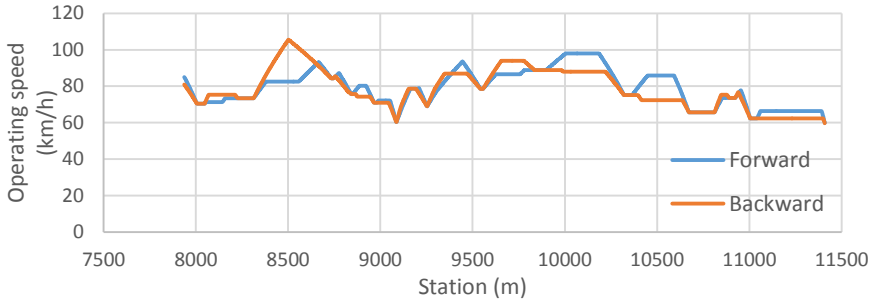

CCR	178.9797 gon/km	$\overline{\Delta v_{85}}$	13.113043 km/h
$\bar{v}_{85}$	78.77468 km/h	d_{85}	1.2769417 m/s^2
$\sigma_{v_{85}}$	10.22219 km/h	$\sigma_{\Delta v_{85}}$	7.383678 km/h
R_a	2.421296 km/h	$\sigma_{d_{85}}$	0.2694062 m/s^2
$E_{a,10}$	1.499299 km/h	$\bar{L}_{\Delta v_{85}}$	65.263158 m
$E_{a,20}$	0.11725 km/h	L_d	17.86%
L_{10}	0.371688 m	N	19
L_{20}	0.018001 m		

CONSISTENCY

Polus (2004)	0.41526
Garach (2013)	0.64313
Camacho (2014	2.57813

CRASHES

Observed:	1
Estimated:	
Exposure	3
Polus (2004)	6
Camacho (2009)	4
Garach (2013)	7
Camacho (2014)	3

ROAD SEGMENT: 43.4

Road:	CV-35	
Initial station:	79+780	Free
Final station:	80+730	Free
		Free

AADT:	1062 vpd
Length:	943 m

OPERATIONAL CHARACTERISTICS

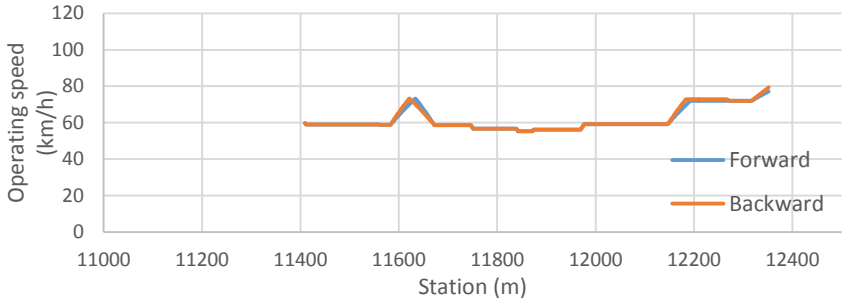

CCR	735.5198 gon/km	$\overline{\Delta v_{85}}$	8.0220368 km/h
$\bar{v}_{85}$	61.8065 km/h	d_{85}	1.8090822 m/s^2
$\sigma_{v_{85}}$	6.12075 km/h	$\sigma_{\Delta v_{85}}$	6.033051 km/h
R_a	1.43356 km/h	$\sigma_{d_{85}}$	0.274198 m/s^2
$E_{a,10}$	0.578024 km/h	$\bar{L}_{\Delta v_{85}}$	23.285714 m
$E_{a,20}$	0 km/h	L_d	8.64%
L_{10}	0.188229 m	N	7
L_{20}	0 m		

CONSISTENCY

Polus (2004)	1.42602
Garach (2013)	1.62332
Camacho (2014	2.11718

CRASHES

Observed:	1
Estimated:	
Exposure	1
Polus (2004)	1
Camacho (2009)	1
Garach (2013)	2
Camacho (2014)	1

ROAD SEGMENT: 43.5

Road:	CV-35	
Initial station:	80+730	Free
Final station:	83+650	Free
		Free

AADT:	1062 vpd
Length:	2893 m

OPERATIONAL CHARACTERISTICS

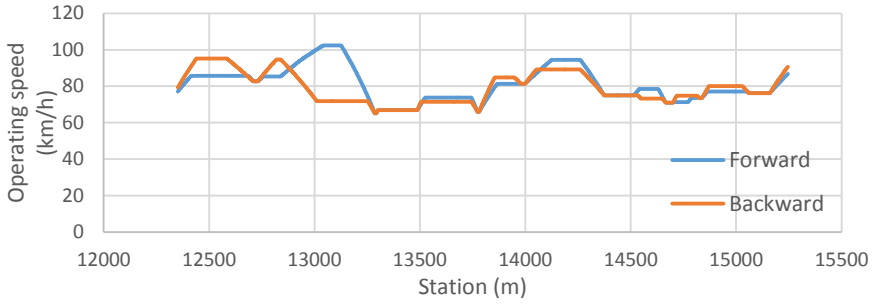

CCR	152.7535 gon/km	$\overline{\Delta v_{85}}$	11.518884 km/h
$\bar{v}_{85}$	80.14981 km/h	d_{85}	1.2141072 m/s^2
$\sigma_{v_{85}}$	8.833038 km/h	$\sigma_{\Delta v_{85}}$	9.3949203 km/h
R_a	2.070932 km/h	$\sigma_{d_{85}}$	0.2010984 m/s^2
$E_{a,10}$	0.957496 km/h	$\overline{L}_{\Delta v_{85}}$	59.142857 m
$E_{a,20}$	0.133186 km/h	L_d	14.31%
L_{10}	0.240754 m	N	14
L_{20}	0.02195 m		

CONSISTENCY

Polus (2004)	0.68378
Garach (2013)	0.98012
Camacho (2014	2.63703

CRASHES

Observed:	2
Estimated:	
Exposure	2
Polus (2004)	5
Camacho (2009)	3
Garach (2013)	5
Camacho (2014)	3

ROAD SEGMENT: 43.6

Road:	CV-35	
Initial station:	83+650	Free
Final station:	86+640	Town
		Constrained

AADT:	1062 vpd
Length:	2995 m

OPERATIONAL CHARACTERISTICS

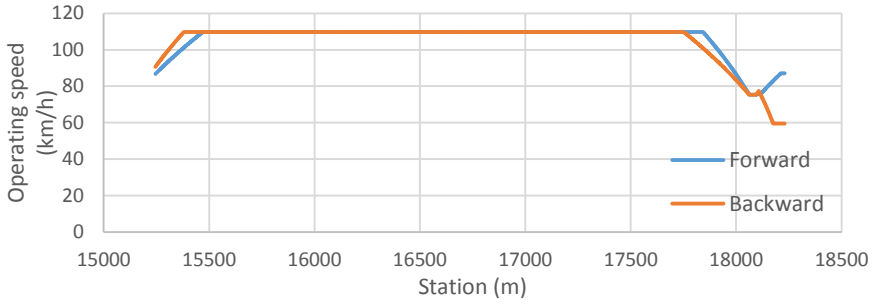

CCR	10.7912 gon/km	$\overline{\Delta v_{85}}$	18.576257 km/h
$\bar{v}_{85}$	105.6611 km/h	d_{85}	1.0907141 m/s^2
$\sigma_{v_{85}}$	10.02328 km/h	$\sigma_{\Delta v_{85}}$	16.180203 km/h
R_a	1.827617 km/h	$\sigma_{d_{85}}$	0.0291543 m/s^2
$E_{a,10}$	0.836391 km/h	$\bar{L}_{\Delta v_{85}}$	122.33333 m
$E_{a,20}$	0.630129 km/h	L_d	6.15%
L_{10}	0.123953 m	N	3
L_{20}	0.074204 m		

CONSISTENCY

Polus (2004)	0.6824
Garach (2013)	0.98663
Camacho (2014	2.99664

CRASHES

Observed:	4
Estimated:	
Exposure	4
Polus (2004)	5
Camacho (2009)	3
Garach (2013)	6
Camacho (2014)	3

ROAD SEGMENT: 44.1

Road:	CV-35	
Initial station:	53+510	Town
Final station:	58+040	Free
		Constrained

AADT:	2258 vpd
Length:	4651 m

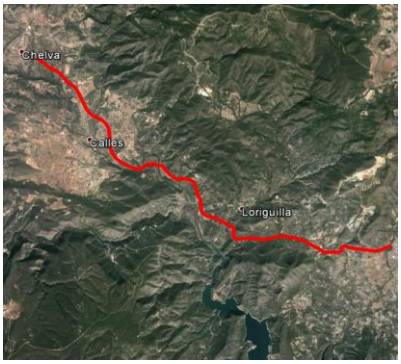

OPERATIONAL CHARACTERISTICS

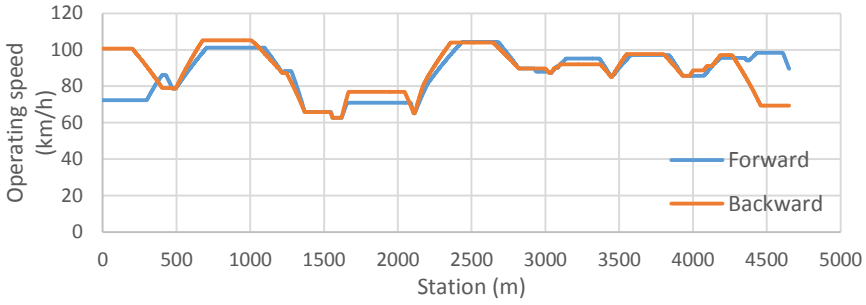

CCR	98.63712 gon/km	$\overline{\Delta v_{85}}$	10.509512 km/h
$\bar{v}_{85}$	88.48449 km/h	d_{85}	1.0159973 m/s^2
$\sigma_{v_{85}}$	11.94102 km/h	$\sigma_{\Delta v_{85}}$	9.6830231 km/h
R_a	2.770455 km/h	$\sigma_{d_{85}}$	0.3199527 m/s^2
$E_{a,10}$	2.027211 km/h	$\bar{L}_{\Delta v_{85}}$	70.25 m
$E_{a,20}$	0.441112 km/h	L_d	15.10%
L_{10}	0.453773 m	N	20
L_{20}	0.068265 m		

CONSISTENCY

Polus (2004)	0.21823
Garach (2013)	0.29604
Camacho (2014	2.89217

CRASHES

Observed:	16
Estimated:	
Exposure	9
Polus (2004)	18
Camacho (2009)	13
Garach (2013)	20
Camacho (2014)	9

ROAD SEGMENT: 44.2

Road:	CV-35	
Initial station:	58+040	Free
Final station:	62+450	Free
		Free

AADT:	2258 vpd
Length:	4421 m

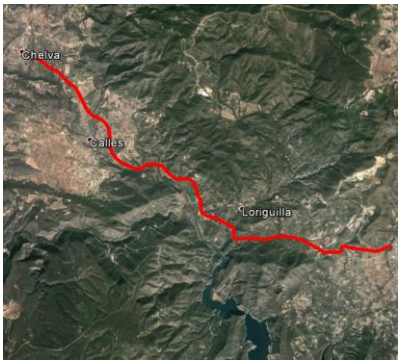

OPERATIONAL CHARACTERISTICS

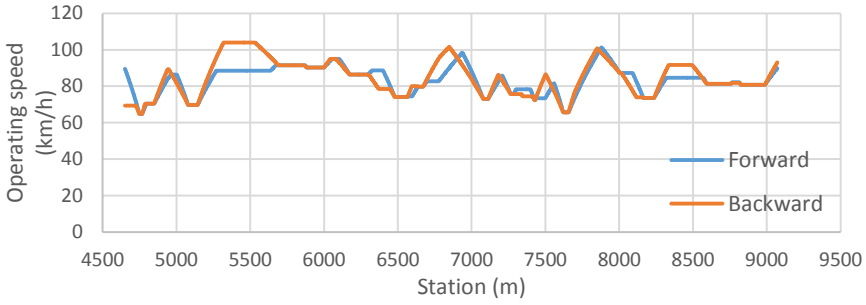

CCR	182.255 gon/km	$\overline{\Delta v_{85}}$	14.14984 km/h
$\bar{v}_{85}$	83.94154 km/h	d_{85}	1.117814 m/s^2
$\sigma_{v_{85}}$	8.574284 km/h	$\sigma_{\Delta v_{85}}$	9.2981333 km/h
R_a	1.949045 km/h	$\sigma_{d_{85}}$	0.221367 m/s^2
$E_{a,10}$	0.967214 km/h	$\bar{L}_{\Delta v_{85}}$	79.708333 m
$E_{a,20}$	0 km/h	L_d	21.64%
L_{10}	0.249152 m	N	24
L_{20}	0 m		

CONSISTENCY

Polus (2004)	0.77256
Garach (2013)	1.07633
Camacho (2014	2.75276

CRASHES

Observed:	12
Estimated:	
Exposure	6
Polus (2004)	14
Camacho (2009)	10
Garach (2013)	17
Camacho (2014)	8

ROAD SEGMENT: 44.3

Road:	CV-35	
Initial station:	62+450	Free
Final station:	67+050	Roundabout
		Constrained

AADT:	2146 vpd
Length:	4499 m

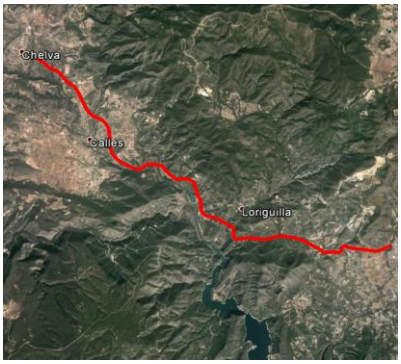

OPERATIONAL CHARACTERISTICS

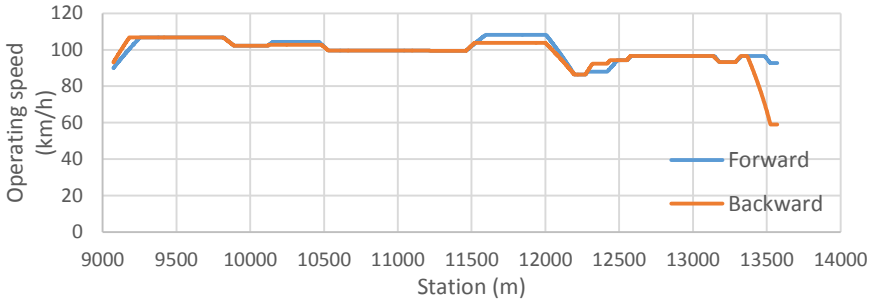

CCR	76.84161 gon/km	$\overline{\Delta v_{85}}$	6.3445184 km/h
$\bar{v}_{85}$	99.591 km/h	d_{85}	0.707512 m/s^2
$\sigma_{v_{85}}$	6.688214 km/h	$\sigma_{\Delta v_{85}}$	6.0872117 km/h
R_a	1.288162 km/h	$\sigma_{d_{85}}$	0.1335763 m/s^2
$E_{a,10}$	0.299199 km/h	$\bar{L}_{\Delta v_{85}}$	63.636364 m
$E_{a,20}$	0.128546 km/h	L_d	7.78%
L_{10}	0.062903 m	N	11
L_{20}	0.01367 m		

CONSISTENCY

Polus (2004)	1.44363
Garach (2013)	1.64244
Camacho (2014	3.39413

CRASHES

Observed:	5
Estimated:	
Exposure	8
Polus (2004)	11
Camacho (2009)	8
Garach (2013)	15
Camacho (2014)	6

ROAD SEGMENT: 45.1

Road:	CV-333	
Initial station:	3+850	Roundabout
Final station:	6+510	Free
		Constrained

AADT:	4076 vpd
Length:	2658 m

OPERATIONAL CHARACTERISTICS

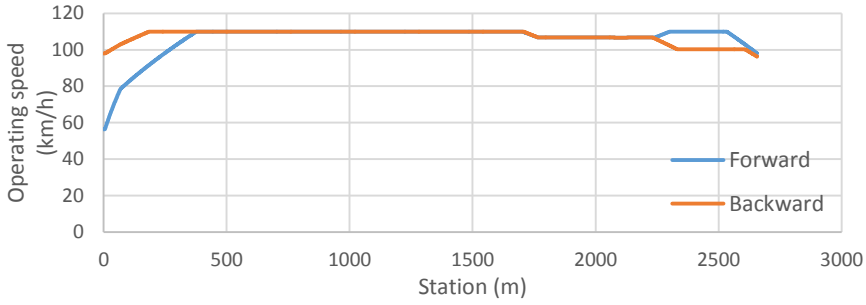

CCR	7.010917 gon/km	$\overline{\Delta v_{85}}$	9.0326406 km/h
$\bar{v}_{85}$	106.8742 km/h	d_{85}	0.5770457 m/s^2
$\sigma_{v_{85}}$	6.626502 km/h	$\sigma_{\Delta v_{85}}$	5.0967729 km/h
R_a	1.051624 km/h	$\sigma_{d_{85}}$	0.1827182 m/s^2
$E_{a,10}$	0.311962 km/h	$\bar{L}_{\Delta v_{85}}$	122 m
$E_{a,20}$	0.233707 km/h	L_d	6.89%
L_{10}	0.045916 m	N	3
L_{20}	0.026534 m		

CONSISTENCY

Polus (2004)	1.63942
Garach (2013)	1.7724
Camacho (2014	3.71923

CRASHES

Observed:	0
Estimated:	
Exposure	7
Polus (2004)	11
Camacho (2009)	8
Garach (2013)	18
Camacho (2014)	4

ROAD SEGMENT: 45.2

Road:	CV-333	
Initial station:	6+510	Free
Final station:	8+390	Roundabout
		Constrained

AADT:	3129 vpd
Length:	1925 m

OPERATIONAL CHARACTERISTICS

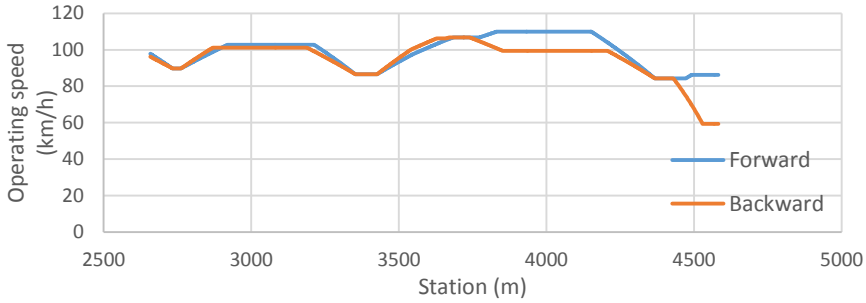

CCR	61.58028 gon/km	$\overline{\Delta v_{85}}$	16.244443 km/h
$\bar{v}_{85}$	96.90831 km/h	d_{85}	0.8059191 m/s^2
$\sigma_{v_{85}}$	9.562018 km/h	$\sigma_{\Delta v_{85}}$	6.8959427 km/h
R_a	2.051671 km/h	$\sigma_{d_{85}}$	0.0663735 m/s^2
$E_{a,10}$	1.090028 km/h	$\bar{L}_{\Delta v_{85}}$	148.2 m
$E_{a,20}$	0.281795 km/h	L_d	19.25%
L_{10}	0.270909 m	N	5
L_{20}	0.031169 m		

CONSISTENCY

Polus (2004)	0.61725
Garach (2013)	0.91646
Camacho (2014	3.22049

CRASHES

Observed:	2
Estimated:	
Exposure	4
Polus (2004)	9
Camacho (2009)	6
Garach (2013)	12
Camacho (2014)	3

ROAD SEGMENT: 46.1

Road:	CV-801	
Initial station:	0+420	Town
Final station:	3+700	Free
		Constrained

AADT:	547 vpd
Length:	3280 m

OPERATIONAL CHARACTERISTICS

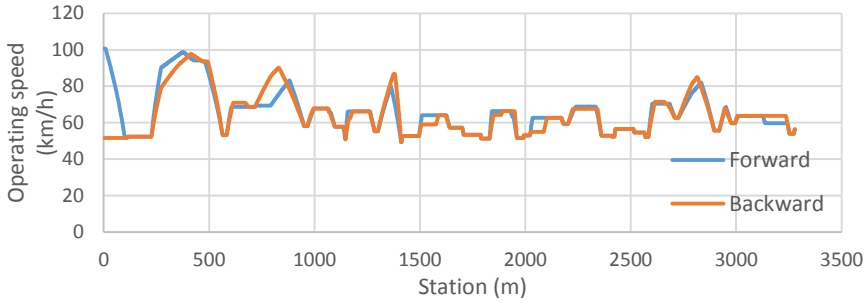

CCR	737.4441 gon/km	$\overline{\Delta v_{85}}$	11.66509 km/h
$\bar{v}_{85}$	65.28338 km/h	d_{85}	2.1863206 m/s^2
$\sigma_{v_{85}}$	11.45658 km/h	$\sigma_{\Delta v_{85}}$	11.964109 km/h
R_a	2.403775 km/h	$\sigma_{d_{85}}$	0.5947886 m/s^2
$E_{a,10}$	1.69914 km/h	$\bar{L}_{\Delta v_{85}}$	29.521739 m
$E_{a,20}$	0.650733 km/h	L_d	20.71%
L_{10}	0.374199 m	N	46
L_{20}	0.084782 m		

CONSISTENCY

Polus (2004)	0.33482
Garach (2013)	0.53413
Camacho (2014	2.02424

CRASHES

Observed:	3
Estimated:	
Exposure	3
Polus (2004)	3
Camacho (2009)	2
Garach (2013)	3
Camacho (2014)	3

ROAD SEGMENT: 46.2

Road:	CV-801	
Initial station:	3+700	Free
Final station:	5+580	Free
		Free

AADT:	547 vpd
Length:	1979 m

OPERATIONAL CHARACTERISTICS

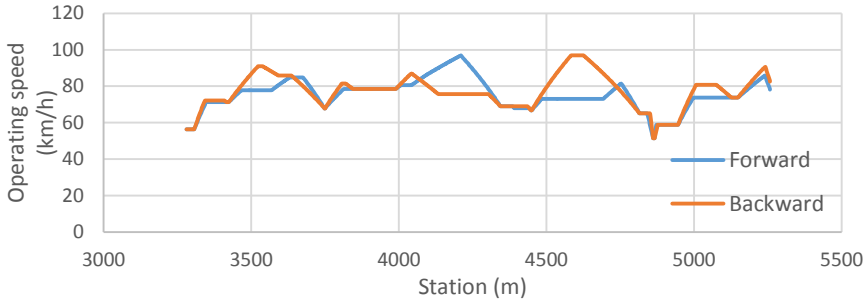

CCR	229.7443 gon/km	$\overline{\Delta v_{85}}$	15.572845 km/h
$\bar{v}_{85}$	76.45764 km/h	d_{85}	1.7711595 m/s^2
$\sigma_{v_{85}}$	8.743197 km/h	$\sigma_{\Delta v_{85}}$	7.9394431 km/h
R_a	1.862119 km/h	$\sigma_{d_{85}}$	0.720529 m/s^2
$E_{a,10}$	0.974192 km/h	$\bar{L}_{\Delta v_{85}}$	61.142857 m
$E_{a,20}$	0.209014 km/h	L_d	21.64%
L_{10}	0.223711 m	N	14
L_{20}	0.035895 m		

CONSISTENCY

Polus (2004)	0.7987
Garach (2013)	1.10757
Camacho (2014	2.28887

CRASHES

Observed:	1
Estimated:	
Exposure	1
Polus (2004)	2
Camacho (2009)	1
Garach (2013)	2
Camacho (2014)	1

ROAD SEGMENT: 46.3

Road:	CV-801	
Initial station:	5+580	Free
Final station:	9+070	Intersection
		Constrained

AADT:	822 vpd
Length:	3218 m

OPERATIONAL CHARACTERISTICS

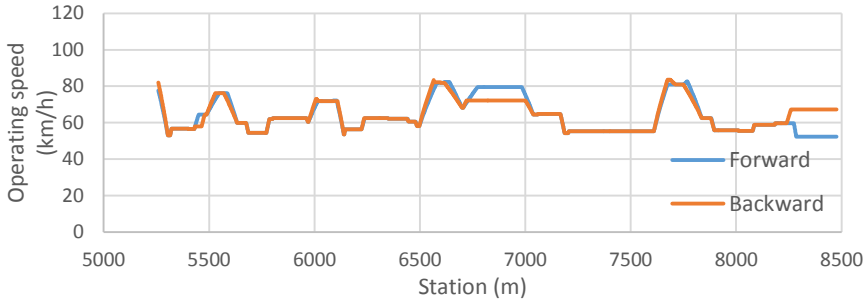

CCR	564.9896 gon/km	$\overline{\Delta v_{85}}$	9.9101269 km/h
$\bar{v}_{85}$	63.85205 km/h	d_{85}	2.0498463 m/s^2
$\sigma_{v_{85}}$	8.446486 km/h	$\sigma_{\Delta v_{85}}$	7.9703032 km/h
R_a	1.964503 km/h	$\sigma_{d_{85}}$	0.4329887 m/s^2
$E_{a,10}$	0.737696 km/h	$\bar{L}_{\Delta v_{85}}$	25.925926 m
$E_{a,20}$	0 km/h	L_d	10.88%
L_{10}	0.183499 m	N	27
L_{20}	0 m		

CONSISTENCY

Polus (2004)	0.77967
Garach (2013)	1.0806
Camacho (2014	2.05298

CRASHES

Observed:	0
Estimated:	
Exposure	3
Polus (2004)	4
Camacho (2009)	3
Garach (2013)	4
Camacho (2014)	4

ROAD SEGMENT: 47.1

Road:	CV-820	
Initial station:	8+950	Town
Final station:	10+860	Roundabout
		Constrained

AADT:	4476 vpd
Length:	1791 m

OPERATIONAL CHARACTERISTICS

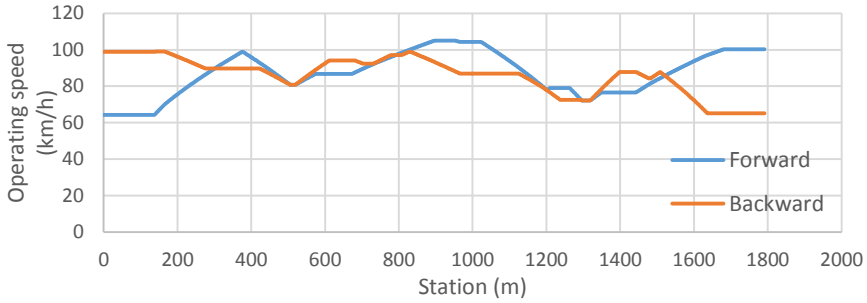

CCR	68.53882 gon/km	$\overline{\Delta v_{85}}$	11.309754 km/h
$\bar{v}_{85}$	86.76453 km/h	d_{85}	0.9507217 m/s^2
$\sigma_{v_{85}}$	10.8279 km/h	$\sigma_{\Delta v_{85}}$	8.5160406 km/h
R_a	2.410896 km/h	$\sigma_{d_{85}}$	0.2046541 m/s^2
$E_{a,10}$	1.744657 km/h	$\bar{L}_{\Delta v_{85}}$	76.375 m
$E_{a,20}$	0.531776 km/h	L_d	17.06%
L_{10}	0.41541 m	N	8
L_{20}	0.087381 m		

CONSISTENCY

Polus (2004)	0.37403
Garach (2013)	0.5914
Camacho (2014	2.93762

CRASHES

Observed:	5
Estimated:	
Exposure	5
Polus (2004)	13
Camacho (2009)	9
Garach (2013)	18
Camacho (2014)	5

ROAD SEGMENT: 48.1

Road:	CV-755	
Initial station:	0+000	Town
Final station:	0+650	Town
		Constrained

AADT:	871 vpd
Length:	642 m

OPERATIONAL CHARACTERISTICS

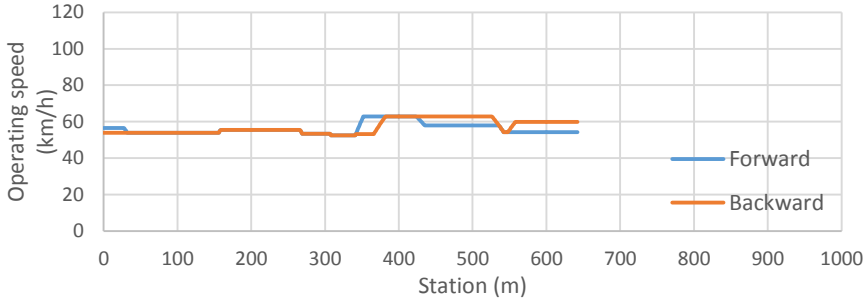

CCR	920.6207 gon/km	$\overline{\Delta v_{85}}$	3.8915478 km/h
$\bar{v}_{85}$	56.629 km/h	d_{85}	2.2622499 m/s^2
$\sigma_{v_{85}}$	3.447652 km/h	$\sigma_{\Delta v_{85}}$	2.8237263 km/h
R_a	0.822928 km/h	$\sigma_{d_{85}}$	0.2379742 m/s^2
$E_{a,10}$	0 km/h	$\bar{L}_{\Delta v_{85}}$	7.375 m
$E_{a,20}$	0 km/h	L_d	4.60%
L_{10}	0 m	N	8
L_{20}	0 m		

CONSISTENCY

Polus (2004)	2.25552
Garach (2013)	2.22436
Camacho (2014	1.90867

CRASHES

Observed:	1
Estimated:	
Exposure	1
Polus (2004)	0
Camacho (2009)	0
Garach (2013)	1
Camacho (2014)	1

ROAD SEGMENT: 49.1

Road:	CV-50	
Initial station:	42+210	Town
Final station:	46+310	Free
		Constrained

AADT:	2676	vpd
Length:	4101	m

OPERATIONAL CHARACTERISTICS

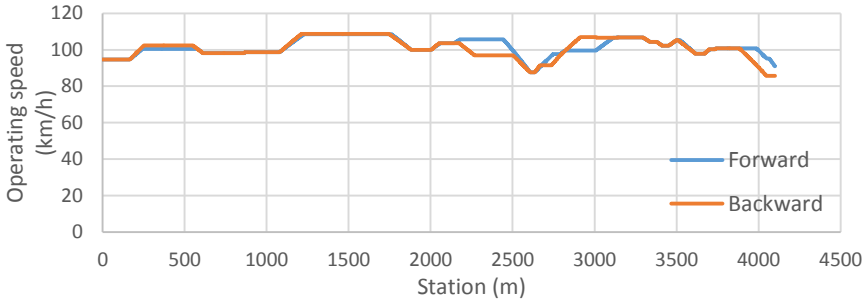

CCR	57.09453	gon/km	$\overline{\Delta v_{85}}$	6.4953652	km/h
$\bar{v}_{85}$	101.2864	km/h	d_{85}	0.6379439	m/s^2
$\sigma_{v_{85}}$	5.065899	km/h	$\sigma_{\Delta v_{85}}$	4.9182688	km/h
R_a	1.128826	km/h	$\sigma_{d_{85}}$	0.1274539	m/s^2
$E_{a,10}$	0.136919	km/h	$\bar{L}_{\Delta v_{85}}$	76.6	m
$E_{a,20}$	0	km/h	L_d	14.01%	
L_{10}	0.038049	m	N	15	
L_{20}	0	m			

CONSISTENCY

Polus (2004)	1.80557
Garach (2013)	1.89953
Camacho (2014	3.5331

CRASHES

Observed:	5
Estimated:	
Exposure	8
Polus (2004)	11
Camacho (2009)	8
Garach (2013)	16
Camacho (2014)	6

ROAD SEGMENT: 49.2

Road:	CV-50	
Initial station:	46+310	Free
Final station:	48+830	Town
		Constrained

AADT:	2676	vpd
Length:	2498	m

OPERATIONAL CHARACTERISTICS

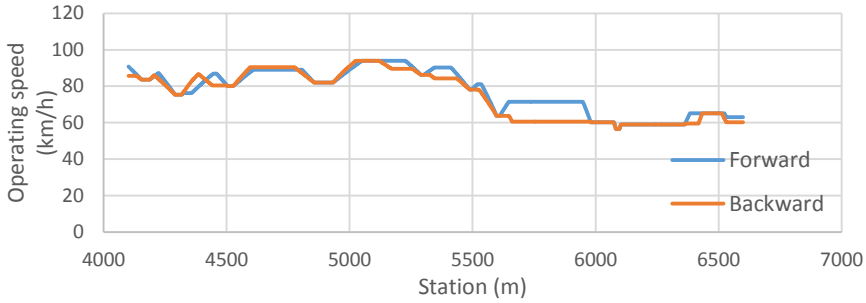

CCR	180.6309	gon/km	$\overline{\Delta v_{85}}$	8.2019988	km/h
$\bar{v}_{85}$	76.26199	km/h	d_{85}	1.2664339	m/s^2
$\sigma_{v_{85}}$	12.3033	km/h	$\sigma_{\Delta v_{85}}$	4.3451534	km/h
R_a	3.112134	km/h	$\sigma_{d_{85}}$	0.4334404	m/s^2
$E_{a,10}$	2.497054	km/h	$\bar{L}_{\Delta v_{85}}$	45.625	m
$E_{a,20}$	0	km/h	L_d	14.61%	
L_{10}	0.608687	m	N	16	
L_{20}	0	m			

CONSISTENCY

Polus (2004)	0.14597
Garach (2013)	0.08383
Camacho (2014	2.55745

CRASHES

Observed:	11
Estimated:	
Exposure	5
Polus (2004)	12
Camacho (2009)	8
Garach (2013)	15
Camacho (2014)	6

ROAD SEGMENT: 50.1

Road:	CV-15	
Initial station:	17+850	Town
Final station:	21+490	Free
		Constrained

AADT:	2703 vpd
Length:	3635 m

OPERATIONAL CHARACTERISTICS

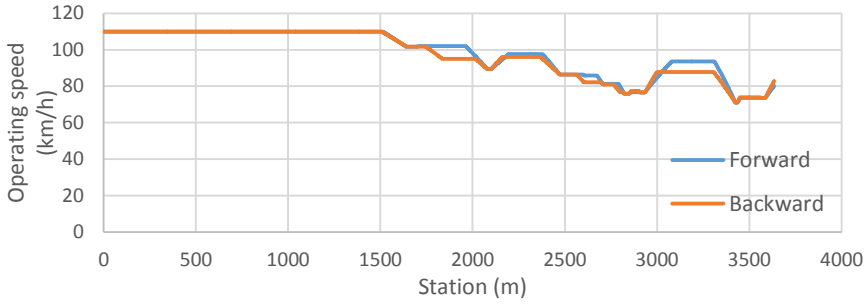

CCR	59.99343 gon/km	$\overline{\Delta v_{85}}$	8.8114694 km/h
$\bar{v}_{85}$	98.0124 km/h	d_{85}	0.9720493 m/s^2
$\sigma_{v_{85}}$	12.48263 km/h	$\sigma_{\Delta v_{85}}$	5.7793331 km/h
R_a	3.062892 km/h	$\sigma_{d_{85}}$	0.2212505 m/s^2
$E_{a,10}$	2.732883 km/h	$\bar{L}_{\Delta v_{85}}$	65.181818 m
$E_{a,20}$	0.657164 km/h	L_d	9.86%
L_{10}	0.705227 m	N	11
L_{20}	0.102613 m		

CONSISTENCY

Polus (2004)	0.14661
Garach (2013)	0.09802
Camacho (2014	3.0369

CRASHES

Observed:	9
Estimated:	
Exposure	7
Polus (2004)	18
Camacho (2009)	12
Garach (2013)	21
Camacho (2014)	7

ROAD SEGMENT: 50.2

Road:	CV-15	
Initial station:	21+490	Free
Final station:	26+140	Free
		Free

AADT:	2703	vpd
Length:	4647	m

OPERATIONAL CHARACTERISTICS

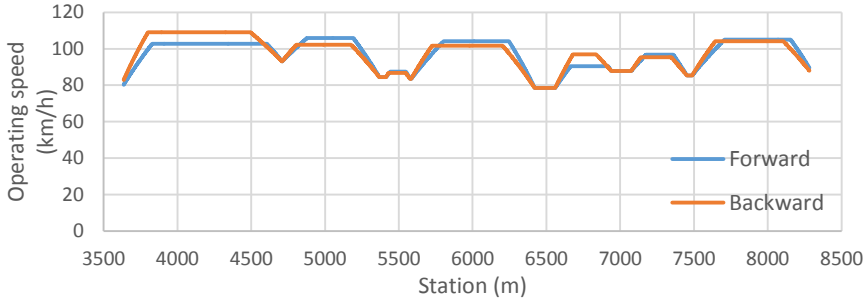

CCR	45.7016	gon/km	$\overline{\Delta v_{85}}$	13.626671	km/h
$\bar{v}_{85}$	97.52856	km/h	d_{85}	0.8906583	m/s^2
$\sigma_{v_{85}}$	8.046829	km/h	$\sigma_{\Delta v_{85}}$	8.1408728	km/h
R_a	1.912596	km/h	$\sigma_{d_{85}}$	0.1251332	m/s^2
$E_{a,10}$	0.798017	km/h	$\bar{L}_{\Delta v_{85}}$	106.64286	m
$E_{a,20}$	0	km/h	L_d	16.06%	
L_{10}	0.221433	m	N	14	
L_{20}	0	m			

CONSISTENCY

Polus (2004)	0.85556
Garach (2013)	1.15132
Camacho (2014	3.12157

CRASHES

Observed:	7
Estimated:	
Exposure	7
Polus (2004)	18
Camacho (2009)	12
Garach (2013)	21
Camacho (2014)	8

ROAD SEGMENT: 50.3

Road:	CV-15	
Initial station:	26+140	Free
Final station:	28+480	Free
		Free

AADT:	2703	vpd
Length:	2333	m

OPERATIONAL CHARACTERISTICS

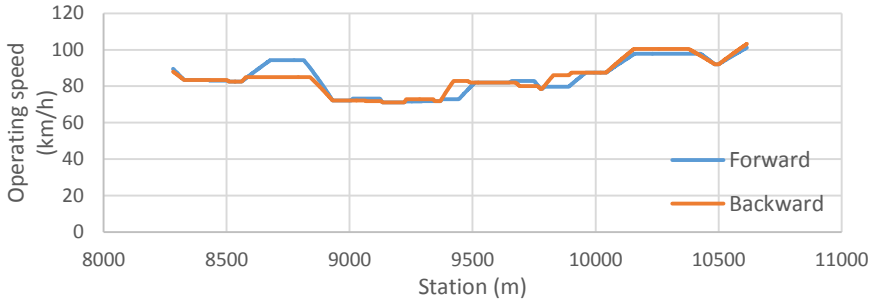

CCR	164.1135	gon/km	$\overline{\Delta v_{85}}$	7.3954055	km/h
$\bar{v}_{85}$	84.65727	km/h	d_{85}	0.9833548	m/s^2
$\sigma_{v_{85}}$	9.011418	km/h	$\sigma_{\Delta v_{85}}$	6.1107533	km/h
R_a	2.030549	km/h	$\sigma_{d_{85}}$	0.1828051	m/s^2
$E_{a,10}$	1.453001	km/h	$\bar{L}_{\Delta v_{85}}$	51.833333	m
$E_{a,20}$	0	km/h	L_d	13.33%	
L_{10}	0.399486	m	N	12	
L_{20}	0	m			

CONSISTENCY

Polus (2004)	0.68349
Garach (2013)	0.98509
Camacho (2014	2.88105

CRASHES

Observed:	3
Estimated:	
Exposure	4
Polus (2004)	9
Camacho (2009)	7
Garach (2013)	12
Camacho (2014)	5

ROAD SEGMENT: 50.4

Road:	CV-15	
Initial station:	28+480	Free
Final station:	32+110	Free
		Free

AADT:	2703 vpd
Length:	3617 m

OPERATIONAL CHARACTERISTICS

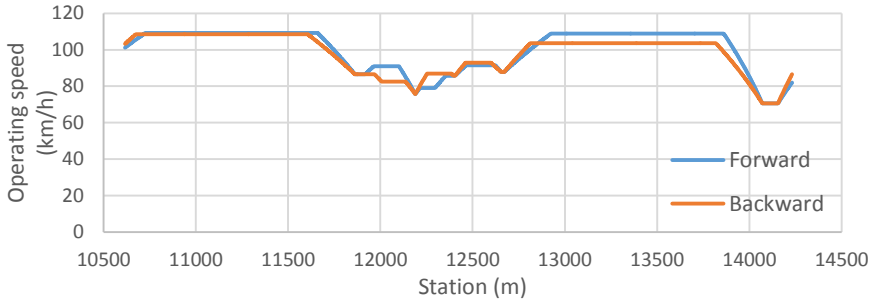

CCR	52.58624 gon/km	$\overline{\Delta v_{85}}$	15.036173 km/h
$\bar{v}_{85}$	99.04696 km/h	d_{85}	0.9757665 m/s^2
$\sigma_{v_{85}}$	11.25187 km/h	$\sigma_{\Delta v_{85}}$	10.644505 km/h
R_a	2.733023 km/h	$\sigma_{d_{85}}$	0.2089017 m/s^2
$E_{a,10}$	1.463951 km/h	$\bar{L}_{\Delta v_{85}}$	103.77778 m
$E_{a,20}$	0.497527 km/h	L_d	12.91%
L_{10}	0.357202 m	N	9
L_{20}	0.073127 m		

CONSISTENCY

Polus (2004)	0.26126
Garach (2013)	0.37446
Camacho (2014	3.04367

CRASHES

Observed:	2
Estimated:	
Exposure	6
Polus (2004)	17
Camacho (2009)	12
Garach (2013)	20
Camacho (2014)	6

ROAD SEGMENT: 50.5

Road:	CV-15	
Initial station:	32+110	Free
Final station:	36+130	Free
		Free

AADT:	1836	vpd
Length:	4000	m

OPERATIONAL CHARACTERISTICS

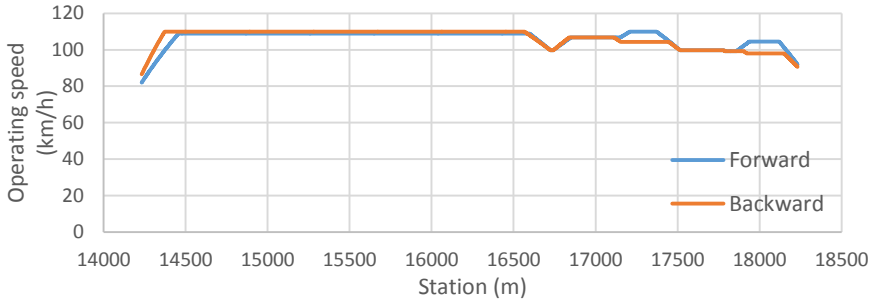

CCR	14.31232	gon/km	$\overline{\Delta v_{85}}$	12.508718	km/h
$\bar{v}_{85}$	106.2254	km/h	d_{85}	0.7679839	m/s^2
$\sigma_{v_{85}}$	4.777876	km/h	$\sigma_{\Delta v_{85}}$	6.4553301	km/h
R_a	1.069342	km/h	$\sigma_{d_{85}}$	0.304177	m/s^2
$E_{a,10}$	0.137198	km/h	$\bar{L}_{\Delta v_{85}}$	124.6	m
$E_{a,20}$	0.023841	km/h	L_d	7.79%	
L_{10}	0.03325	m	N	5	
L_{20}	0.003875	m			

CONSISTENCY

Polus (2004)	1.89256
Garach (2013)	1.96098
Camacho (2014	3.37436

CRASHES

Observed:	3
Estimated:	
Exposure	5
Polus (2004)	7
Camacho (2009)	5
Garach (2013)	10
Camacho (2014)	4

ROAD SEGMENT: 50.6

Road:	CV-15	
Initial station:	36+130	Free
Final station:	38+020	Free
		Free

AADT:	2008	vpd
Length:	1885	m

OPERATIONAL CHARACTERISTICS

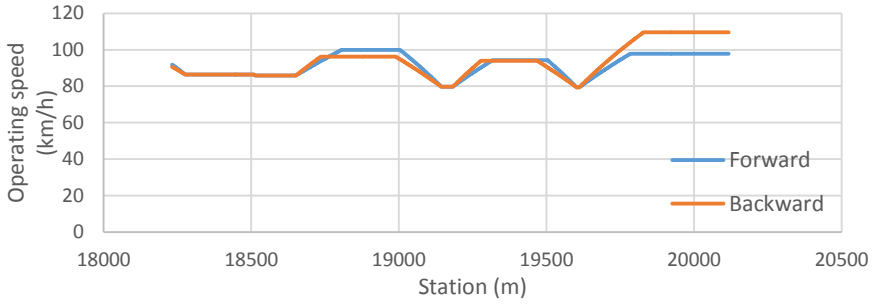

CCR	75.59115	gon/km	$\overline{\Delta v_{85}}$	15.912726	km/h
$\bar{v}_{85}$	92.4749	km/h	d_{85}	0.9517252	m/s^2
$\sigma_{v_{85}}$	7.615103	km/h	$\sigma_{\Delta v_{85}}$	8.6013825	km/h
R_a	1.735001	km/h	$\sigma_{d_{85}}$	0.077162	m/s^2
$E_{a,10}$	0.658923	km/h	$\bar{L}_{\Delta v_{85}}$	114	m
$E_{a,20}$	0	km/h	L_d	18.14%	
L_{10}	0.163395	m	N	6	
L_{20}	0	m			

CONSISTENCY

Polus (2004)	1.01227
Garach (2013)	1.29763
Camacho (2014	2.99965

CRASHES

Observed:	8
Estimated:	
Exposure	3
Polus (2004)	5
Camacho (2009)	4
Garach (2013)	7
Camacho (2014)	3

ROAD SEGMENT: 51.1

Road:	CV-50	
Initial station:	76+240	Town
Final station:	83+740	Roundabout
		Constrained

AADT:	4722 vpd
Length:	7509 m

OPERATIONAL CHARACTERISTICS

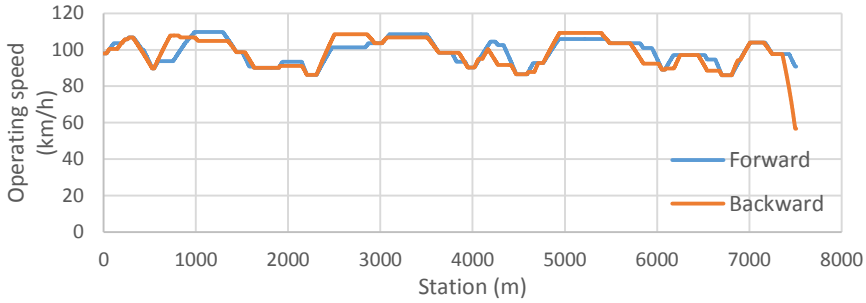

CCR	70.24882 gon/km	$\overline{\Delta v_{85}}$	7.0398458 km/h
$\bar{v}_{85}$	98.80843 km/h	d_{85}	0.6858695 m/s^2
$\sigma_{v_{85}}$	7.342475 km/h	$\sigma_{\Delta v_{85}}$	5.2953366 km/h
R_a	1.721418 km/h	$\sigma_{d_{85}}$	0.1324725 m/s^2
$E_{a,10}$	0.464068 km/h	$\bar{L}_{\Delta v_{85}}$	74.151515 m
$E_{a,20}$	0.046655 km/h	L_d	16.29%
L_{10}	0.136503 m	N	33
L_{20}	0.005194 m		

CONSISTENCY

Polus (2004)	1.05805
Garach (2013)	1.33371
Camacho (2014	3.42045

CRASHES

Observed:	9
Estimated:	
Exposure	21
Polus (2004)	46
Camacho (2009)	33
Garach (2013)	54
Camacho (2014)	20

ROAD SEGMENT: 52.1

Road:	CV-16	
Initial station:	8+890	Roundabout
Final station:	10+050	Roundabout
		Constrained

AADT:	10325	vpd
Length:	1252	m

OPERATIONAL CHARACTERISTICS

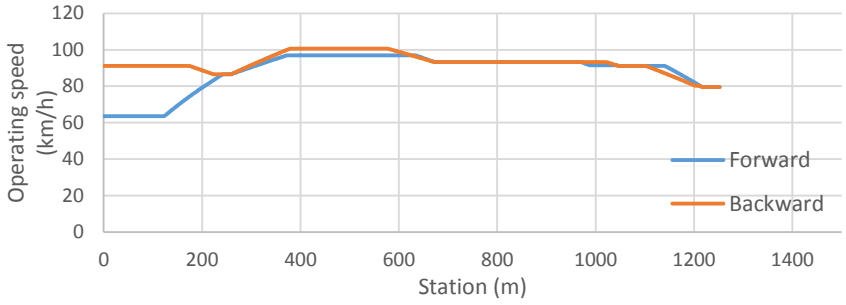

CCR	103.2663	gon/km	$\overline{\Delta v_{85}}$	7.8225803	km/h
$\bar{v}_{85}$	90.50983	km/h	d_{85}	0.812976	m/s^2
$\sigma_{v_{85}}$	8.601183	km/h	$\sigma_{\Delta v_{85}}$	5.9853068	km/h
R_a	1.62719	km/h	$\sigma_{d_{85}}$	0.1411642	m/s^2
$E_{a,10}$	0.879252	km/h	$\bar{L}_{\Delta v_{85}}$	63.75	m
$E_{a,20}$	0.454494	km/h	L_d	10.18%	
L_{10}	0.200879	m	N	4	
L_{20}	0.0623	m			

CONSISTENCY

Polus (2004)	0.95284
Garach (2013)	1.25092
Camacho (2014	3.13886

CRASHES

Observed:	3
Estimated:	
Exposure	5
Polus (2004)	17
Camacho (2009)	12
Garach (2013)	29
Camacho (2014)	6

ROAD SEGMENT: 53.1

Road:	CV-18	
Initial station:	3+350	Roundabout
Final station:	8+000	Roundabout
		Constrained

AADT:	14640	vpd
Length:	4522	m

OPERATIONAL CHARACTERISTICS

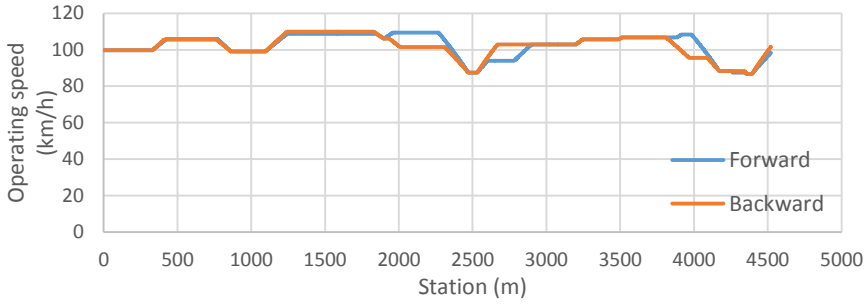

CCR	49.48173	gon/km	$\overline{\Delta v_{85}}$	10.198325	km/h
$\bar{v}_{85}$	102.1906	km/h	d_{85}	0.6373965	m/s^2
$\sigma_{v_{85}}$	6.232095	km/h	$\sigma_{\Delta v_{85}}$	7.5982335	km/h
R_a	1.382727	km/h	$\sigma_{d_{85}}$	0.1727064	m/s^2
$E_{a,10}$	0.386852	km/h	$\bar{L}_{\Delta v_{85}}$	109	m
$E_{a,20}$	0	km/h	L_d	12.05%	
L_{10}	0.102167	m	N	10	
L_{20}	0	m			

CONSISTENCY

Polus (2004)	1.44344
Garach (2013)	1.63989
Camacho (2014	3.54459

CRASHES

Observed:	49
Estimated:	
Exposure	23
Polus (2004)	75
Camacho (2009)	54
Garach (2013)	113
Camacho (2014)	26

ROAD SEGMENT: 54.1

Road:	CV-18	
Initial station:	2+570	Roundabout
Final station:	3+100	Roundabout
		Constrained

AADT:	14640	vpd
Length:	520	m

OPERATIONAL CHARACTERISTICS

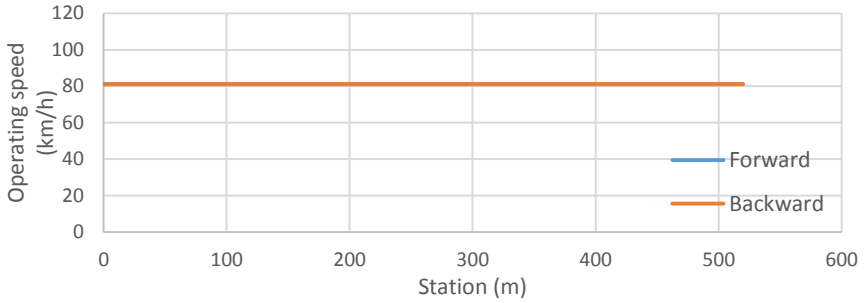

CCR	0 gon/km	$\overline{\Delta v_{85}}$	0 km/h
$\bar{v}_{85}$	0 km/h	d_{85}	0 m/s^2
$\sigma_{v_{85}}$	0 km/h	$\sigma_{\Delta v_{85}}$	0 km/h
R_a	0 km/h	$\sigma_{d_{85}}$	0 m/s^2
$E_{a,10}$	0 km/h	$\bar{L}_{\Delta v_{85}}$	0 m
$E_{a,20}$	0 km/h	L_d	0.00%
L_{10}	0 m	N	0
L_{20}	0 m		

CONSISTENCY

Polus (2004)	2.808
Garach (2013)	2.94029
Camacho (2014	#¡DIV/0!

CRASHES

Observed:	2
Estimated:	
Exposure	3
Polus (2004)	5
Camacho (2009)	4
Garach (2013)	15
Camacho (2014)	#¡DIV/0!

ROAD SEGMENT: 55.1

Road:	CV-439	
Initial station:	0+270	Roundabout
Final station:	9+350	Free
		Constrained

AADT:	371 vpd
Length:	9082 m

OPERATIONAL CHARACTERISTICS

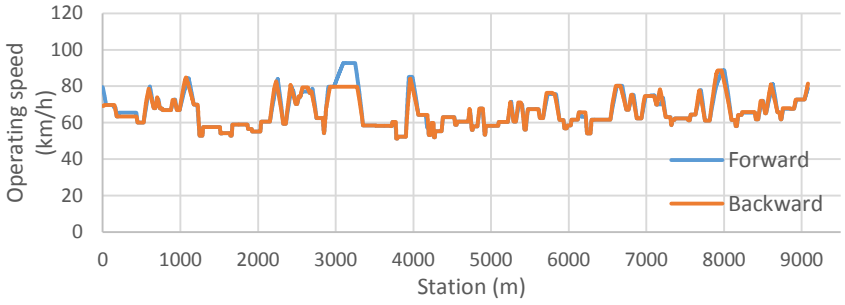

CCR	544.9676 gon/km	$\overline{\Delta v_{85}}$	9.3049259 km/h
$\bar{v}_{85}$	66.24177 km/h	d_{85}	1.8050509 m/s^2
$\sigma_{v_{85}}$	8.299182 km/h	$\sigma_{\Delta v_{85}}$	7.3063349 km/h
R_a	1.870793 km/h	$\sigma_{d_{85}}$	0.4505967 m/s^2
$E_{a,10}$	0.829064 km/h	$\bar{L}_{\Delta v_{85}}$	28.840426 m
$E_{a,20}$	0.139844 km/h	L_d	14.93%
L_{10}	0.212752 m	N	94
L_{20}	0.020923 m		

CONSISTENCY

Polus (2004)	0.84664
Garach (2013)	1.14928
Camacho (2014	2.16827

CRASHES

Observed:	2
Estimated:	
Exposure	6
Polus (2004)	5
Camacho (2009)	3
Garach (2013)	4
Camacho (2014)	7

ROAD SEGMENT: 55.2

Road:	CV-439	
Initial station:	9+350	Free
Final station:	12+590	Free
		Free

AADT:	295 vpd
Length:	2910 m

OPERATIONAL CHARACTERISTICS

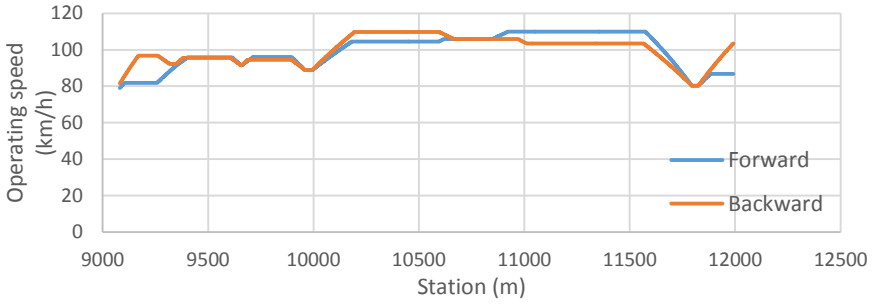

CCR	33.52351 gon/km	$\overline{\Delta v_{85}}$	13.356138 km/h
$\bar{v}_{85}$	99.49988 km/h	d_{85}	0.8685914 m/s^2
$\sigma_{v_{85}}$	8.465608 km/h	$\sigma_{\Delta v_{85}}$	10.411917 km/h
R_a	2.050598 km/h	$\sigma_{d_{85}}$	0.1697059 m/s^2
$E_{a,10}$	1.116472 km/h	$\bar{L}_{\Delta v_{85}}$	105.625 m
$E_{a,20}$	0.003861 km/h	L_d	14.52%
L_{10}	0.325601 m	N	8
L_{20}	0.000687 m		

CONSISTENCY

Polus (2004)	0.73486
Garach (2013)	1.02879
Camacho (2014	3.16885

CRASHES

Observed:	1
Estimated:	
Exposure	1
Polus (2004)	1
Camacho (2009)	1
Garach (2013)	1
Camacho (2014)	1

ROAD SEGMENT: 56.1

Road:	CV-222	
Initial station:	0+530	Roundabout
Final station:	5+470	Free
		Constrained

AADT:	6549 vpd
Length:	4940 m

OPERATIONAL CHARACTERISTICS

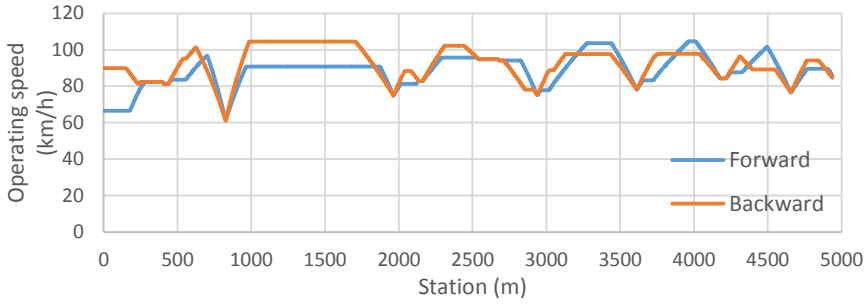

CCR	43.75312 gon/km	$\overline{\Delta v_{85}}$	16.585275 km/h
$\bar{v}_{85}$	90.33578 km/h	d_{85}	1.0493418 m/s^2
$\sigma_{v_{85}}$	8.856828 km/h	$\sigma_{\Delta v_{85}}$	10.90226 km/h
R_a	1.919161 km/h	$\sigma_{d_{85}}$	0.2763836 m/s^2
$E_{a,10}$	1.025443 km/h	$\bar{L}_{\Delta v_{85}}$	100.68421 m
$E_{a,20}$	0.222346 km/h	L_d	19.37%
L_{10}	0.252278 m	N	19
L_{20}	0.033306 m		

CONSISTENCY

Polus (2004)	0.75569
Garach (2013)	1.06381
Camacho (2014	2.88102

CRASHES

Observed:	19
Estimated:	
Exposure	16
Polus (2004)	47
Camacho (2009)	33
Garach (2013)	58
Camacho (2014)	23

ROAD SEGMENT: 56.2

Road:	CV-222	
Initial station:	5+470	Free
Final station:	6+450	Roundabout
		Constrained

AADT:	6549 vpd
Length:	1231 m

OPERATIONAL CHARACTERISTICS

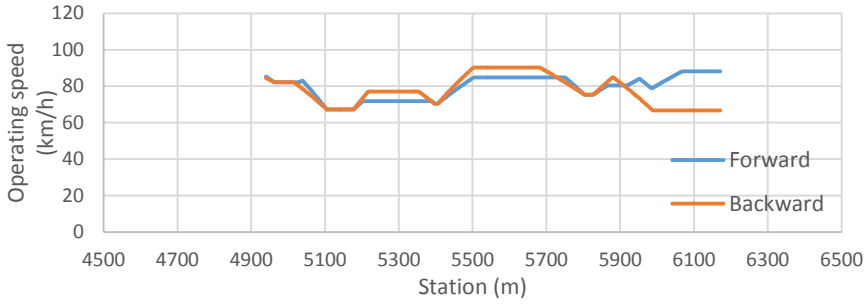

CCR	122.9289 gon/km	$\overline{\Delta v_{85}}$	9.2827241 km/h
$\bar{v}_{85}$	78.5038 km/h	d_{85}	1.1853865 m/s^2
$\sigma_{v_{85}}$	7.276862 km/h	$\sigma_{\Delta v_{85}}$	6.1824411 km/h
R_a	1.741701 km/h	$\sigma_{d_{85}}$	0.1679868 m/s^2
$E_{a,10}$	0.738843 km/h	$\bar{L}_{\Delta v_{85}}$	46.125 m
$E_{a,20}$	0 km/h	L_d	14.99%
L_{10}	0.230707 m	N	8
L_{20}	0 m		

CONSISTENCY

Polus (2004)	1.05522
Garach (2013)	1.32886
Camacho (2014	2.63983

CRASHES

Observed:	3
Estimated:	
Exposure	4
Polus (2004)	11
Camacho (2009)	7
Garach (2013)	18
Camacho (2014)	5

ROAD SEGMENT: 57.1

Road:	CV-245	
Initial station:	0+620	Town
Final station:	3+270	Town
		Constrained

AADT:	209 vpd
Length:	2352 m

OPERATIONAL CHARACTERISTICS

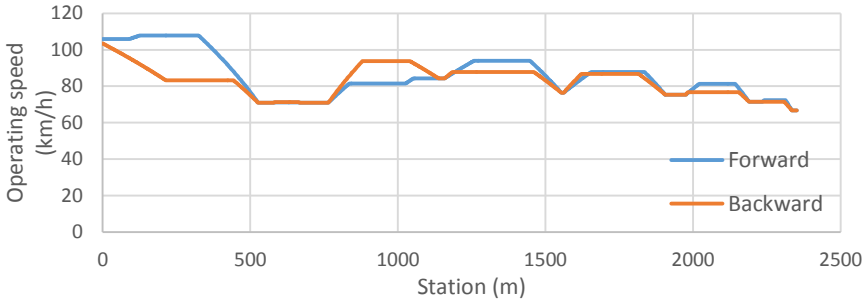

CCR	136.3315 gon/km	$\overline{\Delta v_{85}}$	13.370348 km/h
$\bar{v}_{85}$	84.17251 km/h	d_{85}	1.1470475 m/s^2
$\sigma_{v_{85}}$	10.06696 km/h	$\sigma_{\Delta v_{85}}$	11.135238 km/h
R_a	2.202866 km/h	$\sigma_{d_{85}}$	0.1433173 m/s^2
$E_{a,10}$	1.312672 km/h	$\bar{L}_{\Delta v_{85}}$	73.222222 m
$E_{a,20}$	0.473167 km/h	L_d	14.01%
L_{10}	0.30102 m	N	9
L_{20}	0.074192 m		

CONSISTENCY

Polus (2004)	0.50661
Garach (2013)	0.78103
Camacho (2014	2.73167

CRASHES

Observed:	0
Estimated:	
Exposure	1
Polus (2004)	1
Camacho (2009)	1
Garach (2013)	1
Camacho (2014)	1

ROAD SEGMENT: 58.1

Road:	CV-245	
Initial station:	3+770	Town
Final station:	6+000	Free
		Constrained

AADT:	209 vpd
Length:	2229 m

OPERATIONAL CHARACTERISTICS

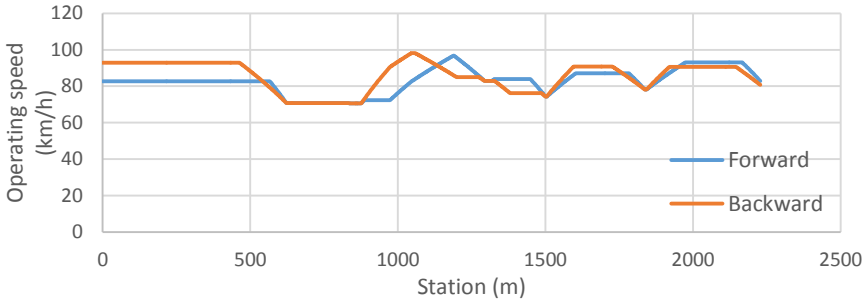

CCR	97.39913 gon/km	$\overline{\Delta v_{85}}$	13.930133 km/h
$\bar{v}_{85}$	84.22491 km/h	d_{85}	1.0870184 m/s^2
$\sigma_{v_{85}}$	7.481862 km/h	$\sigma_{\Delta v_{85}}$	6.0403928 km/h
R_a	1.712146 km/h	$\sigma_{d_{85}}$	0.0987306 m/s^2
$E_{a,10}$	0.657531 km/h	$\bar{L}_{\Delta v_{85}}$	84 m
$E_{a,20}$	0 km/h	L_d	15.08%
L_{10}	0.184919 m	N	8
L_{20}	0 m		

CONSISTENCY

Polus (2004)	1.0442
Garach (2013)	1.3245
Camacho (2014	2.78164

CRASHES

Observed:	1
Estimated:	
Exposure	1
Polus (2004)	1
Camacho (2009)	0
Garach (2013)	1
Camacho (2014)	1

ROAD SEGMENT: 58.2

Road:	CV-245	
Initial station:	6+000	Free
Final station:	6+690	Roundabout
		Constrained

AADT:	209 vpd
Length:	853 m

OPERATIONAL CHARACTERISTICS

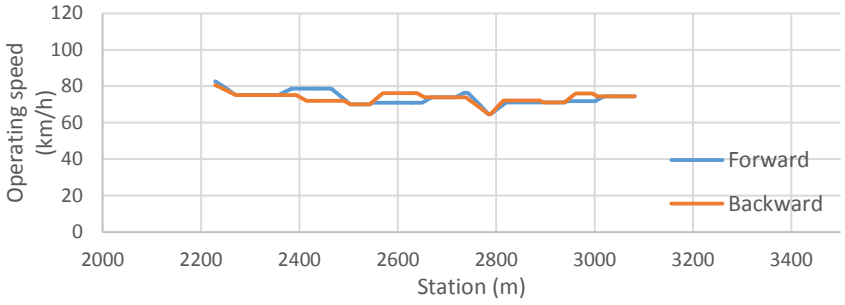

CCR	287.2062 gon/km	$\overline{\Delta v_{85}}$	7.7348988 km/h
$\bar{v}_{85}$	73.40413 km/h	d_{85}	1.3205494 m/s^2
$\sigma_{v_{85}}$	2.944703 km/h	$\sigma_{\Delta v_{85}}$	2.331361 km/h
R_a	0.666671 km/h	$\sigma_{d_{85}}$	0.1619544 m/s^2
$E_{a,10}$	0 km/h	$\bar{L}_{\Delta v_{85}}$	33 m
$E_{a,20}$	0 km/h	L_d	11.61%
L_{10}	0 m	N	6
L_{20}	0 m		

CONSISTENCY

Polus (2004)	2.41301
Garach (2013)	2.35324
Camacho (2014	2.49012

CRASHES

Observed:	0
Estimated:	
Exposure	0
Polus (2004)	0
Camacho (2009)	0
Garach (2013)	0
Camacho (2014)	0

ROAD SEGMENT: 59.1

Road:	CV-585	
Initial station:	0+160	Roundabout
Final station:	3+100	Free
		Constrained

AADT:	3555 vpd
Length:	2944 m

OPERATIONAL CHARACTERISTICS

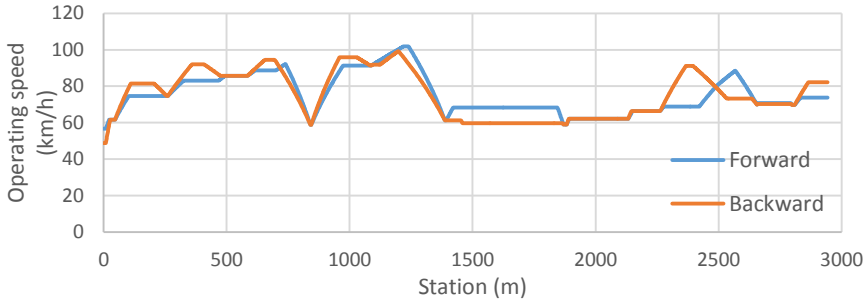

CCR	166.3165 gon/km	$\overline{\Delta v_{85}}$	16.710478 km/h
$\bar{v}_{85}$	75.57426 km/h	d_{85}	1.5672234 m/s^2
$\sigma_{v_{85}}$	11.60069 km/h	$\sigma_{\Delta v_{85}}$	12.419634 km/h
R_a	2.803927 km/h	$\sigma_{d_{85}}$	0.5549415 m/s^2
$E_{a,10}$	2.03269 km/h	$\bar{L}_{\Delta v_{85}}$	65.933333 m
$E_{a,20}$	0.298062 km/h	L_d	16.80%
L_{10}	0.485389 m	N	15
L_{20}	0.04774 m		

CONSISTENCY

Polus (2004)	0.22778
Garach (2013)	0.30603
Camacho (2014	2.37491

CRASHES

Observed:	12
Estimated:	
Exposure	7
Polus (2004)	18
Camacho (2009)	13
Garach (2013)	23
Camacho (2014)	11

ROAD SEGMENT: 59.2

Road:	CV-585	
Initial station:	3+100	Free
Final station:	4+120	Free
		Free

AADT:	3555	vpd
Length:	1018	m

OPERATIONAL CHARACTERISTICS

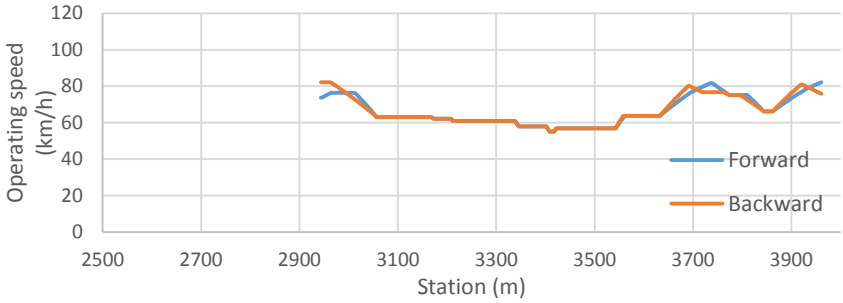

CCR	463.9704	gon/km	$\overline{\Delta v_{85}}$	7.6426985	km/h
$\bar{v}_{85}$	66.41077	km/h	d_{85}	1.6703051	m/s^2
$\sigma_{v_{85}}$	7.769668	km/h	$\sigma_{\Delta v_{85}}$	5.6214187	km/h
R_a	1.89745	km/h	$\sigma_{d_{85}}$	0.3214636	m/s^2
$E_{a,10}$	0.644225	km/h	$\bar{L}_{\Delta v_{85}}$	27.1	m
$E_{a,20}$	0	km/h	L_d	13.32%	
L_{10}	0.19174	m	N	10	
L_{20}	0	m			

CONSISTENCY

Polus (2004)	0.89944
Garach (2013)	1.18829
Camacho (2014	2.22697

CRASHES

Observed:	2
Estimated:	
Exposure	3
Polus (2004)	5
Camacho (2009)	4
Garach (2013)	8
Camacho (2014)	4

ROAD SEGMENT: 59.3

Road:	CV-585	
Initial station:	4+120	Free
Final station:	5+290	Free
		Free

AADT:	3555	vpd
Length:	1169	m

OPERATIONAL CHARACTERISTICS

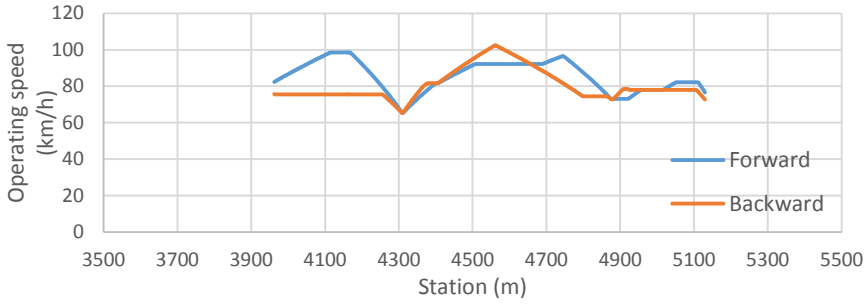

CCR	101.6543	gon/km	$\overline{\Delta v_{85}}$	17.540921	km/h
$\bar{v}_{85}$	83.13869	km/h	d_{85}	1.333034	m/s^2
$\sigma_{v_{85}}$	8.774073	km/h	$\sigma_{\Delta v_{85}}$	10.762101	km/h
R_a	2.135704	km/h	$\sigma_{d_{85}}$	0.2917141	m/s^2
$E_{a,10}$	0.900752	km/h	$\bar{L}_{\Delta v_{85}}$	90	m
$E_{a,20}$	0	km/h	L_d	23.12%	
L_{10}	0.240582	m	N	6	
L_{20}	0	m			

CONSISTENCY

Polus (2004)	0.66062
Garach (2013)	0.94837
Camacho (2014	2.58754

CRASHES

Observed:	1
Estimated:	
Exposure	3
Polus (2004)	6
Camacho (2009)	4
Garach (2013)	9
Camacho (2014)	4

ROAD SEGMENT: 59.4

Road:	CV-585	
Initial station:	5+290	Free
Final station:	5+980	Roundabout
		Constrained

AADT:	3555 vpd
Length:	676 m

OPERATIONAL CHARACTERISTICS

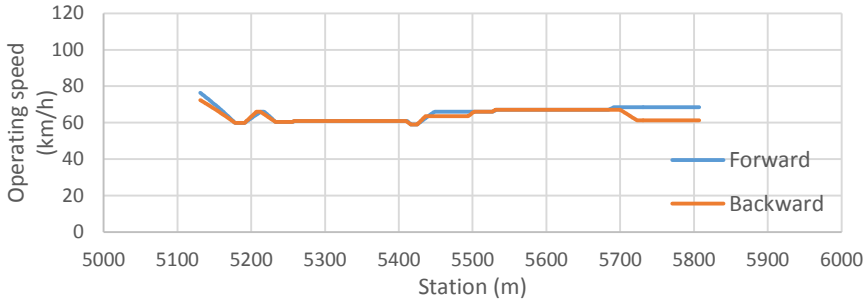

CCR	458.3786 gon/km	$\overline{\Delta v_{85}}$	5.4446061 km/h
$\bar{v}_{85}$	64.2747 km/h	d_{85}	1.6764443 m/s^2
$\sigma_{v_{85}}$	3.29149 km/h	$\sigma_{\Delta v_{85}}$	5.2090828 km/h
R_a	0.835853 km/h	$\sigma_{d_{85}}$	0.1637607 m/s^2
$E_{a,10}$	0.015977 km/h	$\bar{L}_{\Delta v_{85}}$	15.571429 m
$E_{a,20}$	0 km/h	L_d	8.06%
L_{10}	0.005178 m	N	7
L_{20}	0 m		

CONSISTENCY

Polus (2004)	2.27054
Garach (2013)	2.23309
Camacho (2014	2.20014

CRASHES

Observed:	6
Estimated:	
Exposure	2
Polus (2004)	2
Camacho (2009)	1
Garach (2013)	5
Camacho (2014)	2

ROAD SEGMENT: 60.1

Road:	CV-790	
Initial station:	0+020	Intersection
Final station:	1+990	Free
		Constrained

AADT:	1966 vpd
Length:	1966 m

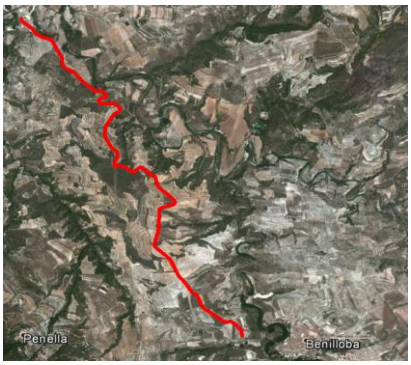

OPERATIONAL CHARACTERISTICS

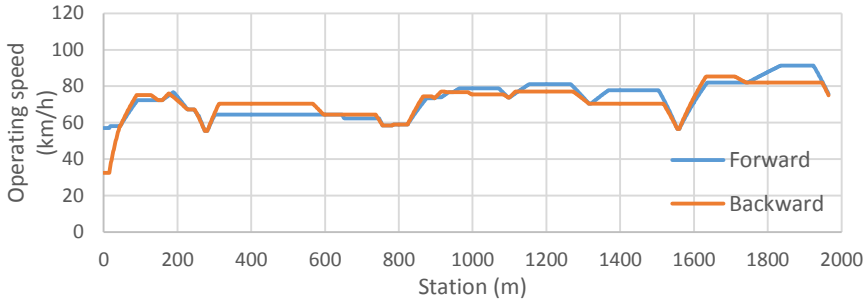

CCR	242.5701 gon/km	$\overline{\Delta v_{85}}$	11.339735 km/h
$\bar{v}_{85}$	72.22365 km/h	d_{85}	1.7891807 m/s^2
$\sigma_{v_{85}}$	8.857718 km/h	$\sigma_{\Delta v_{85}}$	8.4095942 km/h
R_a	1.981135 km/h	$\sigma_{d_{85}}$	0.5605714 m/s^2
$E_{a,10}$	0.791273 km/h	$\bar{L}_{\Delta v_{85}}$	30.882353 m
$E_{a,20}$	0.085825 km/h	L_d	13.36%
L_{10}	0.187786 m	N	17
L_{20}	0.00916 m		

CONSISTENCY

Polus (2004)	0.72423
Garach (2013)	1.02888
Camacho (2014	2.23824

CRASHES

Observed:	1
Estimated:	
Exposure	3
Polus (2004)	6
Camacho (2009)	4
Garach (2013)	8
Camacho (2014)	5

ROAD SEGMENT: 60.2

Road:	CV-790	
Initial station:	1+990	Free
Final station:	5+890	Roundabout
		Constrained

AADT:	2541 vpd
Length:	3908 m

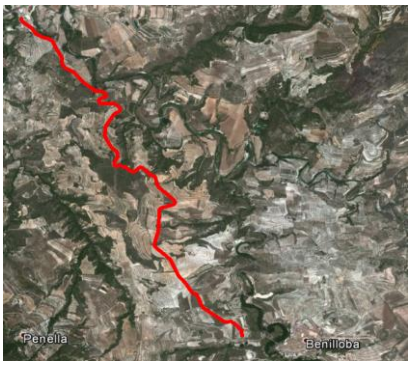

OPERATIONAL CHARACTERISTICS

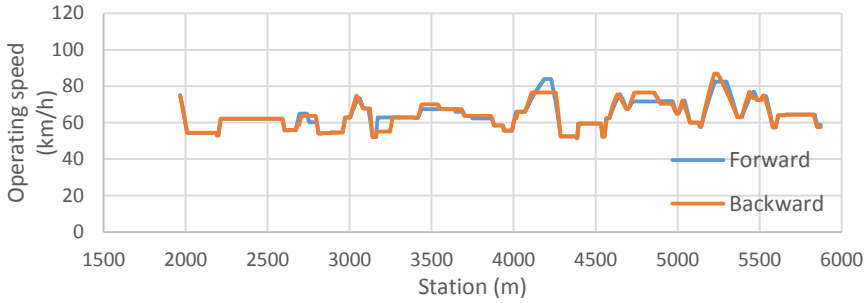

CCR	547.8734 gon/km	$\overline{\Delta v_{85}}$	8.1322063 km/h
$\bar{v}_{85}$	64.4139 km/h	d_{85}	1.9199261 m/s^2
$\sigma_{v_{85}}$	7.275906 km/h	$\sigma_{\Delta v_{85}}$	6.8407465 km/h
R_a	1.583891 km/h	$\sigma_{d_{85}}$	0.5360635 m/s^2
$E_{a,10}$	0.60241 km/h	$\bar{L}_{\Delta v_{85}}$	21.666667 m
$E_{a,20}$	0.033346 km/h	L_d	12.47%
L_{10}	0.16607 m	N	45
L_{20}	0.005502 m		

CONSISTENCY

Polus (2004)	1.1532
Garach (2013)	1.41823
Camacho (2014	2.10441

CRASHES

Observed:	3
Estimated:	
Exposure	8
Polus (2004)	13
Camacho (2009)	9
Garach (2013)	16
Camacho (2014)	13

ROAD SEGMENT: 61.1

Road:	CV-11	
Initial station:	10+660	Town
Final station:	17+920	Free
		Constrained

AADT:	3267	vpd
Length:	7218	m

OPERATIONAL CHARACTERISTICS

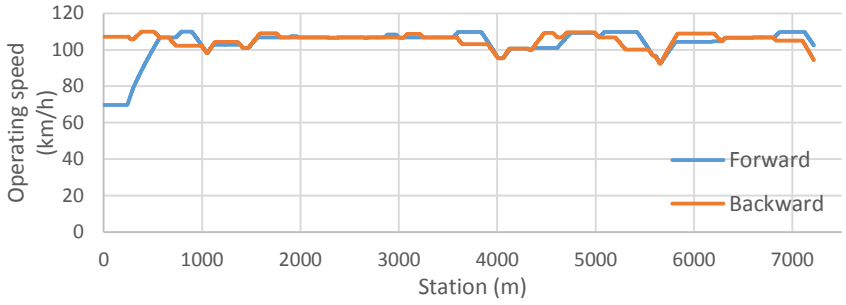

CCR	20.8147	gon/km	$\overline{\Delta v_{85}}$	6.6803662	km/h
$\bar{v}_{85}$	104.5467	km/h	d_{85}	0.5554363	m/s^2
$\sigma_{v_{85}}$	6.33371	km/h	$\sigma_{\Delta v_{85}}$	4.8512242	km/h
R_a	1.077902	km/h	$\sigma_{d_{85}}$	0.1139729	m/s^2
$E_{a,10}$	0.266643	km/h	$\bar{L}_{\Delta v_{85}}$	89.705882	m
$E_{a,20}$	0.216934	km/h	L_d	10.56%	
L_{10}	0.037961	m	N	17	
L_{20}	0.024106	m			

CONSISTENCY

Polus (2004)	1.65743
Garach (2013)	1.79133
Camacho (2014	3.73931

CRASHES

Observed:	15
Estimated:	
Exposure	16
Polus (2004)	25
Camacho (2009)	18
Garach (2013)	33
Camacho (2014)	12

ROAD SEGMENT: 61.2

Road:	CV-11	
Initial station:	17+920	Free
Final station:	19+320	Roundabout
		Constrained

AADT:	3267 vpd
Length:	1390 m

OPERATIONAL CHARACTERISTICS

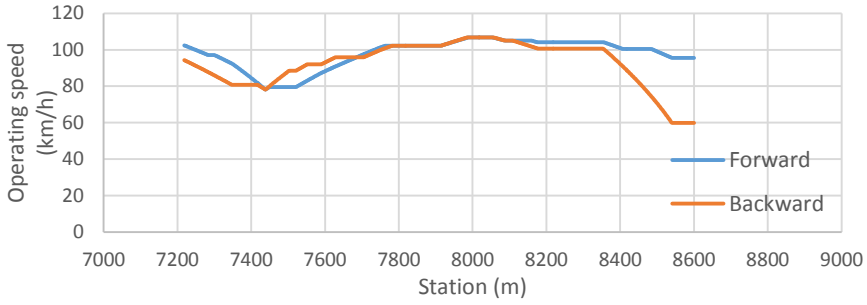

CCR	61.47359 gon/km	$\overline{\Delta v_{85}}$	6.3106973 km/h
$\bar{v}_{85}$	95.30684 km/h	d_{85}	0.6887512 m/s^2
$\sigma_{v_{85}}$	10.64031 km/h	$\sigma_{\Delta v_{85}}$	4.9770563 km/h
R_a	2.345338 km/h	$\sigma_{d_{85}}$	0.1865231 m/s^2
$E_{a,10}$	1.216188 km/h	$\bar{L}_{\Delta v_{85}}$	62.8 m
$E_{a,20}$	0.37923 km/h	L_d	22.72%
L_{10}	0.273155 m	N	10
L_{20}	0.043415 m		

CONSISTENCY

Polus (2004)	0.40876
Garach (2013)	0.6455
Camacho (2014	3.37484

CRASHES

Observed:	5
Estimated:	
Exposure	3
Polus (2004)	7
Camacho (2009)	5
Garach (2013)	11
Camacho (2014)	2

ROAD SEGMENT: 62.1

Road:	CV-17	
Initial station:	0+230	Roundabout
Final station:	3+370	Roundabout
		Constrained

AADT:	16339	vpd
Length:	3117	m

OPERATIONAL CHARACTERISTICS

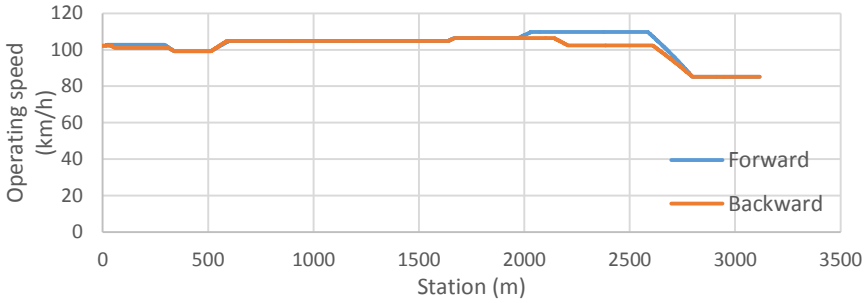

CCR	73.20549	gon/km	$\overline{\Delta v_{85}}$	8.8091013	km/h
$\bar{v}_{85}$	102.0421	km/h	d_{85}	0.6155283	m/s^2
$\sigma_{v_{85}}$	6.745556	km/h	$\sigma_{\Delta v_{85}}$	10.665212	km/h
R_a	1.328241	km/h	$\sigma_{d_{85}}$	0.1893926	m/s^2
$E_{a,10}$	0.554383	km/h	$\bar{L}_{\Delta v_{85}}$	91	m
$E_{a,20}$	0	km/h	L_d	5.84%	
L_{10}	0.122714	m	N	4	
L_{20}	0	m			

CONSISTENCY

Polus (2004)	1.40577
Garach (2013)	1.6148
Camacho (2014	3.58434

CRASHES

Observed:	12
Estimated:	
Exposure	17
Polus (2004)	59
Camacho (2009)	42
Garach (2013)	94
Camacho (2014)	18

ROAD SEGMENT: 63.1

Road:	CV-403	
Initial station:	2+050	Roundabout
Final station:	3+320	Roundabout
		Constrained

AADT:	14176	vpd
Length:	1228	m

OPERATIONAL CHARACTERISTICS

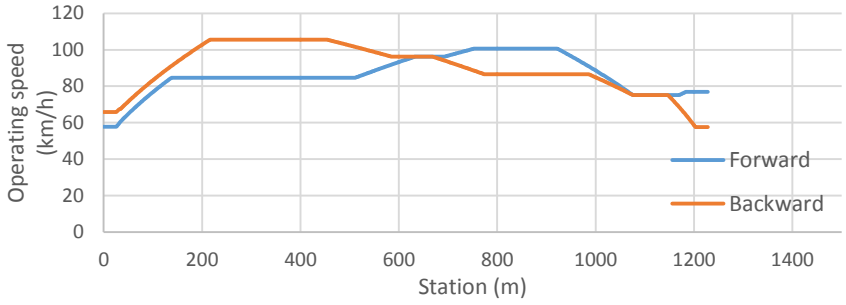

CCR	96.73083	gon/km	$\overline{\Delta v_{85}}$	21.74007	km/h
$\bar{v}_{85}$	88.11065	km/h	d_{85}	1.2930735	m/s^2
$\sigma_{v_{85}}$	11.83297	km/h	$\sigma_{\Delta v_{85}}$	18.541096	km/h
R_a	2.671884	km/h	$\sigma_{d_{85}}$	0.146355	m/s^2
$E_{a,10}$	2.021895	km/h	$\bar{L}_{\Delta v_{85}}$	114.33333	m
$E_{a,20}$	0.463253	km/h	L_d	13.97%	
L_{10}	0.461319	m	N	3	
L_{20}	0.063925	m			

CONSISTENCY

Polus (2004)	0.24438
Garach (2013)	0.35781
Camacho (2014	2.66502

CRASHES

Observed:	4
Estimated:	
Exposure	6
Polus (2004)	30
Camacho (2009)	21
Garach (2013)	48
Camacho (2014)	10

ROAD SEGMENT: 64.1

Road:	CV-407	
Initial station:	0+500	Town
Final station:	2+160	Roundabout
		Constrained

AADT:	13149 vpd
Length:	1633 m

OPERATIONAL CHARACTERISTICS

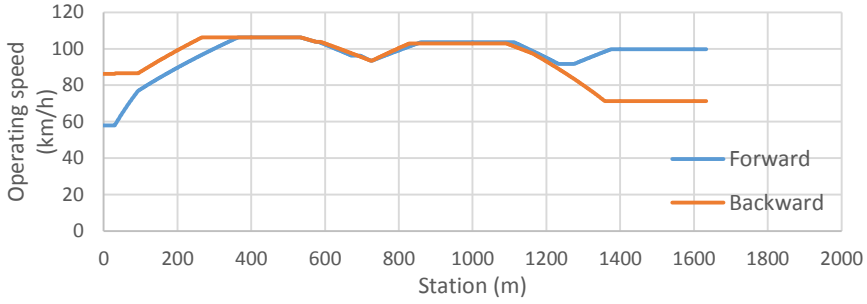

CCR	50.01479 gon/km	$\overline{\Delta v_{85}}$	9.0433008 km/h
$\bar{v}_{85}$	95.40375 km/h	d_{85}	0.682072 m/s^2
$\sigma_{v_{85}}$	11.51004 km/h	$\sigma_{\Delta v_{85}}$	6.4524532 km/h
R_a	2.479066 km/h	$\sigma_{d_{85}}$	0.1279558 m/s^2
$E_{a,10}$	1.482098 km/h	$\bar{L}_{\Delta v_{85}}$	93.833333 m
$E_{a,20}$	0.851916 km/h	L_d	17.24%
L_{10}	0.312309 m	N	6
L_{20}	0.119412 m		

CONSISTENCY

Polus (2004)	0.31006
Garach (2013)	0.48943
Camacho (2014	3.38697

CRASHES

Observed:	3
Estimated:	
Exposure	8
Polus (2004)	37
Camacho (2009)	25
Garach (2013)	55
Camacho (2014)	8

ROAD SEGMENT: 65.1

Road:	CV-720	
Initial station:	0+020	Town
Final station:	2+380	Town
		Constrained

AADT:	363 vpd
Length:	2367 m

OPERATIONAL CHARACTERISTICS

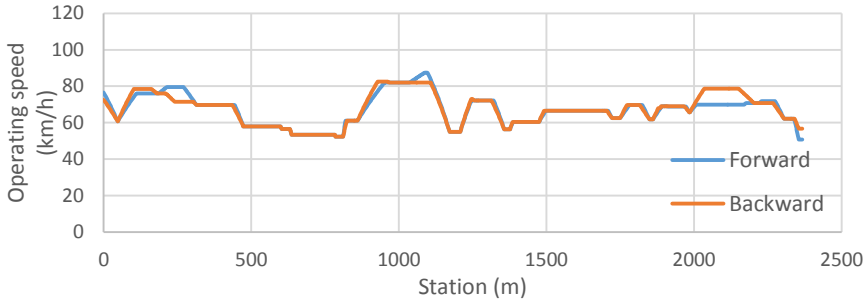

CCR	464.3329 gon/km	$\overline{\Delta v_{85}}$	10.068865 km/h
$\bar{v}_{85}$	67.43309 km/h	d_{85}	1.9075136 m/s^2
$\sigma_{v_{85}}$	8.245858 km/h	$\sigma_{\Delta v_{85}}$	7.6352851 km/h
R_a	1.843024 km/h	$\sigma_{d_{85}}$	0.4923494 m/s^2
$E_{a,10}$	1.014593 km/h	$\bar{L}_{\Delta v_{85}}$	27.652174 m
$E_{a,20}$	0 km/h	L_d	13.43%
L_{10}	0.273764 m	N	23
L_{20}	0 m		

CONSISTENCY

Polus (2004)	0.8684
Garach (2013)	1.17057
Camacho (2014	2.14142

CRASHES

Observed:	1
Estimated:	
Exposure	2
Polus (2004)	1
Camacho (2009)	1
Garach (2013)	1
Camacho (2014)	2

IV. Statistical adjustments

IV.1. Model considering exposure

```
> summary(Complete)

Call:
glm.nb(formula = SPFData$Accidents ~ log(SPFData$Length) + log(SPFData
$AADT),
    init.theta = 3.501506578, link = log)

Deviance Residuals:
    Min       1Q   Median       3Q      Max
-2.7199  -0.8797  -0.3313   0.3208   2.6802

Coefficients:
                     Estimate Std. Error z value Pr(>|z|)
(Intercept)         -4.16565    0.48437   -8.60   <2e-16 ***
log(SPFData$Length)  0.97389    0.09068   10.74   <2e-16 ***
log(SPFData$AADT)    0.61301    0.06078   10.09   <2e-16 ***
---
Signif. codes:  0 ‘***’ 0.001 ‘**’ 0.01 ‘*’ 0.05 ‘.’ 0.1 ‘ ’ 1

(Dispersion parameter for Negative Binomial(3.5015) family taken to be
 1)

    Null deviance: 442.48  on 152  degrees of freedom
Residual deviance: 154.28  on 150  degrees of freedom
AIC: 712.27

Number of Fisher Scoring iterations: 1


              Theta:  3.502
          Std. Err.:  0.721

 2 x log-likelihood:  -704.265


> summary(ModelFree)

Call:
glm.nb(formula = Free$Accidents ~ log(Free$Length) + log(Free$AADT),
    init.theta = 7.509376904, link = log)

Deviance Residuals:
    Min       1Q   Median       3Q      Max
-2.1056  -1.0484  -0.1022   0.4856   2.4154

Coefficients:
                 Estimate Std. Error z value Pr(>|z|)
(Intercept)       -5.5596     0.8777  -6.334 2.39e-10 ***
log(Free$Length)   0.7370     0.1385   5.321 1.03e-07 ***
log(Free$AADT)     0.8080     0.1159   6.972 3.13e-12 ***
---
Signif. codes:  0 ‘***’ 0.001 ‘**’ 0.01 ‘*’ 0.05 ‘.’ 0.1 ‘ ’ 1

(Dispersion parameter for Negative Binomial(7.5094) family taken to be
 1)
```

```
    Null deviance: 183.877  on 60  degrees of freedom
Residual deviance:  64.556  on 58  degrees of freedom
AIC: 234.45

Number of Fisher Scoring iterations: 1


              Theta:  7.51
          Std. Err.:  4.79

 2 x log-likelihood:  -226.448


> summary(ModelConstrained)

Call:
glm.nb(formula = Constrained$Accidents ~ log(Constrained$Length) +
    log(Constrained$AADT), init.theta = 3.356820922, link = log)

Deviance Residuals:
    Min       1Q   Median       3Q      Max
-2.7193  -0.9188  -0.3770   0.3052   2.2852

Coefficients:
                      Estimate Std. Error z value Pr(>|z|)
(Intercept)           -3.65890    0.58817  -6.221 4.95e-10 ***
log(Constrained$Length)  1.00638    0.11387   8.838  < 2e-16 ***
log(Constrained$AADT)    0.55137    0.07053   7.818 5.37e-15 ***
---
Signif. codes:  0 ‘***’ 0.001 ‘**’ 0.01 ‘*’ 0.05 ‘.’ 0.1 ‘ ’ 1

(Dispersion parameter for Negative Binomial(3.3568) family taken to be
 1)

    Null deviance: 253.70  on 91  degrees of freedom
Residual deviance:  93.61  on 89  degrees of freedom
AIC: 477.7

Number of Fisher Scoring iterations: 1


              Theta:  3.357
          Std. Err.:  0.796

 2 x log-likelihood:  -469.701
```

IV.2. Models considering one operational parameter

CCR

```
> summary(Completo)

Call:
glm.nb(formula = SPFData$Accidents ~ log(SPFData$Length) + log(SPFData
$AADT) +
    SPFData$CCR, init.theta = 3.751857224, link = log)

Deviance Residuals:
    Min       1Q   Median       3Q      Max
-2.6622  -0.8939  -0.3067   0.3969   2.6235

Coefficients:
```

```
                      Estimate Std. Error z value Pr(>|z|)
(Intercept)         -5.2596612  0.6314302  -8.330  < 2e-16 ***
log(SPFData$Length)  1.0229543  0.0907238  11.275  < 2e-16 ***
log(SPFData$AADT)    0.7250004  0.0731651   9.909  < 2e-16 ***
SPFData$CCR          0.0010109  0.0003607   2.802  0.00507 **
---
Signif. codes:  0 ‘***’ 0.001 ‘**’ 0.01 ‘*’ 0.05 ‘.’ 0.1 ‘ ’ 1

(Dispersion parameter for Negative Binomial(3.7519) family taken to be
 1)

    Null deviance: 459.56  on 152  degrees of freedom
Residual deviance: 152.11  on 149  degrees of freedom
AIC: 707.16

Number of Fisher Scoring iterations: 1


              Theta:  3.752
          Std. Err.:  0.791

 2 x log-likelihood:  -697.157


> summary(ModelFree)

Call:
glm.nb(formula = Free$Accidents ~ log(Free$Length) + log(Free$AADT) +
    Free$CCR, init.theta = 9.50154796, link = log)

Deviance Residuals:
    Min       1Q   Median       3Q      Max
-1.9950  -0.9752  -0.0889   0.4537   2.5535

Coefficients:
                  Estimate Std. Error z value Pr(>|z|)
(Intercept)      -6.631065   0.991070  -6.691 2.22e-11 ***
log(Free$Length)  0.851248   0.145182   5.863 4.54e-09 ***
log(Free$AADT)    0.909525   0.121670   7.475 7.70e-14 ***
Free$CCR          0.001157   0.000525   2.204   0.0275 *
---
Signif. codes:  0 ‘***’ 0.001 ‘**’ 0.01 ‘*’ 0.05 ‘.’ 0.1 ‘ ’ 1

(Dispersion parameter for Negative Binomial(9.5015) family taken to be
 1)

    Null deviance: 196.703  on 60  degrees of freedom
Residual deviance:  63.333  on 57  degrees of freedom
AIC: 232.04

Number of Fisher Scoring iterations: 1


              Theta:  9.50
          Std. Err.:  6.99

 2 x log-likelihood:  -222.039


> summary(ModelConstrained)

Call:
glm.nb(formula = Constrained$Accidents ~ log(Constrained$Length) +
    log(Constrained$AADT) + Constrained$CCR, init.theta = 3.421453062,

    link = log)
```

```
Deviance Residuals:
    Min       1Q   Median       3Q      Max
-2.6650  -0.9228  -0.3574   0.3322   2.2008

Coefficients:
                        Estimate Std. Error z value Pr(>|z|)
(Intercept)            -4.4255976  0.8197535  -5.399 6.71e-08 ***
log(Constrained$Length)  1.0280685  0.1142116   9.001  < 2e-16 ***
log(Constrained$AADT)    0.6311256  0.0922515   6.841 7.84e-12 ***
Constrained$CCR          0.0006884  0.0004847   1.420    0.156
---
Signif. codes:  0 ‘***’ 0.001 ‘**’ 0.01 ‘*’ 0.05 ‘.’ 0.1 ‘ ’ 1

(Dispersion parameter for Negative Binomial(3.4215) family taken to be
 1)

    Null deviance: 256.685  on 91  degrees of freedom
Residual deviance:  92.767  on 88  degrees of freedom
AIC: 477.89

Number of Fisher Scoring iterations: 1


              Theta:  3.421
          Std. Err.:  0.817

 2 x log-likelihood:  -467.892
```

Average Operating Speed (SpeedAvg)

```
> summary(Complete)

Call:
glm.nb(formula = SPFData$Accidents ~ log(SPFData$Length) + log(SPFData
$AADT) +
    SPFData$SpeedAvg, init.theta = 4.295215794, link = log)

Deviance Residuals:
    Min       1Q   Median       3Q      Max
-2.5121  -0.9772  -0.2559   0.5250   2.6070

Coefficients:
                     Estimate Std. Error z value Pr(>|z|)
(Intercept)          -3.77054    0.46981  -8.026 1.01e-15 ***
log(SPFData$Length)   1.09419    0.09232  11.853  < 2e-16 ***
log(SPFData$AADT)     0.80858    0.07516  10.758  < 2e-16 ***
SPFData$SpeedAvg     -0.02322    0.00556  -4.177 2.95e-05 ***
---
Signif. codes:  0 ‘***’ 0.001 ‘**’ 0.01 ‘*’ 0.05 ‘.’ 0.1 ‘ ’ 1

(Dispersion parameter for Negative Binomial(4.2952) family taken to be
 1)

    Null deviance: 493.72  on 152  degrees of freedom
Residual deviance: 151.94  on 149  degrees of freedom
AIC: 697.75

Number of Fisher Scoring iterations: 1


              Theta:  4.295
          Std. Err.:  0.964
```

```
 2 x log-likelihood:  -687.747
```

```
> summary(ModelFree)

Call:
glm.nb(formula = Free$Accidents ~ log(Free$Length) + log(Free$AADT) +
    Free$SpeedAvg, init.theta = 11.67072641, link = log)

Deviance Residuals:
    Min       1Q   Median       3Q      Max
-1.9889  -1.1195  -0.1351   0.6070   2.3992

Coefficients:
                  Estimate Std. Error z value Pr(>|z|)
(Intercept)      -5.156144   0.854020  -6.037 1.57e-09 ***
log(Free$Length)  0.913649   0.150779   6.060 1.37e-09 ***
log(Free$AADT)    0.980499   0.129028   7.599 2.98e-14 ***
Free$SpeedAvg    -0.021021   0.008467  -2.483    0.013 *
---
Signif. codes:  0 ‘***’ 0.001 ‘**’ 0.01 ‘*’ 0.05 ‘.’ 0.1 ‘ ’ 1

(Dispersion parameter for Negative Binomial(11.6707) family taken to b
e 1)

    Null deviance: 207.162  on 60  degrees of freedom
Residual deviance:  64.502  on 57  degrees of freedom
AIC: 230.8

Number of Fisher Scoring iterations: 1


              Theta:  11.67
          Std. Err.:  9.91

 2 x log-likelihood:  -220.804
```

```
> summary(ModelConstrained)

Call:
glm.nb(formula = Constrained$Accidents ~ log(Constrained$Length) +
    log(Constrained$AADT) + Constrained$SpeedAvg, init.theta = 3.87878
9256,
    link = log)

Deviance Residuals:
    Min       1Q   Median       3Q      Max
-2.4984  -0.9054  -0.2066   0.5247   2.1252

Coefficients:
                       Estimate Std. Error z value Pr(>|z|)
(Intercept)           -3.416705   0.573888  -5.954 2.62e-09 ***
log(Constrained$Length)  1.110393   0.116797   9.507  < 2e-16 ***
log(Constrained$AADT)    0.742510   0.095728   7.756 8.74e-15 ***
Constrained$SpeedAvg    -0.021276   0.007197  -2.956  0.00311 **
---
Signif. codes:  0 ‘***’ 0.001 ‘**’ 0.01 ‘*’ 0.05 ‘.’ 0.1 ‘ ’ 1

(Dispersion parameter for Negative Binomial(3.8788) family taken to be
 1)

    Null deviance: 276.811  on 91  degrees of freedom
Residual deviance:  92.421  on 88  degrees of freedom
AIC: 471.38

Number of Fisher Scoring iterations: 1
```

```
              Theta:  3.879
          Std. Err.:  0.978

 2 x log-likelihood:  -461.383
```

Operating speed dispersion (SpeedDisp)

```
> summary(Complete)

Call:
glm.nb(formula = SPFData$Accidents ~ log(SPFData$Length) + log(SPFData
$AADT) +
    SPFData$SpeedDisp, init.theta = 3.866818868, link = log)

Deviance Residuals:
    Min       1Q   Median       3Q      Max
-2.7041  -0.9394  -0.2758   0.3034   2.7766

Coefficients:
                    Estimate Std. Error z value Pr(>|z|)
(Intercept)         -4.87450    0.56786  -8.584   <2e-16 ***
log(SPFData$Length)  1.00084    0.09167  10.918   <2e-16 ***
log(SPFData$AADT)    0.64333    0.06067  10.603   <2e-16 ***
SPFData$SpeedDisp    0.05347    0.02313   2.312   0.0208 *
---
Signif. codes:  0 ‘***’ 0.001 ‘**’ 0.01 ‘*’ 0.05 ‘.’ 0.1 ‘ ’ 1

(Dispersion parameter for Negative Binomial(3.8668) family taken to be
 1)

    Null deviance: 467.10  on 152  degrees of freedom
Residual deviance: 156.07  on 149  degrees of freedom
AIC: 709

Number of Fisher Scoring iterations: 1


              Theta:  3.867
          Std. Err.:  0.837

 2 x log-likelihood:  -698.996


> summary(ModelFree)

Call:
glm.nb(formula = Free$Accidents ~ log(Free$Length) + log(Free$AADT) +
    Free$SpeedDisp, init.theta = 8.478517675, link = log)

Deviance Residuals:
     Min        1Q    Median        3Q       Max
-2.00598  -0.98520  -0.08207   0.37216   2.16949

Coefficients:
                  Estimate Std. Error z value Pr(>|z|)
(Intercept)      -6.48090    1.21362  -5.340 9.29e-08 ***
log(Free$Length)  0.75908    0.13667   5.554 2.79e-08 ***
log(Free$AADT)    0.88819    0.13679   6.493 8.42e-11 ***
Free$SpeedDisp    0.04066    0.03609   1.127     0.26
---
Signif. codes:  0 ‘***’ 0.001 ‘**’ 0.01 ‘*’ 0.05 ‘.’ 0.1 ‘ ’ 1
```

```
(Dispersion parameter for Negative Binomial(8.4785) family taken to be
 1)

    Null deviance: 190.598  on 60  degrees of freedom
Residual deviance:  65.093  on 57  degrees of freedom
AIC: 235.28

Number of Fisher Scoring iterations: 1


              Theta:  8.48
          Std. Err.:  5.82

 2 x log-likelihood:  -225.28


> summary(ModelConstrained)

Call:
glm.nb(formula = Constrained$Accidents ~ log(Constrained$Length) +
    log(Constrained$AADT) + Constrained$SpeedDisp, init.theta = 3.9412
34404,
    link = log)

Deviance Residuals:
    Min       1Q   Median       3Q      Max
-2.6713  -0.8636  -0.2150   0.3218   2.7855

Coefficients:
                      Estimate Std. Error z value Pr(>|z|)
(Intercept)           -4.57360    0.71713  -6.378  1.8e-10 ***
log(Constrained$Length)  1.07050    0.11878   9.013  < 2e-16 ***
log(Constrained$AADT)    0.58012    0.06945   8.353  < 2e-16 ***
Constrained$SpeedDisp    0.06990    0.03181   2.197    0.028 *
---
Signif. codes:  0 ‘***’ 0.001 ‘**’ 0.01 ‘*’ 0.05 ‘.’ 0.1 ‘ ’ 1

(Dispersion parameter for Negative Binomial(3.9412) family taken to be
 1)

    Null deviance: 279.429  on 91  degrees of freedom
Residual deviance:  96.625  on 88  degrees of freedom
AIC: 474.83

Number of Fisher Scoring iterations: 1


              Theta:  3.94
          Std. Err.:  1.01

 2 x log-likelihood:  -464.825
```

Ra

```
> summary(Complete)

Call:
glm.nb(formula = SPFData$Accidents ~ log(SPFData$Length) + log(SPFData
$AADT) +
    SPFData$Ra, init.theta = 3.902715077, link = log)

Deviance Residuals:
    Min       1Q   Median       3Q      Max
```

```
-2.6268  -0.9937  -0.2748   0.3503   2.8044

Coefficients:
                  Estimate Std. Error z value Pr(>|z|)
(Intercept)       -4.88365    0.56286  -8.676   <2e-16 ***
log(SPFData$Length)  1.00394    0.09133  10.993   <2e-16 ***
log(SPFData$AADT)    0.64700    0.06091  10.622   <2e-16 ***
SPFData$Ra           0.22486    0.09203   2.443   0.0145 *
---
Signif. codes:  0 ‘***’ 0.001 ‘**’ 0.01 ‘*’ 0.05 ‘.’ 0.1 ‘ ’ 1

(Dispersion parameter for Negative Binomial(3.9027) family taken to be
 1)

    Null deviance: 469.42  on 152  degrees of freedom
Residual deviance: 156.20  on 149  degrees of freedom
AIC: 708.48

Number of Fisher Scoring iterations: 1


              Theta:  3.903
          Std. Err.:  0.849

 2 x log-likelihood:  -698.485


> summary(ModelFree)

Call:
glm.nb(formula = Free$Accidents ~ log(Free$Length) + log(Free$AADT) +
    Free$Ra, init.theta = 8.157342718, link = log)

Deviance Residuals:
    Min       1Q   Median       3Q      Max
-1.9683  -1.0321  -0.1034   0.3678   2.2425

Coefficients:
                 Estimate Std. Error z value Pr(>|z|)
(Intercept)       -6.2434     1.1829  -5.278 1.31e-07 ***
log(Free$Length)   0.7502     0.1370   5.476 4.35e-08 ***
log(Free$AADT)     0.8691     0.1360   6.390 1.66e-10 ***
Free$Ra            0.1264     0.1423   0.888    0.375
---
Signif. codes:  0 ‘***’ 0.001 ‘**’ 0.01 ‘*’ 0.05 ‘.’ 0.1 ‘ ’ 1

(Dispersion parameter for Negative Binomial(8.1573) family taken to be
 1)

    Null deviance: 188.483  on 60  degrees of freedom
Residual deviance:  65.011  on 57  degrees of freedom
AIC: 235.73

Number of Fisher Scoring iterations: 1


              Theta:  8.16
          Std. Err.:  5.48

 2 x log-likelihood:  -225.727


> summary(ModelConstrained)

Call:
glm.nb(formula = Constrained$Accidents ~ log(Constrained$Length) +
```

```
    log(Constrained$AADT) + Constrained$Ra, init.theta = 4.10185959,
    link = log)

Deviance Residuals:
    Min       1Q   Median       3Q      Max
-2.5622  -0.8869  -0.2540   0.3382   2.8025

Coefficients:
                       Estimate Std. Error z value Pr(>|z|)
(Intercept)            -4.66454    0.69593  -6.703 2.05e-11 ***
log(Constrained$Length)  1.08446    0.11683   9.282  < 2e-16 ***
log(Constrained$AADT)    0.58732    0.06915   8.493  < 2e-16 ***
Constrained$Ra           0.32074    0.12267   2.615  0.00893 **
---
Signif. codes:  0 ‘***’ 0.001 ‘**’ 0.01 ‘*’ 0.05 ‘.’ 0.1 ‘ ’ 1

(Dispersion parameter for Negative Binomial(4.1019) family taken to be
 1)

    Null deviance: 286.028  on 91  degrees of freedom
Residual deviance:  96.757  on 88  degrees of freedom
AIC: 473.08

Number of Fisher Scoring iterations: 1


              Theta:  4.10
          Std. Err.:  1.07

 2 x log-likelihood:  -463.077
```

Ea,10

```
> summary(Complete)

Call:
glm.nb(formula = SPFData$Accidents ~ log(SPFData$Length) + log(SPFData
$AADT) +
    SPFData$Ea10, init.theta = 3.886545311, link = log)

Deviance Residuals:
    Min       1Q   Median       3Q      Max
-2.6613  -0.8697  -0.2735   0.2720   2.9262

Coefficients:
                     Estimate Std. Error z value Pr(>|z|)
(Intercept)          -4.60077    0.51370  -8.956   <2e-16 ***
log(SPFData$Length)   0.99307    0.09049  10.975   <2e-16 ***
log(SPFData$AADT)     0.63982    0.06047  10.582   <2e-16 ***
SPFData$Ea10          0.21017    0.08959   2.346    0.019 *
---
Signif. codes:  0 ‘***’ 0.001 ‘**’ 0.01 ‘*’ 0.05 ‘.’ 0.1 ‘ ’ 1

(Dispersion parameter for Negative Binomial(3.8865) family taken to be
 1)

    Null deviance: 468.38  on 152  degrees of freedom
Residual deviance: 156.38  on 149  degrees of freedom
AIC: 708.96

Number of Fisher Scoring iterations: 1


              Theta:  3.887
```

```
          Std. Err.:  0.845

 2 x log-likelihood:  -698.957


> summary(ModelFree)

Call:
glm.nb(formula = Free$Accidents ~ log(Free$Length) + log(Free$AADT) +
    Free$Ea10, init.theta = 7.570256423, link = log)

Deviance Residuals:
     Min        1Q    Median        3Q       Max
-2.09274  -1.06878  -0.08167   0.46557   2.39255

Coefficients:
                Estimate Std. Error z value Pr(>|z|)
(Intercept)     -5.68251    1.09152  -5.206 1.93e-07 ***
log(Free$Length)  0.73825    0.13844   5.333 9.68e-08 ***
log(Free$AADT)    0.82081    0.13449   6.103 1.04e-09 ***
Free$Ea10         0.03218    0.16603   0.194    0.846
---
Signif. codes:  0 ‘***’ 0.001 ‘**’ 0.01 ‘*’ 0.05 ‘.’ 0.1 ‘ ’ 1

(Dispersion parameter for Negative Binomial(7.5703) family taken to be
 1)

    Null deviance: 184.330  on 60  degrees of freedom
Residual deviance:  64.638  on 57  degrees of freedom
AIC: 236.41

Number of Fisher Scoring iterations: 1


             Theta:  7.57
         Std. Err.:  4.85

 2 x log-likelihood:  -226.413


> summary(ModelConstrained)

Call:
glm.nb(formula = Constrained$Accidents ~ log(Constrained$Length) +
    log(Constrained$AADT) + Constrained$Ea10, init.theta = 4.11184083,

    link = log)

Deviance Residuals:
    Min       1Q   Median       3Q      Max
-2.6174  -0.8865  -0.2472   0.3316   2.7169

Coefficients:
                      Estimate Std. Error z value Pr(>|z|)
(Intercept)             -4.2861     0.6167  -6.950 3.66e-12 ***
log(Constrained$Length)   1.0706     0.1136   9.422  < 2e-16 ***
log(Constrained$AADT)     0.5799     0.0685   8.465  < 2e-16 ***
Constrained$Ea10          0.3067     0.1106   2.773  0.00555 **
---
Signif. codes:  0 ‘***’ 0.001 ‘**’ 0.01 ‘*’ 0.05 ‘.’ 0.1 ‘ ’ 1

(Dispersion parameter for Negative Binomial(4.1118) family taken to be
 1)

    Null deviance: 286.432  on 91  degrees of freedom
Residual deviance:  96.132  on 88  degrees of freedom
```

```
AIC: 472.34

Number of Fisher Scoring iterations: 1


              Theta:  4.11
          Std. Err.:  1.07

 2 x log-likelihood:  -462.338
```

Ea,20

```
> summary(Complete)

Call:
glm.nb(formula = SPFData$Accidents ~ log(SPFData$Length) + log(SPFData
$AADT) +
    SPFData$Ea20, init.theta = 3.525857563, link = log)

Deviance Residuals:
    Min       1Q   Median       3Q      Max
-2.7301  -0.9102  -0.3212   0.2974   2.7568

Coefficients:
                    Estimate Std. Error z value Pr(>|z|)
(Intercept)         -4.20791    0.48644  -8.650   <2e-16 ***
log(SPFData$Length)  0.97814    0.09192  10.641   <2e-16 ***
log(SPFData$AADT)    0.61398    0.06067  10.119   <2e-16 ***
SPFData$Ea20         0.16215    0.26867   0.604    0.546
---
Signif. codes:  0 ‘***’ 0.001 ‘**’ 0.01 ‘*’ 0.05 ‘.’ 0.1 ‘ ’ 1

(Dispersion parameter for Negative Binomial(3.5259) family taken to be
 1)

    Null deviance: 444.19  on 152  degrees of freedom
Residual deviance: 154.42  on 149  degrees of freedom
AIC: 713.9

Number of Fisher Scoring iterations: 1


              Theta:  3.526
          Std. Err.:  0.728

 2 x log-likelihood:  -703.901


> summary(ModelFree)

Call:
glm.nb(formula = Free$Accidents ~ log(Free$Length) + log(Free$AADT) +
    Free$Ea20, init.theta = 8.765886202, link = log)

Deviance Residuals:
    Min       1Q   Median       3Q      Max
-2.2026  -1.0425  -0.1337   0.5774   2.4521

Coefficients:
                  Estimate Std. Error z value Pr(>|z|)
(Intercept)       -5.1568     0.9041  -5.704 1.17e-08 ***
log(Free$Length)   0.7207     0.1347   5.352 8.71e-08 ***
log(Free$AADT)     0.7660     0.1171   6.540 6.14e-11 ***
Free$Ea20         -0.9263     0.6861  -1.350    0.177
```

```
---
Signif. codes:  0 ‘***’ 0.001 ‘**’ 0.01 ‘*’ 0.05 ‘.’ 0.1 ‘ ’ 1

(Dispersion parameter for Negative Binomial(8.7659) family taken to be
 1)

    Null deviance: 192.406  on 60  degrees of freedom
Residual deviance:  64.888  on 57  degrees of freedom
AIC: 234.63

Number of Fisher Scoring iterations: 1


              Theta:  8.77
          Std. Err.:  6.07

 2 x log-likelihood:  -224.63


> summary(ModelConstrained)

Call:
glm.nb(formula = Constrained$Accidents ~ log(Constrained$Length) +
    log(Constrained$AADT) + Constrained$Ea20, init.theta = 3.412380897
,
    link = log)

Deviance Residuals:
    Min       1Q   Median       3Q      Max
-2.7260  -0.8843  -0.2996   0.2600   2.3721

Coefficients:
                       Estimate Std. Error z value Pr(>|z|)
(Intercept)            -3.75117    0.59658  -6.288 3.22e-10 ***
log(Constrained$Length)  1.02325    0.11777   8.688  < 2e-16 ***
log(Constrained$AADT)    0.55315    0.07035   7.863 3.74e-15 ***
Constrained$Ea20         0.25024    0.31802   0.787    0.431
---
Signif. codes:  0 ‘***’ 0.001 ‘**’ 0.01 ‘*’ 0.05 ‘.’ 0.1 ‘ ’ 1

(Dispersion parameter for Negative Binomial(3.4124) family taken to be
 1)

    Null deviance: 256.267  on 91  degrees of freedom
Residual deviance:  93.822  on 88  degrees of freedom
AIC: 479.08

Number of Fisher Scoring iterations: 1


              Theta:  3.412
          Std. Err.:  0.815

 2 x log-likelihood:  -469.081
```

L10

```
> summary(Complete)

Call:
glm.nb(formula = SPFData$Accidents ~ log(SPFData$Length) + log(SPFData
$AADT) +
    SPFData$L10, init.theta = 3.838478712, link = log)
```

```
Deviance Residuals:
    Min       1Q   Median       3Q      Max
-2.6416  -0.8734  -0.2984   0.2836   2.9263

Coefficients:
                  Estimate Std. Error z value Pr(>|z|)
(Intercept)        -4.58400    0.51729  -8.862   <2e-16 ***
log(SPFData$Length)  0.98974    0.09044  10.943   <2e-16 ***
log(SPFData$AADT)    0.63965    0.06083  10.515   <2e-16 ***
SPFData$L10          0.81590    0.37306   2.187   0.0287 *
---
Signif. codes:  0 ‘***’ 0.001 ‘**’ 0.01 ‘*’ 0.05 ‘.’ 0.1 ‘ ’ 1

(Dispersion parameter for Negative Binomial(3.8385) family taken to be
 1)

    Null deviance: 465.26  on 152  degrees of freedom
Residual deviance: 156.24  on 149  degrees of freedom
AIC: 709.68

Number of Fisher Scoring iterations: 1


              Theta:  3.838
          Std. Err.:  0.829

 2 x log-likelihood:  -699.677


> summary(ModelFree)

Call:
glm.nb(formula = Free$Accidents ~ log(Free$Length) + log(Free$AADT) +
    Free$L10, init.theta = 7.514758404, link = log)

Deviance Residuals:
    Min       1Q   Median       3Q      Max
-2.1041  -1.0506  -0.0998   0.4857   2.4132

Coefficients:
                Estimate Std. Error z value Pr(>|z|)
(Intercept)      -5.57375    1.10183  -5.059 4.22e-07 ***
log(Free$Length)  0.73706    0.13850   5.322 1.03e-07 ***
log(Free$AADT)    0.80945    0.13558   5.970 2.37e-09 ***
Free$L10          0.01469    0.68401   0.021    0.983
---
Signif. codes:  0 ‘***’ 0.001 ‘**’ 0.01 ‘*’ 0.05 ‘.’ 0.1 ‘ ’ 1

(Dispersion parameter for Negative Binomial(7.5148) family taken to be
 1)

    Null deviance: 183.917  on 60  degrees of freedom
Residual deviance:  64.566  on 57  degrees of freedom
AIC: 236.45

Number of Fisher Scoring iterations: 1


              Theta:  7.51
          Std. Err.:  4.79

 2 x log-likelihood:  -226.448


> summary(ModelConstrained)
```

```
Call:
glm.nb(formula = Constrained$Accidents ~ log(Constrained$Length) +
    log(Constrained$AADT) + Constrained$L10, init.theta = 4.07625688,
    link = log)

Deviance Residuals:
    Min       1Q   Median       3Q      Max
-2.5861  -0.8689  -0.2843   0.3855   2.6916

Coefficients:
                       Estimate Std. Error z value Pr(>|z|)
(Intercept)            -4.27334    0.61514  -6.947 3.73e-12 ***
log(Constrained$Length)  1.06566    0.11293   9.437  < 2e-16 ***
log(Constrained$AADT)    0.57967    0.06861   8.449  < 2e-16 ***
Constrained$L10          1.26371    0.45725   2.764  0.00571 **
---
Signif. codes:  0 ‘***’ 0.001 ‘**’ 0.01 ‘*’ 0.05 ‘.’ 0.1 ‘ ’ 1

(Dispersion parameter for Negative Binomial(4.0763) family taken to be
 1)

    Null deviance: 284.989  on 91  degrees of freedom
Residual deviance:  95.824  on 88  degrees of freedom
AIC: 472.44

Number of Fisher Scoring iterations: 1


              Theta:  4.08
          Std. Err.:  1.05

 2 x log-likelihood:  -462.437
```

L20

```
> summary(Complete)

Call:
glm.nb(formula = SPFData$Accidents ~ log(SPFData$Length) + log(SPFData
$AADT) +
    SPFData$L20, init.theta = 3.535639524, link = log)

Deviance Residuals:
    Min       1Q   Median       3Q      Max
-2.7241  -0.9121  -0.3152   0.2894   2.7670

Coefficients:
                     Estimate Std. Error z value Pr(>|z|)
(Intercept)          -4.21671    0.48695  -8.659   <2e-16 ***
log(SPFData$Length)   0.97814    0.09180  10.656   <2e-16 ***
log(SPFData$AADT)     0.61454    0.06061  10.139   <2e-16 ***
SPFData$L20           1.25313    1.81554   0.690     0.49
---
Signif. codes:  0 ‘***’ 0.001 ‘**’ 0.01 ‘*’ 0.05 ‘.’ 0.1 ‘ ’ 1

(Dispersion parameter for Negative Binomial(3.5356) family taken to be
 1)

    Null deviance: 444.87  on 152  degrees of freedom
Residual deviance: 154.50  on 149  degrees of freedom
AIC: 713.79

Number of Fisher Scoring iterations: 1
```

```
              Theta:  3.536
          Std. Err.:  0.732

 2 x log-likelihood:  -703.789


> summary(ModelFree)

Call:
glm.nb(formula = Free$Accidents ~ log(Free$Length) + log(Free$AADT) +
    Free$L20, init.theta = 8.698961489, link = log)

Deviance Residuals:
    Min       1Q   Median       3Q      Max
-2.1992  -1.0449  -0.1511   0.5792   2.4485

Coefficients:
                Estimate Std. Error z value Pr(>|z|)
(Intercept)      -5.1634     0.9089  -5.681 1.34e-08 ***
log(Free$Length)   0.7208     0.1350   5.341 9.25e-08 ***
log(Free$AADT)     0.7667     0.1176   6.520 7.03e-11 ***
Free$L20          -5.7771     4.5006  -1.284    0.199
---
Signif. codes:  0 ‘***’ 0.001 ‘**’ 0.01 ‘*’ 0.05 ‘.’ 0.1 ‘ ’ 1

(Dispersion parameter for Negative Binomial(8.699) family taken to be
1)

    Null deviance: 191.992  on 60  degrees of freedom
Residual deviance:  64.974  on 57  degrees of freedom
AIC: 234.82

Number of Fisher Scoring iterations: 1


              Theta:  8.70
          Std. Err.:  6.01

 2 x log-likelihood:  -224.817


> summary(ModelConstrained)

Call:
glm.nb(formula = Constrained$Accidents ~ log(Constrained$Length) +
    log(Constrained$AADT) + Constrained$L20, init.theta = 3.43047467,
    link = log)

Deviance Residuals:
    Min       1Q   Median       3Q      Max
-2.7168  -0.8777  -0.2926   0.2602   2.3813

Coefficients:
                      Estimate Std. Error z value Pr(>|z|)
(Intercept)           -3.76157    0.59658  -6.305 2.88e-10 ***
log(Constrained$Length)  1.02320    0.11723   8.728  < 2e-16 ***
log(Constrained$AADT)    0.55365    0.07026   7.880 3.27e-15 ***
Constrained$L20           1.89543    2.14344   0.884    0.377
---
Signif. codes:  0 ‘***’ 0.001 ‘**’ 0.01 ‘*’ 0.05 ‘.’ 0.1 ‘ ’ 1

(Dispersion parameter for Negative Binomial(3.4305) family taken to be
 1)

    Null deviance: 257.099  on 91  degrees of freedom
```

```
Residual deviance:  93.929  on 88  degrees of freedom
AIC: 478.92

Number of Fisher Scoring iterations: 1


              Theta:  3.430
          Std. Err.:  0.822

 2 x log-likelihood:  -468.922
```

Average operating speed reduction (SpeedReductionAvg)

```
> summary(Complete)

Call:
glm.nb(formula = SPFData$Accidents ~ log(SPFData$Length) + log(SPFData
$AADT) +
    SPFData$SpeedReductionAvg, init.theta = 3.685361797, link = log)

Deviance Residuals:
    Min       1Q   Median       3Q      Max
-2.6514  -0.9292  -0.2934   0.3822   2.6136

Coefficients:
                          Estimate Std. Error z value Pr(>|z|)
(Intercept)               -4.54928    0.55150  -8.249   <2e-16 ***
log(SPFData$Length)        0.99114    0.09107  10.883   <2e-16 ***
log(SPFData$AADT)          0.63181    0.06187  10.212   <2e-16 ***
SPFData$SpeedReductionAvg  0.02175    0.01436   1.514     0.13
---
Signif. codes:  0 ‘***’ 0.001 ‘**’ 0.01 ‘*’ 0.05 ‘.’ 0.1 ‘ ’ 1

(Dispersion parameter for Negative Binomial(3.6854) family taken to be
 1)

    Null deviance: 455.11  on 152  degrees of freedom
Residual deviance: 155.77  on 149  degrees of freedom
AIC: 712.08

Number of Fisher Scoring iterations: 1


              Theta:  3.685
          Std. Err.:  0.779

 2 x log-likelihood:  -702.079


> summary(ModelFree)

Call:
glm.nb(formula = Free$Accidents ~ log(Free$Length) + log(Free$AADT) +
    Free$SpeedReductionAvg, init.theta = 7.756268426, link = log)

Deviance Residuals:
    Min       1Q   Median       3Q      Max
-2.0868  -1.0652  -0.1310   0.4838   2.3646

Coefficients:
                          Estimate Std. Error z value Pr(>|z|)
(Intercept)             -5.689924   1.001522  -5.681 1.34e-08 ***
log(Free$Length)         0.745747   0.141044   5.287 1.24e-07 ***
```

```
log(Free$AADT)           0.815948   0.119531   6.826 8.72e-12 ***
Free$SpeedReductionAvg   0.006053   0.021985   0.275    0.783
---
Signif. codes:  0 ‘***’ 0.001 ‘**’ 0.01 ‘*’ 0.05 ‘.’ 0.1 ‘ ’ 1

(Dispersion parameter for Negative Binomial(7.7563) family taken to be
 1)

    Null deviance: 185.688  on 60  degrees of freedom
Residual deviance:  64.952  on 57  degrees of freedom
AIC: 236.38

Number of Fisher Scoring iterations: 1


              Theta:  7.76
          Std. Err.:  5.05

 2 x log-likelihood:  -226.377


> summary(ModelConstrained)

Call:
glm.nb(formula = Constrained$Accidents ~ log(Constrained$Length) +
    log(Constrained$AADT) + Constrained$SpeedReductionAvg, init.theta
= 3.596689639,
    link = log)

Deviance Residuals:
    Min       1Q   Median       3Q      Max
-2.6299  -0.9449  -0.3138   0.3601   2.2976

Coefficients:
                           Estimate Std. Error z value Pr(>|z|)
(Intercept)                -4.16802    0.66104  -6.305 2.88e-10 ***
log(Constrained$Length)     1.02456    0.11361   9.018  < 2e-16 ***
log(Constrained$AADT)       0.57642    0.07131   8.083 6.30e-16 ***
Constrained$SpeedReductionAvg  0.02934    0.01762   1.665   0.0959 .
---
Signif. codes:  0 ‘***’ 0.001 ‘**’ 0.01 ‘*’ 0.05 ‘.’ 0.1 ‘ ’ 1

(Dispersion parameter for Negative Binomial(3.5967) family taken to be
 1)

    Null deviance: 264.603  on 91  degrees of freedom
Residual deviance:  94.425  on 88  degrees of freedom
AIC: 477.06

Number of Fisher Scoring iterations: 1


              Theta:  3.597
          Std. Err.:  0.879

 2 x log-likelihood:  -467.056
```

Average deceleration rate (DecelAvg)

```
> summary(Complete)

Call:
glm.nb(formula = SPFData$Accidents ~ log(SPFData$Length) + log(SPFData
$AADT) +
```

```
    SPFData$DecelAvg, init.theta = 4.475674855, link = log)

Deviance Residuals:
    Min       1Q   Median       3Q      Max
-2.5259  -0.8421  -0.2180   0.4949   2.7055

Coefficients:
                  Estimate Std. Error z value Pr(>|z|)
(Intercept)       -6.81776    0.74856  -9.108  < 2e-16 ***
log(SPFData$Length)  1.08378    0.08982  12.067  < 2e-16 ***
log(SPFData$AADT)    0.83601    0.07565  11.052  < 2e-16 ***
SPFData$DecelAvg    -0.72692    0.15627  -4.652 3.29e-06 ***
---
Signif. codes:  0 ‘***’ 0.001 ‘**’ 0.01 ‘*’ 0.05 ‘.’ 0.1 ‘ ’ 1

(Dispersion parameter for Negative Binomial(4.4757) family taken to be
 1)

    Null deviance: 504.28  on 152  degrees of freedom
Residual deviance: 151.46  on 149  degrees of freedom
AIC: 694.57

Number of Fisher Scoring iterations: 1


              Theta:  4.48
          Std. Err.:  1.02

 2 x log-likelihood:  -684.568


> summary(ModelFree)

Call:
glm.nb(formula = Free$Accidents ~ log(Free$Length) + log(Free$AADT) +
    Free$DecelAvg, init.theta = 9.146345757, link = log)

Deviance Residuals:
    Min       1Q   Median       3Q      Max
-2.0642  -0.9248  -0.1757   0.4842   2.4425

Coefficients:
                 Estimate Std. Error z value Pr(>|z|)
(Intercept)       -7.4849     1.2545  -5.966 2.43e-09 ***
log(Free$Length)   0.8956     0.1581   5.666 1.46e-08 ***
log(Free$AADT)     0.9586     0.1329   7.215 5.40e-13 ***
Free$DecelAvg     -0.6084     0.2887  -2.107   0.0351 *
---
Signif. codes:  0 ‘***’ 0.001 ‘**’ 0.01 ‘*’ 0.05 ‘.’ 0.1 ‘ ’ 1

(Dispersion parameter for Negative Binomial(9.1463) family taken to be
 1)

    Null deviance: 194.685  on 60  degrees of freedom
Residual deviance:  63.112  on 57  degrees of freedom
AIC: 232.3

Number of Fisher Scoring iterations: 1


              Theta:  9.15
          Std. Err.:  6.57

 2 x log-likelihood:  -222.30
```

```
> summary(ModelConstrained)

Call:
glm.nb(formula = Constrained$Accidents ~ log(Constrained$Length) +
    log(Constrained$AADT) + Constrained$DecelAvg, init.theta = 4.12848
111,
    link = log)

Deviance Residuals:
    Min       1Q   Median       3Q      Max
-2.5093  -0.8595  -0.2175   0.4657   2.0297

Coefficients:
                          Estimate Std. Error z value Pr(>|z|)
(Intercept)              -6.35827    0.97664  -6.510 7.50e-11 ***
log(Constrained$Length)   1.11084    0.11326   9.808  < 2e-16 ***
log(Constrained$AADT)     0.78187    0.09585   8.158 3.42e-16 ***
Constrained$DecelAvg     -0.68247    0.19273  -3.541 0.000398 ***
---
Signif. codes:  0 ‘***’ 0.001 ‘**’ 0.01 ‘*’ 0.05 ‘.’ 0.1 ‘ ’ 1

(Dispersion parameter for Negative Binomial(4.1285) family taken to be
 1)

    Null deviance: 287.104  on 91  degrees of freedom
Residual deviance:  92.219  on 88  degrees of freedom
AIC: 468.24

Number of Fisher Scoring iterations: 1


              Theta:  4.13
          Std. Err.:  1.06

 2 x log-likelihood:  -458.238
```

Speed reduction dispersion (SpeedReductionDisp)

```
> summary(Complete)

Call:
glm.nb(formula = SPFData$Accidents ~ log(SPFData$Length) + log(SPFData
$AADT) +
    SPFData$SpeedReductionDisp, init.theta = 3.728231795, link = log)

Deviance Residuals:
    Min       1Q   Median       3Q      Max
-2.7076  -0.9623  -0.2579   0.2958   2.6577

Coefficients:
                           Estimate Std. Error z value Pr(>|z|)
(Intercept)               -4.81451    0.56748  -8.484   <2e-16 ***
log(SPFData$Length)        0.98276    0.09016  10.900   <2e-16 ***
log(SPFData$AADT)          0.65601    0.06312  10.393   <2e-16 ***
SPFData$SpeedReductionDisp 0.03952    0.01841   2.147   0.0318 *
---
Signif. codes:  0 ‘***’ 0.001 ‘**’ 0.01 ‘*’ 0.05 ‘.’ 0.1 ‘ ’ 1

(Dispersion parameter for Negative Binomial(3.7282) family taken to be
 1)

    Null deviance: 457.99  on 152  degrees of freedom
Residual deviance: 154.39  on 149  degrees of freedom
AIC: 709.88
```

```
Number of Fisher Scoring iterations: 1


              Theta:  3.728
          Std. Err.:  0.788

 2 x log-likelihood:  -699.876


> summary(ModelFree)

Call:
glm.nb(formula = Free$Accidents ~ log(Free$Length) + log(Free$AADT) +
    Free$SpeedReductionDisp, init.theta = 9.480212182, link = log)

Deviance Residuals:
    Min       1Q   Median       3Q      Max
-2.0645  -0.9412  -0.1691   0.4227   2.1448

Coefficients:
                         Estimate Std. Error z value Pr(>|z|)
(Intercept)              -6.78255    1.16826  -5.806 6.41e-09 ***
log(Free$Length)          0.76373    0.13409   5.696 1.23e-08 ***
log(Free$AADT)            0.91413    0.13227   6.911 4.80e-12 ***
Free$SpeedReductionDisp   0.05256    0.03312   1.587    0.113
---
Signif. codes:  0 ‘***’ 0.001 ‘**’ 0.01 ‘*’ 0.05 ‘.’ 0.1 ‘ ’ 1

(Dispersion parameter for Negative Binomial(9.4802) family taken to be
 1)

    Null deviance: 196.585  on 60  degrees of freedom
Residual deviance:  65.367  on 57  degrees of freedom
AIC: 234.1

Number of Fisher Scoring iterations: 1


              Theta:  9.48
          Std. Err.:  6.92

 2 x log-likelihood:  -224.10


> summary(ModelConstrained)

Call:
glm.nb(formula = Constrained$Accidents ~ log(Constrained$Length) +
    log(Constrained$AADT) + Constrained$SpeedReductionDisp, init.theta
 = 3.571452713,
    link = log)

Deviance Residuals:
    Min       1Q   Median       3Q      Max
-2.7046  -0.9223  -0.2797   0.3263   2.2569

Coefficients:
                                Estimate Std. Error z value Pr(>|z|)

(Intercept)                     -4.22264    0.67397  -6.265 3.72e-10 **
*
log(Constrained$Length)          1.01515    0.11343   8.949  < 2e-16 **
*
log(Constrained$AADT)            0.58622    0.07241   8.095 5.71e-16 **
*
```

```
Constrained$SpeedReductionDisp  0.03581    0.02165   1.654   0.0981 .
---
Signif. codes:  0 ‘***’ 0.001 ‘**’ 0.01 ‘*’ 0.05 ‘.’ 0.1 ‘ ’ 1

(Dispersion parameter for Negative Binomial(3.5715) family taken to be
 1)

    Null deviance: 263.479  on 91  degrees of freedom
Residual deviance:  94.028  on 88  degrees of freedom
AIC: 477.01

Number of Fisher Scoring iterations: 1


              Theta:  3.571
          Std. Err.:  0.870

 2 x log-likelihood:  -467.008
```

Deceleration dispersion (DecelDisp)

```
> summary(Complete)

Call:
glm.nb(formula = SPFData$Accidents ~ log(SPFData$Length) + log(SPFData
$AADT) +
    SPFData$DecelDisp, init.theta = 3.729959037, link = log)

Deviance Residuals:
    Min       1Q   Median       3Q      Max
-2.7290  -0.8833  -0.3022   0.3280   2.8284

Coefficients:
                    Estimate Std. Error z value Pr(>|z|)
(Intercept)         -4.44833    0.49534  -8.980   <2e-16 ***
log(SPFData$Length)  0.97826    0.08937  10.946   <2e-16 ***
log(SPFData$AADT)    0.63874    0.06112  10.450   <2e-16 ***
SPFData$DecelDisp    0.22905    0.09615   2.382   0.0172 *
---
Signif. codes:  0 ‘***’ 0.001 ‘**’ 0.01 ‘*’ 0.05 ‘.’ 0.1 ‘ ’ 1

(Dispersion parameter for Negative Binomial(3.73) family taken to be 1
)

    Null deviance: 458.10  on 152  degrees of freedom
Residual deviance: 154.01  on 149  degrees of freedom
AIC: 709.46

Number of Fisher Scoring iterations: 1


              Theta:  3.730
          Std. Err.:  0.788

 2 x log-likelihood:  -699.463


> summary(ModelFree)

Call:
glm.nb(formula = Free$Accidents ~ log(Free$Length) + log(Free$AADT) +
    Free$DecelDisp, init.theta = 7.530272348, link = log)
```

```
Deviance Residuals:
    Min       1Q   Median       3Q      Max
-2.0030  -1.0187  -0.1150   0.4192   2.5113

Coefficients:
                 Estimate Std. Error z value Pr(>|z|)
(Intercept)       -6.4790     1.2368  -5.239 1.62e-07 ***
log(Free$Length)   0.7728     0.1433   5.393 6.95e-08 ***
log(Free$AADT)     0.9034     0.1469   6.149 7.82e-10 ***
Free$DecelDisp     0.6842     0.6281   1.089    0.276
---
Signif. codes:  0 ‘***’ 0.001 ‘**’ 0.01 ‘*’ 0.05 ‘.’ 0.1 ‘ ’ 1

(Dispersion parameter for Negative Binomial(7.5303) family taken to be
 1)

    Null deviance: 184.033  on 60  degrees of freedom
Residual deviance:  63.437  on 57  degrees of freedom
AIC: 235.29

Number of Fisher Scoring iterations: 1


              Theta:  7.53
          Std. Err.:  4.81

 2 x log-likelihood:  -225.289


> summary(ModelConstrained)

Call:
glm.nb(formula = Constrained$Accidents ~ log(Constrained$Length) +
    log(Constrained$AADT) + Constrained$DecelDisp, init.theta = 3.5855
91832,
    link = log)

Deviance Residuals:
    Min       1Q   Median       3Q      Max
-2.7242  -0.8812  -0.3534   0.2829   2.2537

Coefficients:
                         Estimate Std. Error z value Pr(>|z|)
(Intercept)             -3.92685    0.60171  -6.526 6.75e-11 ***
log(Constrained$Length)  1.01502    0.11213   9.052  < 2e-16 ***
log(Constrained$AADT)    0.57446    0.07102   8.089 6.00e-16 ***
Constrained$DecelDisp    0.19665    0.10085   1.950   0.0512 .
---
Signif. codes:  0 ‘***’ 0.001 ‘**’ 0.01 ‘*’ 0.05 ‘.’ 0.1 ‘ ’ 1

(Dispersion parameter for Negative Binomial(3.5856) family taken to be
 1)

    Null deviance: 264.109  on 91  degrees of freedom
Residual deviance:  93.553  on 88  degrees of freedom
AIC: 476.34

Number of Fisher Scoring iterations: 1


              Theta:  3.586
          Std. Err.:  0.871

 2 x log-likelihood:  -466.338
```

Average deceleration length (DecrLengthAvg)

```
> summary(Complete)

Call:
glm.nb(formula = SPFData$Accidents ~ log(SPFData$Length) + log(SPFData
$AADT) +
    SPFData$DecrLengthAvg, init.theta = 3.589327932, link = log)

Deviance Residuals:
    Min       1Q   Median       3Q      Max
-2.7658  -0.8653  -0.3054   0.3711   2.9098

Coefficients:
                          Estimate Std. Error z value Pr(>|z|)
(Intercept)             -4.263719   0.482151  -8.843   <2e-16 ***
log(SPFData$Length)      0.991764   0.090880  10.913   <2e-16 ***
log(SPFData$AADT)        0.657077   0.064104  10.250   <2e-16 ***
SPFData$DecrLengthAvg -0.003949   0.002155  -1.832    0.067 .
---
Signif. codes:  0 ‘***’ 0.001 ‘**’ 0.01 ‘*’ 0.05 ‘.’ 0.1 ‘ ’ 1

(Dispersion parameter for Negative Binomial(3.5893) family taken to be
 1)

    Null deviance: 448.58  on 152  degrees of freedom
Residual deviance: 152.73  on 149  degrees of freedom
AIC: 710.92

Number of Fisher Scoring iterations: 1


              Theta:  3.589
          Std. Err.:  0.744

 2 x log-likelihood:  -700.923


> summary(ModelFree)

Call:
glm.nb(formula = Free$Accidents ~ log(Free$Length) + log(Free$AADT) +
    Free$DecrLengthAvg, init.theta = 7.350210106, link = log)

Deviance Residuals:
    Min       1Q   Median       3Q      Max
-2.0789  -1.0505  -0.1147   0.4409   2.5270

Coefficients:
                        Estimate Std. Error z value Pr(>|z|)
(Intercept)           -5.544843   0.879675  -6.303 2.91e-10 ***
log(Free$Length)       0.747961   0.140561   5.321 1.03e-07 ***
log(Free$AADT)         0.824520   0.118267   6.972 3.13e-12 ***
Free$DecrLengthAvg -0.002145   0.003138  -0.683    0.494
---
Signif. codes:  0 ‘***’ 0.001 ‘**’ 0.01 ‘*’ 0.05 ‘.’ 0.1 ‘ ’ 1

(Dispersion parameter for Negative Binomial(7.3502) family taken to be
 1)

    Null deviance: 182.669  on 60  degrees of freedom
Residual deviance:  63.767  on 57  degrees of freedom
AIC: 235.97

Number of Fisher Scoring iterations: 1
```

```
              Theta:  7.35
          Std. Err.:  4.61

 2 x log-likelihood:  -225.974


> summary(ModelConstrained)

Call:
glm.nb(formula = Constrained$Accidents ~ log(Constrained$Length) +
    log(Constrained$AADT) + Constrained$DecrLengthAvg, init.theta = 3.
439095168,
    link = log)

Deviance Residuals:
    Min       1Q   Median       3Q      Max
-2.7551  -0.8623  -0.3607   0.4443   2.1573

Coefficients:
                           Estimate Std. Error z value Pr(>|z|)
(Intercept)               -3.806904   0.593737  -6.412 1.44e-10 ***
log(Constrained$Length)    1.030065   0.114423   9.002  < 2e-16 ***
log(Constrained$AADT)      0.598613   0.077570   7.717 1.19e-14 ***
Constrained$DecrLengthAvg -0.003847   0.002764  -1.392    0.164
---
Signif. codes:  0 ‘***’ 0.001 ‘**’ 0.01 ‘*’ 0.05 ‘.’ 0.1 ‘ ’ 1

(Dispersion parameter for Negative Binomial(3.4391) family taken to be
 1)

    Null deviance: 257.494  on 91  degrees of freedom
Residual deviance:  92.962  on 88  degrees of freedom
AIC: 477.83

Number of Fisher Scoring iterations: 1


              Theta:  3.439
          Std. Err.:  0.822

 2 x log-likelihood:  -467.828
```

Deceleration length divided by total length (DecrLengthDivLength)

```
> summary(Complete)

Call:
glm.nb(formula = SPFData$Accidents ~ log(SPFData$Length) + log(SPFData
$AADT) +
    SPFData$DecrLengthDivLength, init.theta = 3.67912553, link = log)

Deviance Residuals:
    Min       1Q   Median       3Q      Max
-2.6568  -0.8444  -0.2774   0.3362   2.4614

Coefficients:
                            Estimate Std. Error z value Pr(>|z|)
(Intercept)                -4.64714    0.57650  -8.061 7.57e-16 ***
log(SPFData$Length)         0.99224    0.09112  10.890  < 2e-16 ***
log(SPFData$AADT)           0.64154    0.06326  10.141  < 2e-16 ***
SPFData$DecrLengthDivLength  1.74170    1.09660   1.588    0.112
---
```

```
Signif. codes:  0 ‘***’ 0.001 ‘**’ 0.01 ‘*’ 0.05 ‘.’ 0.1 ‘ ’ 1

(Dispersion parameter for Negative Binomial(3.6791) family taken to be
 1)

    Null deviance: 454.69  on 152  degrees of freedom
Residual deviance: 155.54  on 149  degrees of freedom
AIC: 711.97

Number of Fisher Scoring iterations: 1


              Theta:  3.679
          Std. Err.:  0.777

 2 x log-likelihood:  -701.968


> summary(ModelFree)

Call:
glm.nb(formula = Free$Accidents ~ log(Free$Length) + log(Free$AADT) +
    Free$DecrLengthDivLength, init.theta = 9.340742801, link = log)

Deviance Residuals:
    Min       1Q   Median       3Q      Max
-2.2588  -1.0166  -0.1688   0.4735   2.2694

Coefficients:
                          Estimate Std. Error z value Pr(>|z|)
(Intercept)               -6.2227     1.0112  -6.154 7.57e-10 ***
log(Free$Length)           0.7910     0.1409   5.612 2.00e-08 ***
log(Free$AADT)             0.8526     0.1179   7.232 4.75e-13 ***
Free$DecrLengthDivLength   1.8367     1.4884   1.234    0.217
---
Signif. codes:  0 ‘***’ 0.001 ‘**’ 0.01 ‘*’ 0.05 ‘.’ 0.1 ‘ ’ 1

(Dispersion parameter for Negative Binomial(9.3407) family taken to be
 1)

    Null deviance: 195.80  on 60  degrees of freedom
Residual deviance:  66.21  on 57  degrees of freedom
AIC: 235.13

Number of Fisher Scoring iterations: 1


              Theta:  9.34
          Std. Err.:  6.88

 2 x log-likelihood:  -225.13


> summary(ModelConstrained)

Call:
glm.nb(formula = Constrained$Accidents ~ log(Constrained$Length) +
    log(Constrained$AADT) + Constrained$DecrLengthDivLength,
    init.theta = 3.501604715, link = log)

Deviance Residuals:
    Min       1Q   Median       3Q      Max
-2.6552  -0.9087  -0.2945   0.3755   2.2254

Coefficients:
                                Estimate Std. Error z value Pr(>|z|)
```

```
(Intercept)                          -4.12959    0.68544  -6.025 1.69e-09 *
**
log(Constrained$Length)               1.00745    0.11335   8.888  < 2e-16 *
**
log(Constrained$AADT)                 0.57920    0.07287   7.948 1.89e-15 *
**
Constrained$DecrLengthDivLength       1.91272    1.43588   1.332    0.183

---
Signif. codes:  0 ‘***’ 0.001 ‘**’ 0.01 ‘*’ 0.05 ‘.’ 0.1 ‘ ’ 1

(Dispersion parameter for Negative Binomial(3.5016) family taken to be
 1)

    Null deviance: 260.340  on 91  degrees of freedom
Residual deviance:  94.122  on 88  degrees of freedom
AIC: 478.08

Number of Fisher Scoring iterations: 1


              Theta:  3.502
          Std. Err.:  0.849

 2 x log-likelihood:  -468.085
```

Number of decelerations (DecelNum)

```
> summary(Complete)

Call:
glm.nb(formula = SPFData$Accidents ~ log(SPFData$Length) + log(SPFData
$AADT) +
    SPFData$DecelNum, init.theta = 3.888070963, link = log)

Deviance Residuals:
    Min       1Q   Median       3Q      Max
-2.7040  -0.9247  -0.2418   0.4263   2.4596

Coefficients:
                     Estimate Std. Error z value Pr(>|z|)
(Intercept)         -4.905256   0.551530  -8.894  < 2e-16 ***
log(SPFData$Length)  0.780094   0.109119   7.149 8.74e-13 ***
log(SPFData$AADT)    0.706399   0.068482  10.315  < 2e-16 ***
SPFData$DecelNum     0.012243   0.004599   2.662  0.00777 **
---
Signif. codes:  0 ‘***’ 0.001 ‘**’ 0.01 ‘*’ 0.05 ‘.’ 0.1 ‘ ’ 1

(Dispersion parameter for Negative Binomial(3.8881) family taken to be
 1)

    Null deviance: 468.48  on 152  degrees of freedom
Residual deviance: 154.49  on 149  degrees of freedom
AIC: 707.04

Number of Fisher Scoring iterations: 1


              Theta:  3.888
          Std. Err.:  0.845

 2 x log-likelihood:  -697.043
```

```
> summary(ModelFree)

Call:
glm.nb(formula = Free$Accidents ~ log(Free$Length) + log(Free$AADT) +
    Free$DecelNum, init.theta = 8.602614455, link = log)

Deviance Residuals:
    Min       1Q   Median       3Q      Max
-1.9730  -1.0687  -0.1278   0.5281   2.3107

Coefficients:
                 Estimate Std. Error z value Pr(>|z|)
(Intercept)      -6.49767    0.99887  -6.505 7.77e-11 ***
log(Free$Length)  0.54443    0.16927   3.216   0.0013 **
log(Free$AADT)    0.90899    0.12560   7.237 4.57e-13 ***
Free$DecelNum     0.02520    0.01342   1.878   0.0603 .
---
Signif. codes:  0 ‘***’ 0.001 ‘**’ 0.01 ‘*’ 0.05 ‘.’ 0.1 ‘ ’ 1

(Dispersion parameter for Negative Binomial(8.6026) family taken to be
 1)

    Null deviance: 191.388  on 60  degrees of freedom
Residual deviance:  63.072  on 57  degrees of freedom
AIC: 233.06

Number of Fisher Scoring iterations: 1


              Theta:  8.60
          Std. Err.:  5.74

 2 x log-likelihood:  -223.064


> summary(ModelConstrained)

Call:
glm.nb(formula = Constrained$Accidents ~ log(Constrained$Length) +
    log(Constrained$AADT) + Constrained$DecelNum, init.theta = 3.53138
2337,
    link = log)

Deviance Residuals:
    Min       1Q   Median       3Q      Max
-2.7001  -0.8889  -0.2577   0.4019   2.3053

Coefficients:
                       Estimate Std. Error z value Pr(>|z|)
(Intercept)           -4.195333   0.689482  -6.085 1.17e-09 ***
log(Constrained$Length)  0.863701   0.138199   6.250 4.11e-10 ***
log(Constrained$AADT)    0.620386   0.083169   7.459 8.69e-14 ***
Constrained$DecelNum     0.007890   0.005225   1.510    0.131
---
Signif. codes:  0 ‘***’ 0.001 ‘**’ 0.01 ‘*’ 0.05 ‘.’ 0.1 ‘ ’ 1

(Dispersion parameter for Negative Binomial(3.5314) family taken to be
 1)

    Null deviance: 261.683  on 91  degrees of freedom
Residual deviance:  93.827  on 88  degrees of freedom
AIC: 477.37

Number of Fisher Scoring iterations: 1
```

```
              Theta:  3.531
          Std. Err.:  0.863

 2 x log-likelihood:  -467.367
```

IV.3. Final consistency model

```
> summary(Complete)

Call:
glm.nb(formula = SPFData$Accidents ~ log(SPFData$Length) + log(SPFData
$AADT) +
    Consistency, init.theta = 4.598038918, link = log)

Deviance Residuals:
    Min       1Q   Median       3Q      Max
-2.4009  -0.8944  -0.2016   0.4772   2.5665

Coefficients:
                    Estimate Std. Error z value Pr(>|z|)
(Intercept)         -4.26225    0.46140  -9.238  < 2e-16 ***
log(SPFData$Length)  1.13196    0.09322  12.143  < 2e-16 ***
log(SPFData$AADT)    0.85298    0.07643  11.161  < 2e-16 ***
Consistency         -0.42896    0.09064  -4.733 2.22e-06 ***
---
Signif. codes:  0 ‘***’ 0.001 ‘**’ 0.01 ‘*’ 0.05 ‘.’ 0.1 ‘ ’ 1

(Dispersion parameter for Negative Binomial(4.598) family taken to be
1)

    Null deviance: 511.24  on 152  degrees of freedom
Residual deviance: 151.74  on 149  degrees of freedom
AIC: 693.12

Number of Fisher Scoring iterations: 1


              Theta:  4.60
          Std. Err.:  1.06

 2 x log-likelihood:  -683.117


> summary(ModelFree)

Call:
glm.nb(formula = Free$Accidents ~ log(Free$Length) + log(Free$AADT) +
    ConsistencyFree, init.theta = 10.19672396, link = log)

Deviance Residuals:
    Min       1Q   Median       3Q      Max
-2.0183  -0.9682  -0.1648   0.5800   2.2641

Coefficients:
                  Estimate Std. Error z value Pr(>|z|)
(Intercept)       -5.5819     0.8553  -6.526 6.76e-11 ***
log(Free$Length)   0.9265     0.1611   5.750 8.95e-09 ***
log(Free$AADT)     0.9934     0.1388   7.159 8.11e-13 ***
ConsistencyFree   -0.3403     0.1553  -2.191   0.0285 *
---
Signif. codes:  0 ‘***’ 0.001 ‘**’ 0.01 ‘*’ 0.05 ‘.’ 0.1 ‘ ’ 1
```

```
(Dispersion parameter for Negative Binomial(10.1967) family taken to b
e 1)

    Null deviance: 200.379  on 60  degrees of freedom
Residual deviance:  64.045  on 57  degrees of freedom
AIC: 231.89

Number of Fisher Scoring iterations: 1


              Theta:  10.20
          Std. Err.:  7.76

 2 x log-likelihood:  -221.887


> summary(ModelConstrained)

Call:
glm.nb(formula = Constrained$Accidents ~ log(Constrained$Length) +
    log(Constrained$AADT) + ConsistencyConstrained, init.theta = 4.286
998094,
    link = log)

Deviance Residuals:
    Min       1Q   Median       3Q      Max
-2.4362  -0.8906  -0.2156   0.4802   2.1867

Coefficients:
                         Estimate Std. Error z value Pr(>|z|)
(Intercept)              -3.91602    0.57004  -6.870 6.43e-12 ***
log(Constrained$Length)   1.16103    0.11667   9.952  < 2e-16 ***
log(Constrained$AADT)     0.80150    0.09504   8.433  < 2e-16 ***
ConsistencyConstrained   -0.41954    0.11116  -3.774 0.000161 ***
---
Signif. codes:  0 ‘***’ 0.001 ‘**’ 0.01 ‘*’ 0.05 ‘.’ 0.1 ‘ ’ 1

(Dispersion parameter for Negative Binomial(4.287) family taken to be
1)

    Null deviance: 293.405  on 91  degrees of freedom
Residual deviance:  92.119  on 88  degrees of freedom
AIC: 466.4

Number of Fisher Scoring iterations: 1


              Theta:  4.29
          Std. Err.:  1.12

 2 x log-likelihood:  -456.399
```